frontiers | Research Topics

Updates in ocular therapeutics and surgery, volume II

Edited by
Georgios D. Panos and Horace Massa

Published in
Frontiers in Medicine

ISSN 1664-8714
ISBN 978-2-8325-4497-6
DOI 10.3389/978-2-8325-4497-6

About Frontiers

Frontiers is more than just an open access publisher of scholarly articles: it is a pioneering approach to the world of academia, radically improving the way scholarly research is managed. The grand vision of Frontiers is a world where all people have an equal opportunity to seek, share and generate knowledge. Frontiers provides immediate and permanent online open access to all its publications, but this alone is not enough to realize our grand goals.

Frontiers journal series

The Frontiers journal series is a multi-tier and interdisciplinary set of open-access, online journals, promising a paradigm shift from the current review, selection and dissemination processes in academic publishing. All Frontiers journals are driven by researchers for researchers; therefore, they constitute a service to the scholarly community. At the same time, the *Frontiers journal series* operates on a revolutionary invention, the tiered publishing system, initially addressing specific communities of scholars, and gradually climbing up to broader public understanding, thus serving the interests of the lay society, too.

Dedication to quality

Each Frontiers article is a landmark of the highest quality, thanks to genuinely collaborative interactions between authors and review editors, who include some of the world's best academicians. Research must be certified by peers before entering a stream of knowledge that may eventually reach the public - and shape society; therefore, Frontiers only applies the most rigorous and unbiased reviews. Frontiers revolutionizes research publishing by freely delivering the most outstanding research, evaluated with no bias from both the academic and social point of view. By applying the most advanced information technologies, Frontiers is catapulting scholarly publishing into a new generation.

What are Frontiers Research Topics?

Frontiers Research Topics are very popular trademarks of the *Frontiers journals series*: they are collections of at least ten articles, all centered on a particular subject. With their unique mix of varied contributions from Original Research to Review Articles, Frontiers Research Topics unify the most influential researchers, the latest key findings and historical advances in a hot research area.

Find out more on how to host your own Frontiers Research Topic or contribute to one as an author by contacting the Frontiers editorial office: frontiersin.org/about/contact

Updates in ocular therapeutics and surgery, volume II

Topic editors

Georgios D. Panos — Nottingham University Hospitals NHS Trust, United Kingdom

Horace Massa — Hôpitaux universitaires de Genève (HUG), Switzerland

Citation

Panos, G. D., Massa, H., eds. (2024). *Updates in ocular therapeutics and surgery, volume II*. Lausanne: Frontiers Media SA. doi: 10.3389/978-2-8325-4497-6

Table of contents

frontiers | Frontiers in Medicine

TYPE Editorial
PUBLISHED 08 February 2024
DOI 10.3389/fmed.2024.1370515

OPEN ACCESS

EDITED AND REVIEWED BY
Jodhbir Mehta,
Singapore National Eye Center, Singapore

*CORRESPONDENCE
Georgios D. Panos
✉ gdpanos@gmail.com

RECEIVED 14 January 2024
ACCEPTED 22 January 2024
PUBLISHED 08 February 2024

CITATION
Panos GD and Massa H (2024) Editorial: Updates in ocular therapeutics and surgery, volume II. *Front. Med.* 11:1370515. doi: 10.3389/fmed.2024.1370515

Editorial: Updates in ocular therapeutics and surgery, volume II

Georgios D. Panos[1,2]* and Horace Massa[3]

[1]Department of Ophthalmology, Queen's Medical Centre, Nottingham University Hospitals, Nottingham, United Kingdom, [2]Division of Ophthalmology and Visual Sciences, School of Medicine, University of Nottingham, Nottingham, United Kingdom, [3]Department of Ophthalmology, Geneva University Hospitals, Geneva, Switzerland

KEYWORDS

cornea, macular oedema, uveitis, glaucoma, vitreoretinal surgery, machine learning, eyelid surgery, paediatric ophthalmology

Editorial on the Research Topic
Updates in ocular therapeutics and surgery, volume II

Introduction

It is with great pleasure that we introduce Volume II of "*Updates in Ocular Therapeutics and Surgery*," building upon the success of its predecessor in the ever-evolving field of ophthalmology. This volume emerges at a pivotal time when the landscape of eye care is being redefined by novel treatments and advanced surgical techniques, particularly for conditions like age-related macular degeneration, glaucoma, and diabetic macular oedema, among others.

Recent technological advancements have revolutionised ocular surgery, making procedures safer, faster, and more precise. This Research Topic aims to highlight these transformative therapeutic and surgical approaches, offering a comprehensive overview of the current state-of-the-art and setting a direction for future research. Each article in this Research Topic not only enriches our understanding but also underscores the rapid progress in ocular medicine.

As we delve into this volume, we invite our readers to explore the significant strides made in treating and understanding ocular diseases, marking another milestone in the journey of ophthalmology.

Anterior segment

In this Research Topic, we explore a range of groundbreaking studies in the field of anterior segment ocular therapeutics and surgery. Swain and Eliassi-Rad present a five-year retrospective study on selective laser trabeculoplasty (SLT) in glaucoma patients, revealing mixed long-term efficacy with half of the eyes achieving controlled intraocular pressure (IOP), but an increase in glaucoma medications and progression in Humphrey visual field (HVF) parameters.

Cai et al. investigate the efficacy and safety of oral voriconazole (VCZ) as primary treatment for fungal keratitis (FK). Their study demonstrates significant healing and visual acuity improvement in most cases, although larger ulcers and hypopyon were linked to reduced treatment response, highlighting the need for individualised therapeutic approaches.

The global impact of the COVID-19 pandemic on corneal donor tissue harvesting and transplantation is reviewed by Mousavi et al.. They report a worldwide decline in donor tissue volume and elective corneal transplant procedures during lockdowns, with regional variations in the extent of impact, underscoring the pandemic's significant influence on ophthalmic services.

Deshmukh et al. provide an updated review on the management of keratoconus, covering the latest advancements in treatments ranging from corneal cross-linking to gene therapy. The review also discusses the emerging role of artificial intelligence in early detection and management of the condition.

Xu C. et al.'s study on the effects of resveratrol in rat models of corneal allograft rejection (CGR) reveals its potential in prolonging graft survival and reducing inflammation, implicating the PI3K/Akt pathway as a key mechanism.

Onoe et al. compare the outcomes of microhook ab interno trabeculotomy (μLOT) combined with phacoemulsification and iStent inject W implantation in primary open-angle glaucoma patients. Their findings suggest comparable efficacy between the two surgical methods, with significant improvements in IOP and reduced medication requirements.

Finally, Huang et al. explore the relationships between lens diameter (LD) and ocular biometric parameters through ultrasound biomicroscopy. They find that larger LD is associated with elder age, male gender, and larger white-to-white distance, particularly in eyes without extreme myopia, providing valuable insights for personalised surgical planning and visual outcome enhancement.

Posterior segment

In the domain of posterior segment ocular therapeutics and surgery, this Research Topic presents a series of insightful studies contributing significantly to our understanding and management of various conditions.

Fan S. et al. conduct a systematic review and meta-analysis on the efficacy and safety of a single-dose intravitreal dexamethasone (DEX) implant in treating non-infectious uveitic macular oedema. Their analysis, encompassing 201 eyes, demonstrates notable improvements in visual acuity and central macular thickness with manageable increased intraocular pressure, highlighting the potential of this treatment in uveitic macular oedema.

Shi et al. delve into the outcomes of revision surgery for persistent idiopathic macular hole (PIMH) post-failed primary vitrectomy. The study evaluates the effectiveness of extended internal limiting membrane (ILM) peeling combined with silicone oil (SiO) or air tamponade. Results show promising closure rates, especially for macular holes $\leq$650 μm in diameter, suggesting the viability of this approach in PIMH treatment.

In a groundbreaking effort, Wang et al. aim to develop a theoretical formula for intraocular lens power calculation in silicone oil-dependent eyes. Testing their formula on 32 patients, they find a strong correlation with actual clinical outcomes, offering a valuable guide for clinicians in selecting appropriate intraocular lenses in these complex cases.

Klaas et al.'s study compares the risk of transient vision loss (TVL) in intravitreal aflibercept injections using a novel prefilled syringe (PFS) against the traditional vial system (VS). Their findings indicate a higher risk associated with the PFS, underscoring the importance of informed consent and careful consideration when using this formulation.

Lastly, Fan W. et al. present a retrospective study aimed at developing a predictive model for elevated intraocular pressure following vitreoretinal surgery with silicone oil tamponade. Employing machine learning techniques, they analyse various predictive factors in over a thousand eyes, culminating in a model with significant accuracy. This model could potentially aid clinicians in anticipating and mitigating the risk of high intraocular pressure postoperatively.

Adnexa and paediatric ophthalmology

In the Adnexa and Pediatric Ophthalmology field of this Research Topic, we explore diverse and significant advancements in the field. Chaurasia et al. investigate the relationship between eccentric downward eye movement and depth of anaesthesia in paediatric ophthalmic surgeries. Their study, which combines retrospective and prospective data, reveals a notable correlation between the depth of sevoflurane anaesthesia and the occurrence of eccentric downward eye positioning, highlighting the critical need for precise anaesthesia monitoring in paediatric ocular procedures.

Zhou et al. conduct a retrospective analysis to assess the impact of pre-operative axial length on the myopic shift in children undergoing congenital or developmental cataract surgery. The study finds that children with longer pre-operative axial lengths experience slower myopic shifts post-surgery, providing valuable insights for targeted refraction planning in paediatric cataract procedures.

In a pioneering effort, Xu P. et al. develop biomimetic poly(lactic-co-glycolic acid) scaffolds for eyelid reconstruction, aiming to replicate the microstructure of the natural eyelid. Their study introduces three types of scaffolds, including one with azithromycin loading, and demonstrates their efficacy *in vitro* and *in vivo*, suggesting their potential as promising alternatives for eyelid tarsal plate substitutes.

Li et al.'s retrospective study compares the long-term efficacy of botulinum toxin type A (BTXA) injections and surgery in treating acute acquired comitant esotropia. They discover that while both treatments are effective, surgery provides more precise and enduring results. Importantly, the study also finds that patients who respond well to BTXA initially have better long-term outcomes.

Lastly, Song et al. evaluate the effectiveness of optimal pulse technology (OPT) in the treatment of chalazions. Their study shows significant improvements in chalazion size and meibomian gland area following two sessions of OPT treatment. This non-invasive approach also leads to decreased conjunctival congestion, positioning OPT as an effective non-surgical option for adult chalazion treatment.

This Research Topic has traversed a wide spectrum of groundbreaking research and innovative practices in the field of ophthalmology. From the nuanced complexities of anterior and posterior segment treatments to the delicate intricacies of adnexa and paediatric ophthalmology, each article contributes profoundly to our expanding knowledge base. The insights offered here not only reflect the current state-of-the-art but also pave the way for future explorations and advancements. As we close this issue, we extend our heartfelt gratitude to the authors, reviewers, and readers who have contributed to and engaged with these pivotal discussions. It is our collective endeavor that continues to drive the frontiers of ophthalmic research and clinical practice, with the ultimate goal of enhancing patient care and vision health globally.

Author contributions

GP: Conceptualisation, Data curation, Formal analysis, Funding acquisition, Investigation, Methodology, Project administration, Resources, Software, Supervision, Validation, Visualisation, Writing – original draft, Writing – review & editing. HM: Methodology, Validation, Writing – review & editing.

Funding

The author(s) declare that no financial support was received for the research, authorship, and/or publication of this article.

Conflict of interest

The authors declare that the research was conducted in the absence of any commercial or financial relationships that could be construed as a potential conflict of interest.

The author(s) declared that they were an editorial board member of Frontiers, at the time of submission. This had no impact on the peer review process and the final decision.

Publisher's note

frontiers | Frontiers in Medicine

TYPE Original Research
PUBLISHED 11 January 2023
DOI 10.3389/fmed.2022.1093276

OPEN ACCESS

EDITED BY
Georgios Panos,
Nottingham University Hospitals NHS Trust, United Kingdom

REVIEWED BY
Sudarshan Khokhar,
All India Institute of Medical Sciences, India
Ane Murueta-Goyena,
University of the Basque Country, Spain

*CORRESPONDENCE
Yi Luo
✉ yi.luo@fdeent.org

†These authors have contributed equally to this work and share first authorship

SPECIALTY SECTION
This article was submitted to Ophthalmology, a section of the journal Frontiers in Medicine

RECEIVED 08 November 2022
ACCEPTED 28 December 2022
PUBLISHED 11 January 2023

CITATION
Zhou X, Fan F, Liu X, Yang J, Yang T and Luo Y (2023) The impact of pre-operative axial length on myopic shift 3 years after congenital and developmental cataract surgery and intraocular lens implantation. *Front. Med.* 9:1093276. doi: 10.3389/fmed.2022.1093276

The impact of pre-operative axial length on myopic shift 3 years after congenital and developmental cataract surgery and intraocular lens implantation

Xiyue Zhou†, Fan Fan†, Xin Liu, Jianing Yang, Tianke Yang and Yi Luo*

Department of Ophthalmology, Eye Institute, Eye and ENT Hospital, Fudan University, Shanghai, China

Purpose: To investigate the impact of the pre-operative axial length (AL) on myopic shift (MS) 3 years after primary intraocular lens (IOL) implantation in congenital/developmental cataract patients.

Methods: A retrospective study of patients who underwent congenital/developmental cataract surgery and primary IOL implantation at age 2–3 years at EENT Hospital was conducted. All patients were followed up regularly for at least 3 years after surgery. Refractive outcomes, including spherical equivalent (SE) and MS, were collected at each follow-up.

Results: Forty eyes from 40 patients were included. The mean age at surgery was 2.56 ± 0.57 years old, and the mean follow-up time was 3.05 ± 0.22 years. Patients were divided into two groups: Group 1 included 20 patients with longer pre-operative ALs (≥22 mm), and Group 2 included 20 patients with average pre-operative ALs (<22 mm). By the last follow-up, the MS was 2.13 (0.38, 2.63) D in Group 1 and 3.88 (2.85, 5.72) D in Group 2. The post-operative MS in Group 2 was statistically greater than that in Group 1 at 3 years after surgery ($P < 0.001$).

Conclusion: In congenital/developmental cataract patients who underwent cataract extraction and primary IOL implantation at age 2–3 years, eyes with longer pre-operative ALs had a slower MS than those with average pre-operative ALs 3 years after surgery. This finding could have implications for the target refraction decision in congenital/developmental cataract surgery.

KEYWORDS

myopic shift, pre-operative axial length, congenital/developmental cataract, cataract surgery, IOL implantation

Introduction

Myopic shift (MS) occurs after congenital/developmental cataract extraction and intraocular lens (IOL) implantation in most children. MS usually increases with age, and the rate of MS is most rapid during the first 1.5 years of life (1). Considering that MS increases with age, most clinicians choose an under corrected target diopter when performing IOL implantation in children (2–5).

Due to the rapid growth of children's eyeballs and the great individual differences in children with congenital/developmental cataracts, MS can be quite unpredictable in childhood and varies substantially among patients, which can lead to large refractive errors or even high myopia. Although target diopter selection takes age into consideration, many children still require additional refractive correction within a few years, and even IOL replacement is needed in some situations to correct anisometropia and improve visual acuity (6–8). Therefore, other factors related to MS should be taken into account when selecting the target diopter, and pre-operative axial length (AL) is quite important.

An increasing number of congenital/developmental cataract patients are being diagnosed with myopia before surgery or have a longer pre-operative AL than average. However, there has been little previous research on the impact of the pre-operative AL on post-operative MS.

In this study, we reviewed the visual and refractive outcomes of children with different ALs who underwent congenital/developmental cataract extraction and primary IOL implantation at 2–3 years old. Additionally, the impact of the pre-operative AL on MS was investigated 3 years after primary IOL implantation in congenital/developmental cataract patients.

Materials and methods

Ethic declaration

The Institutional Review Board of the Eye and ENT Hospital of Fudan University, Shanghai, China, approved this retrospective cohort study. All procedures were conducted in agreement with the tenets of the Declaration of Helsinki. Written consent forms were signed by the guardians of the patients for the use of their medical data for research purposes before surgery.

Study population

This retrospective cohort study was performed on the medical records of children who underwent congenital/developmental cataract surgery at Eye and ENT Hospital of Fudan University between 2014 and 2018. The age at diagnosis and surgery had to be 2–3 years old, and the patients were followed up regularly for at least 3 years after surgery. Diseased eyes were included in children with unilateral congenital/developmental cataract, and only right eyes were included in children with bilateral congenital/developmental cataract.

The exclusion criteria were other eye diseases, such as severe posterior and combined persistent fetal vasculature (9), congenital microcornea, congenital iris defects and congenital glaucoma; systemic diseases, such as cerebral palsy and congenital heart disease; serious post-operative complications, such as uveitis; and failure to follow regular follow-up or amblyopia training.

Surgical technique

All surgeries were performed by the same experienced surgeon. Lensectomy, anterior vitrectomy and primary IOL implantation were performed, and the IOLs were implanted in the capsular bag. The IOL power was calculated on the basis of the SRK/T formula and the Hoffer Q formula. For patients who failed to cooperate with the keratometry measurement, we used an average keratometry (45 D for 2 year olds, 44 D for 2.5 year olds, 43.5 D for 3 year olds) when calculating the IOL power (10, 11). The target diopter was (7-age) D, targeting an hyperopia under correction based on the age at surgery.

Post-operative assessment

All patients were referred to the same pediatric amblyopia expert within one week after the operation. They had optometric assessments, lenses with best refractive correction and individualized amblyopia training plans. Follow-up was performed 1 day, 1 week, 1 month and every 4 months after surgery for at least 3 years. During the follow-up, all patients kept the individualized amblyopia training plan and changed the glasses when necessary. Post-operative complications, adherence to amblyopia training, and visual and refractive outcomes were collected at each follow-up. Children with unilateral congenital/developmental cataract had an extra covering on the contralateral eye every day, lasting 3–6 h according to the follow-up age and the amblyopia severity (12–15).

Statistical analysis

Statistical analyses were performed using IBM SPSS statistics (version 25.0; IBM Corp., Somers, NY, USA). Descriptive statistics were used to analyse the demographics and clinical

characteristics of the population. Continuous variables are presented as the mean ± standard or median (quartile). Independent-samples *t*-tests were used to compare the means. Mann–Whitney U test was applied to compare the medians. The linear regression model was used to analysis the impact of pre-operative AL on MS. A *P*-value < 0.05 was considered statistically significant difference.

Results

Basic characteristics

From 2014 to 2018, a total of 98 congenital/developmental cataract patients treated by Dr. Luo's team underwent primary IOL implantation at 2–3 years of age at Eye and ENT Hospital of Fudan University. Of the 98 patients, we included 40 patients who met the inclusion criteria. Twenty-one (52.5%) had bilateral cataracts, and nineteen (47.5%) had unilateral cataracts. The percentage of males to females was 22 (55.0%) versus 18 (45.0%). The mean age at surgery was 2.56 ± 0.57 years old. The mean follow-up time was 3.05 ± 0.22 years.

The patients were divided into two groups according to the pre-operative AL. Group 1 included 20 patients with longer pre-operative ALs (≥22 mm), and Group 2 included 20 patients with average pre-operative ALs (<22 mm). The mean pre-operative AL was 23.17 ± 0.81 mm in Group 1 and 20.85 ± 0.69 mm in Group 2. Table 1 shows the characteristics of the two groups. There was no significant difference in the follow-up time ($P = 0.095$) or basic characteristics except for AL.

Comparison of MS between the two different AL groups

Table 2 shows the refractive outcomes of the two groups. One year after surgery, the MS of Group 1 and Group 2 was significantly different [0.63 (0.5, 1.13) D vs. 1.44 (1.04, 2.44) D, $P < 0.001$]. The MS at two years after surgery was 1.50 (0.19, 1.98) D in Group 1 and 3.07 (2.38, 4.53) D in Group 2. By the time of last follow-up (3 years after surgery), the MS of Group 1 and Group 2 were 2.13 (0.38, 2.63) D and 3.88 (2.85, 5.72) D, respectively. The post-operative MS in Group 2 was statistically greater than that in Group 1 at two and three years after surgery ($P < 0.001$). Figure 1 shows the comparison of MS at 1–3 years after surgery between Group 1 and Group 2.

Comparison of MS between the unilateral and bilateral cases

Table 3 and Figure 2 present the comparison of MS between unilateral and bilateral congenital/developmental cataracts in the same group of pre-operative AL. No statistically significant difference was found in MS between unilateral and bilateral cataracts in the same group of pre-operative AL ($P > 0.05$).

The impact of pre-operative AL on MS

The linear regression model was used to analysis the impact of pre-operative AL on MS, with MS 3 years after surgery as the outcome variable and pre-operative AL as the main predictor. The confounding factors included laterality, gender and type of cataract.

The linear regression model turned out to be MS = 20.60 −0.76*pre-operational AL ($R^2 = 0.337$, F = 4.445, $P = 0.005$). As the linear regression model showed, the impact of pre-operational AL on MS was statistically significant (b = −0.76, $t = 2.80$, $P = 0.008$). However, the impact of laterality, gender and

TABLE 1 Characteristics of the two groups.

	Group 1	Group 2	*P*-value
Eyes (*n*)	20	20	–
Male/female (*n*)	13/7	9/11	0.204
Unilateral/bilateral (eyes)	8/12	11/9	0.342
Cataract morphology (eyes)			
Total white	2	2	–
Nuclear	1	1	–
Cortical	4	1	–
Posterior subcapsular	1	6	–
Mixed	2	4	–
Others*	10	6	–
Age at surgery (y)	2.53 ± 0.60	2.59 ± 0.56	0.737
Pre-operative AL (mm)	23.17 ± 0.81	20.85 ± 0.69	<0.001*
Follow-up time (y)	3.00 ± 0.15	3.11 ± 0.26	0.095
Age at the last follow-up (y)	5.53 ± 0.61	5.70 ± 0.60	0.362

n, number of patients; y, years.
*$P < 0.05$. *Others include point-like, perinuclear, lamellar, anterior polar, and other opacity.

TABLE 2 Refractive outcomes of the two groups.

	Group 1	Group 2	*P*-value
Eyes (*n*)	20	20	–
Initial SE (D)	3.59 ± 2.67	3.76 (3.06, 5.00)	0.569
SE at last follow-up (D)	2.29 ± 2.99	−0.01 ± 2.59	0.009*
MS 1 year after surgery (D)	0.63 (0.5, 1.13)	1.44 (1.04, 2.44)	<0.001*
MS 2 years after surgery (D)	1.50 (0.19, 1.98)	3.07 (2.38, 4.53)	<0.001*
MS 3 years after surgery (D)	2.13 (0.38, 2.63)	3.88 (2.85, 5.72)	<0.001*

n, number of patients; D, diopter; SE, spherical equivalent.
*$P < 0.05$.

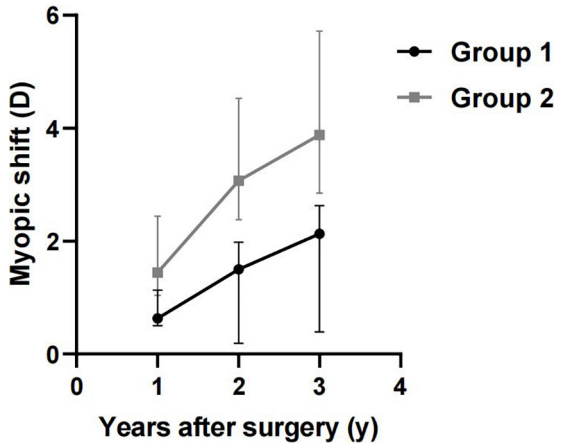

FIGURE 1
Comparison of myopic shift (MS) at 1–3 years after surgery in Group 1 and Group 2.

type of cataract on MS was not statistically significant ($P = 0.136$, 0.334, and 0.108).

Discussion

There is little previous research on the impact of the pre-operative AL on post-operative MS. An earlier retrospective study conducted in Peru (16) found no statistically significant relationship between the initial AL and MS 3 years after IOL implantation. The MS was 3.2 ± 3.3 D in children with longer ALs and 3.9 ± 3.2 D in those with shorter ALs ($P = 0.359$). This earlier study included congenital cataracts in children younger than 4 years old and chose an AL of 21.5 mm as the group division. As numerous studies have observed, the growth of AL was the most significant during the first 2 years of life and tended to be stable as age increased (17–21). Therefore, the mixing of children under 12 months with children aged 3–4 years old in the earlier study may have led to deviation of the results. In our study, we only included patients aged 2–3 years old, which not only captured the period of greater ocular growth but also controlled the impact of operative age on post-operative MS.

With reference to a 3-year-old Asian cohort (349 children) and another study in 4,350 Chinese children aged 3 to 4 years, which found average ALs of 21.73 ± 0.66 mm (95% CI: 21.6–21.80 mm) (22) and 22.10 ± 0.79 mm (95% CI: 20.55 –23.65 mm) (23), we chose an AL of 22 mm as the standard for grouping patients aged 2–3 years old in our study.

Myopic shift after congenital/developmental cataract surgery and IOL implantation is quite complicated and difficult to predict. The Eye and ENT Hospital of Fudan University is the largest tertiary referral center for pediatric cataracts in East China and receives almost all pediatric cataracts in this region (24). Based on the 3-year clinical data of congenital/developmental cataract patients with primary IOL implantation between 2 and 3 years old in our center, we observed that eyes with longer pre-operative ALs (≥22 mm) tended to have a slower MS than those with average pre-operative ALs (<22 mm) 3 years after surgery.

Axial length growth is associated with MS and myopia, (25) and a longer AL can be used to identify those at high risk of myopia in both pre-school and school-aged children (26, 27). However, in our study, a longer pre-operative AL led to a slower MS in children with congenital/developmental cataracts with pseudophakic eyes. The opposite result may be related to the impact of congenital/developmental cataracts on eyeball growth. Seven et al. (28) found a lower growth rate of AL in pseudophakic eyes than in phakic eyes, while Wilson et al. (18) found that eyes treated for monocular cataracts in infancy had axial growth similar to that of fellow eyes. This finding and the reasons behind it remain to be solved in further studies.

Compared with that of bilateral congenital/developmental cataract patients, the prognosis of unilateral congenital/developmental cataract patients is usually worse (29–31). Earlier studies have already found that children with unilateral congenital cataracts had greater MS after surgery (20, 32). Additionally, studies have shown that the growth of AL in unilateral patients tends to be greater than that in bilateral patients (33). Children with unilateral congenital cataracts are more likely to have high myopia and great anisometropia in the long term after the operation, (28) the mean of which can be

TABLE 3 Comparison of myopic shift (MS) in patients with unilateral and bilateral cataracts in the same pre-operative axial length (AL) group.

	Group 1		*P*-value	Group 2		*P*-value
	Unilateral	Bilateral		Unilateral	Bilateral	
Eyes (*n*)	8	12	–	9	11	–
MS 1 year after surgery (D)	1.07 (0.41, 1.34)	0.41 (−0.22, 0.88)	0.054	2.00 (0.75, 2.60)	1.38 (1.07, 1.69)	0.304
MS 2 years after surgery (D)	1.57 (0.75, 1.98)	0.94 (−0.06, 1.91)	0.316	3.75 (1.88, 5.00)	2.88 (2.38, 3.44)	0.424
MS 3 years after surgery (D)	2.20 (1.09, 2.69)	1.13 (0.03, 2.63)	0.279	4.50 (2.75, 6.25)	3.76 (2.69, 4.75)	0.595

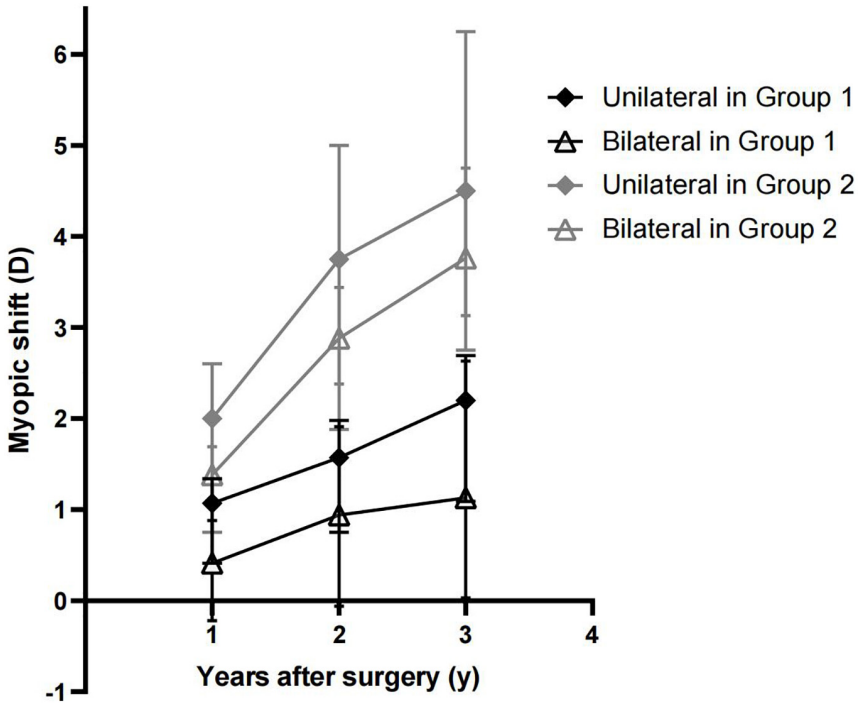

FIGURE 2
Comparison of myopic shift (MS) in patients with unilateral and bilateral cataracts in the same pre-operative axial length (AL) group.

up to −3.50 D (−19.63 D–+2.75 D) at the age of five. In our study, the MS in unilateral congenital cataracts was numerically larger, but no statistically significant difference was found in MS between unilateral and bilateral congenital/developmental cataracts of each group. The results of the linear regression model also showed that there was no statistical relevance between laterality and MS (P = 0.136). In our study, all unilateral congenital/developmental cataract patients had an extra covering on the contralateral eye every day, which may have reduced the differences in MS between children with unilateral and bilateral congenital/developmental cataracts.

Keratometry is another refractive-related biometry characteristic. It has been widely acknowledged that infants have a steeper corneal curvature than older children. A study showed a linear decline in mean keratometry during the first 6 months of life, while no significant change was found in the keratometry value with increasing age beyond 6 months (10). That is, the corneal curvature decreased with age and stabilized after 6 months of age (34). With this growth pattern of keratometry, patients aged 2–3 years old would have a relatively stable keratometry at surgery, and keratometry and its influence on post-operative MS could be insignificant or minimally significant in our study. Thus, for patients who failed to cooperate with the examination, an average keratometry from those of the same age was used to calculate the IOL power.

To the best of our knowledge, our study is the first to demonstrate the impact of the pre-operative AL on MS in children with congenital/developmental cataracts. As the age of the global myopia population decreases, this result can help to guide the prediction and control of MS in congenital/developmental cataract patients with longer ALs. However, our study still has its limitations. Long-term changes of MS cannot be observed during 3-year follow-up, as some patients with high and pathological myopia tend to grow even further. The number of participants was not large enough. We did not include the anterior chamber depth in the analysis, which was also an important variable in biometry measurement. Also, we were unable to measure the post-operative AL of all patients. Future studies for long-term outcomes will enlarge the sample size, incorporate anterior chamber depth and post-operative AL changes.

In conclusion, in congenital/developmental cataract patients who underwent surgery at 2–3 years old, eyes with longer pre-operative ALs had a slower MS than those with average pre-operative ALs. This finding could have implications for the target refraction decision in congenital/developmental cataract surgery. Accurate prediction of post-operative MS in congenital/developmental cataract patients remains challenging. Studies on MS and the pre-operative factors influencing it, such as post-operative AL, will be helpful to better predict and control MS after congenital/developmental cataract surgery and can help clinicians to make optimal treatment decisions.

Data availability statement

The raw data supporting the conclusions of this article will be made available by the authors, without undue reservation.

Ethics statement

The studies involving human participants were reviewed and approved by the Institutional Review Board of the Eye and ENT Hospital of Fudan University, Shanghai, China. Written informed consent to participate in this study was provided by the participants or their legal guardian/next of kin.

Author contributions

XZ was responsible for conception and design, analysis and interpretation of data, and writing the manuscript. FF was responsible for conception and design, analysis and interpretation of data, critical revision of the manuscript, and supervision. XL, JY, and TY were responsible for data collection. YL was responsible for conception and design, technical support, and critical revision of the manuscript. All authors contributed to the article and approved the submitted version.

Conflict of interest

The authors declare that the research was conducted in the absence of any commercial or financial relationships that could be construed as a potential conflict of interest.

Publisher's note

All claims expressed in this article are solely those of the authors and do not necessarily represent those of their affiliated organizations, or those of the publisher, the editors and the reviewers. Any product that may be evaluated in this article, or claim that may be made by its manufacturer, is not guaranteed or endorsed by the publisher.

References

1. Weakley D Jr, Lynn M, Dubois L, Cotsonis G, Wilson M, Buckley E, et al. Myopic shift 5 years after intraocular lens implantation in the Infant Aphakia Treatment Study. *Ophthalmology.* (2017) 124:822–7. doi: 10.1016/j.ophtha.2016.12.040

2. VanderVeen D. Predictability of intraocular lens calculation and early refractive status. *Arch Ophthalmol.* (2012) 130:293. doi: 10.1001/archophthalmol.2011.358

3. Wilson M Jr, Trivedi R, Hoxie J, Bartholomew L. Treatment outcomes of congenital monocular cataracts: the effects of surgical timing and patching compliance. *J Pediatr Ophthalmol Strabismus.* (2003) 40:323–9; quiz 53–4. doi: 10.3928/0191-3913-20031101-04

4. Hutchinson A, Drews-Botsch C, Lambert S. Myopic shift after intraocular lens implantation during childhood. *Ophthalmology.* (1997) 104:1752–7. doi: 10.1016/S0161-6420(97)30031-1

5. Dahan E, Drusedau M. Choice of lens and dioptric power in pediatric pseudophakia. *J Cataract Refract Surg.* (1997) 23(Suppl. 1):618–23. doi: 10.1016/S0886-3350(97)80043-0

6. Yangzes S, Kaur S, Gupta P, Sharma M, Jinagal J, Singh J, et al. Intraocular lens implantation in children with unilateral congenital cataract in the first 4 years of life. *Eur J Ophthalmol.* (2019) 29:304–8. doi: 10.1177/1120672118790193

7. Tadros D, Trivedi R, Wilson M. Primary versus secondary IOL implantation following removal of infantile unilateral congenital cataract: outcomes after at least 5 years. *J Am Assoc Pediatr Ophthalmol Strabismus.* (2016) 20:25–9. doi: 10.1016/j.jaapos.2015.10.010

8. Kraus C, Trivedi R, Wilson M. Intraocular lens exchange for high myopia in pseudophakic children. *Eye.* (2016) 30:1199–203. doi: 10.1038/eye.2016.152

9. Chen C, Xiao H, Ding X. Persistent fetal vasculature. *Asia Pac J Ophthalmol.* (2019) 8:86–95.

10. Lin D, Chen J, Liu Z, Wu X, Long E, Luo L, et al. Prevalence of corneal astigmatism and anterior segmental biometry characteristics before surgery in Chinese congenital cataract patients. *Sci Rep.* (2016) 6:22092. doi: 10.1038/srep22092

11. Trivedi R, Wilson M. Keratometry in pediatric eyes with cataract. *Arch Ophthalmol.* (2008) 126:38–42. doi: 10.1001/archophthalmol.2007.22

12. Stewart C, Stephens D, Fielder A, Moseley M, Cooperative R. Objectively monitored patching regimens for treatment of amblyopia: randomised trial. *BMJ.* (2007) 335:707. doi: 10.1136/bmj.39301.460150.55

13. Pediatric Eye Disease Investigator Group. The course of moderate amblyopia treated with patching in children: experience of the amblyopia treatment study. *Am J Ophthalmol.* (2003) 136:620–9. doi: 10.1016/S0002-9394(03)00392-1

14. Holmes J, Kraker R, Beck R, Birch E, Cotter S, Everett D, et al. A randomized trial of prescribed patching regimens for treatment of severe amblyopia in children. *Ophthalmology.* (2003) 110:2075–87. doi: 10.1016/j.ophtha.2003.08.001

15. Drews-Botsch C, Celano M, Kruger S, Hartmann E, Infant Aphakia Treatment Study. Adherence to occlusion therapy in the first six months of follow-up and visual acuity among participants in the Infant Aphakia Treatment Study (IATS). *Invest Ophthalmol Vis Sci.* (2012) 53:3368–75. doi: 10.1167/iovs.11-8457

16. Valera Cornejo D, Flores Boza A. Relationship between preoperative axial length and myopic shift over 3 years after congenital cataract surgery with primary intraocular lens implantation at the National Institute of Ophthalmology of Peru, 2007-2011. *Clin Ophthalmol.* (2018) 12:395–9. doi: 10.2147/OPTH.S152560

17. Wilson M, Trivedi R, Weakley D Jr, Cotsonis G, Lambert S. Globe axial length growth at age 10.5 years in the Infant Aphakia Treatment Study. *Am J Ophthalmol.* (2020) 216:147–55. doi: 10.1016/j.ajo.2020.04.010

18. Wilson M, Trivedi R, Weakley D Jr, Cotsonis G, Lambert S. Globe axial length growth at age 5 years in the Infant Aphakia Treatment Study. *Ophthalmology.* (2017) 124:730–3. doi: 10.1016/j.ophtha.2017.01.010

19. Valeina S, Heede S, Erts R, Sepetiene S, Skaistkalne E, Radecka L, et al. Factors influencing myopic shift in children after intraocular lens implantation. *Eur J Ophthalmol.* (2019) 30:933–40. doi: 10.1177/1120672119845228

20. Koch C, Kara-Junior N, Serra A, Morales M. Long-term results of secondary intraocular lens implantation in children under 30 months of age. *Eye.* (2018) 32:1858–63. doi: 10.1038/s41433-018-0191-3

21. Sachdeva V, Katukuri S, Kekunnaya R, Fernandes M, Ali M. Validation of guidelines for undercorrection of intraocular lens power in children. *Am J Ophthalmol.* (2017) 174:17–22. doi: 10.1016/j.ajo.2016.10.017

22. Foo V, Verkicharla P, Ikram M, Chua S, Cai S, Tan C, et al. Axial length/corneal radius of curvature ratio and myopia in 3-year-old children. *Transl Vis Sci Technol.* (2016) 5:5. doi: 10.1167/tvst.5.1.5

23. Zhao K, Yang Y, Wang H, Li L, Wang Z, Jiang F, et al. Axial length/corneal radius of curvature ratio and refractive development evaluation in 3- to 4-year-old children: the Shanghai Pudong Eye Study. *Int J Ophthalmol.* (2019) 12:1021–6. doi: 10.18240/ijo.2019.06.23

24. Zhu X, He W, Du Y, Kraus C, Xu Q, Sun T, et al. Presence of posterior staphyloma in congenital cataract children. *Curr Eye Res.* (2019) 44:1319–24. doi: 10.1080/02713683.2019.1637437

25. Lambert S, Cotsonis G, DuBois L, Wilson M, Plager D, Buckley E, et al. Comparison of the rate of refractive growth in aphakic eyes versus pseudophakic eyes in the Infant Aphakia Treatment Study. *J Cataract Refract Surg.* (2016) 42:1768–73. doi: 10.1016/j.jcrs.2016.09.021

26. Liu L, Li R, Huang D, Lin X, Zhu H, Wang Y, et al. Prediction of premyopia and myopia in Chinese preschool children: a longitudinal cohort. *BMC Ophthalmol.* (2021) 21:283. doi: 10.1186/s12886-021-02045-8

27. Sanz Diez P, Yang L, Lu M, Wahl S, Ohlendorf A. Growth curves of myopia-related parameters to clinically monitor the refractive development in Chinese schoolchildren. *Graefes Arch Clin Exp Ophthalmol.* (2019) 257:1045–53. doi: 10.1007/s00417-019-04290-6

28. Seven E, Tekin S, Batur M, Artuç T, Yaşar T. Evaluation of changes in axial length after congenital cataract surgery. *J Cataract Refract Surg.* (2019) 45:470–4. doi: 10.1016/j.jcrs.2018.11.012

29. Nystrom A, Almarzouki N, Magnusson G, Zetterberg M. Phacoemulsification and primary implantation with bag-in-the-lens intraocular lens in children with unilateral and bilateral cataract. *Acta Ophthalmol.* (2018) 96:364–70. doi: 10.1111/aos.13626

30. Solebo A, Russell-Eggitt I, Cumberland P, Rahi J. Risks and outcomes associated with primary intraocular lens implantation in children under 2 years of age: the IoLunder2 cohort study. *Br J Ophthalmol.* (2015) 99:1471–6. doi: 10.1136/bjophthalmol-2014-306394

31. Gouws P, Hussin H, Markham R. Long term results of primary posterior chamber intraocular lens implantation for congenital cataract in the first year of life. *Br J Ophthalmol.* (2006) 90:975–8. doi: 10.1136/bjo.2006.094656

32. Hoevenaars N, Polling J, Wolfs R. Prediction error and myopic shift after intraocular lens implantation in paediatric cataract patients. *Br J Ophthalmol.* (2011) 95:1082–5. doi: 10.1136/bjo.2010.183566

33. Lambert S, Lynn M, DuBois L, Cotsonis G, Hartmann E, Wilson M. Axial elongation following cataract surgery during the first year of life in the Infant Aphakia Treatment Study. *Invest Ophthalmol Vis Sci.* (2012) 53:7539–45. doi: 10.1167/iovs.12-10285

34. Prado R, Silva V, Schellini S, Rodrigues A. Congenital and developmental cataract: axial length and keratometry study in Brazilian children. *Arq Bras Oftalmol.* (2016) 79:19–23. doi: 10.5935/0004-2749.20160007

frontiers | Frontiers in Medicine

TYPE Original Research
PUBLISHED 12 January 2023
DOI 10.3389/fmed.2022.1039195

OPEN ACCESS

EDITED BY
Georgios Panos,
Nottingham University Hospitals NHS Trust, United Kingdom

REVIEWED BY
Tomaž Gračner,
Maribor University Medical Centre, Slovenia
Parul Ichhpujani,
Government Medical College and Hospital, India

*CORRESPONDENCE
David L. Swain
✉ dlswain@bu.edu
Babak Eliassi-Rad
✉ babak.eliassirad@gmail.com

SPECIALTY SECTION
This article was submitted to Ophthalmology, a section of the journal Frontiers in Medicine

RECEIVED 07 September 2022
ACCEPTED 27 December 2022
PUBLISHED 12 January 2023

CITATION
Swain DL and Eliassi-Rad B (2023) Five-year outcomes of selective laser trabeculoplasty: A retrospective study.
Front. Med. 9:1039195.
doi: 10.3389/fmed.2022.1039195

Five-year outcomes of selective laser trabeculoplasty: A retrospective study

David L. Swain[1,2]* and Babak Eliassi-Rad[1]*

[1]Department of Ophthalmology, Boston University School of Medicine, Boston, MA, United States, [2]Department of Anatomy and Neurobiology, Boston University School of Medicine, Boston, MA, United States

Introduction: Studies have shown the efficacy of selective laser trabeculoplasty (SLT) to lower intraocular pressure (IOP) as adjuvant therapy during short-term follow-up. However, few studies have assessed the long-term efficacy of SLT on preventing worsening Humphrey visual field (HVF) parameters and thinning of the retinal nerve fiber layer (RNFL) with continued medical therapy.

Methods: A retrospective chart review was conducted of 51 eyes of 39 patients with glaucoma treated with SLT at Boston Medical Center between 2012 and 2016 with 3- and 5-year follow-up. Outcome measures included IOP, visual acuity, number of glaucoma medications, number of months to subsequent surgical intervention. HVF outcome measures included mean deviation (MD) and pattern standard deviation (PSD). Optical coherence tomography (OCT) outcome measures included RNFL mean thickness, and superior and inferior thicknesses.

Results: Twenty-five eyes received subsequent surgical intervention (mean time to intervention = 33.6 ± 20.0 months). In the eyes that did not receive another intervention, mean IOP was significantly decreased by 3.2 and 3.5 mmHg at 3- and 5-year after SLT, respectively. Mean number of glaucoma medications was significantly increased at 5-year (2.7 ± 1.6; $P = 0.04$), compared to pre-SLT (2.0 ± 1.1). Mean HVF MD was significantly higher at 5-year (−7.64 ± 6.57 dB) compared to pre-SLT (−5.61 ± 3.90 dB). Mean PSD significantly increased at 3-year (5.30 ± 2.91 dB) and 5-year (6.84 ± 2.62 dB), compared to pre-SLT (4.63 ± 2.70 dB; $P = 0.04$ and ≤0.01, respectively). On OCT, inferior quadrant RNFL thickness decreased significantly at 5-year (88.5 ± 19.3 μm), compared to pre-SLT (94.0 ± 23.2 μm).

Discussion: Although 51% of eyes had IOP controlled at 5-year post-SLT, mean number of glaucoma medications was significantly higher. Also, there was progression of MD and PSD on HVF and inferior quadrant thinning on OCT at 5-year. We found a significant association between age at SLT and risk of

subsequent surgical intervention over 5-year follow-up. Our study adds to our understanding of long-term outcomes of adjuvant SLT for glaucoma patients receiving medical therapy.

KEYWORDS

selective laser trabeculoplasty, intraocular pressure, glaucoma, retrospective chart review, optical coherence tomography, retinal nerve fiber thickness

1. Introduction

Glaucoma is one of the leading causes of irreversible blindness worldwide with an estimated prevalence of 79.6 million in 2020 with 74% of cases being primary open-angle glaucoma (POAG) (1, 2). Glaucoma is characterized by degeneration of the retinal ganglion cells and their axons (3). The only modifiable risk factor for glaucoma is intraocular pressure (IOP) (4). Current first-line intervention to lower IOP is medications (i.e., eyedrops); however, laser procedures, including selective laser trabeculoplasty (SLT), have been shown to be effective at lowering IOP in the short-term follow-up period and are most commonly used for adjuvant and first-line therapy (5).

Selective laser trabeculoplasty utilizes a Q-switched, frequency-doubled Nd:YAG laser to target pigmented cells of the trabecular meshwork selectively that leads to acute changes in the anterior angle ultrastructure, including disruption of the uveal trabecular beams (6, 7). SLT has also been shown to lead to increased activity of metalloproteinases that remodel the juxtacanalicular connective tissue matrix (8) and increased permeability of Schlemm's canal endothelial cells (9). Both of these changes lead to increased aqueous humor outflow and lower IOP to prevent progression of glaucomatous damage.

Many studies have investigated the clinical value of first line or adjuvant SLT in the short-term period following treatment and have found that SLT is effective at lowering IOP in patients with glaucoma (10–17). Many studies of adjuvant SLT therapy have reported decreases in IOP of ∼29% up to 4 years following treatment (13). However, only a few studies have explored the long-term (>4 years) outcomes of SLT on lowering IOP and even fewer have examined functional analyses of vision, including Humphrey visual fields (HVF) and retinal nerve fiber layer (RNFL).

Although SLT has been shown to be an effective method in lowering IOP in patients with glaucoma, there is not a consensus and not enough literature to assess whether SLT works in all clinical settings and whether its effects on IOP are long-lasting and prevent further loss of function on HVF and OCT exams. Therefore, in this study, we investigated the long-term outcomes of SLT after 3- and 5-year on patient parameters including IOP, visual acuity (VA), HVF parameters, and RNFL thickness on OCT using a retrospective chart review of glaucoma patients with continued medical therapy at Boston Medical Center.

Abbreviations: CCT, central corneal thickness; HVF, Humphrey visual field; IOP, intraocular pressure; MD, mean deviation; NTG, normal tension glaucoma; OCT, optical coherence tomography; POAG, primary open-angle glaucoma; PSD, pattern standard deviation; SD, standard deviation; SLT, selective laser trabeculoplasty; RNFL, retinal nerve fiber layer; VA, visual acuity.

2. Materials and methods

2.1. Study design

A single-center retrospective review evaluated patients with glaucoma who underwent SLT from 2012 to 2016 at Boston Medical Center, Boston, MA. This study adhered to tenets of the Declaration of Helsinki and was approved by the Institutional Review Board of Boston University (IRB: H-39121). Four hundred and thirty-nine charts were examined to identify patients with a diagnosis of glaucoma (POAG, borderline, suspect with ocular hypertension, normal tension glaucoma, or uveitic) with follow-up within 6 months of 3- and 5-year following SLT (**Figure 1**). We excluded patients with other forms of secondary open-angle glaucoma and angle-closure glaucoma, and we excluded patients who had received previous laser procedures, including argon laser trabeculoplasty or SLTs performed before treatment at Boston Medical Center. Fifty-one eyes of 39 patients (20 male, 19 female) followed for a mean of 68.2 ± 12.4 months following SLT at Boston Medical Center were identified and used in this study (**Figure 1**). Data were recorded from pre-SLT and at 3- and 5-year follow-ups. Data included age at SLT, gender, self-identified ethnicity, IOP, VA (reported as a decimal), number of glaucoma medications, HVF mean deviation (MD) and pattern standard deviation (PSD), OCT RNFL mean thickness, and superior and inferior thicknesses.

2.2. Selective laser trabeculoplasty and functional assessments

Lower intraocular pressure was measured before SLT, immediately after SLT, 6 weeks after SLT, and then typically

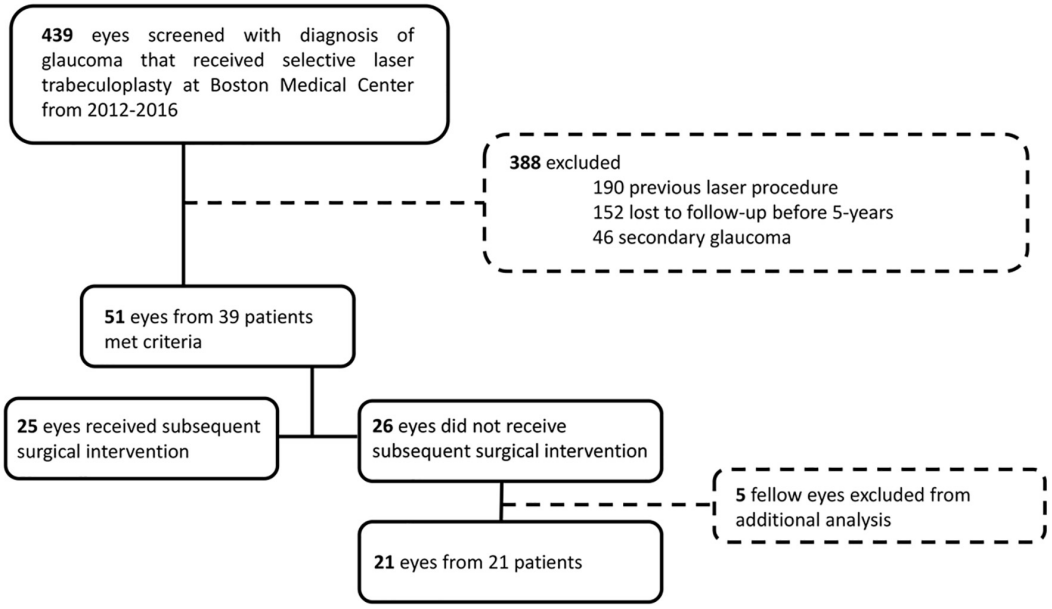

FIGURE 1
CONSORT diagram for retrospective chart review. We retrospectively screened 439 charts of eyes with diagnosis of glaucoma that received SLT at Boston Medical Center from 2012 to 2016. We excluded 388 eyes that had a previous laser procedure, were lost to follow-up within 5-year, or had secondary open-angle glaucoma or angle-closure glaucoma. We included 51 eyes, who had sufficient 5-year follow-up, of which 25 received subsequent surgical intervention and 26 did not. For analysis of the outcome measures of the patients that did not receive subsequent surgical intervention, we excluded fellow eyes to only analyze one eye per patient.

every 6–12 months. SLTs were performed at Boston Medical Center from 2012 to 2016 using a Lumenis Selecta® Trio™ (Lumenis Inc., CA, USA), which is a Q-switched Nd:YAG laser. Laser wavelength was 532 nm with a spot size of 400 μm and pulse duration of 3 ns. Energy levels ranged from 0.4 to 1.2 mJ per pulse. All eyes received 50–62 adjacent, non-overlapping pulses to 180° of the trabecular meshwork, except one eye which received 100 pulses to 360° of meshwork. If the eyes received a second SLT, the previously untreated 180° of trabecular meshwork were treated. Factors that were weighed between physician and patient when assessing need for subsequent surgical intervention included IOP not at target, patient adherence to medications, patient on maximally tolerated medical treatment, risk of surgical complications, patient preference for or against surgery.

For functional assessments, HVF was performed with a Humphrey Field Analyzer 750i (Carl Zeiss Meditec, Inc., Dublin, CA, USA), and RNFL measurements were taken using a Cirrus HD-OCT 5000 (Carl Zeiss Meditec, Inc., Dublin, CA, USA).

2.3. Statistical analysis

All statistical analyses were performed using R Statistical Computing Package (v3,5,1l R Foundation for Statistical Computing, Vienna, Austria). All data are summarized as means ± SD. VA is reported as a decimal. For survival analysis, we performed a multilevel Cox proportional hazards regression analysis, with clustering by patient to account for the potential intraclass correlation from including both eyes for some patients, to calculate the survival probability of patients that received a subsequent surgical intervention over time in months during the follow-up period. For each eye, the amount of time (months) was calculated from SLT treatment to date of subsequent intervention, and eyes that did not receive subsequent intervention were censored at timepoint of last follow-up. This multilevel model with clustering also estimated hazard ratios for risk of receiving subsequent surgical procedure during the 5-year follow-up, while adjusting for confounding factors, including fellow eyes, age, sex, and pre-SLT IOP. In this model, we used a central corneal thickness (CCT) value of <555 μm, based on previous studies (18). Lastly, using the eyes that did not receive further surgical intervention following SLT to control IOP, we excluded fellow eyes, only including one eye per patient. We excluded fellow eyes by using a random number generator to randomly select the right or left eye to exclude. For these eyes, we examined differences in mean IOP, number of glaucoma medications, HVF MD and PSD, and OCT RNFL thickness using paired Student's *t*-tests to compare the means at 3-year or 5-year to baseline values. A value of $P < 0.05$ was considered significant.

3. Results

Patient demographics are summarized in Table 1. The mean age at SLT treatment was 69.4 ± 8.0-year, and 69.8 ± 7.8 years for males and 69.0 ± 8.3 years for females. Of these patients, 82.3% self-identified as black or African American. Most eyes were diagnosed with POAG (40/51, 78.4%) or normal tension glaucoma (NTG) (5/51, 9.8%).

TABLE 1 Baseline demographic and clinical characteristics of eyes.

Characteristic	Mean or count
Age at SLT (years)	69.4 ± 8.0
Gender	
Male	25 (49.0%)
Female	26 (51.0%)
Self-reported ethnicity	
Black or African American	42 (82.3%)
Hispanic or Latino	3 (5.9%)
White	4 (7.8%)
Declined	2 (3.9%)
Diagnosis	
POAG	40 (78.4%)
Borderline	3 (5.9%)
Suspect	1 (2.0%)
NTG	5 (9.8%)
Uveitic	2 (3.9%)

POAG, primary open-angle glaucoma; NTG, normal tension glaucoma.

3.1. Time to subsequent glaucoma surgical intervention

Time to subsequent glaucoma surgical intervention was calculated for each eye from the SLT date. Of the 51 eyes, 25 (49%) received subsequent surgical intervention to lower IOP, and 26 (51%) did not receive further surgical intervention. Survival probability calculated by multilevel Cox proportional hazard model analysis was 79.6% at 36 months (3-year) and 60.7% at 60 months (5-year) (Figure 2). Of the eyes that received subsequent surgical intervention, 52% (13/25) underwent a repeat SLT. The counts of each type of first subsequent surgical intervention over the 5-year follow-up period are summarized in Table 2. Of the 25 eyes that received a subsequent surgical intervention, seven of them (28%) received more than one intervention (six eyes received two interventions; and one eye received three interventions total) within the 5-year follow-up period. None of the eyes received more than one additional SLT.

3.2. Factors influencing time to subsequent surgical procedure

To identify factors that potentially contributed to receiving a subsequent surgical intervention within the 5-year follow-up period, we calculated hazard ratios of certain characteristics (Table 3). We found that central corneal thickness < 555 μm, female gender, and pre-SLT IOP, and left eye (OS) were not significantly associated with increased risk of subsequent surgical procedure over the 5-year follow-up period (all $P > 0.05$; Table 3). However, we found that higher patient age at SLT was significantly associated with an increased risk of receiving a subsequent surgical procedure ($P = 0.04$) (Table 3).

3.3. IOP, VA, and number of glaucoma medications

We further examined the eyes that did not receive a subsequent surgical intervention within the 5-year follow-up period and only used one eye from each patient ($n = 21$) in order to examine the effect of SLT alone with continued medical therapy. The outcome measures for these 21 eyes were analyzed to determine the effects of SLT provided over 5-year (Table 4). Mean IOP was significantly reduced at 3-year (14.8 ± 2.8 mmHg) and 5-year (14.5 ± 3.3 mmHg), compared to pre-SLT IOP (18.0 ± 3.7 mmHg; paired Student's t-test; both $P \leq 0.01$). VA (reported as a decimal) was not significantly different at 3-year (0.8 ± 0.2; $P = 0.84$) or 5-year (0.8 ± 0.2; $P = 0.74$), compared to pre-SLT VA (0.8 ± 0.2; paired Student's t-tests). Number of glaucoma medications was significantly higher at 5-year (2.7 ± 1.6) compared to pre-SLT (2.0 ± 1.1; $P = 0.04$), but it was not different at 3-year (2.5 ± 1.3), compared to pre-SLT ($P = 0.07$) (Table 4).

3.4. Humphrey visual field parameters

For the eyes that did not receive a surgical intervention in the follow-up period that had complete HVF data, we used only one eye from each patient ($n = 20$) to compare MD and PSD before and after SLT treatment. The outcomes are summarized in Table 5. Mean HVF MD was significantly higher at 5-year (−7.64 ± 6.57 dB) compared to pre-SLT (−5.61 ± 3.90 dB; $P = 0.02$) with a difference of −2.03 dB over 5-year. PSD was significantly increased at 3-year (5.30 ± 2.91 dB) and 5-year (6.84 ± 2.62 dB), compared to pre-SLT (4.63 ± 2.70 dB; $P = 0.04$ and ≤0.01, respectively) (Table 5).

3.5. OCT parameters

The OCT parameters are summarized in Table 6 for the 19 eyes that did not receive a subsequent surgical intervention

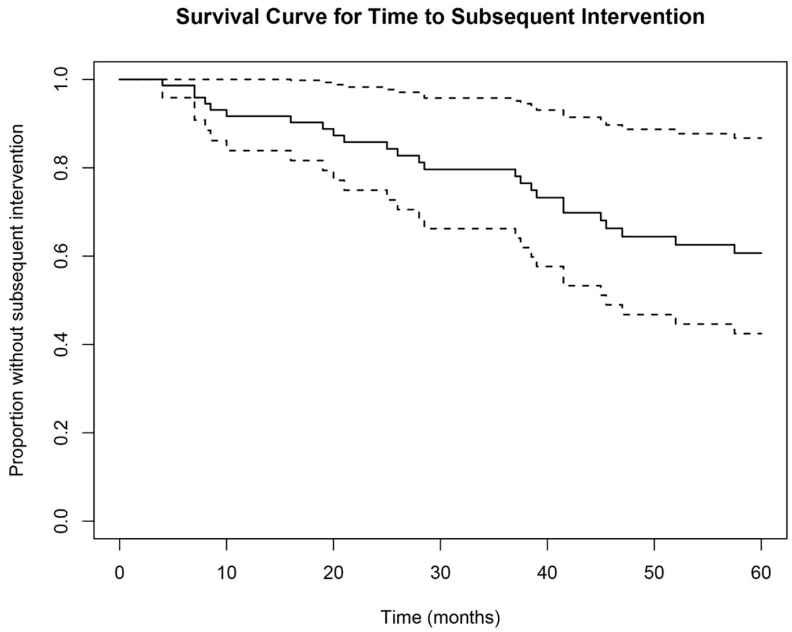

FIGURE 2
Cox proportional hazard survival curve for time to subsequent surgical intervention. Survival analysis showed a 79.6% survival probability at 36 months and a 60.7% survival probability at 60 months. Dotted lines represent upper and lower 95% confidence intervals.

in the 5-year follow-up period and had complete OCT data. While average RNFL thickness and superior quadrant RNFL thickness were unchanged at 3-year and 5-year (both $P > 0.05$), the inferior quadrant RNFL thickness decreased significantly at 3-year (89.7 ± 20.5 μm) and 5-year (88.5 ± 19.3 μm), compared to pre-SLT RNFL thickness (94.0 ± 23.2 μm; both $P \leq 0.01$, respectively) (Table 6).

4. Discussion

In this study, we examined the long-term outcomes of adjuvant SLT treatment on glaucomatous eyes that were receiving medical therapy. One of our main findings was that we found that a large percentage (49%) of eyes received a subsequent surgical intervention within the 5-year follow-up period after SLT treatment. Another main finding was that although IOP was significantly lower than baseline after 5 years in the eyes that did not receive a subsequent surgical intervention, the number of glaucoma medications was significantly increased, the HVF MD and PSD were significantly more deviated, and the inferior quadrant RNFL thickness was significantly decreased at 5 years compared to pre-SLT. Finally, we also found that patient age $\geq$ 69 years was significantly associated with increased risk of receiving subsequent surgical procedure to control IOP over the 5-year period after SLT treatment.

Although SLT has been shown to provide significant IOP reduction for glaucomatous eyes receiving concurrent medical

TABLE 2 Counts of subsequent surgical interventions.

Type of surgical intervention	Count
None	26
Repeat SLT	13
Ahmed valve implant	5
Trabeculectomy	3
MicroPulse™	2
CE	2
Total	51

SLT, selective laser trabeculoplasty; CE, cataract extraction.

TABLE 3 Summary of hazard ratio analysis.

Characteristic	Hazard ratio over 5-year	95% confidence interval	*P*-value
Age at SLT	1.05	[1.01, 1.09]	**0.04**
CCT*	1.01	[0.99, 1.01]	0.24
Female gender	1.79	[0.70, 4.54]	0.22
Pre-SLT IOP	1.02	[0.91, 1.14]	0.76
OS	0.92	[0.49, 1.74]	0.80

CCT, central corneal thickness; OS, left eye. *Forty-one eyes were used for this analysis that had available CCT data pre-SLT. All other hazard ratios were determined using all 51 eyes included in this study with clustering among patients. Bold values indicate the *p*-value <0.05.

TABLE 4 Outcome measures in eyes that did not receive subsequent surgical intervention.

		Mean*	SD	*P*-value†
IOP (mmHg)	Pre-SLT	18.0	3.7	–
	3-year	14.8	2.8	**≤0.01**
	5-year	14.5	3.3	**≤0.01**
VA	Pre-SLT	0.8	0.2	–
	3-year	0.8	0.2	0.84
	5-year	0.8	0.2	0.74
# Glaucoma medications	Pre-SLT	2.0	1.1	–
	3-year	2.5	1.3	0.07
	5-year	2.7	1.6	**0.04**

*Twenty-one eyes that did not receive subsequent surgical intervention in the 5-year follow-up period were used in this analysis. Only one eye from each patient was used in this analysis. †*P*-values refer to comparison with pre-SLT values. Bold values indicate the *p*-value <0.05.

TABLE 5 Humphrey visual field parameters in eyes that did not receive subsequent surgical intervention.

		Mean (dB)*	SD	*P*-value†
HVF MD	Pre-SLT	−5.61	3.90	–
	3-year	−6.84	5.84	0.05
	5-year	−7.64	6.57	**0.02**
HVF PSD	Pre-SLT	4.63	2.70	–
	3-year	5.30	2.91	**0.04**
	5-year	6.84	2.62	**≤0.01**

*Twenty eyes that did not receive subsequent surgical intervention in the 5-year follow-up period were used in this analysis. Two eyes were missing one or more HVF. Only one eye from each patient was used in this analysis. †*P*-values refer to comparison with pre-SLT values. Bold values indicate the *p*-value <0.05.

therapy during the short-term follow-up period (10, 11, 19–21), we found that 49% of eyes received a subsequent surgical intervention in addition to continued medical therapy within 5 years to control IOP in response to progressively decreasing visual function. For the other 51% of eyes, one-time SLT with continued medical therapy significantly lowered IOP without subsequent surgical intervention. However, this group had a significant increase in the number of glaucoma medications (2.7 ± 1.6 at 5-year compared to 2.0 ± 1.1 before SLT) (**Table 4**). These data suggest that SLT may have some value as an adjuvant therapy for glaucomatous patients in lowering IOP; however, additional medical management (e.g., increased number of glaucoma medications) may be necessary to continue to observe the IOP-lowering effects of SLT at 5 years following treatment.

In comparison to previous studies that looked at the long-term effects of SLT on glaucomatous eyes, our study had a similar or lower rate of subsequent surgical intervention. One retrospective chart review study of 90° SLT had a low success rate of 24% after 4 years, where failure was defined as having repeat SLT, change in medical treatment, or other surgery (22). Our study looked at eyes receiving 180°, so we cannot directly compare with this study. However, previous studies suggest that 180° SLT is more efficacious at lowering IOP than 90° SLT after 1 year (20, 23). Other studies using 180° SLT showed low survival rates of 25% after 5 years, with survival being defined as at least 20% lowering of IOP with no additional surgical or medical intervention (24). In our study, we specifically examined whether eyes received additional surgical or laser intervention and excluded an increase in medical therapy from our survival analysis, which may explain our higher cumulative survival rate of 51% at 5 years. In another long-term study following early glaucoma patients treated with first line SLT, the re-treatment rate for receiving a repeat SLT was 60% over 10 years, which was slightly higher than ours of 49% over 5 years (14). Nonetheless, our data agree with previous studies that the rate of having a subsequent intervention is nearly half of patients receiving SLT over long-term follow-up.

Many previous studies have examined predictors of success of SLT. In this study, we examined factors that may be associated with having a subsequent surgical intervention by calculating hazard ratios over the 5-year follow-up period. We found that older age was significantly associated with greater risk of receiving a subsequent surgical intervention within 5-year (**Table 3**). A previous study reported that higher baseline IOP was associated with increased risk of re-treatment with 360° SLT within the 10-year follow-up period (14). In our study, baseline IOP was not significantly associated with risk of subsequent surgical intervention (**Table 3**). This previous study also did not find an association between age at SLT and risk of re-treatment. One difference between this previous study and ours that could account for these different findings is that our study examined adjuvant use of 180° SLT in glaucoma patients with continued medical therapy, while the previous study looked at first-line 360° SLT in treatment-naïve early glaucoma patients. Another factor that may account for our findings is the relatively small sample size of 51 eyes in our study. Further study is needed to elucidate the factors associated with risk of further surgical treatment in eyes receiving adjuvant SLT with continued medical therapy.

One of the strengths of this study is that we examined functional assessments (HVF and OCT) over the follow-up period, whereas previous long-term studies have not thoroughly examined such parameters. We found significant decreases in the functional assessments (HVF and OCT) over the 5-year follow-up period, specifically in patients who did not receive a subsequent surgical intervention. We had 20 eyes from 20 patients who did not receive a subsequent surgical intervention with complete HVF data, and we found mean MD declined from −5.61 to −7.64 dB over 5-year, or −0.41 dB per year if consistent rate of decline. One previous retrospective study examined early POAG patients receiving first-line SLT and found a steep decline in MD on HVF during years 6–10 of follow-up but only a slight decline over the first 6 years of follow-up, with a mean visual

field MD change of −0.2 dB per year (14). The authors stated that this could have been due to the significant drop-out rate of patients over the follow-up period; the study started with 105 patients and only had 18 patients by the 10-year follow-up. The difference between our rates of MD decline is likely due to different patient populations; we examined glaucomatous eyes receiving medical therapy and adjuvant SLT in a mostly black/African American population, whereas Ansari's study examined early glaucomatous eyes receiving first-line SLT in an unspecified patient population in the United Kingdom. We additionally examined the PSD and found a significant increase in PSD at 3- and 5-year compared to pre-SLT. These data suggest that HVF parameters may still decline, despite having significantly lower IOP and not receiving a subsequent surgical intervention.

We also examined the RNFL *via* OCT and found a significant decrease in inferior quadrant RNFL thickness at 3- and 5-year compared to pre-SLT in our 19 eyes from 19 patients with complete OCT data of the eyes that did not receive a subsequent surgical intervention. Previous studies found no significant change in RNFL in the short-term follow-up period of 6 months to 1 year after SLT (25, 26). To our knowledge, no other long-term studies have examined RNFL thickness in glaucomatous eyes receiving adjuvant SLT with continued medical therapy. Our data suggest that even with significantly lower IOP at 5-year follow-up, patients may have continued decreasing visual function as observed through decreasing RNFL thickness in the inferior quadrant (Table 6). Our findings on HVF and OCT exams suggest that patients who do not receive a subsequent surgical intervention to manage IOP may still be having statistically significant functional decline even with continued medical management.

There were some limitations in our study. First, this study was retrospective, meaning that no specific management protocol was followed among surgeons at Boston Medical Center. Additionally, because this study was retrospective, not all patients had every HVF or OCT parameter, therefore, analysis was conducted with those who had sufficient data. Also, our study contained a limited number of eyes from single healthcare center. In order to capture more patients with SLT, we included five eyes with NTG and two with uveitic glaucoma, so not all of our patients had the same glaucoma diagnosis; however, we included these, because statistical outcomes were not different when these eyes were excluded from analysis. Lastly, while we defined survival as not receiving a subsequent surgical procedure to control IOP, there were factors that this metric did not capture, such as if the patient did not wish to have a subsequent procedure.

In summary, this study found that a large percentage (49%) of eyes received a subsequent surgical intervention within the 5-year follow-up period after SLT treatment, with higher risk associated with higher age at time of SLT. Unlike previous studies on the efficacy of adjuvant SLT, we examined RNFL and HVF parameters and found that for the eyes that did not receive further surgical treatment, there was progression of MD and PSD on HVF and inferior quadrant RNFL thinning on OCT at 5-year follow-up with a significant increase in number of glaucoma medications. Our findings suggest that SLT may have some long-term benefit to lowering IOP with continued medical therapy; however, a significant number of patients received subsequent laser/surgical procedures to lower and prevent worsening visual function. Overall, our study adds to the understanding of the long-term effectiveness of SLT.

TABLE 6 OCT parameters in eyes that did not receive subsequent surgical intervention.

RFNL thickness		Mean (μm)*	SD	*P*-value†
Mean	Pre-SLT	74.6	13.2	–
	3-year	73.3	11.8	0.21
	5-year	72.5	11.8	0.10
Superior	Pre-SLT	89.8	20.6	–
	3-year	87.7	20.0	0.28
	5-year	85.9	19.3	0.12
Inferior	Pre-SLT	94.0	23.2	–
	3-year	89.7	20.5	**≤0.01**
	5-year	88.5	19.3	**≤0.01**

*Nineteen eyes that did not receive subsequent surgical intervention in the 5-year follow-up period were used in this analysis. Three eyes were missing one or more OCT. Only one eye from each patient was used in this analysis. †*P*-values refer to comparison with pre-SLT values. Bold values indicate the *p*-value <0.05.

Data availability statement

The original contributions presented in this study are included in this article/supplementary material, further inquiries can be directed to the corresponding authors.

Ethics statement

The studies involving human participants were reviewed and approved by Boston University Institutional Review Board (IRB: H-39121). Written informed consent for participation was not required for this study in accordance with the national legislation and the institutional requirements.

Author contributions

BE-R: conceptualization, resources, and supervision. DLS: data collection, analysis, and writing original draft. Both authors: writing, reviewing, editing, and approve the submitted version.

Funding

DLS was supported in part by training grant EY030318 from the National Institutes of Health (NIH). The funders had no role in the study design, data collection and analysis, decision to publish, or the preparation of the manuscript.

Acknowledgments

We thank Michael P. LaValley at Boston University School of Public Health for assistance with statistical analysis and Emily Swain for assistance with R coding.

Conflict of interest

The authors declare that the research was conducted in the absence of any commercial or financial relationships that could be construed as a potential conflict of interest.

Publisher's note

All claims expressed in this article are solely those of the authors and do not necessarily represent those of their affiliated organizations, or those of the publisher, the editors and the reviewers. Any product that may be evaluated in this article, or claim that may be made by its manufacturer, is not guaranteed or endorsed by the publisher.

References

1. Quigley H, Broman A. The number of people with glaucoma worldwide in 2010 and 2020. *Br J Ophthalmol.* (2006) 90:262–7. doi: 10.1136/bjo.2005.081224

2. Tham Y, Li X, Wong T, Quigley H, Aung T, Cheng C. Global prevalence of glaucoma and projections of glaucoma burden through 2040: a systematic review and meta-analysis. *Ophthalmology.* (2014) 121:2081–90. doi: 10.1016/j.ophtha.2014.05.013

3. Weinreb R, Aung T, Medeiros F. The pathophysiology and treatment of glaucoma: a review. *JAMA.* (2014) 311:1901–11. doi: 10.1001/jama.2014.3192

4. The AGIS Investigators. The advanced glaucoma intervention study (AGIS): 7. The relationship between control of intraocular pressure and visual field deterioration. *Am J Ophthalmol.* (2000) 130:429–40. doi: 10.1016/s0002-9394(00)00538-9

5. Garg A, Gazzard G. Selective laser trabeculoplasty: past, present, and future. *Eye (Lond).* (2018) 32:863–76. doi: 10.1038/eye.2017.273

6. Cvenkel B, Hvala A, Drnovsek-Olup B, Gale N. Acute ultrastructural changes of the trabecular meshwork after selective laser trabeculoplasty and low power argon laser trabeculoplasty. *Lasers Surg Med.* (2003) 33:204–8. doi: 10.1002/lsm.10203

7. Gupta M, Heo J, Gong H, Cha E, Latina M, Rhee D. Morphologic and cellular changes induced by selective laser trabeculoplasty. *Clin Ophthalmol.* (2022) 16:1383–90. doi: 10.2147/opth.S342787

8. Lee J, Kagan D, Roumeliotis G, Liu H, Hutnik C. Secretion of matrix metalloproteinase-3 by co-cultured pigmented and non-pigmented human trabecular meshwork cells following selective laser trabeculoplasty. *Clin Exp Ophthalmol.* (2016) 44:33–42. doi: 10.1111/ceo.12591

9. Alvarado J, Iguchi R, Martinez J, Trivedi S, Shifera A. Similar effects of selective laser trabeculoplasty and prostaglandin analogs on the permeability of cultured schlemm canal cells. *Am J Ophthalmol.* (2010) 150:254–64. doi: 10.1016/j.ajo.2010.03.012

10. Cvenkel B. One-year follow-up of selective laser trabeculoplasty in open-angle glaucoma. *Ophthalmologica.* (2004) 218:20–5. doi: 10.1159/000074562

11. Schlote T, Kynigopoulos M. Selective laser trabeculoplasty (Slt): 1-year results in early and advanced open angle glaucoma. *Int Ophthalmol.* (2016) 36:55–61. doi: 10.1007/s10792-015-0079-1

12. Patel V, El Hawy E, Waisbourd M, Zangalli C, Shapiro D, Gupta L, et al. Long-term outcomes in patients initially responsive to selective laser trabeculoplasty. *Int J Ophthalmol.* (2015) 8:960–4. doi: 10.3980/j.issn.2222-3959.2015.05.19

13. Weinand F, Althen F. Long-term clinical results of selective laser trabeculoplasty in the treatment of primary open angle glaucoma. *Eur J Ophthalmol.* (2006) 16:100–4.

14. Ansari E. 10-Year outcomes of first-line selective laser trabeculoplasty (Slt) for primary open-angle glaucoma (Poag). *Graefes Arch Clin Exp Ophthalmol.* (2021) 259:1597–604. doi: 10.1007/s00417-021-05098-z

15. Garg A, Vickerstaff V, Nathwani N, Garway-Heath D, Konstantakopoulou E, Ambler G, et al. Primary selective laser trabeculoplasty for open-angle glaucoma and ocular hypertension: clinical outcomes, predictors of success, and safety from the laser in glaucoma and ocular hypertension trial. *Ophthalmology.* (2019) 126:1238–48. doi: 10.1016/j.ophtha.2019.04.012

16. Gazzard G, Konstantakopoulou E, Garway-Heath D, Garg A, Vickerstaff V, Hunter R, et al. Selective laser trabeculoplasty versus eye drops for first-line treatment of ocular hypertension and glaucoma (Light): a multicentre randomised controlled trial. *Lancet.* (2019) 393:1505–16. doi: 10.1016/s0140-6736(18)32213-x

17. Lai J, Chua J, Tham C, Lam D. Five-year follow up of selective laser trabeculoplasty in Chinese eyes. *Clin Exp Ophthalmol.* (2004) 32:368–72. doi: 10.1111/j.1442-9071.2004.00839.x

18. Shazly T, Latina M, Daagianis J, Chitturi S. Effect of central corneal thickness on the long-term outcome of selective laser trabeculoplasty as primary treatment for ocular hypertension and primary open-angle glaucoma. *Cornea.* (2011) 31:883–6. doi: 10.1097/ICO.0b013e318243f684

19. Nirappel A, Klug E, Ye R, Hall N, Chachanidze M, Chang T, et al. Effectiveness of selective laser trabeculoplasty applied to 360 degrees Vs. 180 degrees of the angle. *J Ophthalmol.* (2021) 2021:8860601. doi: 10.1155/2021/8860601

20. Nagar M, Ogunyomade A, O'Brart D, Howes F, Marshall J. A randomised, prospective study comparing selective laser trabeculoplasty with latanoprost for the control of intraocular pressure in ocular hypertension and open angle glaucoma. *Br J Ophthalmol.* (2005) 89:1413–7. doi: 10.1136/bjo.2004.052795

21. Miki A, Kawashima R, Usui S, Matsushita K, Nishida K. Treatment outcomes and prognostic factors of selective laser trabeculoplasty for open-angle glaucoma receiving maximal-tolerable medical therapy. *J Glaucoma.* (2016) 25:785–9. doi: 10.1097/IJG.0000000000000411

22. Ayala M, Chen E. Long-term outcomes of selective laser trabeculoplasty (Slt) treatment. *Open Ophthalmol J.* (2011) 5:32–4.

23. Chen E, Golchin S, Blomdhal S. A comparison between 90 degrees and 180 degrees selective laser trabeculoplasty. *J Glaucoma.* (2004) 13:62–5. doi: 10.1097/00061198-200402000-00012

24. Bovell A, Damji K, Hodge W, Rock W, Buhrmann R, Pan Y. Long term effects on the lowering of intraocular pressure: selective laser or argon laser trabeculoplasty? *Can J Ophthalmol.* (2011) 46:408–13. doi: 10.1016/j.jcjo.2011.07.016

25. Gillmann K, Rao H, Mansouri K. Changes in peripapillary and macular vascular density after laser selective trabeculoplasty: an optical coherence tomography angiography study. *Acta Ophthalmol.* (2022) 100:203–11. doi: 10.1111/aos.14805

26. Wong M, Lai I, Chan P, Chan N, Chan A, Lai G, et al. Efficacy and safety of selective laser trabeculoplasty and pattern scanning laser trabeculoplasty: a randomised clinical trial. *Br J Ophthalmol.* (2021) 105:514–20. doi: 10.1136/bjophthalmol-2020-316178

frontiers | Frontiers in Medicine

TYPE Systematic Review
PUBLISHED 17 February 2023
DOI 10.3389/fmed.2023.1126724

OPEN ACCESS

EDITED BY
Georgios Panos,
Nottingham University Hospitals NHS Trust,
United Kingdom

REVIEWED BY
Manisha Agarwal,
Dr Shroff Charity Eye Hospital,
India
Mehmet Cem Sabaner,
Kutahya Evliya Celebi Training and
Research Hospital,
Türkiye

*CORRESPONDENCE
Xia Li
✉ tuotuo19840411@163.com
Jun Li
✉ drliwpp@163.com

†These authors have contributed equally to this work

SPECIALTY SECTION
This article was submitted to
Ophthalmology,
a section of the journal
Frontiers in Medicine

RECEIVED 18 December 2022
ACCEPTED 23 January 2023
PUBLISHED 17 February 2023

CITATION
Fan S, Shi X-Y, Zhao C-F, Chen Z, Ying J, Yu S-P, Li J and Li X (2023) Efficacy and safety of single-dose intravitreal dexamethasone implant in non-infectious uveitic macular edema: A systematic review and meta-analysis.
Front. Med. 10:1126724.
doi: 10.3389/fmed.2023.1126724

Efficacy and safety of single-dose intravitreal dexamethasone implant in non-infectious uveitic macular edema: A systematic review and meta-analysis

Shipei Fan[1†], Xing-yu Shi[2†], Chao-fu Zhao[1], Zhen Chen[1], Jia Ying[1], Song-ping Yu[1], Jun Li[1*] and Xia Li[1*]

[1]Department of Ophthalmology, Lishui Municipal Central Hospital, The Fifth Affiliated Hospital of Wenzhou Medical University, Lishui, Zhejiang, China, [2]Department of Nephrology, Lishui Municipal Central Hospital, The Fifth Affiliated Hospital of Wenzhou Medical University, Lishui, Zhejiang, China

Purpose: We conducted a systematic review and meta-analysis to investigate the efficacy and safety of single-dose intravitreal dexamethasone (DEX) implant for treating non-infectious uveitic macular edema (UME).

Methods: Studies including clinical outcomes of the DEX implant in UME were comprehensively searched in PubMed, Embase, and Cochrane databases for potential studies from inception to July 2022. The primary outcomes were best corrected visual acuity (BCVA) and central macular thickness (CMT) during the follow-up period. Stata 12.0 was used to perform the statistical analyses.

Results: Six retrospective studies and one prospective investigation involving 201 eyes were ultimately included. Significantly improved BCVA was observed from baseline to 1month (WMD=−0.15, 95%CI=−0.24, −0.06), 3months (WMD=−0.22, 95%CI=−0.29, −0.15), and 6months (WMD=−0.24, 95%CI=−0.35, −0.13), after single-dose DEX implant. When considering CMT, macular thickness of 1month (WMD=−179.77, 95%CI=−223.45, −136.09), 3months (WMD=−179.13, 95%CI=−232.63, −125.63), and 6months (WMD=−140.25, 95%CI=−227.61, −52.88) decreased in comparison with baseline, with statistical significance.

Conclusion: Based on the current results, this meta-analysis confirmed favorable visual prognosis and anatomical improvement in patients with UME, after receiving the single-dose DEX implant. The most common adverse event is increased intraocular pressure, which could be controlled with topical medications.

Systematic Review Registration: https://www.crd.york.ac.uk/PROSPERO/, identifier CRD42022325969.

KEYWORDS

macular edema, intravitreal implant, dexamethasone, meta-analysis, non-infectious uveitis

Introduction

Uveitis accounts for 10–15% of blindness in developed countries, with an estimated prevalence of 9–730 cases per 100,000 population (1, 2). Uveitic macular edema (UME) is the most frequent clinical complication of non-infectious uveitis and could persist for a long period despite various treatment modalities and adequate control of ocular inflammation, leading to structural retinal damage and irreversible vision impairment (3).

Large publications have focused on various aspects of UME, yet the detailed and comprehensive pathogenesis remains not fully understood. Prior investigations have found increased pro-inflammatory cytokine levels such as interleukin-6 (IL-6), IL-8, tumor necrosis factor-α, and vascular endothelial growth factor (VEGF), which might play an essential role in UME (4, 5). A recent study demonstrates that the regulatory T cell is positively associated with persistent anatomical improvement and might be a prognostic factor for patients with UME (5). In short, breakdown of the outer and inner blood-retinal barrier results in increased permeability of the microvasculature and pigment epithelium, leading to fluid accumulation and macular edema. Therefore, exploring effective and acceptable therapeutic strategies is a persistent challenge.

Local and systemic uses of corticosteroids are the first-line treatment option for UME, while long-term use may be burdened by multiple side effects, including poor blood glucose control, osteoporosis, cataract progression, and ocular hypertension (6). Therefore, different interventions including immunomodulatory agents, anti-VEGF, and pars plana vitrectomy are also adopted for UME (7). However, the prognosis remains unsatisfactory in patients with chronic and refractory UME. Thus, there has been a growing body of studies that focus on intravitreal implants to improve visual outcomes and minimize ocular side effects in recent years.

The intravitreal dexamethasone (DEX) implant (Ozurdex; Allergan, Inc., Irvine, CA) is a sustained-release implant designed to deliver 0.7 mg of dexamethasone in vitreous (8). A recently published network meta-analysis manifested that the DEX implant could improve the anatomical structure and vitreous haze of non-infectious uveitis (9). In addition, the HURON study had demonstrated significantly reduced central macular thickness (CMT) and improved visual acuity with duration for 6 months in non-infectious uveitis after a single DEX implantation (10). Although multiple publications have manifested the efficacy of the DEX implant in UME, the precise conclusion remains unclear. To elucidate the potential benefits and drawbacks of this treatment option, this meta-analysis was performed to systematically determine the effectiveness and safety of a single-dose DEX implant for macular edema secondary to non-infectious uveitis.

Methods

The present meta-analysis was conducted based on the principles proposed by the Cochrane Handbook (11) and the Preferred Reporting Items for Systematic reviews and Meta-Analyses (PRISMA) statement (12). No ethical approval and informed consent were required. This analysis has already been registered in Prospero.

Search strategy

In total, three electronic databases, including PubMed, Embase, and Cochrane library, were searched comprehensively in July 2022 by two independent investigators (FSP and SXY). The search strategy was performed in accordance with the following terms: ((“uveitic” [tiab]) OR (“uveitis” [tiab]) OR (“UME” [tiab]) OR (“Uveitides” [tiab]) OR (“panuveitis” [tiab]) OR (“iridocyclitis” [tiab]) OR (“vasculitis” [tiab]) OR (“(retinal vasculitis” [tiab]) OR (“ocular inflammation” [tiab])) AND ((“macular edema” [tiab]) OR (“(macular oedema” [tiab])) AND ((“intravitreal dexamethasone implant” [tiab]) OR (“(dexamethasone” [tiab]) OR (“ozurdex” [tiab])). The references of associated publications were further screened thoroughly for additional relevant investigations.

Inclusion and exclusion criteria

Eligible studies were required to accord with the following criteria: (1) original investigation focusing on non-infectious UME; (2) chronic macular edema refractory to previous treatments; (3) the age of patients >18 years; (4) sample size of included eyes in each study was at least 20; (5) acceptance of DEX implant with at least 3 months follow-up period; and (6) the main outcomes were expressed as mean ± standard deviation (SD). The exclusion was adopted as follows: (1) patients with other fundus diseases such as diabetic retinopathy, age-related macular degeneration, and choroidal neovascularization; (2) case reports, reviews, letters, editorials, and comments without data; and (3) patients who underwent prior pars plana vitrectomy.

Data extraction and quality assessment

Overall, two investigators (FSP and SXY) separately screened the titles and abstracts of eligible studies and assessed entire articles to evaluate the finally included investigations. The data extraction was conducted by two independent researchers (FSP and SXY) from eligible studies. From each publication, the following demographic information and clinical characteristics were extracted: first author, publication date, location and study period, study type, duration of uveitis, follow-up time, mean number of DEX implants, previous systemic and local treatments, incidence of adverse events, best corrected visual acuity (BCVA), and CMT change after single-dose DEX implant. The criteria reported by the Methodological Index for Non-randomized Studies (Minors) were adopted to evaluate the evidence quality of included studies, which contained eight items specifically for non-comparative studies (13). A third reviewer (LX) was involved in case of any disagreement to reach a consensus.

Quantitative analysis

Stata 12.0 (Stata Corporation, College Station, TX, United States) was applied to conduct all data analyses. The inverse-variance model was utilized to determine the weight mean difference (WMD) with a 95% confidence interval (CI) for continuous outcomes in the present meta-analysis. The evaluation of statistical heterogeneity was assessed using Cochran's Q test and I^2 test. Based on the meta-analysis principle, a value of $I^2 < 50\%$ indicated relatively low heterogeneity across studies, while $I^2 > 75\%$ represented substantial heterogeneity. When significant heterogeneity was determined, a random-effect model was used; otherwise, a fixed-effect model was applied. Publication bias was calculated by the Egger test. A two-sided p value <0.05 was adopted as statistically significant.

Results

Selection of studies

As illustrated in Figure 1, a total of 445 records were identified in accordance with the search strategy from electronic databases (PubMed = 265, Embase = 180), of which 155 duplicates were excluded. After screening the titles and abstracts of the remaining 290 publications,

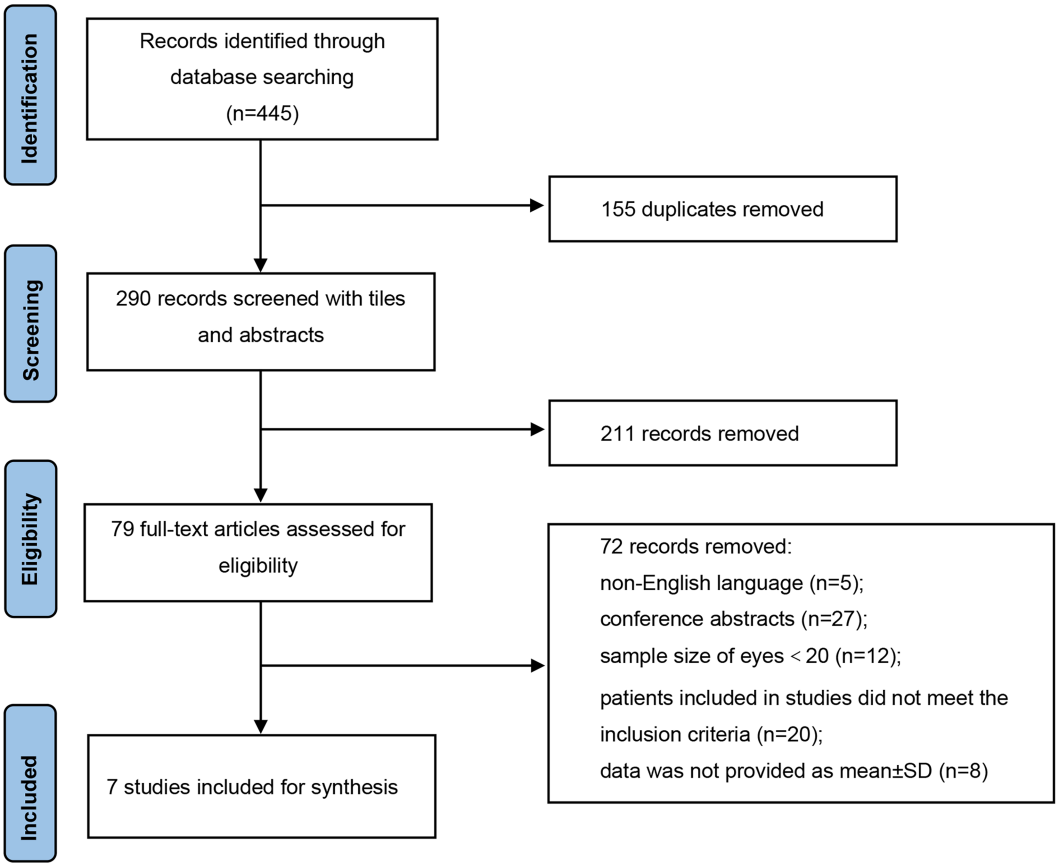

FIGURE 1
Flow diagram of the study selection process.

211 studies were ruled out. Among the 79 potentially eligible records for full-text review, 72 articles were excluded. Finally, seven studies were included and pooled together for further data synthesis (14–20). Studies were ruled out for the following reasons: non-English language, conference abstracts, sample size of included eyes was less than 20, patients included in studies did not meet the inclusion criteria, and data were not provided as mean ± SD.

Baseline characteristics

Detailed baseline demographics and clinical information are summarized in Tables 1, 2. Among seven publications, a total of 201 eyes were retrieved in accordance with the inclusion criteria. The sample size of included studies ranged from 22 to 41 eyes. In total, six studies were designed as retrospective and one study was designed as prospective. The clinical diagnoses of included studies were summarized in Supplementary Table S1. The methodologic score of eligible studies ranged from 11 to 14, indicating relatively high quality and reliability of results from included studies (Table 3).

Best corrected vision acuity and central macular thickness

Data from five studies, six studies, and four studies were pooled together to determine the average change of BCVA from baseline to 1, 3, and 6 months, respectively. After the DEX implant, BCVA significantly increased at 1 month, compared to the baseline (Figure 2A, WMD = −0.15, 95%CI = −0.24, −0.06, $p = 0.013$, $I^2 = 68.2\%$). At 3 months, significantly improved BCVA was determined (Figure 2B, WMD = −0.22, 95%CI = −0.29, −0.15, $p = 0.012$, $I^2 = 65.9\%$). When considering 6 months, BCVA improved from the baseline with an average of −0.24 logMAR (Figure 2C, WMD = −0.24, 95%CI = −0.35, −0.13, $p = 0.211$, $I^2 = 33.6\%$).

Regarding the CMT of 1 month, results from seven articles identified significantly reduced thickness with an average of −179.77 μm, compared with baseline data (Figure 3A, WMD = −179.77, 95%CI = −223.45, −136.09, $p < 0.001$, $I^2 = 91.0\%$). In addition, significantly decreased CMT was observed at 3 months in comparison with baseline (Figure 3B, WMD = −179.13, 95%CI = −232.63, −125.63, $p < 0.001$, $I^2 = 92.8\%$). Significant difference between the CMT of 6 months and baseline was determined (Figure 3C, WMD = −140.25, 95%CI = −227.61, −52.88, $p < 0.001$, $I^2 = 85.7\%$).

Adverse events and publication bias

Based on this meta-analysis, it had been revealed that the incidence of ocular hypertension (IOP > 21 mmHg) and cataract formation after single-dose DEX implant were 13.6 (Figure 4A, 95%CI = 3.1, 29.0%, $p = 0.001$, $I^2 = 79.7\%$) and 5.4% (Figure 4B, 95%CI = 0.6, 13.3%, $p = 0.085$, $I^2 = 51.1\%$), respectively. All eyes with intraocular hypertension could be controlled with topical treatments. Two

TABLE 1 Clinical demographics of included studies.

Study	Year	Country	Survey period	Study type	Eyes (patients)	Age (years)	Duration of uveitis (years)	Follow-up period (months)
Bansal et al. (14)	2015	India	NA	Prospective	30 (27)	46.1 ± 15.7	1.4 ± 0.6	5.6
Garweg et al. (15)	2016	Switzerland	NA	Retrospective	26 (19)	NA	NA	NA
Fabiani et al. (16)	2017	Italy	NA	Retrospective	22 (22)	49.0 ± 20.1	3.5 ± 2.5	6
Cardoso et al. (17)	2017	France	2012–2013	Retrospective	41 (31)	57.9 ± 13.1	NA	13.4 ± 5.9
Tsang et al. (18)	2017	Canada	2012–2014	Retrospective	25 (15)	46.8	NA	9
Nagpal et al. (19)	2018	India	2013–2016	Retrospective	30 (NA)	NA	NA	6
Yalcinbayir et al. (20)	2019	Turkey	2013–2016	Retrospective	27 (20)	35.6 ± 12.1	NA	24.4 ± 9.9

NA, Not applicable.

TABLE 2 Demographics of included studies.

Study	Mean number of implants	Previous systemic treatments			Prior ocular treatments		
		Steroid	Immunosuppressant	Biological agent	Anti-VEGF	IV steroid	ST steroid
Bansal et al. (14)	1.1	27 patients	8 patients	NA	11 patients	NA	NA
Garweg et al. (15)	NA	NA	NA	NA	NA	NA	NA
Fabiani et al. (16)	1	19 patients	13 patients	10 patients	NA	NA	NA
Cardoso et al. (17)	1.4	21 patients	12 patients	4 patients	NA	NA	2 patients
Tsang et al. (18)	1.4	5 patients	5 patients	1 patient	No	3 patients	11 patients
Nagpal et al. (19)	1	NA	NA	NA	2 patients	NA	NA
Yalcinbayir et al. (20)	1.2	NA	12 patients	8 patients	NA	NA	NA

VEGF, Vascular endothelial growth factor; IV, Intravitreal; ST, Sub-tenon; NA, Not applicable.

TABLE 3 The quality of included studies based on the MINORS.

Study	–1	–2	–3	–4	–5	–6	–7	–8	Total
Bansal et al. (14)	2	2	2	2	2	2	2	0	14
Garweg et al. (15)	2	2	0	2	2	1	2	0	11
Fabiani et al. (16)	2	2	0	2	2	2	2	0	12
Cardoso et al. (17)	2	2	0	2	2	2	1	0	11
Tsang et al. (18)	2	2	0	2	2	2	2	0	12
Nagpal et al. (19)	2	2	0	2	2	2	2	0	12
Yalcinbayir et al. (20)	2	2	0	2	2	2	2	0	12

Studies fulling the criteria of: (1) clearly stated aim; (2) consecutive patients; (3) prospective data collection; (4) endpoints appropriate to the aim of the study; (5) unbiased assessment of the study endpoint; (6) follow-up period appropriate to the aim of the study; (7) loss to follow up less than 5%; (8) prospective calculation of the study size. MINORS, Methodological item for non-randomized studies; 0 = not reported; 1 = reported, but inadequate; 2 = reported and adequate.

unexpected adverse events including vitreous hemorrhage and lens injury were observed immediately after implantation, which were successfully treated with vitrectomy (Supplementary Table S2). There were no reported cases of endophthalmitis and retinal detachment during the follow-up period. The Egger test demonstrated no significant publication bias of visual and structural outcomes in the present meta-analysis (Supplementary Table S3).

Discussion

In the present meta-analysis, favorable visual prognosis and significant anatomical improvement were demonstrated after a single-dose DEX implant in patients with refractory UME. No serious adverse events were recorded in the follow-up period. Based on the results, the DEX implant could be an effective therapeutic option for chronic and refractory patients with UME who had previously undergone systemic therapy.

Uveitis occurs in population of all ages but frequently affects working-age individuals, thus posing a substantial socioeconomic burden on the healthcare system (21). Macular edema is the most frequent and sight-threatening complication of non-infectious uveitis, which leads to central visual impairment. Taking the adverse events and side effects of systemic corticosteroid into account, some scholars advocated the intravitreal dexamethasone implant for chronic and refractory UME.

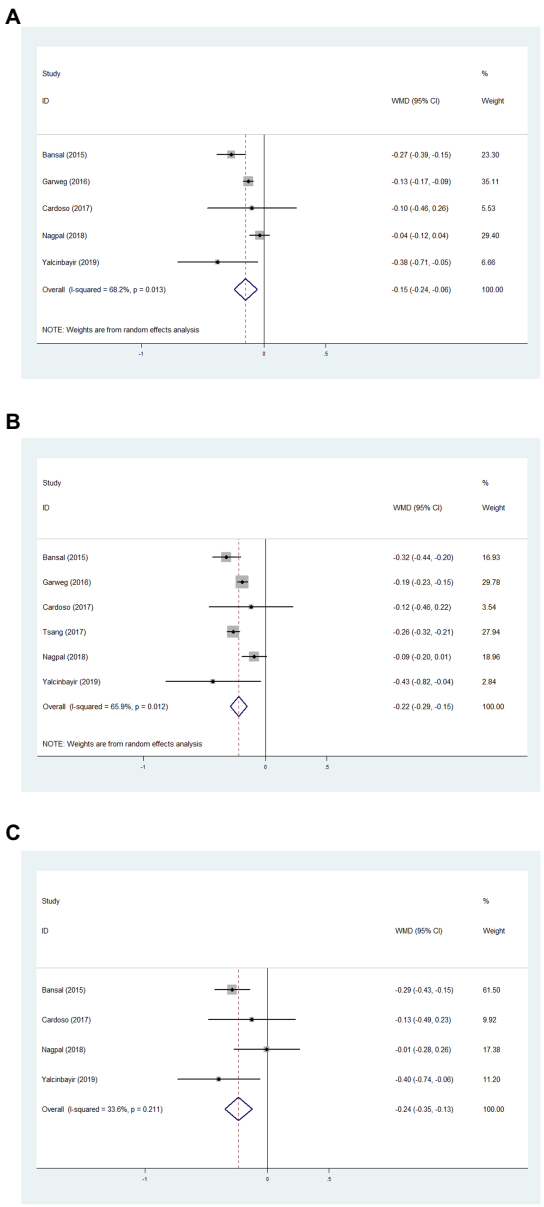

FIGURE 2
Forest plot showing best corrected visual acuity changes from baseline to 1 **(A)**, 3 **(B)**, and 6months **(C)**.

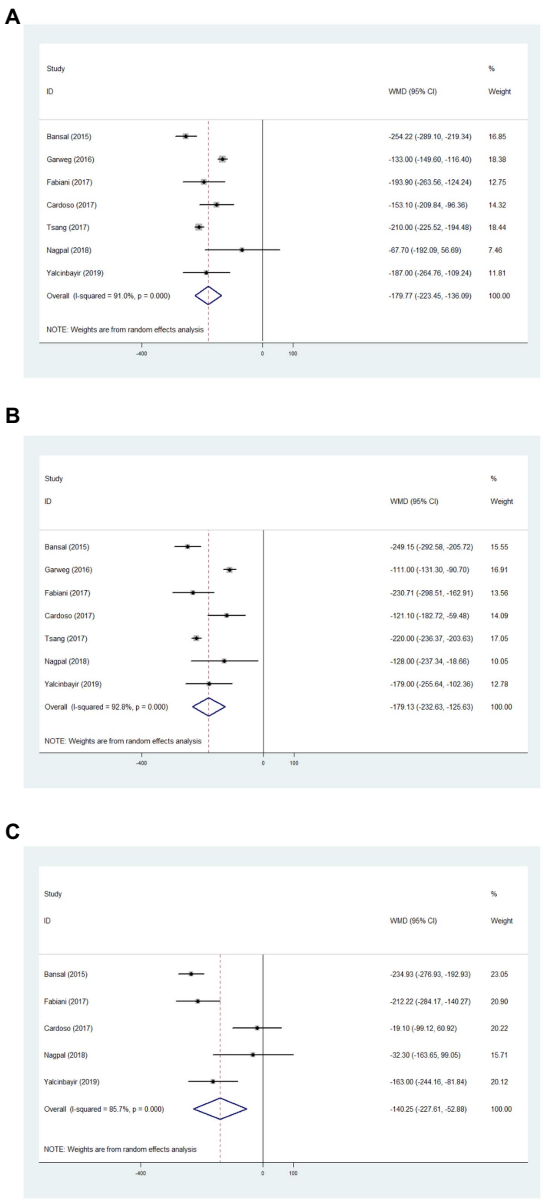

FIGURE 3
Forest plot showing central macular thickness changes from baseline to 1 **(A)**, 3 **(B)**, and 6months **(C)**.

The most noteworthy result emerging from the present meta-analysis was significantly improved BCVA and reduced CMT after the implant of single-dose DEX, indicating the strong ability in inhibiting inflammation and edema during the 6-month follow-up period. Similar findings were also reported in an earlier systematic review, which showed that the DEX implant was an effective option for posterior uveitis and improved the final visual outcome significantly (22). In addition, the therapeutic effects of the DEX implant can maintain for 1 year for macular edema in quiescent uveitis (23). For patients with persistent and chronic UME whose response is unsatisfactory, the DEX implant has the ability to reduce the incidence of visual loss (24). A possible explanation is that dexamethasone can reduce the expression of VEGF, pro-inflammatory cytokines, and chemokines efficiently and then promote the repair of the blood–retinal barrier. It is worthwhile to point out that a small group of patients in included studies underwent repeated injections of the DEX implant due to elevated CMT or deteriorated visual acuity, and most investigations did not provide the relevant results after repeated implants. Longitudinal cohort trials with longer follow-ups are desirable to ensure the reliability and stability of the DEX implant in chronic UME.

Adverse events were relatively rare in the included studies. The most common side effects are ocular hypertension and cataract formation. Previous network meta-analysis including random controlled trials confirmed that the DEX implant had a lower incidence of cataract progressing in non-infectious uveitis (9). Data analyzed from another meta-analysis confirmed that the incidence of increased IOP and cataract were 20.6 and 11%, respectively (22). Thus, it is essential to inform the patients of the potential risks and monitor the lens status and IOP fluctuation after the DEX implant. However, the incidence of cataract formation should be interpreted with caution. It remains

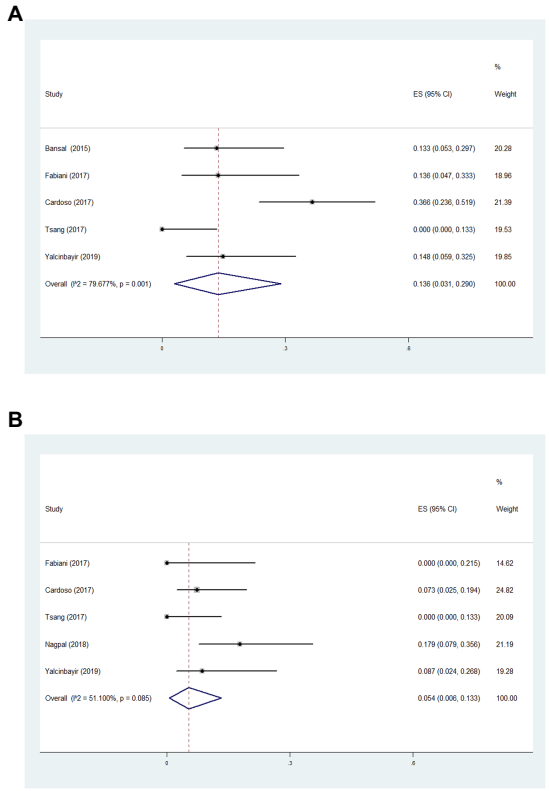

FIGURE 4
Forest plot of incidence of ocular hypertension **(A)** and cataract formation **(B)** during follow-up.

unclear whether the cataract was attributed to the DEX implant or related to the natural course of uveitis. In addition, taking the potentially severe complications into consideration, patients with a history of glaucoma and active ocular infection should not be allowed to receive the DEX implant.

Substantial heterogeneity in meta-analyses of this study was identified, which may be due to the various clinical demographics of included participants. The mean disease duration of uveitis or macular edema varied widely and was not reported in some studies, which may contribute to the heterogeneity. Second, the previous systemic and local treatment options varied extensively among studies, which contained oral steroids, immunosuppressants, biological agents, anti-VEGF, etc., also leading to clinical heterogeneity. Another critical concern is the lack of a precise grading method to define and assess the degree of UME, and the significant heterogeneity of statistical analyses is unavoidable. Further investigations, which consider these variables, will need to be conducted.

Several limitations of the present analysis should be considered. First, six studies were designed as retrospective studies and one was a prospective study, and all of the included studies lacked a control group, limiting the reliability of evidence and leading to inevitable inclusion criteria bias. The previous therapeutic strategies were not reported by Nagpal et al., which could also result in selection bias (19). In addition, the relatively small size of the included studies limited the ability to draw definitive conclusions. Moreover, considering the limited data extracted from the included articles, further detailed analysis such as subgroup analysis cannot be performed.

In conclusion, this meta-analysis demonstrated that the DEX implant may play a promising role in the management of patients with persistent and chronic UME. Taking present findings into account, further investigations featuring multicenter and random control should be performed to evaluate the long-term effect and potential complications of repeated injections of DEX.

Data availability statement

The original contributions presented in the study are included in the article/Supplementary material, further inquiries can be directed to the corresponding authors.

Author contributions

SF and X-yS designed the review and extracted the data. C-fZ, ZC, JY, and S-pY contributed to the analysis of data. SF drafted the article. JL and XL reviewed and edited the manuscript. All authors contributed to the article and approved the submitted version.

Funding

This study was supported by the Lishui Municipal Science and Technology Project (2023GYX66) and the Youth Fund Program of Lishui Municipal Central Hospital (2022qnjj15).

Acknowledgments

We would like to thank all of the donors that participated in the present study.

Conflict of interest

The authors declare that the research was conducted in the absence of any commercial or financial relationships that could be construed as a potential conflict of interest.

Publisher's note

Supplementary material

The Supplementary material for this article can be found online at: https://www.frontiersin.org/articles/10.3389/fmed.2023.1126724/full#supplementary-material

References

1. Mccluskey, PJ, Towler, HM, and Lightman, S. Management of chronic uveitis. *BMJ*. (2000) 320:555–8. doi: 10.1136/bmj.320.7234.555

2. García-Aparicio, Á, García De Yébenes, MJ, Otón, T, and Muñoz-Fernández, S. Prevalence and incidence of uveitis: a systematic review and meta-analysis. *Ophthalmic Epidemiol*. (2021) 28:461–8. doi: 10.1080/09286586.2021.1882506

3. Lardenoye, CW, Van Kooij, B, and Rothova, A. Impact of macular edema on visual acuity in uveitis. *Ophthalmology*. (2006) 113:1446–9. doi: 10.1016/j.ophtha.2006.03.027

4. Jeon, S, Lee, WK, and Jung, Y. Changes in the intraocular cytokine levels after intravitreal bevacizumab in uveitic macular edema. *Ocul Immunol Inflamm*. (2012) 20:360–4. doi: 10.3109/09273948.2012.709576

5. Matas, J, Llorenç, V, Fonollosa, A, Díaz-Valle, D, Esquinas, C, De La Maza, MTS, et al. Systemic regulatory T cells and IL-6 as prognostic factors for anatomical improvement of uveitic macular edema. *Front Immunol*. (2020) 11:579005. doi: 10.3389/fimmu.2020.579005

6. Koronis, S, Stavrakas, P, Balidis, M, Kozeis, N, and Tranos, PG. Update in treatment of uveitic macular edema. *Drug Des Devel Ther*. (2019) 13:667–80. doi: 10.2147/dddt.S166092

7. Teper, SJ. Update on the management of uveitic macular edema. *J Clin Med*. (2021) 10:4133. doi: 10.3390/jcm10184133

8. Chang-Lin, JE, Attar, M, Acheampong, AA, Robinson, MR, Whitcup, SM, Kuppermann, BD, et al. Pharmacokinetics and pharmacodynamics of a sustained-release dexamethasone intravitreal implant. *Invest Ophthalmol Vis Sci*. (2011) 52:80–6. doi: 10.1167/iovs.10-5285

9. Vieira, R, Sousa-Pinto, B, and Figueira, L. Efficacy and safety of corticosteroid implants in non-infectious uveitis: a systematic review with network meta-analysis. *Ocul Immunol Inflamm*. (2022) 30:215–22. doi: 10.1080/09273948.2020.1787463

10. Lowder, C, Belfort, R Jr, Lightman, S, Foster, CS, Robinson, MR, Schiffman, RM, et al. Dexamethasone intravitreal implant for noninfectious intermediate or posterior uveitis. *Arch Ophthalmol*. (2011) 129:545–53. doi: 10.1001/archophthalmol.2010.339

11. Cumpston, M, Li, T, Page, MJ, Chandler, J, Welch, VA, Higgins, JP, et al. Updated guidance for trusted systematic reviews: a new edition of the cochrane handbook for systematic reviews of interventions. *Cochrane Database Syst Rev*. (2019) 10:142. doi: 10.1002/14651858.Ed000142

12. Shamseer, L, Moher, D, Clarke, M, Ghersi, D, Liberati, A, Petticrew, M, et al. Preferred reporting items for systematic review and meta-analysis protocols (PRISMA-P) 2015: elaboration and explanation. *BMJ*. (2015) 349:g7647. doi: 10.1136/bmj.g7647

13. Slim, K, Nini, E, Forestier, D, Kwiatkowski, F, Panis, Y, and Chipponi, J. Methodological index for non-randomized studies (minors): development and validation of a new instrument. *ANZ J Surg*. (2003) 73:712–6. doi: 10.1046/j.1445-2197.2003.02748.x

14. Bansal, P, Agarwal, A, Gupta, V, Singh, R, and Gupta, A. Spectral domain optical coherence tomography changes following intravitreal dexamethasone implant, Ozurdex® in patients with uveitic cystoid macular edema. *Indian J Ophthalmol*. (2015) 63:416–22. doi: 10.4103/0301-4738.159870

15. Garweg, JG, Baglivo, E, Freiberg, FJ, Pfau, M, Pfister, IB, Michels, S, et al. Response of postoperative and chronic uveitic cystoid macular edema to a dexamethasone-based intravitreal implant (Ozurdex). *J Ocul Pharmacol Ther*. (2016) 32:442–50. doi: 10.1089/jop.2016.0035

16. Fabiani, C, Vitale, A, Emmi, G, Lopalco, G, Vannozzi, L, Bacherini, D, et al. Systemic steroid sparing effect of intravitreal dexamethasone implant in chronic noninfectious uveitic macular edema. *J Ocul Pharmacol Ther*. (2017) 33:549–55. doi: 10.1089/jop.2017.0034

17. Nobre-Cardoso, J, Champion, E, Darugar, A, Fel, A, Lehoang, P, and Bodaghi, B. Treatment of non-infectious uveitic macular edema with the intravitreal dexamethasone implant. *Ocul Immunol Inflamm*. (2017) 25:447–54. doi: 10.3109/09273948.2015.1132738

18. Tsang, AC, Virgili, G, Abtahi, M, and Gottlieb, CC. Intravitreal dexamethasone implant for the treatment of macular edema in chronic non-infectious uveitis. *Ocul Immunol Inflamm*. (2017) 25:685–92. doi: 10.3109/09273948.2016.1160130

19. Nagpal, M, Mehrotra, N, Juneja, R, and Jain, H. Dexamethasone implant (0.7 mg) in indian patients with macular edema: real-life scenario. *Taiwan J Ophthalmol*. (2018) 8:141–8. doi: 10.4103/tjo.tjo_62_17

20. Yalcinbayir, O, Caliskan, E, Ucan Gunduz, G, Gelisken, O, Kaderli, B, and Yucel, AA. Efficacy of dexamethasone implants in uveitic macular edema in cases with behçet disease. *Ophthalmologica*. (2019) 241:190–4. doi: 10.1159/000490674

21. Acharya, NR, Tham, VM, Esterberg, E, Borkar, DS, Parker, JV, Vinoya, AC, et al. Incidence and prevalence of uveitis: results from the pacific ocular inflammation study. *JAMA Ophthalmol*. (2013) 131:1405–12. doi: 10.1001/jamaophthalmol.2013.4237

22. Saincher, SS, and Gottlieb, C. Ozurdex (dexamethasone intravitreal implant) for the treatment of intermediate, posterior, and panuveitis: a systematic review of the current evidence. *J Ophthalmic Inflamm Infect*. (2020) 10:1. doi: 10.1186/s12348-019-0189-4

23. Khurana, RN, Bansal, AS, Chang, LK, Palmer, JD, Wu, C, and Wieland, MR. Prospective evaluation of a sustained-release dexamethasone intravitreal implant for cystoid macular edema in quiescent uveitis. *Retina*. (2017) 37:1692–9. doi: 10.1097/iae.0000000000001406

24. Cao, JH, Mulvahill, M, Zhang, L, Joondeph, BC, and Dacey, MS. Dexamethasone intravitreal implant in the treatment of persistent uveitic macular edema in the absence of active inflammation. *Ophthalmology*. (2014) 121:1871–6. doi: 10.1016/j.ophtha.2014.04.012

frontiers | Frontiers in Medicine

TYPE Original Research
PUBLISHED 11 May 2023
DOI 10.3389/fmed.2023.1174264

OPEN ACCESS

EDITED BY
Horace Massa,
Hôpitaux universitaires de Genève (HUG), Switzerland

REVIEWED BY
Darren Shu Jeng Ting,
University of Nottingham, United Kingdom
Margarita Samudio,
Universidad del Pacífico, Paraguay

*CORRESPONDENCE
Wenjin Zou
✉ zouwj168@gmail.com

RECEIVED 26 February 2023
ACCEPTED 20 April 2023
PUBLISHED 11 May 2023

CITATION
Cai Y, Song S, Chen Y, Xu X and Zou W (2023) Oral voriconazole monotherapy for fungal keratitis: efficacy, safety, and factors associated with outcomes.
Front. Med. 10:1174264.
doi: 10.3389/fmed.2023.1174264

Oral voriconazole monotherapy for fungal keratitis: efficacy, safety, and factors associated with outcomes

Youran Cai, Shimei Song, Yiying Chen, Xuyang Xu and Wenjin Zou*

Department of Ophthalmology, The First Affiliated Hospital of Guangxi Medical University, Nanning, China

Purpose: To provide preliminary data on the efficacy and safety of oral voriconazole (VCZ) as a primary treatment for fungal keratitis (FK).

Method: We performed a retrospective histopathological analysis of data on 90 patients with FK at The First Affiliated Hospital of Guangxi Medical University between September 2018 and February 2022. We recorded three outcomes: corneal epithelial healing, visual acuity (VA) improvement, and corneal perforation. Independent predictors were identified using univariate analysis, and multivariate logistic regression analysis was used to identify independent predictive factors associated with the three outcomes. The area under the curve was used to evaluate the predictive value of these factors.

Results: Ninety patients were treated with VCZ tablets as the only antifungal drug. Overall, 71.1% (n=64) of the patients had extreme corneal epithelial healing, 56.7% (n=51) showed an improvement in VA, and 14.4% (n=13) developed perforation during treatment. Non-cured patients were more likely to have large ulcers (≥5×5mm^2) and hypopyon.

Conclusion: The results indicated that oral VCZ monotherapy was successful in the patients with FK in our study. Patients with ulcers larger than 5×5mm^2 and hypopyon were less likely to respond to this treatment.

KEYWORDS

fungal keratitis, voriconazole, treatment, efficacy, safety

Introduction

Fungal keratitis (FK) is a serious infection of the cornea that often causes blindness and vision loss (1). The main cause is corneal trauma due to vegetable matter, organic materials and animal products that occur during agricultural work in developing countries (2). Previous studies have shown that the most common organisms that cause FK are *Fusarium* and *Aspergillus* (molds) and *Candida* (yeast) (3). The incidence of FK is >30% in developing countries (4, 5) and between 6 and 20% in developed countries for all microbial keratitis cases (6, 7). Although several new treatments have been developed, there is little evidence to guide treatment because there is a lack of effective antifungal agents (8).

Topical natamycin (5%) is the standard medical therapy recommended for FK. While it has broad activity, it has a poor ability to penetrate the intact corneal epithelium (9).

Systemic antifungal agents have previously been used as an adjunct to topical treatment for ulcers and are thought to involve up to 50% of the stromal depth (10). Voriconazole (VCZ) is a triazole antifungal agent that is administered orally and intravenously. In recent years, corneal stromal injections of antifungal drugs have achieved good clinical results in the treatment of FK (11). However, whether VCZ improves clinical efficacy remains controversial (12). There has been no clinical research on oral VCZ as the primary antifungal therapy for FK. Our study was conducted to identify the effectiveness and safety of oral VCZ as the primary treatment for FK and the predictive factors of this monotherapy.

Materials and methods

Study design and population

This single-center retrospective study adhered to the tenets of the Declaration of Helsinki. This study was approved by the Ethics Review Board of the First Affiliated Hospital of Guangxi Medical University (E-2022-066). All data were anonymized and collected retrospectively, and the requirement for written informed consent was therefore waived. Between September 2018 and February 2022, patients diagnosed with FK and aged ≥18 years were recruited from the Department of Ophthalmology, the First Affiliated Hospital of Guangxi Medical University. We excluded any patients with a mixed infection in the history or on examination (bacterial, viral or parasitic), contraindications for the medication (allergic or cannot tolerate), an willingness to undergo regular review, a history of having received any antifungal treatment previously, and had an impending or a full thickness corneal perforation at an initial consultation.

Clinical assessment and treatment

All eligible patients underwent slit-lamp examination by two experienced cornea specialists. The depth of ulcer infiltration and location of the ulcer were categorized at the slit lamp by a single ophthalmologist. Anterior augmented photographs (Topcon slit lamp and camera; Topcon Corp. Tokyo, Japan) were acquired at each visit for all patients. Corneal scrapings were collected from all suspected patients with clinical signs and symptoms suggestive of FK. All specimens were subjected to bacterial smears, bacterial cultures (blood agar), fungal smears, fungal cultures (agar slant Sabouraud medium), and fungal fluorescence staining. We also performed *in vivo* confocal microscopy (HRT III/RCM Heidelberg Engineering, Germany) in the suspected patients to confirm the diagnosis.

All the patients were administered oral VCZ (Chengdu Huashen Group Corp., China) tablets once the infection was confirmed. VCZ was administered at a loading dose of 400 mg twice daily for 24 h. Subsequently, a maintenance dose of 200 mg twice daily was administered until 2 weeks after the ulcer had healed. VCZ therapy did not exclude the use of other non-antifungal concomitant treatments, such as antibiotic agents or artificial tears when considered necessary by the cornea specialists. Patients had weekly monitoring of electrolyte and liver function tests.

Data collection

All data were recorded using a standard protocol, including the demographics, visual acuity (VA, logMAR), history of trauma, presence of systemic disease, and duration of symptoms at the initial diagnosis. The signs of corneal ulcers were also recorded, including the ulcer size, ulcer location, depth of ulcer infiltration, and depth of hypopyon. The ulcer size and hypopyon depth were measured using Photoshop software. The location of the ulcer was categorized as the central area where the ulcer was located only in the center of the cornea (6 mm × 6 mm). A safety assessment was performed to evaluate and record any adverse events or complications that appeared during VCZ administration, including visual disturbances, neurological disorders (mental disorders and nervous system abnormalities), skin disorders, abnormal liver function and electrolyte disturbances.

In this study, we examined three primary outcomes: corneal epithelial healing, VA improvement, and corneal perforation. All patients were followed up for a minimum of 6 months after the initial oral VCZ. During the follow-up period, we recorded corneal ulcer healing, the VA, and corneal perforation at any time.

Statistical analysis

All statistical analyses were performed using the IBM Statistical Package for Social Sciences (SPSS) version 26.0 (IBM, NY, USA). Data are presented as mean ± standard deviations/medians (minimum–maximum) and frequency percentages, as appropriate. Univariate analyses for proportions were compared using the chi-square test, independent *t*-test, or exact test, as appropriate. The prediction accuracy was measured using the area under the curve (AUC). For all the analyses, two-sided *p*-values were calculated. Statistical significance was set at $p < 0.05$. All graphs were prepared using GraphPad Prism 9.0 (GraphPad Software).

Results

Ninety patients (53 men and 37 women) with a mean age of 56.74 ± 10.95 years (range: 28–83 years) and a mean duration of symptoms of 20 days (range: 1–90 days) were enrolled in the study. All patients were treated unilaterally. The most prevalent risk factor identified in these patients was injury due to vegetable matter ($n = 29$). Moreover, definite risk factors were not identified in any of the 22 patients. The preoperative demographic and clinical characteristics of the 90 patients are shown in Table 1.

The fungal culture tested positive in 54 patients, with Fusarium species being the most common microorganism isolated ($n = 24$), followed by Aspergillus species (Table 2). There were no significant differences in efficacy and adverse events among the culture-positive and culture-negative populations ($p > 0.05$). Re-infection was noted in two eyes, which tested positive for *Dematiaceous* spp.

All patients who had not used any antifungal drugs previously were administered oral VCZ tablets after the microbiological results of corneal scrapings or confocal microscopy results were obtained. The cure rate of corneal epithelial healing with oral VCZ as primary therapy was 71.1%. Vision improved in 51 (56.7%) patients and remained unchanged in 23 (25.6%) patients (Figure 1). The perforation

rate throughout the treatment course was 14.4%. The results of the univariate analysis of the factors affecting the three outcomes are shown in Table 3. At three months, the VA baseline <2.40 (OR = 3.34, $p < 0.05$), the depth of ulcer infiltration <1/2CT (OR = 3.18, $p < 0.05$), the ulcer size <5 × 5 mm^2 (OR = 4.07, $p < 0.001$) were more likely to achieve corneal epithelial healing. While patients with hypopyon were less likely to obtain corneal epithelial healing (OR = 0.10, $p < 0.001$).

TABLE 1 Demographic and clinical characteristics in patients with fungal keratitis (Patients, *n* [%]).

Characteristics	
Age, years	56.74 ± 10.95
Gender	
Male	53 (58.9)
Female	37 (41.1)
Eye	
Right	49 (54.4)
Left	41 (45.6)
VA baseline (logMAR)	2.16 ± 0.64
Duration of symptoms, days	20.00 (1.00–90.00)
Trauma	44 (48.9)
Vegetables	29 (32.2)
Brick	5 (5.6)
Animals	3 (3.3)
Wood	1 (1.1)
Chemical material	4 (4.4)
Dust	2 (2.2)
Systemic disease*	9 (10.0)
Hypertension	6 (6.7)
Diabetes	3 (3.3)
Hyperlipidemia	1 (1.1)
Hyperthyroidism	1 (1.1)
Medication time, days	53.00 (14.00–186.00)

VA, vision acuity; logMAR, logarithm of the minimum angle resolution; mm, millimeter.
*Two patients had both hypertension and diabetes.

The difference in VA before and after treatment was statistically significant in all the patients ($p < 0.001$). injury due to vegetable matter and ulcer size were significant ($p < 0.05$). The depths of ulcer infiltration and hypopyon were nearly statistically significant ($p = 0.056$). Regarding corneal perforation, patients with corneal perforation showed significant differences in their age ($p < 0.05$). Perforation was negatively correlated to the depth of infiltration <1/2CT (OR = 0.12, $p < 0.05$) and ulcer size <5 × 5 mm^2 (OR = 0.09, $p < 0.001$), and positively associated with hypopyon (OR = 11.44, $p < 0.001$). On multivariate logistic regression (Table 4), the ulcer size and hypopyon depth were independent predictors for 3-month corneal healing and corneal perforation ($p < 0.05$). For the 3-month VA improvement, only the depth of infiltration was an independent predictive factor. The number of patients with an ulcer size less than 5 × 5 mm^2 was 4.17-fold higher than that with an ulcer size greater than 5 × 5 mm^2 in terms of corneal healing and 0.14-fold lower in terms of perforation. The number of patients with a depth of corneal ulcer greater than 1/2CT was 3.54-fold higher than that with a depth less than 1/2CT in terms of an improvement in VA in three months.

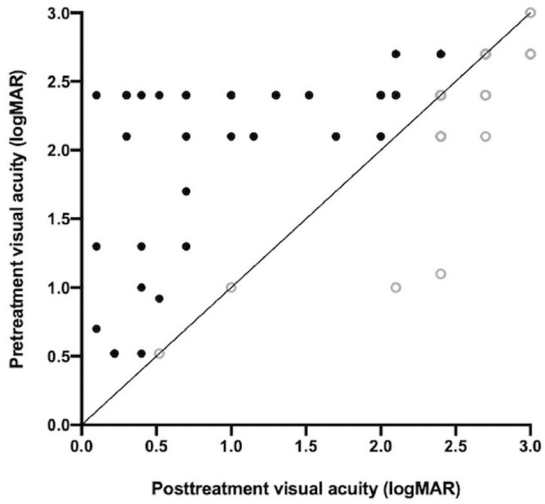

FIGURE 1
Scatter plot of pre-treatment and post-treatment visual acuity. Solid circles represent patients with improved vision, and hollow circles represent patients with unchanged or reduced vision after treatment.

TABLE 2 Causative organisms of fungi cultured results of corneal ulcers.

Organisms	*N* (%)	Cornea healing	VA improved	Perforation
Fusarium species	24 (26.7)	15	10	5
Aspergillus flavus	10 (11.1)	7	7	2
Aspergillus fumigatus	6 (6.7)	4	5	0
Curvularia species	2 (2.2)	1	0	0
Purpureocillium secies.	1 (1.1)	1	0	0
Bipolaris secies.	1 (1.1)	1	1	0
Acremonium secies.	1 (1.1)	1	1	0
Candida species	1 (1.1)	1	1	0
Unidentified dematiaceous fungus	8 (8.9)	6	4	1
Microscopy positive (no growth)	36 (40.0)	27	22	5

TABLE 3 Univariate analyses for three outcome variables.

Predict factor	*n*=90	3-month epithelial healing			3-month visual acuity improved			3-month cornea perforation		
		n (%)	Coefficient (95% CI)	*p*	*n* (%)	Coefficient (95% CI)	*p*	*n* (%)	Coefficient (95% CI)	*p*
Age		NA	NA	0.08[b]	NA	NA	0.06[b]	NA	NA	**0.044[b]**
Gender			1.07 (0.43–2.70)	0.53[a]		0.82 (0.35–1.93)	0.67[a]		0.55 (0.17–1.79)	0.37[a]
Male	53	38 (71.7)			29 (54.7)			6 (11.3)		
Female	37	26 (70.3)			22 (59.5)			7 (18.9)		
VA baseline			3.34 (1.26–8.87)	**0.005[a]**		0.48 (0.20–1.16)	0.10[a]		3.91 (0.81–18.86)	0.120[d]
<2.40	34	30 (88.2)			23 (67.6)			2 (5.9)		
≥2.40	56	34 (60.7)			28 (50.0)			11 (19.6)		
Duration of symptoms		NA	NA	0.25[c]	NA	NA	0.98[c]	NA	NA	0.62[c]
Systemic disease			0.78 (0.59–1.02)	0.44[d]		0.70 (0.47–1.04)	0.29[d]		0.84 (0.76–0.92)	0.35[d]
Yes	9	8 (88.9)			7 (77.8)			0 (0)		
No	81	56 (69.1)			44 (54.3)			13 (16.0)		
Trauma			1.17 (0.47–2.91)	0.82[a]		1.75 (0.75–4.07)	0.21[a]		0.88 (0.27–2.86)	0.83[a]
Yes	44	32 (72.7)			28 (63.6)			6 (13.6)		
No	46	32 (69.6)			2 (50.0)			7 (15.2)		
Injury with vegetable			1.42 (0.52–3.90)	0.62[a]		2.71 (1.04–7.06)	**0.038[a]**		0.92 (0.26–3.29)	0.90[d]
Yes	29	22 (75.9)			21 (72.4)			4 (13.8)		
No	61	42 (68.9)			30 (49.2)			9 (14.8)		
Culture positive			0.73 (0.28–1.87)	0.64[a]		0.74 (0.31–1.74)	0.52[a]		0.94 (0.33–2.64)	0.90[a]
Yes	54	37 (68.5)			29 (53.7)			8 (14.8)		
No	36	27 (75.0)			22 (61.1)			5 (13.9)		
Central ulcer			1.75 (0.67–4.61)	0.26[a]		0.64 (0.27–1.49)	0.30[a]		0.40 (0.10–1.57)	0.18[a]
Yes	36	28 (77.8)			18 (50.0)			3 (8.3)		
No	54	36 (66.7)			33 (61.1)			10 (18.5)		
Depth of infiltrate			3.18 (1.20–8.44)	**0.008[a]**		2.65 (1.32–5.31)	**0.001[a]**		0.12 (0.02–0.95)	**0.027[a]**
<1/2CT	33	29 (87.9)			26 (78.8)			1 (3.0)		
≥1/2CT	57	35 (61.4)			25 (43.9)			12 (21.1)		
Size of ulcer			4.07 (1.91–8.68)	**<0.001[a]**		2.30 (0.97–5.46)	**0.056[a]**		0.09 (0.02–0.43)	**0.001[a]**
<5*5mm^2	54	47 (87.0)			35 (64.8)			2 (3.7)		
≥5*5mm^2	36	17 (47.2)			16 (44.4)			11 (30.6)		
Hypopyon			0.10 (0.03–0.29)	**<0.001[a]**		0.43 (0.18–1.03)	**0.056[a]**		11.44 (2.36–55.56)	**0.001[a]**
Yes	36	16 (44.4)			16 (44.4)			11 (30.6)		
No	54	48 (88.9)			35 (64.8)			2 (3.7)		

Statistically significant values are bolded.
[a]Chi-Square test. [b]Independent samples *t*-test. [c]Mann–Whitney test. [d]Fisher's test. NA, Not Applicable; CT, Cornea Thickness.

The receiver-operating characteristic curve showed that the AUCs based on the ulcer size were 0.73 for predicting 3-month corneal healing and 0.76 for predicting corneal perforation. The AUCs based on the hypopyon depth were 0.76 for predicting 3-month corneal healing and 0.76 for predicting corneal perforation. The AUC based on ulcer infiltration was 0.67 for predicting 3-month VA improvement. In terms of combinations of two factors, the combined ulcer size and hypopyon depth were more accurate than only one factor for predicting both corneal healing (0.83) and perforation (0.84) (Figure 2).

Three patients healed spontaneously after perforation. We were able to improve perforation in five patients by performing conjunctival flap coverage, and the remaining patients underwent corneal transplantation. In two cases, the ulcers improved but did not heal, and we administered intrastromal injections of VCZ, which resulted in healing.

Overall, adverse events were reported in 7.8% of the patients ($n=7$) during the study period. Four patients developed ocular hypertension, and all the patients responded to antiglaucoma medications. Liver function abnormalities were observed in one patient, which resolved two weeks after VCZ withdrawal. Two patients reported auditory or visual hallucinations, and none discontinued the medication because of adverse events. Symptoms in all the patients disappeared quickly after discontinuing treatment.

Discussion

FK can present as superficial keratitis, corneal ulcers, or endothelial plaques. Fungal corneal ulcers are difficult to cure and

TABLE 4 Multivariable analyses for three outcomes.

Predict factor	3-month corneal healing		3-month visual acuity		Perforation	
	Coefficient (95% CI)	*p*	Coefficient (95% CI)	*p*	Coefficient (95% CI)	*p*
Age					0.94 (0.87–1.02)	0.127
VA baseline	2.63 (0.68–10.10)	0.160				
Injury with vegetable			2.52 (0.90–7.09)	0.079		
Depth of infiltrate	1.79 (0.45–7.13)	0.410	3.54 (1.25–10.06)	**0.018**	0.49 (0.05–5.06)	0.553
Size of ulcer	4.17 (1.31–13.26)	**0.016**	1.55 (0.58–4.15)	0.380	0.14 (0.03–0.83)	**0.030**
Hypopyon	0.18 (0.55–0.58)	**0.004**	0.66 (0.25–1.76)	0.405	5.94 (1.09–32.47)	**0.040**

Statistically significant values are bolded.

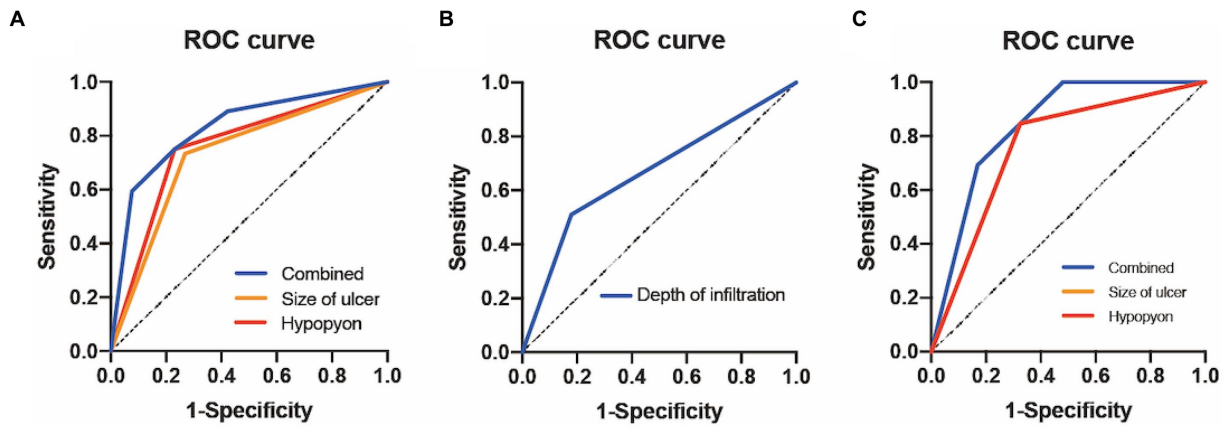

FIGURE 2
ROC curve analysis of FK for different outcomes. **(A)** ROC curve of 3-month corneal epithelial healing. **(B)** ROC curve of 3-month improved visual acuity. **(C)** ROC curve of 3-month corneal perforation. ROC, receiver-operating characteristic; FK, fungal keratitis.

contribute to blindness. Early detection and diagnosis of fungal corneal ulcers are significant. Currently, antifungal drug therapy remains the primary treatment option. VCZ has also been shown to have a broad spectrum and is the most promising treatment for FK (13). Additionally, oral VCZ may benefit patients who exhibit suboptimal responses to natamycin (14). Only a few cases have been reported on the effectiveness of using only oral VCZ for FK (15). To our knowledge, this is the first large case series to describe the effectiveness and safety in patients with FK using oral VCZ as a first-line antifungal drug.

VCZ can be administered topically (eye drops or injections) or systemically (oral tablets or injections). Topical VCZ eye drops have been used in many studies and have shown effective outcomes. However, eye drops should be produced on the day of treatment and remain stable during long-term storage (16). Oral VCZ has high bioavailability and can penetrate several parts of the eye (17). VCZ is a broad-spectrum antifungal agent that is effective against Candida, dematiaceous, and filamentous fungi (18). However, VCZ eye drops may be effective in most cases of FK but fail in cases involving Fusarium spp. (19). The Mycotic Ulcer Treatment Trial also revealed that natamycin is associated with better outcomes than those associated with voriconazole for the treatment of *Fusarium* keratitis (20). Our data suggest that oral VCZ monotherapy can cure 62.5% of cases caused by *Fusarium* spp., which is similar to the cure rate with *Aspergillus* spp. This may be affected by the small samples and low rate of culture positivity in our study. Voriconazole has been suggested as the first-line treatment for *Paecilomyces/Purpureocillium* keratitis (21). There was also one patient with *Purpureocillium* spp. in our study, in whom the cornea healed successfully, but the VA did not improve. Among culture-negative and positive patients, the corneal epithelial healing rate was 75.0 and 68.5%, respectively. This result is consistent with the previous studies about microbial keratitis (22, 23). However, studies regarding the comparison between culture-negative and positive fungal keratitis remain rare. Further investigations in this direction are required. The most dominant factor in our research was corneal trauma, which is consistent with results from China and other developing countries (24, 25). Oral VCZ is superior to other antifungal oral drugs, such as ketoconazole and fluconazole, providing a safe adjunct to topical therapy with good systemic absorption and high intraocular concentrations (26).

Similar to previous studies on FK (20, 27, 28), we used corneal epithelial healing as the primary outcome measure, with VA improvement and corneal perforation as the secondary outcome measures. We chose these because they provide the most objective and reproducible effect of therapy. Approximately 31% of patients with FK fail to respond to antifungal drugs, and some patients develop severe effects during the treatment (13). In our study, the overall cure rate of oral VCZ as the primary therapy was 77.1%. Ramakrishnan et al. studied 26 cases and found that only 50% of patients responded to topical VCZ. They summarized that peripheral infiltrates and

hypopyon are possible predictive factors of the outcomes of topical VCZ treatment (29). Ting et al. studied patients with FK in the UK over a 10-year period and found that age > 50 years, VA <1.0logMAR, and an infiltration depth > 3 mm result in poor corneal epithelial healing (30). Chow et al. studied the visual prognosis of 103 patients with FK and found that a large ulcer size (> 4 mm), fungal ulcers in the central area, the presence of pus, and high intraocular pressure (> 21 mmHg) at the time of presentation are predictors of poor final visual outcomes (31). Our study demonstrated the statistical significance of systemic VCZ with a larger case series compared with previous research. Hung et al. reported that the presenting time, poor VA at the initial presentation, and trauma are significantly associated with VA recurrence (32). This is in contrast to our observations. We also suggest that hypopyon in the anterior chamber is an important independent predictor of corneal healing and perforation. However, this factor has rarely been mentioned in the literature on FK. Hypopyon may be a key factor not only in monotherapy but also in other antifungal therapies. Our data confirm that patients with hypopyon are less likely to exhibit corneal healing and non-perforation. To predict VA improvement, patients with ulcer infiltration of less than 1/2 CT will be more likely to approach VA improvement. A previous study revealed that the combination of oral VCZ and topical natamycin can cure 80% of patients with severe FK (10). The results of our analysis showed a significant difference in the size of the corneal ulcer and hypopyon depth. This demonstrates that using only oral VCZ as an antiulcer agent may be effective in patients with early and mild FK ulcers. Therefore, therapeutic options for patients with moderate-to-severe signs remain limited. To evaluate the factors for predicting the outcomes of VCZ monotherapy, we pursued the approach of combining two factors. The predictive value of these factors can be further enhanced by combining more than one predictor. Further research is required to assess the predictive value of other parameters associated with FK for other causes of curing, as these could further improve the prediction.

In addition to its therapeutic effects, we should also focus on the safety profile and side effects of oral VCZ medication. Hepatotoxicity, visual disturbances, photosensitivity, and skin rashes have been reported (33). In our study, an uncomfortable appearance was observed in 7.8% of the patients, including ocular hypertension, liver function abnormality, and hallucinations. After appropriate drug treatment, all the patients recovered after two weeks of drug distribution. Therefore, oral VCZ treatment usually requires hospitalization, placement in a quiet room, and observation for the development of complications. Since fungal keratitis occurs mostly in developing countries, some regions inevitably face difficulties in obtaining topical antifungal drugs promptly. Our study provides an alternative treatment choice to traditional topical antifungal therapy. Further studies comparing the method of oral antifungal tablets with conventional topical antifungal eyedrops are needed to fully evaluate its efficacy.

The sample size in our study was small, the patients were all from a developing country, and the pathogenesis was mainly agricultural trauma. Therefore, a larger sample size and diverse populations from different countries are needed. Our low positive fungal culture rate cannot exclude the possibility of false negatives. This resulted in our findings being unclear about which organisms are more suitable for this treatment. Additionally, there were some insufficiencies in the measurement approaches. The infiltration of the ulcer was judged subjectively by a specialist without objective measurements. Further investigations are required to confirm these factors and to gain a better understanding of possible factors.

Conclusion

In summary, the results of the present study may provide a new treatment option for patients with FK. We confirmed that oral VCZ monotherapy is an effective treatment for fungal corneal ulcers and can induce good-quality remission with acceptable toxicity in most patients. We should consider a combination of these three factors, including the size of the ulcer greater than $5 \times 5\ mm^2$, infiltration of the ulcer, and presence of hypopyon, while discussing the treatment modality with patients. We recommend considering hospitalization for patients to take prompt action to manage side effects. Further studies on predictors of different antifungal medications in diverse populations should be conducted. This will help provide more standards for choosing drugs for patients with FK under various conditions.

Data availability statement

The raw data supporting the conclusions of this article will be made available by the authors, without undue reservation.

Ethics statement

This study was approved by the Ethics Review Board of the First Affiliated Hospital of Guangxi Medical University (E-2022-066). All data were anonymized and collected retrospectively, and the requirement for written informed consent was therefore waived.

Author contributions

YRC designed the study and drafted the initial manuscript. SMS and YYC collected information and analyzed the data. XYX collated and interpreted the data. WJZ critically revised the manuscript. All authors have read and approved the final manuscript.

Funding

This study was supported by the National Natural Science Foundation of China (81160119) and the Key Research and Development Program in Guangxi (AB20238003).

Conflict of interest

The authors declare that the research was conducted in the absence of any commercial or financial relationships that could be construed as a potential conflict of interest.

Publisher's note

References

1. Brown L, Leck AK, Gichangi M, Burton MJ, Denning DW. The global incidence and diagnosis of fungal keratitis. *Lancet Infect Dis*. (2021) 21:e49–57. doi: 10.1016/s1473-3099(20)30448-5

2. Ting DSJ, Ho CS, Deshmukh R, Said DG, Dua HS. Infectious keratitis: an update on epidemiology, causative microorganisms, risk factors, and antimicrobial resistance. *Eye (Lond)*. (2021) 35:1084–101. doi: 10.1038/s41433-020-01339-3

3. Ozdemir HB, Kalkanci A, Bilgihan K, Gocun PU, Ogut B, Karakurt F, et al. Comparison of corneal collagen cross-linking (PACK-CXL) and voriconazole treatments in experimental fungal keratitis. *Acta Ophthalmol*. (2019) 97:e91–6. doi: 10.1111/aos.13829

4. Keay LJ, Gower EW, Iovieno A, Oechsler RA, Alfonso EC, Matoba A, et al. Clinical and microbiological characteristics of fungal keratitis in the United States, 2001-2007: a multicenter study. *Ophthalmology*. (2011) 118:920–6. doi: 10.1016/j.ophtha.2010.09.011

5. Gopinathan U, Garg P, Fernandes M, Sharma S, Athmanathan S, Rao GN. The epidemiological features and laboratory results of fungal keratitis: a 10-year review at a referral eye care center in South India. *Cornea*. (2002) 21:555–9. doi: 10.1097/00003226-200208000-00004

6. Li X, Wang L, Dustin L, Wei Q. Age distribution of various corneal diseases in China by histopathological examination of 3112 surgical specimens. *Invest Ophthalmol Vis Sci*. (2014) 55:3022–8. doi: 10.1167/iovs.13-13805

7. Tuli SS. Fungal keratitis. *Clin Ophthalmol*. (2011) 5:275–9. doi: 10.2147/opth.S10819

8. Austin A, Lietman T, Rose-Nussbaumer J. Update on the Management of Infectious Keratitis. *Ophthalmology*. (2017) 124:1678–89. doi: 10.1016/j.ophtha.2017.05.012

9. Thomas PA. Current perspectives on ophthalmic mycoses. *Clin Microbiol Rev*. (2003) 16:730–97. doi: 10.1128/CMR.16.4.730-797.2003

10. Sharma N, Singhal D, Maharana PK, Sinha R, Agarwal T, Upadhyay AD, et al. Comparison of Oral Voriconazole versus Oral ketoconazole as an adjunct to topical Natamycin in severe fungal keratitis: a randomized controlled Trial. *Cornea*. (2017) 36:1521–7. doi: 10.1097/ico.0000000000001365

11. Jain V, Borse N, Shome D, Natarajan S. Recalcitrant fungal tunnel infection treated with intrastromal injection of voriconazole. *Int Ophthalmol*. (2010) 30:723–5. doi: 10.1007/s10792-010-9354-3

12. Prajna NV, Krishnan T, Rajaraman R, Patel S, Srinivasan M, Das M, et al. Effect of Oral Voriconazole on fungal keratitis in the Mycotic ulcer treatment Trial II (MUTT II): a randomized clinical Trial. *JAMA Ophthalmol*. (2016) 134:1365–72. doi: 10.1001/jamaophthalmol.2016.4096

13. Wang JY, Wang DQ, Qi XL, Cheng J, Xie LX. Modified ulcer debridement in the treatment of the superficial fungal infection of the cornea. *Int J Ophthalmol*. (2018) 11:223–9. doi: 10.18240/ijo.2018.02.07

14. Prajna NV, Krishnan T, Rajaraman R, Patel S, Shah R, Srinivasan M, et al. Adjunctive Oral Voriconazole treatment of Fusarium keratitis: a secondary analysis from the Mycotic ulcer treatment Trial II. *JAMA Ophthalmol*. (2017) 135:520–5. doi: 10.1001/jamaophthalmol.2017.0616

15. Chen D, Tan S, Zou W. Treating fungal keratitis with Oral Voriconazole only: a case series. *Klin Monatsbl Augenheilkd*. (2021) 238:55–9. doi: 10.1055/a-1268-9168

16. Amoros-Reboredo P, Bastida-Fernandez C, Guerrero-Molina L, Soy-Muner D, Lopez-Cabezas C. Stability of frozen 1% voriconazole ophthalmic solution. *Am J Health Syst Pharm*. (2015) 72:479–82. doi: 10.2146/ajhp140127

17. Hariprasad SM, Mieler WF, Holz ER, Gao H, Kim JE, Chi J, et al. Determination of vitreous, aqueous, and plasma concentration of orally administered voriconazole in humans. *Arch Ophthalmol*. (2004) 122:42–7. doi: 10.1001/archopht.122.1.42

18. Marangon FB, Miller D, Giaconi JA, Alfonso EC. In vitro investigation of voriconazole susceptibility for keratitis and endophthalmitis fungal pathogens. *Am J Ophthalmol*. (2004) 137:820–5. doi: 10.1016/j.ajo.2003.11.078

19. Neoh CF, Leung L, Chan E, Al-Badriyeh D, Fullinfaw RO, Jhanji V, et al. Open-label study of absorption and clearance of 1% Voriconazole eye drops. *Antimicrob Agents Chemother*. (2016) 60:6896–8. doi: 10.1128/AAC.00683-16

20. Prajna NV, Krishnan T, Mascarenhas J, Rajaraman R, Prajna L, Srinivasan M, et al. The mycotic ulcer treatment trial: a randomized trial comparing natamycin vs voriconazole. *JAMA Ophthalmol*. (2013) 131:422–9. doi: 10.1001/jamaophthalmol.2013.1497

21. Chen YT, Yeh LK, Ma DHK, Lin HC, Sun CC, Tan HY, et al. Paecilomyces/Purpureocillium keratitis: a consecutive study with a case series and literature review. *Med Mycol*. (2020) 58:293–9. doi: 10.1093/mmy/myz059

22. Yarımada S, Barut Selver Ö, Palamar M, Eğrilmez S, Aydemir S, Hilmioğlu Polat S, et al. Comparison of culture-positive and -negative microbial keratitis. *Turk J Ophthalmol*. (2022) 52:1–5. doi: 10.4274/tjo.galenos.2021.98046

23. Bhadange Y, Das S, Kasav MK, Sahu SK, Sharma S. Comparison of culture-negative and culture-positive microbial keratitis: cause of culture negativity, clinical features and final outcome. *Br J Ophthalmol*. (2015) 99:1498–502. doi: 10.1136/bjophthalmol-2014-306414

24. Xie L, Zhong W, Shi W, Sun S. Spectrum of fungal keratitis in North China. *Ophthalmology*. (2006) 113:1943–8. doi: 10.1016/j.ophtha.2006.05.035

25. Ghosh AK, Gupta A, Rudramurthy SM, Paul S, Hallur VK, Chakrabarti A. Fungal keratitis in North India: Spectrum of agents, Risk Factors and Treatment. *Mycopathologia*. (2016) 181:843–50. doi: 10.1007/s11046-016-0042-3

26. Jurkunas UV, Langston DP, Colby K. Use of voriconazole in the treatment of fungal keratitis. *Int Ophthalmol Clin*. (2007) 47:47–59. doi: 10.1097/IIO.0b013e318036bd47

27. Prajna NV, Srinivasan M, Lalitha P, Krishnan T, Rajaraman R, Ravindran M, et al. Differences in clinical outcomes in keratitis due to fungus and bacteria. *JAMA Ophthalmol*. (2013) 131:1088–9. doi: 10.1001/jamaophthalmol.2013.1612

28. Hung N, Yeh LK, Ma DH, Lin HC, Tan HY, Chen HC, et al. Filamentous fungal keratitis in Taiwan: based on molecular diagnosis. *Transl Vis Sci Technol*. (2020) 9:32. doi: 10.1167/tvst.9.8.32

29. Ramakrishnan T, Constantinou M, Jhanji V, Vajpayee RB. Factors affecting treatment outcomes with voriconazole in cases with fungal keratitis. *Cornea*. (2013) 32:445–9. doi: 10.1097/ICO.0b013e318254a41b

30. Ting DSJ, Galal M, Kulkarni B, Elalfy MS, Lake D, Hamada S, et al. Clinical characteristics and outcomes of fungal keratitis in the United Kingdom 2011-2020: a 10-year study. *J Fungi (Basel)*. (2021) 7:966. doi: 10.3390/jof7110966

31. Tze-Suen C, Chew-Ean T, Md DN. Fungal keratitis in a tertiary Hospital in Malaysia. *Cureus*. (2021) 13:e18389. doi: 10.7759/cureus.18389

32. Hung N, Shih AK, Lin C, Kuo MT, Hwang YS, Wu WC, et al. Using slit-lamp images for deep learning-based identification of bacterial and fungal keratitis: model development and validation with different convolutional neural networks. *Diagnostics (Basel)*. (2021) 11:1246. doi: 10.3390/diagnostics11071246

33. Zonios DI, Gea-Banacloche J, Childs R, Bennett JE. Hallucinations during voriconazole therapy. *Clin Infect Dis*. (2008) 47:e7–e10. doi: 10.1086/588844

frontiers | Frontiers in Medicine

TYPE Original Research
PUBLISHED 16 May 2023
DOI 10.3389/fmed.2023.1129606

OPEN ACCESS

EDITED BY
Horace Massa,
Hôpitaux universitaires de Genève (HUG), Switzerland

REVIEWED BY
Ming Lin,
Shanghai Jiao Tong University, China
Lindsay Elizabeth Fitzpatrick,
Queen's University, Canada

*CORRESPONDENCE
Juan Ye
✉ yejuan@zju.edu.cn

†These authors have contributed equally to this work

RECEIVED 22 December 2022
ACCEPTED 26 April 2023
PUBLISHED 16 May 2023

CITATION
Xu P, Chen P, Gao Q, Sun Y, Cao J, Wu H and Ye J (2023) Azithromycin-carrying and microtubule-orientated biomimetic poly (lactic-co-glycolic acid) scaffolds for eyelid reconstruction.
Front. Med. 10:1129606.
doi: 10.3389/fmed.2023.1129606

Azithromycin-carrying and microtubule-orientated biomimetic poly (lactic-co-glycolic acid) scaffolds for eyelid reconstruction

Peifang Xu†, Pengjie Chen†, Qi Gao, Yiming Sun, Jing Cao, Han Wu and Juan Ye*

Eye Center, The Second Affiliated Hospital, School of Medicine, Zhejiang University, Zhejiang Provincial Key Laboratory of Ophthalmology, Zhejiang Provincial Clinical Research Center for Eye Diseases, Zhejiang Provincial Engineering Institute on Eye Diseases, Hangzhou, Zhejiang, China

Introduction: Tarsal plate repair is the major challenge of eyelid reconstruction for the oculoplastic surgeon. The ideal synthetic tarsal plate substitute should imitate the microstructure and mechanical strength of the natural eyelid. The aim of this work was to develop a novel bionic substitute for eyelid reconstruction.

Methods: Three types of poly(lactic-co-glycolic acid) (PLGA) scaffolds (random, oriented, and azithromycin-loaded oriented scaffolds) were prepared using an improved thermal-induced phase separation technique. The microstructure of the scaffolds was examined by scanning electron microscopy. In vitro cytotoxicity was assessed using scaffold extracts. Fibroblast and primary rat meibomian gland epithelial cells (rMGCs) were cultured within the scaffolds, and their behavior was observed using fluorescence staining. Three types of PLGA scaffolds were implanted into rabbit eyelid defect in vivo to evaluate their inductive tissue repair function.

Results: We successfully fabricated three types of PLGA scaffolds with varying pore architectures, and the axially aligned scaffold demonstrated interconnected and vertically parallel channels. In vitro cytotoxicity tests using scaffold extracts revealed no apparent cytotoxicity. Fluorescence staining showed that both Fibroblast and rMGCs could adhere well onto the pore walls, with fibroblast elongating along the axially aligned porous structure. At 8 weeks post-implantation, all scaffolds were well integrated by fibrovascular tissue. The axially aligned scaffold groups exhibited faster degradation compared to the random scaffold group, with smaller fragments surrounded by mature collagen fibers.

Conclusion: The study found that the axially aligned scaffolds could well support and guide cellular activities in vitro and in vivo. Moreover, the axially aligned scaffold group showed a faster degradation rate with a matched integration rate compared to the random scaffold group. The findings suggest that the oriented scaffold is a promising alternative for eyelid tarsal plate substitutes.

KEYWORDS

eyelid reconstruction, biomimetic, tarsal plate substitute, oriented structure, poly(lactic-co-glycolic acid)

1. Introduction

Eyelids is an important functional structure of eye, which can provide corneal protection and offer good cosmesis (1). Eyelid defects usually result from congenital anomalies, trauma, tumor excision, burns, or autoimmune disease (2). The goal of eyelid reconstruction is to restore structural and functional integrity of the eyelid. The posterior lamella is the key of eyelid reconstruction, which can provide structural support and a mucosal surface that allows for corneal protection. To reconstruct this layer, various tarsal substitute materials have been developed. Homologous grafts such as contralateral eyelid (3), hard-plate mucosa (4), nasal or ear cartilage grafts (5) were most often used. However, surgery is needed to harvest the homologous grafts, which may cause additional injury to the donor site. Xenogenic substitutes such as allogeneic sclera, acellular dermal matrix (ADM) (6), and scleral patches (7) were restricted in application for infection and immunologic rejection. Therefore, synthetic tarsal substitute may be an effective solution to alleviate donor shortage, immune rejection and infection risks.

An ideal scaffold for tarsal substitute should exhibit similar structural and mechanical properties to the targeted tissue (8). Previous studies have revealed the effect of pore size and geometry in promoting tissue regeneration using porous scaffolds with radially aligned or axially aligned pores. The scaffolds with regular pores were designed to better mimic the microenvironments of the target tissues, which possess oriented structure. Xu, et al. designed a scaffold with microstructure orientation for cartilage tissue engineering. By optimizing the freezing box and temperature, the manufacture PLGA scaffold has a mechanical strength and microstructure close to that of real cartilage (9). Dai. et al. applied the oriented PLGA scaffolds into rabbit articular osteochondral defect models, and the results confirmed an *in situ* inductive osteochondral regeneration without pre-seeding cells (10). Tarsal plate is very superficial, and located between two very thin tissues, the conjunctiva and eyelid skin. Too hard or non-degradable materials, such as Medpor, may cause cornea irritation, exposure or thick fibrous encapsule in long term observation (11). So far, few researches have tried degradable or materials with oriented microstructure to eyelid reconstruction. Therefore, oriented PLGA scaffolds may be a promising material for eyelid repair for its regular structure and similar mechanical strength with cartilage (12).

Azithromycin (AZM) is a potent broad-spectrum macrolide antibiotic. Studies have proved the potentials of AZM for localized therapy, which enables the delivery of antibiotic to the site of action at lower doses while escaping systemic drug effects and reducing the risk of developing microbial resistance (13, 14). What's more, AZM was available at the surgical site for a longer period of time than amoxicillin, and patients taking azithromycin exhibited lower levels of specific proinflammatory cytokines (15). As for eyelid, AZM acts directly on meibomian gland epithelial cells to stimulate their differentiation, enhance the quality and quantity of their lipid production, and promote their holocrine secretion (16). Thus, AZM may enhance resolution of postoperative inflammation and enhance the local meibomian gland function, simultaneously.

The aim of this work was the development of a bionic tarsal plate substitute. By using ice particulate templates and freeze-drying, an AZM-carrying and microtubule-orientated PLGA scaffolds can be prepared successfully. The behaviors of two target cells of tarsal plate in the PLGA scaffolds were evaluated. Moreover, we intend to investigate the effects of the different pore architectures of the three scaffolds on the repair of eyelid defects *in vivo*. It is expected that this study will contribute towards the development of a novel substitute for eyelid reconstruction.

2. Materials and methods

2.1. Materials

PLGA (molar ratio of lactyl/glycotyl = 75/25, Mw = 1.22kd) was purchased from China Textile Academy. 1,4-Dioxane, ethanol, and other reagents of analytical grade were directly used in this study. Dulbecco's modified Eagle's medium (DMEM, Gibco, United States) and fetal bovine serum (FBS, Gibco, United States) were used for *in vitro* cell culture.

2.2. Preparation of PLGA scaffolds

The PLGA scaffolds were prepared by ice-templated assembly and temperature gradient-guided thermally-induced phase separation, which controlled the direction of crystal growth (17). The mold structures used to fabricate the random, axially aligned PLGA scaffolds are shown in Supplementary Figure S1. In brief, 5% w/v PLGA in dioxane solution, and PE and PTFE molds were preheated at 37.0°C for 1 h. To prepare the random PLGA scaffold, the PLGA solution in the PE mold was transferred into a freezer at −20°C overnight to form randomly distributed crystals. To fabricate the axially aligned scaffold, PE molds containing the PLGA solution were mounted into the holes of a larger PTFE mold, which was placed between two −20°C precooled aluminum molds. The system was maintained at −20°C overnight to ensure temperature transduction in an axially directional manner. After the PLGA solution was absolutely frozen, it was lyophilized to remove dioxane solution and preserve the formed porous structure. 1 mg Azithromycin was dissolved into 400 μL 5% w/v PLGA solution. The mixture solution was used to fabricate the Azithromycin-carrying, axially aligned scaffold at the same method. Finally, three types of scaffolds were fabricated with different pore architectures, namely R-PLGA, O-PLGA, and AZM@O-PLGA. R-PLGA refers to PLGA scaffolds with random pores. O-PLGA refers to PLGA scaffolds with axially aligned pores. AZM@O-PLGA refers to oriented PLGA scaffolds loaded with AZM.

2.3. Characterization of PLGA scaffolds

The microstructure of three types of PLGA scaffolds was characterized using a field emission scanning electron microscope (FESEM; S4800, Hitachi, Japan). The Azithromycin loading efficacy was determined by color reaction of sulfuric acid. Firstly, AZM@O-PLGA scaffolds were prepared according to the description of section 2.2. Secondly, an Azim solution standard curve was plotted Supplementary Figure S2. To this end, different concentrations of AZM (0, 7.5, 10, 15, 20, 25, and 30 μg/mL) were prepared and the standard curve was then established based on the relationship between the azithromycin standard solution and the corresponding absorbance

at 482 nm. To measure the encapsulation efficiency of AZM on the PLGA scaffolds, each of the AZM loaded samples were placed in a 1.5 mL Eppendorf tube. Then, 500 mL of ethanol was added to dissolve the AZM in the samples. Afterwards, the supernatant was collected by centrifugation at 8000 rpm for 5 min. To determine the content of AZM in each sample, the absorbance of supernatant at 482 nm was measured and the AZM loading efficacy was calculated using the following equation:

$$\text{AZM loading efficacy} = W_r / W_i$$

where W_i is the initial added amount of AZM and W_r is the remaining amount of AZM encapsulated in the samples.

2.4. Cell culture

Human dermal fibroblasts (HDFs, kindly provided by Faculty of Burn, Second Affiliated Hospital of Zhejiang University, Hangzhou, China). HDFs were cultured in DMEM, supplemented with 10% FBS and penicillin/streptomycin (100/100 U) at 37°C and 5% CO2. The primary rat meibomian gland epithelial cells (rMGCs) were isolated according to the previous study (18). In brief, the eyelid tissues were obtained freshly from ~120 g Sprague–Dawley (SD) rats. The tarsal plates were isolated from eyelid tissues under a dissecting microscope by removing skin, subcutaneous tissue, muscle, and palpebral conjunctiva. Small pieces of tarsal plates, which contained two to five meibomian glands, were further digested with 0.25% collagenase I (Biosharp, China) and 0.9 U/mL dispase II (Roche Applied Science, Indianapolis, IN) at 37°C for 5 h. Single glands were then isolated under a dissecting microscope and were dissociated into a single-cell suspension by 0.05% trypsin- EDTA treatment for 5 min. Isolated cells were centrifuged at 1000 rpm for 5 min resuspended and cultured in keratinocyte serum-free medium (SFM) (Invitrogen-Gibco, United States) for 5 to 7 days before subculture. To detect the neutral lipid expression, the cells were stained with 0.3% Oil red O (Beyotime Biotechnology, China) and lipophilic dye Nile red (MedChemExpresss, United States).

2.5. RNA extraction and RT-PCR

The gene expression of keratin 14 (Krt 14), keratin 5 (Krt 5), p63, Sox9 and PPAR- γ in rMGCs was identified by RT-PCR. Total RNA of cells was extracted using FlaPure Animal Tissue/Cell DNA Extraction Kit (Genesand Biotech, China) according to the manufacturer's protocol. The RNA was reverse transcribed into cDNA using a PrimeScript RT Reagent Kit (Takara, China), and the resulting cDNA was utilized for PCR amplification. Real-time PCR (RT-PCR) reactions were conducted using the SYBR Premix EX TaqTM kit (Takara, China) and the CFX96 system (Bio-Rad, United States), with the reaction conditions of 95°C for 30 s, followed by 40 cycles of 95°C for 5 s and 60°C for 30 s. The expression of β-actin was used as a reference gene to normalize the real-time PCR results, and the relative mRNA expression was calculated using the comparative cycle threshold method (ΔΔCT method). The primer sequences utilized in RT-PCR studies are provided in Supplementary Table S1. All the experiments were conducted in triplicate.

2.6. *In vitro* cytotoxicity

To evaluate the potential cytotoxicity of scaffolds, three scaffolds were first immersed in DMEM or SFM at an approximate concentration of 0.1 g/mL and incubated at 37°C for 24 h to obtain the scaffold extraction solutions. The extracted solutions were then collected and was filtered by a 0.22 μm bacteria-retentive filter. The HDFs and rMGCs were seeded into a 96-well plate at a density of 5×10^3 and 8×10^3 cells per well, respectively. After 24 h of incubation, the medium was removed and replaced with the extracts with the same supplements as negative control(fresh medium with no extracts). After another 24 h continuous cultivation, 100 μL cell culture medium supplemented with 10 μL CCK-8 solution(Dojindo Laboratories, China) was added to each well. After 2 h incubation at 37°C, the absorbance at 450 nm was assessed using a SpectraMax iD5 microplate reader (Molecular Devices, United States).

2.7. Cell behaviors *in vitro*

The distribution and morphology of HDFs and rMGCs in the PLGA scaffolds were visualized using an inverted fluorescence microscope (Leica, German) and a confocal laser scanning microscope (CLSM; LSM780, ZEISS, Germany). HDFs and rMGCs with a concentration of 5×10^6 mL^{-1} were introduced into the PLGA composite scaffolds under negative pressure, respectively. Then, the cell seeded scaffolds were maintained at 37°C and 5% CO_2 for 3 h to allow initial adhesion of onto the scaffolds. The complete DMEM was then added to the HDFs seeded scaffolds, and keratinocyte SFM to the rMGCs seeded scaffolds. Following 2 days of cultivation, cell viability was assessed using the Live/Dead assay. Specifically, the PLGA scaffolds were incubated with calcein-AM/propidium iodide (PI; Beyotime Biotechnology, China) for 30 min at 37°C and evaluated using a fluorescence microscope. After 5 days cultivation for HDFs and 7 days for rMGCs, the PLGA scaffolds were fixed with 4% w/v paraformaldehyde at 37°C for 1 h. The cells were permeabilized in 0.1% w/v Triton X-100 at 4°C for 10 min, followed by blocking with 1% BSA at 37°C for 1 h. The nucleus and cytoskeleton of HDFs were stained with Hoechst 33342 and FITC-labeled phalloidin at 4°C overnight for fluorescence microscope observation. The nucleus and cytoskeleton of rMGCs were stained with DAPI and rhodamine phalloidin at 4°C overnight for CLSM observation.

2.8. *In vivo* rabbit eyelid defect model and scaffolds transplantation

Three groups of PLGA scaffolds were cut into pieces at an average size of 8.0 × 4.0 mm, which were sterilized in 75% ethanol for 4 h, and then displaced with sterile normal saline before use.

All animal procedures were performed in accordance with the Guidelines for Care and Use of Laboratory Animals of Hangzhou Medical College and approved by the Animal Ethics Committee of Hangzhou Medical College. Twelve male New Zealand white rabbits weighing between 2.5 and 3.0 kg were divided into three groups (4 eyes per group). The rabbit eyelid defect model was stablished according to our previous study (19). In brief, the rabbits were anesthetized by an intravenous injection of pentobarbital sodium

(30 mg kg^{-1}), followed by local anesthesia with 1% lidocaine. The lower eyelid was everted to expose the palpebral conjunctiva. An 8.0 × 4.0 mm defect was created inside the lid with a micro scissor to completely remove the conjunctival epithelium and substantia propria. PLGA scaffold was grafted to the wound bed by interrupted sutures using 7–0 polyglactin. The usage of ofloxacin ointment in the conjunctival sac was performed after surgery. At the end of 1 and 2 month, the morphology of repaired eyelid was observed. All rabbits were euthanized at 2 months after surgery to harvest the eyelid tissues containing the defect and normal area for further histological analysis.

2.9. Statistical analysis

GraphPad Prism 8.0 Software (GraphPad Software Inc., United States) was used to analyze the data. The differences between groups were examined with One-way ANOVA. A value of $p < 0.05$ was considered statistically significant.

3. Results

In this study, three types of scaffolds, i.e., R-PLGA, O-PLGA, and AZM@O-PLGA were prepared, and their ability to repair eyelid defects were compared *in vivo*.

3.1. Microstructure of three types of PLGA scaffolds

The methods used to prepare the three types of PLGA scaffolds are shown in Supplementary Figure S1. The random scaffold was obtained by phase-separation at low temperature of −20°C, whereas the axially aligned scaffolds were prepared by thermally induced phase separation under an axial temperature gradient, followed by lyophilization. The morphology of the three kinds of PLGA scaffolds is shown in Figures 1A–C, confirming the desired types of architectures. The random scaffold exhibited an evenly irregular porous structure in the vertical section (Figures 1A1–A3). The axially aligned scaffold showed interconnected and vertically parallel channels (Figures 1B1, B2, C1–C3), validating the good efficacy of preparation of the axially aligned scaffolds by this method. The average AZM loading efficacy is 84.86 ± 6.15%. There was no significant difference in the architectures of the axially aligned scaffold with or without AZM loading.

3.2. Cultivation and identification of primary rat meibomian gland epithelial cells (rMGCs)

The primary rMGCs had cobblestone morphology day 5 days (Figure 2A). Neutral lipid droplets in primary human meibomian gland epithelial cells were detected by Nile red and Oil red O staining. Nile red staining (Figure 2B) was predominantly localized to the cell membrane and showed weak intracellular staining, indicating a lower presence of lipid droplets in the cells cultured in SFM. Additionally, the results of Oil red O staining (Figure 2C) showed that there was minimal intracellular lipid staining in SFM-cultured cells. The phenotype of rMGCs (Figure 2D) was identified by RT-qPCR with positive expression of keratin-related genes krt 14 and krt 5. Very low expression of lipid-related gene PPAR-γ, as well as positive expression of stem cell marker sox9 and p63 showed that the harvested cell could proliferate well *in vitro*, maintaining the proliferation characteristic of progenitor cells.

3.3. *In vitro* cytotoxicity of PLGA scaffolds

The cytotoxicity of the three scaffolds was assessed through the CCK-8 assay. The extracted solutions of the scaffolds were incubated with HCFs and rMGCs, and the OD values were measured and compared to normal medium. The extraction solutions of the three scaffolds did not induce significant changes in cell viability of HDFs (Figure 3A) and rMGCs (Figure 3B).

3.4. Cell behavior of HDFs and rMGCs on PLGA scaffolds

The distribution and morphology of HDFs and rMGCs in the scaffolds were observed by an inverted fluorescence microscope (Leica, Japan) and a confocal laser scanning microscopy (CLSM; LSM780, ZEISS, Germany), respectively. Fluorescence microscope observation revealed that HDFs could adhere and spread onto the three PLGA scaffolds (Figure 4) with a high degree of viability, as confirmed by Live/dead assay (Supplementary Figure S3) which showed minimal cell death. Moreover, the HDFs distributed randomly on the random PLGA scaffold (Figures 4A1–A3), while they were spread completely and elongated along the axially aligned porous structure on the O-PLGA (Figures 4B1–B3), and AZM@O-PLGA (Figures 4C1–C3) scaffolds. Similarly, Live/dead assay indicated that nearly all rMGCs on the three scaffolds were alive (Supplementary Figure S4). The rMGCs were uniformly distributed in the three types of PLGA scaffolds, after 7 days cultivation. CLSM observation showed the rMGCs could adhere well onto the pore walls (Figure 5).

3.5. Reconstruction of eyelid defect by PLGA scaffolds.

As three types of PLGA scaffolds would well support both HDFs and rMGCs, we further applied the scaffolds as grafts to reconstruct the eyelid defect in a rabbit model. Rabbits in all groups ate normally and behaved regularly in the weeks after operation. Though at 1 m of post-operation, the eyelid grafted with R-PLGA and O-PLGA scaffolds formed a noticeable notch at the wound site. All grafted eyelid showed acceptable defect repair with mild scar at 2 m of post-operation (Figure 6). The eyelid grafted with AZM@O-PLGA scaffolds showed good wound healing without noticeable scar formation or other abnormality. Historically, at 2 m of post-operation, all PLGA scaffolds started to degrade into pieces and were well integrated by fibrovascular tissue. The R-PLGA degraded slower than O-PLGA scaffolds, with more PLGA material and less collagen deposition inside scaffolds

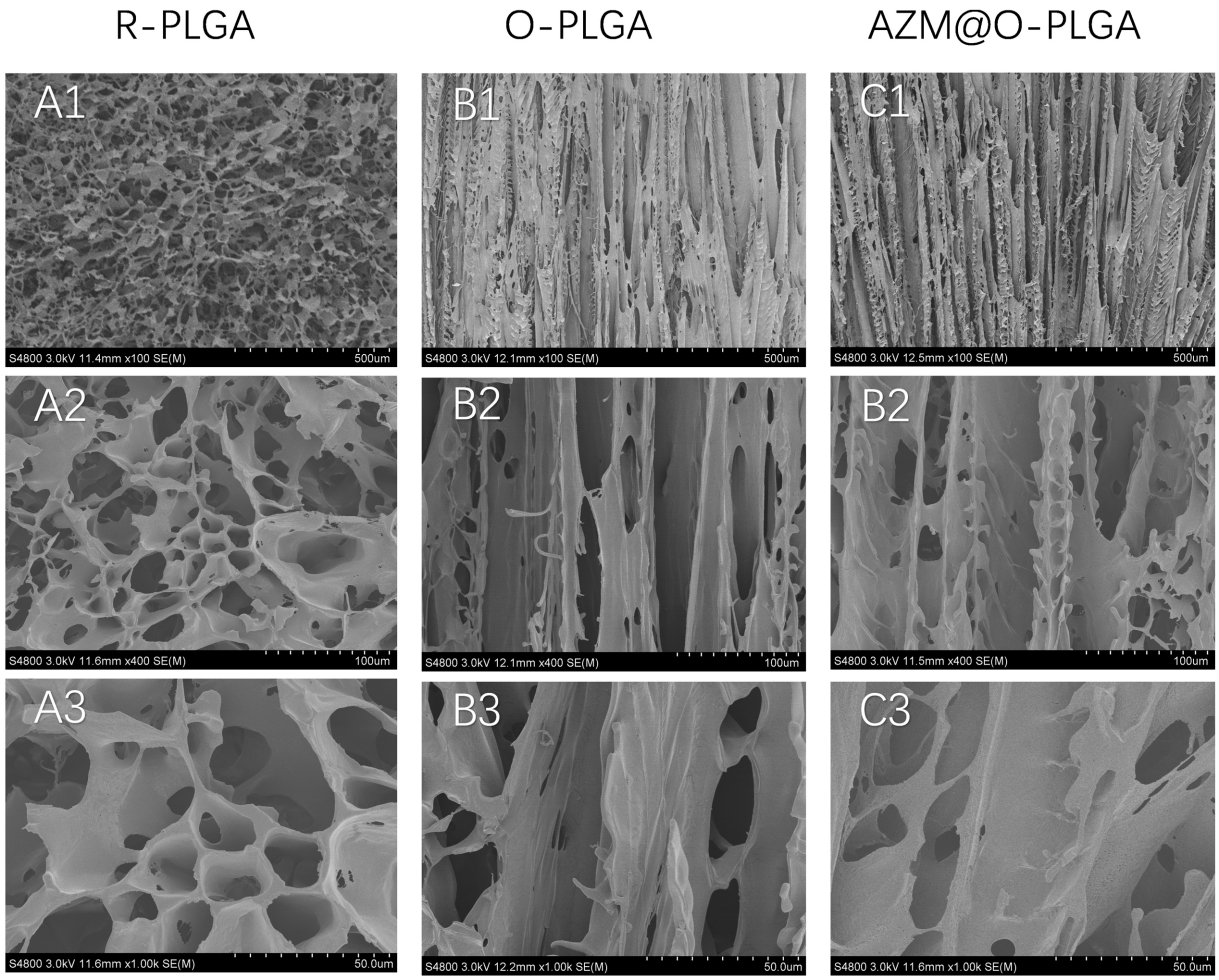

FIGURE 1
SEM images showing the morphology of random structured **(A1–A3)**, and orientation-structured PLGA scaffolds **(B,C)**. Azithromycin loading **(C1–C3)** did not influent the orientated structure.

(Figures 7A1–A3; Supplementary Figures S5A1,A2; Supplementary Figures S6A1,A2). The O-PLGA scaffolds and AZM@O-PLGA scaffolds were markedly degraded into small fragments surrounded by mature collagen fibers (Figures 7B1–C3; Supplementary Figures S5B1–C2; Supplementary Figures S6B1–C2), simulating the structure of natural tarsal plate (Figures 7D1–D3; Supplementary Figures S6D1,D2), while the untreated defected tissue showed a denser collagen deposition (Supplementary Figures S6D1–E2).

4. Discussion

Tarsal plate is an essential structure that support and maintain shape of eyelid. The structure of tarsus is composed of regularly arranged meibomian glands and surrounding ECM. Because of the particularity of tissue component and regularity of tissue distribution, there is a lack of suitable eyelid tarsus tissue substitutes, making it a big challenge in eyelid defect reconstruction. In this study we tried to construct an axially aligned PLGA scaffold which is structurally similar to the native tarsus ECM. *In vitro* study showed that the O-PLGA scaffolds are able to support the growth of the two target cells, fibroblasts and meibomian glands cells. In addition, after transplanted into the defect site of eyelid, the O-PLGA, especially AZM@O-PLGA could well maintain the normal shape of eyelid with mild scare formation, and be well integrated by the local tarsus tissue.

Many native tissues had oriented structures, such as tendon, cartilage, nerve, bone and so on. The oriented structures are closely related to their physiological and mechanical properties (10). Scaffolds were fabricated with oriented structures to mimic the microenvironment of native tissue, and were proved to facilitate cell promotion, differentiation, spatial organization and tissue formation (20). To a certain degree, tarsus has its own oriented structure caused by axially arrangements of meibomian glands. We conjectured that oriented scaffolds may induce eyelid ECM remodeling. To enable injured eyelid tissue to recover its normal function and promote tissue repair, tissue engineering eyelid tarsus tissue substitutes should mimic native tissue, both mechanically and physiologically. Therefore, we fabricated three types of PLGA scaffolds for eyelid defect

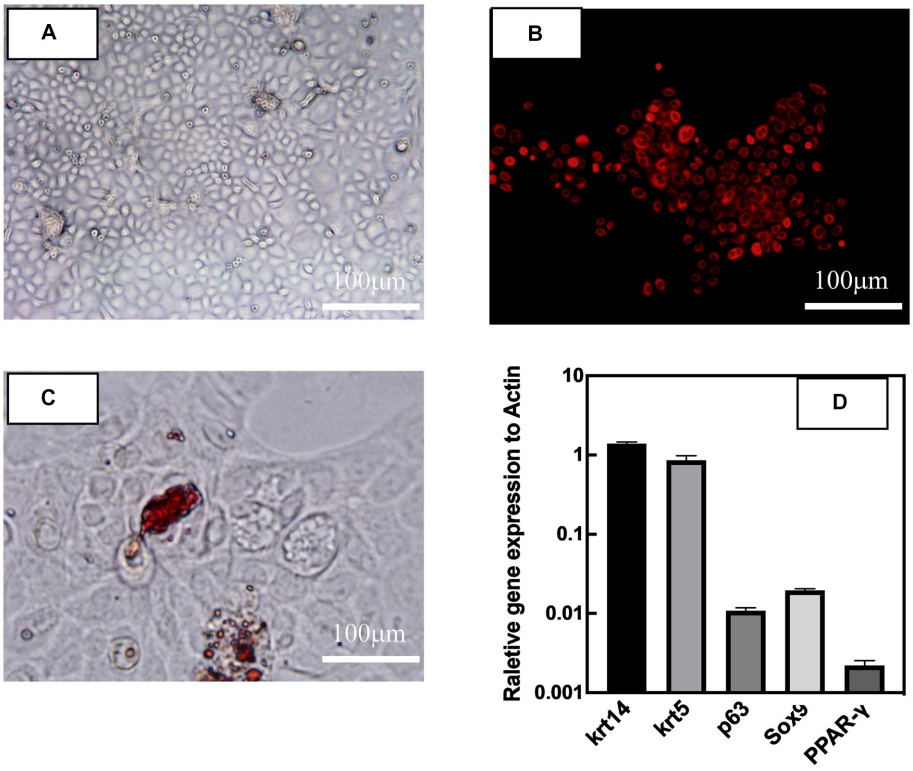

FIGURE 2
Appearance of primary rat meibomian gland epithelial cells (passage 2) after culturing in SFM for 5days. Light microscopy image **(A)**, Nile red staining **(B)**, oil O staining**(C)** of meibomian gland epithelial cells, respectively. Gene expression patterns **(D)** of rat meibomian gland epithelial cells. Data are shown as mean±SD and each sample was tested in triplicate.

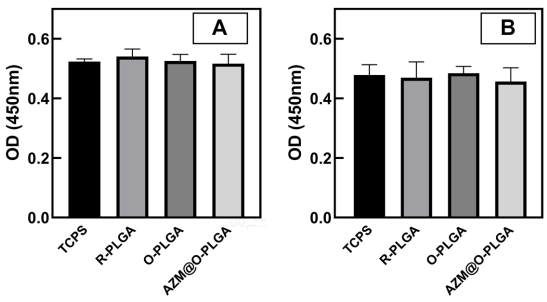

FIGURE 3
Cytotoxicity of the scaffolds. CCK-8 assay of human fibroblast cells **(A)** and rat meibomian gland epithelial cells **(B)** cultured with extracts of scaffolds. Data are shown as mean±SD and each sample was tested in triplicate.

reconstruction. The axially aligned PLGA was designed to mimic the natural structure of eyelid tarsus tissue.

Some researchers have attempted to develop a synthetic tarsal substitute for eyelid defect reconstruction caused by tumor resection, trauma, or congenital diseases. Synthesized materials such as porous HDPE (Medpor), poly(3-hydroxybutyrate-co-3-hydroxyhexanoate) (21), and poly(propylene fumarate)-2-hydroxyethyl methacrylate copolymers (22) have been explored as tarsus substitutes. However, these synthesized materials were rigid and hardly degradable. Long-term implantation may lead to complications, such as exposure through the skin, unexplained pain, poor mobility and eyelid abnormal shape (11). Very few studies tried degradable biomaterials for eyelid reconstruction. Michelle T. Sunat al. developed a macro-porous chitosan scaffold for eyelid tarsus tissue engineering, which could support the attachment and proliferation human orbital skin fibroblasts *in vitro* (23). But the authors did not investigate the scaffolds for further *in-vivo* repair effects.

In clinical, a lid-sharing technique was wildly used for large eyelid defects. The shared lid is usually divided about 2 months after the initial surgical repair to allow enough time for the reconstructed lid to develop a new blood supply and to counteract the downward contractile forces of scar maturation and gravity (24). Therefore, scaffolds should have a good balance between degradation rate and tarsus tissue repair after implanted in defect sites, except for good biocompatibility and mechanical intensity. PLGA are the most popular polymers in tissue engineering, such as bone (25), tendon (26), cartilage (27) and so on, due to their biodegradability and biocompatibility. Oriented PLGA scaffolds have shown great potential for the practical application in cartilage regeneration, for biomimetic structure and mechanical property (28). Based on the axially aligned structure of tarsus tissue and specific mechanical property similar to cartilage (12), we suspected that the multiple-bionic oriented PLGA scaffolds may have great potential in eyelid defect repair. After 2-month *in vivo* observation, the implanted oriented PLGA substitute was well degraded into fragments and surrounded with collagenous

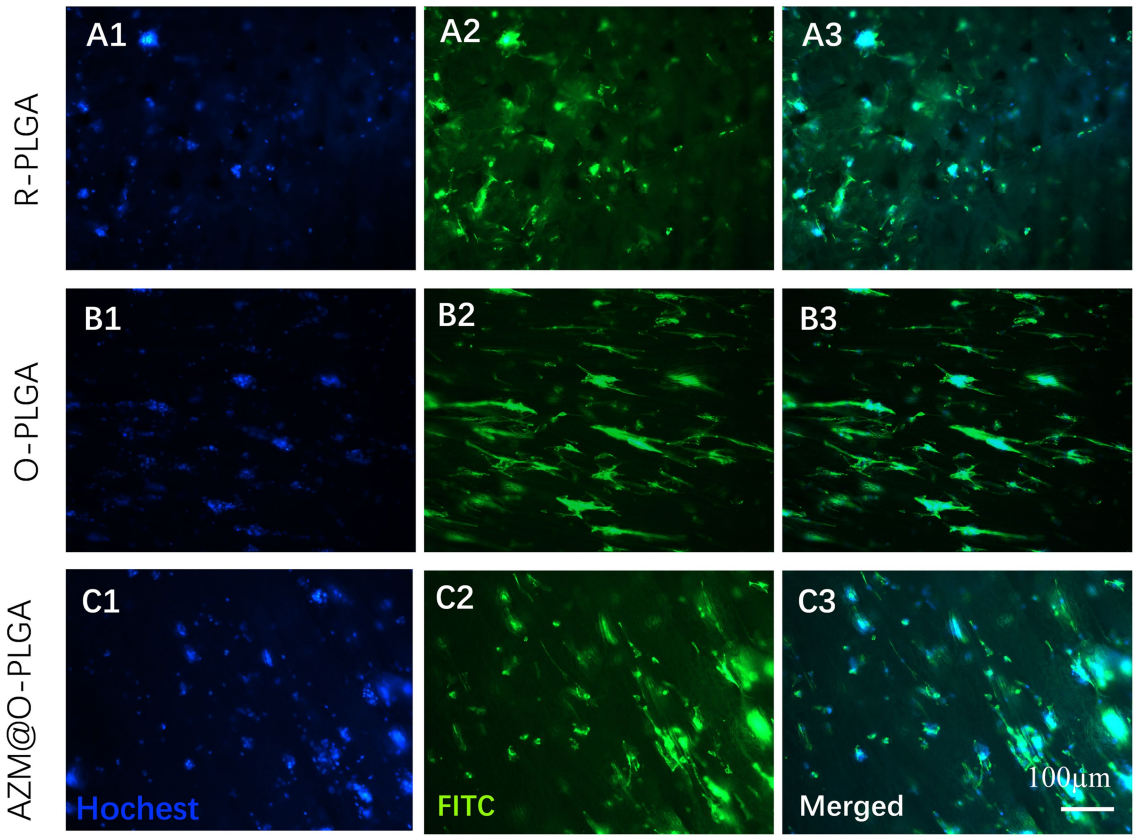

FIGURE 4
Fluorescence staining showing the morphology and distribution of human fibroblast cells inside **(A)** R-PLGA, **(B)** O-PLGA and **(C)** AZM@O-PLGA scaffolds after 5 days culture *in vitro*. The nuclei and actin were stained with hochest-33342 (blue) and FITC phalloidin (green), respectively..

fiber, which was similar with natural eyelid in morphological character (Figure 6). The relatively slower degradation of R-PLGA substitute may due to pore structure and interconnectivity. Preliminary observation showed a matched rate between oriented PLGA degradation and eyelid tissue integration.

As foreign materials that have been introduced into the body, biomaterials would also be a potential source of infection (29) and associated with triggering inflammation and immune reactions (30). Therefore, multifunctional biomaterials with combined properties that can combat infections, modulate inflammation, and promote regeneration is the real quest. Azithromycin antibiotics have been reported to have anti-inflammatory properties in blepharitis and meibomian gland dysfunction, by suppressing the expression of proinflammatory mediator, such as IL-1β, IL-8, and MMP-9 (31). In this study, AZM was loaded into the microtubule-orientated biomimetic PLGA scaffolds. This biomaterial was developed not only as a substitute of eyelid tarsus, but also as a mediator to prevent biodevices-related infections and improve the local environment of eyelid defect. Preliminary results of animal experiments showed that AZM@O-PLGA scaffolds have a batter eyelid repair effects after 1 month and 2 months transplantation. However, this article is only a first attempt to evaluate the *in vivo* repair effect of oriented scaffolds loaded with AZM as eyelid tarsus substitutes. In the future study, longer observation *in vivo* and more functional characterization of the two target cells response to the scaffolds *in vitro* will be carried out.

5. Conclusion

Three kinds of PLGA scaffolds with different pore architectures were successfully fabricated to assess their repair ability for eyelid defects in a rabbit model. The axially aligned scaffold presented bionic structure mechanical property. The axially aligned scaffolds could well support and guide cellular activities *in vitro* and *in vivo*. The *in vivo* infiltration of reparative tissue into the scaffolds could be significantly enhanced in the axially aligned scaffolds, contributing to better repair effects compared with those of the random scaffold. Structural and functional repair of eyelid was realized with fibrous connective tissue integration in the two types of axially aligned scaffold groups，O-PLGA and AZM@O-PLGA scaffolds at 8 weeks post-surgery. Overall, a faster degradation with matched integration rate was found in the axially aligned scaffold group. By loading Azithromycin, the AZM@O-PLGA scaffolds showed a better appearance of eyelid with milder scar. In conclusion, the axially aligned PLGA scaffolds, especially the ones loaded with Azithromycin, provide a promising alternative for eyelid tarsal plate substitutes, and possess greater potential to be translated into medical devices for applications in the future.

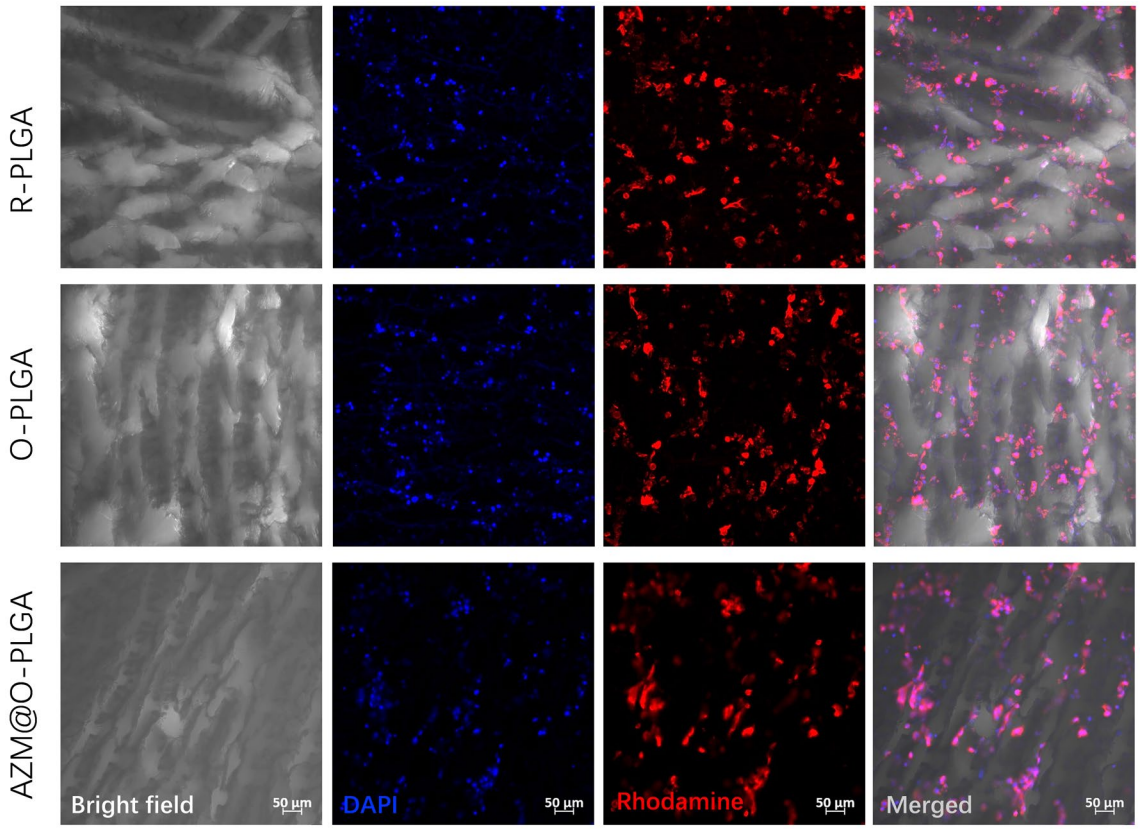

FIGURE 5
CLSM images showing the morphology and rat meibomian gland epithelial cells inside three scaffolds after 7d three-dimension culture *in vitro*. The nuclei and actin were stained with DAPI (blue) and rhodamine phalloidin (red), respectively.

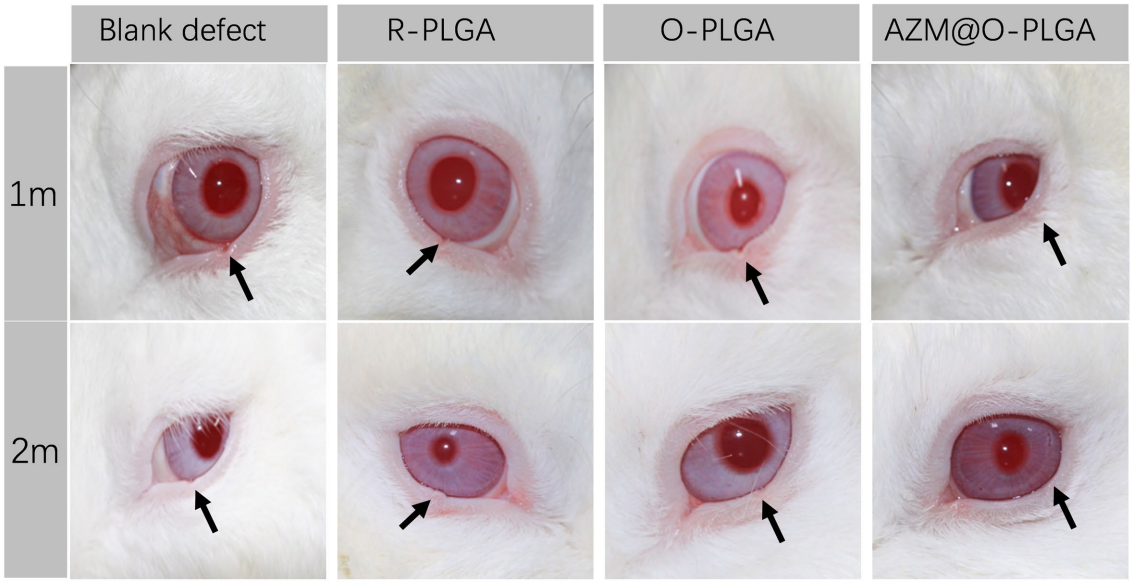

FIGURE 6
Post-surgery appearance of repaired eyelid after the full thickness defects (6.0×3.0mm) were reconstructed by R-PLGA, O-PLGA and AZM@O-PLGA scaffolds at 1 and 2months. The black arrows point to the defect sites.

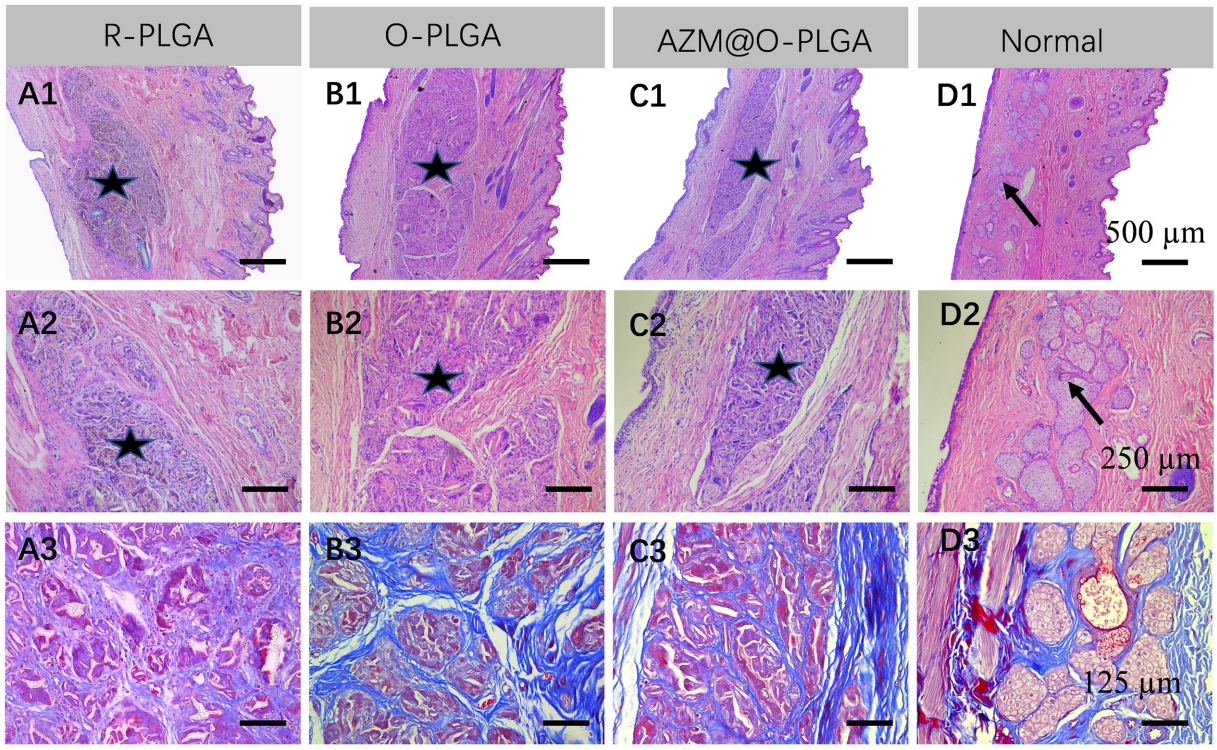

FIGURE 7
Histological analysis of the repaired eyelid implanted by **(A)** R-PLGA, **(B)** O-PLGA and **(C)** AZM@O-PLGA scaffolds for 8 w, respectively. H&E staining **(A1–D1,A2-D2)** and Masson staining **(A3-D3)** of the repaired and normal eyelid tissues. Asterisks represent scaffolds. Black arrows point to the normal meibomian glands.

Data availability statement

The original contributions presented in the study are included in the article/Supplementary material, further inquiries can be directed to the corresponding author.

Ethics statement

The animal study was reviewed and approved by the Animal Ethics Committee of Hangzhou Medical College.

Author contributions

JY designed this study and provided technical support. PX and PC performed the experiments and wrote the manuscript. YS and JC helped cell culture and animal experiments. QG and HW helped revised manuscript. All authors contributed to the article and approved the submitted version.

Funding

This study is financially supported by the National Natural Science Foundation of China (82101080, 82000857) and the Natural Science Foundation of Zhejiang province (LQ22H120001).

Acknowledgments

The authors sincerely appreciate the technical support of the Facility of Histomorphology, Core Facilities, Zhejiang University School of Medicine.

Conflict of interest

The authors declare that the research was conducted in the absence of any commercial or financial relationships that could be construed as a potential conflict of interest.

Publisher's note

Supplementary material

The Supplementary material for this article can be found online at: https://www.frontiersin.org/articles/10.3389/fmed.2023.1129606/full#supplementary-material

References

1. Chang EI, Esmaeli B, Butler CE. Eyelid reconstruction. *Plast Reconstr Surg*. (2017) 140:724e–35e. doi: 10.1097/PRS.0000000000003820

2. Mukit M, Anbar F, Dadireddy K, Konofaos P. Eyelid reconstruction: an algorithm based on defect location. *J Craniofac Surg*. (2022) 33:821–6. doi: 10.1097/SCS.0000000000008433

3. Tenland K, Berggren J, Engelsberg K, Bohman E, Dahlstrand U, Castelo N, et al. Successful free Bilamellar eyelid grafts for the repair of upper and lower eyelid defects in patients and laser speckle contrast imaging of revascularization. *Ophthalmic Plast Reconstr Surg*. (2021) 37:168–72. doi: 10.1097/IOP.0000000000001724

4. Patel BC, Patipa M, Anderson RL, McLeish W. Management of postblepharoplasty lower eyelid retraction with hard palate grafts and lateral tarsal strip. *Plast Reconstr Surg*. (1997) 99:1251–60. doi: 10.1097/00006534-199705000-00007

5. Miotti G, Zeppieri M, Rodda A, Salati C, Parodi PC. How and when of eyelid reconstruction using autologous transplantation. *World J Transplant*. (2022) 12:175–83. doi: 10.5500/wjt.v12.i7.175

6. Li J, Li L, Ren BC. Experimental study of the eyelid reconstruction in situ with the acellular xenogeneic dermal matrix. *Zhonghua Zheng Xing Wai Ke Za Zhi*. (2007) 23:154–7. doi: 10.3760/j.issn:1009-4598.2007.02.025

7. Sabater-Cruz N, Figueras-Roca M, Gonzalez Ventosa A, Padro-Pitarch L, Tort J, Casaroli-Marano RP. Current clinical application of sclera and amniotic membrane for ocular tissue bio-replacement. *Cell Tissue Bank*. (2020) 21:597–603. doi: 10.1007/s10561-020-09848-x

8. Diaz-Gomez L, Kontoyiannis PD, Melchiorri AJ, Mikos AG. Three-dimensional printing of tissue engineering scaffolds with horizontal pore and composition gradients. *Tissue Eng Part C Methods*. (2019) 25:411–20. doi: 10.1089/ten.tec.2019.0112

9. Xu Y, Guo X, Yang S, Li L, Zhang P, Sun W, et al. Construction of bionic tissue engineering cartilage scaffold based on three-dimensional printing and oriented frozen technology. *J Biomed Mater Res A*. (2018) 106:1664–76. doi: 10.1002/jbm.a.36368

10. Dai Y, Shen T, Ma L, Wang D, Gao C. Regeneration of osteochondral defects in vivo by a cell-free cylindrical poly (lactide-co-glycolide) scaffold with a radially oriented microstructure. *J Tissue Eng Regen Med*. (2018) 12:e1647–61. doi: 10.1002/term.2592

11. Tan J, Olver J, Wright M, Maini R, Neoh C, Dickinson AJ. The use of porous polyethylene (Medpor) lower eyelid spacers in lid heightening and stabilisation. *Br J Ophthalmol*. (2004) 88:1197–200. doi: 10.1136/bjo.2003.029397

12. Tanaka T, Furutani-Miura S, Nakamura M, Nishida T. Immunohistochemical study of localization of extracellular matrix after holmium YAG laser irradiation in rat cornea. *Jpn J Ophthalmol*. (2000) 44:482–8. doi: 10.1016/S0021-5155(00)00223-9

13. Vanić Ž, Rukavina Z, Manner S, Fallarero A, Uzelac L, Kralj M, et al. Azithromycin-liposomes as a novel approach for localized therapy of cervicovaginal bacterial infections. *Int J Nanomedicine*. (2019) 14:5957–76. doi: 10.2147/IJN.S211691

14. Pradeep AR, Bajaj P, Agarwal E, Rao NS, Naik SB, Kalra N, et al. Local drug delivery of 0.5% azithromycin in the treatment of chronic periodontitis among smokers. *Aust Dent J*. (2013) 58:34–40. doi: 10.1111/adj.12019

15. Escalante MG, Eubank TD, Leblebicioglu B, Walters JD. Comparison of azithromycin and amoxicillin before dental implant placement: an exploratory study of bioavailability and resolution of postoperative inflammation. *J Periodontol*. (2015) 86:1190–200. doi: 10.1902/jop.2015.150024

16. Liu Y, Kam WR, Ding J, Sullivan DA. Effect of azithromycin on lipid accumulation in immortalized human meibomian gland epithelial cells. *JAMA Ophthalmol*. (2014) 132:226–8. doi: 10.1001/jamaophthalmol.2013.6030

17. Feng X, Xu P, Shen T, Zhang Y, Ye J, Gao C. Influence of pore architectures of silk fibroin/collagen composite scaffolds on the regeneration of osteochondral defects in vivo. *J Mater Chem B*. (2020) 8:391–405. doi: 10.1039/C9TB01558B

18. Liu S, Hatton MP, Khandelwal P, Sullivan DA. Culture, immortalization, and characterization of human meibomian gland epithelial cells. *Invest Ophthalmol Vis Sci*. (2010) 51:3993–4005. doi: 10.1167/iovs.09-5108

19. Xu P, Gao Q, Feng X, Lou L, Zhu T, Gao C, et al. A biomimetic Tarso-conjunctival biphasic scaffold for eyelid reconstruction in vivo. *Biomater Sci*. (2019) 7:3373–85. doi: 10.1039/C9BM00431A

20. Li L, Zhao M, Li J, Zuo Y, Zou Q, Li Y. Preparation and cell infiltration of lotus-type porous nano-hydroxyapatite/polyurethane scaffold for bone tissue regeneration. *Mater Lett*. (2015) 149:25–8. doi: 10.1016/j.matlet.2015.02.106

21. Zhou J, Peng SW, Wang YY, Zheng SB, Wang Y, Chen GQ. The use of poly(3-hydroxybutyrate-co-3-hydroxyhexanoate) scaffolds for tarsal repair in eyelid reconstruction in the rat. *Biomaterials*. (2010) 31:7512–8. doi: 10.1016/j.biomaterials.2010.06.044

22. Gao Q, Hu B, Ning Q, Ye C, Xie J, Ye J, et al. A primary study of poly(propylene fumarate)-2-hydroxyethyl methacrylate copolymer scaffolds for tarsal plate repair and reconstruction in rabbit eyelids. *J Mater Chem B*. (2015) 3:4052–62. doi: 10.1039/C5TB00285K

23. Sun MT, O'Connor AJ, Milne I, Biswas D, Casson R, Wood J, et al. Development of macroporous chitosan scaffolds for eyelid Tarsus tissue engineering. *Tissue Eng Regen Med*. (2019) 16:595–604. doi: 10.1007/s13770-019-00201-2

24. Eah KS, Sa H-S. Reconstruction of large upper eyelid defects using the reverse Hughes flap combined with a Sandwich graft of an acellular dermal matrix. *Ophthalmic Plast Reconstr Surg*. (2021) 37:S27–30. doi: 10.1097/IOP.0000000000001779

25. Sokolova V, Kostka K, Shalumon KT, Prymak O, Chen JP, Epple M. Synthesis and characterization of PLGA/HAP scaffolds with DNA-functionalised calcium phosphate nanoparticles for bone tissue engineering. *J Mater Sci Mater Med*. (2020) 31:102. doi: 10.1007/s10856-020-06442-1

26. Chachlioutaki K, Karavasili C, Adamoudi E, Bouropoulos N, Tzetzis D, Bakopoulou A, et al. Silk sericin/PLGA electrospun scaffolds with anti-inflammatory drug-eluting properties for periodontal tissue engineering. *Biomater Adv*. (2022) 133:112723. doi: 10.1016/j.msec.2022.112723

27. Xie Y, Lee K, Wang X, Yoshitomi T, Kawazoe N, Yang Y, et al. Interconnected collagen porous scaffolds prepared with sacrificial PLGA sponge templates for cartilage tissue engineering. *J Mater Chem B*. (2021) 9:8491–500. doi: 10.1039/D1TB01559A

28. Dai Y, Gao Z, Ma L, Wang D, Gao C. Cell-free HA-MA/PLGA scaffolds with radially oriented pores for in situ inductive regeneration of full thickness cartilage defects. *Macromol Biosci*. (2016) 16:1632–42. doi: 10.1002/mabi.201600218

29. Buhmann MT, Stiefel P, Maniura-Weber K, Ren Q. In vitro biofilm models for device-related infections. *Trends Biotechnol*. (2016) 34:945–8. doi: 10.1016/j.tibtech.2016.05.016

30. Griffith M, Islam MM, Edin J, Papapavlou G, Buznyk O, Patra HK. The quest for anti-inflammatory and anti-infective biomaterials in clinical translation. *Front Bioeng Biotechnol*. (2016) 4:71. doi: 10.3389/fbioe.2016.00071

31. Zhang L, Su Z, Zhang Z, Lin J, Li DQ, Pflugfelder SC. Effects of azithromycin on gene expression profiles of proinflammatory and anti-inflammatory mediators in the eyelid margin and conjunctiva of patients with meibomian gland disease. *JAMA Ophthalmol*. (2015) 133:1117–23. doi: 10.1001/jamaophthalmol.2015.2326

frontiers | Frontiers in Medicine

TYPE Original Research
PUBLISHED 15 June 2023
DOI 10.3389/fmed.2023.1029952

OPEN ACCESS

EDITED BY
Georgios D. Panos,
Nottingham University Hospitals NHS Trust, United Kingdom

REVIEWED BY
Giulio Vicini,
Careggi University Hospital, Italy
Beniamin Oskar Grabarek,
Academy of silesia, Poland

*CORRESPONDENCE
Shweta Chaurasia
✉ shweta84omns@yahoo.com

RECEIVED 02 September 2022
ACCEPTED 11 May 2023
PUBLISHED 15 June 2023

CITATION
Chaurasia S, Soni SL, Ganesh V, Ram J, Sukhija J, Chaurasia S and Takkar A (2023) Tonic down-rolling and eccentric down-positioning of eyes under sevoflurane anesthesia without non-depolarizing muscle relaxant and its relationship with depth of anesthesia. *Front. Med.* 10:1029952. doi: 10.3389/fmed.2023.1029952

Tonic down-rolling and eccentric down-positioning of eyes under sevoflurane anesthesia without non-depolarizing muscle relaxant and its relationship with depth of anesthesia

Shweta Chaurasia[1]*, Shiv Lal Soni[2], Venkata Ganesh[2], Jagat Ram[1], Jaspreet Sukhija[1], Swati Chaurasia[3] and Aastha Takkar[4]

[1]Department of Ophthalmology, Advanced Eye Centre, Post Graduate Institute of Medical Education and Research, Chandigarh, India, [2]Department of Anaesthesiology, Post Graduate Institute of Medical Education and Research, Chandigarh, India, [3]Department of Medicine, Sanjay Gandhi Memorial Hospital, New Delhi, India, [4]Department of Neurology, Post Graduate Institute of Medical Education and Research, Chandigarh, India

Purpose: To analyze the relationship between eccentric downward eye movement/eccentric downward eye-positioning (EDEM/EDEP) encountered in patients undergoing ophthalmic surgeries and its return to a centralized position under general anesthesia (GA) with the depth of anesthesia (DOA).

Methods: Patients undergoing ophthalmic surgeries (6 months-12 years) under sevoflurane anesthesia without non-depolarizing muscle relaxant (NDMR) who witnessed a sudden tonic EDEM/EDEP were both retrospectively (R-group) and prospectively (P-group) enrolled (ambispective study). R-group included data-points after induction (AI) till the time surgery lasted while P-group compiled data both during induction (DI) and AI. DOA in terms of MAC (minimum alveolar concentration) at the time of EDEM/EDEP and centralization of eyeball and their timings were noted and compared for both AI and DI data-points. Also, vertical eccentric eye positions were scored and correlated with MAC.

Results: AI data included 22 (14R+8P) events and their mean MAC of EDEM/EDEP and centralization were 1.60 ± 0.25 and 1.18 ± 0.17 respectively ($p = 0.000$). DI data included 62 (P) cases and its mean MAC of EDEM/EDEP and centralization was 2.19 ± 0.43 and 1.39 ± 0.26 respectively ($p = 0.000$). Median (IQR) eye positions during down-positioning in 84 events was −3 (−3.9 to −2.5). It was preceded by an eccentric upward drift of eyes in 10/22 (6R+4P) AI cases. A strong negative correlation was seen between DOA and eccentric eye positions ($r = -0.77$, $p = 0.000$).

Conclusions: Tonic down-rolling of eyes is not uncommon in children seen without NDMR with higher depths of sevoflurane anesthesia compared to point of centralization and fluctuations in DOA should be avoided to circumvent inadvertent complications during ocular surgery.

KEYWORDS

tonic down-rolling, minimal alveolar concentration, general anesthesia, downward eye movement, sevoflurane, laryngeal mask, eccentric eye positioning, non-depolarizing muscle relaxant

1. Introduction

Anesthetized patients go through Guedel's (1) stages of general anesthesia (GA). Guedel described how, as depth of anesthesia increases and the third stage of surgical anesthesia is reached, the extraocular muscles become flaccid and the eyeball movement ceases (1). But eye movements on the operating table are not uncommon in stage 3 anesthesia (2–4). Investigators found that during ocular surgery under GA, 18% of patients had eccentric eye movements (3). In a developing nation like ours with limited resources and high patients' volume, it is routine to perform short surgeries under sevoflurane anesthesia using a laryngeal mask without non-depolarizing muscle relaxant (NDMR). This newer drugs' rapid manipulation of anesthetic planes allows patients to move quickly between deeper and superficial planes (5). For an ophthalmologist, eccentric eye movements can pose a surgical challenge due to constriction of the field of surgery and sudden jerks which can cause inadvertent iatrogenic complications at different steps in the surgical procedures like cataracts, squints, etc. Slightly divergent and elevated eye positions during GA is a known finding (2, 6). But only a few studies have described fixed vertically deviated eye positions during ocular surgery under GA and discussed its definite relationship with anesthetic depth (2–4). According to a quantitative study, lighter planes of anesthesia without NDMR correlate with higher eye position, (4) which has been explained on the basis of natural Bell's phenomenon. Only a few authors have mentioned deeper levels of anesthesia with the down positioning of eyes (2, 4). To the best of our knowledge, there is no literature on the detailed documentation of tonic downward movement of the eyes and their eccentric positioning in down gaze in their relation to anesthetic depth.

So, we here aimed to investigate relationship DOA (in terms of MAC) with the abrupt downward eccentric eye movement/eccentric down-positioning (EDEM/EDEP) and its return to normal centralized position under sevoflurane in the absence of NDMR. Also, we aimed to evaluate their timings and correlate eye positions (eye score) with fluctuation in DOA. This study aims to raise awareness of this not uncommon ocular finding in children under SA that has important consequences in ophthalmic surgery when done without NDMR. Using our study's findings, we hope to evaluate the literature and gain insight into the intricacy of neuronal processes in subcortical regions mediating tonic eye movements under GA.

Abbreviations: P, prospective; R, retrospective; MAC, minimal alveolar concentration; DOA, depth of anesthesia; R, retrospective; P, prospective; GA, general anesthesia; NDMR, non-depolarizing muscle-relaxant; SA, sevoflurane anesthesia; EDEM/EDEP, eccentric downward eye-movement/eccentric downward eye-positioning; AI, after induction; DI, during induction; IQR, inter quartile range; CBF, cerebral blood flow; OCR, oculo-cardiac reflex; LMA, Laryngeal mask anesthesia; LC, Locus Coeruleus; CNS, central nervous system; BIS, Bispectral index; REM, Rapid eye movement; NREM, Non-rapid eye movement; ROC, Receiver Operating characteristics; EEG, electro encephalogram.

2. Materials and methods

2.1. Study type

We experienced EDEM/EDEP during surgery in a few retrospective cases, so we decided to prospectively recruit subjects and follow them from induction to end of surgery to witness sudden down-rolling events. Data-points during induction were included in prospective series to understand the relationship of eye movements with different DOA as maximum flow of sevoflurane and its fluctuation occur during induction. So, this was an ambispective observational study which was approved by our Institutional Ethics committee (retrospective IEC NK/7068/Study/068; prospective IEC NK/5860/Study/542 with CTRI no 2021/2021/10/037578S). This adhered to the tenets of the Declaration of Helsinki and written informed consent was obtained from all patients' parents or guardians regarding their study participation.

2.2. Study population

2.2.1. Retrospective

Operative records of pediatric patients aged 6 months to 12 years of age who underwent surgeries (operated by single surgeon SC) under GA with a supraglottic airway device without NDMR between January 2018 and August 2021 were retrospectively reviewed from the recorded intra-operative data base of ophthalmic surgeries (cataract/squint/botulinum toxin) and cases in which vertically downward movement was witnessed intra-operatively by the ophthalmic surgeon with or without an accompanying upward movement under direct observation during surgery were included in our study.

2.2.2. Prospective

Patients aged 6 months to 12 years of age who underwent squint surgery/botulinum toxin under GA with a supraglottic airway device without NDMR between November 2021 to December 2022 were prospectively recruited to record and study the eye movement and eye positions during both process of induction and intra-operatively after induction for any eccentric eye-movements. It is to be noted that patients were prospectively monitored from the start of induction because maximum anesthetic depth and its fluctuation occurs during induction and there would be greater chance to witness them. And the patients who witnessed down-rolling of eyes and/or downward eccentric eye positioning during induction or intra-operatively after induction were recruited in the study.

Exclusion criteria were patients with neurological disorders like cerebral palsy, seizure disorder, or paralytic or restrictive squints, patients with eccentric upward movement alone (without accompanying downward movement or down-positioning), and in cases without anesthetic details or details of intra-operative of eye movements.

2.3. Study methodology

Inhalational induction was started with 8% sevoflurane in a 50% oxygen/nitrous-oxide mixture (N2O) mixture and an intravenous line was placed both in prospective and retrospective cases. After attaining jaw relaxation, the supraglottic airway device (laryngeal mask airway) was inserted. Synchronous intermittent mechanical ventilation was started with pressure support on "GE Datex-Ohmeda Avance S5 (USA) Anesthesia machine." Tidal volume, frequency, and pressure support was adjusted to achieve an end tidal carbon-dioxide (ETCO2) between 35 mmHg and 40 mgHg. Venous access was obtained once the child was sedated with inhalational induction. After establishing the intra-venous line, fentanyl (0.5–2 μg/kg) and propofol (if required) was injected as an inducing agent to increase depth of anesthesia. Once the laryngeal mask airway was secured, sevoflurane was reduced to maintain airway along with oxygen and nitrous oxide (50:50) without a muscle relaxant. Corresponding values of minimum alveolar concentration (MAC) (7) (as calculated by the anesthetic machine from ET sevoflurane of the anesthetic agent) at the time of onset of down drift and its centralization were noted along with their timings. This included data-points during induction (prospective data) and after induction during surgery (both retrospective and prospective data). MAC is defined as the concentration of inhaled anesthetic within alveoli at which 50% of people show immobility in response to any nociceptive stimulus (7). Also sequence of events prior and following downward eye movements in different cases were noted in both retrospective and prospective data-points. Timings of anesthetic agents, such as intra-venous agents like fentanyl and propofol (if given) during or after induction in relation to down-drifted eye movements, were noted. Types and duration of surgery were also noted. Any oculo-cardiac reflex if present and any change in heart rate and pupil size were also noted.

2.4. Recording of eye movement

Details of eye movement recordings (for the retrospective study) were available from our recorded intra-operative data base. Pre-operative recordings of GA induction were done using smart-phone cameras (I phone 13) for our prospective series. Eye movements and timings during induction were recorded and noted by the ophthalmologist starting from the point the child was sedated from the awake condition. The ophthalmologist continually monitored the eye positions by retracting both lids and opening the eyes together. Vitals and sevoflurane concentration (in terms of MAC) were simultaneously recorded from the monitor by separate observers from induction till the airway was secured by a laryngeal mask (Supplementary Video 1).

2.5. Scoring of eye movement

Records of eccentric down-positioning of eyes from the recordings were evaluated in both inferior positions of eyes (toward inferior fornix) in relation to the medial canthus; superior limbus/superior half of cornea was scored on an ordinal scale from −4 to 0 (Figure 1).

−4 = line joining medial and lateral canthi passes above the superior limbus

−3 = line joining medial and lateral canthi passes via superior limbus

−2 = line joining medial and lateral canthi passes between superior limbus to superior one-fourth cornea

−1 = line joining medial and lateral canthi passes between superior half to one-fourth cornea

0 = pupil position aligning medial canthus

Similarly, positive values (0 to +4) reflected superior positions of eyes (toward superior fornix) in relation to the medial canthus and inferior limbus or inferior half of the cornea.

2.6. Definition of eccentric eye movement and positioning

"**Eccentric eye movement**" is defined as the off-axis vertical movement of the eye from its central position in a quick-rolling/drifting fashion. "**Eccentric position**" is defined as off-axis vertically deviated positioning of the eye from its central position after the vertical eye movement. This eccentricity is either described as upward or downward depending on the movement/position of the eye toward the upper fornix or lower fornix respectively. In our study, the term "**drift"** and **"rolling**" have been interchangeably used for the upward and downward movements as these movements were smooth and slow similar to the drifts seen in dissociated vertical deviation or slow rolling eye movements seen during sleep onset/Bells phenomenon. Also, both terms describe sweeping eye movements with marginally slow speed (encountered in our study) which differentiates them from rapid eye movements/saccades of the awake state. An electronic search was performed using keywords: eye movement, general anesthesia, eccentric eye position, anesthetic depth, sleep, and anesthesia. The search of published literature for the review was made via PubMed, Med line, Google Scholar, and Ovid along with checking for cross-references.

2.7. Sample size calculation and statistics analysis

Sample size calculation was done using G*Power software (version 3.1.9.4). In order to get a statistically significant mean difference of 0.4 MAC (with SD of 1) between down-rolling and centralization at 80% power of study and 95% confidence interval, sample size for down-rolling events came out to be 52 patients. Anticipating a 10% iteration rate, we recruited 60 patients.

Data sets (events of EDEM/EDEP) were divided into two parts: (a) **during induction (DI)** from prospective data and (b) **after induction (AI)** from start to end of surgery (both prospective and retrospective data). The statistical analysis was carried out using Statistical Package for Social Sciences (SPSS Inc., Version 22.0. IBM Corp., Armonk, NY for Windows). Normality of quantitative data like age, HR, MAC, duration, down-rolled and up-rolled eye position score, etc. were checked by Shapiro Wilk test

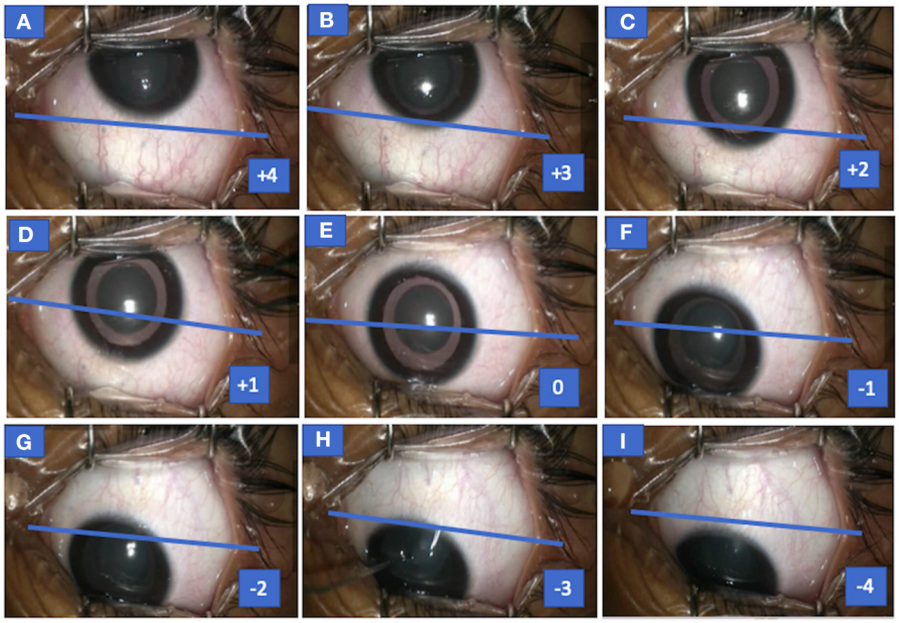

FIGURE 1
Photograph of the left eye of case 1 (congenital cataract) showing both up and down drift with scores for various eye positions. Eye seen in up-drifted position (+4) before the start of surgery (MAC = 1), following which sevoflurane concentration was increased and eye slowly drifted down (+4 to +1) **(A–D)**, became centralized momentarily **(E)** but overshot or drifted in downgaze **(F–I)**, and eye assumed an eccentric position in downgaze (−1 to −4) at MAC = 1.8. MAC, minimum alveolar concentration.

and Kolmogorov-Smirnov test of normality. Normally distributed quantitative variables were presented as mean and SD whereas skewed data were represented as median IQR (Interquartile range). Qualitative or categorical variables like gender, number of down and up movement, propofol given (yes/no), etc. were described as frequencies and proportions. Mean ± SD of MAC and median (IQR) of eye score both during down-rolling and centralization were calculated for both PI and AI data and mean difference and median difference of the two were calculated using paired *t*-test and Wilcoxon Signed Rank test respectively. Median difference of two independent variables (age of PI vs. DI data; eye scores of right vs. left eye, MAC during induction without propofol vs. with propofol before down-drift) were calculated by independent Mann Whitney U test.

Additionally, Median MAC (IQR) during up-rolling and its relationship with down-rolling were studied from AI data. All eye positions including up (4 to >0), central (0), and down (−4 to <0) eye positions with various scores correlated were with DOA (in terms of MAC) for both AI and DI data via Spearman's rank correlation. ROC curve analysis was performed on both AI and DI data to find out MAC cut off value for down movement in two age groups: ≤2 years and >2 years. All inferential statistical tests were two-sided and were performed at a significance level of $p < 0.05$ with 95% confidence Interval (95% CI).

3. Results

In retrospective (R) series, a total of 48 patients were identified to have up-rolling/down-rolling eccentric eye movements or eccentric eye positions intra-operatively among a total of 249 children over 59 weeks. Among them, only 12 patients with downward eccentric position of eyes (with or without upward eccentric eye position) were enrolled. As two patients re-encountered tonic down-rolling during subsequent surgeries, **14** down-rolling events (**after induction/AI**) were included in the study for final analysis.

A total of 62/131 patients were included in the **prospective (P) series**, out of which data of **70** abrupt down-rolling events were populated (**8** events **after induction** from start to end of surgery and **62** events **during induction/DI** of anesthesia).

So, a total of **22 AI** (14 retrospective and 8 prospective) and **62 DI** were included in the final analysis (Table 1). The median age of 74 (62P+ 12R) patients was 2 years (IQR 1–5). There were 32 male and 42 female participants. HR (Median 120; IQR 110–124) was maintained throughout the event. The demographic profile of both retrospective and prospective data is shown in Table 1.

3.1. Depth of anesthesia during down-rolling and centralization

3.1.1. After induction (from start of surgery to end)

Mean MAC of EDEM/EDEP and centralization after induction in 22 events were 1.60 ± 0.25 and 1.18 ± 0.17, respectively, ($p = 0.000$) (Table 2).

3.1.2. During induction

Mean MAC of EDEM/EDEP and centralization during induction in 62 patients was 2.19 ± 0.43 and 1.39 ± 0.26, respectively, ($p = 0.000$). Mean total time passed from start of stage

3 anesthesia (when child got unconscious) to start of down-drift event was 112.79 ± 36.21 s (Table 2).

3.1.3. ROC curve for both DI and AI data

The cut off value of MAC for EDEM/EDEP from ROC curve came out to be 1.65 in ≤2 years (71.7% sensitivity and 95% specificity) and 1.75 in >2 years (78.9%sensitivity and 92.9 % specificity) (Figure 2).

TABLE 1 Demographic profile of retrospective and prospective data.

	Retrospective	Prospective
Number of children analyzed	249	131
Number of patients witnessing down-drift	12	62
Number of down-drift events	14	74
M/F	8:4	24:38
Age	1.375 ± 0.85 years	3.52 ± 2.97 years
Type of ocular surgery	Phacoemulsification-3 Botox injection-8 Posterior capsulotomy-1 Squint Sx-2	Squint Sx-46 Botox injection-16
Distribution of EDEM/DP events	Before start of Sx-7 (2*) During Sx-6 (4*) End of Sx-1(0*)	Before Start of Sx-5 (3*) During Sx-2 (1*) End of Sx-1 (0*)

Sx, surgery; M, male; F, female; EDEM/EDEP, eccentric downward eye movement/eccentric downward eye-positioning.
*Refer to number of patients with up-rolling events preceding down-rolling among them.

3.2. Correlation between DOA and eye position

The median (IQR) eye score at the time of down-drift and correlation between MAC (DOA) and various eye position (scores −4 to +4) for both **AI** and **DI** data-points is shown in Table 2. All eyes were slightly adducted during eccentric positioning in down gaze (opposite of upward and outward positioning in up-gaze). Strong negative correlations between MAC (DOA) and various eye positions for both AI and DI data have been shown in Table 2.

3.3. Age and DOA during EDEM/EDEP

Median age of AI and DI have been shown in Table 2. Their median difference was statistically significant ($p = 0.001$).

3.4. Time duration of down-rolling and return of down-drifted to the central position

3.4.1. After induction

Eccentric down-positioning of eyes partially interrupted the ongoing surgical procedure. When down-positioning of eyes was encountered, anesthetists usually decreased the DOA slightly, on a trial basis toward the recommended lower limit by decreasing the volatile agent. Eccentric downward eye position was maintained till anesthetic depth was slightly lightened when eyes returned to their resting position. All the movements were smooth throughout. Tonic downward

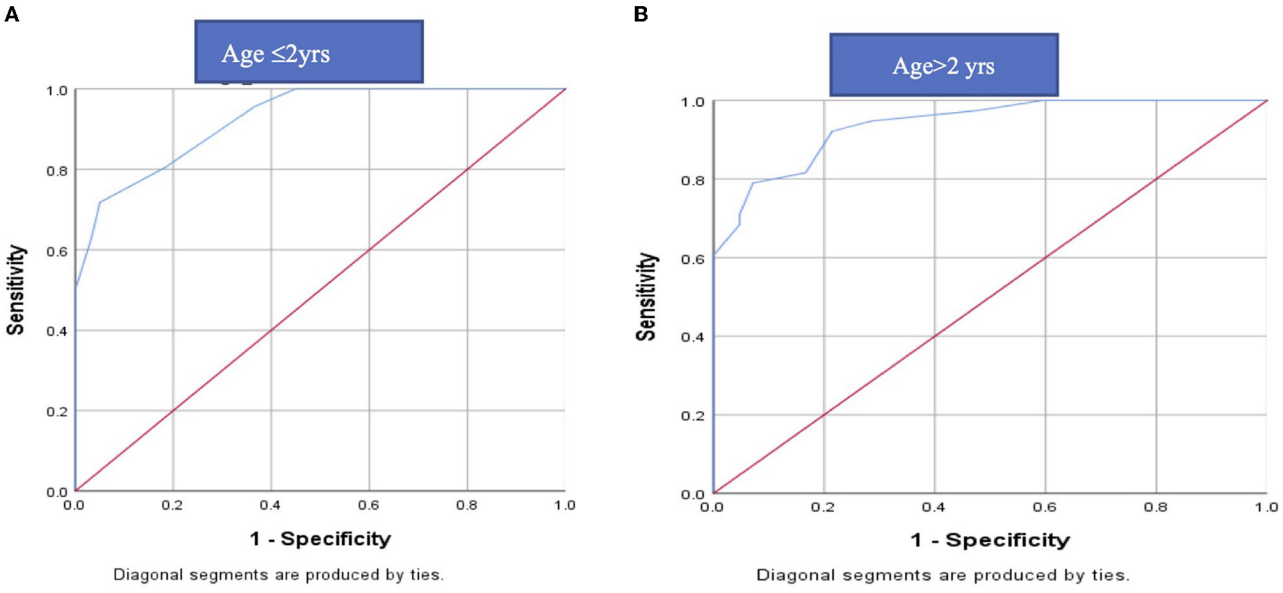

FIGURE 2
ROC curve of MAC for DEEM/EDP in **(A)** ≤2 years and **(B)** > 2 years: The cut off value of MAC for EDEM/ EDEP from ROC curve came out to be 1.65 in ≤2 years (71.7% sensitivity and 95% specificity) and 1.75 in >2 years (78.9%sensitivity and 92.9 % specificity). ROC, receiver operating characteristics; EDEM/EDEP-eccentric downward eye movement/eccentric downward eye-positioning; MAC-minimal alveolar concentration.

TABLE 2 Details of data-sets both after induction (AI) and during induction (DI).

		After induction/AI	During induction/DI	
No of patients analyzed		131 (P)+245 (R) = 376	131 (P)	
No of down-rolling events (patients enrolled)		8 (P) + 14 (R) = 22	62 (P)	
Number of up-rolling events preceding down-rolling		12 (6P+6R)	54	
Median Age (IQR) in years		1.05 (IQR 1–1.5)	3 (IQR 1.06–6)	
		$p = 0.001$		
DOA (Mean MAC)	During start of induction	-*	2.65 ± 0.48	
	During down-roll	1.60 ± 0.25	2.19 ± 0.43	
	centralization	1.18 ± 0.17	1.39 ± 0.26	
	Up-rolling	1 (IQR 0.98–1.1)	NA**	
Mean MAC (IQR) of down-rolling events witnessed immediately after propofol ($n = 20$)		-***	2.0 (1.63–2.3)	$p = 0.022$
Mean MAC (IQR) of down-rolling events witnessed immediately without/before propofol ($n = 42$)			2.25 (2–2.6)	
Recurrence of down-rolling event in same patient		2	2	
Timing (median, IQR)	Time elapsed during induction from the time child loses consciousness (stage 3) to start of down-rolling mean	*	112.79 ± 36.21 s	
	Total time taken in down-rolling from centralized position	10 (8–14) s	9 (8–12) s	
	Total time taken in centralization from down-rolled position	85 (60–117) s	120 (80–165) s	
	Time elapsed from propofol injection to down-rolling of eyes ($n = 20$)	***	10 (8–12) s	
pupil size during down-rolling		2.5(IQR 2–3.5) mm	2(IQR 1.5–2.5) mm	
Eye score	Down-rolling	−3 (IQR −2 to −4)	−3 (IQR −2.5 to −4)	
	Number of asymmetricity	4/22	23/62	
	Up-rolling	2 (1–2.25)	NA**	
correlation between eye position (scores −4 to +4) and DOA (MAC)		−0.714; $p = 0.000$	−0.832; $p = 0.000$	

P, prospective; R, retrospective; M, minimal alveolar concentration; DOA, depth of anesthesia; EDEM/EDEP, eccentric downward eye movement or eccentric downward eye-positioning, IQR, interquartile range.

*Not part of inclusion criteria.

**NA-not applicable as up-rolling of eyes occur transiently during induction, and MAC value at the time of up-rolling do not denote the corresponding depth of anesthesia and hence eye score of up-rolling for induction was not measured.

***Propofol was not given.

movement was quick but the return was comparatively slow and variable depending on varying rates at which the individual anesthetist adjusted DOA and how fast MAC was changed. Median time taken in down rolling from centralized eye position was 10 s (IQR 8–14) and time taken in centralization from eccentric downward position was 85 (IQR 60–117) s (Table 2).

3.4.2. During Induction

Median time taken in down rolling from centralized eye position was 9 (IQR 8–12) s and time taken in centralization from eccentric downward position was 120 (IQR 80–165) s (Table 2).

3.5. Timing of onset of down-rolling and its relationship with upward drift

3.5.1. After induction: down-rolling/positioning of eyes was seen either (a) with upward drift or (b) without upward drift

(a) In 10 events **(4P+6R),** downward drift during surgery was preceded by an **upward drift** (Table 1). In five events, eyes were found up-rolled **before the start of surgery** after cleaning, draping, and using an eye speculum (Figure 1; Supplementary Video 2) and in five events, patients encountered up-rolling after the start of surgery with application of noxious stimuli (e.g., traction, during conjunctival incision). This upward drift was seen when the DOA was on the borderline lighter side in all cases. Documented median

(IQR) MAC in 10 cases at the time of upward drift was **1 (IQR 0.98–1.1)** (Table 2). When anesthetists were informed of the up-rolling of eyes, increase in sevoflurane concentration (increasing MAC) was used as a measure to resolve the problem in all cases. Within a few minutes of increasing MAC, the eye returned to its primary position but, as the procedure was about to be re-started, eyes overshot in down gaze at the same time (Figure 1; Supplementary Video 2).

(b) Downward eye eccentric position of eyes **without upward drift** was seen in 12 patients (8R+4P; Table 1). Seven events of downward eccentric down-positioning were encountered **before the start of surgery** after cleaning and draping when eyes were found eccentrically down-positioned (Figures 3A, E; Supplementary Video 3). Three events occurred **after the start of surgery** during intermittent withdrawal of traction in eye (at the same MAC, when eyes were central and surgery was started; Figure 3D). Eyes also down-rolled during important steps in a few patients e.g., just before re-introducing phacoemulsification probe, injection of Botulinum toxin in medial rectus etc. but fortunately no complications were encountered as during these movements, no instruments were close to important structures of the eye. And two events of downward rolling were witnessed in a patient **at the end of surgery** (Supplementary Figure 5; Supplementary Video 4).

When the surgeons tried to manually rotate the eyes to the central position, difficulty was felt as the tonic downward force was experienced by the surgeons in all cases. The surgical procedure was abandoned for a few minutes as in the presence of an eccentric eye position the continuation of the surgical procedure became unexpectedly difficult.

3.5.2. During induction

At the time of induction all patients witnessed transient up-rolling and outward drift following which down-rolling was witnessed in all cases. But MAC during transient up-rolling in DI data was not analyzed because it was witnessed transiently during beginning of induction when sevoflurane flow was high.

3.6. Relationship of downward drift with anesthetic agent used

3.6.1. After induction

21 episodes of down-rolling which occurred during surgery were maintained on sevoflurane. Only one patient who witnessed down-rolling during switching of sevoflurane to isoflurane (when anesthetic concentration inside lungs became momentarily high) was also included in the study. None of the patients were injected with any intra-venous anesthetic agent (like propofol) prior to witnessing a down-rolling event.

3.6.2. During induction

Induction was performed with sevoflurane and fentanyl in all cases. Propofol was given in 28 out of 62 patients among which 20 patients experienced episodes of down-rolling immediately after propofol injection (median time 10 s) while down-rolling event was noted prior to propofol injection in eight patients. MAC at which downdrift was witnessed immediately after propofol injection was lower compared to MAC at which downdrift was witnessed without/before propofol injection ($p = 0.022$; Table 2).

3.7. Relationship of repeated anesthetic exposure on the incidence of downdrift

3.7.1. After induction

15 patients underwent repeat surgeries under GA without NDMR out of which recurrence of event was seen in five patients.

3.8. Relationship of pupil size with EDEM/EDEP event

No change in pupil size was noted during EDEM/EDEP in both AI and DI data.

3.8.1. After induction

Proparacaine was given to all patients before the start of the procedure. The median pupil size during EDEM/EDEP was 2.5 mm (IQR 1.5–3.5).

3.8.2. During induction

In four patients (three pediatric cataracts and one pseudophakia with posterior capsular opacification), change in pupil size could not be estimated as pupils were pharmacologically dilated for the surgical procedure. In the remaining 18 patients, the median pupil size during EDEM/EDEP was 1.75 mm (IQR 1.5–2 mm).

3.9. Symmetry of eye position between two eyes

3.9.1. After induction

Downward drift was asymmetrical in four patients (Figure 4A). Pre-operative records of one patient revealed eye dissociated in a vertical deviation (Figure 4B).

3.9.2. Before induction

Mild asymmetry in downward drift was seen in 23 patients during down-drift and in extreme eccentric down-drifted position. The median eye score was -2.68 ± 0.99 in the right eye and -2.87 ± 1.01 in the left eye in 23 patients ($p = 0.939$).

4. Discussion

4.1. Depth of anesthesia during down-rolling and centralization

Our study showed that, in absence of muscle relaxant, down rolling of eyes occurred at relatively deeper depths of sevoflurane

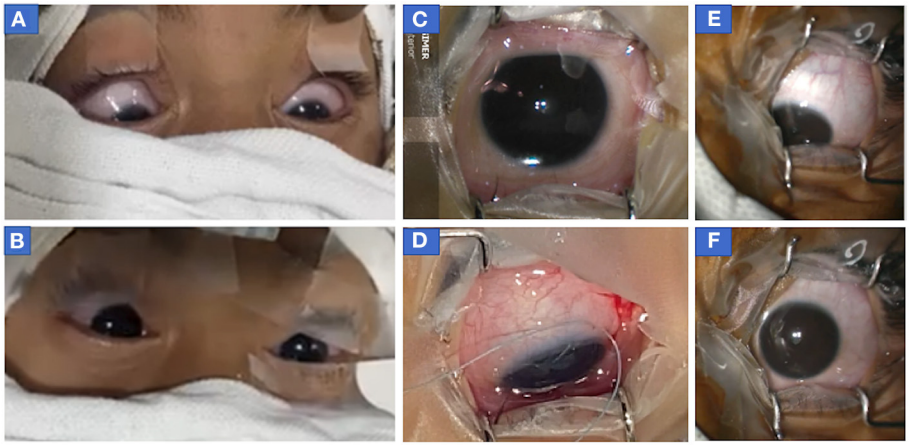

FIGURE 3
Photograph of eyes of patients who showed downdrift alone without updrift. **(A, B)** Both eyes of case 2 (before botulinum injection) showed **(A)** symmetric down-positioning of eyes before the start of surgery (MAC 1.4) when eyes were cleaned, draped, and opened following which **(B)** sevoflurane concentration was decreased and eyes returned to the central position (MAC = 1.2) within a minute of decreasing sevoflurane concentration. It should be noted that recorded values of MAC at the time of intubation were 1.7 and MAC was stabilized to 1.4 within a few minutes of decreasing sevoflurane concentration after intubation when eyes were opened to see their position at the time of cleaning and draping. **(C, D)** The right eye of patient 2 (before second botulinum injection) at 14 months of age in the central position (MAC = 1) at the time of the start of surgery **(C)** but as anesthesia was deepened (to improve oxygen saturation as patient was not able to maintain spontaneous breathing), eye turned in and down **(D)** after temporary release of muscle traction during surgery following passage of traction suture, conjunctival incision, and hooking of muscle. (at MAC = 1.4) **(E, F)** Photographs of eccentric eye positioning in downgaze with slight adduction (toward the nose) in left eye before start of surgery in case 3 (infantile esotropia) (MAC = 1.6) **(E)** and after eye achieved centralized position when the depth of anesthesia was decreased (MAC 1.3). MAC, minimum alveolar concentration.

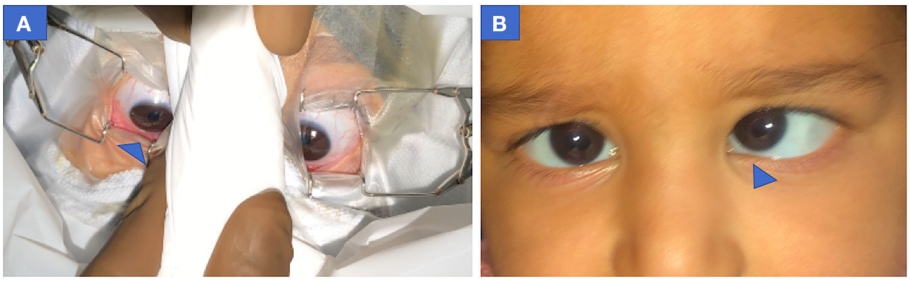

FIGURE 4
Pre-operative photograph of both eyes showing asymmetric down-positioning of eyes in case 4 (infantile esotropia) **(A)** Right eye more down-positioned than left eye at MAC = 2. **(B)** Pre-operative clinical profile of same patient showing esotropia with left eye Dissociated vertical deviation. MAC, minimum alveolar concentration.

anesthesia compared to anesthetic depths at which eyes were centralized. This was demonstrated by the higher value of MAC for EDEM/EDP relative to centralized position ($p = 0.001$) in all cases (both DI and AI data; Table 2). Results of our study matched the finding of Kook's study which mentioned downward eye drift with BIS values below 35 or deep anesthesia (4). Anesthetic depths (MAC) at which these fluctuations in eye position appeared was within permissible anesthetic limits of induction (8) as well as surgery (stage 3 anesthesia). Inhalational agents are known to cause a dose-dependent suppression of reflexes and movements (6). It is said that a complete lack of electrical discharge in the extraocular muscles occurs during deep sleep or deep anesthesia, (6) but our study confirmed that the increasing DOA may not always be effective in centralization of eyes or in reducing eye movements (9).

4.2. Correlation between DOA and eye position

A significant negative correlation of eye score (-4 to +4) with DOA signified that eyes up-rolled in lighter planes, (4) centralized on slight increase, and down-rolled on further deepening the DOA (4). In his study of 32 patients, Kook et al. (2) scored the vertical position of each eye on an ordinal scale from −2 to +6, according to its height in relation to the medial canthus, and studied the relationship between fixed eccentric eye elevation and DOA during surgery. He encountered elevation of the eyes in 83% and downward position of eyes in 2% (one child) with BIS values <35, probably because he maintained a lower concentration of sevoflurane for induction. We did not include BIS in our study because the majority of our children were younger than 2 years old

and values of BIS in infants and young children do not indicate a similar concentration of sevoflurane like adults and hence may not be always reliable (10). Lower values of BIS generally indicate deeper levels of anesthesia which can also be corroborated from the higher values of MAC used in our study.

4.3. Relationship of Age with DOA during down-drift

Average age of children who witnessed a down-rolling event during surgery was lower compared to the age of children witnessing down drift during induction (Table 2). It could be because infants and smaller children are more susceptible to fluctuations in DOA and a higher depth is reached with lower MAC in a very short time. This is also supported by the lower cut off level in infants and younger children than older children shown in ROC curve in our study. Reasons for greater down-drifts in smaller children could be because of the (1) lower threshold for sevoflurane, (2) start of sevoflurane induction prior to placement of intravenous line (as injection of intra-venous agents not possible without sedation) and (3) extended period of high sevoflurane flow due to difficult cannulation in small children. Intravenous agents which are injected in co-operative older children by placing an intra-venous line before starting sevoflurane increase depth of anesthesia and decrease the requirement of sevoflurane. Few older children also witnessed down-drift during induction in our study. Hence the results of our study showed that even though smaller children are more susceptible, there remains risk to older children as well specially with high flow of sevoflurane (high MAC) for prolonged periods like delay in intra-venous cannulation etc.

4.4. Time duration of down-rolling, downward eye positioning, and return of down-drifted to the central position

Our study showed that these movements are swift and the ophthalmologist has to be careful to identify such movement and withdraw instruments carefully if such movements are encountered. Also, the anesthetist must avoid fluctuation in DOA in short surgeries without NDMR and should be aware that eyes shall remain in this down-rolled position till sevoflurane flow, and in turn anesthetic depth, is decreased.

4.5. Timing of onset of down-rolling during GA

4.5.1. During induction

In his study under different depths of general anesthesia, Power et al. (9) observed final eye position in downward direction after induction in a few patients but details including timing, number of down-rolling events, and DOA were never described. Our P-study showed that tonic EDEM/EDEP occurred during induction in 62 out of 132 patients. Such high numbers of down-rolling were witnessed during induction in our study because in general, induction with sevoflurane is rapid (alveolar concentration approaches inspired concentration much more rapidly) and because its flow to lungs is generally kept high during induction. The mean concentration of sevoflurane during induction at which EDEM/EDEP occurred prior to LMA insertion was high (median MAC = 2.65; IQR 2.28–3.0) which matched with other studies (8). In children, where it is common to use a volatile induction, sevoflurane is the preferred choice. In a busy tertiary center like ours with high volume cases it is not uncommon to see reduction of the time for inhalational induction by using a concentration in excess of 1 MAC to speed-up induction as it would take some time for the patient to go to sleep if 1 MAC of volatile was used to induce anesthesia. It is then slowly decreased to the desired level once the child is cannulated and other intra-venous anesthetic agents are given to increase depth of anesthesia which decreases requirement of sevoflurane flow. This is when the supra-glottic device is inserted and then lower flow is sevoflurane is maintained while eyes are centralized and the child is handed to the ophthalmic surgeon.

4.5.2. After induction

Quick induction and failure to lower sevoflurane (below the threshold value for that age group) explains why few children witnessed downward eye-positioning following handing over to the ophthalmic surgeon as it was the extension of down-rolling events during induction which was evident when eyes were opened after cleaning and draping before the start of surgery. Power et al. (9), while studying the DOA in young adults via sevoflurane induction, compared eye signs with EEG polysomnography and showed that the deepest level of sleep was reached on average 3 min before the onset of eccentric ocular positioning, thereby suggesting that eccentric eye movements may occur even when a patient appears satisfactorily anesthetized. This also points toward an understandable lag between anesthetic depth reached at the level of lungs and its effect seen at the level of CNS (eccentric eye positioning). This could be why many of our patients (n = 11) experienced downward movement **before or at the start of surgery** because of the lag between change in anesthetic depth (increase) after induction and start of surgery which might overlap as most of the children witnessed downward movement before/at the start of surgery, depending on DOA and the child's threshold value.

Some children witnessed downward rolling **in the middle or at the end of surgery** potentially because DOA (although MAC was kept constant) varies with the level of stimulus (like traction on eye) the patient is experiencing. This may be illustrated by the fact that one of our patients experienced downward movement at the end of surgery (during conjunctival suturing) on the same MAC eyes were central and was being operated upon. Oculo-cardiac reflex was noticed in two cases following which depth of anesthesia was increased which in turn caused the down-rolling event in one patient.

4.6. Up-rolling and its timing with down-rolling

Many children experienced down-rolling during surgery immediately after up-rolling (Table 1). In our case series, upward drifting of the eyeball was also seen under lighter planes of

anesthesia during surgery in response to any noxious stimuli in the form of pressure on the globe or any manipulation of the eyeball as demonstrated by lower MAC values (median 1.0) (4, 11). Though literature describes slight up-rolling of eyes with the cessation of voluntary eye movement as the point of sufficient anesthetic depth, (12) ocular surgeries are not performed under this anesthetic depth. Rossiter et al. (3) reported its substantial increased incidence without the use of muscle relaxants. Harrad and Stoddart suggested that Bell's phenomenon, a natural protective reflex, which occurs both in the awake state and with lighter planes of anesthesia (though the patient is not awake), may explain the entity (11, 13). The exact neural mechanism is unknown but involves brainstem pathways between the seventh cranial nerve nucleus in the pons and the third cranial nerve nuclear complex in the rostral midbrain. Hiraoka et al. (14) have suggested that the mesencephalic reticular nucleus may play an important role in integrating these two patterns of movement (bilateral lid closure and upward movement of both eyes).

Bell's reflex is extinguished with deep planes of anesthesia, such that the eye remains in the neutral gaze (13, 15). And this upward drift triggered by traction during surgery prompted the anesthetist in our study to increase the DOA to make the eyes return from the upward position following which tonic down shoot of eyes was encountered. This was seen in a few cases and could be because of the attempt to rapidly increase the flow of sevoflurane and rapidly deepen/optimize the anesthetic depth which crossed the threshold for that child.

4.7. Relationship of down-rolling with propofol

4.7.1. During induction

Propofol was given in 28/62 patients in which a down-rolling event was seen immediately after injection in 20 children. Time interval elapsed from propofol injection to down-drift (10 s) matched with the onset of action of propofol (16) (Table 2). Median MAC during which EDEM/EDEP was witnessed immediately after propofol was slightly lower than MAC at which down-rolling was experienced without propofol (Table 2), thereby suggesting a synergistic effect of high sevoflurane flow and propofol in increasing DOA and causing sudden EDEM/EDEP. The remaining 72 patients who did not experience down-rolling and hence were not recruited in the study may have received a low flow of sevoflurane (low MAC during induction) from the start due to quick cannulation or prior injection of propofol and fentanyl before starting induction in co-operative older children.

4.8. Relationship of repeated anesthetic exposure to the incidence of downdrift

Our study showed that the same patient may or may not experience such events again and it depends on sevoflurane flow used during induction and maintained in surgery, threshold for that age, and rapidity at which DOA is changed.

4.9. Relationship of pupil size with anesthetic depth

No change in pupil size (or no dilatation of pupils) occurred throughout the study whether the eyes were centralized or down-rolled, which implies MAC at which down-rolling occurred (highest depth of anesthesia in our study) was also within permissible limits of surgical anesthesia (stage 3) (8). Our study showed that eyes rolled up in the lighter plane of stage 3 anesthesia and down-rolled during deeper planes of stage 3 anesthesia without muscle relaxant. So, there is a **narrow band of anesthetic depth** in which ocular surgery has to be performed. If anesthetic depth goes too low eyes shall roll up and if it gets too deep eyes shall roll down.

4.10. Symmetry between two eyes

Our study showed eyes generally move symmetrically in a downward position but can move asymmetrically (Figure 4). In a majority of cases the difference remained insignificant. Though we could not understand the exact reason for asymmetry, we suspected asymmetric dissociated vertical deviation in the child to alter the eye position in two cases.

4.11. Probable pathophysiology behind downward drift

The pathophysiology of down-rolling under GA is unknown. We tried to hypothesize based on the shared neurochemical and behavioral features of sleep and general anesthesia (17, 18). Various anesthetics have been demonstrated to alter brain systems involved in sleep-wake control (17–19). Many medicines produce general anesthesia that is very comparable to NREM sleep, (20) including a breakdown in efficient cortical communication (21, 22) and inactivation of the thalamus and midbrain reticular formation along with loss of awareness (23). Anesthetized patients' brains may be trapped in an NREM-like state, preventing access to REM sleep and waking (22, 24). In a wakeful state, the mesencephalic reticular development is critical in creating a vertical saccade (25). REM sleep activates cholinergic neurons in the reticular formation (26). The similar velocity-amplitude correlations of rapid eye movements during REM sleep and spontaneous saccades in the dark when awake suggest a shared neural circuit (27). Since eye movements changed with MAC, we hypothesize that a sudden increase in anesthetic concentration (which might have been potentiated with use of prolonged high sevoflurane flow during induction for deepening DOA) caused temporary irritative effects in the central nervous system, causing temporary switching (28) of non-REM to a REM sleep-like state or isolated REM sleep-like traits being expressed during non-REM sleep-like state (29) with activation of the mesencephalic reticular formation and neurons.

The irritative effect of increased anesthetic concentration can be many-fold, although prospective studies are required to evaluate these theories.

1. An increase in sevoflurane concentration (higher MAC) and differential sensitivity of cortical and subcortical areas to sevoflurane concentrations (30). In adults, Mourisse and colleagues (31) found that the blink reflex (brainstem function) was more susceptible to sevoflurane than BIS (forebrain function). The interstitial nucleus of Cajal, the mesencephalic reticular formation, and the posterior commissure are all located at the meso-diencephalic junction (32). Forced downward gaze is prominent in this area's lesions, indicating a vertical gaze plane imbalance (33). In our cases, down gaze neurons in the midbrain were possibly selectively irritated by high flow of sevoflurane (34, 35). Younger children's higher sensitivity to sevoflurane for specific subcortical areas (i.e. mesencephalic control) than older subjects may explain its greater prevalence only in younger children (30) when the threshold was crossed. Different flow rates of anesthetic agent used, different time taken, and different DOA achieved during intubation as well as different DOA (MAC value) on which the patient was stabilized before handing them over to the ophthalmic surgeon for the procedure could be factors influencing the non-occurrence of eye movements during repeat exposures in the same patients.
2. Another potential reason could be related to shortened autoregulation and vasodilatory impact of sevoflurane generating transient reduced cerebral blood flow (CBF) and an irritative effect which reverses when concentration is decreased (36, 37). The lower limits of sevoflurane autoregulation are close to young children's basal mean arterial pressure (38). The fact that our patients' exhibited eye movements beyond 1.5 mean MAC supports this hypothesis, as CBF remains unchanged by sevoflurane up to 1.5 MAC value (36, 39). It is possible that the CBF sensitivity window is quite narrow and specific to each individual. It is likely that the narrow autoregulation limit was violated when the depth went above the child's acceptable limit. The posterior circulation zone supplying the mesencephalic-diencephalic junction comprises structures critical for vertical sight and vergence, (40) and may be transiently impaired, manifesting eye movements. The concentrations at which these downward movements were seen in our cases do not necessarily lead to cerebral ischemia in healthy children. As thousands of sevoflurane inductions are performed every day in children, and neurologic complications are quite rare. The movement occurred only when the MAC level was below or beyond the narrow limit in sensitive children.
3. A third possibility is that sevoflurane is known to excite the neurons in Locus Coeruleus (LC) (41). The LC is a pontine nucleus, with the largest group of noradrenergic neurons in the brain, and is responsible for the tonic maintenance of the wakeful state (42). This nucleus has very widespread projections to cortical and subcortical regions and to the spinal cord (43). In addition, it also projects to the oculomotor nucleus which has been shown to have a high density of α1-adrenoceptors (44, 45). It is plausible that sevoflurane, at higher concentrations, induces the activation of the LC leading to the tonic contraction of the muscles innervated by the oculomotor nerve. As the LC is also involved in maintaining the wakeful state, once the DOA is on the lighter side it is possible that the same scenario of LC activation repeats itself. LC activity, through effects on α2-adrenoceptors in the Edinger-Westphal Nucleus (46, 47), can inhibit pupillary constriction by attenuating the light reflex. This might be the reason why we noticed ocular movement without any pupillary change. The interindividual differences in the specificity of these projections, in addition to the fact that MAC per se has been defined for producing immobility to surgical stimulus in 50% of the population, (48) may explain why these ocular movements are not noticed in every case.

The limitations of our study are the small sample size and absence of EEG monitoring in participants. The sample size limits generalization of reported median MAC values and the usefulness of the association between DOA (MAC value) and eye-positioning score. The sevoflurane flow was changed by anesthetist as per requirement in a child for quick induction which might have influenced the eye movements. Separate studies are required to be done with and without propofol to look for the impact on eye movements. Also, more research is needed on the link between eccentric downward movement, eccentric upward movement, level of anesthesia (using BIS and MAC values), and electrical activity of brain (Electro-encephalogram). In addition to electro-oculogram, we need to explore the tonic force in the inferior rectus to understand the pathophysiology of these eye movements, giving clues into ongoing subcortical processes. Further research is required on the entity's link to anesthetic depth and age. It will be fascinating to see if an anesthetic drug plays a role in halting these motions.

5. Conclusions

Our study concludes that sudden tonic down-drifts of eyes can occur in children without NDMR with the deeper plane of stage 3 sevoflurane anesthesia compared to depths at which eyes are centralized though both depths are adequate and under safe limits of anesthetic depth. This article intends to educate ophthalmologists and anesthetists about this unexpected eye movement during general anesthesia. Knowledge of this is important in short ocular procedures or surgeries under GA, especially without NDMR. In intra-ocular surgeries involving critical steps, muscle relaxants may be used for novices. Our study demonstrates the importance of keeping a stable DOA throughout and avoiding fluctuations. In the event of eye movement, the anesthesia team should be contacted immediately and the surgery should be restarted after the eye movements have stopped, and the eyes have returned to their centralized position.

Data availability statement

The original contributions presented in the study are included in the article/Supplementary material, further inquiries can be directed to the corresponding author.

Ethics statement

The studies involving human participants were reviewed and approved by Institutional Ethics Committee of the Postgraduate Institute of Medical Education and Research, Chandigarh, India. Written informed consent to participate in this study was provided by the participants' legal guardian/next of kin. Written informed consent was obtained from the minor(s)' legal guardian/next of kin for the publication of any potentially identifiable images or data included in this article.

Author contributions

ShC, SLS, SwC, and JR contributed to conception and design of the study. ShC, JS, and SwC organized the database. ShC wrote the first draft of the manuscript. SLS and VG wrote sections of the manuscript. All authors contributed to the article and approved the submitted version.

Acknowledgments

The authors thank Dr. Ashok Kumar for statistical assistance.

Conflict of interest

The authors declare that the research was conducted in the absence of any commercial or financial relationships that could be construed as a potential conflict of interest.

Publisher's note

All claims expressed in this article are solely those of the authors and do not necessarily represent those of their affiliated organizations, or those of the publisher, the editors and the reviewers. Any product that may be evaluated in this article, or claim that may be made by its manufacturer, is not guaranteed or endorsed by the publisher.

Supplementary material

The Supplementary Material for this article can be found online at: https://www.frontiersin.org/articles/10.3389/fmed.2023.1029952/full#supplementary-material

References

1. Guedel AE. *Inhalation Anaesthesia: A Fundamental Guide*. 1st ed. New York, NY: Macmillan (1937). p. 63–4.

2. Kook KH, Chung SA, Park S, Kim DH. Use of the bispectral index to predict eye position of children during general anesthesia. *Korean J Ophthalmol.* (2018) 32:234–40. doi: 10.3341/kjo.2017.0104

3. Rossiter JD, Wood M, Lockwood A, Lewis K. Operating conditions for ocular surgery under general anesthesia: an eccentric problem. *Eye.* (2006) 20:55–8. doi: 10.1038/sj.eye.6701789

4. Chung SA, Jang S, Kook K, Lee JB. Prediction of eye position during general anesthesia using bispectral index monitoring. *Invest Ophthalmol Vis Sci.* (2014) 55:2560.

5. Sakai EM, Connolly LA, Klauck JA. Inhalation anesthesiology and volatile liquid anesthetics: focus on isoflurane, desflurane, and sevoflurane. *Pharmacotherapy.* (2005) 25:1773–88. doi: 10.1592/phco.2005.25.12.1773

6. von Noorden GK, Campos EC. Classification of neuromuscular anomalies of the eyes. In: von Noorden GK, Campos EC, editors. *Binocular Vision and Ocular Motility: Theory and Management of Strabismus*. 6th ed. St. Louis: CV Mosby (2002). p. 110–28.

7. Eger EI, Saidman LJ, Brandstater B. Minimum alveolar anesthetic concentration: a standard of anesthetic potency. *Anesthesiology.* (1965) 26:756–63. doi: 10.1097/00000542-196511000-00010

8. Mudakanagoudar MS, Santhosh MC. Comparison of sevoflurane concentration for insertion of proseal laryngeal mask airway and tracheal intubation in children (correlation with BIS). *Braz J Anesthesiol.* (2016) 66:24–8. doi: 10.1016/j.bjane.2014.07.011

9. Power C, Crowe C, Higgins P, Moriarty DC. Anaesthetic depth at induction: an evaluation using clinical eye signs and EEG polysomnography. *Anaesthesia.* (1998) 53:736–43. doi: 10.1046/j.1365-2044.1998.00468.x

10. Sciusco A, Standing JF, Sheng Y, Raimondo P, Cinnella G, Dambrosio M. Effect of age on the performance of bispectral and entropy indices during sevoflurane pediatric anesthesia: a pharmacometric study. *Paediatr Anaesth.* (2017) 27:399–408. doi: 10.1111/pan.13086

11. Francis IC, Lough head JA. Bell's phenomenon. A study of 508 patients. *Aust J Ophthalmol.* (1984) 12:15–21.

12. Snow JD. On the inhalation of the vapour of ether in surgical operations. *Br J Anaesth.* (1953) 25:253–67. doi: 10.1093/bja/25.3.253

13. Harrad RA, Stoddart P. Operating conditions for ocular surgery under general anaesthesia: an eccentric problem. *Eye.* (2007) 21:256–7. doi: 10.1038/sj.eye.6702487

14. Hiraoka M. Physiological study of the Bell's phenomenon in human. *Acta SOC Ophthalmol Japan.* (1979) 83:2184–90.

15. Griffiths AN, Marshall RW, Richens A. Saccadic eye movement analysis as a measure of drug effects on human psychomotor performance. *Br J Clin Pharmacol.* (1984) 18 Suppl 1:73S—82S. doi: 10.1111/j.1365-2125.1984.tb02584.x

16. Condello I, Santarpino G, Fiore F, Di Bari N, Speziale G, Moscarelli M, et al. Propofol pharmacokinetics and pharmacodynamics-a perspective in minimally invasive extracorporeal circulation. *Interact Cardiovasc Thorac Surg.* (2021) 33:625–7. doi: 10.1093/icvts/ivab143

17. Lydic R, Baghdoyan HA. Sleep, anesthesiology, and the neurobiology of arousal state control. *Anesthesiology.* (2005) 103:1268–95. doi: 10.1097/00000542-200512000-00024

18. Franks NP. General anaesthesia: From molecular targets to neuronal pathways of sleep and arousal. *Nat Rev Neurosci.* (2008) 9:370–86. doi: 10.1038/nrn2372

19. Lu J, Nelson LE, Franks N, Maze M, Chamberlin NL, Saper CB. Role of endogenous sleep-wake and analgesic systems in anesthesia. *J Comp Neurol.* (2008) 508:648–62. doi: 10.1002/cne.21685

20. Karan SB, Perlis M, Ward D. Anesthesia and sleep medicine: An opportunity to be mutually informative? *Semin Anesth Perioper Med Pain.* (2007) 26:42–8. doi: 10.1053/j.sane.2007.06.002

21. Ferrarelli F, Massimini M, Sarasso S, Casali A, Riedner BA, Angelini G, et al. Breakdown in cortical effective connectivity during midazolam-induced loss of consciousness. *Proc Natl Acad Sci U S A.* (2010) 107:2681–6. doi: 10.1073/pnas.0913008107

22. Massimini M, Ferrarelli F, Huber R, Esser SK, Singh H, Tononi G. Breakdown of cortical effective connectivity during sleep. *Science.* (2005) 309:2228–32. doi: 10.1126/science.1117256

23. Alkire MT, Haier RJ, Fallon JH. Toward a unified theory of narcosis: brain imaging evidence for a thalamocortical switch as the neurophysiologic basis of anesthetic-induced unconsciousness. *Conscious Cogn.* (2000) 9:370–86. doi: 10.1006/ccog.1999.0423

24. Mashour GA, Lipinski WJ, Matlen LB, Walker AJ, Turner AM, Schoen W, et al. Isoflurane anesthesia does not satisfy the homeostatic need for rapid eye movement sleep. *Anesth Analg.* (2010) 110:1283–9. doi: 10.1213/ANE.0b013e3181d3e861

25. King WM, Fuchs AF. Reticular control of vertical saccadic eye movements by mesencephalic burst neurons. *J Neurophysiol.* (1979) 42:861–76. doi: 10.1152/jn.1979.42.3.861

26. Brown RE, Basheer R, McKenna JT, Strecker RE, McCarley RW. Control of sleep and wakefulness. *Physiol Rev.* (2012) 92:1087–187. doi: 10.1152/physrev.00032.2011

27. Bahill AT, Clark MR, Stark L. The main sequence, a tool for studying human eye movements. *Math Biosci.* (1975) 24:191–204. doi: 10.1016/0025-5564(75)90075-9

28. Hayashi Y, Kashiwagi M, Yasuda K, Ando R, Kanuka M, Sakai K, Itohara S. Cells of a common developmental origin regulate REM/non-REM sleep and wakefulness in mice. *Science.* (2015) 350:957–61. doi: 10.1126/science.aad1023

29. Mashour GA. Rapid eye movement sleep and general anesthesia. *Anesthesiology.* (2010) 112:1053. doi: 10.1097/ALN.0b013e3181d3d3c3

30. Bourgeois E, Sabourdin N, Louvet N, Donette FX, Guye ML, Constant I. Minimal alveolar concentration of sevoflurane inhibiting the reflex pupillary dilatation after noxious stimulation in children and young adults. *Br J Anaesth.* (2012) 108:648–54. doi: 10.1093/bja/aer459

31. Mourisse J, Lerou J, Struys M, Zwarts M, Booij L. Multi-level approach to anaesthetic effects produced by sevoflurane or propofol in humans: 1. BIS and blink reflex. *Br J Anaesth.* (2007) 98:737–45. doi: 10.1093/bja/aem104

32. Bhidayasiri R, Plant GT, Leigh RJ. A hypothetical scheme for the brainstem control of vertical gaze. *Neurology.* (2000) 54:1985–93. doi: 10.1212/WNL.54.10.1985

33. Keane JR. The pretectal syndrome: 206 patients. *Neurology.* (1990) 40:684–90. doi: 10.1212/WNL.40.4.684

34. Sharpe JA. Neural control of ocular motor systems. In: Miller NR, Newman NJ, editors. *Walsh and Hoyt's Clinical Neuro-Ophthalmology.* 5th edition. Baltimore:, Williams & Wilkins (1998). P. 1101–88.

35. Pierrot-Deseilligny C, Chain F, Gray F, Serdaru M, Escourolle R, Lhermitte F. Parinaud's syndrome: electro-oculographic and anatomical analyses of six vascular cases with deductions about vertical gaze organization in the premotor structures. *Brain.* (1982) 105:667–96. doi: 10.1093/brain/105.4.667

36. Rhondali O, Mahr A, Simonin-Lansiaux S, De Queiroz M, Rhzioual-Berrada K, Combet S, et al. Impact of sevoflurane anesthesia on cerebral blood flow in children younger than 2 years. *Paediatr Anaesth.* (2013) 23:946–51. doi: 10.1111/pan.12166

37. Goettel N, Patet C, Rossi A, Burkhart CS, Czosnyka M, Strebel SP, et al. Monitoring of cerebral blood flow autoregulation in adults undergoing sevoflurane anesthesia: a prospective cohort study of two age groups. *J Clin Monit Comput.* (2016) 30:255–64. doi: 10.1007/s10877-015-9754-z

38. Vavilala MS, Lee LA, Lam AM. The lower limit of cerebral autoregulation in children during sevoflurane anesthesia. *J Neurosurg Anesthesiol.* (2003) 15:307–12. doi: 10.1097/00008506-200310000-00003

39. Fairgrieve R, Rowney DA, Karsli C et al. The effect of sevoflurane on cerebral blood flow velocity in children. *Acta Anaesthesiol Scand.* (2003) 47:1226–30. doi: 10.1046/j.1399-6576.2003.00248.x

40. Choi KD, Jung DS, Kim JS. Specificity of "peering at the tip of the nose" for a diagnosis of thalamic hemorrhage. *Arch Neurol.* (2004) 61:417–22. doi: 10.1001/archneur.61.3.417

41. Yasui Y, Masaki E, Kato F. Sevoflurane directly excites locus coeruleus neurons of rats. *Anesthesiology.* (2007) 107:992–1002. doi: 10.1097/01.anes.0000291453.78823.f4

42. Jones BE. The role of noradrenergic locus coeruleus neurons and neighboring cholinergic neurons of the pontomesencephalic tegmentum in sleep-wake states. *Prog Brain Res.* (1991) 88:533–43. doi: 10.1016/S0079-6123(08)63832-7

43. Loughlin SE, Foote SL, Fallon JH. Locus coeruleus projections to cortex: topography, morphology and collateralization. *Brain Res Bull.* (1982) 9:287–94. doi: 10.1016/0361-9230(82)90142-3

44. Carpenter MB, Periera AB, Guha N. Immunocytochemistry of oculomotor afferents in the squirrel monkey (Saimirisciureus). *J Hirnforsch.* (1992) 33:151–67.

45. Day HE, Campeau S, Watson SJ Jr, Akil H. Distribution of alpha 1a-, alpha 1b- and alpha 1d-adrenergic receptor mRNA in the rat brain and spinal cord. *J Chem Neuroanat.* (1997) 3:115–39. doi: 10.1016/S0891-0618(97)00042-2

46. Heal DJ, Prow MR, Butler SA, Buckett WR. Mediation of mydriasis in conscious rats by central postsynaptic alpha 2-adrenoceptors. *Pharmacol Biochem Behav.* (1995) 50:219–24. doi: 10.1016/0091-3057(94)00299-X

47. Costa VD, Rudebeck PH. More than meets the eye: the relationship between pupil size and locus Coeruleus activity. *Neuron.* (2016) 89:8–10. doi: 10.1016/j.neuron.2015.12.031

48. Szabo EZ, Luginbuehl I, Bissonnette B. Impact of anesthetic agents on cerebrovascular physiology in children. *Pediatr Anesth.* (2009) 19:108–18. doi: 10.1111/j.1460-9592.2008.02826.x

frontiers | Frontiers in Medicine

TYPE Review
PUBLISHED 20 June 2023
DOI 10.3389/fmed.2023.1212314

OPEN ACCESS

EDITED BY
Horace Massa,
Hôpitaux Universitaires de Genève (HUG), Switzerland

REVIEWED BY
Davide Borroni,
Riga Stradiņš University, Latvia
Prema Padmanabhan,
Sankara Nethralaya, India

*CORRESPONDENCE
Darren Shu Jeng Ting
✉ ting.darren@gmail.com

RECEIVED 26 April 2023
ACCEPTED 30 May 2023
PUBLISHED 20 June 2023

CITATION
Deshmukh R, Ong ZZ, Rampat R, Alió del Barrio JL, Barua A, Ang M, Mehta JS, Said DG, Dua HS, Ambrósio R Jr and Ting DSJ (2023) Management of keratoconus: an updated review.
Front. Med. 10:1212314.
doi: 10.3389/fmed.2023.1212314

Management of keratoconus: an updated review

Rashmi Deshmukh[1], Zun Zheng Ong[2], Radhika Rampat[3], Jorge L. Alió del Barrio[4,5], Ankur Barua[6], Marcus Ang[7], Jodhbir S. Mehta[7], Dalia G. Said[2,8], Harminder S. Dua[2,8], Renato Ambrósio Jr[9,10,11] and Darren Shu Jeng Ting[6,8,12]*

[1]Department of Cornea and Refractive Surgery, LV Prasad Eye Institute, Hyderabad, India, [2]Department of Ophthalmology, Queen's Medical Centre, Nottingham, United Kingdom, [3]Department of Ophthalmology, Royal Free London NHS Foundation Trust, London, United Kingdom, [4]Cornea, Cataract and Refractive Surgery Unit, Vissum (Miranza Group), Alicante, Spain, [5]Division of Ophthalmology, School of Medicine, Universidad Miguel Hernández, Alicante, Spain, [6]Birmingham and Midland Eye Centre, Birmingham, United Kingdom, [7]Singapore National Eye Centre, Singapore Eye Research Institute, Singapore, Singapore, [8]Academic Ophthalmology, School of Medicine, University of Nottingham, Nottingham, United Kingdom, [9]Department of Cornea and Refractive Surgery, Instituto de Olhos Renato Ambrósio, Rio de Janeiro, Brazil, [10]Department of Ophthalmology, Federal University of the State of Rio de Janeiro (UNIRIO), Rio de Janeiro, Brazil, [11]Federal University of São Paulo (UNIFESP), São Paulo, Brazil, [12]Academic Unit of Ophthalmology, Institute of Inflammation and Ageing, College of Medical and Dental Sciences, University of Birmingham, Birmingham, United Kingdom

Keratoconus is the most common corneal ectatic disorder. It is characterized by progressive corneal thinning with resultant irregular astigmatism and myopia. Its prevalence has been estimated at 1:375 to 1:2,000 people globally, with a considerably higher rate in the younger populations. Over the past two decades, there was a paradigm shift in the management of keratoconus. The treatment has expanded significantly from conservative management (e.g., spectacles and contact lenses wear) and penetrating keratoplasty to many other therapeutic and refractive modalities, including corneal cross-linking (with various protocols/techniques), combined CXL-keratorefractive surgeries, intracorneal ring segments, anterior lamellar keratoplasty, and more recently, Bowman's layer transplantation, stromal keratophakia, and stromal regeneration. Several recent large genome-wide association studies (GWAS) have identified important genetic mutations relevant to keratoconus, facilitating the development of potential gene therapy targeting keratoconus and halting the disease progression. In addition, attempts have been made to leverage the power of artificial intelligence-assisted algorithms in enabling earlier detection and progression prediction in keratoconus. In this review, we provide a comprehensive overview of the current and emerging treatment of keratoconus and propose a treatment algorithm for systematically guiding the management of this common clinical entity.

KEYWORDS

artificial intelligence, refractive surgery, contact lens, cornea, corneal cross-linking, corneal transplant, intracorneal ring segment, keratoconus

1. Introduction

Keratoconus was first reported by Benedict Duddell in 1736 (1). Following its first description, various terminologies such as prolapses corneae, cornea conica, sugar-loaf cornea, and procidentia corneae, were introduced in the early literature (2). Around a century later, John Nottingham provided the first detailed description of the disease in his landmark publication in 1854 (2, 3). Pickford described the conical cornea as a disease that is "intractable in nature and fatal to vision" and one in which "the pathology and treatment are so little understood." Around 170 years later, keratoconus remains an enigmatic disease.

Over the past few decades, rapid advancement in diagnosing and managing keratoconus has been observed. Originally described as a rare disease by the National Institute of Health with an incidence of less than 1 per 2,000 people (4), it is now known that keratoconus is much more common than originally thought. The reported prevalence is highly variable from 0.2 per 100,000 in Russia (5) to 33 per 1,000 in Iran (6). A meta-analysis from 15 countries reported a global prevalence of 1.4 per 1,000 (7). A higher prevalence is noted in Asian and Middle Eastern populations. Pediatric populations have a higher prevalence rate, with a reported prevalence rate ranging from 5.2 per 1,000 people in New Zealand to 47.9 per 1,000 people in Saudi Arabia (8, 9). In addition, it is one of the most common indications for keratoplasty in many countries (10, 11). Nonetheless, some countries have reported a decreasing trend in the number of keratoplasty for keratoconus in view of the implementation of corneal cross-linking (12, 13).

Etiology of keratoconus is multifactorial, with environmental and genetic factors playing important roles (14, 15). Atopy, eye rubbing, and exposure to ultraviolet rays are some of the recognized risk factors. Familial aggregation of the disease has been noted in several studies indicating a genetic transmission (16). In the Collaborative Longitudinal Evaluation of Keratoconus (CLEK) study, around 13.5% of the patients reported a positive family history (17). The most common mode of inheritance described is autosomal dominant with incomplete penetrance and variable expression (18). However, a study based on a segregation analysis on 95 families suggested a possibility of autosomal recessive inheritance (19). Offspring of consanguineous marriages are also reportedly affected more than those of non-consanguineous marriages, indicating an autosomal recessive inheritance (20). The recent discovery and characterization of pre-Descemet's layer has also improved the understanding of keratoconus and acute corneal hydrops, a rare but well-recognized complication of keratoconus (21–24).

Until the end of the 21st century, the management of keratoconus has been largely restricted to spectacles, rigid contact lens (CL) and keratoplasty (in advanced cases) for refractive and visual correction. Wollensak et al. (25) described a highly innovative and minimally invasive technique – corneal cross-linking (CXL) using the Dresden protocol – to halt the progression of keratoconus and reduce the need for keratoplasty. Since then, a variety of treatment protocols and techniques have been introduced to further optimize the clinical efficacy, efficiency, and safety of CXL. These include modifications such as accelerated CXL, transepithelial CXL, Epi-Flap CXL, pulsed UV light, and many others (26–34). Other surgical techniques, particularly intrastromal corneal ring segments (ICRS) and anterior lamellar keratoplasty (ALK), have been developed. In addition, there has also been a recent increased interest in the refractive surgical management of patients with keratoconus.

In this review, we aim to: (1) provide a comprehensive overview of the current therapeutic modalities of keratoconus; (2) propose a systematic and practical treatment algorithm; and (3) discuss the future directions of the management of keratoconus.

2. Important factors for consideration for treatment

The choice of treatment is contingent upon a combination of factors, including host factors (e.g., age, atopy, tolerance to CL, and visual requirement/expectations), clinical factors (e.g., severity and progression of keratoconus, location of the cone, corneal thickness, and presence of scarring or previous hydrops), and surgeons' experience and expertise (35). A number of classifications have been proposed and used in the clinic to enable a more consistent grading of the severity of keratoconus, including the commonly used Amsler-Krumeich classification (36), Belin ABCD grading system (37), Keratoconus Severity Score (38), and several others (**Table 1**) (15, 39). The diagnosis of keratoconus has been well covered by a few recent excellent review articles (15, 35), and is beyond the scope of our article.

The progression of keratoconus has been defined in several ways based on a combination of visual acuity, refraction, and tomographic/topographic indexes. Various parameters have been used in the literature and clinic to define progression (33, 40–42). These include:

- *Visual acuity:* subjective or objective decrease in vision by 1 Snellen line or more
- *Refraction:* increase in cylinder on manifest refraction by 1 D or more over 1 year
- *Keratometry:* increase in K2 (keratometry at the steepest meridian) or Kmax (maximum keratometry) by 1 D or more over 1 year
- *Corneal thickness:* progressive decrease (no definite quantitative value provided).

In 2015, the Global Delphi Panel of Keratoconus and Ectatic Disease has established a global consensus on the definition, concepts, diagnosis, clinical management, and surgical treatment of keratoconus and ectatic diseases (43). They have defined ectasia progression by a consistent change in at least two of the following parameters:

(1) Progressive steepening of the anterior corneal surface;
(2) Progressive steepening of the posterior corneal surface; and
(3) Progressive thinning and/or an increase in the rate of corneal thickness change from the periphery to the thinnest point.

More recently, the Belin ABCD Progression Display has also been introduced as an extension of the Belin ABCD grading system to detect and monitor the progression of keratoconus (44). This progression grading system considers both the anterior

TABLE 1 Classification and grading of keratoconus based on Amsler-Krumeich classification and Belin ABCD grading system.

Amsler-Krumeich classification					
	Eccentric CS	Refraction*	Mean central keratometry	CT	Scarring
Stage 1	Yes	<5 D	<48 D	>400 μm	No
Stage 2	Yes	5–8 D	<53 D	>400 μm	No
Stage 3	Yes	8–10 D	>53 D	300–400 μm	No
Stage 4	Yes	Not measurable	>55 D	200 μm	Yes
Belin ABCD grading system					
	A (ARC; 3 mm zone)	B (PRC; 3 mm zone)	C (thinnest pachymeter)	D (BDVA)	Scarring
Stage 0	>7.25 mm (<46.5 D)	>5.90 mm (<57.25 D)	>490 μm	= 20/20	–
Stage 1	>7.05 mm (<48.0 D)	>5.70 mm (<59.25 D)	>450 μm	<20/20	–, +, ++
Stage 2	>6.35 mm (<53.0 D)	>5.15 mm (<65.5 D)	>400 μm	<20/40	–, +, ++
Stage 3	>6.15 mm (<55.0 D)	>4.95 mm (<68.5 D)	>300 μm	<20/100	–, +, ++
Stage 4	<6.15 mm (>55.0 D)	<4.95 mm (>68.5 D)	≤300 μm	<20/400	–, +, ++

CS, corneal steepening; CT, corneal thickness; ARC, anterior radius of curvature in the 3.0 mm zone centered on the thinnest location of cornea; PRC, posterior radius of curvature in the 3.0 mm zone centered on the thinnest location of cornea; BDVA, best-corrected-distance-visual-acuity. *Refraction refers to myopia and/or astigmatism.

and the posterior corneal surfaces, which increases the sensitivity for detecting any early progression of the disease. Based on all the factors mentioned above, we propose a treatment algorithm as a practical (instead of prescriptive) guidance for managing keratoconus (**Figure 1**).

3. Conservative treatment

Eye rubbing, often in the context of ocular allergy, is often the main underlying predisposing factor for the development and progression of keratoconus (45–47). Therefore, avoidance of eye rubbing and a reasonable control of the underlying ocular allergy is crucial during the management of keratoconus. Studies have shown that a good control of ocular allergy can reduce the risk of disease progression, development of acute hydrops, and post-keratoplasty complications such as loose corneal graft sutures, persistent epithelial defect, and steroid-induced cataract (48–50). In recognition of the importance of patient education, a public awareness campaign, named the Violet June, was started in Brazil in 2018 to raise awareness of keratoconus and importance of avoiding eye rubbing in reducing the disease severity and its wider impact on the society (51). In addition, dry eye management is often required as the condition is common among patients with keratoconus who wear CL, irrespective of the types of CL used (52).

In the early stages of keratoconus, spectacles or soft CL may serve as a useful, first-line conservative treatment in providing satisfactory refractive and visual corrections. Refractive errors are commonly measured with manifest clinical refraction but may be objectively aided by ocular wavefront analysis (35). However, as the disease often affects the eyes asymmetrically, many affected individuals remain asymptomatic until one eye is significantly affected or both eyes are considerably affected, rendering the above treatment options unsatisfactory. Occasionally, early detection of the disease may occur by chance during routine eye screening by optometrists in the community and/or ophthalmologists.

The use of CL in cases with keratoconus was first introduced by Fick (53). Since then, significant advancement has been made in the designs of CL used for keratoconus. In general, the use of CL in keratoconus depends on the stage of keratoconus, the location of the cone, and patient's variable tolerance to CL. Soft toric CL offers the advantage of increased comfort. However, they cannot correct higher order aberrations (HOAs) and are best suited for early keratoconus (54). When used in advanced stages, conflicting results have been reported, with some authors finding it difficult to fit these CLs (55) while others report good results (56, 57). Rigid gas permeable (RGP) CL is the preferred option for keratoconic corneas. Customized RGP CL has been introduced to address the challenges in the fitting of traditional RGP CL (58). Studies have shown good RGP CL fitting in stage 2 and stage 3 keratoconus (56), though the vision-related quality of life (VR-QoL) is reduced when they were used for corneas with keratometry values exceeding 52 D (58).

When RGP CL wear is not tolerated, several other options are available to improve CL tolerance in patients with keratoconus. Hybrid CLs consist of a central rigid zone with a peripheral soft skirt, which provides better comfort and potentially better visual acuity than those using RGP CLs (59). They are better fitted for patients with stage 1 and stage 2 keratoconus and have been shown to improve their VR-QoL (59). However, hybrid CLs are associated with potential increased risks of giant papillary conjunctivitis, corneal edema, and vascularization (60, 61). Mini-scleral and scleral CLs are strong alternatives to RGP corneal CLs in patients with very steep or irregular corneas seen in advanced keratoconus (62). These CLs have a larger diameter and rest on the sclera without touching the limbus and the cornea, building a fluid reservoir between the posterior surface of the CL and the cornea that helps in evening out the irregularities and maintaining epithelial health. The prosthetic replacement of ocular surface ecosystem (PROSE) CL has been shown to be highly effective in patients with excessive HOAs (63). They are also particularly beneficial in patients with keratoconus having co-existing ocular surface disease (64). Piggyback CL, consisting of a soft bandage CL and an overlying RGP CL, also serves as another valuable option for vision

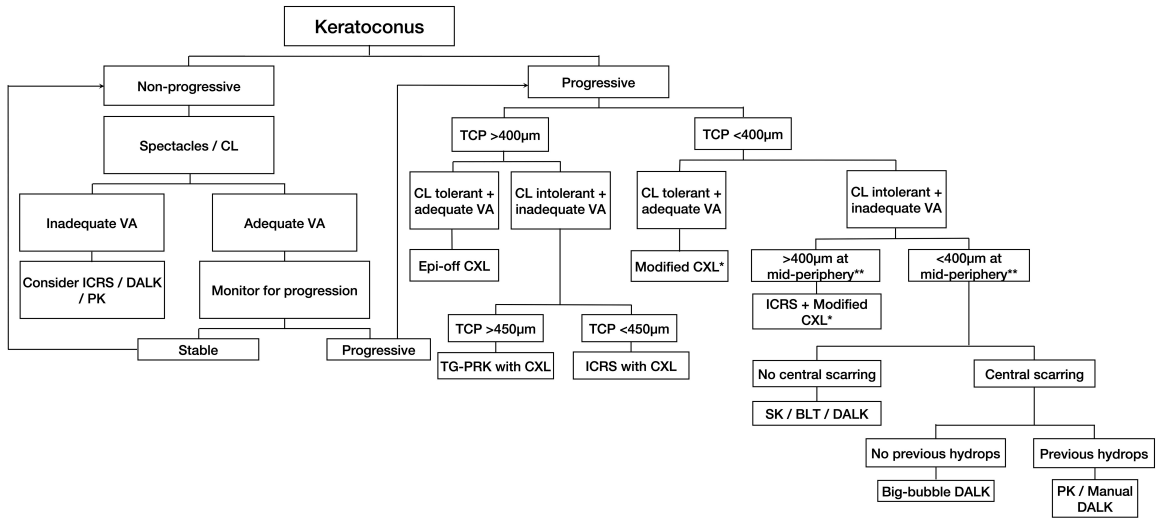

FIGURE 1
A proposed treatment algorithm for guiding the management of keratoconus. CL, contact lens; VA, visual acuity; ICRS, intracorneal ring segments; DALK, deep anterior lamellar keratoplasty; PK, penetrating keratoplasty; TCP, thinnest corneal pachymetry; CXL, corneal cross-linking; TG-PRK, topographic guided-photorefractive keratectomy; SK, stromal keratophakia; BLT, Bowman's layer transplantation; DM, Descemet membrane. *Modified CXL includes transepithelial, iontophoresis-assisted, lenticule-assisted, CL-assisted, and adapted fluence CXL. **Corneal thickness at the mid-periphery/tunneling site for ICRS implantation.

correction in patients with keratoconus who are intolerant to RGP CL and scleral lens (65).

4. Surgical treatment

4.1. Corneal cross-linking

Corneal cross-linking (CXL) refers to the formation of covalent bonds between collagen molecules which results in biomechanical tissue strengthening (66). Physiological age-related collagen cross-linking has been shown to occur naturally whereby the diameter of the corneal collagen fibrils increases by up to 4.5% in an individual's lifetime (67). Researchers noted that diabetic patients rarely developed keratoconus due to glycosylation-related collagen cross-linking and developed a technique for chemical CXL in biomechanically weaker corneas such as in keratoconus (68). The University of Dresden described the process of CXL using riboflavin and ultraviolet (UV-A) as a treatment modality for keratoconus. A complex photochemical reaction consisting of aerobic and anaerobic phases leads to the formation crosslinks between collagen molecules (69). Studies have also shown that CXL strengthens the cornea via cross-linking of the collagen molecules and non-collagen molecules (70, 71); therefore, the term "corneal cross-linking," instead of "corneal collagen cross-linking," is more commonly used in current practice.

Since the original CXL technique was described, several modifications have been described and used to reduce the time and increase the efficiency of CXL in stabilizing keratoconus. The long-term efficacy and safety of CXL have also been well-established (71, 72), though postoperative complications such as infectious keratitis, reactivation of herpes simplex keratitis, acute hydrops, endothelial damage, and corneal haze/scar may occur (**Figure 2**) (73, 74).

4.1.1. Epithelium-off techniques

4.1.1.1. Dresden protocol (conventional protocol)

The Dresden protocol or the conventional protocol of CXL (C-CXL) was originally described by Wollensak et al. (25). Since then, several prospective and retrospective studies have established the efficacy of C-CXL in halting the progression of keratoconus (42, 75, 76). The technique involves epithelial debridement in the central 8–9 mm zone followed by soaking the cornea in 0.1% riboflavin solution for 30 min before irradiating the cornea with 370 nm UV-A light (3 mW/cm^2 for 30 min) to achieve a surface dose of 5.4 J/cm^2. This technique is currently considered as the standard for CXL and is often performed in outpatient settings. The corneal epithelium can be removed using alcohol (33, 77, 78), hockey knife (79), Amoils brush (80), or transepithelial phototherapeutic keratectomy (PTK) (81, 82). Removal of the hydrophobic corneal epithelium facilitates adequate riboflavin penetration and imbibition into the stroma, allowing for effective UV-A induced photochemical reactions and subsequent CXL. The degree of riboflavin penetration affects the depth of UV-A radiation absorption thereby affecting the extent of CXL. Immediate post-CXL corneal haze and/or apoptosis of keratocytes in the anterior and middle stroma, which is often observed as a demarcation line in the anterior segment optical coherence tomography (AS-OCT), may serve a surrogate marker for the depth of CXL (83, 84).

Studies on corneal biomechanics have proven the stiffening effect of CXL on animal as well as human corneas (85, 86). C-CXL has also been shown to improve the corneal curvature reducing the corneal steepening and improving visual acuity (87, 88). Corneal thinning is noted up to 3 months post-surgery after C-CXL, which slowly recovers by 1 year (89–91). However, Kim et al. (92) demonstrated that even after 5 years, there was a

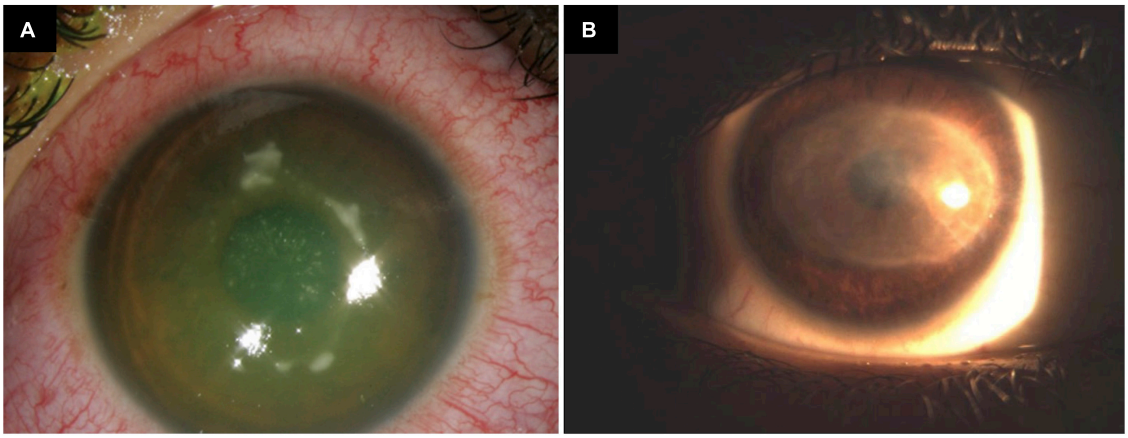

FIGURE 2
Infectious keratitis following epithelium-off corneal cross-linking for progressive keratoconus. **(A)** Active infection. **(B)** Resolved infection with a visual debilitating corneal scar.

statistically significant reduction in corneal thickness as compared to the pre-CXL values. In general, CXL achieves better efficacy when performed in early keratoconus as compared to advanced keratoconus (33, 93). Innovative approach such as Epi-Flap CXL has also been described, which is shown to be associated with less postoperative pain and anterior stromal haze when compared to conventional epithelium-off CXL (34).

4.1.1.2. Accelerated protocol

The concept of accelerated CXL (A-CXL) is based on the Bunsen-Roscoe law of photochemical reciprocity, which states that the total energy remains unchanged if the irradiation duration is reduced with a corresponding increase in the intensity of irradiation (69). The main advantages of A-CXL include reduced treatment duration and a possible reduced risk of infection (94). Several protocols for A-CXL have been described, including the use of 9 mW/cm^2 for 10 min, 18 mW/cm^2 for 5 min, and 30 mW/cm^2 for 3 min, all of which result in a surface dose of 5.4 J/cm^2 (33, 95, 96). Larger dose of radiation such as 7.2 J/cm^2 (with 30 mW/cm^2 radiation for 3 min) has been described, though it may lead to increased risk of corneal haze (97). Laboratory studies analyzing the corneal stiffening following CXL have shown comparable efficacy of C-CXL with A-CXL (98, 99). A large *ex vivo* study showed that the Bunsen-Roscoe law of reciprocity is valid only up to irradiation intensities of 40–50 mW/cm^2 and for more than 2 min. At higher intensities and shorter duration, the biomechanical stiffening can rapidly decrease (100).

Many large clinical studies have demonstrated the clinical efficacy and safety of A-CXL in halting progressive keratoconus in adult patients (33, 101–103). The potential benefit and safety of A-CXL has also recently been substantiated in pediatric patients with progressive keratoconus. Larkin et al. (104) recently conducted the KERALINK study, a phase 3 clinical trial which included 60 patients aged 10–16 years with progressive keratoconus. It demonstrated a significantly beneficial effect of A-CXL [using continuous UV light with 10 mW/cm^2 over 9 min (total energy of 5.4 J/cm^2)] in halting the progression of pediatric keratoconus when compared to those receiving standard care (which included refraction testing with provision of glasses and/or CL fitting). CXL was offered to the standard care group if there was confirmed disease progression but this was not provided earlier than 9 months after randomization. The reported follow-up period was 18 months.

A meta-analysis of 11 studies evaluating the efficacy and safety between A-CXL and C-CXL demonstrated similar postoperative outcomes, in terms of mean keratometry (K_{mean}), uncorrected-distance-visual-acuity (UDVA), and corrected-distance-visual-acuity (CDVA) (105). However, A-CXL was shown to achieve less reduction in maximum keratometry (K_{max}) but with less impact on corneal thickness and endothelial cell density when compared to C-CXL. The observed difference in the effect (in K_{max}) may be attributed to less energy penetration into the cornea hence less corneal biomechanical stiffening in the A-CXL group, evidenced by shallower corneal demarcation line in A-CXL when compared to C-CXL (69, 84). Touboul et al. (106) reported a corneal demarcation line at a depth of 100–150 μm using a 30 mW/cm^2 irradiance protocol for 3 min. This is possibly due to the shorter riboflavin soaking time of 10 min in their study. Studies with riboflavin soakage for 15 min have reported the demarcation line to be deeper than 200 μm (26, 107). Kymionis et al. (108) found a demarcation line at a mean of 288–290 μm, using a protocol of 9 mW/cm^2 for 10 min. A study comparing the depth of demarcation lines in two groups of patients undergoing A-CXL with 18 mW/cm^2 for 5 min and different riboflavin soakage times (20 and 30 min) found that it was deeper in the group with longer soakage time before UV-A irradiation (109).

Favorable outcomes have also been reported in terms of keratometric flattening and improvement in visual acuity using A-CXL (110, 111). Razmjoo et al. (112) reported comparable improvement in visual acuity and refractive astigmatism after A-CXL and C-CXL. The photochemical reaction during CXL is known to be oxygen-dependent (113). Accelerated protocols with higher fluence raised concerns about oxygen depletion during CXL, resulting in a reduced stiffening effect. This led to the concept of using pulsed light during irradiation instead of continuous light. Pulsing the light allows more oxygen availability and more singlet oxygen release for CXL (30). Comparative studies of continuous

light A-CXL and pulsed light A-CXL have revealed a deeper demarcation line when pulsed light was used, with the latter achieving a better efficacy (30, 114). Studies have shown that pulsed light A-CXL is effective in halting the progression of keratoconus up to 2 years after the procedure (115, 116).

4.1.2. Epithelium-on techniques

4.1.2.1. Transepithelial CXL

CXL without epithelial debridement has been described to reduce the risk of infectious keratitis and improve patient comfort after the procedure (74, 117–119). However, riboflavin, a hydrophilic substance with a high molecular weight, does not penetrate through an intact hydrophobic epithelium easily (120). This issue is overcome by using permeability enhancers like ethylene-diamine-tetra-acetic acid (EDTA), benzalkonium chloride (BAC), trometamol, and gentamicin (121, 122). The riboflavin-soaked epithelium also absorbs UV radiation resulting in an attenuated effect of CXL (123). Studies have shown that transepithelial CXL is less effective in halting progression in keratoconus than C-CXL (124). Bottós et al. (125) suggested that the reduced effect of transepithelial CXL is due to inadequate stromal concentration of riboflavin rather than reduced UV transmittance. Reduced oxygen diffusion into the stroma due to an intact epithelium also attenuates the effect of CXL (126). It has been estimated that corneal biomechanics improves by 64% following transepithelial CXL as compared to 320% after C-CXL (127). The demarcation line after transepithelial CXL is also reportedly shallower than C-CXL (127). The use of pulsed treatment (1 s on, 1 s off) to improve oxygen concentration has improved the results at 1-year follow-up (128). A study by Caporossi et al. (28) reported that the UDVA and CDVA improved up to 3–6 months then gradually returned to the preoperative level. Keratoconus was noted to be stable up to 1 year, however there was a subsequent worsening noted at 2-year follow-up. They used riboflavin with dextran and EDTA, and trometamol as the permeability enhancers. Another study done using riboflavin with BAC 0.01% reported a progression of keratoconus in 46% eyes at 1-year follow-up (129). Other studies have concluded that, although limited, there is a definite favorable effect of transepithelial CXL (130, 131). A recent Cochrane review of 11 studies reported that transepithelial CXL and epithelium-off CXL confer similar efficacy on keratoconus stabilization (132). Another approach recently described by Mazzotta et al. (133) is to increase the fluence to 7 J/cm^2 and use pulsed UV light. This approach has been termed as Transepithelial Enhanced Fluence Pulsed M Accelerated Crosslinking (EFPL-M-CXL).

4.1.2.2. Iontophoresis-assisted CXL

Riboflavin is a negatively charged, small molecule with a molecular weight of 376.4 g/mol. Penetration of riboflavin into the corneal stroma (via an intact layer of epithelium) can be enhanced using iontophoresis, a non-invasive technique employed to facilitate the movement of ionized molecules (134). In this technique, the active electrode is placed over the cornea with a suction ring, while the passive electrode is placed on the cervical vertebrae or on the patient's forehead. The annular suction ring on the cornea is then rinsed with 0.1% riboflavin in distilled water until the grid is submerged. A small current of 1 mA is then applied for 5 min. Once adequate stromal soakage by riboflavin is confirmed through slit-lamp examination, the cornea is then irradiated with UV-A light (135, 136).

Studies have shown that iontophoresis-assisted CXL (I-CXL) was effective in halting progression at 1-year follow-up (135, 137). The depth of the corneal demarcation line has been reported to be at 210 μm with no significant corneal haze (135). Studies comparing C-CXL and I-CXL in early keratoconus have shown comparable effects in stabilizing progressive keratoconus (138, 139). Another study reported that at a 2-year follow-up, I-CXL could halt keratoconus, albeit less efficiently than C-CXL (80 vs. 92.5%). They reported a demarcation line at a depth of 216 μm observed in 35% of cases. The failure rate reported was 20% with I-CXL as compared to 7.5% with conventional CXL (140). Similar to transepithelial CXL, the efficacy of I-CXL is reduced by the presence of intact corneal epithelium due to decreased oxygen diffusion. Secondly, the riboflavin-soaked epithelium is likely to reduce the UV transmittance. A study by Mastropasqua et al. (141) showed that riboflavin saturation achieved in I-CXL was deeper than transepithelial approach, but shallower than the conventional epithelium-off CXL approach.

Some potential advantages do exist with I-CXL. Studies have shown that contrast sensitivity function was transiently better after I-CXL than C-CXL during early postoperative period (first 3 days), which is likely attributed to the inflammatory effect during the wound healing process following epithelial debridement in C-CXL (142, 143). However, the significant difference observed between the two groups was normalized by 1 week postoperative. In addition to the reduction of the riboflavin soakage time to 5 min, it also offers the advantages of intact epithelium such as reduced pain and lower chances of infectious keratitis (118, 144).

4.1.3. Modified techniques for thin corneas

4.1.3.1. Lenticule-assisted CXL

Sachdev et al. (145) first described an innovative lenticule-assisted CXL technique in three patients where tailored stromal expansion was used for corneas <400 μm, utilizing lenticules extracted from patients undergoing small incision lenticule extraction (SMILE). Following epithelial debridement, a stromal lenticule of appropriate thickness derived from a patient undergoing SMILE for myopic correction was placed on the cornea to be cross-linked. The lenticule was centered over the apex of the cone. Riboflavin 0.1% was instilled every 5 min for 30 min, and UV-A radiation was given as in the Dresden protocol. The effectiveness and safety of this technique was observed throughout their 6-month study, evidenced by the keratometric stability, minimal/no effect on the endothelial cell density, and a corneal demarcation line of 280–300 μm (suggesting that the posterior stroma and endothelium is spared). The thickness of the lenticule can also be customized according to the corneal thickness of the treated eye. Further modification was described by Cagini et al. (146) where they prepared the lenticule using femtosecond laser (FSL) on donor corneas and standardized the lenticule thickness to 100 μm. Their study included 10 eyes of eight patients, and the demarcation line at 1 month was comparable to C-CXL technique. Further studies are needed to determine the efficacy and safety of this technique.

4.1.3.2. Contact lens-assisted CXL

The technique of CL-assisted CXL (CL-CXL) was first described by Jacob et al. (147) in 2014 in their pilot study of 14 eyes with thin cornea. In this technique, the cornea was soaked with riboflavin for 30 min after epithelial debridement. A CL was also soaked in riboflavin solution simultaneously for 30 min. This riboflavin-soaked CL was then placed on the cornea before UV irradiation was started. Intra-operative pachymetry was done to confirm the thickness to be >400 μm. UV-A irradiation was then given as in the Dresden protocol. Placing a CL on the thin cornea increases the available thickness of the cornea by approximately 100 μm. Usually a CL with negligible power is chosen. The hydrophilicity of the CL is another factor to be considered. A more hydrophilic CL absorbs more riboflavin and hence more UV-A radiation, thereby reducing the transmission of UV-A to the stroma and affecting the effect of CXL (148). Wollensak et al. (148) compared the biomechanical efficacy of CL-CXL with C-CXL in porcine eyes and found that CL-CXL was about one-third less efficacious than C-CXL. Using Brillouin microscopy, Zhang et al. (149) reported that the localized corneal stiffening effect after CL-CXL was up to 70% that after standard CXL. Both groups showed a higher cross-linking effect in the anterior cornea than in the middle and posterior cornea. Knyazer et al. (150) performed CL-CXL using the accelerated protocol on 24 eyes with keratoconus. Progression was halted in 80% of cases with no evidence of damage to the corneal endothelium.

4.1.3.3. Adapted fluence CXL

Approaches like CL-CXL and hypotonic riboflavin have their drawbacks of having limited biomechanical strengthening (151). Kling and Hafezi (152) suggested that the rate-limiting factor in CXL is the irradiation time rather than the UV fluence or irradiance. If the fluence or irradiance is varied, it would be possible to perform CXL in corneas thinner than 400 μm since the threshold for endothelial cell toxicity would not be surpassed. Based on this theory, they proposed an algorithm for CXL in thin corneas where the fluence was adapted according to the pre-irradiation thickness. In their retrospective analysis of 39 eyes, they found a significant correlation between the irradiation time and the demarcation line depth. At 1-year follow-up, progression of keratoconus was halted in 90% of the patients and none of the patients developed endothelial decompensation (153). Further studies are needed to assess the long-term stability of such cases.

4.2. Intracorneal ring segments

In 1949, Dr. Barraquer explored the placement of an intracorneal device to correct a patient's myopia, though this approach has become obsolete for this indication (154). It was only in 2000 that Colin et al. (155) reported the ability of implanted devices, now known as ICRS, to reduce corneal steepening in keratoconic eyes with some improvement in UDVA, CDVA, and tolerance to CL wear.

This technique works on the principle that adding tissues at the corneal periphery confers a centrally flattening effect (known as the arc shortening effect) (154). Patients with keratoconus whose vision can no longer be corrected adequately with spectacles or those intolerant to CL wear may benefit from this minimally invasive and reversible procedure. Other less common indications for ICRS include irregular astigmatism post-penetrating keratoplasty (PK) or deep anterior lamellar keratoplasty (DALK), post excimer laser corneal ectasia, astigmatism post radial keratotomy, and pellucid marginal degeneration. Whilst PK and DALK can be the next surgical step in keratoconus patients with visual impairment not correctable by spectacles or CLs, ICRS serves as a useful surgery to bridge the gap, delay or even eliminate the need for keratoplasty (**Figure 3**). There has also been some debate on whether or not ICRS prevents disease progression, with some studies supporting its long-term stabilizing effect whilst the others did not (156–160).

Since the first human ICRS implantation report in the early nineties (161), various types of polymethyl methacrylate (PMMA)-based ICRS have now become widely available globally (**Table 2**). When considering ICRS implantation in keratoconus patients, ideally the cornea should be without scarring, though recent evidence suggests that corneas with mild apical haze may still benefit from ICRS (162).

Pre-operatively, one may consider an implantation checklist including but not exhaustive of the following: (1) CDVA of 20/30 or worse; (2) CL intolerance; (3) corneal thickness of more than 400 μm at the site of the tunnel; (4) steep keratometry less than 62 D; (5) adequate stromal bed around the rings (thickness of the ring cannot exceed half that of the corneal thickness); and (6) patient's acceptance of a moderate and slow improvement in CDVA as management of the patient's expectation is key (163, 164). Though pediatric patients have been implanted with ICRS, it is more commonly accepted to be placed in patients 18 years of age or older (165, 166).

So far, ICRS has been shown to be an effective method in managing keratoconus, with many recent studies reporting a significant improvement in UDVA, CDVA, refraction, and keratometric readings (**Table 3**) (159, 167–175). In a sizeable multi-centered study of 611 eyes with varying degree of keratoconus, Vega-Estrada et al. (176) observed a significant improvement in UDVA in all cases of keratoconus and CDVA in the majority of cases (except for mild keratoconus with 0.1 logMAR vision or better). This suggests that ICRS is most beneficial in grade I to III keratoconus. In addition to symmetric ICRS implantation, there have recently been some studies reporting the potential benefit of asymmetric ICRS implantation for keratoconus. However, the evidence is largely limited to short follow-up and small sample size (177, 178). Furthermore, novel progressive thickness ICRS (i.e., one end of the ring is thicker than the other end) has been successfully used to treat keratoconic eyes with non-uniform irregularities, resulting in a progressive corneal flattening effect (179, 180). Recently, Alfonso-Bartolozzi et al. (181) also reported using FSL-assisted, Ferrara-type ICRS to effectively correct astigmatism (≥3.00 D) following DALK.

There are a few contraindications to ICRS implantation, including advanced keratoconus with more than 65 D keratometry (62–65 D being a gray area), corneal opacity, severe atopic disease, eye rubbing, immunological diseases, corneal dystrophy, pregnancy, and breastfeeding (164). Patients with a history of herpetic eye disease as well as those on isotretinoin, amiodarone, and sumatriptan are not favorable candidates. Wound healing may be affected in patients with diabetes and severe atopic disease. It is also preferable to avoid patients with large pupils, as the chances

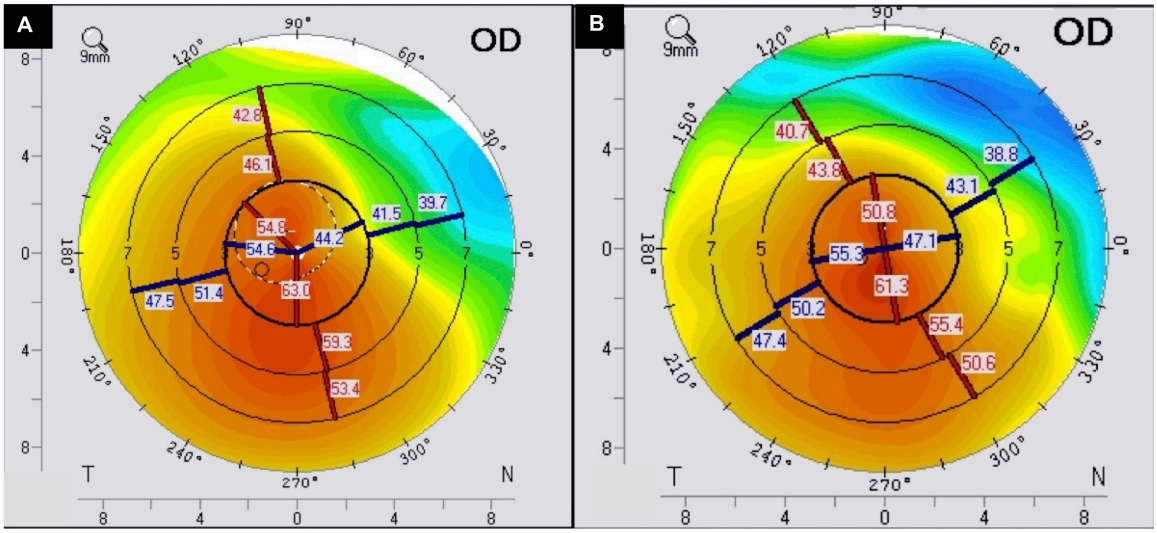

FIGURE 3
A case of intracorneal ring segments (ICRS) implantation for treating stable moderate keratoconus. The **(A)** preoperative and **(B)** postoperative corneal topography demonstrates an improvement in the regularity of the cornea following ICRS.

TABLE 2 A summary of different types of intracorneal segment rings.

Type/company	Number of segments	Cross section	Size (μm)	Diameters (Int/Ext)	Arc length (degree)	Optical zones (mm)
Keraring, Mediphacos, Brazil	2	Triangle	150–350 (50 steps)	5/6	90, 120, 150, 160, 210, 340, 355	5, 5.5, 6
Ferrara, Ferrara Ophthalmics, Brazil	2	Triangle	150–350 (50 steps)	4.4/5.6	90, 100, 110, 120, 130, 140, 150, 160, 170, 180, 190, 210, 320	5, 6
Intacs, Addition Technology, Lombard, IL, USA	2	Hexagon	250–450 (50 steps)	6.7/8.1	150, 210	7
Intacs SK, Addition Technology, Lombard, IL, USA	2	Oval	210–500 (50 steps)	6/7	90, 130, 150	6
Corneal Ring, VisionTech, Brazil	2	Fusiform	150–350	4.7/6	155–220	5, 6
MyoRing, Dioptex GmbH, Austria	1	Triangle	200–320	5–8	360	5–8
KentacX, Plus (Imperial Medical Technologies Europe GmBH)	2	Triangle with rounded corners	100–450 (25 steps)	4.5–5.7	45, 90, 120, 160, 210, 320, 355	5.4–5.6
Bisantis (Opticon 2000 SpA y Soleko SpA)	Up to 4	Oval	150	3.5	80	3.5, 4, 4.5

of inducing HOAs are high. Corneal topography, aberrometry and assessment of the corneal biomechanics are helpful.

Different nomograms exist for each type of ring, with the size and position usually planned by the manufacturers based on refraction and tomography (Figure 4). For example, for Kerarings, one must send the refraction and tomography, including the four refractive maps, four topometric maps, one color map, and a corneal Zernike analysis to the 6th order over a maximum 6 mm pupil. It is thought that refractive and topographic cylinders should be within 15° of each other for a better result (look at K1 and refractive cylinder axis) (164). Usually, two segments are placed, with thinner segments for mild cases. ICRS may be placed by manual dissection or FSL dissection, where a tunnel or channel is created in the deep corneal stroma. Studies have shown that both FSL and manual dissection techniques result in similar improvement in visual, refractive and topographic outcomes, though the FSL technique has a better safety profile with a lower complication rate (164, 182).

Complications of ICRS include ring exposure or extrusion (Figure 5), broken ring segments, segment migration, recurrent erosion, corneal melt, perforation, vascularization, and infectious keratitis (183–185). Coskunseven et al. (186) reported 1.3% of cases had segment migration, 0.2% cases of corneal melting, and 0.1% case of mild infection, with an overall complication rate of 5.7% (49 out of 850 eyes). Long-term stability has been shown in adults but less so in the pediatric population, associated with a higher chance of progression (156, 187–192). Variable thickness ICRS and Long Arc Length ICRS are both being explored, though their effectiveness is less in advanced keratoconus, which is similarly observed in ICRS in general (172, 178). The explantation rate due to complications or poor visual outcomes (including halo and glare) is considered relatively low.

TABLE 3 A summary of the recent studies evaluating the effectiveness and stability of intracorneal ring segment (ICRS) for keratoconus.

References	Number of eyes	Intervention	Visual outcomes	K change (D)	Stability	Follow-up duration
Costa et al. (159)	124	Ferrara	UDVA (logMAR): 0.91 ± 0.36 (preop) to 0.46 ± 0.32 (postop), CDVA (logMAR): 0.40 ± 0.27 (preop) to 0.22 ± 0.20 (postop)	K_{max}: −1.8	Stability: 90.3%	5 years
Peris-Martínez et al. (171)	61	Ferrara	UDVA (logMAR): 0.89 ± 0.52 (preop) to 0.44 ± 0.34 (postop)	K_{max}: −4.0	Stable (8.2% extrusion)	2 years
de Araujo et al. (169)	34	Ferrara	CDVA (logMAR): 0.32 ± 0.19 (preop) to 0.46 ± 0.27 (postop)	K_{max}: −3.1	Stability: 74%	5 years
Warrak et al. (175)	932	Intacs	Both UDVA and CDVA improved significantly	K_{max}: −3.8	Stability: 97.3%, extrusion rate: 0.4%	3 years
Prisant et al. (172)	82	Keraring	UDVA (logMAR): 0.82 (preop) to 0.46 (postop), CDVA (logMAR): 0.31 (preop) to 0.21 (postop), Mean change in SE: 0.8 D	K_{max}: −3.3	Stable (but short follow-up)	3 months
Abdellah and Ammar, (168)	38	Keraring 355	UDVA (logMAR): 0.93 ± 0.21 (preop) to 0.63 ± 0.21 (postop), Mean change in SE: 2.9 D	K_{max}: −3.4	High rate of extrusion (31.5%) and instability	3 years
Kang et al. (170)	30	Intacs	UDVA (logMAR): 0.86 ± 0.46 (preop) to 0.74 ± 0.37 (postop), CDVA (logMAR): 0.52 ± 0.30 (preop) to 0.40 ± 0.30 (postop), Mean change in SE: 1.1 D	K_{mean}: −2.9	Only stable cases were included in this study.	5 years
Torquetti et al. (174)	138	Ferrara 320	UDVA (logMAR): 1.1 (preop) to 0.3 (postop), CDVA (logMAR): 0.7 (preop) to 0.3 (postop), Mean change in SE: 3.7 D	K_{mean}: −5.5	Stable (but short follow-up)	6 months
Abd Elaziz et al. (167)	30	Keraring 355	CDVA (decimal): 0.22 ± 0.17 (preop) to 0.49 ± 0.22 (postop), Mean change in SE: 7.6 D	K_{max}: −8.6	Stability: 90%, migration/extrusion: 10%	6 months
Sandes et al. (173)	58	Ferrara 140	CDVA (logMAR): 0.5 ± 0.2 (preop) to 0.3 ± 0.21 (postop)	K_{mean}: −2.5	Good stability with 88% retainment rate	17 months

UDVA, uncorrected-distance-visual-acuity; CDVA, corrected-distance-visual-acuity.

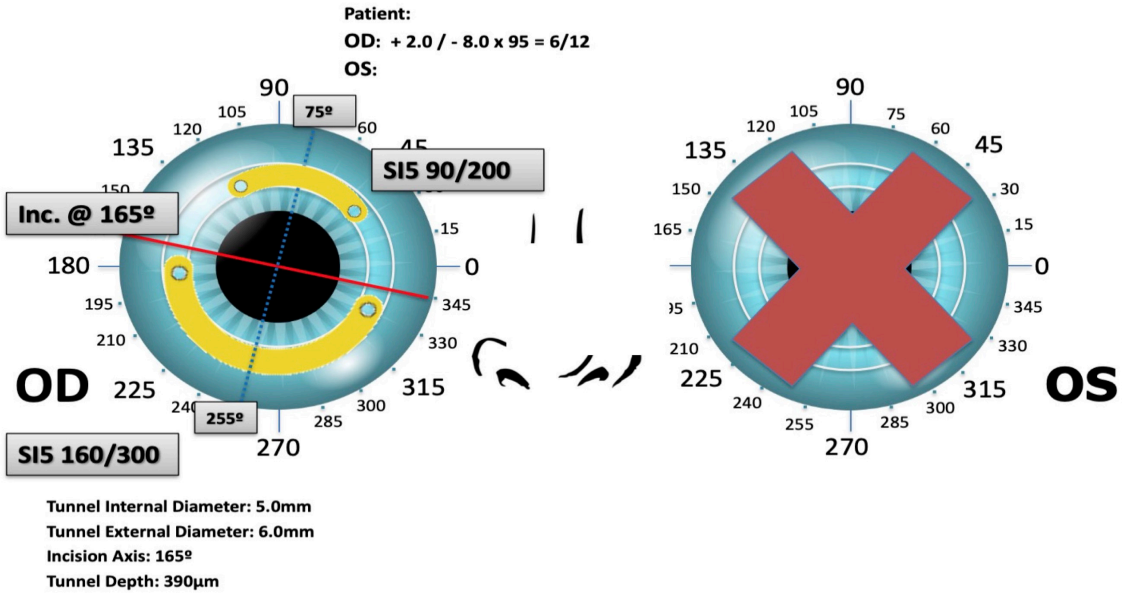

FIGURE 4
Surgical planning of Keraring intracorneal ring segments implantation based on preoperative refraction and tomography.

To improve the biocompatibility and biointegration of ICRS within the host cornea, Jacob et al. (193) described a novel technique of corneal allogenic intrastromal ring segments (CAIRS) combined with CXL to manage patients with stage I to IV keratoconus. A customized double-bladed trephine with outer diameter 7.5 mm and inner diameter 6.7 mm was used to cut the donor corneal rims into ring-like segments. The lenticules were crosslinked and cut into two halves akin to INTACS segments and

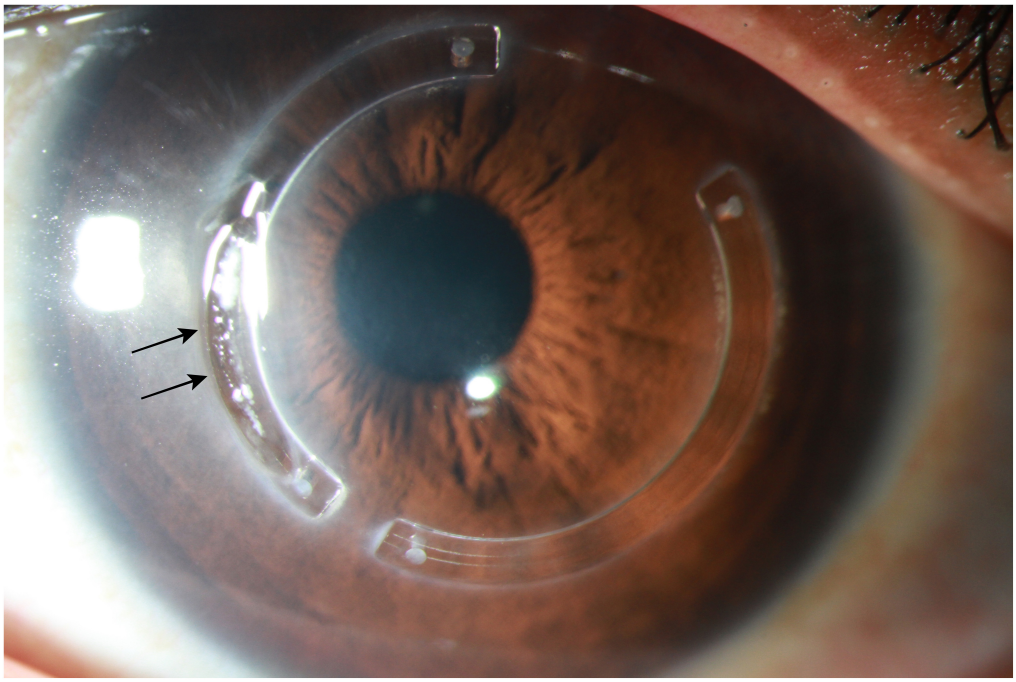

FIGURE 5
Slit-lamp photograph demonstrating an extrusion of intracorneal ring segments (black arrows), which is a well-recognized complication.

inserted intrastromally at 50% depth of the thinnest pachymetry at 7 mm zone. Their study of 24 eyes (20 patients) showed a significant improvement in UDVA, CDVA, and steepest keratometry values at 18 months after the procedure. None of the patients had displaced or extruded segments. Transient dehydration of the CAIRS before insertion has also been described to reduce the surgical learning curve and aid insertion of thicker segments for more severe keratoconus (where the cornea is very thin and insertion of thick segments are technically challenging) (194). Another similar study was conducted by Jafarinasab and Hadi (195) where they created ring-like stromal segments from the anterior lamellae left after preparing DSAEK lenticules. The authors reported an improvement in CDVA without a significant difference in refractive or topographic astigmatism.

In summary, ICRS, based on either synthetic material or human donor cornea, serves a safe, effective, reversible, and adjustable surgical option for managing keratoconus, with variable outcomes dependent on the differing experiences between surgeons and units.

4.3. Combined CXL-keratorefractive surgeries

It is well known that keratorefractive surgeries may result in postoperative corneal ectasia, particularly in patients with underlying undetected mild keratoconus or forme fruste keratoconus (196). Therefore, keratorefractive surgery is traditionally contraindicated for eyes with keratoconus. However, with the growing experience in CXL and refractive surgery over the past decade, more clinicians are combining these two procedures, simultaneously (on the same day) or sequentially, to visually and refractively rehabilitate patients with keratoconus (35, 197, 198). "CXL plus" is a term coined in 2011 to refer to any CXL combined with refractive surgery to treat corneal ectasia (199). CXL and ICRS, either coupled or decoupled, have shown a significant improvement in keratometry (200). The results of this can be enhanced further with refractive surgery such as topography-guided photorefractive keratectomy (TG-PRK) (201).

Multiple combinations exist for CXL plus, including PRK, transepithelial PRK (t-PRK), TG-PRK, transepithelial TG-PRK, and wavefront-guided PRK (WG-PRK). Combined with varying CXL protocols and intra- and inter-person variability (as part of the nature of the disease), it is understandable why optimum parameters are difficult to determine. However, there is cumulative evidence in the literature demonstrating the long-term effectiveness and safety of various CXL plus procedures, including CXL + ICRS (189, 202–204), CXL + PRK/PTK (205–212), and CXL + PRK/PTK ± phakic IOL implantation (**Table 4**) (213–217).

To date, several protocols of CXL plus have been developed and implemented:

- TG-PRK (max 80 μm) then high-fluence CXL (known as the Athens protocol) (218)
- tPTK then CXL (known as the Cretan protocol) (219)
- tPTK then PRK + CXL (known as the Cretan Plus protocol) (220)
- Selective transepithelial TG-PRK with simultaneous accelerated CXL (STARE-X) (221)
- CXL + ICRS (203)
- CXL + ICRS + transepithelial TG-PRK (214)
- CXL + ICRS + toric phakic IOL + TG-PRK (222)
- CXL + ICRS + TG-tPRK (I-TRESK/CXL) (217).

TABLE 4 A summary of some of the recent studies examining the effectiveness and safety of corneal cross-linking (CXL) plus procedures for managing keratoconus (this is not an exhaustive list).

References	Number of eyes	Intervention	Visual outcome	Refractive/K changes	Complications	F/U (months)
CXL + ICRS						
Hersh et al. (203)	198	CXL + ICRS (concurrent vs. sequential)	Concurrent: UDVA improved 0.17 logMAR, CDVA improved 0.09 logMAR, Sequential: UDVA improved 0.24 logMAR, CDVA improved 0.14 logMAR	K_{max}: −2.2 D (concurrent) vs. −2.7 (sequential)	2 (1%) cases of microbial keratitis (1 in each group)	6
Renesto Ada et al. (204)	39	Intacs vs. CXL then Intacs	Intacs: UDVA improved 0.16 logMAR, CDVA improved 0.13 logMAR, CXL/Intacs: UDVA improved 0.33 logMAR, CDVA improved 0.22 logMAR	No difference between groups for all K values	Nil	24
Kilic et al. (189)	131	Same-day Intacs + epi-on CXL	UDVA improved 0.26 ± 0.16 logMAR, CDVA improved 0.24 ± 0.16 logMAR	Kmean: −4.5 D	Nil	1–25
Coskunseven et al. (202)	48	CXL then ICRS vs. ICRS then CXL	CXL/ICRS: UDVA improved 0.18 decimal, CDVA improved 0.17 decimal, ICRS/CXL: UCVA improved 0.21 decimal, BCVA improved 0.33 decimal	CXL/ICRS: K_{mean}: −4.2 D ICRS/CXL: K_{mean}: −4.0 D	8 eyes with stromal edema (resolved by 3 months)	13
CXL + PRK/PTK						
Iqbal et al. (207)	125	PRK + CXL (Athens) vs. CXL alone	CXL: UDVA improved 0.54 logMAR, PRK + CXL: SE reduced 2.3 D, UDVA improved 0.68 logMAR	CXL: K_{mean}: −2.1 D, SE reduced 2.3 D, PRK + CXL: K_{mean}: −1.4 D, SE reduced 2.3 D	CXL: 12.1% haze, 1.7% stromal scar CXL + PRK: 5.9% haze, 1.3% stromal scar	24
Ohana et al. (212)	98	Athens	UDVA improved 1.23 logMAR, CDVA no improvement	K_{mean}: −4.0 D	5% significant haze	12–36
Nattis et al. (211)	62	CXL then TG-PRK	Ref: UDVA 20/100 to 20/60 CDVA 20/50 to 20/30	Ref: K_{mean}: −0.4 D, Topo: no change	Nil	6
Gore et al. (206)	47	Athens	CDVA improved 0.13 logMAR	K1: −1.1 D, K2: −5.4 D	Microbial keratitis (2%)	24
Kontadakis et al. (210)	60	TG-tPRK + CXL vs. CXL alone	PRK + CXL: CDVA improved 0.17 logMAR, CXL: CDVA improved 0.09 logMAR	Significant improvement in K1 and K2 in the PRK + CXL group	Nil	39
Kanellopoulos and Asimellis (209)	231	Athens	UDVA improved 0.38 ± 0.31 logMAR, CDVA improved 0.20 ± 0.21 logMAR	K1: −3.4 D	Nil	36
Alessio et al. (205)	34	PRK + CXL vs. CXL alone	PRK + CXL: UDVA improved 0.44 logMAR, CDVA improve 0.03 logMAR, CXL: UDVA improved 0.07 logMAR, CDVA improved 0.02 logMAR	Significant improvement in SE, K1, K2, and Kmax in PRK + CXL group but not in CXL group	Nil	24
Kanellopoulos (208)	325	Athens (simultaneous vs. sequential)	Sequential: UDVA improved 0.41 logMAR, CDVA improved 0.25 logMAR Simultaneous: UDVA improved 0.66 logMAR, CDVA improved 0.28 logMAR	Sequential: K_{mean}: −2.8 ± 1.3 D Simultaneous: K_{mean}: −3.5 ± 1.3 D	Stromal haze: 13.4% (sequential) vs. 1% (simultaneous)	24–68
CXL plus (3 or more procedures)						
Shetty et al. (217)	48	ICRS followed by CXL + TG-tPTK	UDVA improved 0.53 logMAR, CDVA improved 0.11 logMAR	SE: 4.6 D, Cyl: 1.7 D	2% lost 1 line of CDVA	12
Rocha et al. (216)	55	Simultaneous ICRS + PTK + CXL	UDVA Improved 0.39 logMAR, CDVA improved 0.08 logMAR	Cyl: −2.1 D	1 eye (2%) lost >3 lines CDVA (haze)	6
Assaf and Kotb (213)	22	Sequential Athens protocol then PIOL	UDVA improved 0.87 logMAR, CDVA improved 0.34 logMAR	K_{mean} reduced −1.8 D	Nil	6–14
Coskunseven et al. (214)	16	ICRS then TG-tPRK then CXL	UDVA improved 0.89 logMAR, CDVA improved 0.62 logMAR	SE: 4.7 D, K1: −3.1 D, K2: −8.7 D	Nil	6
Kremer et al. (215)	45	Sequential Intacs then same-day PRK + CXL	UDVA improved 0.35 decimal, CDVA improved 0.19 decimal	K_{max}: −4.3 D	11.1% mild haze	12

K, keratometry; F/U, follow-up; TG, topography-guided; PRK/PTK, photorefractive/phototherapeutic keratectomy; tPTK, transepithelial phototherapeutic keratectomy; ICRS, intrastromal corneal ring segments; PIOL, phakic intraocular lens; SE, spherical equivalent; CDVA, corrected-distance-visual-acuity; UDVA, uncorrected-distance-visual-acuity.

With the recent advances in refractive surgery and the tools available to refractive surgeons, it is now more common for patients who are having CXL plus procedures to have customized treatment targeting wavefront guided HOAs with no compromise to optical zones. This ablation pattern allows regularization of the cornea, overcoming their otherwise inefficient optical system to allow for an improvement in their functional vision.

The timing of ICRS implantation, in the context of combined CXL, is still being debated, though in clinical setting it is not always a choice to make. Often patients may have already undergone CXL, other times they have had ICRS but are progressing. There is a logic that ICRS should precede CXL as it may be easier to insert the rings from a biomechanical point of view (202). Same day simultaneous ICRS and CXL has also gained support (223). In a recent randomized clinical trial evaluating the timing of CXL and ICRS for keratoconus (n = 198 eyes of 198 patients), Hersh et al. (203) reported a similar safety and effectiveness between concurrent surgery (same day for ICRS then CXL) and sequential surgery (ICRS then CXL 3 months later). Overall, there was a mean improvement in UDVA (by two logMAR lines), CDVA (by 1.1 logMAR line), and maximum topographic keratometry (by 7.5 D).

Several studies have demonstrated that combined PRK and CXL are able to achieve significant improvement in vision and corneal regularity when compared to CXL alone, with long-term stabilization of the disease progression (**Figure 6**) (205, 210). However, combined PRK with CXL may result in a deeper penetration of the UV-A radiation during CXL [potentially attributed to the ablation of the Bowman's layer (BL)], which needs to be considered during the preoperative planning to avoid any undesirable damage to the corneal endothelium (210). In addition, the timing of PRK in relation to CXL, whether to be performed simultaneously or sequentially (where PRK is performed 6–12 months post-CXL), is another important clinical question. Several factors need to be considered during combined PRK + CXL. First, the ablation effect of PRK on crosslinked corneas may differ from non-crosslinked corneas, potentially affecting the predictability and outcome of the combined treatment if performed sequentially (i.e., CXL then PRK). Second, the crosslinked corneal tissues (particularly the anterior portion of the stroma) are removed by the PRK if performed later, which may increase the risk of progression of keratoconus in the long-term. Third, the risk of postoperative stromal haze may be different between two approaches. CXL is known to induce apoptosis of the stromal keratocyte (224), which may reduce the risk of postoperative haze formation if PRK is applied simultaneously. With a sequential approach, the crosslinked stroma becomes repopulated by host keratocytes, which may result in a higher rate of postoperative haze formation.

Kanellopoulos et al. (208) previously conducted a clinical study comparing the outcome of same-day simultaneous versus sequential CXL and TG-PRK in 325 eyes with progressive keratoconus. Although both approaches offered beneficial effects, the same-day simultaneous approach was shown to exhibit significantly better improvement in UDVA, CDVA, refraction, and topographic keratometric measurements, with lesser risk of postoperative stromal haze. Recently, selective transepithelial topography-guided photorefractive keratectomy combined with accelerated corneal crosslinking (STARE-X) protocol has been described to achieve good corneal regularity and improve both visual acuity and corneal aberrations at 2 years after the procedure (221).

Corneal stromal haze remains a recognized postoperative risk in combined CXL and PRK, especially in cases with sequential approach (208) and in patients with a history of atopy (225). Intraoperative topical mitomycin C (MMC) 0.02% is commonly used to reduce the risk of corneal haze following PRK (226) and is also used in the Athens protocol (i.e., TG-PRK followed by high-fluence CXL) (209). However, a study showed that topical MMC may increase the risk of stromal haze following CXL, for which the mechanism is poorly understood (227). On the other hand, the Cretan protocol does not use any MMC intraoperatively and the rate of stromal haze is similar to those that undergo CXL alone.

Multiple CXL plus procedures such as CXL, ICRS and PRK showed benefit regardless of the sequence of events. However, the common approach is to first perform ICRS implantation followed by combined PRK/PTK and CXL (**Table 4**) (214, 216, 228). Surgical success is dependent on patient selection, intraoperative factors such as the proper depth of ring pavement, and reliability of the nomogram used. As CXL leads to gradual changes in the anterior corneal curvature for up to a year postoperatively, there is a valid question over the exact refraction target in combined procedures. Nonetheless, promising results are still observed in specific protocols without any adjustment for such refractive changes (229).

Early detection and treatment of patients with aggressive medical management of co-existing atopic disease, avoidance of eye rubbing, and CXL in an early stage of the disease may reduce the need for additional refractive procedures (230, 231). On the other hand, management of cases of moderate to advanced disease is more challenging, and as refractive surgery continues to advance, it is envisaged that customized CXL-keratorefractive surgery tailored to each individual's need and disease severity is likely to take place in the future (232–234).

4.4. Stromal keratophakia (allogeneic)

Tissue addition techniques or keratophakia has been described as a vision correction technique for aphakia, hyperopia, and myopia via the change of the anterior corneal curvature (235–237). To allow for the addition of a donor lenticule into the stroma, the host stromal pocket needs to be fashioned, either with microkeratome or with FSL. However, the use of microkeratome has been shown to produce inconsistent anatomic and refractive outcomes (238), which explains the lack of uptake of this approach. Jonas et al. (239) first explored and demonstrated the feasibility of FSL in safely preparing the host bed for intrastromal lamellar keratoplasty without disturbing the recipient's corneal epithelium and BL, using an *ex vivo* porcine corneal model. Subsequently, Tan et al. (240) described a new technique named "intralamellar keratoplasty," which is a type of stromal additive keratoplasty that involves the insertion of a laser-fashioned donor stromal lenticule into an FSL-assisted intrastromal pocket created in the host cornea. They reported an improvement in refractive and topographic astigmatism (by 1–2 D) and CL tolerance (50% with successful CL fitting) at 6 months follow-up.

More recently, Mastropasqua et al. (241) implanted +8 D hyperopic lenticules from donor corneas into corneas with

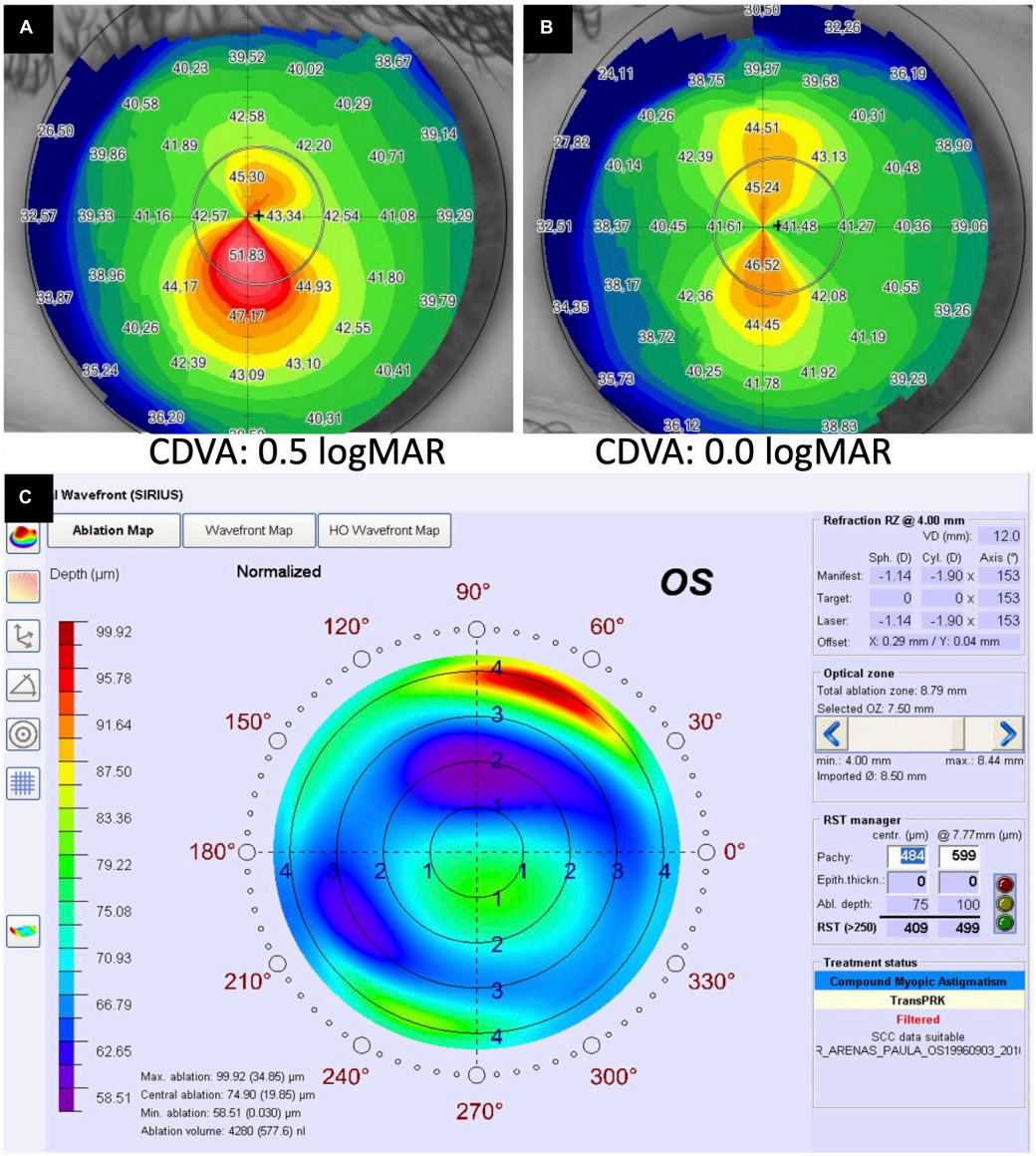

FIGURE 6
A case of corneal cross-linking (CXL) plus [with wavefront transepithelial photorefractive keratectomy (tPRK) followed by simultaneous same-day conventional CXL] for treating moderate progressive keratoconus. **(A)** Preoperative corneal topography demonstrating a significant irregular astigmatism [with high inferior-superior (IS) asymmetry] and a corrected-distance-visual-acuity (CDVA) of 0.5 logMAR. **(B)** Postoperative corneal topography demonstrating a significant improvement in irregular astigmatism and CDVA to 0.0 logMAR following the treatment. **(C)** The ablation map demonstrating the setting of the tPRK used in this patient.

stage III and IV keratoconus with central cones. The negative meniscus lenticules were inserted at a depth of 120 mm and centered on the apex of the cone. The study showed significant cornea flattening, asphericity reduction, and corneal biomechanical strength improvement. It has been shown that the lenticule addition into the stroma leads to stromal remodeling, corneal flattening and restoration of epithelial thickness (242). Similarly, Alio Del Barrio et al. (243) reported an innovative stromal keratophakia technique using 9 mm diameter, 120 µm thick, FSL-assisted lenticules of decellularized human donor corneal stroma, with or without autologous adipose-derived adult stem cells (ADASCs) recellularization, for treating advanced keratoconus. At 6 months postoperative, there was an improvement in UDVA, CDVA, refractive spheres, HOAs, and corneal thickness. Decellularization of the donor corneal stroma helps reduce the risk of allograft corneal stromal rejection. In addition, corneal stromal cell density is shown to increase following the implantation of the decellularized lenticules, especially when they are recellularized with ADASCs, at 1-year postoperative (244).

Several other stromal keratophakia techniques have also been described. In a case reported by Pradhan et al. (245), a 400 µm stromal lenticule was prepared by performing a DALK on a donor cornea. Excimer laser ablation was then done to remove 50 µm of the tissue to help regularize the host cornea. This lenticule was inserted in a patient with progressive keratoconus and thinnest pachymetry of 425 µm. The intrastromal space

was created by combining LASIK and DALK, leaving 125 μm of anterior stromal tissue and 140 μm of posterior tissue. At 1 year follow-up, the authors reported a reduction of steepest keratometry (by >7 D) and Q value (by 0.6). Successful tissue additive procedures have also been reported in pediatric patients with advanced keratoconus (246, 247). Jadidi and Mosavi (248) successfully implanted planar lenticules of thickness 140–250 μm at a depth of 250 μm in a series of four patients with advanced keratoconus. The technique of stromal keratophakia with excimer laser-assisted donor keratomileusis has also been described (249), with improvement in the mean simulated keratometric values and myopia.

Stromal addition to the mid-peripheral cornea represents another approach for stromal keratophakia. Ganesh and Brar (250) described the use of cryopreserved stromal lenticules derived from patients undergoing SMILE to create a donut-shaped lenticule. This lenticule was soaked in riboflavin and inserted in ectatic cornea at a depth of 100 μm centered on the first Purkinje image, followed by simultaneous accelerated CXL. This procedure, termed as femtosecond intrastromal lenticule implantation (FILI), results in tissue addition in the mid-periphery. At 6 months follow-up, the authors reported a significant improvement in UDVA, CDVA, Q values, and corneal aberrations in 5 eyes with moderate keratoconus. One eye with advanced keratoconus did not show improvement which led the authors to conclude that FILI worked best for patients with keratometry values <58 D.

In addition, a recent meta-analysis of 10 studies by Riau et al. (251) demonstrated that FSL-assisted stromal keratophakia serves as a feasible technique to expand corneal volume, correct refractive errors, and regularize corneal curvature in patients with keratoconus. However, further studies are required to help standardize the technique, including the choice of lenticules (concave vs. convex), the need and timing for combined CXL, and mathematical modeling to account for the long-term epithelial changes and stromal modeling that will have an important impact on the outcome of the technique.

4.5. Keratoplasty

As discussed above, keratoconus can be managed conservatively with spectacles and/or CL and corneal interventions such as CXL, ICRS, and keratophakia. With disease progression, visual correction with these measures may become insufficient or infeasible. It is estimated that up to 20% of patients with keratoconus will eventually need a keratoplasty (252–254).

Keratoconus is the leading indication for keratoplasty worldwide but the trend varies among different countries. In European countries such as France and Ireland, nationwide studies reported that keratoconus is their top indication for keratoplasty, accounting for around 19% cases (255, 256). In New Zealand, 28% of all keratoplasty were performed for eyes with keratoconus in 2019 (257). In a study specifically looking at the trend of PK in US, keratoconus accounted for 16% of their transplantation cases (11). However, studies conducted in Asia (e.g., China and Singapore) demonstrated a lower proportion of keratoplasty for keratoconus (~10% of the national corneal transplantation activity) (258, 259), highlighting the geographical variations in the indication for keratoplasty and potentially the prevalence of keratoconus.

For more than 100 years, PK was the only surgical option for patients with keratoconus. However, over the past two decades, there has been a paradigm shift in the surgical technique from PK to DALK for treating advanced keratoconus worldwide (10, 11, 255–257, 259–262). Moreover, a new technique, Bowman's layer transplantation (BLT), has recently been proposed to treat advanced keratoconus and delay or reduce the need for DALK or PK (263, 264).

In view of the potential complications and the shortage of donor corneas, keratoplasty is usually reserved as the last resort for treating advanced keratoconus. In general, DALK is the technique of choice when Descemet's membrane remains free of scarring or opacity and corneal endothelium remains healthy (10, 43, 253, 254, 265–267). On the other hand, PK is indicated when there is significant, full-thickness corneal scarring (e.g., following acute corneal hydrops or perforation), extremely thin cornea (<150–200 μm, though technically is still possible for DALK), or in cases with co-existing endothelial dysfunctions (43, 265, 266).

4.5.1. Penetrating keratoplasty

Despite being out favored by newer techniques, PK is well-established and long-term data has shown that PK has a high success rate in managing advanced keratoconus. The Australian Corneal Graft Registry Study (one of the most extensive corneal transplant studies which included 4,834 eyes) reported a relatively favorable long-term outcome for PK performed for keratoconus, with a graft survival rate of 89 and 49% at 10 and 20 years postoperative, respectively (268). This is similarly to the finding observed in the recent Singapore Corneal Transplant Study where the PK survival rate was 44% at 20 years (258). In addition, 74% of the eyes that had undergone PK for advanced keratoconus achieved a CDVA of 20/40 or better at their last follow-up as compared to only 8% of the eyes preoperatively (268). Several other studies also showed that long-term visual acuity after PK can improve to 20/30–20/40 with only spectacle correction (269–271). However, as many of the keratoconus patients undergo PK at a relatively young age, it is likely that these patients will require more than one graft in their lifetime, for which the risk of graft rejection is increased with repeated grafts (272, 273).

Graft rejection is the main reason for graft failure in PK, and it occurs most frequently in the first few years after PK, with around 50% of graft rejection occurring within the first year and 90% within the first 4 years (268). Recurrence of corneal ectasia, usually at the graft-host junction, is another recognized cause for "graft failure" in long-term surviving PK where the graft is anatomically clear but not functionally useful (268). The risk is estimated at 10–30% at 10–20 years postoperative and is higher in more advanced keratoconus (274–276). Significant post-keratoplasty astigmatism represents another important factor that may limit the visual outcome despite an anatomically clear graft. In the Australian Corneal Graft Registry Study, 61% of the patients who had PK needed refractive correction with spectacles and/or CL, and significant astigmatism (≥5 D) was prevalent among 77% of the patients (268). In addition, acute hydrops may also manifest following post-PK in keratoconic patients (277).

4.5.2. Anterior lamellar keratoplasty

In advanced keratoconus without any previous acute corneal hydrops, DALK with big bubble techniques is the most common

type of lamellar keratoplasty performed, accounting for more than 50% of the corneal transplantations in some countries (43, 266, 278). There are many other ALK techniques, such as manual layer-by-layer pre-descemetic DALK (pdDALK), dDALK with viscodissection, pdDALK with the Melles technique, and FSL-assisted DALK. Still, all of these are less commonly performed (43, 254, 265, 267, 278, 279). With the demonstration of the Dua's layer/pre-Descemet's layer (PDL) and the associated Type-1, Type-2, and mixed big bubbles, the different planes of cleavage achieved during DALK are now well-defined (280, 281).

DALK has become the treatment of choice because it has several advantages over PK. With DALK, the host corneal endothelial cells are retained, eliminating the risk of corneal endothelial rejection and graft failure (253, 254, 265, 266, 282). Other benefits of DALK include lower risk of endophthalmitis, reduced dependence on long-term topical corticosteroids [hence lesser risk of ocular hypertension (OHT) and glaucoma], faster recovery, and stronger graft-host junction (282, 283).

Literature comparing the clinical outcomes of PK and DALK has shown inconclusive results. In a French Study, it was found that the predicted graft survival period of DALK was almost three times of PK (49.0 vs. 17.3 years) (284). This difference is possibly explained by the higher endothelial cell density and elimination of the risk of endothelial rejection after DALK (267, 283, 285). However, a Cochrane review, which only included two randomized controlled trials (RCTs), concluded that there was no difference in CDVA, graft survival or keratometric outcomes between PK and DALK for keratoconus (286), though the findings were of low evidence due to small sample size. These results were supported by two subsequent systematic reviews and meta-analyses, which demonstrated no significant difference in graft survival and keratometric astigmatism between PK and DALK (283, 285). However, in terms of BCVA at 6 months or longer post-transplantation, these two studies showed conflicting results, with one showing DALK being superior to PK and vice versa (283, 285). This difference can be possibly explained by the heterogeneity of DALK techniques employed in the included studies. For instance, DALK with a successful big bubble technique may lead to a superior visual acuity and quality of vision compared to manual dissection technique, as the latter technique could result in more graft-host interface irregularity and undesirable ocular aberrations, especially when the residual stromal thickness is high (267, 287, 288). However, similar postoperative results have been demonstrated between big-bubble and manual dissection techniques when the latter achieves relatively thin residual stromal host bed (289). More importantly, studies have consistently demonstrated a lower graft rejection in DALK than PK (283, 285).

Long-term use of topical corticosteroids has been linked to OHT and/or glaucoma. It was reported that up to 46% of post-PK keratoconic eyes experienced OHT (290–293). With a lower requirement of topical steroid in DALK, eyes following DALK are less prone to developing OHT or glaucoma. Studies have shown that only 1–36% of keratoconic eyes develop OHT after DALK, with a significantly lower risk of developing secondary glaucoma than post-PK (278, 293–296). Compared to PK, DALK may offer a faster rehabilitation postoperatively due to stronger graft-host junction (297), which allows for earlier suture removal (without affecting the graft-host junction) and reduces the risk of suture-related post-keratoplasty infectious keratitis (298, 299). In addition, the risk of recurrence of keratoconus in the graft is considerably less common after DALK than PK (275, 300).

However, DALK is associated with a relatively steep learning curve and the surgical outcome is highly surgeon-dependent. A retrospective London study found that intraoperative perforation of DM occurred in 45.4% of eyes, and their conversion rate to PK was 24.1% (278). This considerably higher complication rate was likely attributed to a relative lack of relevant surgical experience among surgeons. Most cases were performed by trainee surgeons, and none of the surgeons in this study conducted more than 20 DALK cases per year (278). In other previous studies where more than 100 cases were performed by high-volume corneal surgeons, a considerably lower complication rate was reported, with ∼10% intraoperative micro/macroperforation of the Descemet membrane and ∼0.3–3% conversion rate to PK (265, 286, 288, 301, 302). Intra-operative imaging and use of assistive techniques such as FSL may improve the consistency and outcomes of DALK in keratoconus (303–306).

In addition to the graft-host junction (which is along the circumference as with PK), DALK has another graft-host interface which exists between the anterior surface of the host DM or PDL and the posterior surface of the transplanted donor tissue. This interface corresponds to the diameter/surface area of the donor tissue. This graft-host interface provides a plane for implantation of debris intraoperatively, interface haze, the spread of ingrowing blood vessels, inflammatory debris and organisms following suture-related infections. These issues are not seen with PK but do not override the advantages of DALK.

4.5.3. Bowman's layer transplantation

Bowman's layer fragmentation is seen early in the course of keratoconus and it is a sensitive and specific indicator of disease (307–309). It is postulated that further deterioration of vision or disease progression can be prevented by replacing the BL. Isolated BLT for 10 eyes with advanced keratoconus (ineligible for conservative treatments such as CXL or ICRS) was first attempted by Van Dijk et al. (263). The same group further expanded the cohort to include 22 eyes in 2015, with no intra- or post-operative complications reported in these two studies (263, 310). At 6-month post-operatively, the mean maximum keratometry (K max) reduced by 6–8 D and remained stable after that with a mean follow-up period of 21 months (263, 310). The mean best spectacle-corrected visual acuity (BSCVA) improved from 1.27 to 0.90 logMAR post-operatively, with a stable contact lens-corrected-visual-acuity (CLVA) (310). No cases of progression of keratoconus, graft rejection, or allograft reaction were reported (310). These promising early results sparked interest among surgeons in performing BLT as an alternative to PK or DALK for eyes with advanced keratoconus.

Similar results were reported in a later study of BLT of 15 eyes with advanced keratoconus, with a mean BSCVA improving from 1.35 logMAR preoperative to 0.96 logMAR at 12 months postoperative (311). It was also found that the corneal HOAs, especially spherical aberration, improved on both anterior and posterior corneal surfaces after BLT (311). There are also studies which modify the original techniques such as with the use of FSL or intraoperative optical coherence topography (iOCT), to improve the reproducibility of BLT by aiming to reduce the risk of stromal perforation (312, 313). However, Tong et al. (313) found

that with the help of iOCT, their results were no better than those achieved without iOCT.

Long-term follow-up of the original cohort of eyes that underwent BLT reported that the estimated success rate of BLT at 5 years was 84% (264). Kmax continued to be stable at 5 years after the initial drop postoperatively (264, 314). At 5–7 years follow-up, BSCVA also remained stable after the initial improvement but CLVA did not improve as compared to preoperatively (264, 314). No complications were reported except three acute corneal hydrops developed in between 4.5 and 6.5 years postoperatively, and these two patients had a history of atopy and severe eye rubbing (264, 314, 315).

This limited evidence to date suggests BLT may preserve the CDVA in patients with advanced keratoconus, potentially serving as an alternative to PK or DALK. One limitation of the adoption of BLT as treatment for advanced keratoconus is the technical difficulty but successful attempts from surgeons around the world have supported the feasibility of this technique (264, 311, 314, 316). More studies are needed to further determine the long-term efficacy and safety of BLT in treating advanced keratoconus.

5. Future directions

5.1. Corneal stromal regeneration

Keratoconus is a corneal disease that primarily affects the corneal stroma and BL, with these structures being severely diseased in advanced cases (309). Thus, current research is partially focusing on whether advanced keratoconic eyes can be rehabilitated by minimally invasive procedures that efficiently regenerate the corneal stroma to improve vision and reduce the risk of complications associated with PK or DALK (317–320).

Recently, several studies have reported the preliminary safety and efficacy results of corneal stromal stem cell therapy for patients with advanced keratoconus (243, 321, 322). Autologous mesenchymal stem cells (MSCs), in the form of suspension containing quiescent autologous adipose derived adult stem cells (ADASCs; obtained by elective liposuction), were transplanted into a mid-stroma FSL-assisted lamellar pocket in patients with advanced (stage IV) keratoconus (321). They could confirm, in a clinical setting, what was previously demonstrated in the animal model (323). ADASCs were capable of surviving *in vivo*, showing a perfect biointegration without any clinical inflammatory response or rejection, generating new collagen production within the corneal stroma (**Figure 7A**), and improving the vision. However, the creation of the stromal pocket may induce some aberrometric and keratometric changes, partially interfering with visual improvement (321). Moreover, they reported a case where preoperative stromal scars at the cone apex improved after the implantation of such MSC. This correlates well with the acquired knowledge from the experimental data in animals, which demonstrates the potential of stem cell therapy in alleviating pre-existing mild stromal scars (324, 325). Nevertheless, according to the clinical and pre-clinical available evidence, the direct intrastromal implantation of MSCs within the cornea achieves the production of new extracellular matrix but is not expected to be quantitatively enough to restore the thickness of a severely thin human cornea (like in severe keratoconus). On the other hand, this approach may provide a promising treatment modality for corneal dystrophies, and for the modulation of corneal scars (320).

In this context, the addition of decellularized human corneal sections repopulated by autologous MSC with the purpose of enhancing the anatomic rehabilitation of the keratoconic cornea has also been studied (243, 326). Both experimental and clinical studies have demonstrated good biointegration of such implants within the host corneal stroma, mimicking the normal natural strength and transparency of cornea with no risk of rejection reported so far (**Figure 7B**). *In vivo* confocal biomicroscopy studies have also shown that the transplanted MSCs can survive and differentiate into corneal keratocytes, while the decellularized implants show cellular repopulation starting from 3 months postoperative (244). Long-term studies (up to 3 years) demonstrated a moderate efficacy (a mean visual improvement by two Snellen lines) and a moderate flattening effect, with no reported postoperative complications (325). This innovative technique may also help reduce the need for donor human corneas as one donor corneal tissue can be used for up to three patients (324).

Nevertheless, the presented data is so far preliminary and limited to small samples, though additional studies are underway. Moreover, MSCs have proven to exhibit immunomodulatory properties on even xenogeneic transplants, though this capacity differs among different individuals (324). This raises the question about the ideal approach, since the autologous MSCs will carry the same genetic defects that precipitated the disease on first instance, and so their use may increase the risk of disease recurrence in long-term. The creation of cellular banks that could select the best donor cells with the greater biological effect may enhance these initial clinical outcomes. The future will bring further answers that can help establish this stromal cellular therapy as a potential therapeutic alternative to keratoplasty in some early cases of keratoconus.

5.2. Stromal keratophakia (xenogeneic)

In the previous section "4.4. Stromal keratophakia (allogeneic)," we highlighted the use of allogeneic stromal keratophakia as a novel treatment for keratoconus to obviate the need for DALK and PK. However, this technique is dependent on the availability of human donor corneas, which is currently limited by the global shortage. To overcome this issue, Rafat et al. (327) recently described an innovative xenogeneic stromal keratophakia technique using a "bioengineered cell-free porcine construct, double cross-linked (BPCDX)." The porcine construct is made of medical-grade type 1 porcine dermal collagen (to mimic the human corneal stroma with abundant type 1 collagen) and is double cross-linked to improve the strength and stability of the implantable hydrogel. In a recently completed phase 1 open-label clinical trial of 20 patients with advanced keratoconus, the authors reported a mean improvement in the corneal thickness (by 200–300 μm) and visual acuity (final vision was around 20/30–20/60) and a decrease in maximum keratometry (by ∼11–14 D), with no adverse event, over a 24-month follow-up period. These promising results highlight the potential of xenogeneic

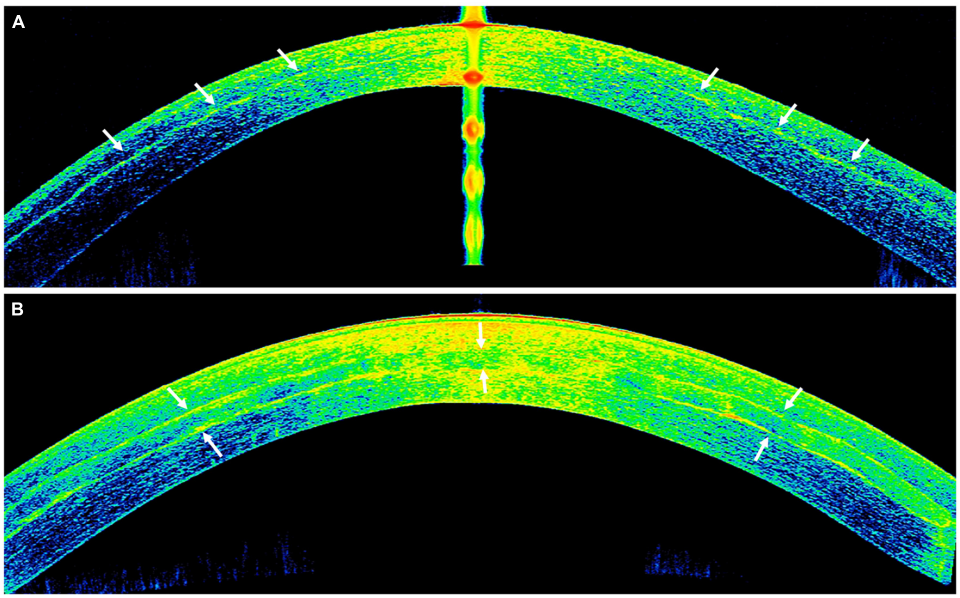

FIGURE 7
Anterior segment optical coherence tomography (AS-OCT) images demonstrating the outcome of implanted autologous adipose derived adult stem cells (ADASCs) in advanced keratoconus. **(A)** An ASOCT image showing the effect of the cellular therapy of the corneal stroma by an intrastromal implantation of autologous ADASCs in a patient with advanced keratoconus at 6 months post-treatment. Observe the hyperreflective band of neo-collagen (around 15 μm thickness) at the level of the stromal pocket (arrows). **(B)** An ASOCT image showing the corneal stromal enhancement by an intrastromal implantation of a decellularized lamina of human corneal stroma (arrows) colonized with autologous ADASC in a patient with advanced keratoconus at 12 months post-treatment.

stromal keratophakia, using BPCDX, as a safe, minimally invasive and donor-independent technique for advanced keratoconus. This may also serve as a useful alternative to the current conventional keratoplasty and overcome the barrier of the shortage of human donor corneas.

5.3. Gene therapy

The recent advent of next generation sequencing (NGS) has significantly advanced the ability to accurately sequence any genome of interest with reduced time and cost (328). This technology has enabled the detection of many previously unknown genetic mutations and has greatly deepened the understanding of various diseases (329). In addition, identification of these genetic mutations may serve as important biomarkers to predict the severity and progression of the disease and open the door to gene therapy targeting the underlying mutations to prevent or deter the disease progression (329).

Emerging studies have demonstrated important genetic implications on the pathogenesis and progression of keratoconus (330, 331). Lu et al. (332) previously conducted a meta-analysis of >20,000 individuals in European and Asian populations and identified two central corneal thickness-associated loci, FOXO1 and FNDC3B, that are strongly linked to the development of keratoconus. Several genome-wide linkage studies (GWLS) and genome-wide association studies (GWAS) have mapped out a wide array of genetic mutations linked to keratoconus. These include *LOX* gene (which encodes for lysyl oxidase, an enzyme that is involved in the cross-linking of extracellular proteins), *COL5A1* gene (which encodes for collagen type V). *TGFBI* gene (which encodes for transforming growth factor beta induced protein), *ZNF469* gene (which regulates corneal collagen structure and synthesis), *VSX1* gene (which encodes for visual system homeobox 1), and many others (333). So far, gene therapy has demonstrated promise as a novel therapy for treating a wide range of inherited retinal degeneration (334, 335). It is possible that the successful development and translation of these retinal gene therapies will pave the way for similar gene therapy for many other ocular diseases (with genetic predisposition) in the future, including keratoconus. However, as keratoconus is a polygenic disease, the development of effective gene therapy for keratoconus will undoubtedly be more complex than for monogenic disease like certain inherited retinal degeneration (336).

5.4. Artificial intelligence

Over the past decade, there has been an explosion of artificial intelligence (AI) research in healthcare, primarily owing to the significant improvement in computer processing power, advancement in deep learning techniques, and increased availability of big data, electronic health records and open-source databases (337–342). The development of AI-power platforms and telemedicine in healthcare, including ophthalmology, was further fueled by the recent COVID-19 pandemic to address the unprecedented rise in the healthcare backlog and to reduce the

need for conventional face-to-face consultation as part of the containment and mitigation strategy (343–346).

To date, AI has demonstrated its potential for the diagnosis of keratoconus (347–351). Furthermore, clinical applicability in the management of keratoconus, ranging from early detection of the disease, including sub-clinical keratoconus (or forme fruste keratoconus), preoperative screening and prediction of postoperative ectasia following keratorefractive surgery, and guiding and predicting the need for surgery (352–356). As corneal tomography (e.g., Oculus Pentacam) and AS-OCT (e.g., swept-source CASIA) are two most common modalities used in screening and diagnosing keratoconus (357), these images are most commonly utilized to train and develop the AI algorithms for keratoconus. So far, various AI approaches have been described and used, including artificial neural network (ANN), random forest, automated decision-tree classification, support vector machine (SVM) learning, convolutional neural network (CNN), and unsupervised learning (351, 352, 358–368).

Yousefi et al. (369) previously developed an unsupervised AI algorithm using swept-source AS-OCT images (CASIA) of ∼3,000 eyes to identify the stages and severity of keratoconus. The algorithm successfully identified four clusters of patients (ranging from normal eyes, forme fruste keratoconus to advanced keratoconus), and correlated well with the Ectasia Status Index. KeratoDetect, a CNN-based algorithm, has been shown to be able to automatically distinguish keratoconic eyes from normal eyes using topographic maps obtained from Scheimpflug imaging (370). By using 3,000 corneal topographic images (with a mixture of healthy cornea and keratoconus images), the algorithm was able to accurately diagnose keratoconus with 99.3% accuracy. Similarly, Chen et al. (351) developed a CNN-based algorithm to accurately detect and grade keratoconus based on the color-coded Scheimpflug topography maps. More recently, Gao et al. (360) developed an artificial neural network, named KeratoScreen, based on Zernike coefficient obtained from Scheimpflug corneal tomography. By using images of 208 patients, the algorithm was able to accurately distinguish normal eyes from subclinical keratoconus and keratoconus in >95% cases. AI has also been shown to be able to efficiently predict local and global progression of keratoconus based on Pentacam parameters, which may facilitate an earlier treatment for keratoconic eyes that are at higher risk of progression (371).

In addition, AI has demonstrated its usefulness in guiding implantation of ICRS in keratoconic corneas and predicting surgical outcomes. Valdés-Mas et al. (368) proposed an ANN based on multilayer perceptron to predict the postoperative improvement in corneal curvature and astigmatism following ICRS, with a predictive error of less than 1 D for both parameters. Another study demonstrated that an ANN-based algorithm was able to guide the ICRS implantation better than the manufacturer's nomogram and resulted in better visual outcome and less HOAs (372). It is also likely that AI may be used to optimize the planning for CXL-plus treatment (e.g., CXL + PRK) and improve the visual and refractive outcomes (233). Furthermore, based on ∼12,000 ASOCT images, Yousefi et al. (356) were able to develop an accurate unsupervised AI system that may help identify patients with corneal disease who are at a higher risk for future keratoplasty, including DALK for keratoconus.

6. Conclusion

The management of keratoconus has evolved significantly over the past century. As with most diseases, the approach has evolved from treating the disease to preventing and early diagnosis. The advent of CXL has rendered it possible to halt the progression of keratoconus. Recent years have seen several modifications of CXL to extend the treatment eligibility to thinner corneas. Efforts have been made to combine CXL with keratorefractive procedures to regularize the cornea and improve visual and refractive outcomes. While not yet widely performed, allogeneic stromal keratophakia and BLT have shown favorable short- to mid-term results. DALK has emerged as the preferred choice of keratoplasty over PK (when DM/PDL is not affected), and autologous stem cells and BPCDX are being investigated to avoid keratoplasty and its associated complications and reduce/eliminate the need for human donor corneas.

7. Methods of literature search

Electronic databases, including MEDLINE and EMBASE, were searched to identify relevant studies on the management of keratoconus. Only English articles were included in this review article. Key words used were "keratoconus," "corneal ectasia," "contact lens," "corneal cross-linking," "intracorneal ring segment," "keratorefractive surgery," "keratoplasty," "stromal keratophakia," "corneal stromal regeneration," "gene therapy," "artificial intelligence," and "machine learning." The bibliographies of included articles were manually screened to identify further relevant studies. The final search was last updated on 31 December 2022.

Author contributions

DT: study conceptualization and supervision. DT, RD, ZO, RR, and JA: literature review, data collection and curation, and drafting of initial manuscript. AB, MA, JM, DS, HD, and RA: critical revision of manuscript. All authors: data analysis, interpretation, and final approval of manuscript.

Funding

DT acknowledged support from the Medical Research Council/Fight for Sight Clinical Research Fellowship (MR/T001674/1).

Conflict of interest

The authors declare that the research was conducted in the absence of any commercial or financial relationships that could be construed as a potential conflict of interest.

Publisher's note

References

1. Wyman A. Benedict Duddell: pioneer oculist of the 18th century. *J R Soc Med.* (1992) 85:412–5.

2. Grzybowski A, McGhee C. The early history of keratoconus prior to Nottingham's landmark 1854 treatise on conical cornea: a review. *Clin Exp Optom.* (2013) 96:140–5. doi: 10.1111/cxo.12035

3. Gokul A, Patel D, McGhee CN. John Nottingham's 1854 landmark treatise on conical cornea considered in the context of the current knowledge of keratoconus. *Cornea.* (2016) 35:673–8. doi: 10.1097/ICO.0000000000000801

4. Ferrari G, Rama P. The keratoconus enigma: a review with emphasis on pathogenesis. *Ocul Surf.* (2020) 18:363–73. doi: 10.1016/j.jtos.2020.03.006

5. Gorskova E, Sevost'ianov E. Epidemiology of keratoconus in the Urals. *Vestn Oftalmol.* (1998) 114:38–40.

6. Hashemi H, Khabazkhoob M, Fotouhi A. Topographic keratoconus is not rare in an Iranian population: the Tehran Eye Study. *Ophthalmic Epidemiol.* (2013) 20:385–91.

7. Hashemi H, Heydarian S, Hooshmand E, Saatchi M, Yekta A, Aghamirsalim M, et al. The Prevalence and risk factors for keratoconus: a systematic review and meta-analysis. *Cornea.* (2020) 39:263–70.

8. Torres Netto E, Al-Otaibi W, Hafezi N, Kling S, Al-Farhan H, Randleman J, et al. Prevalence of keratoconus in paediatric patients in Riyadh, Saudi Arabia. *Br J Ophthalmol.* (2018) 102:1436–41. doi: 10.1136/bjophthalmol-2017-311391

9. Papali'i-Curtin A, Cox R, Ma T, Woods L, Covello A, Hall R. Keratoconus prevalence among high school students in New Zealand. *Cornea.* (2019) 38:1382–9. doi: 10.1097/ICO.0000000000002054

10. Ting D, Sau C, Srinivasan S, Ramaesh K, Mantry S, Roberts F. Changing trends in keratoplasty in the West of Scotland: a 10-year review. *Br J Ophthalmol.* (2012) 96:405–8. doi: 10.1136/bjophthalmol-2011-300244

11. Park C, Lee J, Gore P, Lim C, Chuck R. Keratoplasty in the United States. *Ophthalmology.* (2015) 122:2432–42.

12. Sandvik G, Thorsrud A, Råen M, Østern A, Sæthre M, Drolsum L. Does corneal collagen cross-linking reduce the need for keratoplasties in patients with keratoconus? *Cornea.* (2015) 34:991–5.

13. Godefrooij D, Gans R, Imhof S, Wisse R. Nationwide reduction in the number of corneal transplantations for keratoconus following the implementation of cross-linking. *Acta Ophthalmol.* (2016) 94:675–8. doi: 10.1111/aos.13095

14. Dua H, Ting D, Al-Aqaba M, Said D. Pathophysiology of keratoconus. In: Izquierdo LH, Mannis M editors. *Keratoconus: Diagnosis and management.* Amsterdam: Elsevier (2023).

15. Santodomingo-Rubido J, Carracedo G, Suzaki A, Villa-Collar C, Vincent S, Wolffsohn J. Keratoconus: an updated review. *Cont Lens Anterior Eye.* (2022) 45:101559.

16. Rong S, Ma S, Yu X, Ma L, Chu W, Chan T, et al. Genetic associations for keratoconus: a systematic review and meta-analysis. *Sci Rep.* (2017) 7:4620.

17. Zadnik K, Barr J, Edrington T, Everett D, Jameson M, McMahon T, et al. Baseline findings in the collaborative longitudinal evaluation of keratoconus (CLEK) Study. *Invest Ophthalmol Vis Sci.* (1998) 39:2537–46.

18. Mas Tur V, MacGregor C, Jayaswal R, O'Brart D, Maycock N. A review of keratoconus: diagnosis, pathophysiology, and genetics. *Surv Ophthalmol.* (2017) 62:770–83.

19. Wang Y, Rabinowitz Y, Rotter J, Yang H. Genetic epidemiological study of keratoconus: evidence for major gene determination. *Am J Med Genet.* (2000) 93:403–9.

20. Gordon-Shaag A, Millodot M, Essa M, Garth J, Ghara M, Shneor E. Is consanguinity a risk factor for keratoconus? *Optom Vis Sci.* (2013) 90:448–54.

21. Dua H, Faraj L, Said D, Gray T, Lowe J. Human corneal anatomy redefined: a novel pre-Descemet's layer (Dua's layer). *Ophthalmology.* (2013) 120:1778–85. doi: 10.1016/j.ophtha.2013.01.018

22. Lewis P, White T, Young R, Bell J, Winlove C, Meek K. Three-dimensional arrangement of elastic fibers in the human corneal stroma. *Exp Eye Res.* (2016) 146:43–53.

23. Parker J, Birbal R, van Dijk K, Oellerich S, Dapena I, Melles G. Are descemet membrane ruptures the root cause of corneal hydrops in keratoconic eyes? *Am J Ophthalmol.* (2019) 205:147–52.

24. Ting D, Said D, Dua H. Are descemet membrane ruptures the root cause of corneal hydrops in keratoconic eyes? *Am J Ophthalmol.* (2019) 205:204.

25. Wollensak G, Spoerl E, Seiler T. Riboflavin/ultraviolet-a-induced collagen crosslinking for the treatment of keratoconus. *Am J Ophthalmol.* (2003) 135:620–7.

26. Ozgurhan E, Akcay B, Kurt T, Yildirim Y, Demirok A. Accelerated corneal collagen cross-linking in thin keratoconic corneas. *J Refract Surg.* (2015) 31:386–90.

27. Deshmukh R, Hafezi F, Kymionis G, Kling S, Shah R, Padmanabhan P, et al. Current concepts in crosslinking thin corneas. *Indian J Ophthalmol.* (2019) 67:8–15. doi: 10.4103/ijo.IJO_1403_18

28. Caporossi A, Mazzotta C, Paradiso A, Baiocchi S, Marigliani D, Caporossi T. Transepithelial corneal collagen crosslinking for progressive keratoconus: 24-month clinical results. *J Cataract Refract Surg.* (2013) 39:1157–63.

29. Mazzotta C, Raiskup F, Hafezi F, Torres-Netto E, Armia Balamoun A, Giannaccare G, et al. Long term results of accelerated 9?mW corneal crosslinking for early progressive keratoconus: the Siena Eye-Cross Study 2. *Eye Vis.* (2021) 8:16. doi: 10.1186/s40662-021-00240-8

30. Mazzotta C, Traversi C, Paradiso A, Latronico M, Rechichi M. Pulsed light accelerated crosslinking versus continuous light accelerated crosslinking: one-year results. *J Ophthalmol.* (2014) 2014:604731. doi: 10.1155/2014/604731

31. Vinciguerra P, Rosetta P, Legrottaglie E, Morenghi E, Mazzotta C, Kaye S, et al. Iontophoresis CXL with and without epithelial debridement versus standard cxl: 2-year clinical results of a prospective clinical study. *J Refract Surg.* (2019) 35:184–90. doi: 10.3928/1081597X-20190128-01

32. Beckman K. Epithelium-on corneal collagen cross-linking with hypotonic riboflavin solution in progressive keratoconus. *Clin Ophthalmol.* (2021) 15:2921–32.

33. Ting D, Rana-Rahman R, Chen Y, Bell D, Danjoux J, Morgan S, et al. Effectiveness and safety of accelerated (9mW/cm(2)) corneal collagen cross-linking for progressive keratoconus: a 24-month follow-up. *Eye.* (2019) 33:812–8.

34. Borroni D, Bonzano C, Hristova R, Rachwani-Anil R, Sánchez-González J, de Lossada C. Epithelial flap corneal cross-linking. *J Refract Surg.* (2021) 37:741–5.

35. Salomão M, Hofling-Lima A, Gomes Esporcatte L, Correa F, Lopes B, Sena N, et al. Ectatic diseases. *Exp Eye Res.* (2021) 202:108347.

36. Amsler M. Classic keratocene and rough keratocene; Unitary arguments. *Ann Ocul.* (1947) 180:112.

37. Belin M, Duncan J. Keratoconus: the ABCD grading system. *Klin Monbl Augenheilkd.* (2016) 233:701–7.

38. McMahon T, Szczotka-Flynn L, Barr J, Anderson R, Slaughter M, Lass J, et al. A new method for grading the severity of keratoconus: the Keratoconus Severity Score (KSS). *Cornea.* (2006) 25:794–800. doi: 10.1097/01.ico.0000226359.26678.d1

39. Alió J, Shabayek M. Corneal higher order aberrations: a method to grade keratoconus. *J Refract Surg.* (2006) 22:539–45.

40. Duncan J, Belin M, Borgstrom M. Assessing progression of keratoconus: novel tomographic determinants. *Eye Vis.* (2016) 3:6.

41. Raiskup-Wolf F, Hoyer A, Spoerl E, Pillunat L. Collagen crosslinking with riboflavin and ultraviolet-A light in keratoconus: long-term results. *J Cataract Refract Surg.* (2008) 34:796–801.

42. Wittig-Silva C, Chan E, Islam F, Wu T, Whiting M, Snibson GR. A randomized, controlled trial of corneal collagen cross-linking in progressive keratoconus: three-year results. *Ophthalmology.* (2014) 121:812–21. doi: 10.1016/j.ophtha.2013.10.028

43. Gomes J, Tan D, Rapuano C, Belin M, Ambrósio R Jr, Guell J, et al. Global consensus on keratoconus and ectatic diseases. *Cornea.* (2015) 34:359–69.

44. Belin M, Kundu G, Shetty N, Gupta K, Mullick R, Thakur P. ABCD: a new classification for keratoconus. *Indian J Ophthalmol.* (2020) 68:2831–4.

45. Bawazeer A, Hodge W, Lorimer B. Atopy and keratoconus: a multivariate analysis. *Br J Ophthalmol.* (2000) 84:834–6.

46. Shajari M, Eberhardt E, Müller M, Al Khateeb G, Friderich S, Remy M, et al. Effects of atopic syndrome on keratoconus. *Cornea.* (2016) 35:1416–20.

47. Sharma N, Rao K, Maharana P, Vajpayee R. Ocular allergy and keratoconus. *Indian J Ophthalmol.* (2013) 61:407–9.

48. Egrilmez S, Sahin S, Yagci A. The effect of vernal keratoconjunctivitis on clinical outcomes of penetrating keratoplasty for keratoconus. *Can J Ophthalmol.* (2004) 39:772–7.

49. Sharma R, Titiyal J, Prakash G, Sharma N, Tandon R, Vajpayee R. Clinical profile and risk factors for keratoplasty and development of hydrops in north Indian patients with keratoconus. *Cornea.* (2009) 28:367–70. doi: 10.1097/ICO.0b013e31818cd077

50. Wagoner M, Ba-Abbad R. Penetrating keratoplasty for keratoconus with or without vernal keratoconjunctivitis. *Cornea.* (2009) 28:14–8.

51. Ambrósio R. Violet June: the global keratoconus awareness campaign. *Ophthalmol Ther.* (2020) 9:685–8. doi: 10.1007/s40123-020-00283-5

52. Shorter E, Harthan J, Nau A, Fogt J, Cao D, Schornack M, et al. Dry eye symptoms in individuals with keratoconus wearing contact lenses. *Eye Contact Lens.* (2021) 47:515–9.

53. Fick AE. A contact-lens. 1888 (translation). *Arch Ophthalmol.* (1988) 106: 1373–7.

54. Downie L, Lindsay R. Contact lens management of keratoconus. *Clin Exp Optom.* (2015) 98:299–311.

55. Rathi V, Mandathara P, Dumpati S. Contact lens in keratoconus. *Indian J Ophthalmol.* (2013) 61:410–5.

56. Saraç Ö, Kars M, Temel B, Çağıl N. Clinical evaluation of different types of contact lenses in keratoconus management. *Cont Lens Anterior Eye.* (2019) 42:482–6.

57. Sultan P, Dogan C, Iskeleli G. A retrospective analysis of vision correction and safety in keratoconus patients wearing Toris K soft contact lenses. *Int Ophthalmol.* (2016) 36:799–805. doi: 10.1007/s10792-016-0200-0

58. Wu Y, Tan Q, Zhang W, Wang J, Yang B, Ma W, et al. Rigid gas-permeable contact lens related life quality in keratoconic patients with different grades of severity. *Clin Exp Optom.* (2015) 98:150–4. doi: 10.1111/cxo.12237

59. Hashemi H, Shaygan N, Asgari S, Rezvan F. ClearKone-synergeyes or rigid gas-permeable contact lens in keratoconic patients: a clinical decision. *Eye Contact Lens.* (2014) 40:95–8.

60. Fernandez-Velazquez F. Severe epithelial edema in Clearkone SynergEyes contact lens wear for keratoconus. *Eye Contact Lens.* (2011) 37:381–5. doi: 10.1097/ICL.0b013e31822a33a6

61. Rico-Del-Viejo L, Garcia-Montero M, Hernández-Verdejo J, García-Lázaro S, Gómez-Sanz F, Lorente-Velázquez A. Nonsurgical procedures for keratoconus management. *J Ophthalmol.* (2017) 2017:9707650.

62. Suarez C, Madariaga V, Lepage B, Malecaze M, Fournié P, Soler V, et al. First experience with the ICD 16.5 mini-scleral lens for optic and therapeutic purposes. *Eye Contact Lens.* (2018) 44:44–9. doi: 10.1097/ICL.0000000000000293

63. Rathi V, Mandathara P, Taneja M, Dumpati S, Sangwan V. Scleral lens for keratoconus: technology update. *Clin Ophthalmol.* (2015) 9:2013–8.

64. Rathi V, Taneja M, Dumpati S, Mandathara P, Sangwan V. Role of scleral contact lenses in management of coexisting keratoconus and stevens-johnson syndrome. *Cornea.* (2017) 36:1267–9. doi: 10.1097/ICO.0000000000001310

65. Sengor T, Kurna S, Aki S, Ozkurt Y. High Dk piggyback contact lens system for contact lens-intolerant keratoconus patients. *Clin Ophthalmol.* (2011) 5:331–5. doi: 10.2147/OPTH.S16727

66. Raiskup F, Spoerl E. Corneal crosslinking with riboflavin and ultraviolet A. Part II. Clinical indications and results. *Ocul Surf.* (2013) 11:93–108.

67. Daxer A, Misof K, Grabner B, Ettl A, Fratzl P. Collagen fibrils in the human corneal stroma: structure and aging. *Invest Ophthalmol Vis Sci.* (1998) 39:644–8.

68. Dahl B, Spotts E, Truong J. Corneal collagen cross-linking: an introduction and literature review. *Optometry.* (2012) 83:33–42.

69. Mastropasqua L. Collagen cross-linking: when and how? A review of the state of the art of the technique and new perspectives. *Eye Vis.* (2015) 2:19.

70. McCall A, Kraft S, Edelhauser H, Kidder G, Lundquist R, Bradshaw H, et al. Mechanisms of corneal tissue cross-linking in response to treatment with topical riboflavin and long-wavelength ultraviolet radiation (UVA). *Invest Ophthalmol Vis Sci.* (2010) 51:129–38. doi: 10.1167/iovs.09-3738

71. Randleman J, Khandelwal S, Hafezi F. Corneal cross-linking. *Surv Ophthalmol.* (2015) 60:509–23.

72. Angelo L, Gokul Boptom A, McGhee C, Ziaei M. Corneal crosslinking: present and future. *Asia Pac J Ophthalmol.* (2022) 11:441–52.

73. Dhawan S, Rao K, Natrajan S. Complications of corneal collagen cross-linking. *J Ophthalmol.* (2011) 2011:869015.

74. Ting D, Bandyopadhyay J, Patel T. Microbial keratitis complicated by acute hydrops following corneal collagen cross-linking for keratoconus. *Clin Exp Optom.* (2019) 102:434–6. doi: 10.1111/cxo.12856

75. Caporossi A, Mazzotta C, Baiocchi S, Caporossi T. Long-term results of riboflavin ultraviolet a corneal collagen cross-linking for keratoconus in Italy: the Siena eye cross study. *Am J Ophthalmol.* (2010) 149:585–93.

76. Tiveron M, Pena C, Hida R, Moreira L, Branco F, Kara-Junior N. Topographic outcomes after corneal collagen crosslinking in progressive keratoconus: 1-year follow-up. *Arq Bras Oftalmol.* (2017) 80:93–6.

77. Choi M, Kim J, Kim E, Seo K, Kim T. Comparison of the conventional dresden protocol and accelerated protocol with higher ultraviolet intensity in corneal collagen cross-linking for keratoconus. *Cornea.* (2017) 36:523–9. doi: 10.1097/ICO.0000000000001165

78. Dua H, Deshmukh R, Ting D, Wilde C, Nubile M, Mastropasqua L, et al. Topical use of alcohol in ophthalmology - Diagnostic and therapeutic indications. *Ocul Surf.* (2021) 21:1–15.

79. Wollensak G, Wilsch M, Spoerl E, Seiler T. Collagen fiber diameter in the rabbit cornea after collagen crosslinking by riboflavin/UVA. *Cornea.* (2004) 23:503–7.

80. Amoils S. Using a nidek excimer laser with a rotary epithelial brush and corneal chilling: clinical results. *J Cataract Refract Surg.* (1999) 25:1321–6. doi: 10.1016/s0886-3350(99)00198-4

81. Kymionis G, Grentzelos M, Karavitaki A, Kounis G, Kontadakis G, Yoo S, et al. Transepithelial phototherapeutic keratectomy using a 213-nm solid-state laser system followed by corneal collagen cross-linking with riboflavin and UVA irradiation. *J Ophthalmol.* (2010) 2010:146543. doi: 10.1155/2010/146543

82. Kymionis G, Grentzelos M, Kounis G, Diakonis V, Limnopoulou A, Panagopoulou S. Combined transepithelial phototherapeutic keratectomy and corneal collagen cross-linking for progressive keratoconus. *Ophthalmology.* (2012) 119:1777–84.

83. Seiler T, Hafezi F. Corneal cross-linking-induced stromal demarcation line. *Cornea.* (2006) 25:1057–9. doi: 10.1097/01.ico.0000225720.38748.58

84. Mazzotta C, Wollensak G, Raiskup F, Pandolfi A, Spoerl E. The meaning of the demarcation line after riboflavin-UVA corneal collagen crosslinking. *Expert Rev Ophthalmol.* (2019) 14:115–31.

85. Kohlhaas M, Spoerl E, Schilde T, Unger G, Wittig C, Pillunat L. Biomechanical evidence of the distribution of cross-links in corneas treated with riboflavin and ultraviolet A light. *J Cataract Refract Surg.* (2006) 32:279–83. doi: 10.1016/j.jcrs.2005.12.092

86. Wollensak G, Iomdina E. Long-term biomechanical properties of rabbit cornea after photodynamic collagen crosslinking. *Acta Ophthalmol.* (2009) 87:48–51. doi: 10.1111/j.1755-3768.2008.01190.x

87. Ghanem R, Santhiago M, Berti T, Netto M, Ghanem V. Topographic, corneal wavefront, and refractive outcomes 2 years after collagen crosslinking for progressive keratoconus. *Cornea.* (2014) 33:43–8.

88. Steinberg J, Ahmadiyar M, Rost A, Frings A, Filev F, Katz T, et al. Anterior and posterior corneal changes after crosslinking for keratoconus. *Optom Vis Sci.* (2014) 91:178–86.

89. Greenstein S, Shah V, Fry K, Hersh P. Corneal thickness changes after corneal collagen crosslinking for keratoconus and corneal ectasia: one-year results. *J Cataract Refract Surg.* (2011) 37:691–700.

90. Kymionis G, Kounis G, Portaliou D, Grentzelos M, Karavitaki A, Coskunseven E, et al. Intraoperative pachymetric measurements during corneal collagen cross-linking with riboflavin and ultraviolet A irradiation. *Ophthalmology.* (2009) 116:2336–9.

91. Subasinghe S, Ogbuehi K, Dias G. Current perspectives on corneal collagen crosslinking (CXL). *Graefes Arch Clin Exp Ophthalmol.* (2018) 256:1363–84.

92. Kim T, Kim K, Han J, Jin K. The long-term clinical outcome after corneal collagen cross-linking in korean patients with progressive keratoconus. *Korean J Ophthalmol.* (2016) 30:326–34. doi: 10.3341/kjo.2016.30.5.326

93. Arora R, Gupta D, Goyal J, Jain P. Results of corneal collagen cross-linking in pediatric patients. *J Refract Surg.* (2012) 28:759–62.

94. Kymionis G, Kontadakis G, Hashemi K. Accelerated versus conventional corneal crosslinking for refractive instability: an update. *Curr Opin Ophthalmol.* (2017) 28:343–7. doi: 10.1097/ICU.0000000000000375

95. Ashena Z, Doherty S, Gokul A, McGhee C, Ziaei M, Nanavaty M. Flattening of central, paracentral, and peripheral cones after non-accelerated and accelerated epithelium-off CXL in keratoconus: a multicenter study. *J Refract Surg.* (2022) 38:310–6. doi: 10.3928/1081597X-20220404-02

96. Medeiros C, Giacomin N, Bueno R, Ghanem R, Moraes H, Santhiago M. Accelerated corneal collagen crosslinking: technique, efficacy, safety, and applications. *J Cataract Refract Surg.* (2016) 42:1826–35. doi: 10.1016/j.jcrs.2016.11.028

97. Said D, Ross A, Messina M, Mohammed I, Dua H. Localised corneal haze and scarring following pulsed accelerated collagen cross-linking for keratoconus. *Eye.* (2019) 33:167–8. doi: 10.1038/s41433-018-0211-3

98. Krueger R, Herekar S, Spoerl E. First proposed efficacy study of high versus standard irradiance and fractionated riboflavin/ultraviolet a cross-linking with equivalent energy exposure. *Eye Contact Lens.* (2014) 40:353–7. doi: 10.1097/ICL.0000000000000095

99. Schumacher S, Oeftiger L, Mrochen M. Equivalence of biomechanical changes induced by rapid and standard corneal cross-linking, using riboflavin and ultraviolet radiation. *Invest Ophthalmol Vis Sci.* (2011) 52:9048–52. doi: 10.1167/iovs.11-7818

100. Wernli J, Schumacher S, Spoerl E, Mrochen M. The efficacy of corneal cross-linking shows a sudden decrease with very high intensity UV light and short treatment time. *Invest Ophthalmol Vis Sci.* (2013) 54:1176–80.

101. Brittingham S, Tappeiner C, Frueh B. Corneal cross-linking in keratoconus using the standard and rapid treatment protocol: differences in demarcation line and 12-month outcomes. *Invest Ophthalmol Vis Sci.* (2014) 55:8371–6. doi: 10.1167/iovs.14-15444

102. Hashemi H, Miraftab M, Seyedian M, Hafezi F, Bahrmandy H, Heidarian S, et al. Long-term results of an accelerated corneal cross-linking protocol (18 mW/cm2) for the treatment of progressive keratoconus. *Am J Ophthalmol.* (2015) 160:1164–70.e1. doi: 10.1016/j.ajo.2015.08.027

103. Mita M, Waring G, Tomita M. High-irradiance accelerated collagen crosslinking for the treatment of keratoconus: six-month results. *J Cataract Refract Surg.* (2014) 40:1032–40. doi: 10.1016/j.jcrs.2013.12.014

104. Larkin D, Chowdhury K, Burr J, Raynor M, Edwards M, Tuft S, et al. Effect of corneal cross-linking versus standard care on keratoconus progression in young patients: the keralink randomized controlled trial. *Ophthalmology.* (2021) 128:1516–26. doi: 10.1016/j.ophtha.2021.04.019

105. Wen D, Li Q, Song B, Tu R, Wang Q, O'Brart D, et al. Comparison of standard versus accelerated corneal collagen cross-linking for keratoconus: a meta-analysis. *Invest Ophthalmol Vis Sci.* (2018) 59:3920–31. doi: 10.1167/iovs.18-24656

106. Touboul D, Efron N, Smadja D, Praud D, Malet F, Colin J. Corneal confocal microscopy following conventional, transepithelial, and accelerated corneal collagen cross-linking procedures for keratoconus. *J Refract Surg.* (2012) 28:769–76.

107. Tomita M, Mita M, Huseynova T. Accelerated versus conventional corneal collagen crosslinking. *J Cataract Refract Surg.* (2014) 40:1013–20.

108. Kymionis G, Tsoulnaras K, Grentzelos M, Plaka A, Mikropoulos D, Liakopoulos D, et al. Corneal stroma demarcation line after standard and high-intensity collagen crosslinking determined with anterior segment optical coherence tomography. *J Cataract Refract Surg.* (2014) 40:736–40.

109. Ozgurhan E, Sezgin Akcay B, Yildirim Y, Karatas G, Kurt T, Demirok A. Evaluation of corneal stromal demarcation line after two different protocols of accelerated corneal collagen cross-linking procedures using anterior segment optical coherence tomography and confocal microscopy. *J Ophthalmol.* (2014) 2014:981893. doi: 10.1155/2014/981893

110. Aixinjueluo W, Usui T, Miyai T, Toyono T, Sakisaka T, Yamagami S. Accelerated transepithelial corneal cross-linking for progressive keratoconus: a prospective study of 12 months. *Br J Ophthalmol.* (2017) 101:1244–9.

111. Artola A, Piñero D, Ruiz-Fortes P, Soto-Negro R, Pérez-Cambrodí R. Clinical outcomes at one year following keratoconus treatment with accelerated transepithelial cross-linking. *Int J Ophthalmol.* (2017) 10:652–5.

112. Razmjoo H, Peyman A, Rahimi A, Modrek H. Cornea collagen cross-linking for keratoconus: a comparison between accelerated and conventional methods. *Adv Biomed Res.* (2017) 6:10.

113. Richoz O, Hammer A, Tabibian D, Gatzioufas Z, Hafezi F. The biomechanical effect of corneal collagen cross-linking (CXL) with riboflavin and UV-A is oxygen dependent. *Transl Vis Sci Technol.* (2013) 2:6.

114. Moramarco A, Iovieno A, Sartori A, Fontana L. Corneal stromal demarcation line after accelerated crosslinking using continuous and pulsed light. *J Cataract Refract Surg.* (2015) 41:2546–51.

115. Belviranli S, Oltulu R. Efficacy of pulsed-light accelerated crosslinking in the treatment of progressive keratoconus: two-year results. *Eur J Ophthalmol.* (2020) 30:1256–60. doi: 10.1177/1120672119872375

116. Ziaei M, Vellara H, Gokul A, Patel D, McGhee C. Prospective 2-year study of accelerated pulsed transepithelial corneal crosslinking outcomes for keratoconus. *Eye.* (2019) 33:1897–903. doi: 10.1038/s41433-019-0502-3

117. Khoo P, Cabrera-Aguas M, Watson S. Microbial keratitis after corneal collagen cross-linking for corneal ectasia. *Asia Pac J Ophthalmol.* (2021) 10:355–9.

118. Shalchi Z, Wang X, Nanavaty M. Safety and efficacy of epithelium removal and transepithelial corneal collagen crosslinking for keratoconus. *Eye.* (2015) 29:15–29.

119. Ting D, Cairns J, Gopal B, Ho C, Krstic L, Elsahn A, et al. Risk factors, clinical outcomes, and prognostic factors of bacterial keratitis: the nottingham infectious keratitis study. *Front Med.* (2021) 8:715118. doi: 10.3389/fmed.2021.715118

120. Baiocchi S, Mazzotta C, Cerretani D, Caporossi T, Caporossi A. Corneal crosslinking: riboflavin concentration in corneal stroma exposed with and without epithelium. *J Cataract Refract Surg.* (2009) 35:893–9.

121. Chang S, Chi R, Wu C, Su M. Benzalkonium chloride and gentamicin cause a leak in corneal epithelial cell membrane. *Exp Eye Res.* (2000) 71:3–10. doi: 10.1006/exer.2000.0849

122. Majumdar S, Hippalgaonkar K, Repka M. Effect of chitosan, benzalkonium chloride and ethylenediaminetetraacetic acid on permeation of acyclovir across isolated rabbit cornea. *Int J Pharm.* (2008) 348:175–8. doi: 10.1016/j.ijpharm.2007.08.017

123. Wollensak G, Aurich H, Wirbelauer C, Sel S. Significance of the riboflavin film in corneal collagen crosslinking. *J Cataract Refract Surg.* (2010) 36:114–20.

124. Kobashi H, Rong S, Ciolino J. Transepithelial versus epithelium-off corneal crosslinking for corneal ectasia. *J Cataract Refract Surg.* (2018) 44:1507–16.

125. Bottós K, Schor P, Dreyfuss J, Nader H, Chamon W. Effect of corneal epithelium on ultraviolet-A and riboflavin absorption. *Arq Bras Oftalmol.* (2011) 74:348–51.

126. Hersh P, Lai M, Gelles J, Lesniak S. Transepithelial corneal crosslinking for keratoconus. *J Cataract Refract Surg.* (2018) 44:313–22.

127. Wollensak G, Iomdina E. Biomechanical and histological changes after corneal crosslinking with and without epithelial debridement. *J Cataract Refract Surg.* (2009) 35:540–6. doi: 10.1016/j.jcrs.2008.11.036

128. Sun L, Li M, Zhang X, Tian M, Han T, Zhao J, et al. Transepithelial accelerated corneal collagen cross-linking with higher oxygen availability for keratoconus: 1-year results. *Int Ophthalmol.* (2018) 38:2509–17. doi: 10.1007/s10792-017-0762-5

129. Gatzioufas Z, Raiskup F, O'Brart D, Spoerl E, Panos G, Hafezi F. Transepithelial corneal cross-linking using an enhanced riboflavin solution. *J Refract Surg.* (2016) 32:372–7.

130. Filippello M, Stagni E, O'Brart D. Transepithelial corneal collagen crosslinking: bilateral study. *J Cataract Refract Surg.* (2012) 38:283–91.

131. Leccisotti A, Islam T. Transepithelial corneal collagen cross-linking in keratoconus. *J Refract Surg.* (2010) 26:942–8.

132. Ng S, Ren M, Lindsley K, Hawkins B, Kuo I. Transepithelial versus epithelium-off corneal crosslinking for progressive keratoconus. *Cochrane Database Syst Rev.* (2021) 3:CD013512.

133. Mazzotta C, Balamoun A, Chabib A, Rechichi M, D'Oria F, Hafezi F, et al. Transepithelial enhanced fluence pulsed light m accelerated crosslinking for early progressive keratoconus with chemically enhanced riboflavin solutions and air room oxygen. *J Clin Med.* (2022) 11:5039. doi: 10.3390/jcm11175039

134. Cassagne M, Laurent C, Rodrigues M, Galinier A, Spoerl E, Galiacy S, et al. Iontophoresis transcorneal delivery technique for transepithelial corneal collagen crosslinking with riboflavin in a rabbit model. *Invest Ophthalmol Vis Sci.* (2016) 57:594–603. doi: 10.1167/iovs.13-12595

135. Bikbova G, Bikbov M. Transepithelial corneal collagen cross-linking by iontophoresis of riboflavin. *Acta Ophthalmol.* (2014) 92:e30–4.

136. Jia H, Pang X, Fan Z, Li N, Li G, Peng X. Iontophoresis-assisted corneal crosslinking using 0.1% riboflavin for progressive keratoconus. *Int J Ophthalmol.* (2017) 10:717–22.

137. Vinciguerra P, Randleman J, Romano V, Legrottaglie E, Rosetta P, Camesasca F, et al. Transepithelial iontophoresis corneal collagen cross-linking for progressive keratoconus: initial clinical outcomes. *J Refract Surg.* (2014) 30:746–53. doi: 10.3928/1081597X-20141021-06

138. Bikbova G, Bikbov M. Standard corneal collagen crosslinking versus transepithelial iontophoresis-assisted corneal crosslinking, 24 months follow-up: randomized control trial. *Acta Ophthalmol.* (2016) 94:e600–6. doi: 10.1111/aos.13032

139. Cantemir A, Alexa A, Anton N, Ciuntu R, Danielescu C, Chiselita D, et al. Evaluation of iontophoretic collagen cross-linking for early stage of progressive keratoconus compared to standard cross-linking: a non-inferiority study. *Ophthalmol Ther.* (2017) 6:147–60. doi: 10.1007/s40123-017-0076-8

140. Jouve L, Borderie V, Sandali O, Temstet C, Basli E, Laroche L, et al. Conventional and iontophoresis corneal cross-linking for keratoconus: efficacy and assessment by optical coherence tomography and confocal microscopy. *Cornea.* (2017) 36:153–62.

141. Mastropasqua L, Nubile M, Calienno R, Mattei P, Pedrotti E, Salgari N, et al. Corneal cross-linking: intrastromal riboflavin concentration in iontophoresis-assisted imbibition versus traditional and transepithelial techniques. *Am J Ophthalmol.* (2014) 157:623–30.e1. doi: 10.1016/j.ajo.2013.11.018

142. Lombardo M, Serrao S, Raffa P, Rosati M, Lombardo G. Novel technique of transepithelial corneal cross-linking using iontophoresis in progressive keratoconus. *J Ophthalmol.* (2016) 2016:7472542.

143. Lombardo M, Giannini D, Lombardo G, Serrao S. Randomized controlled trial comparing transepithelial corneal cross-linking using iontophoresis with the dresden protocol in progressive keratoconus. *Ophthalmology.* (2017) 124:804–12.

144. Jia H, Peng X. Efficacy of iontophoresis-assisted epithelium-on corneal cross-linking for keratoconus. *Int J Ophthalmol.* (2018) 11:687–94.

145. Sachdev M, Gupta D, Sachdev G, Sachdev R. Tailored stromal expansion with a refractive lenticule for crosslinking the ultrathin cornea. *J Cataract Refract Surg.* (2015) 41:918–23. doi: 10.1016/j.jcrs.2015.04.007

146. Cagini C, Riccitelli F, Messina M, Piccinelli F, Torroni G, Said D, et al. Epi-off-lenticule-on corneal collagen cross-linking in thin keratoconic corneas. *Int Ophthalmol.* (2020) 40:3403–12. doi: 10.1007/s10792-020-01526-x

147. Jacob S, Kumar D, Agarwal A, Basu S, Sinha P. Contact lens-assisted collagen cross-linking (CACXL): a new technique for cross-linking thin corneas. *J Refract Surg.* (2014) 30:366–72. doi: 10.3928/1081597X-20140523-01

148. Wollensak G, Spörl E, Herbst H. Biomechanical efficacy of contact lens-assisted collagen cross-linking in porcine eyes. *Acta Ophthalmol.* (2019) 97:e84–90.

149. Zhang H, Roozbahani M, Piccinini A, Golan O, Hafezi F, Scarcelli G, et al. Depth-dependent reduction of biomechanical efficacy of contact lens-assisted corneal cross-linking analyzed by brillouin microscopy. *J Refract Surg.* (2019) 35:721–8. doi: 10.3928/1081597X-20191004-01

150. Knyazer B, Kormas R, Chorny A, Lifshitz T, Achiron A, Mimouni M. Corneal cross-linking in thin corneas: 1-year results of accelerated contact lens-assisted treatment of keratoconus. *J Refract Surg.* (2019) 35:642–8. doi: 10.3928/1081597X-20190903-01

151. Kling S, Richoz O, Hammer A, Tabibian D, Jacob S, Agarwal A, et al. Increased biomechanical efficacy of corneal cross-linking in thin corneas due to higher oxygen availability. *J Refract Surg.* (2015) 31:840–6. doi: 10.3928/1081597X-20151111-08

152. Kling S, Hafezi F. An algorithm to predict the biomechanical stiffening effect in corneal cross-linking. *J Refract Surg.* (2017) 33:128–36. doi: 10.3928/1081597X-20161206-01

153. Hafezi F, Kling S, Gilardoni F, Hafezi N, Hillen M, Abrishamchi R, et al. Individualized corneal cross-linking with riboflavin and UV-A in ultrathin corneas: the Sub400 protocol. *Am J Ophthalmol.* (2021) 224:133–42.

154. Barraquer J. Modification of refraction by means of intracorneal inclusions. *Int Ophthalmol Clin.* (1966) 6:53–78.

155. Colin J, Cochener B, Savary G, Malet F. Correcting keratoconus with intracorneal rings. *J Cataract Refract Surg.* (2000) 26:1117–22.

156. Torquetti L, Ferrara G, Almeida F, Cunha L, Araujo L, Machado A, et al. Intrastromal corneal ring segments implantation in patients with keratoconus: 10-year follow-up. *J Refract Surg.* (2014) 30:22–6.

157. Vega-Estrada A, Alió J, Brenner L, Burguera N. Outcomes of intrastromal corneal ring segments for treatment of keratoconus: five-year follow-up analysis. *J Cataract Refract Surg.* (2013) 39:1234–40.

158. Vega-Estrada A, Alió J, Plaza-Puche A. Keratoconus progression after intrastromal corneal ring segment implantation in young patients: five-year follow-up. *J Cataract Refract Surg.* (2015) 41:1145–52. doi: 10.1016/j.jcrs.2014.08.045

159. Costa J, Monteiro T, Franqueira N, Faria-Correia F, Alfonso J, Vaz F. Five-year long-term outcomes of intrastromal corneal ring segment implantation using the manual technique for keratoconus management. *J Cataract Refract Surg.* (2021) 47:713–21. doi: 10.1097/j.jcrs.0000000000000500

160. Moscovici B, Rodrigues P, Rodrigues R, Rios L, Simoncelli R, Freitas M, et al. Evaluation of keratoconus progression and visual improvement after intrastromal corneal ring segments implantation: a retrospective study. *Eur J Ophthalmol.* (2021) 31:3483–9.

161. Nosé W, Neves R, Schanzlin D, Belfort Júnior R. Intrastromal corneal ring–one-year results of first implants in humans: a preliminary nonfunctional eye study. *Refract Corneal Surg.* (1993) 9:452–8.

162. Elalfy M, Maqsood S, Reinhold A, Panos G, Khine A, Lake D, et al. Clinical outcomes after intracorneal ring segment implantation for keratoconus management in corneas with mild apical haze. *Ther Adv Ophthalmol.* (2021) 13:25158414211003378. doi: 10.1177/25158414211003378

163. Azar D. *Refractive Surgery E-Book*. Amsterdam: Elsevier (2019).

164. Sakellaris D, Balidis M, Gorou O, Szentmary N, Alexoudis A, Grieshaber M, et al. Intracorneal ring segment implantation in the management of keratoconus: an evidence-based approach. *Ophthalmol Ther.* (2019) 8(Suppl. 1):5–14. doi: 10.1007/s40123-019-00211-2

165. Abreu A, Malheiro L, Coelho J, Neves M, Gomes M, Oliveira L, et al. Implantation of intracorneal ring segments in pediatric patients: long-term follow-up. *Int Med Case Rep J.* (2018) 11:23–7. doi: 10.2147/IMCRJ.S151383

166. Alfonso J, Fernández-Vega-Cueto L, Lisa C, Monteiro T, Madrid-Costa D. Long-Term Follow-up of Intrastromal Corneal Ring Segment Implantation in Pediatric Keratoconus. *Cornea.* (2019) 38:840–6.

167. Abd Elaziz M, El Saebay Sarhan A, Ibrahim A, Elshafy HH. Anterior segment changes after femtosecond laser-assisted implantation of a 355-degree intrastromal corneal ring segment in advanced keratoconus. *Cornea.* (2018) 37:1438–43. doi: 10.1097/ICO.0000000000001702

168. Abdellah M, Ammar H. Femtosecond laser implantation of a 355-degree intrastromal corneal ring segment in keratoconus: a three-year follow-up. *J Ophthalmol.* (2019) 2019:6783181. doi: 10.1155/2019/6783181

169. de Araujo B, Kubo L, Marinho D, Kwitko S. Keratoconus progression after intrastromal corneal ring segment implantation according to age: 5-year follow-up cohort study. *Int Ophthalmol.* (2020) 40:2847–54. doi: 10.1007/s10792-020-01468-4

170. Kang M, Byun Y, Yoo Y, Whang W, Joo C. Long-term outcome of intrastromal corneal ring segments in keratoconus: five-year follow up. *Sci Rep.* (2019) 9:315.

171. Peris-Martínez C, Hernández-Díaz M, Roig-Revert M, Alfonso-Muñoz E, Montolío-Marzo S, Monsálvez-Romín D. Two-year follow-up of intracorneal ring segments implantation in adolescent patients with keratoconus. *J Refract Surg.* (2021) 37:91–7. doi: 10.3928/1081597X-20201123-03

172. Prisant O, Pottier E, Guedj T, Hoang Xuan T. Clinical outcomes of an asymmetric model of intrastromal corneal ring segments for the correction of keratoconus. *Cornea.* (2020) 39:155–60.

173. Sandes J, Stival L, de Ávila M, Ferrara P, Ferrara G, Magacho L, et al. Clinical outcomes after implantation of a new intrastromal corneal ring with 140-degree of arc in patients with corneal ectasia. *Int J Ophthalmol.* (2018) 11:802–6. doi: 10.18240/ijo.2018.05.14

174. Torquetti L, Cunha P, Luz A, Kwitko S, Carrion M, Rocha G, et al. Clinical outcomes after implantation of 320°-arc length intrastromal corneal ring segments in keratoconus. *Cornea.* (2018) 37:1299–305. doi: 10.1097/ICO.0000000000001709

175. Warrak E, Serhan H, Ayash J, Wahab C, Baban T, Daoud R, et al. Long-term follow up of intracorneal ring segment implantation in 932 keratoconus eyes. *J Fr Ophtalmol.* (2020) 43:1020–4. doi: 10.1016/j.jfo.2020.03.019

176. Vega-Estrada A, Alio J, Brenner L, Javaloy J, Plaza Puche A, Barraquer R, et al. Outcome analysis of intracorneal ring segments for the treatment of keratoconus based on visual, refractive, and aberrometric impairment. *Am J Ophthalmol.* (2013) 155:575–84.e1.

177. Baptista P, Marques J, Neves M, Gomes M, Oliveira L. Asymmetric thickness intracorneal ring segments for keratoconus. *Clin Ophthalmol.* (2020) 14:4415–21.

178. Vega-Estrada A, Chorro E, Sewelam A, Alio J. Clinical outcomes of a new asymmetric intracorneal ring segment for the treatment of keratoconus. *Cornea.* (2019) 38:1228–32.

179. Coşkunseven E, Ambrósio R Jr, Smorádková A, Sánchez León F, Sahin O, Kavadarli I, et al. Visual, refractive and topographic outcomes of progressive thickness intrastromal corneal ring segments for keratoconic eyes. *Int Ophthalmol.* (2020) 40:2835–44.

180. Coskunseven E, Kayhan B. Clinical, tomographic, and topometric outcomes of progressive thickness intracorneal ring segment implantations in duck-type keratoconus. *Indian J Ophthalmol.* (2022) 70:2939–45. doi: 10.4103/ijo.IJO_2770_21

181. Alfonso-Bartolozzi B, Fernández-Vega-Cueto L, Poo-López A, Lisa C, Madrid-Costa D, Alfonso J. Intrastromal corneal ring segments implantation after deep anterior lamellar keratoplasty for astigmatism correction: mid-term and long-term follow-up. *Cornea.* (2022) [Epub ahead of print]. doi: 10.1097/ICO.0000000000003110

182. Monteiro T, Alfonso J, Franqueira N, Faria-Correira F, Ambrósio R Jr, Madrid-Costa D. Comparison of clinical outcomes between manual and femtosecond laser techniques for intrastromal corneal ring segment implantation. *Eur J Ophthalmol.* (2020) 30:1246–55. doi: 10.1177/1120672119872367

183. Giacomin N, Mello G, Medeiros C, Kiliç A, Serpe C, Almeida H, et al. Intracorneal ring segments implantation for corneal ectasia. *J Refract Surg.* (2016) 32:829–39.

184. Kanellopoulos A, Pe L, Perry H, Donnenfeld ED. Modified intracorneal ring segment implantations (INTACS) for the management of moderate to advanced keratoconus: efficacy and complications. *Cornea.* (2006) 25:29–33. doi: 10.1097/01.ico.0000167883.63266.60

185. Zare M, Hashemi H, Salari M. Intracorneal ring segment implantation for the management of keratoconus: safety and efficacy. *J Cataract Refract Surg.* (2007) 33:1886–91.

186. Coskunseven E, Kymionis G, Tsiklis N, Atun S, Arslan E, Siganos C, et al. Complications of intrastromal corneal ring segment implantation using a femtosecond laser for channel creation: a survey of 850 eyes with keratoconus. *Acta Ophthalmol.* (2011) 89:54–7. doi: 10.1111/j.1755-3768.2009.01605.x

187. Bedi R, Touboul D, Pinsard L, Colin J. Refractive and topographic stability of Intacs in eyes with progressive keratoconus: five-year follow-up. *J Refract Surg.* (2012) 28:392–6. doi: 10.3928/1081597X-20120509-01

188. Colin J. European clinical evaluation: use of Intacs for the treatment of keratoconus. *J Cataract Refract Surg.* (2006) 32:747–55. doi: 10.1016/j.jcrs.2006.01.064

189. Kilic A, Kamburoglu G, Akıncı A. Riboflavin injection into the corneal channel for combined collagen crosslinking and intrastromal corneal ring segment implantation. *J Cataract Refract Surg.* (2012) 38:878–83. doi: 10.1016/j.jcrs.2011.11.041

190. Kymionis G, Grentzelos M, Diakonis V, Pallikaris A, Pallikaris I. Nine-year follow-up of intacs implantation for keratoconus. *Open Ophthalmol J.* (2009) 3:77–81. doi: 10.2174/1874364100903010077

191. Piñero D, Alio J. Intracorneal ring segments in ectatic corneal disease - a review. *Clin Exp Ophthalmol.* (2010) 38:154–67.

192. Saelens I, Bartels M, Bleyen I, Van Rij G. Refractive, topographic, and visual outcomes of same-day corneal cross-linking with Ferrara intracorneal ring segments in patients with progressive keratoconus. *Cornea.* (2011) 30:1406–8. doi: 10.1097/ICO.0b013e3182151ffc

193. Jacob S, Patel S, Agarwal A, Ramalingam A, Saijimol A, Raj J. Corneal allogenic intrastromal ring segments (CAIRS) combined with corneal cross-linking for keratoconus. *J Refract Surg.* (2018) 34:296–303. doi: 10.3928/1081597X-20180223-01

194. Parker J, Dockery P, Jacob S, Parker J. Preimplantation dehydration for corneal allogenic intrastromal ring segment implantation. *J Cataract Refract Surg.* (2021) 47:e37–9. doi: 10.1097/j.jcrs.0000000000000582

195. Jafarinasab M, Hadi Y. Femtosecond laser-assisted peripheral additive stromal keratoplasty for treatment of primary corneal ectasia: preliminary outcomes. *Indian J Ophthalmol.* (2021) 69:2663–8. doi: 10.4103/ijo.IJO_3206_20

196. Ambrosio R Jr, Faria-Correia F, Silva-Lopes Í, Azevedo-Wagner A, Tanos F, Lopes B, et al. Paradigms, paradoxes, and controversies on keratoconus and corneal ectatic diseases. *Int J Keratoconus Ectatic Corneal Dis.* (2018) 7:35–49.

197. Ambrósio R Jr, Lopes B, Amaral J, Correia F, Canedo A, Salomão M, et al. Keratoconus: breaking paradigms and contradictions of a new subspecialty. *Rev Brasil Oftalmol.* (2019) 78:81–5.

198. Al-Mohaimeed M. Combined corneal CXL and photorefractive keratectomy for treatment of keratoconus: a review. *Int J Ophthalmol.* (2019) 12:1929–38.

199. Kymionis G. Corneal collagen cross linking - PLUS. *Open Ophthalmol J.* (2011) 5:10.

200. El-Raggal T. Sequential versus concurrent KERARINGS insertion and corneal collagen cross-linking for keratoconus. *Br J Ophthalmol.* (2011) 95:37–41. doi: 10.1136/bjo.2010.179580

201. Fernández-Vega-Cueto L, Romano V, Zaldivar R, Gordillo C, Aiello F, Madrid-Costa D, et al. Surgical options for the refractive correction of keratoconus: myth or reality. *J Ophthalmol.* (2017) 2017:7589816.

202. Coskunseven E, Jankov M, Hafezi F, Atun S, Arslan E, Kymionis G. Effect of treatment sequence in combined intrastromal corneal rings and corneal collagen crosslinking for keratoconus. *J Cataract Refract Surg.* (2009) 35:2084–91.

203. Hersh P, Issa R, Greenstein S. Corneal crosslinking and intracorneal ring segments for keratoconus: a randomized study of concurrent versus sequential surgery. *J Cataract Refract Surg.* (2019) 45:830–9.

204. Renesto Ada C, Melo L., Sartori Mde F, Campos M. Sequential topical riboflavin with or without ultraviolet a radiation with delayed intracorneal ring segment insertion for keratoconus. *Am J Ophthalmol.* (2012) 153:982–93.e3.

205. Alessio G, L'Abbate M, Sborgia C, La Tegola M. Photorefractive keratectomy followed by cross-linking versus cross-linking alone for management of progressive keratoconus: two-year follow-up. *Am J Ophthalmol.* (2013) 155:54–65.e1. doi: 10.1016/j.ajo.2012.07.004

206. Gore D, Leucci M, Anand V, Fernandez-Vega Cueto L, Arba Mosquera S, Allan B. Combined wavefront-guided transepithelial photorefractive keratectomy and corneal crosslinking for visual rehabilitation in moderate keratoconus. *J Cataract Refract Surg.* (2018) 44:571–80.

207. Iqbal M, Elmassry A, Tawfik A, Elgharieb M, Nagy K, Soliman A, et al. Standard cross-linking versus photorefractive keratectomy combined with accelerated cross-linking for keratoconus management: a comparative study. *Acta Ophthalmol.* (2019) 97:e623–31. doi: 10.1111/aos.13986

208. Kanellopoulos A. Comparison of sequential vs same-day simultaneous collagen cross-linking and topography-guided PRK for treatment of keratoconus. *J Refract Surg.* (2009) 25:S812–8. doi: 10.3928/1081597X-20090813-10

209. Kanellopoulos A, Asimellis G. Keratoconus management: long-term stability of topography-guided normalization combined with high-fluence CXL stabilization (the Athens Protocol). *J Refract Surg.* (2014) 30:88–93. doi: 10.3928/1081597X-20140120-03

210. Kontadakis G, Kankariya V, Tsoulnaras K, Pallikaris A, Plaka A, Kymionis G. Long-term comparison of simultaneous topography-guided photorefractive keratectomy followed by corneal cross-linking versus corneal cross-linking alone. *Ophthalmology.* (2016) 123:974–83.

211. Nattis A, Rosenberg ED, Donnenfeld E. One-year visual and astigmatic outcomes of keratoconus patients following sequential crosslinking and topography-guided surface ablation: the topolink study. *J Cataract Refract Surg.* (2020) 46:507–16. doi: 10.1097/j.jcrs.0000000000000110

212. Ohana O, Kaiserman I, Domniz Y, Cohen E, Franco O, Sela T, et al. Outcomes of simultaneous photorefractive keratectomy and collagen crosslinking. *Can J Ophthalmol.* (2018) 53:523–8.

213. Assaf A, Kotb A. Simultaneous corneal crosslinking and surface ablation combined with phakic intraocular lens implantation for managing keratoconus. *Int Ophthalmol.* (2015) 35:411–9. doi: 10.1007/s10792-014-9963-3

214. Coskunseven E, Jankov M, Grentzelos M, Plaka A, Limnopoulou A, Kymionis G. Topography-guided transepithelial PRK after intracorneal ring segments implantation and corneal collagen CXL in a three-step procedure for keratoconus. *J Refract Surg.* (2013) 29:54–8. doi: 10.3928/1081597X-20121217-01

215. Kremer I, Aizenman I, Lichter H, Shayer S, Levinger S. Simultaneous wavefront-guided photorefractive keratectomy and corneal collagen crosslinking after intrastromal corneal ring segment implantation for keratoconus. *J Cataract Refract Surg.* (2012) 38:1802–7.

216. Rocha G, Ibrahim T, Gulliver E, Lewis K. Combined phototherapeutic keratectomy, intracorneal ring segment implantation, and corneal collagen cross-linking in keratoconus management. *Cornea.* (2019) 38:1233–8. doi: 10.1097/ICO.0000000000002073

217. Shetty R, Israni N, Ramuka S, Dadachanji Z, Roy A, Mehra R, et al. Intracorneal ring segments followed by simultaneous topography-guided removal of epithelium and stroma with accelerated collagen cross-linking for keratoconus (I-TRESK/CXL). *Asia Pac J Ophthalmol.* (2020) 10:152–60. doi: 10.1097/APO.0000000000000342

218. Kanellopoulos A, Binder P. Management of corneal ectasia after LASIK with combined, same-day, topography-guided partial transepithelial PRK and collagen cross-linking: the athens protocol. *J Refract Surg.* (2011) 27:323–31. doi: 10.3928/1081597X-20101105-01

219. Kymionis G, Grentzelos M, Kankariya V, Liakopoulos D, Karavitaki A, Portaliou D, et al. Long-term results of combined transepithelial phototherapeutic keratectomy and corneal collagen crosslinking for keratoconus: cretan protocol. *J Cataract Refract Surg.* (2014) 40:1439–45.

220. Grentzelos M, Kounis G, Diakonis V, Siganos C, Tsilimbaris M, Pallikaris I, et al. Combined transepithelial phototherapeutic keratectomy and conventional photorefractive keratectomy followed simultaneously by corneal crosslinking for keratoconus: cretan protocol plus. *J Cataract Refract Surg.* (2017) 43:1257–62.

221. Rechichi M, Mazzotta C, Oliverio G, Romano V, Borroni D, Ferrise M, et al. Selective transepithelial ablation with simultaneous accelerated corneal crosslinking for corneal regularization of keratoconus: STARE-X protocol. *J Cataract Refract Surg.* (2021) 47:1403–10. doi: 10.1097/j.jcrs.0000000000000640

222. Coskunseven E, Sharma D, Grentzelos M, Sahin O, Kymionis G, Pallikaris I. Four-stage procedure for keratoconus: icrs implantation, corneal cross-linking, toric phakic intraocular lens implantation, and topography-guided photorefractive keratectomy. *J Refract Surg.* (2017) 33:683–9. doi: 10.3928/1081597X-20170807-01

223. Yeung S, Ku J, Lichtinger A, Low S, Kim P, Rootman D. Efficacy of single or paired intrastromal corneal ring segment implantation combined with collagen crosslinking in keratoconus. *J Cataract Refract Surg.* (2013) 39:1146–51.

224. Wollensak G, Spoerl E, Wilsch M, Seiler T. Keratocyte apoptosis after corneal collagen cross-linking using riboflavin/UVA treatment. *Cornea.* (2004) 23:43–9.

225. Moraes R, Ghanem R, Ghanem V, Santhiago M. Haze and visual acuity loss after sequential photorefractive keratectomy and corneal cross-linking for keratoconus. *J Refract Surg.* (2019) 35:109–14. doi: 10.3928/1081597X-20190114-01

226. Chang Y, Liang C, Weng T, Chien K, Lee C. Mitomycin C for the prevention of corneal haze in photorefractive keratectomy: a meta-analysis and trial sequential analysis. *Acta Ophthalmol.* (2021) 99:652–62. doi: 10.1111/aos.14704

227. Awwad S, Chacra L, Helwe C, Dhaini A, Telvizian T, Torbey J, et al. Mitomycin C application after corneal cross-linking for keratoconus increases stromal haze. *J Refract Surg.* (2021) 37:83–90. doi: 10.3928/1081597X-20201124-01

228. Iovieno A, Légaré M, Rootman D, Yeung S, Kim P, Rootman D. Intracorneal ring segments implantation followed by same-day photorefractive keratectomy and corneal collagen cross-linking in keratoconus. *J Refract Surg.* (2011) 27:915–8.

229. Tamayo G, Castell C, Vargas P, Polania E, Tamayo J. High-resolution wavefront-guided photorefractive keratectomy and accelerated corneal crosslinking for stabilization and visual rehabilitation of keratoconus eyes. *Clin Ophthalmol.* (2020) 14:1297–305. doi: 10.2147/OPTH.S248787

230. Gatinel D. Challenging the « no rub, no cone » keratoconus conjecture. D Gatinel. *Int J Kerat Ect Cor Dis.* (2018) 7:66–81.

231. Mazharian A, Panthier C, Courtin R, Jung C, Rampat R, Saad A, et al. Incorrect sleeping position and eye rubbing in patients with unilateral or highly asymmetric keratoconus: a case-control study. *Graefes Arch Clin Exp Ophthalmol.* (2020) 258:2431–9.

232. Kanellopoulos A. Management of progressive keratoconus with partial topography-guided PRK combined with refractive, customized CXL - a novel technique: the enhanced Athens protocol. *Clin Ophthalmol.* (2019) 13:581–8. doi: 10.2147/OPTH.S188517

233. Kanellopoulos A. Keratoconus management with customized photorefractive keratectomy by artificial intelligence ray-tracing optimization combined with higher fluence corneal crosslinking: the ray-tracing athens protocol. *Cornea.* (2021) 40:1181–7. doi: 10.1097/ICO.0000000000002739

234. Shafik Shaheen M, Shalaby A. Excimer Laser Ablation in Keratoconus Treatment: Sequential High Definition Wavefront-Guided PRK After CXL. In: Alio J editor. *Keratoconus essentials in ophthalmology*. Berlin: Springer (2017).

235. Binder P, Zavala E, Deg J, Baumgartner S. Hydrophilic lenses for refractive keratoplasty: the use of factory lathed materials. *CLAO J.* (1984) 10:105–11.

236. Riau A, Liu Y, Yam G, Mehta J. Stromal keratophakia: corneal inlay implantation. *Prog Retin Eye Res.* (2020) 75:100780.

237. Swinger C, Barraquer J. Keratophakia and keratomileusis–clinical results. *Ophthalmology.* (1981) 88:709–15. doi: 10.1016/s0161-6420(81)34958-6

238. Coullet J, Fournié P, Malecaze F, Arné J. Inadequate results for microkeratome-assisted additive stromal keratoplasty for management of keratoconus. *J Refract Surg.* (2008) 24:166–72. doi: 10.3928/1081597X-20080201-07

239. Jonas J. Intrastromal lamellar femtosecond laser keratoplasty with superficial flap. *Br J Ophthalmol.* (2003) 87:1195. doi: 10.1136/bjo.87.9.1195

240. Tan B, Purcell T, Torres L, Schanzlin D. New surgical approaches to the management of keratoconus and post-LASIK ectasia. *Trans Am Ophthalmol Soc.* (2006) 104:212–20.

241. Mastropasqua L, Nubile M, Salgari N, Mastropasqua R. Femtosecond laser-assisted stromal lenticule addition keratoplasty for the treatment of advanced

keratoconus: a preliminary study. *J Refract Surg.* (2018) 34:36–44. doi: 10.3928/1081597X-20171004-04

242. Nubile M, Salgari N, Mehta J, Calienno R, Erroi E, Bondì J, et al. Epithelial and stromal remodelling following femtosecond laser-assisted stromal lenticule addition keratoplasty (SLAK) for keratoconus. *Sci Rep.* (2021) 11:2293. doi: 10.1038/s41598-021-81626-5

243. Alio Del Barrio J, El Zarif M, Azaar A, Makdissy N, Khalil C, Harb W, et al. Corneal stroma enhancement with decellularized stromal laminas with or without stem cell recellularization for advanced keratoconus. *Am J Ophthalmol.* (2018) 186:47–58.

244. El Zarif M, A Jawad K, Alió Del Barrio J, A Jawad Z, Palazón-Bru A, de Miguel M, et al. Corneal stroma cell density evolution in keratoconus corneas following the implantation of adipose mesenchymal stem cells and corneal laminas: an in vivo confocal microscopy study. *Invest Ophthalmol Vis Sci.* (2020) 61:22. doi: 10.1167/iovs.61.4.22

245. Pradhan K, Reinstein D, Vida R, Archer T, Dhungel S, Dhungana P, et al. Femtosecond laser-assisted small incision sutureless intrastromal lamellar keratoplasty (silk) for corneal transplantation in keratoconus. *J Refract Surg.* (2019) 35:663–71. doi: 10.3928/1081597X-20190826-01

246. Almodin E, Ferrara P, Motta F, Colallilo J. Femtosecond laser–assisted intrastromal corneal lenticule implantation for treatment of advanced keratoconus in a child's eye. *JCRS Online Case Rep.* (2018) 6:25–9.

247. Jadidi K, Hasanpour H. Unilateral keratectasia treated with femtosecond fashioned intrastromal corneal inlay. *J Ophthalmic Vis Res.* (2017) 12:333–7. doi: 10.4103/jovr.jovr_227_15

248. Jadidi K, Mosavi S. Keratoconus treatment using femtosecond-assisted intrastromal corneal graft (FAISCG) surgery: a case series. *Int Med Case Rep J.* (2018) 11:9–15. doi: 10.2147/IMCRJ.S152884

249. Jafarinasab M, Hadi Y, Espandar G. Femtosecond laser-assisted allogenic additive stromal keratoplasty with or without excimer laser donor keratomileusis for management of keratoconus. *J Ophthalmic Vis Res.* (2021) 16:691–7.

250. Ganesh S, Brar S. Femtosecond intrastromal lenticular implantation combined with accelerated collagen cross-linking for the treatment of keratoconus–initial clinical result in 6 eyes. *Cornea.* (2015) 34:1331–9. doi: 10.1097/ICO.0000000000000539

251. Riau A, Htoon H, Alió Del Barrio J, Nubile M, El ZM, Mastropasqua L, et al. Femtosecond laser-assisted stromal keratophakia for keratoconus: a systemic review and meta-analysis. *Int Ophthalmol.* (2021) 41:1965–79. doi: 10.1007/s10792-021-01745-w

252. Hwang S, Chung T, Han J, Kim K, Lim D. Corneal transplantation for keratoconus in South Korea. *Sci Rep.* (2021) 11:12580.

253. McGhee C, Kim B, Wilson P. Contemporary treatment paradigms in keratoconus. *Cornea.* (2015) 34(Suppl. 10):S16–23. doi: 10.1097/ICO.0000000000000504

254. Mohammadpour M, Heidari Z, Hashemi H. Updates on managements for keratoconus. *J Curr Ophthalmol.* (2018) 30:110–24.

255. Iselin K, Greenan E, Hynes C, Shaw S, Fulcher T, Power W, et al. Changing trends in corneal transplantation: a national review of current practices in the Republic of Ireland. *Irish J Med Sci.* (2021) 190:825–34. doi: 10.1007/s11845-020-02340-1

256. Ricouard F, Puyraveau M, Gain P, Martinache I, Delbosc B, Gauthier A. Regional trends in corneal transplantation from 2004 to 2015 in France: a 12-year review on indications, technique and waiting period. *Cell Tissue Bank.* (2020) 21:65–76. doi: 10.1007/s10561-019-09798-z

257. Chilibeck C, Brookes N, Gokul A, Kim B, Twohill H, Moffatt S, et al. Changing trends in corneal transplantation in Aotearoa/New Zealand, 1991 to 2020: effects of population growth, cataract surgery, endothelial keratoplasty, and corneal cross-linking for keratoconus. *Cornea.* (2022) 41:680–7. doi: 10.1097/ICO.0000000000002812

258. Anshu A, Li L, Htoon H, De Benito-Llopis L, Shuang L, Singh M, et al. Long-term review of penetrating keratoplasty: a 20-year review in asian eyes. *Am J Ophthalmol.* (2021) 224:254–66. doi: 10.1016/j.ajo.2020.10.014

259. Gao H, Huang T, Pan Z, Wu J, Xu J, Hong J, et al. Survey report on keratoplasty in China: a 5-year review from 2014 to 2018. *PLoS One.* (2020) 15:e0239939. doi: 10.1371/journal.pone.0239939

260. Moriyama A, Dos Santos Forseto A, Pereira N, Ribeiro A, de Almeida M, Figueras-Roca M, et al. Trends in Corneal transplantation in a tertiary hospital in Brazil. *Cornea.* (2022) 41:857–66. doi: 10.1097/ICO.0000000000002801

261. Sarezky D, Orlin S, Pan W, VanderBeek B. Trends in corneal transplantation in keratoconus. *Cornea.* (2017) 36:131–7.

262. Sklar J, Wendel C, Zhang A, Chan C, Yeung S, Iovieno A. Did collagen cross-linking reduce the requirement for corneal transplantation in keratoconus? *Can Exp Cornea.* (2019) 38:1390–4.

263. Van Dijk K, Parker J, Tong C, Ham L, Lie J, Groeneveld-Van Beek E, et al. Midstromal isolated bowman layer graft for reduction of advanced keratoconus. *JAMA Ophthalmol.* (2014) 132:495.

264. Van Dijk K, Parker J, Baydoun L, Ilyas A, Dapena I, Groeneveld-Van Beek E, et al. Bowman layer transplantation: 5-year results. *Graefe's Arch Clin Exp Ophthalmol.* (2018) 256:1151–8. doi: 10.1007/s00417-018-3927-7

265. Cassidy D, Beltz J, Jhanji V, Loughnan M. Recent advances in corneal transplantation for keratoconus. *Clin Exp Optom.* (2013) 96:165–72.

266. Oyeniran E, Tauqeer Z. Update in the management of keratoconus. *Adv Ophthalmol Optometry.* (2021) 6:307–24.

267. Parker J, Van Dijk K, Melles G. Treatment options for advanced keratoconus: a review. *Surv Ophthalmol.* (2015) 60:459–80.

268. Kelly T, Williams K, Coster D, Registry A. Corneal transplantation for keratoconus: a registry study. *Arch Ophthalmol.* (2011) 129:691–7.

269. Chamberlain W, Rush S, Mathers W, Cabezas M, Fraunfelder F. Comparison of femtosecond laser-assisted keratoplasty versus conventional penetrating keratoplasty. *Ophthalmology.* (2011) 118:486–91.

270. Cheng Y, Visser N, Schouten J, Wijdh R, Pels E, van Cleynenbreugel H, et al. Endothelial cell loss and visual outcome of deep anterior lamellar keratoplasty versus penetrating keratoplasty: a randomized multicenter clinical trial. *Ophthalmology.* (2011) 118:302–9.

271. Jensen L, Hjortdal J, Ehlers N. Longterm follow-up of penetrating keratoplasty for keratoconus. *Acta Ophthalmol.* (2009) 88:347–51.

272. Barraquer R, Pareja-Aricò L, Gómez-Benlloch A, Michael R. Risk factors for graft failure after penetrating keratoplasty. *Medicine.* (2019) 98:e15274.

273. Ellakwa A, Khairy H, Mohammed Marey H. Epithelium-on corneal cross-linking treatment of progressive keratoconus: a prospective, consecutive study. *Clin Ophthalmol.* (2014) 8:819–23.

274. Alió Del Barrio J, Bhogal M, Ang M, Ziaei M, Robbie S, Montesel A, et al. Corneal transplantation after failed grafts: options and outcomes. *Surv Ophthalmol.* (2021) 66:20–40.

275. Moramarco A, Gardini L, Iannetta D, Versura P, Fontana L. Post penetrating keratoplasty ectasia: incidence, risk factors, clinical features, and treatment options. *J Clin Med.* (2022) 11:2678. doi: 10.3390/jcm11102678

276. Yoshida J, Murata H, Miyai T, Shirakawa R, Toyono T, Yamagami S, et al. Characteristics and risk factors of recurrent keratoconus over the long term after penetrating keratoplasty. *Graefes Arch Clin Exp Ophthalmol.* (2018) 256:2377–83. doi: 10.1007/s00417-018-4131-5

277. Ezra D, Mehta J, Allan B. Late corneal hydrops after penetrating keratoplasty for keratoconus. *Cornea.* (2007) 26:639–40.

278. Gadhvi K, Romano V, Fernández-Vega Cueto L, Aiello F, Day A, Allan B. Deep anterior lamellar keratoplasty for keratoconus: multisurgeon results. *Am J Ophthalmol.* (2019) 201:54–62.

279. Patil M, Mehta J. Lamellar keratoplasty for advanced keratoconus. *Asia Pac J Ophthalmol.* (2020) 9:580–8.

280. Dua HS, Freitas R, Mohammed I, Ting DSJ, Said DG. The pre-Descemet's layer (Dua's layer, also known as the Dua-Fine layer and the pre-posterior limiting lamina layer): Discovery, characterisation, clinical and surgical applications, and the controversy. *Prog Retin Eye Res.* (2023) 101161. doi: 10.1016/j.preteyeres.2022.101161

281. Dua HS, Said DG. Deep anterior lamellar keratoplasty (DALK): Science and surgery. In: Albert DM, Miller JW, Azar DT, editors. *Albert and Jakobiec's Principles and Practice of Ophthalmology*. Cham: Springer International Publishing (2022). p. 469–90.

282. Reinhart W, Musch D, Jacobs D, Lee W, Kaufman S, Shtein R. Deep anterior lamellar keratoplasty as an alternative to penetrating keratoplasty a report by the American Academy of Ophthalmology. *Ophthalmology.* (2011) 118:209–18. doi: 10.1016/j.ophtha.2010.11.002

283. Henein C, Nanavaty M. Systematic review comparing penetrating keratoplasty and deep anterior lamellar keratoplasty for management of keratoconus. *Cont Lens Anterior Eye.* (2017) 40:3–14.

284. Borderie V, Sandali O, Bullet J, Gaujoux T, Touzeau O, Laroche L. Long-term results of deep anterior lamellar versus penetrating keratoplasty. *Ophthalmology.* (2012) 119:249–55.

285. Liu H, Chen Y, Wang P, Li B, Wang W, Su Y, et al. Efficacy and safety of deep anterior lamellar keratoplasty vs. penetrating keratoplasty for keratoconus: a meta-analysis. *PLoS One.* (2015) 10:e0113332. doi: 10.1371/journal.pone.0113332

286. Keane M, Coster D, Ziaei M, Williams K. Deep anterior lamellar keratoplasty versus penetrating keratoplasty for treating keratoconus. *Cochrane Database Syst Rev.* (2014) 22:CD009700.

287. Knutsson K, Rama P, Paganoni G. Modified big-bubble technique compared to manual dissection deep anterior lamellar keratoplasty in the treatment of keratoconus. *Acta Ophthalmol.* (2015) 93:431–8. doi: 10.1111/aos.12705

288. Romano V, Iovieno A, Parente G, Soldani A, Fontana L. Long-term clinical outcomes of deep anterior lamellar keratoplasty in patients with keratoconus. *Am J Ophthalmol.* (2015) 159:505–11.

289. Bhatt UK, Fares U, Rahman I, Said DG, Maharajan SV, Dua HS. Outcomes of deep anterior lamellar keratoplasty following successful and failed 'big bubble'. *Br J Ophthalmol.* (2012) 96:564–9. doi: 10.1136/bjophthalmol-2011-300214

290. Ayyala R. Penetrating keratoplasty and glaucoma. *Survey Ophthalmol.* (2000) 45:91–105.

291. Fan J, Chow K, Patel D, McGhee C. Corticosteroid-induced intraocular pressure elevation in keratoconus is common following uncomplicated penetrating keratoplasty. *Eye.* (2009) 23:2056–62. doi: 10.1038/eye.2008.413

292. Greenlee E, Kwon Y. Graft failure: III. Glaucoma escalation after penetrating keratoplasty. *Int Ophthalmol.* (2008) 28:191–207. doi: 10.1007/s10792-008-9223-5

293. Zhang Y, Wu S, Yao Y. Long-term comparison of full-bed deep anterior lamellar keratoplasty and penetrating keratoplasty in treating keratoconus. *J Zhejiang Univ. Sci B.* (2013) 14:438–50. doi: 10.1631/jzus.B1200272

294. Huang O, Mehta J, Htoon H, Tan D, Wong T. Incidence and risk factors of elevated intraocular pressure following deep anterior lamellar keratoplasty. *Am J Ophthalmol.* (2016) 170:153–60.

295. Musa F, Patil S, Rafiq O, Galloway P, Ball J, Morrell A. Long-term risk of intraocular pressure elevation and glaucoma escalation after deep anterior lamellar keratoplasty. *Clin Exp Ophthalmol.* (2012) 40:780–5. doi: 10.1111/j.1442-9071.2012.02796.x

296. Tan D, Anshu A, Parthasarathy A, Htoon H. Visual acuity outcomes after deep anterior lamellar keratoplasty: a case-control study. *Br J Ophthalmol.* (2010) 94:1295–9.

297. Ang M, Mohamed-Noriega K, Mehta J, Tan D. Deep anterior lamellar keratoplasty: surgical techniques, challenges, and management of intraoperative complications. *Int Ophthalmol Clin.* (2013) 53:47–58.

298. Bahar I, Kaiserman I, Srinivasan S, Ya-Ping J, Slomovic A, Rootman D. Comparison of three different techniques of corneal transplantation for keratoconus. *Am J Ophthalmol.* (2008) 146:905–12.e1.

299. Song A, Deshmukh R, Lin H, Ang M, Mehta J, Chodosh J, et al. Post-keratoplasty infectious keratitis: epidemiology, risk factors, management, and outcomes. *Front Med.* (2021) 8:707242. doi: 10.3389/fmed.2021.707242

300. Feizi S, Javadi M, Rezaei Kanavi M. Recurrent keratoconus in a corneal graft after deep anterior lamellar keratoplasty. *J Ophthalmic Vis Res.* (2012) 7:328–31.

301. Huang O, Htoon H, Chan A, Tan D, Mehta J. Incidence and outcomes of intraoperative descemet membrane perforations during deep anterior lamellar keratoplasty. *Am J Ophthalmol.* (2019) 199:9–18.

302. Kubaloglu A, Sari E, Unal M, Koytak A, Kurnaz E, Cinar Y, et al. Long-term results of deep anterior lamellar keratoplasty for the treatment of keratoconus. *Am J Ophthalmol.* (2011) 151:760–7.e1.

303. Carlà M, Boselli F, Giannuzzi F, Gambini G, Caporossi T, De Vico U, et al. An overview of intraoperative oct-assisted lamellar corneal transplants: a game changer? *Diagnostics.* (2022) 12:727. doi: 10.3390/diagnostics12030727

304. De Benito-Llopis L, Mehta J, Angunawela R, Ang M, Tan D. Intraoperative anterior segment optical coherence tomography: a novel assessment tool during deep anterior lamellar keratoplasty. *Am J Ophthalmol.* (2014) 157:334.e–41.e. doi: 10.1016/j.ajo.2013.10.001

305. Deshmukh R, Stevenson L, Vajpayee R. Laser-assisted corneal transplantation surgery. *Surv Ophthalmol.* (2021) 66:826–37.

306. Gerten G, Oberheide U, Thiée P. Clear cornea femto dalk: a novel technique for performing deep anterior lamellar keratoplasty. *Graefes Arch Clin Exp Ophthalmol.* (2022) 260:2941–8. doi: 10.1007/s00417-022-05582-0

307. Abou Shousha M, Perez V, Fraga Santini Canto A, Vaddavalli P, Sayyad F, Cabot F, et al. The use of bowman's layer vertical topographic thickness map in the diagnosis of keratoconus. *Ophthalmology.* (2014) 121:988–93. doi: 10.1016/j.ophtha.2013.11.034

308. Sherwin T, Brookes N. Morphological changes in keratoconus: pathology or pathogenesis. *Clin Exp Ophthalmol.* (2004) 32:211–7.

309. Ting D, Ramaesh K, Srinivasan S, Sau C, Mantry S, Roberts F. Deep anterior lamellar keratoplasty: challenges in histopathological examination. *Br J Ophthalmol.* (2012) 96:1510–2. doi: 10.1136/bjophthalmol-2012-302150

310. van Dijk K, Liarakos V, Parker J, Ham L, Lie J, Groeneveld-van Beek E, et al. Bowman layer transplantation to reduce and stabilize progressive, advanced keratoconus. *Ophthalmology.* (2015) 122:909–17.

311. Luceri S, Parker J, Dapena I, Baydoun L, Oellerich S, van Dijk K, et al. Corneal densitometry and higher order aberrations after bowman layer transplantation: 1-year results. *Cornea.* (2016) 35:959–66. doi: 10.1097/ICO.0000000000000860

312. García de Oteyza G, González Dibildox L, Vázquez-Romo K, Tapia Vázquez A, Dávila Alquisiras J, Martínez-Báez B, et al. Bowman layer transplantation using a femtosecond laser. *J Cataract Refract Surg.* (2019) 45:261–6.

313. Tong C, Parker J, Dockery P, Birbal R, Melles G. Use of intraoperative anterior segment optical coherence tomography for Bowman layer transplantation. *Acta Ophthalmol.* (2019) 97:e1031–2.

314. Zygoura V, Birbal R, van Dijk K, Parker J, Baydoun L, Dapena I, et al. Validity of Bowman layer transplantation for keratoconus: visual performance at 5-7 years. *Acta Ophthalmol.* (2018) 96:e901–2. doi: 10.1111/aos.13745

315. Dragnea D, Birbal R, Ham L, Dapena I, Oellerich S, van Dijk K, et al. Bowman layer transplantation in the treatment of keratoconus. *Eye Vis.* (2018) 5:24.

316. Blasberg C, Geerling G, Schrader S. Bowman layer transplantation in progressive keratoconus - what is it good for?. *Klin Monbl Augenheilkd.* (2017) 234:776–9.

317. Alio J, Montesel A, El Sayyad F, Barraquer R, Arnalich-Montiel F, Alio Del Barrio J. Corneal graft failure: an update. *Br J Ophthalmol.* (2021) 105:1049–58.

318. Alio Del Barrio J, Alio J. Cellular therapy of the corneal stroma: a new type of corneal surgery for keratoconus and corneal dystrophies. *Eye Vis.* (2018) 5:28.

319. Arnalich-Montiel F, Alio Del Barrio J, Alio J. Corneal surgery in keratoconus: which type, which technique, which outcomes? *Eye Vis.* (2016) 3:2.

320. El Zarif M, Alio J, Alio Del Barrio J, De Miguel M, Abdul Jawad K, Makdissy N. Corneal stromal regeneration: a review of human clinical studies in keratoconus treatment. *Front Med.* (2021) 8:650724. doi: 10.3389/fmed.2021.650724

321. Alio Del Barrio J, El Zarif M, de Miguel M, Azaar A, Makdissy N, Harb W, et al. Cellular therapy with human autologous adipose-derived adult stem cells for advanced keratoconus. *Cornea.* (2017) 36:952–60.

322. Alió J, Alió Del Barrio J, El Zarif M, Azaar A, Makdissy N, Khalil C, et al. Regenerative surgery of the corneal stroma for advanced keratoconus: 1-year outcomes. *Am J Ophthalmol.* (2019) 203:53–68. doi: 10.1016/j.ajo.2019.02.009

323. Arnalich-Montiel F, Pastor S, Blazquez-Martinez A, Fernandez-Delgado J, Nistal M, Alio J, et al. Adipose-derived stem cells are a source for cell therapy of the corneal stroma. *Stem Cells.* (2008) 26:570–9.

324. Alio Del Barrio J, Arnalich-Montiel F, De Miguel M, El Zarif M, Alio J. Corneal stroma regeneration: preclinical studies. *Exp Eye Res.* (2021) 202:108314.

325. El Zarif M, Alió J, Alió Del Barrio J, Abdul JK, Palazón-Bru A, Abdul JZ, et al. Corneal stromal regeneration therapy for advanced keratoconus: long-term outcomes at 3 years. *Cornea.* (2021) 40:741–54. doi: 10.1097/ICO.0000000000002646

326. Alio del Barrio J, Chiesa M, Garagorri N, Garcia-Urquia N, Fernandez-Delgado J, Bataille L, et al. Acellular human corneal matrix sheets seeded with human adipose-derived mesenchymal stem cells integrate functionally in an experimental animal model. *Exp Eye Res.* (2015) 132:91–100. doi: 10.1016/j.exer.2015.01.020

327. Rafat M, Jabbarvand M, Sharma N, Xeroudaki M, Tabe S, Omrani R, et al. Bioengineered corneal tissue for minimally invasive vision restoration in advanced keratoconus in two clinical cohorts. *Nat Biotechnol.* (2023) 41:70–81. doi: 10.1038/s41587-022-01408-w

328. Goodwin S, McPherson J, McCombie W. Coming of age: ten years of next-generation sequencing technologies. *Nat Rev Genet.* (2016) 17:333–51. doi: 10.1038/nrg.2016.49

329. Adams D, Eng C. Next-generation sequencing to diagnose suspected genetic disorders. *N Engl J Med.* (2018) 379:1353–62.

330. Chang H, Chodosh J. The genetics of keratoconus. *Semin Ophthalmol.* (2013) 28:275–80.

331. Ferrari G, Rama P. The keratoconus enigma: a pathogenesis review. *Ocul Surf.* (2020) 18:363–73.

332. Lu Y, Vitart V, Burdon K, Khor C, Bykhovskaya Y, Mirshahi A, et al. Genome-wide association analyses identify multiple loci associated with central corneal thickness and keratoconus. *Nat Genet.* (2013) 45:155–63.

333. Bykhovskaya Y, Margines B, Rabinowitz Y. Genetics in Keratoconus: where are we? *Eye Vis.* (2016) 3:16.

334. Cehajic-Kapetanovic J, Singh M, Zrenner E, MacLaren R. Bioengineering strategies for restoring vision. *Nat Biomed Eng.* (2022) 7:387–404. doi: 10.1038/s41551-021-00836-4

335. Fenner B, Tan T, Barathi A, Tun S, Yeo S, Tsai A, et al. Gene-based therapeutics for inherited retinal diseases. *Front Genet.* (2021) 12:794805. doi: 10.3389/fgene.2021.794805

336. Oliynyk R. Future preventive gene therapy of polygenic diseases from a population genetics perspective. *Int J Mol Sci.* (2019) 20:5013. doi: 10.3390/ijms20205013

337. Acosta J, Falcone G, Rajpurkar P, Topol E. Multimodal biomedical AI. *Nat Med.* (2022) 28:1773–84.

338. Li J, Liu H, Ting D, Jeon S, Chan R, Kim J, et al. Digital technology, tele-medicine and artificial intelligence in ophthalmology: a global perspective. *Prog Retin Eye Res.* (2021) 82:100900. doi: 10.1016/j.preteyeres.2020.100900

339. Matheny M, Whicher D, Thadaney Israni S. Artificial intelligence in health care: a report from the national academy of medicine. *Jama.* (2020) 323:509–10. doi: 10.1001/jama.2019.21579

340. Rajkomar A, Dean J, Kohane I. Machine learning in medicine. *N Engl J Med.* (2019) 380:1347–58.

341. Ting D, Cheung C, Lim G, Tan G, Quang N, Gan A, et al. Development and validation of a deep learning system for diabetic retinopathy and related eye diseases using retinal images from multiethnic populations with diabetes. *Jama.* (2017) 318:2211–23. doi: 10.1001/jama.2017.18152

342. Ting D, Deshmukh R, Ting D, Ang M. Big data in corneal diseases and cataract: current applications and future directions. *Front Big Data.* (2023) 6:1017420. doi: 10.3389/fdata.2023.1017420

343. Portney D, Zhu Z, Chen E, Steppe E, Chilakamarri P, Woodward M, et al. COVID-19 and use of teleophthalmology (CUT Group): trends and diagnoses. *Ophthalmology.* (2021) 128:1483–5. doi: 10.1016/j.ophtha.2021.02.010

344. Tan T, Chodosh J, McLeod S, Parke D II, Yeh S, Wong T, et al. Global Trends in Ophthalmic Practices in Response to COVID-19. *Ophthalmology.* (2021) 128:1505–15.

345. Ting D, Ang M, Mehta J, Ting D. Artificial intelligence-assisted telemedicine platform for cataract screening and management: a potential model of care for global eye health. *Br J Ophthalmol.* (2019) 103:1537–8. doi: 10.1136/bjophthalmol-2019-315025

346. Ting D, Deshmukh R, Said D, Dua H. The impact of COVID-19 pandemic on ophthalmology services: are we ready for the aftermath? *Ther Adv Ophthalmol.* (2020) 12:2515841420964099. doi: 10.1177/2515841420964099

347. Ambrosio R Jr, Lopes B, Faria-Correia F, Salomao M, Buhren J, Roberts C, et al. Integration of scheimpflug-based corneal tomography and biomechanical assessments for enhancing ectasia detection. *J Refract Surg.* (2017) 33:434–43.

348. Ambrosio R Jr, Machado A, Leao E, Lyra J, Salomao M, Esporcatte L, et al. Optimized artificial intelligence for enhanced ectasia detection using scheimpflug-based corneal tomography and biomechanical data. *Am J Ophthalmol.* (2022) 251:126–42. doi: 10.1016/j.ajo.2022.12.016

349. Lopes B, Ramos I, Salomao M, Guerra F, Schallhorn S, Schallhorn J, et al. Enhanced tomographic assessment to detect corneal ectasia based on artificial intelligence. *Am J Ophthalmol.* (2018) 195:223–32.

350. Vinciguerra R, Ambrosio R, Wang Y, Zhang F, Zhou X, Bai J, et al. Detection of keratoconus with a new corvis biomechanical index optimized for Chinese population (cCBI). *Am J Ophthalmol.* (2023) 252:182–8. doi: 10.1016/j.ajo.2023.04.002

351. Chen X, Zhao J, Iselin K, Borroni D, Romano D, Gokul A, et al. Keratoconus detection of changes using deep learning of colour-coded maps. *BMJ Open Ophthalmol.* (2021) 6:e000824. doi: 10.1136/bmjophth-2021-000824

352. Almeida G Jr, Guido R, Balarin Silva H, Brandão C, de Mattos L, Lopes B, et al. New artificial intelligence index based on Scheimpflug corneal tomography to distinguish subclinical keratoconus from healthy corneas. *J Cataract Refract Surg.* (2022) 48:1168–74. doi: 10.1097/j.jcrs.0000000000000946

353. Maile H, Li J, Gore D, Leucci M, Mulholland P, Hau S, et al. Machine learning algorithms to detect subclinical keratoconus: systematic review. *JMIR Med Inform.* (2021) 9:e27363. doi: 10.2196/27363

354. Rampat R, Deshmukh R, Chen X, Ting D, Said D, Dua H, et al. Artificial intelligence in cornea, refractive surgery, and cataract: basic principles, clinical applications, and future directions. *Asia Pac J Ophthalmol.* (2021) 10:268–81. doi: 10.1097/APO.0000000000000394

355. Ting D, Foo V, Yang L, Sia J, Ang M, Lin H, et al. Artificial intelligence for anterior segment diseases: emerging applications in ophthalmology. *Br J Ophthalmol.* (2021) 105:158–68.

356. Yousefi S, Takahashi H, Hayashi T, Tampo H, Inoda S, Arai Y, et al. Predicting the likelihood of need for future keratoplasty intervention using artificial intelligence. *Ocul Surf.* (2020) 18:320–5. doi: 10.1016/j.jtos.2020.02.008

357. Gokul A, Vellara H, Patel D. Advanced anterior segment imaging in keratoconus: a review. *Clin Exp Ophthalmol.* (2018) 46:122–32.

358. Arbelaez M, Versaci F, Vestri G, Barboni P, Savini G. Use of a support vector machine for keratoconus and subclinical keratoconus detection by topographic and tomographic data. *Ophthalmology.* (2012) 119:2231–8. doi: 10.1016/j.ophtha.2012.06.005

359. Cao K, Verspoor K, Sahebjada S, Baird P. Evaluating the performance of various machine learning algorithms to detect subclinical keratoconus. *Transl Vis Sci Technol.* (2020) 9:24.

360. Gao H, Pan Z, Shen M, Lu F, Li H, Zhang X. KeratoScreen: early keratoconus classification with zernike polynomial using deep learning. *Cornea.* (2022) 41:1158–65. doi: 10.1097/ICO.0000000000003038

361. Issarti I, Consejo A, Jiménez-García M, Hershko S, Koppen C, Rozema J. Computer aided diagnosis for suspect keratoconus detection. *Comput Biol Med.* (2019) 109:33–42.

362. Kovács I, Miháltz K, Kránitz K, Juhász É, Takács Á, Dienes L, et al. Accuracy of machine learning classifiers using bilateral data from a Scheimpflug camera for identifying eyes with preclinical signs of keratoconus. *J Cataract Refract Surg.* (2016) 42:275–83. doi: 10.1016/j.jcrs.2015.09.020

363. Silverman R, Urs R, Roychoudhury A, Archer T, Gobbe M, Reinstein D. Epithelial remodeling as basis for machine-based identification of keratoconus. *Investig Ophthalmol Vis Sci.* (2014) 55:1580–7. doi: 10.1167/iovs.13-12578

364. Smadja D, Touboul D, Cohen A, Doveh E, Santhiago M, Mello G, et al. Detection of subclinical keratoconus using an automated decision tree classification. *Am J Ophthalmol.* (2013) 156:237.e–46.e.

365. Smolek M, Klyce S. Current keratoconus detection methods compared with a neural network approach. *Investig Ophthalmol Vis Sci.* (1997) 38:2290–9.

366. Souza M, Medeiros F, Souza D, Garcia R, Alves M. Evaluation of machine learning classifiers in keratoconus detection from orbscan II examinations. *Clinics.* (2010) 65:1223–8. doi: 10.1590/s1807-59322010001200002

367. Twa M, Parthasarathy S, Roberts C, Mahmoud A, Raasch T, Bullimore M. Automated decision tree classification of corneal shape. *Optometry Vis Sci.* (2005) 82:1038–46.

368. Valdés-Mas M, Martín-Guerrero J, Rupérez M, Pastor F, Dualde C, Monserrat C, et al. A new approach based on Machine Learning for predicting corneal curvature (K1) and astigmatism in patients with keratoconus after intracorneal ring implantation. *Comput Methods Programs Biomed.* (2014) 116:39–47. doi: 10.1016/j.cmpb.2014.04.003

369. Yousefi S, Yousefi E, Takahashi H, Hayashi T, Tampo H, Inoda S, et al. Keratoconus severity identification using unsupervised machine learning. *PLoS One.* (2018) 13:e0205998. doi: 10.1371/journal.pone.0205998

370. Lavric A, Valentin P. KeratoDetect: keratoconus detection algorithm using convolutional neural networks. *Comput Intell Neurosci.* (2019) 2019:8162567. doi: 10.1155/2019/8162567

371. Shetty R, Kundu G, Narasimhan R, Khamar P, Gupta K, Singh N, et al. Artificial intelligence efficiently identifies regional differences in the progression of tomographic parameters of keratoconic corneas. *J Refract Surg.* (2021) 37:240–8. doi: 10.3928/1081597X-20210120-01

372. Fariselli C, Vega-Estrada A, Arnalich-Montiel F, Alio J. Artificial neural network to guide intracorneal ring segments implantation for keratoconus treatment: a pilot study. *Eye Vis.* (2020) 7:20. doi: 10.1186/s40662-020-00184-5

frontiers | Frontiers in Medicine

TYPE Original Research
PUBLISHED 27 July 2023
DOI 10.3389/fmed.2023.1169776

OPEN ACCESS

EDITED BY
Georgios D. Panos,
Nottingham University Hospitals NHS Trust, United Kingdom

REVIEWED BY
Youxin Chen,
Peking Union Medical College Hospital (CAMS), China
Hanyi Min,
Peking Union Medical College Hospital (CAMS), China

*CORRESPONDENCE
Yantao Wei
✉ weiyantao75@126.com
Ting Zhang
✉ zhangting@gzzoc.com
Shaochong Zhang
✉ zhangshaochong@gzzoc.com

†These authors share first authorship

RECEIVED 22 February 2023
ACCEPTED 16 May 2023
PUBLISHED 27 July 2023

CITATION
Shi Y, Feng L, Li Y, Jiang Z, Fang D, Han X, Wang L, Wei Y, Zhang T and Zhang S (2023) Outcomes of revision surgery for idiopathic macular hole after failed primary vitrectomy. *Front. Med.* 10:1169776. doi: 10.3389/fmed.2023.1169776

Outcomes of revision surgery for idiopathic macular hole after failed primary vitrectomy

Yunhong Shi[1†], Lujia Feng[2†], Yangyang Li[1], Zhihao Jiang[1], Dong Fang[2], Xiaotong Han[1], Lanhua Wang[1], Yantao Wei[1*], Ting Zhang[1*] and Shaochong Zhang[2*]

[1]State Key Laboratory of Ophthalmology, Zhongshan Ophthalmic Center, Sun Yat-sen University, Guangdong Provincial Key Laboratory of Ophthalmology and Visual Science, Guangdong Provincial Clinical Research Center for Ocular Diseases, Guangzhou, China, [2]Shenzhen Eye Hospital, Jinan University, Shenzhen Eye Institute, Shenzhen, China

Persistent idiopathic macular hole (PIMH), the occurrence of idiopathic macular holes that have failed to close after standard pars plana vitrectomy (PPV) with internal limiting membrane (ILM) peeling, has become a global health threat to the aging population. Because postoperative anatomic closure or restoration of visual acuity is more difficult to achieve in PIMH, surgical approaches that would yield the best outcomes remain to be elucidated. On paper, extended ILM peeling combined with silicone oil (SiO) tamponade is believed to be a feasible option for excellent macular hole closure. However, no studies on this combined treatment for PIMH is compared with simple air tamponade have been conducted. Thus, in this retrospective case series, we used spectral-domain optical coherence tomography (SD-OCT) and other technologies to investigate real-world evidence for the anatomical and functional outcomes of revisional PPV with either SiO or air tamponade for failed primary idiopathic macular hole surgery. We included the records of 76 patients with PIMH who had SD-OCT examinations and best-corrected visual acuity (BCVA). Regression analysis was performed to find factors affecting PIMH fracture closure. Seventy-six participants were allocated to a SiO group (n = 21, with an extended ILM peeling and SiO tamponade) or an air group (n = 55, with extended ILM peeling and air tamponade). Anatomical success was achieved in 18 (85.7%) and 40 (72.7%) eyes in the SiO and air groups, respectively ($p = 0.37$). BCVA was significantly improved in both subgroups of closed PIMH (SiO group: $p = 0.041$; air group: $p < 0.001$). Minimum linear diameter (MLD) was closely related to the closure rate (OR, 1.0; 95% CI (0.985–0.999); $p = 0.03$). MLD = 650 μm seemed like a cut-off point for closure rate (MLD ≤ 650 μm vs. MLD > 650 μm; 88.4% vs. 52%, $p = 0.002$). In conclusion, we demonstrated that extended ILM peeling combined with SiO or air tamponade is effective in PIMH treatment. Moreover, though not statistically significant herein, the anatomic closure rate was better for silicone-operated eyes than for air-operated eyes. MLD is the best predictor of PIMH closure; MLD ≤ 650 μm could achieve a significantly higher closure rate.

KEYWORDS

persistent idiopathic macular hole, revision procedure, optical coherence tomography, visual acuity, pars plana vitrectomy

1. Introduction

Since the initial publication by Kelly and Wendel describing vitrectomy surgery for idiopathic macular hole (iMH), the rate of successful macular hole closure has increased to over 90% (1, 2). However, the most common postoperative complication of iMH surgery is persistent iMH (PIMH). Because postoperative anatomic closure (52–80%) or restoration of visual acuity is more difficult to achieve in PIMH, it remains debatable which surgical approach is the best (3).

To increase the closure rate of PIMH, clinical researchers have focused more on completely relieving residual traction and prolonging effective tamponade to stimulate glial cell proliferation (4). Therefore, studies have described improvements in the standard surgical strategies, such as superior wide-base internal limiting membrane flap transposition (5), extended internal limiting membrane (ILM) peeling (6), use of an inverted ILM flap (7), transplantation of a neurosensory retina (8), and use of vitreous substitutes (9), as well as shown innovations in affiliation procedures to improve macular hole bridging, such as the use of whole blood or blood components (10). Air and silicone oil (SiO) are common tamponades. A series of reports have suggested the pleasantness of air tamponade effects in PIMH (11, 12). SiO, a long-acting vitreous substitute, is applied long-term in complicated vitreoretinal surgeries, and a recent meta-analysis showed its benefits in increasing the closure rate of large macular hole with or without retinal detachment (13). In addition, in recent years, enlarged ILM peeling has been widely used to treat various kinds of refractory macular holes because of its ability to relieve residual macular traction. Theoretically, the combined procedure of extended ILM peeling and SiO tamponade will achieve excellent iMH closure, but there are no reports on this kind of treatment for PIMH comparing it with simple air tamponade. Therefore, we conducted a retrospective case series to evaluate the effects of the two procedures, explore their indications, and determine the optimal intervention for relatively large PIMHs in a cohort of 76 patients.

2. Materials and methods

PIMH refers to the occurrence of iMH that have failed to close after standard pars plana vitrectomy (PPV) with ILM peeling. All patients underwent small-gauge (25–27 gauge) PPV with retrobulbar anesthesia, which was performed by experienced ophthalmologist, under monitored anesthetic care. Patients were allocated to either the SiO or air group at the discretion of the treating surgeon. Normally, by clinical experience, patients with a poor degree of adaptability, monophthalmia, or a planned flight were advised to undergo SiO tamponade.

2.1. Ethics statement

This study was approved by the Institutional Review Board of Zhongshan Ophthalmic Center, which is affiliated with Sun Yat-sen University (Guangzhou, China), and was performed in accordance with the World Medical Association's Declaration of Helsinki. All extracted patient data were anonymized for analysis.

2.2. Inclusion and exclusion criteria

The inclusion criteria were the availability of high-quality spectral-domain-optical coherence tomography (SD-OCT, Heidelberg Engineering, Heidelberg, Germany) images pre-and postoperation and the presence of PIMH, as determined by SD-OCT.

The exclusion criteria were as follows: (1) presence of anamnestic data of previous eye trauma, (2) high myopia (axial length greater than 26.50 mm or refractive error more than 6.00 D), (3) rhegmatogenous retinal detachment with macular hole, (4) history of fundus disease, (5) low-quality SD-OCT image, which was defined as an image with no diameter measurement, (6) postoperative follow-up shorter than 4 months, (7) absence of comprehensive presurgery examination, and (8) glaucoma or other concurrent vision-limiting eye conditions were excluded.

2.3. Outcome measures

Baseline patient demographics include age, sex, ocular characteristics, mean preoperative minimum linear diameter (MLD) of the PIMH, and lens status (Table 1). All patients underwent ophthalmic examination, including Snellen best-corrected visual acuity (BCVA) test, SD-OCT scans, intraocular pressure measurement, slit-lamp biomicroscopy, fundus photography, and

TABLE 1 Baseline patient characteristics (76 patients, *n* = 76 eyes).

Factor	SiO (*n* = 21)	Air (*n* = 55)	*p value*
Demographic characteristics			
Age, years, mean ± SD (range)	60.8 ± 7.8 (43–76)	61 ± 7.0(45–80)	0.94
Sex, female, no.(%)	14 (66.7%)	40 (72.7%)	0.61
Ocular characteristics			
Mean preoperative BCVA, logMAR, mean ± SD	1.1 ± 0.4 (0.4–1.7)	1.2 ± 0.3 (0.5–2.0)	0.18
Mean preoperative MLD, μm, mean ± SD	605.6 ± 258.6 (177–1,040)	628.4 ± 247.1(256–1,363)	0.73
Duration between iMH and PIMH surgeries, months, mean ± SD	3.4 ± 3.2 (0.5–6.0)	5.4 ± 14.7(0.3–108)	0.53
Lens status, Phakic, no.(%)	19 (90.5%)	50 (90.9%)	0.91

MH, macular hole; SD, standard deviation; BCVA, best-corrected visual acuity; logMAR, logarithm of the minimum angle of resolution; MLD, minimum linear diameter. Mean ± SD is the mean diameter of the narrowest part of the hole ± standard deviation.

axial length measurement, pre-and postoperatively. All patients were followed up at outpatient clinics for at least 4 months postoperatively. Complications, such SiO emulsification and raised intraocular pressure (greater than 21 mmHg), were recorded.

The primary outcome was anatomical success defined on OCT. We noted all available OCT examination data at the following time intervals: prior to revision surgery, post-revision surgery, and finally, at the most recent follow-up visit. According to the Manchester large macular hole study in which iMH size was the linear width across the narrowest point of the hole, we defined large PIMH as PIMH with a MLD of larger than 650 µm, and those in the 400–650 µm quartile were graded as medium PIMH (14). We measured PIMH using the available instruments (Spectralis [Heidelberg Engineering GmbH, Heidelberg, Germany]); diameters and widths were measured using the OCT caliper function (Cirrus HD software). OCT analysis was performed manually by one surveyor and the images were confirmed by one specialist, according to the benchmark mentioned above.

Using OCT images, we measured MLD, base diameter (BD), and height (H) to describe the anatomical characters of PIMHs (Figure 1). Hole closure was defined as closure of an PIMH, without exposure of the retinal pigment epithelium (RPE), on OCT, in all radial scan meridians.

Secondary outcomes included functional BCVA and significant gain in BCVA. Snellen visual acuities were converted to the log of the minimum angle of resolution (logMAR) units for statistical analysis, and non-numeric values were changed as follows: count fingers = 1.7 Log MAR, hand movement = 2.0 LogMAR (20/2000 Snellen), light perception = 2.3 LogMAR, and no light perception = 3.0 LogMAR (20/20000 Snellen) (14). Significant gain in BCVA was defined as an increase (from baseline) in visual acuity of ≥2 lines on a Snellen chart, which is equivalent to an increase of ≥0.2 logMAR (16).

2.4. Surgical technique

Primary surgical techniques were performed by standard 25-or 27-gauge PPV, with or without the use of triamcinolone. Standard ILM peeling was performed in all cases after indocyanine green staining. Internal tamponade was given with a fluid-air exchange and an intraocular nonexpansile air tamponade. Reoperations were performed under local anesthesia, using either a 25-or 27-gauge system (Constel-lation® Vision System; Alcon Laboratories, Fort Worth, TX, United States). In the SiO group, standard three-port PPV, followed by enlargement of the ILM peeling with adjunctive 0.125% indocyanine green staining, was performed by the same surgeon. Indocyanine green staining was performed to elucidate the extent of the original ILM peel. Care was taken as 25-gauge or 27-gauge forceps were used to ascertain the presence of residual perifoveal ILM or other additional membranes that required peeling. The fluid-air exchange was then repeated, with drainage of the preretinal fluid over the optic

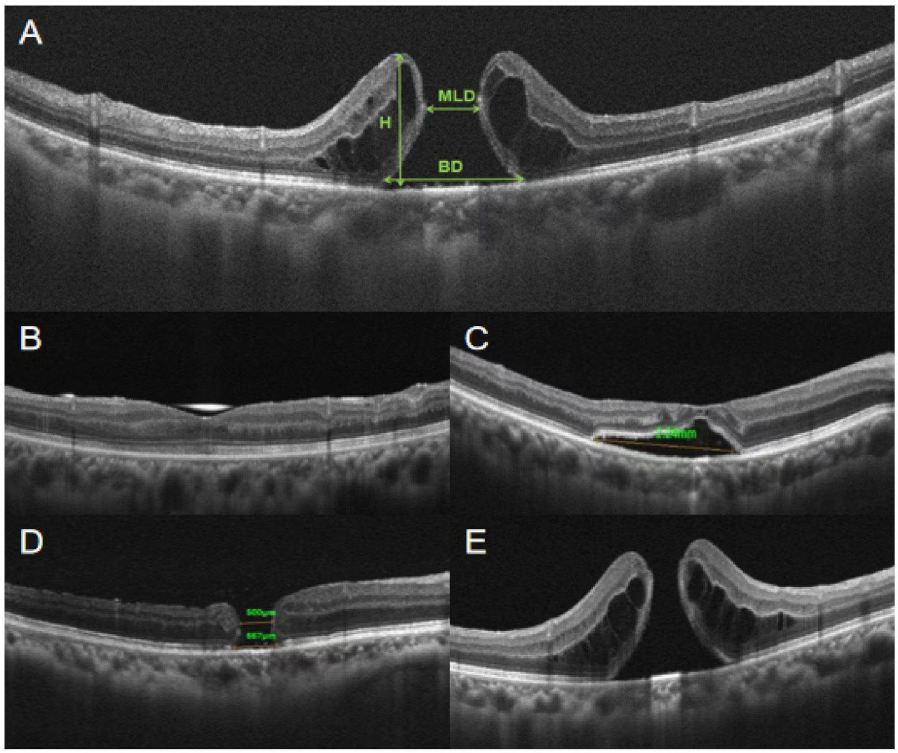

FIGURE 1
Diameters and features of PIMH. **(A)** Minimum linear diameter (MLD) and base diameter (BD) are parallel to the retinal pigment epithelium (RPE) at the nearest point of the retinal apposition, as described by Duker et al. (15). Both widths are measured as a line drawn roughly parallel to the RPE, Height (H) is defined as the distance between the highest edge of the hole and the RPE. **(B)** Flat-closed refers to complete contact between the edges of the hole, with complete coverage of the pigment epithelium layer and no subretinal fluid accumulation. **(C)** Elevated-closed refers to complete contact between the edges of the hole, with no exposure of the pigment epithelium but with a reservoir of subretinal fluid. **(D)** Flat-open refers to a defect of the retina, where PIMH edges attach to the RPE. **(E)** Elevated-open refers to a defect of the retina, where PIMH edges leave the RPE and are upturned.

disc. Air was exchanged for SiO of 5,000 centistoke viscosity. Patients were instructed to maintain a face-down or prone position for 2 weeks postoperatively. Approximately 6 months after the surgery, the SiO was removed through a machine-independent method using a short infusion tube connected to a 10-mL syringe. Residual droplets of SiO were removed by using a flute needle to capture small oil bubbles in the vitreous cavity (17). All patients with phakic eyes underwent SiO removal combined with phacoemulsification and intraocular lens implantation simultaneously. In the air group, the three retina surgeons performed a similar procedure. Reoperation, performed with the standard three-port PPV, extended ILM peeling followed by fluid-air exchange and nonexpansile air tamponade. Patients were instructed to maintain a face-down or prone position for 3 days to 1 week postoperatively.

2.5. Statistical analysis

Statistical analyses were performed using SPSS 22.0 (SPSS for Windows, Chicago, IL). All continuous variables conformed to the normal distribution and were expressed as descriptive statistics, including total numbers, means, standard deviations, and percentages. Descriptive statistics were used to calculate demographic data. Means with standard deviation were presented where relevant. Paired *t*-test, Fisher's exact test, and Bonferroni multiple comparison test were used as appropriate. Logistic regression was performed with the binary dependent variable of "open" or "closed" to assess the impact of the independent variables. A p value less than 0.05 was considered statistically significant. Confidence intervals were calculated to 95%.

3. Results

3.1. Characteristics of the patients

We enrolled 76 patients (21 patients [21 eyes] who underwent extended ILM peeling with SiO tamponade and 55 patients [55 eyes] who underwent extended ILM peeling and air tamponade) from January 2016 to June 2022 at Zhongshan Ophthalmic Center. Average age, sex ratios, ocular characteristics, duration between the iMH and PIMH surgeries, and base lens status were balanced between the two groups. The clinical characteristics of the patients at baseline are shown in Table 1.

3.2. Anatomic outcomes

In the SiO group, a total of 18 eyes of 21 patients (85.7%) achieved anatomical closure (Table 2), with 16 flat-closed and 2 elevated-closed types (Figure 1). All patients received their SD-OCT results on postoperative day one, and most PIMHs were closed. In the air group, 40 eyes (72.7%) achieved closure. There was no statistically significant difference between the two groups.

We found that for all cases of MLD ≤650 μm, extended ILM peeling and SiO tamponade could produce stable anatomical closure success (100%). Further, when the MLD of PIMH was >650 μm, the success rate reduced notably (60.0%, Figure 2). For both groups, 650 μm (MLD) seemed like a cut-off point for closure rate (MLD ≤650 μm vs. MLD >650 μm: 88.4% vs. 52%, $p = 0.002$).

3.3. Effects on vision

In the SiO and air groups, vision significantly increased ($p = 0.038$ and $p < 0.001$), and the mean postoperative BCVA improved in the closed subgroup ($p = 0.041$ vs. $p < 0.001$; Table 3). The visual acuity of all patients in this series was poor before the intervention, but by the final follow-up examination, BCVA had improved in 13 eyes (61.9%), was stable in four eyes (19.1%), and had worsened in four eyes (19.1%) in the SiO group. In addition, in the SiO group, among the 18 patients who obtained anatomical closure success, a significant increase in visual acuity was observed in four patients.

3.4. Analysis of factors affecting PIMH closure

Previous studies have documented that the time between iMH surgery and PIMH surgery influences the anatomical closure rate (18). We also analyzed the duration between the two surgeries but did not get statistically significant results (OR, 1.03; 95% CI [0.94–1.13]; $p = 0.54$) (Table 4). Univariate regression analysis showed that MLD was the only parameter closely related to the closure rate (OR, 1.0; 95% CI (0.985–0.999); $p = 0.03$).

Another structural feature of PIMH we studied based on OCT findings was the elevated edge of the PIMH at baseline (Figure 3). We noted that 14 of 16 patients (87.5%) who had an PIMH with an elevated edge at baseline experienced PIMH closure after surgery, while four of five patients (80.0%) with a flattened PIMH edge experienced closure after the revision surgery. The difference between these groups of patients was non-statistically significant.

TABLE 2 Final anatomic outcome in the two groups.

Final anatomic outcome	Number (%)		*p* value
	SiO (*n* = 21)	Air (*n* = 55)	
Open	3 (14.3)	15 (27.3)	
Closed	18 (85.7)	40 (72.7)	0.37

p value is calculated using Fisher's exact test.

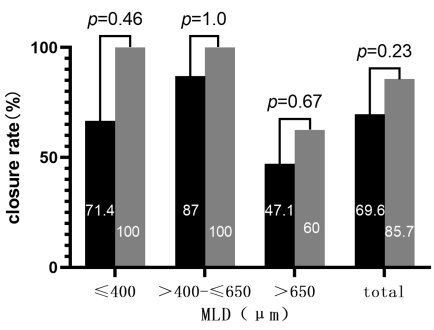

FIGURE 2
Anatomic outcomes of the two groups for different diameters.

TABLE 3 BCVA comparison based on anatomical outcomes in the SiO and air groups.

Macular status	SiO group			Air group		
	Mean BCVA at baseline, LogMAR	Mean BCVA at the final visit, logMAR	*p* value	Mean BCVA at baseline, logMAR	Mean BCVA at the final visit, logMAR	*p* value
Closed	1.11 ± 0.34 (0.6–1.7)	0.87 ± 0.40 (0.3–1.7)	**0.041***	1.57 ± 0.09 (1.4–1.7)	1.05 ± 0.42 (0.5–1.6)	**<0.001***
Open	1.17 ± 0.6 (0.5–1.7)	1.0 ± 0.30 (0.7–1.3)	0.7	1.57 ± 0.12 (1.5–1.7)	1.53 ± 0.06 (1.5–1.6)	0.68
All	1.12 ± 0.4 (0.52–1.70)	0.91 ± 0.40 (0.15–1.7)	**0.038***	1.57 ± 0.10 (1.4–1.7)	1.14 ± 0.42 (0.5–1.6)	**<0.001***

*Significant association (*p* value < 0.05).

TABLE 4 Analysis of factors affecting PIMH fracture closure.

Factor (PIMH)	Odds Ratio (95% Confidence Interval)	*p* Value†
MLD	1.0 (0.985–0.999)	0.03 *
BD	1.0 (0.99–1.001)	0.15
H	1.0 (1.0–1.02)	0.805
MHI	0.0 (0.0–17.6)	0.12
THI	0.41 (0.02–8.82)	0.57
BCVA at baseline	0.71 (0.06–8.92)	0.79
Time duration between iMH and PIMH surgery	1.03 (0.94–1.13)	0.54
Age	0.96 (0.84–1.09)	0.515
Female gender	6.46 (0.81–51.34)	0.08
Tamponade	0.31 (0.01–8.75)	0.49
Binocular iMH	2.53 (0.26–25.03)	0.43

Macular hole index (MHI) is defined as the ratio of height to base diameter, that is MHI=H/BD. Tractional hole index (THI) is defined as the ratio of height to the MLD: THI=H/MLD.
†Univariate regression analysis, $n = 75$, *Significant association (*p* value < 0.05).

3.5. Follow-up and postoperative complications in the SiO tamponade series

Overall, 19 eyes (90.5%) were phakic at baseline, with the remaining eyes having a history of cataract extraction, including intraocular lens implantation. Of the patients with phakic eyes, 16 patients (88.9%) underwent advanced cataract extraction, and a majority (93.8%) underwent SiO removal combined with cataract extraction within 1 year of the repeat surgery (mean 6.2 ± 1.3 months). One patient developed high intraocular pressure after SiO tamponade, which resolved after pharmacotherapy. No other adverse events, such as SiO emulsification or cystoid macular edema, were observed during the follow-up. Two patients in the SiO group experienced subretinal fluid accumulation during the follow-up period, but at the end of the follow-up period, the fluid level had decreased and visual acuity had improved in both patients. In the air group, one patient experienced retinal detachment 9 months after PIMH surgery. The details of three patients that did not achieve anatomical closure success are listed in Table 5.

4. Discussion

Failure of the primary surgery and persistent iMH is the most common complication of iMH surgery. Successful secondary closure of iMH is probably influenced by multiple factors. Several factors have been linked to the failure of primary iMH surgery, including residual traction from ILM, poor patient compliance with proper positioning, and size of iMH > 400 μm. Whether the choice of intraocular gas or SiO as a surgical tamponade in the second iMH surgery affects surgical success is unclear.

We found notable facts: live retinal tissue studies have suggested that the retina is soft and actively mechanoresponsive, approximately 100 times more compliant than soft silicone rubber (19, 20). Broad peeling of a taut ILM may enhance this compliance by relaxing the intrinsically elastic retinal tissue (21). Further, past clinical experience has indicated that prolonged tamponade would lead to a higher rate of effective PIMH closure (18). Thus, we hypothesized that broad peeling of a taut ILM or long-term tamponade, such as using SiO, may be effective. In this study, the surgery of choice for PIMHs was extended ILM peeling and SiO tamponade. We added a matched cohort of patients who underwent air tamponade for its involvement in short-term tamponade and extended ILM peeling to get more information. To the best of our knowledge, this is the first study to evaluate the benefit of these two procedures for PIMH.

The anatomic closure rate in our SiO group was 85.7%, similar to recently reported results in the literature. Conversely, the anatomic closure rate in our air group was 72.7%, which was worse than in a previous study (22, 23). We also noticed a trend toward a higher anatomical closure rate in the SiO group, although this difference was not statistically significant. Conclusively, using SiO and extended ILM peeling does not seem to improve the anatomical and functional outcome of surgery. However, it is difficult to compare the results of our group with those of previously published reports that used SiO because of differences in the MLD basement or in the definition of anatomic closure among the studies. This research employed the evaluation method posited by Kang and colleagues (24); type 1 closure corresponds to flat-closed and elevated-closed, and type 2 closure corresponds to flat-open and elevated-open. Moreover, flat-closed and elevated-closed were defined as forms of an-atomical closure. MLD ≤400 μm has been considered the safest range for anatomical closure. We found that for all cases of MLD ≤650 μm, extended ILM peeling and SiO tamponade could produce stable anatomical success.

In our series, among all cases of anatomical closure, most cases of PIMH were associated with closure on the postoperation first day (16/18, 88.9%). Thus, we can hypothesize that SiO supplies strong tension for aggregating hole margins, and using SiO of 5.000 centistokes of viscosity may elucidate this phenomenon. Because closure detection is via OCT, we could not verify the closure rate in the air tamponade group on the postoperation first day. Therefore, closure speed could not be compared between the two groups.

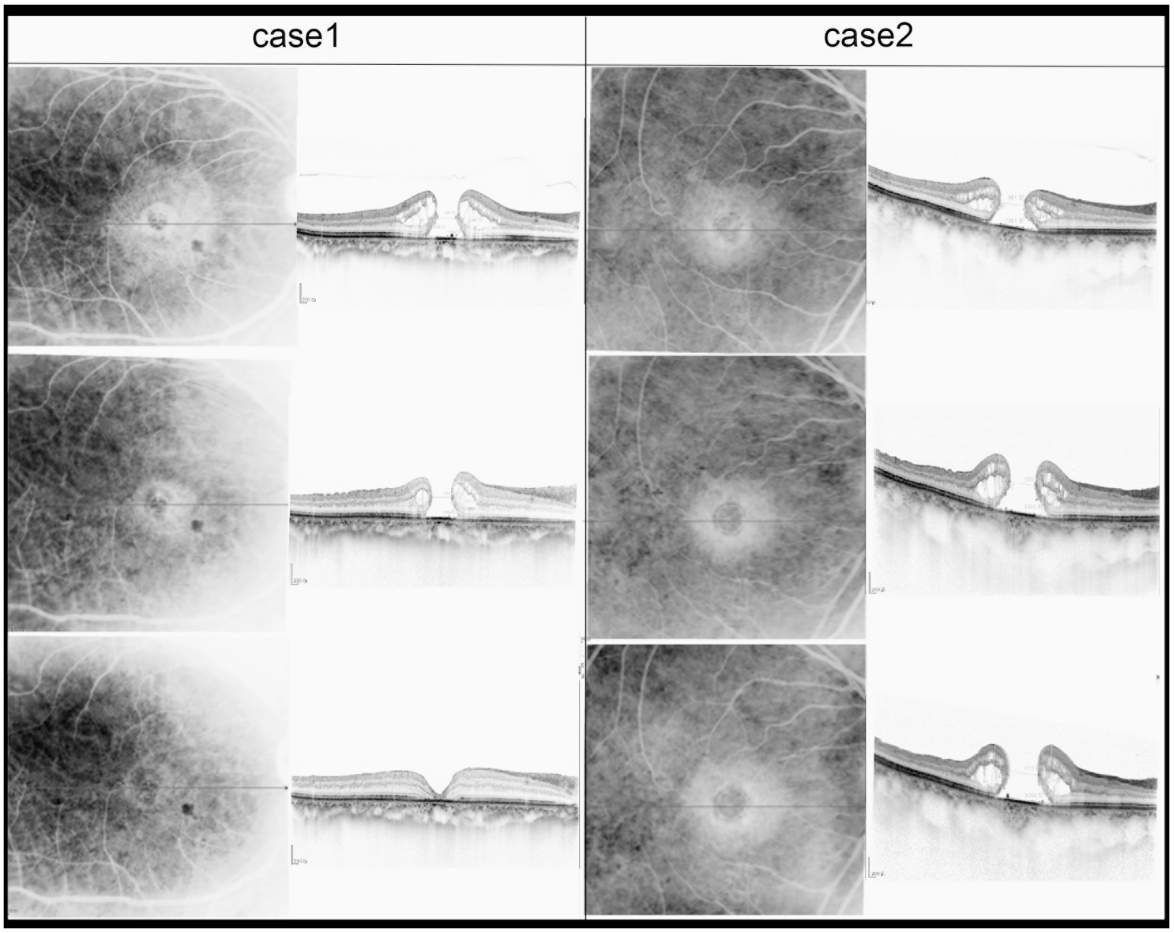

FIGURE 3
Sequential SD-OCT images of two patients were taken before iMH, 1 month after iMH surgery, and 1 month after PIMH surgery. MLD of PIMH of Case 2 is 686 μm. MLD of PIMH of Case 1 is 538 μm.

Functional outcome is typically more important for patients than anatomical closure, although it could be extremely difficult for PIMH. SiO tamponade has been considered less effective in improving vision than gas tamponade. A 2021 study conducted by Li et al. used SiO tamponade in 33 patients with PIMH and reported that 1.00 logMAR (0.60–1.00) at baseline was significantly improved to 0.65 logMAR (0.49–1.00; $p = 0.010$) at the final examination (25). In our study, more than half of the patients in the SiO group experienced vision improvement, and among the 18 patients who achieved anatomic success, four patients obtained a significant increase in visual acuity. Notably, cataract surgery at the time of SiO removal positively influences visual outcomes. Besides, we noted non-improvement in vision in the group that did not achieve anatomical closure. We extensively analyzed the three cases of failed closure and non-improvement in vision after SiO tamponade (Table 5) and only noticed a larger preoperative MLD.

It was important for us to determine the factors that influence operative outcomes. We analyzed factors affecting PIMH fracture closure (Table 4). Although the number of cases in our study may be a limitation, the consistent use of the two different types of surgery for PIMH treatment showed that the final closure rate depends on the MLD of PIMH. We could not find similar studies on PIMH, which may be attributable to the low morbidity associated with PIMH. However, in the iMH field, Chhablani et al. (26) performed a retrospective study of 137 eyes of 137 patients who underwent iMH repair and reached the same conclusion—the minimum diameter between the hole edges and the longest diameter of the hole is the best predictors of hole closure.

There are some disadvantages of SiO tamponade, the most important one being the need for additional surgery. However, cataract formation after PPV, whatever the form of tamponade used, is a well-known and inevitable complication of the surgery. A study reported up to an 81% cataract risk after 6 months and 98 and 100% risk at one and 2 years, respectively, after vitrectomy (27). The incidence of cataract surgery in the present study is comparable to those of other studies investigating cataract occurrence after macular hole surgery (21, 28). Therefore, all our phakic patients in the SiO group proposed to undergo cataract surgery combined with SiO removal. One previous study employed a surgical approach—cataract and SiO removal—and compared them in combination with the two steps, respectively (29). Their results suggest similar visual outcomes and complication rates in both groups. In our cohort, we combined cataract extraction and SiO performed at 6.2 ± 1.3 months after the PIMH operation and observed faster visual rehabilitation with no complication at the final follow-up.

The limitations of this study include the small size and the relatively short follow-up period. For some special reasons in China, we did not get a gas tamponade group for comparison during our research. Table 3 only shows 16 follow-up records in the air group because of the impact of the COVID-19 pandemic. An unforeseen

TABLE 5 Details of three unclosed cases after SiO tamponade ($n = 3$).

MHs that opened in the final examination	Sex	Age	Time interval between MH surgeries (months)	Follow-up Duration (months)	Preoperative BCVA, logMAR	Cataract Treatment	Preoperative MLD, μm	Postoperative MLD, μm	Preoperative MLD, μm (mean ± SD*)	Postoperative MLD, μm (mean ± SD*)	p value†
Case 1	Female	66	2	10	1.7	IOL	970	692	903.67 ± 90.941	776.33 ± 142.620	0.444
Case 2	Female	66	6	11	1.3	NO	941	696			
Case 3	Female	55	1	7.5	0.5	YES	800	941			

MH, macular hole, SD, standard deviation. *mean ± SD is the mean diameter of the narrowest inner ± standard deviation. **All MHs obtained flat-open closure at the final examination after SiO removal, thus, postoperative narrowest inner diameter = postoperative basal diameter †By paired t-test. Significant association (p value < 0.05).

selection bias may have existed for participants who accepted silicone filling because of the surgeon's experience. Generally, PIMHs are more complex, difficult to treat, and filled with SiO. Furthermore, previous studies compared SiO-filled eyes with gas-filled eyes, and variable postoperation BCVA was noted, suggesting that direct macular toxicity related to SiO may adversely affect visual acuity, although there is little supportive evidence. Further studies involving larger patient numbers and longer follow-ups are warranted.

5. Conclusion

In summary, in terms of anatomical and functional outcomes, extended ILM peeling combined with SiO or air tamponade is effective in treating PIMH. Moreover, though not statistically significant in the present study, the anatomic closure rate seems better for silicone-operated eyes than for air-operated eyes in the real world. MLD is the best predictor of PIMH closure, with MLD ≤ 650 μm associated with a significantly higher closure rate. The information in this article can help surgeons and PIMH patients decide whether and how to proceed with a second surgery.

Data availability statement

The original contributions presented in the study are included in the article/supplementary material, further inquiries can be directed to the corresponding authors.

Ethics statement

Written informed consent was obtained from the individual(s) for the publication of any potentially identifiable images or data included in this article.

Author contributions

YS: conceptualization. YS and LW: data curation. LF: formal analysis. LF and XH: methodology. YL: project administration. YS, YL, and DF: resources. DF: visualisation. YS: writing – original draft. YW, TZ, and SZ: writing – review & editing. All authors contributed to the article and approved the submitted version.

Funding

This study was supported by grants Shenzhen Science and Technology Program (KCXFZ20211020163813019) and the Sanming Project of Medicine in Shenzhen (SZSM202011015).

Conflict of interest

The authors declare that the research was conducted in the absence of any commercial or financial relationships that could be construed as a potential conflict of interest.

Publisher's note

References

1. Kelly NE, Wendel RT. Vitreous surgery for idiopathic macular holes. Results of a pilot study. *Arch Ophthalmol.* (1991) 109:654–9. doi: 10.1001/archopht.1991.01080050068031

2. Tabandeh H. Vascularization and reperfusion of autologous retinal transplant for giant macular holes. *JAMA Ophthalmol.* (2020) 138:305–9. doi: 10.1001/jamaophthalmol.2019.5733

3. Hejsek L, Dusova J, Stepanov A, Rozsival P. Re-operation of idiopathic macular hole after failed initial surgery. *Biomed Pap Med Fac Univ Palacky Olomouc Czech Repub.* (2014) 158:596–9. doi: 10.5507/bp.2013.088

4. Thompson JT, Sjaarda RN. Surgical treatment of macular holes with multiple recurrences. *Ophthalmology.* (2000) 107:1073–7. doi: 10.1016/s0161-6420(00)00111-1

5. Tabandeh H, Morozov A, Rezaei KA, Boyer DS. Superior wide-base internal limiting membrane flap transposition for macular holes: flap status and outcomes. *Ophthalmol Retina.* (2021) 5:317–23. doi: 10.1016/j.oret.2020.12.003

6. D'Souza MJ, Chaudhary V, Devenyi R, Kertes PJ, Lam WC. Re-operation of idiopathic full-thickness macular holes after initial surgery with internal limiting membrane peel. *Br J Ophthalmol.* (2011) 95:1564–7. doi: 10.1136/bjo.2010.195826

7. Chou HD, Liu L, Wang CT, Chen KJ, Wu WC, Hwang YS, et al. Single-layer inverted internal limiting membrane flap versus conventional peel for small-or medium-sized full-thickness macular holes. *Am J Ophthalmol.* (2022) 235:111–9. doi: 10.1016/j.ajo.2021.08.016

8. Patel SN, Mahmoud TH, Kazahaya M, Todorich B. Autologous neurosensory retinal transplantation: bridging the gap. *Retina.* (2021) 41:2417–23. doi: 10.1097/IAE.0000000000003210

9. Baino F. Towards an ideal biomaterial for vitreous replacement: historical overview and future trends. *Acta Biomater.* (2011) 7:921–35. doi: 10.1016/j.actbio.2010.10.030

10. Tam ALC, Yan P, Gan NY, Lam WC. The current surgical management of large, recurrent, or persistent macular holes. *Retina.* (2018) 38:1263–75. doi: 10.1097/IAE.0000000000002020

11. Tao J, Chen H, Chen Y, Yu J, Xu J, Mao J, et al. Efficacy of air tamponade treatment of idiopathic macular holes of different diameters and of follow-up intravitreal air tamponade for persistent holes. *Retina.* (2022) 42:877–82. doi: 10.1097/IAE.0000000000003394

12. Yu Y, Liang X, Wang Z, Wang J, Liu X, Chen J, et al. Internal limiting membrane peeling and air tamponade for STAGE III and STAGE IV idiopathic macular hole. *Retina.* (2020) 40:66–74. doi: 10.1097/IAE.0000000000002340

13. Feng X, Li C, Zheng Q, Qian XG, Shao W, Li Y, et al. Risk of silicone oil as vitreous tamponade in pars plana vitrectomy: a systematic review and meta-analysis. *Retina.* (2017) 37:1989–2000. doi: 10.1097/IAE.0000000000001553

14. Ch'ng SW, Patton N, Ahmed M, Ivanova T, Baumann C, Charles S. Jalil AThe Manchester large macular hole study: is it time to reclassify large macular holes? *Am J Ophthalmol.* (2018) 195:36–42. doi: 10.1016/j.ajo.2018.07.027

15. Duker JS, Kaiser PK, Binder S, de Smet MD, Gaudric A, Reichel E, et al. The international vitreomacular traction study group classification of vitreomacular adhesion, traction, and macular hole. *Ophthalmology.* (2013) 120:2611–9. doi: 10.1016/j.ophtha.2013.07.042

16. Mester V, Kuhn F. Internal limiting membrane removal in the management of full-thickness macular holes. *Am J Ophthalmol.* (2000) 129:769–77. doi: 10.1016/s0002-9394(00)00358-5

17. Zhang Z, Zhang S. Novel and easy techniques for 27-gauge silicone oil infusion and removal. *Int Ophthalmol.* (2019) 39:1543–51. doi: 10.1007/s10792-018-0976-1

18. Patel R, Gopalakrishnan M, Giridhar A. Timing and outcome of surgery for persistent macular hole. *Retina.* (2019) 39:314–8. doi: 10.1097/IAE.0000000000001939

19. Bringmann A, Unterlauft JD, Barth T, Wiedemann R, Rehak M, Wiedemann P. Müller cells and astrocytes in tractional macular disorders. *Prog Retin Eye Res.* (2022) 86:100977. doi: 10.1016/j.preteyeres.2021.100977

20. Jones IL, Warner M, Stevens JD. Mathematical modelling of the elastic properties of retina: a determination of Young's modulus. *Eye (Lond Engl).* (1992) 6:556–9. doi: 10.1038/eye.1992.121

21. Iezzi R, Kapoor KG. No face-down positioning and broad internal limiting membrane peeling in the surgical repair of idiopathic macular holes. *Ophthalmology.* (2013) 120:1998–2003. doi: 10.1016/j.ophtha.2013.06.001

22. Romano MR, Rossi T, Borgia A, Catania F, Sorrentino T, Ferrara M. Management of refractory and recurrent macular holes: a comprehensive review. *Surv Ophthalmol.* (2022) 67:908–31. doi: 10.1016/j.survophthal.2022.01.006

23. Valldeperas X, Wong D. Is it worth reoperating on macular holes? *Ophthalmology.* (2008) 115:158–63. doi: 10.1016/j.ophtha.2007.01.039

24. Kang SW, Ahn K, Ham DI. Types of macular hole closure and their clinical implications. *Br J Ophthalmol.* (2003) 87:1015–9. doi: 10.1136/bjo.87.8.1015

25. Li JQ, Brinken R, Holz FG, Krohne TU. Silicone oil tamponade for persistent macular holes. *Eye (Lond Engl).* (2021) 35:2206–12. doi: 10.1038/s41433-020-01228-9

26. Chhablani J, Khodani M, Hussein A, Bondalapati S, Rao HB, Narayanan R, et al. Role of macular hole angle in macular hole closure. *Br J Ophthalmol.* (2015) 99:1634–8. doi: 10.1136/bjophthalmol-2015-307014

27. Jackson TL, Donachie PHJ, Sparrow JM, Johnston RL. United Kingdom national ophthalmology database study of vitreoretinal surgery: report 2, macular hole: report 2. *Ophthalmology.* (2013) 120:629–34. doi: 10.1016/j.ophtha.2012.09.003

28. Pasu S, Bell L, Zenasni Z, Lanz D, Simmonds IA, Thompson A, et al. Facedown positioning following surgery for large full-thickness macular hole: a multicenter randomized clinical trial. *JAMA Ophthalmol.* (2020) 138:725–30. doi: 10.1001/jamaophthalmol.2020.0987

29. Krepler K, Mozaffarieh M, Biowski R, Nepp J, Wedrich A. Cataract surgery and silicone oil removal: visual outcome and complications in a combined vs. two step surgical approach. *Retina.* (2003) 23:647–53. doi: 10.1097/00006982-200310000-00007

frontiers | Frontiers in Medicine

TYPE Original Research
PUBLISHED 04 August 2023
DOI 10.3389/fmed.2023.1219419

OPEN ACCESS

EDITED BY
Georgios D. Panos,
Nottingham University Hospitals NHS Trust, United Kingdom

REVIEWED BY
Donny W. Suh,
University of California, United States
Pradeep Sharma,
Centre for Sight Eye Hospital, India

*CORRESPONDENCE
Fang Zhang
✉ 13757890281@eye.ac.cn

†These authors have contributed equally to this work and share first authorship

RECEIVED 09 May 2023
ACCEPTED 18 July 2023
PUBLISHED 04 August 2023

CITATION
Li Y, Tong L, Chen Y, Zhang B, Wan M, Yin X and Zhang F (2023) The efficacy of botulinum toxin type A treatment and surgery for acute acquired comitant esotropia.
Front. Med. 10:1219419.
doi: 10.3389/fmed.2023.1219419

The efficacy of botulinum toxin type A treatment and surgery for acute acquired comitant esotropia

Yipao Li[1†], Luyao Tong[1,2†], Yuanyuan Chen[1], BinJun Zhang[1], Minghui Wan[1], Xiangping Yin[1] and Fang Zhang[1*]

[1]National Clinical Research Center for Ocular Diseases, Eye Hospital, Wenzhou Medical University, Wenzhou, China, [2]The First Affiliated Hospital of Ningbo University, Ningbo, China

Aim: To compare the long-term efficiency of botulinum toxin type A (BTXA) injection and surgery on acute acquired comitant esotropia (AACE).

Methods: This retrospective study enrolled patients with AACE from January 2020 to August 2022. The horizontal angle of deviation pre- and post-treatment was measured. Deviations in BTXA and surgical treatment were compared. The BTXA group was divided into adequate treatment (AT) and inadequate treatment (inAT) subgroup based on the deviation of no more than 4 prism diopters (at near and distance) or temporary exotropia at the 2 week follow-up. The two subgroups were compared to determine the long-term efficacy of BTXA treatment.

Results: Ninety-two patients with AACE were included. Follow-up was 6 months. The deviations of the surgery and BTXA group were significantly smaller at the 6 month follow-up than at pre-treatment ($p < 0.001$). The deviation before treatment in the surgery group was larger than in the BTXA groups ($p < 0.001$) but smaller at the 6 month follow-up ($p < 0.001$). The deviation was similar in the AT-BTXA and inAT-BTXA subgroups before treatment ($p = 0.322$ for distance and $p = 0.051$ for near) but smaller in the AT-BTXA subgroup at 6 month follow-up ($p < 0.001$ for near and distance).

Conclusion: Surgery and BTXA successfully treat AACE. Surgery has a more precise and lasting therapeutic effect than BTXA. AACE patients adequately treated with BTXA and with deviations of no more than 4 prism diopters at 2 weeks follow-up had better outcomes.

KEYWORDS

acute acquired comitant esotropia, AACE, botulinum toxin type A, BTXA, surgical outcome acute acquired comitant esotropia, surgical outcome

1. Introduction

Acute acquired concomitant esotropia (AACE) is a comitant esotropia characterized by acute onset diplopia in older children and adults (1–3). Excessive near-work and anatomical abnormalities may lead to excessive convergence and induce AACE (4–7). The effects of strabismus surgery and botulinum toxin type A (BTXA) on AACE have been investigated in several studies. Both treatments effectively reduce the degree of strabismus and restore stereoscopic vision (5, 8–10). Accurate surgery dose can be designed according to the pre-surgery deviation (11). BTXA reduces deviation by temporarily blocking the neuromuscular junction without surgical complications (12). Though the efficiency of BTXA and surgery on AACE has

been explored, there is no consensus on whether BTXA can achieve the same success rate as surgery (13–15).

The BTXA treatment is thought to cause less injury and incur fewer costs than other treatments; nevertheless, it is associated with a higher recurrence rate at follow-up (14, 16, 17). BTXA metabolism lasts months, making it challenging to speculate on the long-term (6 months) efficacy in the early follow-up (12). The accurate BTXA dose is also challenging to calculate based on the deviation because of the individual response of BTXA (18). These factors may delay subsequent therapy of recurrence, as it requires a 6 month follow-up to confirm efficacy. An index in the early follow-up period to speculate on the efficacy at 6 months post-injection needs to be developed.

Therefore, we conducted this study to compare the efficacy of BTXA and surgery and to examine the early indexes of long-term BTXA efficacy.

2. Methods

The Ethics Committee of Wenzhou Medical University approved this retrospective study (Approval ID. 2020-148-K-133-01), which adhered to the tenets of the Declaration of Helsinki. Written informed consent was waived because the study was retrospective with anonymized data.

We included patients with AACE from January 2020 to August 2022 at the Affiliated Eye Hospital of Wenzhou Medical University. The inclusion criteria were (1) sudden-onset diplopia, diagnosed with AACE; (2) history of BTXA injection or surgery. The exclusion criteria were (1) history of eye disease, ocular surgery, or ocular trauma; (2) intracranial or neurologic disease; (3) follow-up of less than 6 months. All enrolled patients were examined, treated, and followed by the same ophthalmologist.

The horizontal angle of deviation pre-and post-treatment, with refractive correction, was measured with the prism and cover tests at 6 m (distance) and 40 cm (near) fixation. The spherical equivalents in each eye were averaged and recorded as the value of refractive errors. Ophthalmic examination by ophthalmologists and neurological examination by neurologists were performed to rule out ocular, intracranial, and neurologic diseases. After administration of topical anesthesia, BTXA (Hengli, China) injection (30 gauge × 1/2 in) was performed at about 6 mm posterior to the medial rectus insertion without conjunctival incision and electromyography guidance. The injection doses were 4.0 units for a deviation of more than 35 PD, 3.5 units for 26 PD to 35 PD, and 3.0 units for 10 PD to 25 PD. Unilateral medial rectus recession (no more than 20 PD) or medial rectus recession combined with lateral rectus resection (more than 20 PD) were performed under general anesthesia (patients less than 14 years old) or local anesthesia (patients at least 14 years old).

Patients were divided into a BTXA group and a surgery group. Patients with a deviation of no more than 4 PD can achieve a diplopia-free state by self-control. The patients in both groups who achieved a deviation of no more than 4 PD (at near and distance) or temporary exotropia at the 2 week follow-up were considered adequately treated. The groups were then divided into an adequate treatment (AT) group and an inadequate treatment (inAT) group. Deviation pre-and post-treatment in groups were compared. At the 6 month follow-up, the absence of diplopia throughout the day and horizontal deviation of no more than 8 PD (both at distance and near) was considered a successful treatment. Statistical analyses were performed with SPSS version 26.0 (SPSS, Inc., Chicago, IL, United States). Data were compared using the Mann–Whitney U-test. Spearman's correlation coefficient was calculated to explore relationships between two factors. Differences where $p < 0.05$ were considered statistically significant.

3. Results

We included 92 patients (64 males and 28 females) with AACE, of whom 51 were treated with BTXA and 41 with surgery. All patients were Chinese, ranging from 6 to 50 years old (mean 23.9 years), and had diplopia for 1 month to 10 years (median 1 year).

The clinical characteristics of the two treatment groups are displayed in Table 1 and the deviation in the BTXA group was smaller before treatment ($p < 0.001$) but was larger at the 6 month follow-up

TABLE 1 Clinical characteristics of the BTXA group and surgery group.

Characteristic	BTXA Group (n = 51)	Surgery Group (n = 41)	p-value*
Spherical equivalent (diopters) Pre-treatment	−4.50 (−6.50–−3.25)	−4.00 (−5.50–−0.75)	0.113
Deviation in primary position (PD)			
Pre-treatment			
Distance	20 (15–30)	40 (25–45)	<0.001
Near	18 (12.5–25)	35 (25–40)	<0.001
2week follow-up			
Distance	0 (−5.5–4)	0 (0–0)	0.908
Near	0 (−4.5–2)	0 (0–0)	0.452
6month follow-up			
Distance	6 (4–14)	0 (0–0)	<0.001
Near	4 (2–8)	0 (0–0)	<0.001
Absence of diplopia at 6 month follow-up	58.8% (30/51)	95.1% (39/41)	<0.001

Data are presented as range and median (interquartile range, 25th to 75th percentile). BTXA, botulinum toxin type A; PD, prism diopter. *Mann–Whitney U test. The absence of diplopia means patients worked and lived without diplopia throughout the day.

TABLE 2 Clinical characteristics of the adequately treated patients in two groups.

Characteristic	BTXA Group ($n = 41$)	Surgery Group ($n = 40$)	p-value*
Spherical equivalent (diopters) Pre-treatment	−4.5 (−6.50–−3.50)	−3.5 (−5.375–−0.625)	0.070
Deviation in primary position (PD)			
Pre-treatment			
Distance	20 (15–25)	37.5 (25–45)	<0.001
Near	16 (12–20)	32.5 (25–40)	<0.001
2week follow-up			
Distance	0 (−8–2)	0 (0–0)	0.076
Near	0 (−6–0)	0 (0–0)	0.007
6month follow-up			
Distance	6 (3–9)	0 (0–0)	<0.001
Near	4 (2–5)	0 (0–0)	<0.001
Absence of diplopia at 6 month follow-up	73.2% (30/41)	97.5% (39/40)	<0.001

Data are presented as median (interquartile range, 25th to 75th percentile). BTXA, botulinum toxin type A; PD, prism diopter. *Mann–Whitney U test. "Adequate" means patient without diplopia. Adequate treatment means patients achieved a deviation of no more than 4 PD (at near and distance) or temporary exotropia at the 2 week follow-up.

TABLE 3 Clinical characteristics of the AT-BTXA and inAT-BTXA subgroups.

Characteristic	AT-BTXA Group ($n = 41$)	inAT-BTXA Group ($n = 10$)	p-value*
Spherical equivalent (diopters)			
Pre-treatment	−4.50 (−6.50–−3.50)	−4.00 (−4.00–−3.00)	0.263
Deviation in primary position (PD)			
Pre-treatment			
Distance	20 (15–25)	27.5 (16–35)	0.322
Near	16 (12–20)	25 (16–30)	0.051
2week follow-up			
Distance	0 (−8–2)	10 (8–14)	<0.001
Near	0 (−6–0)	9 (4–10)	<0.001
6month follow-up			
Distance	6 (3–9)	18 (14–25)	<0.001
Near	4 (2–5)	14 (10–20)	<0.001
Absence of diplopia at 6 month follow-up	73.2% (30/41)	0.0% (0/10)	<0.001

Data are presented as median (interquartile range, 25th to 75th percentile). AT, adequate treatment; inAT, inadequate treatment; BTXA, botulinum toxin type A; PD, prism diopter. *Mann–Whitney U test.

than in the surgery group ($p < 0.001$). The success rate was lower in the BTXA group at the 6 month follow-up ($p < 0.001$). At the 2 week follow-up, there was no significant difference between the groups in deviation examined at near ($p = 0.908$) and distance ($p = 0.452$). Compared with deviation before treatment, the deviations of the surgery group ($p < 0.001$ at near and distance) and BTXA group ($p < 0.001$ at near and distance) were significantly smaller at the 6 month follow-up.

BTXA metabolism occurs over time, and its effect develops slowly. We focused on the 2 week follow-up interval, which showed no significant difference in deviation between the two groups. We identified patients in both groups who achieved a deviation of no more than 4 PD (at near and distance) or temporary exotropia at the 2 week follow-up and were considered adequately treated at that time. The clinical characteristics are displayed in Table 2. At the 2 week follow-up, the deviation was similar at distance ($p = 0.076$) in the two groups and smaller at near in the BTXA group ($p = 0.007$). However, the deviations were larger at near and distance in the BTXA group at the 6 month follow-up ($p < 0.001$). The success rate was lower in the BTXA group at the 6 month follow-up ($p < 0.001$). In the BTXA group, the deviation at near and distance at the 6 month follow-up was associated with the deviation at near ($p = 0.001$, $r = 0.447$) and distance ($p < 0.001$, $r = 0.529$) at the 2 week follow-up. In the BTXA group, the success rate at the 6 month follow-up was significantly associated with deviation at near ($p < 0.001$, $r = -0.516$) and distance ($p < 0.001$, $r = -0.529$) at the 2 week follow-up. At the 6 month follow-up, the patients in BTXA group with deviation of no more than 8 PD were free of diplopia.

We divided the BTXA group into the inAT-BTXA and AT-BTXA subgroups based on the deviation at the 2 week follow-up. The two groups' deviations at distance ($p = 0.322$) and near ($p = 0.051$) before treatment were similar. At the 6 month follow-up, deviations were significantly larger in the inAT-BTXA subgroup at near ($p < 0.001$) and distance ($p < 0.001$), as displayed in Table 3. Among the AT-BTXA

subgroup, the success rate was 100% in patients with no more than 15 PD deviations, 83.3% with no more than 25 PD, and 72.3% with no more than 35 PD.

Complications of the BTXA-injected eye, including temporary exotropia and ptosis, were relieved or resolved during the follow-up. No serious severe complications were found in the surgery group, except for intraoperative bleeding.

4. Discussion

This study compared the treatment efficacy of BTXA and surgery at long-term follow-up and revealed that surgery has a more precise and lasting therapeutic effect with a success rate of 95.1%. We also observed that adequate BTXA treatment, with no more than 4 PD deviations at 2 weeks follow-up, was associated with better outcomes.

As the primary treatment of strabismus, surgery was found to be safe and effective in improving ocular alignment, eliminating diplopia, developing binocular fusion, and expanding binocular visual fields (19). Careful surgical planning and operation can prevent severe complications, including scleral perforations, orbital inflammation, muscle slip, and anesthesia complications (20). BTXA was also found to be a safe, effective, and repeatable treatment for AACE, with fewer iatrogenic injuries (10, 17, 21, 22). Because of the individual response of BTXA (18), and limitations of the syringe scale, surgeons cannot precisely administer BTXA doses according to the deviation. Therefore, each BTXA dose corresponds to a range of deviations, which differ from surgery. By comparing the efficiency of the two treatments on AACE, surgery has a similar or better success rate (13–15). In the present study, surgery and BTXA significantly improved ocular alignment at the final follow-up. We then compared the clinical characteristics of the treatment groups. The deviation was more significant in the surgery group before treatment but significantly smaller at the 6 month follow-up, and the success rate was also more significant at the 6 month follow-up. Considering the time required for the BTXA effect and the metabolism, we identified patients in both groups who were adequately treated at the 2 week follow-up. The deviation was also more significant in the BTXA group at the 6 month follow-up. These findings suggest that surgery is more effective, precise, and durable than BTXA.

The BTXA injection is an alternative treatment for AACE. The success at 6 month follow-up ranged from 45 to 90.6% (10, 13–15, 21, 22). The substantial variability in success rates suggests the instability of BTXA in the treatment of AACE. Several months of BTXA metabolism causes a gradual decrease in success rate, which results in a delayed determination of final treatment success after injection (12, 14, 16, 17). It would be beneficial to identify an indicator in the early stage that determines whether the treatment is successful. In this study, the deviation and success rate of the BTXA group at the 6 month follow-up was associated with the deviation at the 2 week follow-up. Based on the deviations at the 2 week follow-up, the BTXA group was divided into AT-BTXA and the-BTXA subgroups. The deviations before treatment were similar in the two groups. At the 6 month follow-up, deviations were significantly larger in the inAT-BTXA subgroup. These results suggest that patients with a deviation of no more than 4 PD after 2 weeks of BTXA injection have a significantly better outcome. A deviation of more than 4 PD at the 2 week follow-up can indicate unsuccessful treatment 6 months after BTXA injection.

Quantitative evidence suggested that augmented-surgery doses should be performed in AACE to obtain a satisfactory outcome (23). In this study, all patients underwent surgery before this concept was proposed; 95.1% of patients were satisfied, and there was no diplopia.

The retrospective and non-randomized design are the primary limitations of this study. Randomized controlled clinical trials need to be designed to increase the evidence strength. The follow-up in this study was 6 months. Longer follow-up will provide more data on treatment efficacy. The surgery group achieved better outcomes with greater deviation before treatment. Though the deviation was different before treatment in both groups, this still indicated a better outcome of surgery.

In conclusion, both surgery and BTXA are efficient for AACE. Surgery has a more precise and lasting therapeutic than BTXA. AACE patients who were adequately treated with BTXA with deviations of no more than 4 PD at 2 weeks follow-up had better outcomes.

Data availability statement

The raw data supporting the conclusions of this article will be made available by the authors, without undue reservation.

Ethics statement

The studies involving human participants were reviewed and approved by Ethics Committee of Wenzhou Medical University. Written informed consent from the participants' legal guardian/next of kin was not required to participate in this study in accordance with the national legislation and the institutional requirements.

Author contributions

YL and FZ conceived and designed the study. YL performed the treatments and follow up with the patients. YL and LT conducted the acquisition and statistical analysis of the data. YL, LT, YC, MW, BZ, and XY drafted the manuscript. FZ supervised the study and critically revised the manuscript. All authors contributed to the article and approved the submitted version.

Conflict of interest

The authors declare that the research was conducted in the absence of any commercial or financial relationships that could be construed as a potential conflict of interest.

Publisher's note

References

1. Clark AC, Nelson LB, Simon JW, Wagner R, Rubin SE. Acute acquired comitant esotropia. *Br J Ophthalmol*. (1989) 73:636–8. doi: 10.1136/bjo.73.8.636

2. Burian HM, Miller JE. Comitant convergent strabismus with acute onset. *Am J Ophthalmol*. (1958) 45:55–64. doi: 10.1016/0002-9394(58)90223-X

3. Fu T, Wang J, Levin M, Xi P, Li D, Li J. Clinical features of acute acquired comitant esotropia in the Chinese populations. *Medicine*. (2017) 96:e8528. doi: 10.1097/MD.0000000000008528

4. Lee HS, Park SW, Heo H. Acute acquired comitant esotropia related to excessive smartphone use. *BMC Ophthalmol*. (2016) 16:37. doi: 10.1186/s12886-016-0213-5

5. Cai C, Dai H, Shen Y. Clinical characteristics and surgical outcomes of acute acquired comitant esotropia. *BMC Ophthalmol*. (2019) 19:173. doi: 10.1186/s12886-019-1182-2

6. Topcu Yilmaz P, Ural Fatihoglu O, Sener EC. Acquired comitant esotropia in children and young adults: clinical characteristics, surgical outcomes, and association with presumed intensive near work with digital displays. *J Pediatr Ophthalmol Strabismus*. (2020) 57:251–6. doi: 10.3928/01913913-20200422-02

7. Neena R, Remya S, Anantharaman G. Acute acquired comitant esotropia precipitated by excessive near work during the COVID-19-induced home confinement. *Indian J Ophthalmol*. (2022) 70:1359–64. doi: 10.4103/ijo.IJO_2813_21

8. Kim DH, Noh HJ. Surgical outcomes of acute acquired comitant esotropia of adulthood. *BMC Ophthalmol*. (2021) 21:45. doi: 10.1186/s12886-020-01793-3

9. Dai Z, Zheng F, Xu M, Zhou J, Wan M, Yu H, et al. Effect of the base-out recovery point as the surgical target for acute acquired comitant esotropia. *Graefes Arch Clin Exp Ophthalmol*. (2021) 259:3787–94. doi: 10.1007/s00417-021-05318-6

10. Huang XQ, Hu XM, Zhao YJ, Ye MH, Yi BX, Zhou LH. Clinical efficacy of botulinum toxin type A on acute acquired comitant esotropia. *Int J Ophthalmol*. (2022) 15:1845–51. doi: 10.18240/ijo.2022.11.16

11. Sefi-Yurdakul N. Clinical features, etiological reasons, and treatment results in patients who developed acute acquired nonaccomodative esotropia. *Int Ophthalmol*. (2023) 43:567–74. doi: 10.1007/s10792-022-02458-4

12. Turton K, Chaddock JA, Acharya KR. Botulinum and tetanus neurotoxins: structure, function and therapeutic utility. *Trends Biochem Sci*. (2002) 27:552–8. doi: 10.1016/S0968-0004(02)02177-1

13. De Alba Campomanes AG, Binenbaum G, Campomanes EG. Comparison of botulinum toxin with surgery as primary treatment for infantile esotropia. *J AAPOS*. (2010) 14:111–6. doi: 10.1016/j.jaapos.2009.12.162

14. Wan MJ, Mantagos IS, Shah AS, Kazlas M, Hunter DG. Comparison of botulinum toxin with surgery for the treatment of acute-onset comitant esotropia in children. *Am J Ophthalmol*. (2017) 176:33–9. doi: 10.1016/j.ajo.2016.12.024

15. Lang LJ, Zhu Y, Li ZG, Zheng GY, Peng HY, Rong JB, et al. Comparison of botulinum toxin with surgery for the treatment of acute acquired comitant esotropia and its clinical characteristics. *Sci Rep*. (2019) 9:13869. doi: 10.1038/s41598-019-50383-x

16. Lueder GT, Galli M, Tychsen L, Yildirim C, Pegado V. Long-term results of botulinum toxin-augmented medial rectus recessions for large-angle infantile esotropia. *Am J Ophthalmol*. (2012) 153:560–3. doi: 10.1016/j.ajo.2011.08.019

17. Tong L, Yu X, Tang X, Zhang Y, Zheng S, Sun Z. Functional acute acquired comitant esotropia: clinical characteristics and efficacy of single botulinum toxin type A injection. *BMC Ophthalmol*. (2020) 20:464. doi: 10.1186/s12886-020-01739-9

18. Morgenstern KE, Evanchan J, Foster JA, Cahill KV, Burns JA, Holck DE, et al. Botulinum toxin type A for dysthyroid upper eyelid retraction. *Ophthalmic Plast Reconstr Surg*. (2004) 20:181–5. doi: 10.1097/00002341-200405000-00001

19. Mills MD, Coats DK, Donahue SP, Wheeler DTAmerican Academy of Ophthalmology. Strabismus surgery for adults: a report by the American Academy of Ophthalmology. *Ophthalmology*. (2004) 111:1255–62. doi: 10.1016/j.ophtha.2004.03.013

20. Simon JW. Complications of strabismus surgery. *Curr Opin Ophthalmol*. (2010) 21:361–6. doi: 10.1097/ICU.0b013e32833b7a3f

21. Xu H, Sun W, Dai S, Cheng Y, Zhao J, Liu Y, et al. Botulinum toxin injection with conjunctival microincision for the treatment of acute acquired comitant esotropia and its effectiveness. *J Ophthalmol*. (2020) 2020:1702695. doi: 10.1155/2020/1702695

22. Huang X, Meng Y, Hu X, Zhao Y, Ye M, Yi B, et al. The effect of different treatment methods on acute acquired concomitant esotropia. *Comput Math Methods Med*. (2022) 2022:5001594. doi: 10.1155/2022/5001594

23. Zhou Y, Ling L, Wang X, Jiang C, Wen W, Zhao C. Augmented-dose unilateral recession-resection procedure in acute acquired comitant esotropia. *Ophthalmology*. (2022) 130:525–32. doi: 10.1016/j.ophtha.2022.12.019

frontiers | Frontiers in Medicine

TYPE Review
PUBLISHED 07 August 2023
DOI 10.3389/fmed.2023.1210293

OPEN ACCESS

EDITED BY
Georgios D. Panos,
Nottingham University Hospitals NHS Trust, United Kingdom

REVIEWED BY
Barbara Burgos-Blasco,
San Carlos University Clinical Hospital, Spain
Kirandeep Kaur,
Dr Om Parkash Eye Hospital, India

*CORRESPONDENCE
Sonia N. Yeung
✉ sonia.y@gmail.com

RECEIVED 22 April 2023
ACCEPTED 24 July 2023
PUBLISHED 07 August 2023

CITATION
Mousavi M, Kahuam-López N, Iovieno A and Yeung SN (2023) Global impact of COVID-19 on corneal donor tissue harvesting and corneal transplantation.
Front. Med. 10:1210293.
doi: 10.3389/fmed.2023.1210293

Global impact of COVID-19 on corneal donor tissue harvesting and corneal transplantation

Morteza Mousavi, Nicolás Kahuam-López, Alfonso Iovieno and Sonia N. Yeung*

Department of Ophthalmology and Visual Sciences, University of British Columbia, Vancouver, BC, Canada

Introduction: The purpose of this review is to consolidate and examine the available literature on the coronavirus disease 2019 pandemic and its effect on corneal transplantation and eye banking.

Methods: A primary literature search was conducted using the PubMed (Medline) database with keywords and MeSH terms such as "corneal transplantation," "eye banks," "keratoplasty" and then were combined with COVID-19. Relevant articles through September 2022 were assessed and 25 articles were included in this review.

Results: Donor tissue volumes declined globally during lockdown periods due to a lower number of referrals and tighter tissue screening guidelines. Rates of elective surgeries decreased in the lockdown period compared to respective periods in previous years. However, changes in rates of emergency procedures were not uniform across different regions. Moreover, rates of different elective corneal grafts [i.e., penetrating keratoplasty (PK), endothelial keratoplasty (EK), or anterior lamellar keratoplasty (ALK)] were affected differently with the pattern of change being dependent on region-specific factors.

Conclusion: Both donor tissue volumes and rates of corneal transplant procedures were affected by lockdown restrictions. The underlying etiology of these changes differed by region. Examining the range of impact across many countries as well as the contributing factors involved will provide guidance for future global pandemics.

KEYWORDS

COVID-19, eye bank, corneal transplant, donor tissue, tissue procurement and processing

1. Introduction

In late 2019, the emergence of the severe acute respiratory syndrome coronavirus 2 (SARS-CoV-2) sparked the beginning of the coronavirus disease 2019 (COVID-19) pandemic. There have been over 450 million confirmed cases and over 6 million confirmed deaths from COVID-19 (1). As countries around the globe were grappling with the fast spread of the disease, several restrictions were put into place to help reduce the growing number of cases. One such restriction was the cancellation of many elective procedures (2, 3). As a result, organ and tissue transplant volumes decreased during the first months of the pandemic (4). This included corneal transplants, as the risk of transmission through ocular tissue transplantation was and still is a

matter of contention (5). Given these challenges and uncertainties, many eye banks experienced decreased donor tissue availability and subsequently, the number of corneal transplantation procedures declined. Based on the statistical report published by the Eye Bank Association of America (EBAA), transplant volumes in 2021 recovered from the decline in 2020. However, the numbers have yet to match the 2019 data (6). Therefore, understanding the differential challenges and responses to the pandemic in different regions is instrumental in planning ahead for similar scenarios in the future. Herein we examine reports of eye banking and corneal transplant statistics during the COVID-19 pandemic and explore the reasons behind the region-specific impact.

2. Materials and methods

A primary literature search was conducted in November 2022 using the PubMed (Medline) database with keywords and MeSH terms such as "corneal transplantation," "eye banks," "keratoplasty," and "COVID-19." There were no publication year or language restrictions. The search yielded a total of 72 articles (Figure 1). Case reports and case series were excluded from the results. Abstracts were reviewed, and literature reporting statistical data on corneal tissue donor volumes and transplantation during the pandemic were selected. Secondary literature was found using pertinent references from the primary articles. A total of 25 relevant papers were identified and reviewed.

3. Results and discussion

3.1. Ocular donor tissue volumes

Studies from the United States (7–9), United Kingdom (10), Canada (11), Germany (12), Italy (13–15), India (16–20), and continental data from Europe (21) showed a decrease in the number of donor corneal tissues procured during their respective lockdown periods in 2020. However, the magnitude of this decline varied among the different regions (Table 1). Interestingly, one survey of members of the European Eye Bank Association (EEBA) found that only one country (Bulgaria) of 19 participating countries showed an increase in the number of tissues procured and distributed from March to May 2020 compared to the same period in 2019. However, this was attributed to the small number of corneas (only 28) procured in this region during and before the period of interest (21).

Several reasons have been reported in the literature to explain this decrease in donor tissue volumes. AlShaker et al. (11) and Ballouz et al. (7) interpreted the decrease in the number of eligible referrals to their respective eye bank as a reflection of an increased number of COVID-19 cases as well as more stringent screening criteria for tissue selection. Moreover, the rate of conversion of those eligible referrals to retrieved tissues for transplantation decreased in the same period in 2020 compared to 2019. This change in conversion rates was thought to reflect logistical challenges due to COVID-19 such as lack of staffing (11). Issues with staffing were also reflected in Thuret et al. (21) survey of EEBA members. The issue of logistical challenges was also highlighted in a survey of eye banks in Germany, where 21 out of the 26 surveyed eye banks reported a decrease in their activity since the beginning of the pandemic compared to before the pandemic (12).

Although donor screening criteria was often reported to account for the decrease in donor tissue volumes, these criteria were variable. A survey of 64 eye bank members of the EEBA reported by Thuret et al. (21) showed that all eye banks in their study contraindicated donations from patients whose confirmed cause of death was COVID-19. However, screening criteria for the rest of the donors, for example, those who had COVID-19 but died of other causes or those who had recovered from a COVID-19 infection and then passed away from other causes later on, varied among the different eye banks. In their survey, the least stringent criteria mandated a 14-day symptom-free period before death, whereas the most stringent criteria mandated a period double that time. Moreover, they reported that the definition of COVID-19 symptoms varied among different exclusion guidelines, with the strictest criteria mandating exclusion of those with "unexplained cough, unexplained asthenia and myalgia, intermittent fever, shortness of breath or unexplained conjunctivitis before death." Such variability in screening criteria was also observed in a survey of Indian eye banks (17), which reported that a fraction of the eye banks avoided tissue retrieval from COVID-19 positive cases (44.4%) or those with suspicious respiratory symptoms (36.7%). In contrast, some eye banks (16.67%) completely halted tissue collection. A survey of German eye banks (12) showed all active banks followed local guidelines. At the same time, a portion of them also followed recommendations made by the Global Alliance of Eye Bank Associations (GAEBA) or the European Center for Disease Prevention and Control (ECDC). The variability in screening criteria is also reflected in the differences in the reported rate of tissue exclusion due to COVID-19 in different studies, which varied from a 2-month rate of 2% in the Italian Society of Eye Banks (SIBO) reports (13) to 35% reported for the month of April in Eye Bank of Canada Ontario Division's (EBCOD) analysis (11). Thuret et al. (21) did establish that higher levels of stringency in the screening criteria often led to a decrease in tissue procurement. This diversity in donor screening criteria not only reflects adherence to the guidelines set forth by different regulatory bodies but is also a product of the timing of when these guidelines were adopted. Furthermore, as our knowledge of SARS-COV2 evolves with time, the guidelines may also be refined to reflect new data (22).

Numbers of procured tissues from the SIBO and Fondazione Banca degli Occhi del Veneto (FBOV eye bank—Venice, Italy) showed some improvement in the first month following lockdown but not large enough to statistically match the comparison periods in previous years (13, 14). A survey conducted by the EBAA showed a similar pattern of improvement in the tissue distribution volume 2 months after lockdown (8). In a study of the Eversight eye bank, Ballouz et al. (9) compared the number of available corneal tissues and corneal transplant surgeries in an 18-month period from July 2020 to December 2021 (when elective surgeries were resumed) to the same period in 2018 and 2019. The number of surgeries requiring corneal tissue significantly increased in this period compared to the pre-pandemic period, and the number of suitable tissues was similar in both periods of comparison. Therefore, though the number of procured tissue increased during this period it was not enough to meet the needs due to the increased demand. This shortage in tissue was handled through an increase in imported tissues (9). Ongoing

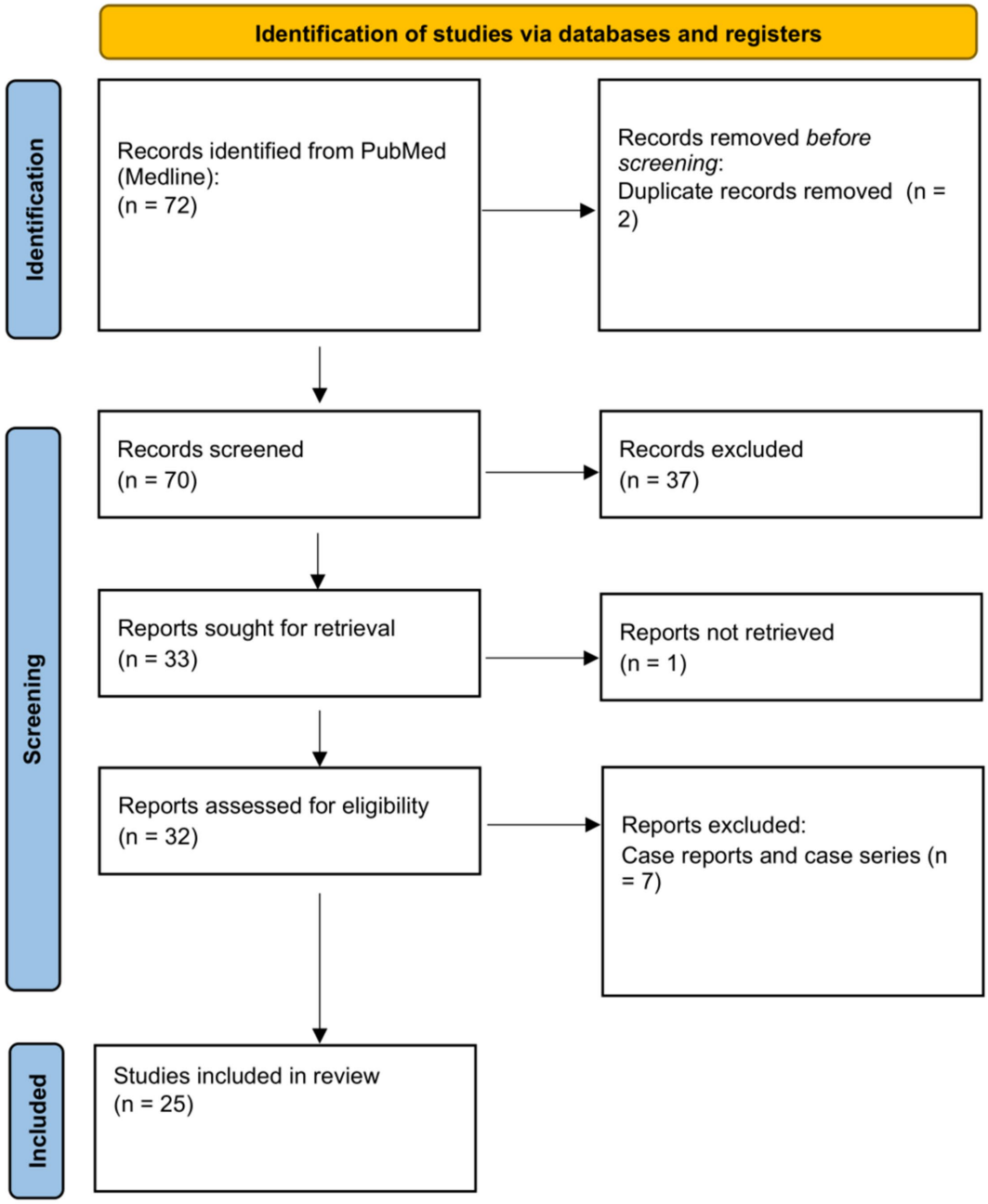

FIGURE 1
PRISMA flow diagram.

efforts to improve the rates of donation of corneal tissue post-pandemic will continue to address the increasing demand for corneal transplantation worldwide.

Lastly, regarding the number of exported tissues the evidence seems to be contradictory. The data from the Eversight eye bank shows a significant decrease in exported tissues which is congruent with the national decline reported by EBAA (7, 8). On the other hand, Aiello et al. (13) reported an increase in the number of exported tissues from SIBO. They attributed this rise to the fact that the lockdown started in Italy before other European countries, and at that time, exports were still happening to those countries where elective surgeries had not stopped (13).

3.2. Transplant volumes

In general, the number of ophthalmic procedures significantly decreased during the lockdown phase in many regions of the world (18, 23–26). Analogous to donor tissue volumes, a decrease in the volume of transplanted tissues and the number of procedures completed during the first wave of the pandemic is reported in the literature (7, 11, 13, 19, 20, 27–30). Similar to the change in donor tissue volumes, the reported decline in transplant volumes varied among regions (Table 2). This was a consequence of non-emergent procedures being shut down due to special considerations in resource reallocation. We will explore these findings in more detail below.

TABLE 1 Studies comparing the number of procured tissues between the lockdown periods in 2020 and respective months in 2019.

Study	Region	Comparison period	No. of procured tissue in 2020	No. of procured tissue in 2019	% decline	*p*
Ballouz et al. (7)	Eversight eye bank facilities (Michigan, Ohio, Illinois, New Jersey, And Connecticut)	March–June	Not reported	Not reported	45	0.031
AlShaker et al. (11)	Eye bank of Canada (Ontario Division)	March–June	267	769	65	Not reported
Trigaux et al. (12)	26-member eye banks of the German Ophthalmological Society	March–April	1,453	1,758	17	Not reported
Aiello et al. (13)	13-member eye banks of the Italian Society of Eye Banks	March–April	1,284	3,088	58	<0.0001
Parekh et al. (14)	Fondazione Banca degli Occhi del Veneto (FBOV – Venice, Italy)	March–April	Not reported	Not reported	41	<0.0001
Agarwal et al. (18)	Apex health institute of India	March–July	Not reported	Not reported	99	<0.001
Nathawat et al. (17)	Eye Banks and Cornea Surgeons' members of the All India Ophthalmological Society (AIOS) and the Eye Bank Association of India (EBAI)	March–May	1,898	8,735	78	Not reported

TABLE 2 Studies comparing the number of surgical procedures between the lockdown periods in 2020 and respective months in 2019.

Study	Region	Comparison period	No. of Surgical procedures in 2020	No. of surgical procedures in 2019	% decline	*p*
Aiello et al. (13)	13-member eye banks of the Italian Society of Eye Banks (SIBO)	March–April	534	1,220	56	<0.0001
AlShaker et al. (11)	Eye bank of Canada Ontario Division (EBCOD)	March–June	207	753	73	Not reported
Ballouz et al. (7)	Eversight eye bank facilities (Michigan, Ohio, Illinois, New Jersey, and Connecticut)	March–June	Not reported	Not reported	53	0.011
Din et al. (29)	Moorfields Eye Hospital (London, UK)	April–June	10	163	92	Not reported

Because mainly elective procedures were subject to cancellations during COVID-19 lockdown periods, the number of emergency procedures would not be expected to change compared to pre-pandemic years (13, 29, 31). Interestingly, Din et al. (29) reported an increase in the number of emergency procedures due to sharp object trauma (29), which was attributed to redirection of all ophthalmic services from other centers to their hospital as well as an increase in domestic incidences due to the lockdown (29). On the other hand, dell'Omo et al. (26) reported a significant decrease in the number of elective and emergency procedures compared to the same period in 2019 in six centers in Italy. Moreover, a 2-month analysis of 39 centers in Italy showed a significant decrease in some subtypes of emergency procedures compared to the same period in 2019 (24), which was reported to be a result of the limitations in access to operating rooms as their availability was reduced in all except one center.

Descriptive statistics drawn from many eye banks around the world showed a decline in transplanted tissue volumes in 2020 compared to 2019 (Figure 2) (7, 11, 13, 20). Specifically, a decline both in donor tissue and transplant volumes was noted. A drop in the rate of unused tissue during the lockdown period compared to the yearly

average in 2019 was reflected in the EBCOD records (11). This was specifically recorded in the months of April and May, when only emergency procedures were done. As a result, a small number of tissues was released for transplant and utilization of retrieved tissues was maximized. However, they reported a surplus of unused tissue in March when operating rooms (ORs) were closed and a return to rates similar to 2019 in the month of June when ORs resumed regular activity. Das et al. (20) reported an increase in the average rate of corneal tissue utilization during and after COVID-19 lockdown in 2020 compared to the same average rate in 2019 due to a shortage of donor tissue availability post-lockdown. As a result, the stringency of their selection criteria was reviewed to improve utilization.

On the other hand, other centers showed a surplus of corneal tissue during the lockdown period due to the reduction in scheduled surgeries and a significant rise in the number of canceled transplants (7, 13). Due to an increase in the number of wasted donor tissues, Busin et al. (27) underlined the importance of exploring alternative procurement techniques that would extend the storage time of procured corneal tissues and reported tissue dehydration as a useful alternative method, especially in the case of deep anterior lamellar keratoplasties. A survey of eye banks and surgeons in India showed a statistically significant increase in the use of long-term tissue preservation methods in the same period in 2020 compared to previous years (17).

When examining the distribution of different types of corneal transplantation surgeries, there was no trend noted. By analyzing Brazilian national data and records from the state of São Paulo, Moriyama et al. (28) found that the proportions of tectonic and/or therapeutic procedures significantly increased. Conversely, the proportions of all 3 optical procedures [penetrating keratoplasty (PK), endothelial keratoplasty (EK), or anterior lamellar keratoplasty (ALK)] significantly decreased, with EK and especially ALK showing more dramatic declines than PK. The analysis of the same proportions after removing the moratorium showed that while the proportions of all 3 optical procedures increased, PK rates showed a significant increase compared to the rates in 2019, whereas EK rates were still below those of 2019 (28). One explanation the authors suggest to account for the change in EK proportions is that EKs are mostly done on elderly patients and during the moratorium as well as after it was released the older population was facing stricter mobility restrictions. The United Kingdom (UK) data did not show any meaningful changes in the patterns of corneal transplants from April 2020 to March 2021 compared to similar periods in previous years (10). The EBAA data revealed a decrease in EK proportions and an increase in PK proportions during the lockdown in the US, however the proportions were once again similar to pre-pandemic values after the restrictions were lifted (28). Mencucci et al. (15) showed a decrease in the rates of both PKs and ALKs due to the suspension of elective surgeries. PKs showed a steeper decline, explained by the general trend of preferring ALKs over PKs in recent years. The increase in the rates of EKs during the lockdown period was attributed to the use of local anesthesia during EKs. In their analysis of data from a tertiary eye care center in India, Das et al. (20) reported a decline in the numbers of PK, EK, and ALK procedures, but a marginal increase in the number of therapeutic penetrating keratoplasty (ThPK) compared to pre-lockdown data (20) due to advanced worsening of visual acuity in patients with infectious keratitis during the pandemic (20).

Data from several eye banks showed an increase in the number of procedures done after the lockdown period, however, those post lockdown numbers were still significantly lower than pre-pandemic rates (13, 20, 28).

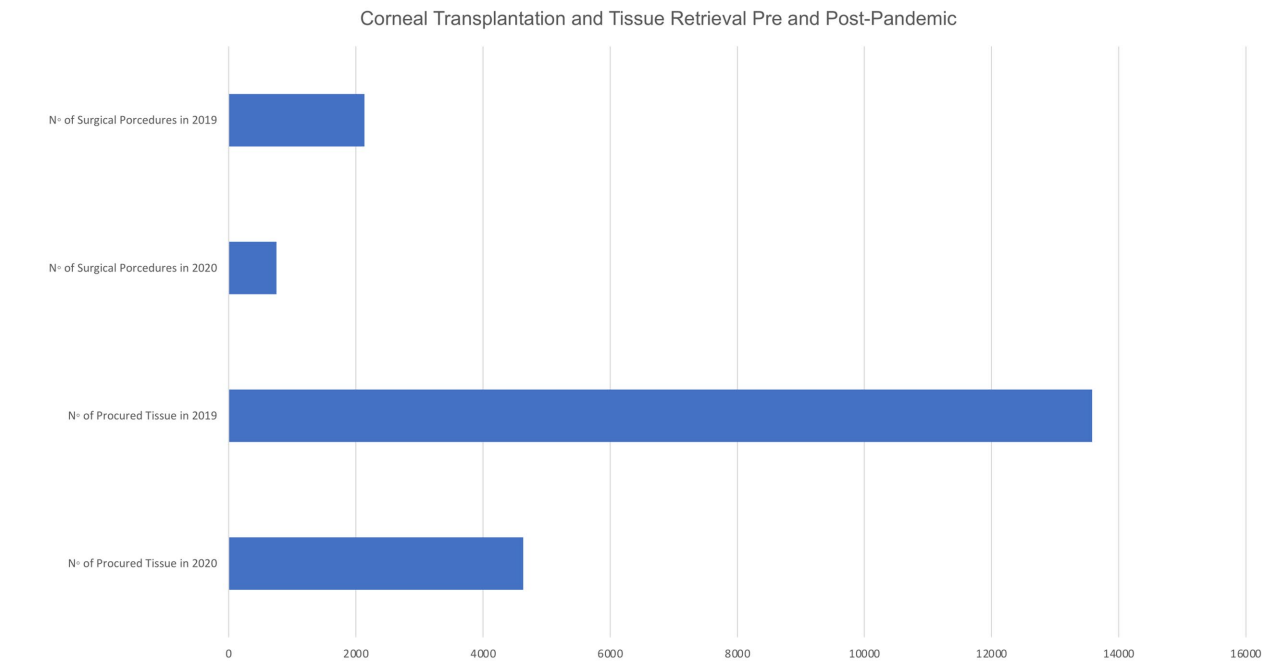

FIGURE 2
Corneal transplantation and tissue retrieval pre- and post-pandemic.

3.3. Patients' challenges

Several studies have analyzed data regarding logistical challenges facing patients requiring corneal transplants.

Data from Moorfields Eye Hospital (MEH) during the lockdown period showed a significant increase in the time between patient's symptom presentation and surgical procedure compared to pre-pandemic period (29). The authors also examined patients' travel distances during the lockdown and found an increasing trend compared to the year before the pandemic. Together, these two results highlighted the fact that during the pandemic corneal procedures were being done in only one of the several centers of the National Health Services (NHS) trust center in London while other centers had been redeployed for COVID-19 care. A geographical barrier was also reported by Das et al. (20). Their analysis of a tertiary eye care center in India showed a decreasing trend in the number of patients who travelled interstate to consult for corneal procedures.

Lastly, in their analysis of the national Brazilian data, Moriyama et al. (28) found a significant decrease in the number of new patients added to corneal surgery waiting list during the lockdown phase when compared to the same period in 2019. The authors suggested this was due to a decrease in the activity of outpatient clinics in that period.

4. Conclusion

This review summarizes the impact of COVID-19 on corneal donor tissue harvesting and corneal transplant in different settings around the world. Both donor tissue and transplant volumes showed a decline during the lockdown times. Moreover, geographical challenges were highlighted which resulted in longer distances traveled by patients to obtain care, as well as delayed care. Eye bank operations during the pandemic have been evolving due to knowledge gained from COVID-19 and the subsequent changes in guidelines over time. Region-specific variability in lockdown timing also affected downstream donor tissue criteria evolution and tissue availability for corneal transplantation. Understanding the impact of this pandemic on eye bank operations around the globe will ultimately allow us to anticipate the disruption to the delivery of corneal tissue for transplantation in future pandemics, and to address the impact more efficiently with the goal of resuming care for our patients. Reports from many regions are valuable to elucidate the region-specific factors with critical roles in providing safe high-quality corneal tissue, optimize eye bank guidelines, improve the efficient use of available tissue, and minimize tissue waste in future similar scenarios.

Author contributions

MM, NK-L, AI, and SY participated in the idea conception, acquisition and data analysis, drafting of the manuscript, and final approval of the version to be published. All authors agree to be accountable for all aspects of the work in ensuring that questions related to the accuracy or integrity of any part of the work are appropriately investigated and resolved.

Conflict of interest

The authors declare that the research was conducted in the absence of any commercial or financial relationships that could be construed as a potential conflict of interest.

Publisher's note

References

1. WHO. WHO coronavirus (COVID-19) dashboard [internet]. (2022). Available at: WHO Coronavirus (COVID-19) Dashboard

2. COVIDSurg Collaborative. Elective surgery cancellations due to the COVID-19 pandemic: global predictive modelling to inform surgical recovery plans. *Br J Surg*. (2020) 107:1440–9. doi: 10.1002/bjs.11746

3. Rosenbaum L. The untold toll — the Pandemic's effects on patients without Covid-19. *N Engl J Med*. (2020) 382:2368–71. doi: 10.1056/NEJMms2009984

4. Heldman MR, Kates OS. COVID-19 in solid organ transplant recipients: a review of the current literature. *Curr Treat Options Infect Dis*. (2021) 13:67–82. doi: 10.1007/s40506-021-00249-6

5. Aldave AJ, DeMatteo J, Chamberlain WD, Philippy B, Farooq A, Buckman N, et al. COVID and the cornea: from controversies to consensus. *Cornea*. (2021) 40:809–16. doi: 10.1097/ICO.0000000000002741

6. Eye Bank Association of America (EBAA). *Eye banking statistical report*. (2021). Available at: https://restoresight.org/wp-content/uploads/2022/03/2021_StatisticalGuide_numbered_FINAL.pdf

7. Ballouz D, Sawant OB, Hurlbert S, Titus MS, Majmudar PA, Kumar A, et al. Impact of the COVID-19 pandemic on Keratoplasty and corneal eye banking. *Cornea*. (2021) 40:1018–23. doi: 10.1097/ICO.0000000000002748

8. AlMutlak M, Li JY, Bin Helayel H, Fairaq R. Future of corneal donation and transplantation: insights from the COVID-19 pandemic. *Cornea*. (2021) 40:274–6. doi: 10.1097/ICO.0000000000002538

9. Ballouz D, Issa R, Sawant OB, Hurlbert S, Titus MS, Zhou Y, et al. COVID-19 and eye banking: ongoing impacts of the pandemic. *Cornea [Internet]*. (2022) 42:89–96. doi: 10.1097/ICO.0000000000003137

10. National health Service Blood and Transplants. Cornea activity [internet]. (2021). Available at: https://nhsbtdbe.blob.core.windows.net/umbraco-assets-corp/23475/section-10-cornea-activity.pdf.

11. AlShaker SM, Humphreys C, Smigielski N, Chan CC. The effect of COVID-19 on corneal donor volumes and eye Bank processes. *Cornea*. (2022);Advance online pub.) 41:757–65. doi: 10.1097/ICO.0000000000003004

12. Trigaux C, Salla S, Schroeter J, Tourtas T, Thomasen H, Maier P, et al. SARS-CoV-2: impact on, risk assessment and countermeasures in German eye banks. *Curr Eye Res*. (2021) 46:666–71. doi: 10.1080/02713683.2020.1828487

13. Aiello F, Genzano Besso F, Pocobelli G, Gallo Afflitto G, Colabelli Gisoldi RAM, Nucci C, et al. Corneal transplant during COVID-19 pandemic: the Italian eye Bank national report. *Cell Tissue Bank*. (2021) 22:697–702. doi: 10.1007/s10561-021-09934-8

14. Parekh M, Ferrari S, Romano V, Myerscough J, Jones GLA, Griffoni C, et al. Impact of COVID-19 on corneal donation and distribution. *Eur J Ophthalmol*. SAGE Publications Ltd. (2022) 32:NP269–70. doi: 10.1177/1120672120948746

15. Mencucci R, Cennamo M, Ponzin D, Genzano Besso F, Pocobelli G, Buzzi M, et al. Impact of the COVID-19 pandemic on corneal transplantation: a report from the Italian Association of eye Banks. *Front Med (Lausanne)*. (2022) 9 Available from: https://www.frontiersin.org/articles/10.3389/fmed.2022.844601

16. Parekh M, Nathawat R, Singh Parihar J, Jhanji V, Sharma N. Impact of COVID-19 restrictions on corneal tissue donation and utilization rate - time to bring reforms? *Indian J Ophthalmol*. (2021) 69:3782–4. doi: 10.4103/ijo.IJO_2714_21

17. Nathawat R, Sharma N, Sachdev M, Sinha R, Mukherjee G. Immediate impact of COVID-19 on eye banking in India. *Indian J Ophthalmol*. (2021) 69:3653–7. doi: 10.4103/ijo.IJO_1171_21

18. Agarwal R, Sharma N, Patil A, Thakur H, Saxena R, Kumar A. Impact of COVID-19 pandemic, national lockdown, and unlocking on an apex tertiary care ophthalmic institute. *Indian J Ophthalmol*. (2020) 68:2391–5. doi: 10.4103/ijo.IJO_2366_20

19. Roy A, Das S, Chaurasia S, Fernandes M, Murthy S. Corneal transplantation and eye banking practices during COVID-19-related lockdown period in India from a network of tertiary eye care centers. *Indian J Ophthalmol*. (2020) 68:2368. doi: 10.4103/ijo.IJO_2258_20

20. Das A, Chaurasia S, Vaddavalli P, Garg P. Year one of COVID-19 pandemic in India: effect of lockdown and unlock on trends in keratoplasty at a tertiary eye Centre. *Indian J Ophthalmol*. (2021) 69:3658–62. doi: 10.4103/ijo.IJO_1740_21

21. Thuret G, Courrier E, Poinard S, Gain P, Baud'Huin M, Martinache I, et al. One threat, different answers: the impact of COVID-19 pandemic on cornea donation and donor selection across Europe. *Br J Ophthalmol*. (2020) 106:312–8. doi: 10.1136/bjophthalmol-2020-317938

22. Ang M, Moriyama A, Colby K, Sutton G, Liang L, Sharma N, et al. Corneal transplantation in the aftermath of the COVID-19 pandemic: an international perspective. *Br J Ophthalmol*. (2020) 104:bjophthalmol-2020-317013–1481. doi: 10.1136/bjophthalmol-2020-317013

23. González-Martín-Moro J, Guzmán-Almagro E, Izquierdo Rodríguez C, Fernández Hortelano A, Lozano Escobar I, Gómez Sanz F, et al. Impact of the COVID-19 lockdown on ophthalmological assistance in the emergency Department at a Spanish Primary Level Hospital. *J Ophthalmol*. (2021) 2021:1–9. doi: 10.1155/2021/8023361

24. dell'Omo R, Filippelli M, Virgili G, Bandello F, Querques G, Lanzetta P, et al. Effect of COVID-19-related lockdown on ophthalmic practice in Italy: a report from 39 institutional centers. *Eur J Ophthalmol*. (2022) 32:695–703. doi: 10.1177/11206721211002442

25. Toro MD, Brézin AP, Burdon M, Cummings AB, Evren Kemer O, Malyugin BE, et al. Early impact of COVID-19 outbreak on eye care: insights from EUROCOVCAT group. *Eur J Ophthalmol*. (2021) 31:5–9. doi: 10.1177/1120672120960339

26. dell'Omo R, Filippelli M, Semeraro F, Avitabile T, Giansanti F, Parmeggiani F, et al. Effects of the first month of lockdown for COVID-19 in Italy: a preliminary analysis on the eyecare system from six centers. *Eur J Ophthalmol*. (2021) 31:2252–8. doi: 10.1177/1120672120953074

27. Busin M, Yu AC, Ponzin D. Coping with COVID-19: an Italian perspective on corneal surgery and eye banking in the time of a pandemic and beyond. *Ophthalmology*. (2020) 127:e68–9. doi: 10.1016/j.ophtha.2020.04.031

28. Moriyama AS, Erbs Pessoa JL, Silva Bessa TR, Pereira NC, Mehta JS, Hofling-Lima AL, et al. The impact of the COVID-19 pandemic on corneal transplantation in Brazil. *Cornea*. (2022) 41:322–7. doi: 10.1097/ICO.0000000000002949

29. Din N, Phylactou M, Fajardo-Sanchez J, Watson M, Ahmad S. The impact of covid-19 on acute and elective corneal surgery at moorfields eye hospital London. *Clin Ophthalmol*. (2021) 15:1639–45. doi: 10.2147/OPTH.S302576

30. Asena L, Dursun Altınörs D, Oto S, Haberal M. Impact of the COVID-19 pandemic on corneal transplantation and cornea procurement. *Exp Clin Transplant [Internet]*. (2022) 20:70–3. doi: 10.6002/ect.DonorSymp.2022.O14

31. Tóth G, Xanthopoulou K, Stachon T, Németh J, Hécz R, Berkó-Göttel B, et al. Impact of COVID-19 pandemic on emergency inpatient volume at a tertiary eye Care Center in Germany with corneal Main specialization. *Klin Monatsbl Augenheilkd*. (2021) 238:715–20. doi: 10.1055/a-1327-3393

frontiers | Frontiers in Medicine

TYPE Original Research
PUBLISHED 29 September 2023
DOI 10.3389/fmed.2023.1266532

OPEN ACCESS

EDITED BY
Georgios D. Panos,
Nottingham University Hospitals NHS Trust, United Kingdom

REVIEWED BY
Junyi Chen,
Fudan University, China
Yinghong Ji,
Fudan University, China

*CORRESPONDENCE
Kazuyuki Hirooka
✉ khirooka9@gmail.com

RECEIVED 25 July 2023
ACCEPTED 18 September 2023
PUBLISHED 29 September 2023

CITATION
Onoe H, Hirooka K, Namiguchi K, Mizoue S, Hosokawa H, Mochizuki H, Okada N, Tokumo K, Okumichi H and Kiuchi Y (2023) Comparison of surgical outcomes between iStent inject W implantation and microhook ab interno trabeculotomy in combination with phacoemulsification in primary open-angle glaucoma patients.
Front. Med. 10:1266532.
doi: 10.3389/fmed.2023.1266532

Comparison of surgical outcomes between iStent inject W implantation and microhook ab interno trabeculotomy in combination with phacoemulsification in primary open-angle glaucoma patients

Hiromitsu Onoe[1], Kazuyuki Hirooka[1]*, Koji Namiguchi[2,3], Shiro Mizoue[2,3], Hiroko Hosokawa[3], Hideki Mochizuki[4], Naoki Okada[1], Kana Tokumo[1], Hideaki Okumichi[1] and Yoshiaki Kiuchi[1]

[1]Department of Ophthalmology and Visual Science, Hiroshima University, Hiroshima, Japan, [2]Department of Ophthalmology, Ehime University Graduate School of Medicine, Toon, Japan, [3]Department of Ophthalmology, Minami-Matsuyama Hospital, Matsuyama, Japan, [4]Kusatsu Eye Clinic, Hiroshima, Japan

Purpose: To examine primary open-angle glaucoma patients after undergoing combined cataract surgery with microhook ab interno trabeculotomy (μLOT-Phaco) or iStent inject W implantation (iStent-Phaco), and then evaluate the surgical outcomes after a minimum of 6 months of follow-up.

Methods: Between October 2020 and July 2022, 39 μLOT-Phaco eyes and 55 iStent-Phaco eyes that underwent surgery were evaluated in this retrospective, multicenter comparative case series. Data that included preoperative and postoperative intraocular pressure (IOP), number of glaucoma medications, and occurrence of complications were collected from medical records and then examined. Surgical failure was defined as patients exhibiting *a* < 20% reduction in the preoperative IOP or an IOP > 18 mmHg on two consecutive follow-up visits, or when patients were required to undergo reoperation. Success rates were determined based on a Kaplan–Meier survival analysis.

Results: At 3, 6 and 12 months postoperatively, there was a significant postoperative reduction in the IOP ($p < 0.001$) and in the medications scores ($p < 0.001$) for both of the groups. In the μLOT-Phaco and iStent-Phaco groups, the probabilities of success at 6 and 12 months were 55.3 and 45.5%, and 48.4 and 45.5% ($p = 0.38$; log-rank test), respectively. In the iStent-Phaco group, there was a significant decrease in the hyphema.

Conclusion: Comparable surgical outcomes occurred for both the μLOT and iStent inject W procedures.

KEYWORDS

iStent inject W, primary open-angle glaucoma, microhook, phacoemulsification, intraocular pressure

Introduction

Glaucoma is a leading cause of irreversible blindness worldwide (1). The use of medications or surgery to lower the intraocular pressure (IOP) are the only ways that have been shown to decrease the speed of the visual field damage progression (2, 3). The first-line therapy normally used includes glaucoma medications and/or selective laser trabeculoplasty. When the IOP cannot be sufficiently lowered or progression prevented after the utilization of the maximum tolerated medical and/or laser treatment, surgery is typically performed.

In mild to moderate glaucoma patients, the interventions available for surgeons have been greatly augmented through the implementation of minimally invasive glaucoma surgery (MIGS) procedure. The iStent trabecular micro-bypass (containing one stent) was the original MIGS device approved by the United Stated Food and Drug Administration (FDA), with the FDA then approving the second-generation iStent inject (containing two stents). As the trabecular meshwork is known to cause resistance to the aqueous humor outflow, in addition to being a major contributor to elevated IOP in glaucoma patients, these stents were both designed to create pathways through this meshwork (4). The iStent inject W (Glaukos Corporation, San Clemente, CA), which is available in Japan, contains a wide flange at its base and is designed to optimize stent visualization and placement. Another trabecular-based device that works by increasing the aqueous humor outflow through Schlemm's canal is the Tanito microhook (Inami & Co., Ltd., Tokyo, Japan).

As there has been continuous expansion of the field of MIGS along with the development of newer techniques, it is important that measurements of the surgical outcome between different procedures be undertaken. Thus, the postoperative outcomes of combined cataract surgery with either microhook ab interno trabeculotomy (μLOT-Phaco) or iStent inject W implantation (iStent-Phaco) were compared in primary open-angle glaucoma (POAG) patients in our current study.

Materials and methods

Patient selection

Eyes undergoing phacoemulsification cataract extraction combined with either μLOT (μLOT-Phaco) or iStent inject W implantation (iStent-Phaco) between October 2020 and July 2022 were evaluated in this retrospective study in the Japanese prefectures of Hiroshima and Ehime at Hiroshima University Hospital, Ehime University Hospital, Minami-Matsuyama Hospital, and Kusatsu Eye Clinic. This study was in accordance with the principles of the Declaration of Helsinki, and was conducted following approval from the Hiroshima university's ethics committee.

Patients that were ≥ 18 years of age, and previously diagnosed with POAG were included in the study. However, patients were excluded from the study if they had other glaucoma types or if they had a history of ocular surgery. Furthermore, a 6-month postoperative observation period was required in all patients. When bilateral surgery was performed in a patient, the analysis only utilized the data from the first eye. A suboptimal IOP and/or slow progression of visual field damage in spite of maximal tolerable glaucoma therapy were the most common and similar indications for the surgeries. Another relevant surgery group included patients who were on more than one glaucoma medications without known intolerance requiring the number of glaucoma medications reduction that were scheduled for cataract surgery. Surgeons were responsible for deciding whether to use the iStent inject W implantation or microhook ab interno trabeculotomy.

Surgical technique

Phacoemulsification was performed using the standard technique. After cataract removal was performed through a temporal corneal incision, intraocular lens was implanted in the capsular bag. Sodium hyaluronate was added to the anterior chamber after the cataract surgery to ensure that there was enhanced visuality of Schlemm's canal. Subsequently, after tilting both the patient's head and microscope, the gonio lens was placed on the cornea to visualize the nasal angle. In the iStent-Phaco group, following the identification of Schlemm's canal, the iStent inject W was implanted as two devices, with the two stents located in the nasal quadrant one to two clock hours apart. After inserting the microhook tip into Schlemm's canal via the main corneal incision in the μLOT-Phaco group, the microhook was circumferentially moved to the 4 clock hour position (nasal quadrant) in order to incise both the trabecular meshwork and the inner wall of the Schlemm's canal. Antibacterial and anti-inflammatory topical medications were prescribed for each of the patients. All of the glaucoma medications were stopped at the time of the surgery, then added in the postoperative follow-up visits performed at the discretion of the surgeon.

Outcome measures

Surgical failure was based on IOP criteria, was defined as the primary outcome. The results of the Kaplan–Meier survival analysis with the two criteria were used to determine the success of the procedure. Surgical failure was defined as $a < 20\%$ reduction in the preoperative IOP or an IOP > 18 mmHg on two consecutive study visits, or when for a patient required a reoperation. However, as it has been reported that there are postoperative IOP fluctuations after trabeculotomy (5), IOPs that met the above criteria for up to 3 months after surgery were not considered to be surgical failures. The number of glaucoma medications used, the presence of any postoperative complications and the mean IOP were all considered to be secondary outcomes. For the mean number of glaucoma medications, 1 point was assigned for each glaucoma eye drop, while 2 points were assigned for the combination eye drops.

Statistical analysis

Statistical analyses were performed using JMP software (version 16; SAS Inc., Cary, NC). An independent *t*-test and a chi-square test were used to analyze the clinical backgrounds of the subjects. A chi-square test was also used to analyze the differences of the postoperative complications. Kaplan–Meier survival curves were used to analyze the probability of success, with the results compared

between the groups using a log-rank test. For continuous variables, the Anderson-Darling test was used to assess the distribution. Based on the results obtained, difference between preoperative and postoperative values were then assessed by either a paired *t*-test or Wilcoxon signed-rank test. All data are expressed as the mean ± standard deviation. *p* values less than 0.05 were defined as being statistically significant.

Results

In the μLOT-Phaco and iStent-Phaco groups in this study, evaluated 39 and 55 eyes, respectively. Evaluations of the age, gender, preoperative IOP, and number of preoperative glaucoma medications found no significant differences between both groups (Table 1). There were 18 eyes (47%) in the μLOT-Phaco group and 36 eyes (65%) in the iStent-Phaco group ($p = 0.08$) in patients with normal-tension glaucoma.

A significant decrease in the IOP was found in both groups when compared to the preoperative levels (Table 2). In the μLOT-Phaco group, the preoperative IOP level was 16.2 ± 4.4 mmHg, while at 3, 6 and 12 months postoperatively, the levels were 12.7 ± 2.9 mmHg, 12.5 ± 2.6 mmHg, and 13.2 ± 3.2 mmHg, respectively. In the iStent-Phaco group, the preoperative IOP level was 15.0 ± 3.8 mmHg, while at 3, 6 and 12 months postoperatively, the levels were 12.4 ± 2.6 mmHg, 12.5 ± 2.3 mmHg, and 13.2 ± 2.4 mmHg, respectively. Significant differences were observed in both groups between the preoperative and postoperative IOP levels at all patient visits. There were no significant differences observed at each visit with regard to the postoperative IOP reduction in these two groups ($p = 0.34$, 0.10, 0.23).

TABLE 1 Clinical characteristics at baseline.

	μLOT-Phaco	iStent-Phaco	*p* value
No. eyes	39	55	
Age (years)	72.5 ± 8.1	72.2 ± 9.8	0.88
Gender (M/F)	21/18	26/29	0.53
Preoperative IOP (mmHg)	16.2 ± 4.4	15.0 ± 3.8	0.18
No. IOP-lowering medication	2.2 ± 1.4	2.1 ± 1.4	0.68
Prostanoid receptor agonist	32	48	
β-blocker	20	27	
Carbonic anhydrase inhibitor	20	22	
α2 agonist	15	14	
ROCK inhibitor	5	4	
Axial length (mm)	25.1 ± 2.1	25.1 ± 2.6	0.93
Central cornea thickness (μm)	507.7 ± 37.7	510.5 ± 37.1	0.72
Visual field MD (dB)	−9.4 ± 6.7	−9.1 ± 7.0	0.87
Visual field PSD (dB)	8.1 ± 4.2	7.5 ± 4.4	0.39
Whole RNFL thickness (μm)	70.1 ± 12.9	70.4 ± 11.6	0.90
Whole GCC thickness (μm)	74.7 ± 14.7	79.6 ± 26.2	0.35

M, male; F, female; IOP, intraocular pressure; ROCK, rho-kinase; MD, mean deviation; PSD, pattern standard deviation; OCT, optical coherence tomography; RNFL, retinal nerve fiber layer; GCC, ganglion cell complex.

In both groups, there was a significant decrease postoperatively in the number of glaucoma medications (Table 3). In the μLOT-Phaco group, the number of preoperative medications was 2.2 ± 1.4, while at 3, 6 and 12 months postoperatively, it was 0.4 ± 1.0, 0.7 ± 1.1, and 0.6 ± 1.0, respectively. In the iStent-Phaco group, the number of preoperative medications was 2.1 ± 1.4, while at 3, 6, and 12 months postoperatively, it was 0.4 ± 0.8, 0.5 ± 0.8, and 0.5 ± 0.8, respectively. In the μLOT-Phaco group, the medication-free rate was 66.7% (26 eyes) and 68.0% (17 eyes) at 6 and 12 months postoperatively, respectively. In the iStent-Phaco group, the medication-free rate was 69.1% (38 eyes) and 69.4% (25 eyes) at 6 and 12 months postoperatively, respectively. The medication-free rate was similar in both groups ($p = 0.78$: 6 months; $p = 0.90$: 12 months). Table 4 shows the category for the postoperative IOP-lowering medications.

The Kaplan–Meier survival curves are seen in Figure 1 for the μLOT-Phaco and iStent-Phaco groups. At 6 and 12 months postoperatively, the survival in the μLOT-Phaco group was 55.3 and 48.4%, while in the iStent-Phaco group it was 45.5 and 45.5%, respectively. Between these two groups, there were no significant differences observed ($p = 0.38$).

Postoperative complications are shown in Table 5. Transient IOP elevation was defined as an elevation of the IOP to ≥30 mmHg within 2 months postoperatively. Hyphema was defined as the presence of the niveau formation. Hyphema was observed in 5 eyes (12.8%) in the μLOT-Phaco group, while in the iStent-Phaco group, 1 eye (1.8%) was found to have hyphema. Analysis indicated that significant differences were noted between the two groups ($p = 0.03$). Transient IOP elevation was observed in 2 eyes (5.1%) of the μLOT-Phaco group. In the μLOT-Phaco group and the iStent-Phaco group, transient IOP elevation occurred in 2 eyes (5.1%) and 2 eyes (3.6%), respectively ($p = 0.72$).

Discussion

This study examined μLOT-Phaco and iStent-Phaco, which are two MIGS technologies, in POAG patients by directly comparing relevant clinical data. Comparable surgical outcomes for both μLOT-Phaco and iStent-Phaco were observed at 12 months. During the 12-month follow-up period, there were significant reductions in both the IOP values and glaucoma medications in the μLOT-Phaco and iStent-Phaco groups.

Surgical outcomes have been evaluated between μLOT and iStent combined with cataract surgery (6, 7) and between goniotomy with Kahook Dual Blade (KDB) or iStent combined with cataract surgery (8) in two previous retrospective studies. Equal or less effectiveness was found for iStent procedures with cataract surgery as compared with μLOT or KDB procedures with cataract surgery. However, the IOP-lowering effects and complications of iStent inject W complications as compared to other MIGS procedures have yet to be definitively evaluated. Thus, this current examination of the

TABLE 2 Differences in postoperative IOP.

		μLOT-Phaco			iStent-Phaco		
	IOP (mmHg)	Change from baseline (%)	*P* value*	IOP (mmHg)	Change from baseline (%)	*P* value*	*P* value** (95% CI)
Baseline	16.2 ± 4.4			15.0 ± 3.8			
Month 3	12.7 ± 2.9	18.4 ± 21.0	<0.001	12.4 ± 2.6	14.4 ± 18.9	<0.001	0.34 (−4.1 ~ 12.6)
Month 6	12.5 ± 2.6	20.4 ± 18.7	<0.001	12.5 ± 2.3	13.8 ± 18.8	<0.001	0.10 (−1.3 ~ 14.5)
Month 12	13.2 ± 3.2	16.2 ± 18.3	<0.001	13.2 ± 2.4	10.0 ± 18.9	<0.001	0.23 (−3.9 ~ 16.3)

IOP, intraocular pressure; CI; confidence interval.
*Calculated using paired *t*-test for IOP between preoperative and postoperative values.
**Calculated using Student's *t*-test for the % changes from baseline at each visit time between the groups.

TABLE 3 Differences postoperative number of glaucoma medication.

	μLOT-Phaco		iStent-Phaco		
	Number of medications	*P* value*	Number of medications	*P* value*	*P* value**(95% CI)
Baseline	2.2 ± 1.4		2.1 ± 1.4		0.68 (−0.46 ~ 0.71)
Month 3	0.4 ± 1.0	<0.001	0.4 ± 0.8	<0.001	0.98 (−0.35 ~ 0.36)
Month 6	0.7 ± 1.1	<0.001	0.5 ± 0.8	<0.001	0.22 (−0.30 ~ 0.77)
Month 12	0.6 ± 1.0	<0.001	0.5 ± 0.8	<0.001	0.51 (−0.31 ~ 0.62)

IOP, intraocular pressure; CI, confidence interval.
*Calculated using Wilcoxon signed-ranks test for number of medications between preoperative and postoperative values.
**Calculated using Student's *t*-test for the % changes from baseline at each visit time between the groups.

TABLE 4 Postoperative IOP-lowering medication.

	μLOT-Phaco	iStent-Phaco
Prostanoid receptor agonist	10	15
β-blocker	7	5
Carbonic anhydrase inhibitor	4	5
α2 agonist	4	2
ROCK inhibitor	1	0

IOP, intraocular pressure; ROCK, rho-kinase.

efficacy of combined phacoemulsification with μLOT and iStent inject W appears to be the first study to compare these procedures. We recently reported that comparable surgical outcomes were found for the use of μLOT and KDB in the combination with cataract surgery (9). Therefore, we assume that comparable surgical outcomes may be obtained for the use of these three different instruments.

When the higher preoperative IOP groups were compared to the lower preoperative IOP groups, a large %IOP reduction was achieved when using the μLOT procedure (10). As our current study found the preoperative IOPs in the μLOT-Phaco and iStent-Phaco groups to be 16.2 mmHg and 15.0 mmHg, respectively, it appears that it would be better to evaluate our current results in line with the similar preoperative IOPs reported in previous papers. In previous studies on open-angle glaucoma patients who underwent the iStent-Phaco procedure, patients who had baseline IOPs of 17.3 mmHg or 17.0 mmHg showed reductions of the IOP of 26.6% or 17.8%, respectively (11, 12). Moreover, these studies reported values of 12.7 mmHg or 14.0 mmHg for the final IOPs. In contrast, procedures in open-angle glaucoma patients who underwent the μLOT-Phaco procedure were found to have a baseline IOP of 16.7 mmHg followed by a 17.8% reduction in the IOP reduction and with a final IOP of 13.6 mmHg (7). The IOP reduction rate and final IOP in the iStent-Phaco and μLOT-Phaco groups in our study were 10.0% and 13.2 mmHg, and 16.2% and 13.2 mmHg, respectively. It should be noted that as compared to the previous study, since we found a lower baseline IOP, this resulted in a tendency for a lower IOP reduction rate in our current study. Even so, as compared to the other previous studies, we found a similar final IOP.

In the μLOT-Phaco group, we found that the hyphema was significantly higher than that observed in the iStent-Phaco group in our current study. Moreover, on postoperative days 1 and 2, the μLOT-Phaco group exhibited a higher postoperative hyphema score as compared to the iStent-Phaco group (13). It has also been reported that there was a significantly higher frequency of layered hyphema in the μLOT group as compared to the iStent group (6). It should be noted, however, that in the current study, the incision of the inner wall of Schlemm's canal produced by μLOT was approximately one third of the circumference. In contrast, this was a much wider range of incision as compared to that observed for the iStent inject W implantation.

In our current study there were several limitations including the fact that this was a retrospective study. As a result, the assignments of subjects to the treatment groups were not random. Furthermore,

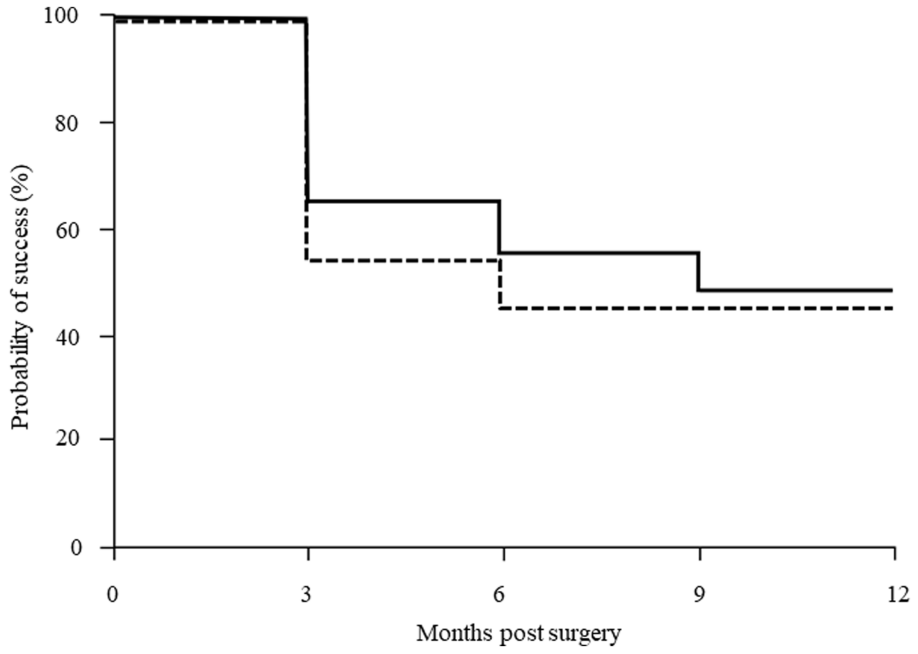

FIGURE 1
Kaplan–Meier survival analysis success rate of IOP control after μLOT and iStent in combination with phacoemulsification. There were no significant differences observed between two groups (p = 0.38, log-rank test). Solid line: μLOT-Phaco group, dashed line: iStent-Phaco group.

TABLE 5 Postoperative complications.

	μLOT-Phaco	iStent-Phaco	*P* value
Hyphema with niveau	5 (12.8%)	1 (1.8%)	0.03
Transient IOP elevation ≥30 mmHg	2 (5.1%)	2 (3.6%)	0.72

IOP, intraocular pressure.

we utilized our routine clinical practice to collect the outcome data. It should also be noted that it was up to the surgeon's discretion to prescribe the IOP-lowering medications at the time of the postoperative follow-up visits. Therefore, to ensure that there is a better collection of data and rigorous comparative evidence, it will be necessary to perform a further randomized and prospective study. Another limitation that needs to be taken into consideration is that there was a relatively low preoperative IOP. Many of the patients that were included in the study had a relatively medically controlled IOP due to being scheduled for the μLOT-Phaco or iStent-Phaco procedures. As a result, there were larger changes in the %IOP reduction in higher preoperative IOP groups when compared to the lower preoperative IOP groups (10). Although it has been recommended that the efficacy of glaucoma surgery be defined based on the combined use of the absolute IOP levels and %IOP reduction (14), the merit of MIGS might be underestimated based on these definitions, especially in eyes having a low preoperative IOP that then undergo surgery.

In conclusion, utilization of the μLOT and iStent inject W procedures resulted in comparable surgical outcomes. Moreover, significant reductions in the IOP were observed when these were combined with cataract surgery, with these POAG patients also showing a reduction in the number of glaucoma medications.

Data availability statement

The raw data supporting the conclusions of this article will be made available by the authors, without undue reservation.

Ethics statement

The studies involving humans were approved by the Institutional Review Board of the Hiroshima University. The studies were conducted in accordance with the local legislation and institutional requirements. The participants provided their written informed consent to participate in this study.

Author contributions

HOn: Writing – original draft, Data curation, Formal analysis, Investigation. KH: Conceptualization, Methodology, Project administration, Writing – original draft, Writing – review & editing. KN: Data curation, Writing – original draft. SM: Data curation, Writing – original draft. HH: Data curation, Writing – original draft. HM: Data curation, Writing – original draft. NO: Project administration, Writing – original draft. KT: Data curation, Writing – original draft. HOk: Data curation, Writing – original draft. YK: Writing – review & editing.

Funding

The author(s) declare that no financial support was received for the research, authorship, and/or publication of this article.

Conflict of interest

The authors declare that the research was conducted in the absence of any commercial or financial relationships that could be construed as a potential conflict of interest.

The author(s) declared that they were an editorial board member of Frontiers, at the time of submission. This had no impact on the peer review process and the final decision.

Publisher's note

References

1. Quigley HA, Broman AT. The number of people with glaucoma worldwide in 2010 and 2020. *Br J Ophthalmol*. (2006) 90:262–7. doi: 10.1136/bjo.2005.081224

2. Chauhan BC, Mikelberg FS, Balaszi AG, LeBlanc RP, Lesk MR, Trope GE, et al. Canadian Glaucoma study: 2. Risk factors for the progression of open-angle glaucoma. *Arch Ophthalmol*. (2008) 126:1030–6. doi: 10.1001/archopht.126.8.1030

3. Heijl A, Leske MC, Bengtsson B, Hyman L, Bengtsson B, Hussein M, et al. Reduction of intraocular pressure and glaucoma progression: results from the early manifest Glaucoma trial. *Arch Ophthalmol*. (2002) 120:1268–79. doi: 10.1001/archopht.120.10.1268

4. Grant WM. Experimental aqueous perfusion in enucleated human eyes. *Arch Ophthalmol*. (1963) 69:783–801. doi: 10.1001/archopht.1963.00960040789022

5. Tanihara H, Negi A, Akimoto M, Terauchi H, Okudaira A, Kozaki J, et al. Surgical effects of trabeculotomy ab externo on adult eyes with primary open angle glaucoma and psedoexfoliaion syndrome. *Arch Ophthalmol*. (1993) 111:1653–61. doi: 10.1001/archopht.1993.01090120075025

6. Takayanagi Y, Ichioka S, Ishida A, Tsutsui A, Tanito M. Fellow-eye comparison between phaco-microhook ab-interno trabeculotomy and phaco-iStent trabecular micro^bypass stent. *J Clin Med*. (2021) 10:2129. doi: 10.3390/jcm10102129

7. Tokuda N, Kitaoka Y, Tsukamoto A, Toyoda Y, Yamada Y, Sase K, et al. Comparison of minimally invasive glaucoma surgery with trabecular micro-bypass stent and microhook ab interno trabeculotomy performed in conjunction with cataract surgery. *Int J Ophthalmol*. (2022) 15:1082–8. doi: 10.18240/ijo.2022.07.07

8. Iwasaki K, Takamura Y, Orii Y, Arimura S, Inatani M. Performance of glaucoma operations with Kahook dual blade or iStent combined with phacoemulsification in Japanese open angle glaucoma patients. *Int J Ophthalmol*. (2020) 13:941–5. doi: 10.18240/ijo.2020.06.13

9. Okada N, Hirooka K, Onoe H, Okumichi H, Kiuchi Y. Comparison of mid-term outcomes between microhook ab interno trabeculotomy and goniotomy with the Kahook dual blade. *J Clin Med*. (2023) 12:558. doi: 10.3390/jcm12020558

10. Tanito M, Sugihara K, Tsutsui A, Hara K, Manabe K, Matsuoka Y. Effects of preoperative intraocular pressure levels on surgical results of microhook ab interno trabeculotomy. *J Clin Med*. (2021) 10:3327. doi: 10.3390/jcm10153327

11. Guedes RAP, Gravina DM, Lake JC, Guedes VMP, Chaoubah A. Intermediate results of iStent or iStent inject implantation combined with cataract surgery in a real-world setting: a longitudinal retrospective study. *Ophthalmol Ther*. (2019) 8:87–100. doi: 10.1007/s40123-019-0166-x

12. Salimi A, Lapointe J, Harasymowycz P. One-year outcomes of second-generation trabecular micro-bypass stent (iStent inject) implantation with cataract surgery in different glaucoma subtypes and severities. *Ophthalmol Ther*. (2019) 8:563–75. doi: 10.1007/s40123-019-00214-z

13. Ishida A, Ichioka S, Takayanagi Y, Tsutsui A, Manabe K, Tanito M. Comparison of postoperative hyphemas between microhook ab interno trabeculotomy and iStent using a new hyphema scoring system. *J Clin Med*. (2021) 10:5541. doi: 10.3390/jcm10235541

14. Heuer DK, Barton K, Grehn F, Fhaaraway T, Sherwood M. Consensus of definitions of success In: TM Shaarawy, MB Sherwood and F Grehn, editors. *Guidelines on design and reporting of surgical trials*. Amsterdam, Netherlands: Kugler Publications (2009). 15–24.

frontiers | Frontiers in Medicine

TYPE Original Research
PUBLISHED 23 October 2023
DOI 10.3389/fmed.2023.1271897

OPEN ACCESS

EDITED BY
Georgios D. Panos,
Nottingham University Hospitals NHS Trust, United Kingdom

REVIEWED BY
Yinghong Ji,
Fudan University, China
Liangbo Shen,
University of California, San Francisco, United States
Qianying Gao,
Vesber Vitreous Institute, China

*CORRESPONDENCE
Yan Cui
✉ qlcyteam@163.com

†These authors have contributed equally to this work and share first authorship

RECEIVED 03 August 2023
ACCEPTED 02 October 2023
PUBLISHED 23 October 2023

CITATION
Wang L, Wang X, Yang X, Si Y, Wu J and Cui Y (2023) Intraocular lens power calculation for silicone oil-dependent eyes.
Front. Med. 10:1271897.
doi: 10.3389/fmed.2023.1271897

Intraocular lens power calculation for silicone oil-dependent eyes

Leyi Wang[1†], Xin Wang[1,2†], Xuepeng Yang[1], Yuanyuan Si[1], Jiayin Wu[1] and Yan Cui[1*]

[1]Department of Ophthalmology, Qilu Hospital of Shandong University, Jinan, Shandong, China, [2]Affiliated Eye Hospital of Shandong University of TCM, Jinan, Shandong, China

Background: Silicone oil tamponade is widely used in vitreoretinal surgery. In some cases, silicone oil may not be extracted for a long time or even permanently and is referred to as silicone oil-dependent eyes. In this study, we aimed to deduce a theoretical formula for calculating intraocular lens power for silicone oil-dependent eyes and compare it with clinical findings.

Methods: A theoretical formula was deduced using strict geometric optical principles and the Gullstrand simplified eye model. The preoperative and postoperative refractive statuses of patients with silicone oil-dependent eyes who underwent intraocular lens implantation were studied (Group A, $n = 13$). To further test our derived theoretical formula, patients with silicone oil tamponade and first-stage intraocular lens implantation were included (Group B, $n = 19$). In total, 32 patients (32 eyes) were included in the study.

Results: In group A, the calculated intraocular lens power based on our formula was 24.96 ± 3.29 diopters (D), and the actual refraction of the patients was 24.02 ± 4.14D. In group B, the theoretical intraocular lens power was 23.10 ± 3.08D, and the clinical intraocular lens power was 22.84 ± 3.42D. There was no significant difference between the theoretical and clinical refractive powers, and the intraclass correlation coefficient was 0.771 for group A and 0.811 for group B (both $p \leq 0.001$). The mean absolute error for silicone oil-dependent eyes of the formula was 1.66 ± 2.09D. After excluding data for two patients with a flat cornea (corneal refractive power < 42D), the mean absolute error decreased to 0.83 ± 0.62D.

Conclusion: A strong correlation between the theoretical and clinical intraocular lens powers was observed, and the formula we deduced can be used to calculate the intraocular lens power for silicone oil-dependent eyes. This formula will help clinicians select a more appropriate intraocular lens for patients with silicone oil-dependent eyes, especially when the corneal refractive power is ≥42D.

KEYWORDS

intraocular lens power, intraocular fillers, silicone oil, theoretical formula, vitreoretinal surgery

1. Introduction

Silicone oil (SO) is one of the most important intraocular fillers used in vitreoretinal surgery (1), which is usually removed 3–6 months after tamponade (2). Retention of SO may lead to complications, including glaucoma, cataracts, band keratopathy, emulsification of SO, and possible neural toxicity (3, 4). However, there is still a distinct group of patients in real-life

practice who, for various reasons, must live with long-term or even permanent SO tamponade. In such patients, retinal re-detachments, severe proliferative vitreoretinopathy (PVR), repeated vitreous hemorrhage, or continually low intraocular pressure occur after SO removal (5, 6). These are called SO-dependent eyes (7).

The intraocular lens (IOL) power calculation for silicon oil-filled eyes has been evaluated. The refractive change associated with SO tamponade in pseudophakic eyes has been studied previously (8), and the ocular biometric parameters in silicone oil-filled eyes have been investigated (9, 10). Recently, a theoretical approach to determining how specific IOL powers would change when silicone oil is used in the vitreous chamber was published (11). However, there is no available formula for calculating the IOL power in SO-dependent eyes. In this study, we aimed to derive a theoretical formula for calculating IOL power according to strict geometric optical principles and compare the calculated power with the clinically determined power.

2. Materials and methods

In this retrospective, single-center, observational case series, we aimed to deduce a theoretical formula for IOL calculation in SO-dependent eyes. This study adheres to the principles of the Declaration of Helsinki and was approved by the ethics committee of Qilu Hospital of Shandong University (reference number: 2019052). All patients signed an informed consent form and received no stipend.

2.1. Theoretical formula deduction

The Gullstrand simplified eye was used to derive the theoretical formula. In this model, the refractive system of the eye is considered a compound system consisting of two coaxially thin lenses: the cornea and a crystalline lens that focus parallel incident light on the retina. The refractive indices of air, aqueous humor, and SO are 1(n_a), 1.336(n_{ah}), and 1.403(n_{SO}), respectively.

The convex lens power formula is as follows:

$$F = \frac{n}{f},$$

where F is the refractive power of a convex lens, n is the refractive index (RI) of the substance containing the lens, and f is the focal length of the lens.

The total refractive power of two coaxial thin lenses in close proximity is calculated as follows:

$$F = F_1 + F_2,$$

where F is the total refractive power and F_1/F_2 is the refractive power of the two lenses.

For the cornea and the crystalline lens separated by a certain distance, we consider the cornea as a thin lens that has moved for a distance d in the direction of the crystalline lens in the aqueous humor to calculate the total power of the two coaxial lenses. The equivalent refractive power of the cornea after movement is given as follows:

$$F_e = \frac{n_{ah} * F_c}{n_{ah} - d * F_c},$$

where F_e is the equivalent refractive power of the cornea after movement, n_{ah} is the RI of aqueous humor, F_c is the original refractive power of the cornea, and d is the distance between the posterior corneal vertex and the optical plane of the IOL on the visual axis.

The 'd' above is also called the effective lens position (ELP) (12), calculated using the Haigis formula: (13)

$$d = ELP = a0 + a1 * AC + a2 * AL,$$

where AC is the preoperative anterior chamber depth; AL is the ocular axial length; and a0, a1, and a2 are the constants for the implanted IOLs. The lens constants were optimized for each type of IOL (available at http://ocusoft.de/ulib/c1.htm, accessed on 18 July 2023). Wang-Koch adjustment of AL was performed for patients with an AL of >26 mm (14).

In SO-dependent eyes, the total refractive power of a pseudophakic eye required to focus parallel incident light on the retina is calculated as follows:

$$F_0 = F_e + F_{IOL} = \frac{n_{SO}}{AL - ELP},$$

where F_0 is the total refractive power of a pseudophakic eye, F_e is the equivalent refractive power of the cornea after moving a distance d in the direction of the crystalline lens in aqueous humor, F_{IOL} is the refractive power of implanted IOL, n_{SO} is the RI of SO, AL is the ocular axial length, and d is the distance between the posterior corneal vertex and IOL posterior surface.

Thus, the refractive power of an implanted IOL is calculated as follows:

$$F_{IOL} = \frac{n_{SO}}{AL - ELP} - Fe = \frac{n_{SO}}{AL - ELP} - \frac{n_{ah} * F_c}{n_{ah} - ELP * F_c}$$

where n_{ah} is the RI of aqueous humor and F_c is the original refractive power of the cornea.

When substituting the constants with some variables ($n_{SO} = 1.403$, $n_{ah} = 1.336$), we obtain the following formula (refractive power is in diopters and length is in meters):

$$F_{IOL} = \frac{1.403}{AL - ELP} - \frac{1.336 * F_c}{1.336 - ELP * F_c}$$

From this formula, we can infer that the IOL power for SO-dependent eyes theoretically depends on ocular axial length, corneal radius of curvature, the refractive power of the cornea, and the IOL constant.

Abbreviations: SO, Silicone oil; PVR, Proliferative vitreoretinopathy; IOL, Intraocular lens; RI, Refractive index; ELP, Effective lens position; PVC, Polypoidal choroidal vasculopathy; RPE, Retinal pigment epithelium; RRD, Rhegmatogenous retinal detachment; AL, Axial length; AC, Anterior chamber depth; FC, Refractive power of the cornea; BCVA, Best-corrected visual acuity; D, Diopters; MAE, Mean absolute error; VA, Visual acuity; PDR, Proliferative diabetic retinopathy; ACD, Anterior chamber depth.

2.2. Clinical observations

Uneventful phacoemulsification, vitrectomy, SO tamponade, and IOL implantation were performed by an experienced surgeon in all patients. The exclusion criteria were as follows: having an unstable fundus (such as macular edema, macular pucker, retinal hemorrhage, or macular hole after SO extraction), SO emulsification obstructing optometric examinations, incomplete filling of the vitreous cavity, posterior capsule rupture, corneal opacity, and incomplete clinical data. A vitrectomy was performed using a standard 3-port 23-G pars plana incision. All incisions were sutured after surgery. To calculate the IOL refractive power required for the patients to achieve emmetropia, the postoperative best spectacle correction (spherical lens) was added to the refractive power of the implanted IOL. Ocular axial length (AL), preoperative anterior chamber (AC) depth, and refractive power of the cornea (F_C) were measured using partial coherence interferometry (IOL Master 5.5xp or IOLMater 700; Carl Zeiss Meditec, Jena, Germany). Six types of IOLs [Rayner (Rayner, Worthing, United Kingdom); Akreos Adapt (Bausch + Lomb, Laval, Canada); 868UV (USIOL, Lexington, KY); Aspira-aA (HumanOptics, Erlangen, Germany); Aaren pal (Aaren Scientific, CA, United States); Tecnis PCB00 (Johnson & Johnson Surgical Vision, Irvine, CA, United States)] were implanted, and all patients were injected with SO (Oxane® 5,700; Bausch + Lomb). Postoperative best-corrected visual acuity (BCVA) and refraction results were collected at least 1 month (1.5 months to 4.5 years) after surgery.

2.3. Statistic analysis

The normal distribution was assessed with the Shapiro–Wilk test, and all data conformed to the normal distribution. Then the paired *t*-test was used for comparison, and correlation analysis was adopted using the intraclass correlation coefficient (ICC). Statistical significance was set at a value of p of <0.05. All analyses were performed using SPSS 25 software (version 25.0; IBM, Armonk, NY).

3. Results

In total, 32 patients (32 eyes) who received care between January 2018 and July 2023 at the Ophthalmology Department of Qilu Hospital of Shandong University were enrolled in this study (21 male and 11 female patients). The refractive power of the implanted IOL ranged from 13 diopters (D) to 31 D.

The SO-dependent group (Group A) included 13 patients (7 male and 6 female patients), and SO cannot be removed because of poor retinal or poor general conditions, or both. Specifically, four patients were diagnosed with polypoidal choroidal vasculopathy (PCV), which characteristically presents as a sub-retinal pigment epithelium (RPE) lesion (15). RPE destruction was also observed in patients with PCV, leading to suboptimal attachment of the neurosensory epithelium and RPE (16). To prevent any further complications and instability of the neuroepithelium, massive old sub-neurosensory-retinal hemorrhage in these four patients prompted the retention of the SO. Another four patients initially underwent vitrectomy with SO tamponade for rhegmatogenous retinal detachment (RRD). Among them, three patients subsequently developed superficial detachment of the peripheral retina, and the fourth patient, who had concurrent renal failure requiring hemodialysis treatment, had a significantly reduced risk of retinal hemorrhage due to the retained SO. Three patients presented with macular holes caused by fibrovascular proliferation of proliferative diabetic retinopathy (PDR) (17). In these cases, retinal detachment at the posterior pole likely or actually occurred once SO was removed. Hence, to prevent further complications, the SO was retained or refilled. The last two patients suffered severe retinal necrosis and repeated retinal detachment due to herpes virus infection. It has been reported that 30% of the patients who undergo vitrectomy with SO tamponade due to RRD following acute retinal necrosis develop recurrent retinal detachment after SO removal (18). To maximize the preservation of the patients' surviving retinal function and vision, the SO was not removed. In fact, SO removal was attempted for a substantial proportion of SO-dependent patients in this study, but the SO had to be refilled in the same way or in a re-operation. The clinical data of the patients are described in Table 1.

In group A, the mean preoperative AC was 2.94 ± 0.31 mm, the mean F_C was 43.91 ± 1.76 mm, and the mean AL was 22.82 ± 1.27 mm. The theoretical IOL refractive power was 24.96 ± 3.29 D. The clinical IOL power required by the patients to achieve emmetropia was 24.02 ± 4.14 D. There was no significant difference between the theoretical and clinical IOL powers (p = 0.205, paired *t*-test; Figure 1A), and the theoretical and clinical IOL powers were strongly correlated (ICC = 0.771, 95% CI: 0.405–0.924, p = 0.001; Figure 2A). For the theoretical formula, a predicted IOL power error of <0.5 D was found in four eyes (30.77%), 1.0–1.5 D in five eyes (38.46%), 1.5–2.0 D in two eyes (15.38%), and ≥ 2.0 D in two eyes (15.38%). The mean absolute error (MAE) for the formula was 1.66 ± 2.09D. After excluding data from the two eyes with a predicted IOL power error ≥ of 2.0 D, the MAE for the formula was 0.83 ± 0.62D.

To further test our derived theoretical formula, which is designed for IOL calculation in eyes with vitreous cavities filled with SO, patients with SO tamponade and first-stage IOL implantation (implantation of the IOL during the same procedure in which vitrectomy, SO filling, and cataract extraction were performed) were included as group B. The choice of filling the vitreous cavity with SO instead of gas was made by the surgeon during the operation according to the condition of the fundus retina. The co-existence of SO and IOL in these eyes was similar to that in the SO-dependent eyes, although the application of SO in group B was eventually stopped. While the postoperative refraction data of group B for the derivation of the formula in our study were collected before the SO was removed, the actual IOL power implanted in group B was based on the recommendation of the IOL Master with the eye status of phakic; in other words, the IOL power was intended to be appropriate after the subsequent SO removal and filling of the vitreous cavity with water. The clinical data of these patients are described in Table 2. Group B included 19 patients (14 male and 5 female patients). In group B, the AC, FC, and AL were 3.03 ± 0.38 mm, 43.64 ± 1.35 mm, and 23.54 ± 1.11 mm, respectively. The theoretical IOL power was 23.10 ± 3.08 D, and the clinical IOL power was 22.84 ± 3.42 D. There was no significant difference between the theoretical and clinical IOL powers (p = 0.577, paired *t*-test; Figure 1B), and the theoretical and clinical IOL powers were strongly correlated (ICC = 0.811, 95% CI: 0.573–0.923, p < 0.001; Figure 2B).

In group A, the visual acuity (VA) was improved from 1.62 ± 0.29 to 1.25 ± 0.39 logMAR after the best refractive correction before IOL

TABLE 1 Data of patients with silicone oil-dependent eyes.

Number			Axial length, mm	Average K, D	Anterior chamber depth, mm	IOL implanted, D	Actual postoperative refraction (spherical), D	Theoretical IOL power	Pre-existing conditions	Visual acuity, logMAR		
	Age range	sex								Preop uncorrected	Preop, corrected	Postop, corrected
1	50s	M	23.91	40.89	2.74	26	−7.0	25.23	PCV	1.40	0.92	0.7
2	70s	F	21.83	46.46	3.01	31	−6.50	26.06	RRD	1.50	1	0.82
3	70s	F	23.98	43.23	3.24	28	−6.25	21.7	PCV	1.40	1.22	0.92
4	70s	M	24.7	41.6	2.95	17	−1.50	21.66	RRD	1.40	1.4	0.6
5	40s	M	22.61	44.35	3.34	18	+8.0	25.99	ARN	2.00	2	0.82
6	70s	F	21.01	45.83	2.68	27.5	+3.0	30.38	RRD	1.22	0.82	0.82
7	20s	F	22.35	42.98	3.04	26	+2.50	28.70	ARN	1.80	1	0.82
8	50s	F	20.37	46.31	3.27	23.5	+4	26.43	PDR	1.60	1.1	0.9
9	60s	F	22.84	42.51	2.38	25	−0.5	26.19	RRD	1.80	1	0.8
10	50s	M	23.78	44.86	2.54	20	+1.0	19.68	PDR	2.00	1.8	1.4
11	60s	M	23.92	42.85	3.27	20.5	+3	22.47	PCV	1.20	0.8	0.5
12	80s	M	21.92	44.07	3.13	23	+4.5	28.54	PCV	1.90	1.6	1.0
13	60s	M	23.4	44.95	2.69	21	+1.5	21.45	PDR	1.90	1.6	1.0

M, male; F, female; K, keratometry; D, diopters; IOL, intraocular lens; PCV, polypoidal choroidal vasculopathy; RRD, rhegmatogenous retinal detachment; ARN, acute retinal necrosis; PDR, proliferative diabetic retinopathy; op, operation.

10.3389/fmed.2023.1271897

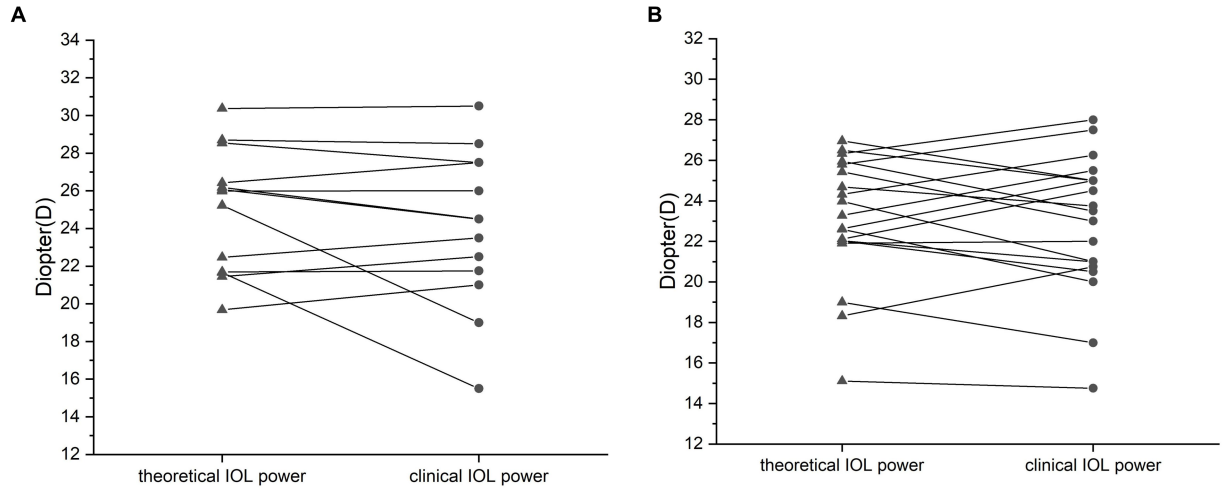

FIGURE 1
Comparison of the calculated and clinical intraocular lens (IOL) refractive powers for the silicone oil (SO)-dependent group **(A)** and the SO tamponade and first-stage IOL implantation group **(B)**. No significant difference between the theoretical and clinical refractive powers was observed. Data are expressed as the mean ± standard deviation. Group A, $p = 0.156$; group B, $p = 0.11$ (paired *t*-test).

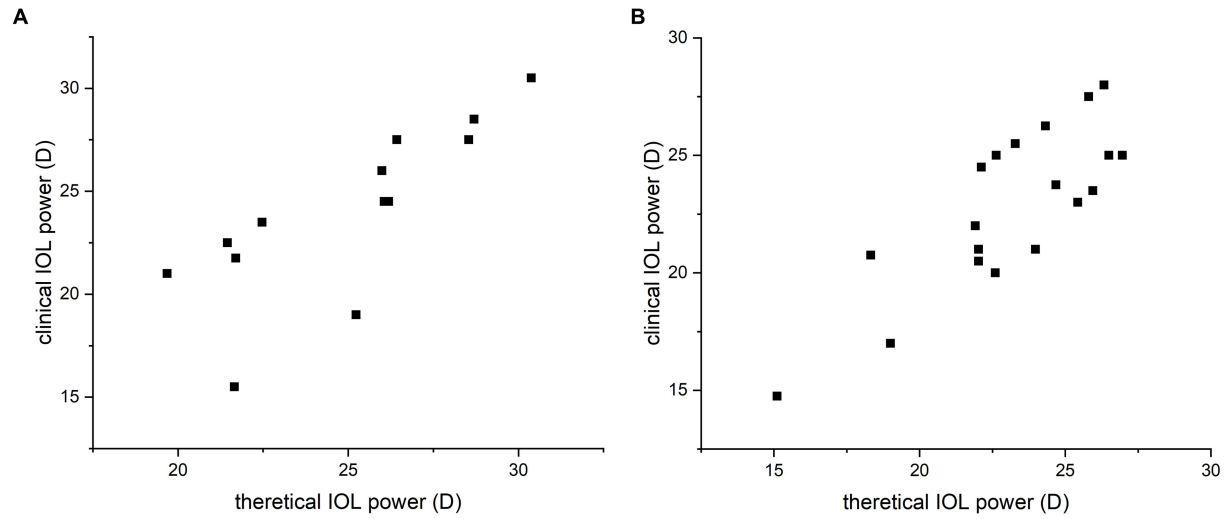

FIGURE 2
Correlation analysis of the calculated and clinical intraocular lens (IOL) refractive powers for the silicone oil (SO)-dependent group **(A)** and the SO tamponade and first-stage IOL implantation group **(B)**. Strong correlation between the theoretical and clinical refractive powers was observed by Spearman's correlation test. Data are expressed as the mean ± standard deviation. Group A, ICC = 0.771, 95% CI: 0.405–0.924, $p = 0.001$; group B, ICC = 0.811, 95% CI: 0.573–0.923, $p < 0.001$.

implantation ($p < 0.001$, paired *t*-test; Figure 3A). After IOL implantation, the BCVA was further improved to 0.85 ± 0.22 logMAR ($p = 0.001$, paired *t*-test; Figure 3B).

4. Discussion

SO-dependent eyes are relatively rare in clinical practice. When SO cannot be removed for various reasons, such as poor retinal condition, poor systemic condition, or both, as in this study, but vision can be improved by spectacle correction, an IOL should be implanted to restore functional VA. The calculation method for the power of the IOLs that should be implanted in these patients has become a real challenge. Our previous attempts based on clinical experience (adding 3D–5D to the IOL power calculated by the formulas implemented in the IOL Master) have been unsuccessful, with a mean refractive error after IOL implantation of 3.79 ± 2.48 D (highest: 8 D, Table 1), creating physiological and psychological distress for both patients and doctors.

However, to our knowledge, the IOL power calculation of existing IOL power formulas, such as SRK-T (19), Haigis (13), and Barrett Universal II (20), is based on the premise that the vitreous cavity is filled with either vitreous or water. Since the refractive indices (RIs) of vitreous and water are the same (1.336), the RIs of the refractive media in contact with the anterior and posterior surfaces of the IOL, which

TABLE 2 Data of patients in group B.

Number	Age	Sex	Axial length, mm	Average K, D	Anterior chamber depth, mm	IOL implanted, D	Actual postoperative refraction (spherical), D	Theoretical IOL power
1	M	70s	23.31	44.61	2.91	20.5	4	22.12
2	M	70s	24.03	42.70	3.38	21	5	22.63
3	M	60s	23.73	43.72	3.22	21	−0.5	22.02
4	M	50s	24.89	43.2	3.51	15	2	18.998
5	F	50s	21.77	45.52	2.31	25	3	26.33
6	F	60s	22.29	47.44	2.65	21.5	0.5	22.02
7	M	50s	23.15	42.32	3.76	22	3	26.5
8	F	50s	23.53	42.59	2.85	22.5	3.75	24.32
9	F	70s	23.56	43.86	3.18	20	0	22.6
10	M	50s	23	43.02	3.06	23	4.5	25.8
11	M	40s	26.53	42.2	3.45	13	1.75	15.11
12	M	60s	22.8	43.47	2.81	24	−0.5	25.95
13	M	60s	24.42	42.24	3.22	21	2.5	21.91
14	F	40s	22.29	45.74	3.15	19.5	1.25	24.68
15	M	60s	22.63	43.64	2.31	22.5	0	25.43
16	M	50s	25.03	43.09	3.27	23	1.75	18.32
17	M	50s	23.43	43.37	2.93	19	3.5	23.28
18	M	70s	23.67	43.58	2.87	22	−1	23.98
19	M	50s	23.16	42.91	2.76	22	1	26.96

M, male; F, female; K, keratometry; D, diopters; IOL, intraocular lens.

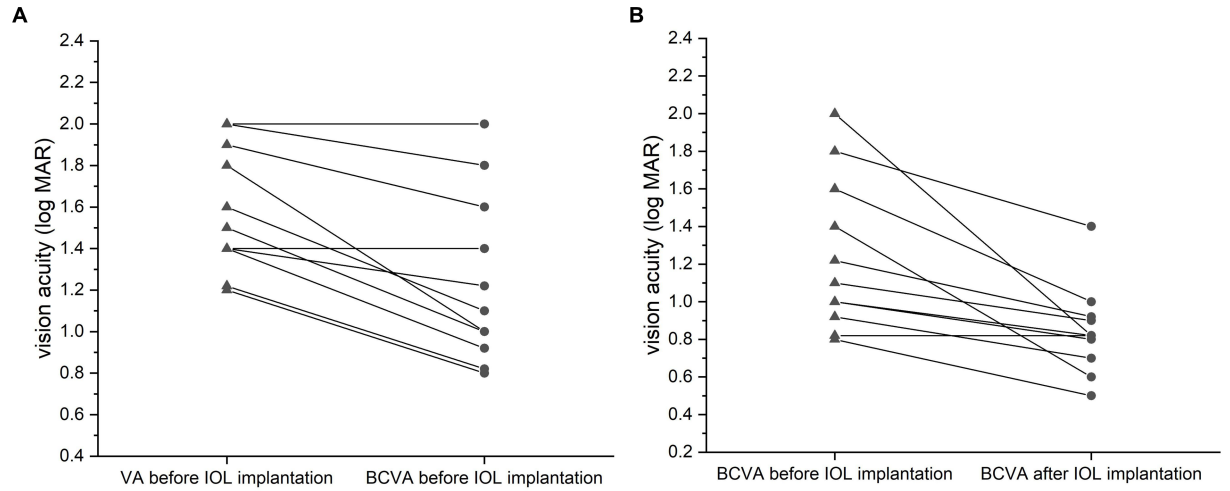

FIGURE 3
Comparison of vision acuities (VA, logMAR) for the silicone oil (SO)-dependent eyes. VA was improved after the best refractive correction before IOL implantation (**A**, $p = 0.035$, paired *t*-test). The best-corrected VA (BCVA) was further improved after the surgery relative to the preoperative BCVA (**B**, $p = 0.043$, paired *t*-test). Data are expressed as the mean ± standard deviation.

are aqueous water and vitreous, respectively, are equal. None of the available IOL power calculation formulas provide a model for the SO-dependent eyes; even when the eye status was set to "silicone filled eye" using the formulas implemented in the IOL Master or other biometer, the calculated IOL power was intended to be appropriate after the SO had been removed and the vitreous cavity filled with water. Therefore, the IOL power for SO-dependent eyes cannot be calculated using the existing formulas. Recently, Atchison et al. applied a theoretical approach to determine how specified IOL powers should change in SO-filled eyes, but it was not clinically proven and

could only be used when complete information about the IOL was released (11), which is uncommon in clinical practice. This is the first study to derive a theoretical formula for calculating the refractive power for IOL implantation in SO-dependent eyes directly using open-access IOL constants. The variables used in the formula, including AL, AC, and F_C, can be easily obtained using the IOL Master (Carl Zeiss Meditec), ultrasonic A-scan, or corneal topography in clinics.

Numerous studies have examined the changes in biometric values of SO-filled eyes. One study found that AL measurement using optical biometry is more accurate than acoustic biometry in SO-filled eyes (9). Liu et al. reported that patients who received vitrectomy with SO tamponade for RRD repair had AL approximately 0.48 mm longer than in RRD status eyes after a mean 4.85-month duration of SO tamponade (21). In the present study, the AL data we used were obtained from the IOL Master with the status of SO-filled eyes. To address potential overestimation by the IOL Master for the AL in long eyes (22), our study applied the Wang-Koch adjustment to the AL of patients with an AL of >26 mm. Regarding anterior chamber depth (ACD), it has been reported that the increase in ACD in SO-injected patients after pars plana vitrectomy returns to preoperative values within 1 month of surgery (23).

To improve the accuracy of the calculation, we replaced the anterior chamber depth with ELP. The ELP algorithm is derived from the Haigis formula, which displays outstanding performance in vitrectomized eyes with optimized constants when predicting the accuracy of implanted IOL power (24). A strong correlation between the theoretical IOL refractive power and the clinical power for SO-dependent eyes was observed. The accuracy of the powers calculated using our formula was further confirmed in patients with SO tamponade and first-stage IOL implantation.

The IOL power calculation for SO-filled eyes has always posed a challenge for ophthalmologists (25). Even when employing optical biometry and correct calculation formulas, only a third of SO-filled eyes might achieve ±1.0 D of the target refraction after SO removal (26). Among the different types of SO-filled eyes, SO-dependent eyes present the most complex fundus conditions and structural damage. However, our study found that the predicted IOL power error was below 0.5D in 30.77% and below 2D in 84.62% of the SO-dependent eyes. These results indicate that our formula was relatively reliable and could instill confidence in ophthalmologists when selecting an IOL for a SO-dependent patient.

Interestingly, we observed that a predicted IOL power error of >2 D was found in two eyes, with both errors being extremely high: 6.23D and 6.16D, respectively (Table 1). These two patients shared a common characteristic of a flat cornea (average K < 42D). Upon excluding the data from these two patients, the MAE decreased from 1.66 ± 2.09D to 0.83 ± 0.62D. This phenomenon may be correlated with the relatively inaccurate performance of the Haigis formula in IOL calculation for eyes with flat keratometry (27). It is essential to note that the sample size of SO-dependent eyes with a flat cornea ($n = 2$) was limited, which hinders us from drawing statistically significant conclusions about the accuracy of the formula derived in this study. However, it still provides a valuable indication of the formula's applicability, necessitating further investigations to better understand its scope of application.

When performing cataract extraction and posterior chamber IOL implantation in SO-dependent eyes, the buoyancy of SO may lead to posterior capsule elevation, additional anterior chamber instability, and an increased risk of posterior capsule rupture (28). To prevent SO leakage into the anterior chamber during surgery, pressure on the eyeball that can lead to the rupture of the suspensory ligament of the lens should be avoided. Once SO drops enter the anterior chamber, a balanced salt solution can be injected in the seated position from the superior corneal incision, and oil drops can be discharged by pressing the posterior lip of the incision.

Several potential limitations exist in this study. First, our study predicted the IOL power using data measured before IOL implantation, although some issues may arise during surgery, such as the effects of the surgical incision and changes in the position of the IOL due to viscoelastic agent residue or laxity of the capsular bag. Second, the state and amount of SO may also impact our calculation (25). However, these issues cannot be predicted; therefore, the influence of these factors is neglected in the derivation of the theoretical formula. Third, as SO-dependent eyes are relatively rare, the sample sizes and postoperative times were limited in our study. Future studies should enroll more cases involving additional postoperative time variables to further verify and improve our formula. Finally, the power of the implanted IOL in this study was calculated based on clinical experience; thus, it is unclear what the refractive error would have been if the IOL power had been calculated using our new formula. Future studies are needed to investigate the refractive error in SO-dependent eyes for which the implanted IOL power is calculated using the theoretical IOL formula proposed in this study.

5. Conclusion

In conclusion, we derived a theoretical formula for calculating IOL power for patients with SO-dependent eyes in this study based on geometric optical principles and the Gullstrand simplified eye model. For these severely damaged eyes, a strong correlation was found between the theoretical and clinical powers, while a predicted IOL power error of <0.5D in 30.77% and ≤ 2 D was found in 84.62% of those eyes. Thus, our formula will help clinicians select a more appropriate IOL for patients with SO-dependent eyes.

Data availability statement

The original contributions presented in the study are included in the article/supplementary material; further inquiries can be directed to the corresponding author.

Ethics statement

The studies involving humans were approved by the Ethics Committee of Qilu Hospital of Shandong University. The studies were conducted in accordance with the local legislation and institutional requirements. The participants provided their written informed consent to participate in this study.

Author contributions

LW: Writing – original draft, Data curation, Formal analysis, Investigation, Methodology, Validation. XW: Data curation, Formal analysis, Investigation, Methodology, Writing – original draft, Project administration. XY: Data curation, Investigation, Methodology, Writing – original draft, Software. YS: Data curation, Investigation, Writing – original draft, Project administration. JW: Writing – original draft, Conceptualization, Funding acquisition, Methodology. YC: Conceptualization, Funding acquisition, Writing – original draft, Project administration, Supervision.

Funding

The author(s) declare financial support was received for the research, authorship, and/or publication of this article. This study was supported by the Natural Science Foundation of Shandong Province [grant number ZR2020MH174], the Medical and Health Development Program of Shandong Province [grant number 2017WS207], and the Qilu Hygiene and Health Leading Personnel Project.

Acknowledgments

The authors thank the patients for their participation in the study. We thank the technicians who provide ophthalmic examinations to patients enrolled in the study.

Conflict of interest

The authors declare that the research was conducted in the absence of any commercial or financial relationships that could be construed as a potential conflict of interest.

Publisher's note

References

1. Ishida Y, Saito S, Tsuboi K, Atsuya M, Kamei M, Wakabayashi T. Head-tilt perfluorocarbon-air exchange technique with heads-up surgery for giant retinal tear-associated retinal detachments to prevent retinal slippage without using silicone oil. *Retina*. (2023). doi: 10.1097/IAE.0000000000003877

2. Rossi T, Canepa P, Cavalleri O, Rolandi R, Querzoli G, D'Agostino I, et al. Silicone oil tamponade removal: which technique is more effective? An x-ray photoemission spectroscopy study. *Transl Vis Sci Technol*. (2023) 12:21. doi: 10.1167/tvst.12.4.21

3. Ferrara M, Coco G, Sorrentino T, Jasani KM, Moussa G, Morescalchi F, et al. Retinal and corneal changes associated with intraocular silicone oil tamponade. *J Clin Med*. (2022) 11:5234. doi: 10.3390/jcm11175234

4. Prathapan M, Shyam P, Pillai GS. Risk factors for secondary ocular hypertension in silicone oil-filled eyes following transconjunctival sutureless vitrectomy—a prospective cohort study. *Indian J Ophthalmol*. (2023) 71:595–600. doi: 10.4103/ijo.IJO_1777_22

5. Zaheer W, Iqbal K, Usman M. Frequency of retinal re-detachment after removal of silicone oil tamponade in cases of proliferative vitreoretinopathy. *J Pak Med Assoc*. (2020) 70:1404–7. doi: 10.5455/JPMA.45900

6. Adhi MI, Siyal N. Retinal re-detachments after removal of silicone oil: frequency and timings in a retrospective clinical study. *J Pak Med Assoc*. (2019) 69:1822–6. doi: 10.5455/JPMA.4988

7. Dong FT, Dai RP, Jia Y. Clinical features of silicone oil dependent eyes. *Zhonghua Yan Ke Za Zhi*. (2008) 44:998–1001.

8. Fang W, Li J, Jin X, Zhai J, Dai Y, Li Y. Refractive shift of silicone oil tamponade in pseudophakic eye. *BMC Ophthalmol*. (2016) 16:144. doi: 10.1186/s12886-016-0243-z

9. Rajurkar K, DaCruz R, Thakar M. Comparison of optical biometry and conventional acoustic biometry in the axial length measurement in silicone oil-filled eyes. *Indian J Ophthalmol*. (2022) 70:2851–4. doi: 10.4103/ijo.IJO_3019_21

10. Xiong Y, Lin Y, Zhao Z, Wang H, Zhang G. Evaluation and comparison of ocular biometric parameters obtained with tomey oa-2000 in silicone oil-filled aphakic eyes. *BMC Ophthalmol*. (2023) 23:218. doi: 10.1186/s12886-023-02962-w

11. Atchison DA, Cooke DL. Determining specified iol powers when silicone oil is to be used in the vitreous chamber. *J Cataract Refract Surg*. (2023) 49:869–73. doi: 10.1097/j.jcrs.0000000000001190

12. Wu P, Sun Y, Peng H, Liu Z, Wen Y, Chen M. Influence of ocular biometric parameters such as effective lens position, keratometry, and axial length on near add power of multifocal intraocular lens. *J Cataract Refract Surg*. (2022) 48:1331–4. doi: 10.1097/j.jcrs.0000000000000947

13. Haigis W, Lege B, Miller N, Schneider B. Comparison of immersion ultrasound biometry and partial coherence interferometry for intraocular lens calculation according to haigis. *Graefes Arch Clin Exp Ophthalmol*. (2000) 238:765–73. doi: 10.1007/s004170000188

14. Wang L, Shirayama M, Ma XJ, Kohnen T, Koch DD. Optimizing intraocular lens power calculations in eyes with axial lengths above 25.0 mm. *J Cataract Refract Surg*. (2011) 37:2018–27. doi: 10.1016/j.jcrs.2011.05.042

15. Zhao J, Chandrasekaran PR, Cheong KX, Wong M, Teo K. New concepts for the diagnosis of polypoidal choroidal vasculopathy. *Diagnostics*. (2023) 13:1680. doi: 10.3390/diagnostics13101680

16. Siedlecki J, Klaas J, Keidel L, Asani B, Schiefelbein J, Knebel D, et al. Optical coherence tomography-based misdiagnosis and morphological distinction in pachychoroid neovasculopathy vs. Polypoidal choroidal vasculopathy. *Eye*. (2023). doi: 10.1038/s41433-023-02529-5

17. Lin A, Xia H, Zhang A, Liu X, Chen H. Vitreomacular interface disorders in proliferative diabetic retinopathy: an optical coherence tomography study. *J Clin Med*. (2022) 11:3266. doi: 10.3390/jcm11123266

18. Dave VP, Pappuru RR, Pathengay A, Tyagi M, Narayanan R, Jalali S. Vitrectomy with silicone oil tamponade in rhegmatogenous retinal detachment following acute retinal necrosis: clinical outcomes and prognostic factors. *Semin Ophthalmol*. (2019) 34:47–51. doi: 10.1080/08820538.2018.1551907

19. Retzlaff JA, Sanders DR, Kraff MC. Development of the srk/t intraocular lens implant power calculation formula. *J Cataract Refract Surg*. (1990) 16:333–40. doi: 10.1016/s0886-3350(13)80705-5

20. Barrett GD. An improved universal theoretical formula for intraocular lens power prediction. *J Cataract Refract Surg*. (1993) 19:713–20. doi: 10.1016/s0886-3350(13)80339-2

21. Liu R, Li Q. Changes in ocular biometric measurements after vitrectomy with silicone oil tamponade for rhegmatogenous retinal detachment repair. *BMC Ophthalmol*. (2020) 20:360. doi: 10.1186/s12886-020-01627-2

22. Zhang J, Han X, Zhang M, Liu Z, Lin H, Qiu X, et al. Comparison of axial length measurements in silicone oil-filled eyes using ss-oct and partial coherence interferometry. *J Cataract Refract Surg*. (2022) 48:1375–80. doi: 10.1097/j.jcrs.0000000000000996

23. Calik B, Ozturk M, Serdarogullari H, Elcioglu M. Evaluation of anterior segment parameters using pentacam in silicone oil-injected patients after pars plana vitrectomy. *Indian J Ophthalmol*. (2013) 61:621–5. doi: 10.4103/0301-4738.123137

24. Tan X, Zhang J, Zhu Y, Xu J, Qiu X, Yang G, et al. Accuracy of new generation intraocular lens calculation formulas in vitrectomized eyes. *Am J Ophthalmol*. (2020) 217:81–90. doi: 10.1016/j.ajo.2020.04.035

25. Lwowski C, Miraka K, Muller M, Singh P, Koch F, Kohnen T. Intraocular lens calculation using 8 formulas in silicone oil-filled eyes undergoing silicone oil removal and phacoemulsification after retinal detachment. *Am J Ophthalmol*. (2022) 244:166–74. doi: 10.1016/j.ajo.2022.07.007

26. Kanclerz P, Grzybowski A. Accuracy of intraocular lens power calculation in eyes filled with silicone oil. *Semin Ophthalmol*. (2019) 34:392–7. doi: 10.1080/08820538.2019.1636097

27. Melles RB, Holladay JT, Chang WJ. Accuracy of intraocular lens calculation formulas. *Ophthalmology*. (2018) 125:169–78. doi: 10.1016/j.ophtha.2017.08.027

28. Kanclerz P, Grzybowski A, Schwartz SG, Lipowski P. Complications of cataract surgery in eyes filled with silicone oil. *Eur J Ophthalmol*. (2018) 28:465–8. doi: 10.1177/1120672117753700

frontiers | Frontiers in Medicine

TYPE Original Research
PUBLISHED 23 October 2023
DOI 10.3389/fmed.2023.1250914

OPEN ACCESS

EDITED BY
Horace Massa,
Hôpitaux universitaires de Genève (HUG), Switzerland

REVIEWED BY
Zhengbo Shao,
The Second Affiliated Hospital of Harbin Medical University, China
Xiaoxiao Lu,
Tianjin Medical University Eye Hospital, China

*CORRESPONDENCE
Ting Huang
✉ thuang@vip.163.com

†These authors share first authorship

RECEIVED 30 June 2023
ACCEPTED 15 September 2023
PUBLISHED 23 October 2023

CITATION
Xu C, Guo R, Hou C, Ma M, Dong X, Ouyang C, Wu J and Huang T (2023) Resveratrol regulates macrophage recruitment and M1 macrophage polarization and prevents corneal allograft rejection in rats.
Front. Med. 10:1250914.
doi: 10.3389/fmed.2023.1250914

Resveratrol regulates macrophage recruitment and M1 macrophage polarization and prevents corneal allograft rejection in rats

Chenjia Xu†, Ruilin Guo†, Chao Hou, Minglu Ma, Xiaojuan Dong, Chen Ouyang, Jing Wu and Ting Huang*

State Key Laboratory of Ophthalmology, Zhongshan Ophthalmic Center, Sun Yat-sen University, Guangdong Provincial Key Laboratory of Ophthalmology and Visual Science, Guangzhou, China

Introduction: Resveratrol is an immune modulator that can reduce M1 macrophage polarization *in vitro*. Reducing macrophage recruitment and M1 polarization can prevent corneal allograft rejection (CGR). In this study, rat corneal allograft rejection models were established to explore the effects of resveratrol on CGR and macrophages and the underlying mechanisms after corneal transplantation.

Methods: Corneal allograft models were established, and 100 mg/kg resveratrol was injected intraperitoneally. The corneal allografts were assessed clinically using the Holland rejection scoring system, anterior segment photography, and anterior segment optical coherence tomography. Corneal macrophages, pro-inflammatory cytokines, and corneal lymphatic vessels were detected using hematoxylin and eosin staining, immunofluorescence staining, and real-time quantitative polymerase chain reaction (qRT-PCR). Dendritic cells (DCs) in cervical lymph nodes were explored using flow cytometry. RNA sequencing experiments were conducted to identify the mechanisms through which resveratrol affected CGR. The results were verified using Simple Western analysis. Pro-inflammatory cytokines by macrophages *in vitro* were measured using qRT-PCR and enzyme-linked immunosorbent assays.

Results: Resveratrol significantly prolonged the survival of corneal grafts and reduced graft edema and central corneal thickness. Corneal macrophage recruitment and M1 macrophage polarization decreased significantly after corneal transplantation in the resveratrol group. Resveratrol also reduced pro-inflammatory cytokines in corneal grafts and suppressed the early generation of cornea lymphatic vessels and the recruitment of cornea inflammatory cells 14 days after surgery. Resveratrol decreased the proportion of DCs in ipsilateral cervical lymph nodes. The effect of resveratrol on CGR was related to the phosphatidylinositol 3-kinase/protein kinase-B (PI3K/Akt) pathway. Resveratrol reduced the secretion of pro-inflammatory cytokines by M1 macrophages *in vitro*.

Conclusion: Our findings suggest that resveratrol can reduce corneal macrophage recruitment and M1 macrophage polarization after corneal transplantation in rats and prevent CGR. The PI3K/Akt pathway may be an important mechanism that warrants further research.

KEYWORDS

resveratrol, macrophages, corneal transplantation, immune rejection, PI3K/Akt pathway

Introduction

Corneal opacity is an important blinding eye condition worldwide. Corneal transplantation surgery remains the main treatment for corneal opacity and has solved most of the blindness caused by corneal opacity (1, 2). The cornea has the highest transplantation success rate of all human organs because of its avascular nature and anterior chamber-associated immune deviation (3, 4). However, corneal allograft rejection (CGR) remains the major reason for the failure of penetrating keratoplasty (5). Although many drugs targeting CGR, such as corticosteroids, tacrolimus, and cyclosporine, play important roles in resisting CGR, they are mostly immunosuppressants, and long-term use may cause many side effects (6, 7). Therefore, there is an urgent need to find new drugs that can prevent or delay CGR.

Macrophages originate from monocytes and play a key role in innate immunity, inflammatory responses, and tissue homeostasis (8). Low expression levels of major histocompatibility complex II (MHC II) co-stimulatory molecules in macrophages in eye tissues enable macrophages to act as antigen-presenting cells (APCs) in CGR (9). After corneal transplantation, the number and function of dendritic cells (DCs), cytotoxic T lymphocyte activity, and corneal neovascularization may decrease with a decrease in the number of macrophages, thereby delaying CGR (10–12). Allograft transplantation leads to the release of many chemicals, triggering the activation of macrophages. Depending on the surrounding inflammatory environment, macrophages can polarize into pro-inflammatory (M1) or anti-inflammatory (M2) macrophages. M1 and M2 macrophages can be derived from M0 macrophages *in vitro* due to different stimuli (13). M1 macrophages can be stimulated, among others, by lipopolysaccharides (LPS) and interferon gamma and can secrete pro-inflammatory cytokines, such as interleukin-6 (IL-6), IL-1β, and tumor necrosis factor alpha (TNF-α) (14, 15). IL-4 can polarize M0 into M2 macrophages, which can secrete anti-inflammatory cytokines, such as IL-10 (15). In mouse corneal transplant rejection models, M1 macrophages have been found to infiltrate the cornea in large numbers, suggesting that they may be directly involved in CGR (16). Previous studies have also shown that inhibiting M1 macrophage polarization can delay CGR (17, 18).

Pathological lymphatic vessels help transport APCs from the transplant site to the corresponding drainage area of lymphatic tissue, thereby accelerating CGR (19). Therefore, inhibiting corneal lymphatic vessels may be a viable strategy for preventing CGR. Researchers have pre-cultured corneal donor tissue *in vitro* and used anti-vascular endothelial growth factor (VEGF) drugs to block postoperative angiogenesis and lymphangiogenesis and maintain the transparency of corneal grafts. This can result in a significant decrease in corneal macrophages (20). Moreover, the inhibition of corneal lymphatic vessel formation can reduce the incidence of corneal transplant rejection, and lymphangiogenesis is associated with macrophages (21).

Resveratrol is a non-flavonoid polyphenol compound found in fruits such as blueberries and many red grape varieties (22, 23). Resveratrol plays an important role in various biological functions, exerting anti-inflammatory, antioxidant, anticancer, and anti-neurodegenerative effects (24–26). A previous study found that resveratrol mainly had anti-inflammatory effects on macrophages (27). Other studies have shown that it can prolong the survival of liver allografts (28, 29). In summary, resveratrol may be a relatively safe drug that can prevent CGR and may act by affecting macrophages. This study aimed to examine whether resveratrol can affect CGR by interfering with the recruitment and polarization of corneal macrophages.

Materials and methods

Animals

Six-to-eight-weeks-old female Sprague Dawley (SD) rats and Wistar rats were purchased from Guangzhou Southern Medical University Experimental Animal Technology Development Co., Ltd. (Guangzhou, Guangdong, China) To avoid the interference of sex hormones with immune responses, only female rats were used. The rats were housed in a specific pathogen free (SPF)-grade standardized feeding room at Zhongshan Ophthalmic Center, Yat-sen University. The experiments were approved by the Institutional Animal Care and Use Committee of Zhongshan Ophthalmic Center (protocol code O2021044).

Corneal transplantation model

Preoperatively, pentobarbital sodium (1%) was used as an anesthetic in intraperitoneal injection doses of 40–45 mg/kg. To establish allograft corneal transplantation models, the SD rats were used as donors, and the Wistar rats were used as recipients. Moreover, corneal autograft operations were performed on Wistar rats. Full-thickness corneal donors 3.5 mm in diameter were sutured to implant beds 3.0 mm in diameter using 10-0 nylon sutures (Alcon, Fort Worth, TX, United States) under a microscope.

Four experimental groups were formed. A normal group of Wistar rats did not undergo corneal transplantation and received no treatment. The Wistar rats in the autograft group underwent only autologous corneal transplantation and received no treatment. A control group of Wistar rats underwent corneal allograft surgery and received saline treatment. The resveratrol group consisted of Wistar rats undergoing corneal allograft surgery and receiving resveratrol treatment. Resveratrol solution (0.6 mL, 100 mg/kg, Sigma-Aldrich, St. Louis, MO, United States) or saline was injected intraperitoneally every day for 30 days postoperatively.

Cell treatments

A human monocytic leukemia cell line (THP-1) was obtained from the cell bank of the Chinese Academy of Sciences in Shanghai. An RPMI-1640 culture medium (Gibco-BRL, Grand Island, NY, United States) with 10% FBS (Thermo Fisher Scientific, Waltham, MA, United States) and 1% penicillin-streptomycin (Sigma-Aldrich, St. Louis, MO, United States) was used. All cells were cultured in a cell incubator containing 5% carbon dioxide at 37°C. After cell line resuscitation, fourth-to-eighth-generation cells were used in the experiments. Adhesive THP-1 cells induced using phorbol 12-myristate-13-acetate (PMA; 100 ng/mL, P1585; Sigma-Aldrich, St. Louis, MO, United States) for 48 h were considered M0 macrophages. M0 macrophages were transformed into M1 macrophages using LPS treatment (1 μg/mL, from Escherichia coli O111:B4, Sigma-Aldrich, St. Louis, MO, United States) for 24 h.

The cells were divided into five groups. The control group consisted of untreated M0 macrophages. The cells in the LPS group

were treated only with LPS. The cells in the resveratrol groups were treated with three resveratrol concentrations: 10, 25, and 50 μM.

Clinical assessment

The rat corneas in the autograft, control, and resveratrol groups were examined using slit-lamp microscopy every other day for 30 days postoperatively. The corneal allografts were assessed clinically using the Holland rejection scoring system (30, 31). Corneal graft clarity, edema, and neovascularization were used as indicators (Table 1). The three parameters were summed to obtain a rejection index (RI). An RI of ≥6 was considered to indicate rejection. Anterior segment photography was performed 7 and 14 days postoperatively to record the condition of the corneal grafts in the control and resveratrol groups. Anterior segment optical coherence tomography (AS-OCT) was performed 14 days postoperatively to measure central corneal thickness (CCT) in the control, resveratrol, and normal groups.

Hematoxylin and eosin staining

On the 14th postoperative day, the eyeballs of rats in the normal, control, and resveratrol groups were removed and placed in 4% paraformaldehyde (PFA; Biosharp, Hefei, Anhui, China) solution at 4°C overnight. After dehydration and paraffin embedding, sections approximately 4 μm thick were cut. After dewaxing and hydration, the sections were stained with hematoxylin and eosin (H&E; Servicebio, Wuhan, Hubei, China). Histological analysis was performed using an inverted microscope (Ts2FL; Nikon, Japan) and CapStudio software.

TABLE 1 Standards of grading for corneal grafts.

Standard	Score	Sign
Clarity	0	Clear cornea
	1	Slight haze
	2	Increased haze but anterior chamber structures still clear
	3	Advanced haze with difficult view of anterior chamber
	4	Opaque cornea without view of anterior chamber
Edema	0	No stromal or epithelial edema
	1	Slight stromal thickness
	2	Diffuse stromal edema
	3	Diffuse stromal edema with microcystic edema of epithelium
	4	Bullous keratopathy
Neovascularization	0	No vascularization
	1	Vascularization of the peripheral cornea
	2	Vascularization to the corneal wound
	3	Vascularization of the peripheral graft
	4	Vascularization of the entire graft

The grafts showing a score of RI ≥6 were defined as rejected.

Immunofluorescence staining

The eyes of rats in the normal, control, and resveratrol groups were removed and fixed with 4% PFA. The tissues were then embedded in paraffin wax and cut into 4 μm thick sections. The sections were stained with mouse anti-cluster of differentiation molecule 11b (CD11b; 1:100, sc-1186; Santa Cruz, CA, United States) and rabbit anti-inducible nitric oxide synthase (iNOS; 1:500, ab283655; Abcam, Cambridge, United Kingdom) primary antibodies at 4°C overnight. Subsequently, they were dyed with Goat anti-Mouse IgG (H + L) Highly Cross-Adsorbed Secondary Antibody (Alexa Fluor Plus 488, 1:200; Invitrogen, Carlsbad, CA, United States) and Goat anti-Rabbit IgG (H + L) Highly Cross-Adsorbed Secondary Antibody (Alexa Fluor Plus 594, 1:200; Invitrogen) for 1 h. The stained slices were analyzed under a Zeiss LSM 880 microscope (Carl Zeiss Meditec, Jena, Germany).

Real-time quantitative polymerase chain reaction

On the seventh postoperative day, corneas from the normal, control, and resveratrol groups were excised and cut into pieces. An RNeasy Fibrous Tissue Mini Kit (Qiagen, Duesseldorf, Germany) was used to extract RNA from the corneas. An RNA Quick Purification Kit (ESscience, Shanghai, China) was used to extract RNA from macrophages. The RNA was then reverse-translated into cDNA using HiScript II QRT SuperMix (Vazyme, Nanjing, Jiangsu, China). A LightCycler 480 SYBR Green I Master (Roche, Basel, Switzerland) was used to perform a real-time quantitative polymerase chain reaction (qRT-PCR). The primers are shown in Tables 2, 3.

Whole-mount corneal immunofluorescence

On the seventh postoperative day, whole corneas from the control and resveratrol groups were excised and fixed with 4% PFA for 1 h. The corneas were then digested by protease K and permeated with methanol. Subsequently, they were blocked at 4°C overnight with 10% Bovine Serum Albumin (BSA; Epizyme, Shanghai, China) blocking solution containing 0.5% Triton X-100. The corneas were then dyed with rabbit anti-rat lymphatic vessel endothelial hyaluronan receptor 1 (LYVE-1; 1:200, 11-036; AngioBio, San Diego, CA, United States) at 4°C overnight. Finally, they were stained with Goat anti-Rabbit IgG (H + L) Highly Cross-Adsorbed Secondary Antibody (Alexa Fluor Plus 594, 1:200, Invitrogen, Carlsbad, CA, United States) at room temperature for 2 h.

Flow cytometry

On the 10th postoperative day, the right cervical lymph nodes on the same side as the surgical eyes of the rats in the normal, control, and resveratrol groups were removed and ground. The obtained cells were resuspended using stain buffer and surface-stained with CD103 (Integrin alpha E) Monoclonal Antibody (OX62), PE, eBioscience (12-1030-82, 0.25 μg per test; Thermo Fisher Scientific, Waltham, MA,

TABLE 2 The primer sequences of the rat genes.

Gene	Primer sequence (5′–3′)
GAPDH	
Forward	TCTCTGCTCCTCCCTGTTC
Reverse	ACACCGACCTTCACCATCT
TNF-α	
Forward	TACTGAACTTCGGGGTGATTGGTCC
Reverse	CAGCCTTGTCCCTTGAAGAGAACC
IL-1β	
Forward	CCCTGCAGCTGGAGAGTGTGG
Reverse	TGTGCTCTGCTTGAGAGGTGCT
IL-6	
Forward	CGAAAGTCAACTCCATCTGCC
Reverse	GGCAACTGGCTGGAAGTCTCT
MCP-1	
Forward	CTGGAGAACTACAAGAGAAT
Reverse	TCTAGTATTCATGGAAGGGA
iNOS	
Forward	CACGACACCCTTCACCACAAG
Reverse	TTGAGGCAGAAGCTCCTCCA
VEGF-C	
Forward	GATTCAGGGGTTGATTTCTTG
Reverse	TTTCCTTAATTCATGTGGAGCC

TABLE 3 The primer sequences of the human genes.

Gene	Primer sequence (5′–3′)
GAPDH	
Forward	GGAGTCCACTGGCGTCTTCA
Reverse	GTCATGAGTCCTTCCACGATACC
TNF-α	
Forward	GAAAGCATGATCCGGGACGTG
Reverse	GATGGCAGAGAGGAGGTTGAC
IL-1β	
Forward	ATGGCTTATTACAGTGGCAATGAG
Reverse	GTAGTGGTGGTCGGAGATTCG
IL-6	
Forward	ACTCACCTCTTCAGAACGAATTG
Reverse	CCATCTTTGGAAGGTTCAGGTTG
MCP-1	
Forward	GATCTCAGTGCAGAGGCTCG
Reverse	TGCTTGTCCAGGTGGTCCAT
VEGF-C	
Forward	CAGCACGAGCTACCTCAGCAAG
Reverse	TTTAGACATGCATCGGCAGGAA

United States) for 20 min. Analyses were then performed using a BD LSRFortessa flow cytometer (BD Biosciences, San Jose, CA, United States).

RNA sequencing

Total RNA was extracted from corneas in the control and resveratrol groups using the method described above. A NanoDrop 2000 spectrophotometer (Thermo Fisher Scientific, Waltham, MA, United States) was used to evaluate the purity and quantification of the extracted RNA. The libraries were sequenced on a NovaSeq 6000 platform (Illumina, San Diego, CA, United States). DESeq25 (Siemens, Berlin, Germany) was used to analyze differential expression. *Q*-values of <0.05 were considered to indicate significant differences in differentially expressed genes (DEGs). R (v 3.2.0) was used to perform the gene ontology (GO) 6 and Kyoto encyclopedia of genes and genomes (KEGG) 7 pathways of DEGs to identify significant enrichment terms and draw a histogram based on the hypergeometric distribution. All RNA sequencing and analyses were performed by Ouyi Biomedical Technology Co., Ltd. (Shanghai, China).

Simple western analysis

On the seventh postoperative day, proteins were isolated from corneas in the control and resveratrol groups. After measuring protein concentrations using the bicinchoninic acid assay (BCA) method, the samples were prepared and denatured at 95°C for 5 min. Following the protocol described in the manual for the 12–230 kDa Wes Separation Module (SM-W004; ProteinSimple, Bio-Techne, San Jose, CA, United States), an automated capillary electrophoresis system was used to separate and detect the proteins. Antibodies targeting the proteins GAPDH, PI3K, Akt and Phospho-Akt (p-Akt) were used [GAPDH (1:50, 5174S; Cell Signaling Technology, Danvers, MA, United States), PI3K (1:50, 4249S; Cell Signaling Technology, Danvers, MA, United States), AKT (1:600, 4691S; Cell Signaling Technology, Danvers, MA, United States), and p-Akt (1:10, 4060S; Cell Signaling Technology, Danvers, MA, United States)]. Horseradish peroxidase (HRP)-conjugated secondary anti-rabbit antibody was used to detect signals. Compass software (ProteinSimple) was used for the quantitative analysis.

Enzyme-linked immunosorbent assay

The cell supernatants of the five groups of cells were extracted separately. Cytokines secreted by macrophages were measured using enzyme-linked immunosorbent assays (ELISA; TNF-α ELISA Kit BMS2034, IL-6 ELISA Kit BMS213-2, MCP-1 ELISA Kit BMS281INST, and VEGF-C ELISA Kit BMS297-2; Thermo Fisher Scientific, Waltham, MA, United States).

Statistical analysis

The data were analyzed using GraphPad Prism 7 software. Kaplan–Meier survival curves were drawn to analyze corneal graft survival. Differences between the two groups were assessed using an

independent-samples *t*-test. *p*-values of <0.05 were considered statistically significant.

Results

Resveratrol prolonged corneal allograft survival

Graft survival time curves were plotted based on three scores, including corneal graft clarity, edema, and neovascularization (Figure 1). At the end of the 30 days observation period, all corneal grafts in the autograft group were still alive. In the control group, all grafts were rejected between days 8 and 12. The median survival time (MST) was 9 days. In the resveratrol group, six grafts were rejected between days 10 and 24. The MST was 17 days. The other four grafts in this group survived until the end of the observation period (Figure 1A). During the observation period, the average corneal graft clarity, edema, and corneal neovascularization scores in the resveratrol group were significantly lower than those in the control group (Figures 1B–E).

Resveratrol reduced postoperative corneal inflammatory responses

Most corneal grafts in the control group showed inflammatory responses soon after surgery, which gradually worsened. In this group, neovascularization reached the periphery of almost all grafts around 7 days after surgery. In contrast, in the resveratrol group, neovascularization grew to the edge of most grafts on the 14th postoperative day. In this group, the grafts remained relatively transparent, with no significant edema and significantly milder rejection reactions (Figure 1F). On the 14th day after surgery, the corneas were used for histological analysis. The H&E staining results showed that inflammatory cells were significantly infiltrated in the corneas of rats with CGR. However, in the allografts of the resveratrol group, inflammatory cell infiltration was significantly decreased (Figure 1G).

Graft CCT

Corneal thickness after corneal transplantation is related to transplant rejection. The average CCT in the control group was 0.345 ± 0.015 mm, whereas the average CCT in the resveratrol group was 0.194 ± 0.012 mm. (Normal rat CCT is 0.158 ± 0.004 mm.) The corneal grafts in the resveratrol group were significantly thinner than those in the control group ($p < 0.01$) (Figures 1H,I).

Effects of resveratrol on macrophages in corneal grafts

To investigate the recruitment and polarization of macrophages in corneas, macrophages were labeled with CD11b, and M1 macrophages were labeled with iNOS on the seventh postoperative day (Figure 2A). No macrophage infiltration was observed in normal corneal tissue. In the control group, the average number of $CD11b^+$-labeled macrophages was 30 cells per field, and the proportion of $CD11b^+$ $iNOS^+$-labeled M1 macrophages was approximately 76.67% (Figure 2B). In the resveratrol group, the average number of $CD11b^+$-labeled macrophages was 17 cells per field, and the proportion of $CD11b^+$ $iNOS^+$-labeled M1 macrophages was approximately 58.82% (Figure 2C). Resveratrol treatment resulted in significantly lower of $CD11b^+$-labeled macrophage recruitment ($p < 0.01$) and a significantly lower polarization ratio of $CD11b^+$ $iNOS^+$-labeled M1 macrophages ($p < 0.01$) than saline treatment (Figures 2B,C). M1 macrophages secreted multiple types of pro-inflammatory cytokines, including TNF-α, iNOS, IL-1β, monocyte chemoattractant protein-1 (MCP-1), IL-6, and VEGF-C. The mRNA expressions of TNF-α, iNOS, IL-1β, MCP-1, IL-6, and VEGF-C were significantly lower in the resveratrol group than in the control group (Figures 2D–I).

Resveratrol inhibited corneal lymphangiogenesis

Previous PCR-based studies have shown that resveratrol can reduce inflammatory cytokines related to the formation of corneal lymphatic vessels, including TNF-α, IL-1β, and VEGF-C. Seven days after surgery, the rats' corneas were removed, and LYVE-1 was used as a lymphatic-specific marker for whole-mount corneal immunofluorescence to clarify the influence of resveratrol on the formation of new lymphatic vessels after corneal transplantation. In the control group, LYVE-1-labeled lymphatic vessels grew considerably from the corneal limbus to the grafts. In contrast, lymphatic vessels grew only slightly in the resveratrol group (Figure 3A).

Transfer of DCs to cervical lymph nodes

After corneal transplant rejection, DCs, a main type of APCs, can be transported to the local lymph nodes on the same side through lymphatic vessels (32). The results reported above confirmed that resveratrol reduced the generation of corneal lymphatic vessels. The changes in APCs in cervical lymph nodes were further investigated using flow cytometry. DCs from the ipsilateral lymph nodes from the different treatment groups were labeled with OX62 (Figure 3B). The results showed a significant increase in the proportion of DCs in the cervical lymph nodes after corneal transplantation. However, on the 10th day after surgery, the resveratrol group showed significantly fewer DCs than the control group (Figure 3C).

RNA sequencing results

Total RNA was extracted from three corneas from the control group and three corneas from the resveratrol group. RNA transcriptome sequencing was performed, and the data were analyzed. A total of 234 DEGs, including 21 upregulated and 213 downregulated genes, were detected (Figure 4A). A differential gene expression heat map was created to visualize the grouping and

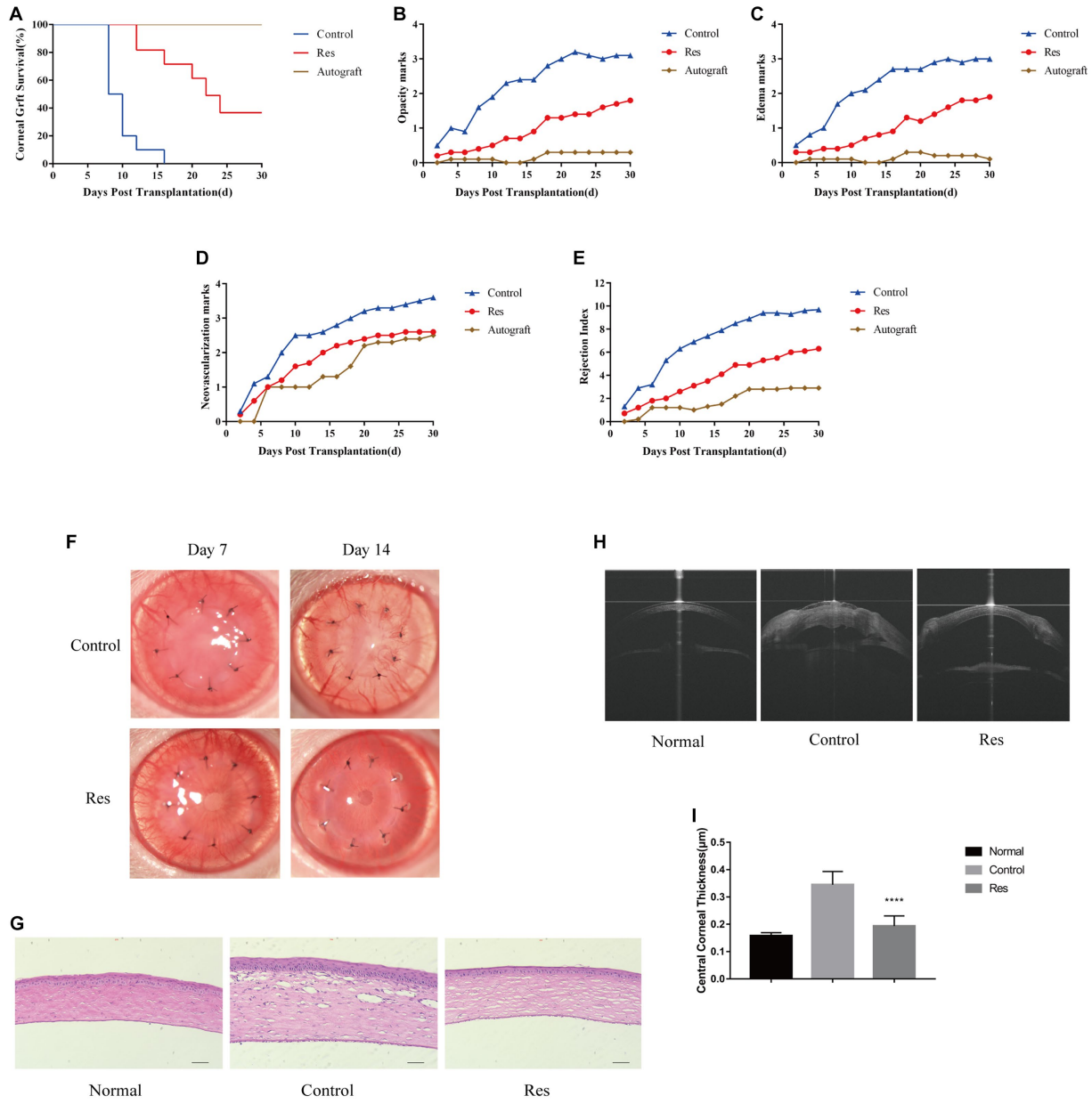

FIGURE 1
Resveratrol prevented CGR and inflammatory responses in rats. **(A)** Kaplan–Meier corneal allograft survival curve ($n = 10$). **(B–E)** The average clarity, edema, neovascularization, and RI scores were considerably lower in the resveratrol group than in the control group. **(F)** Anterior segment photographs of rats in the resveratrol and control groups on postoperative days 7 and 14. **(G)** Comparison of H&E staining images and inflammatory cell expression in the corneas of the normal, control, and resveratrol groups on postoperative day 14 ($n = 3$, magnification: 200×, scale bar: 50 μm). **(H,I)** AS-OCT images of corneas in the normal, control, and resveratrol groups on postoperative day 14. The corneas in the resveratrol group were significantly thinner than those in the control group. The data are shown as mean ± SD. ****$p < 0.0001$ between the resveratrol and control groups.

clustering of DEGs (Figure 4B). The GO analysis showed that among the DEGs in the resveratrol group, immune response (biological process), extracellular matrix (cellular component), and MHC class II protein complex connection (molecular function) exhibited the greatest enrichment (Figure 4C). These results provided references for further research on related signaling pathways, and DEGs were analyzed for this purpose. The results showed that the downregulated genes in the resveratrol group regulated a total of 201 signaling pathways, of which 50 showed significant differences. Notably, in the KEGG analysis, one of the most important pathways of downregulated DEG enrichment in the resveratrol group was allograft rejection, suggesting that resveratrol may act against CGR (Figure 4D). Moreover, antigen processing and presentation of inflammatory-related diseases, Th1 and Th2 cell differentiation, Th17 cell differentiation, PI3K-Akt signaling pathway, and other related pathways were significantly enriched in the downregulation pathway of the resveratrol group. These results suggest that resveratrol may interfere with CGR through multiple pathways, indicating possible directions for follow-up research.

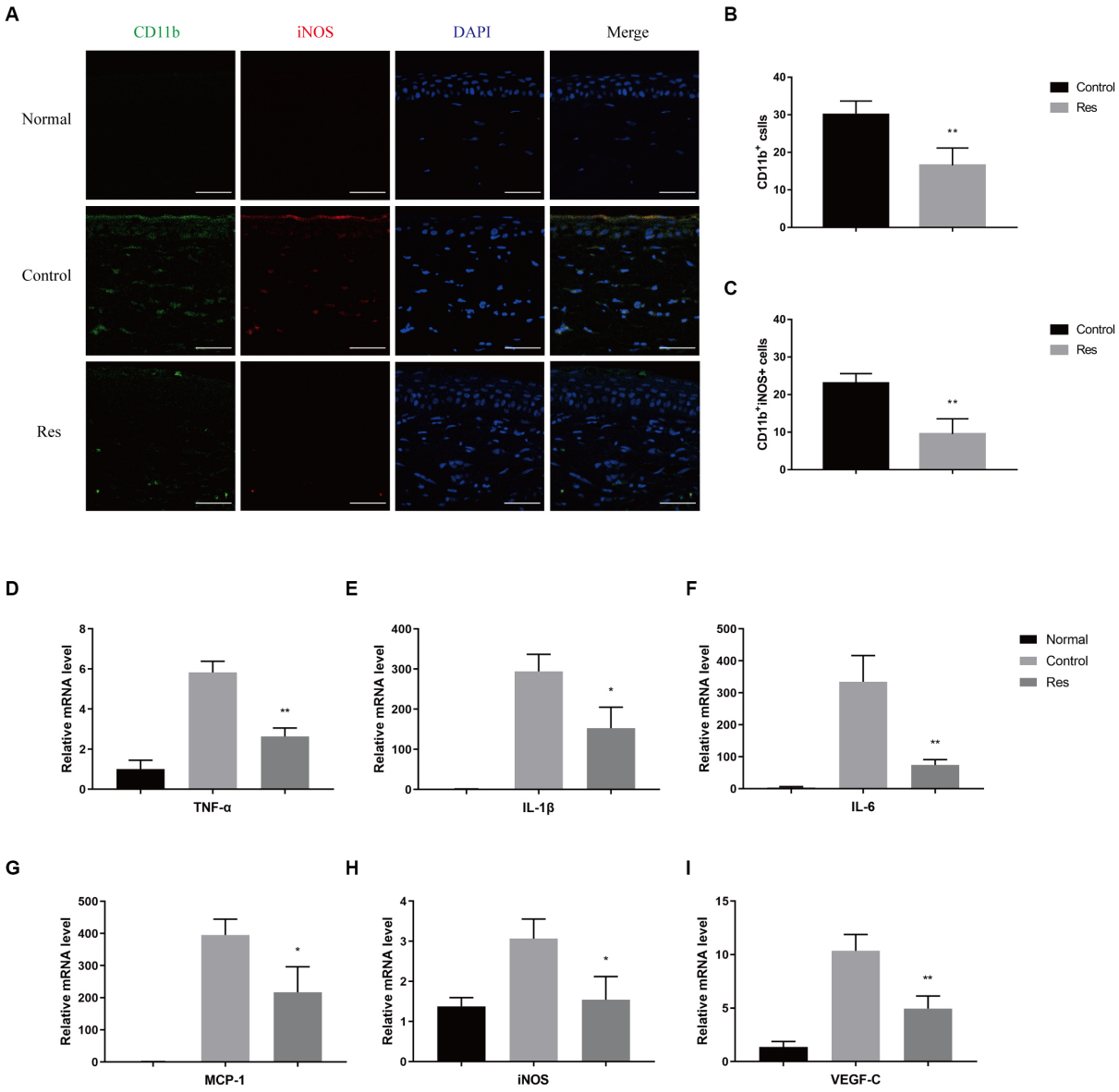

FIGURE 2
Changes in corneal macrophage recruitment and M1 macrophage polarization after resveratrol treatment in rats. **(A–C)** The resveratrol group had significantly lower numbers of CD11b$^+$-labeled macrophages (green) and CD11b$^+$ iNOS$^+$-labeled M1 macrophages (red) than the control group on postoperative day 7 ($n = 4$, magnification: 400×, scale bar: 50 μm). **(D–I)** The resveratrol group had significantly lower mRNA expression levels of TNF-α, IL-1β, IL-6, MCP-1, iNOS, and VEGF-C than the control group on postoperative day 7 ($n = 3$). The data are shown as mean ± SD. *$p < 0.05$ and **$p < 0.01$ between the resveratrol and the control groups.

Resveratrol inhibited PI3K/Akt pathway

Based on the RNA sequencing results reported above, the PI3K/Akt pathway was selected for protein-level pathway validation. The expressions of the PI3K and Akt proteins in the corneas of the rats in the control and resveratrol groups were analyzed using Simple Western. The protein table indicated that the expression levels of PI3K, Akt and p-Akt were significantly lower in the resveratrol group than in the control group (Figure 4E). These results suggest that resveratrol can effectively regulate the PI3K/Akt signaling pathway after corneal transplantation in rats, which may be related to its action against CGR.

Resveratrol inhibited the polarization of M1 macrophages *in vitro*

THP-1 was used to validate the effect of resveratrol on macrophages *in vitro*. After being treated with PMA and LPS, THP-1 cells can be considered M1 macrophages, which express various pro-inflammatory cytokines. The qRT-PCR results showed that resveratrol at concentrations of 10, 25, and 50 μM reduced the production of pro-inflammatory cytokines, such as TNF-α, IL-6, IL-1β, MCP-1, and VEGF-C, by M1 macrophages (Figures 5A–E). The subsequent ELISA results were consistent with the qRT-PCR results

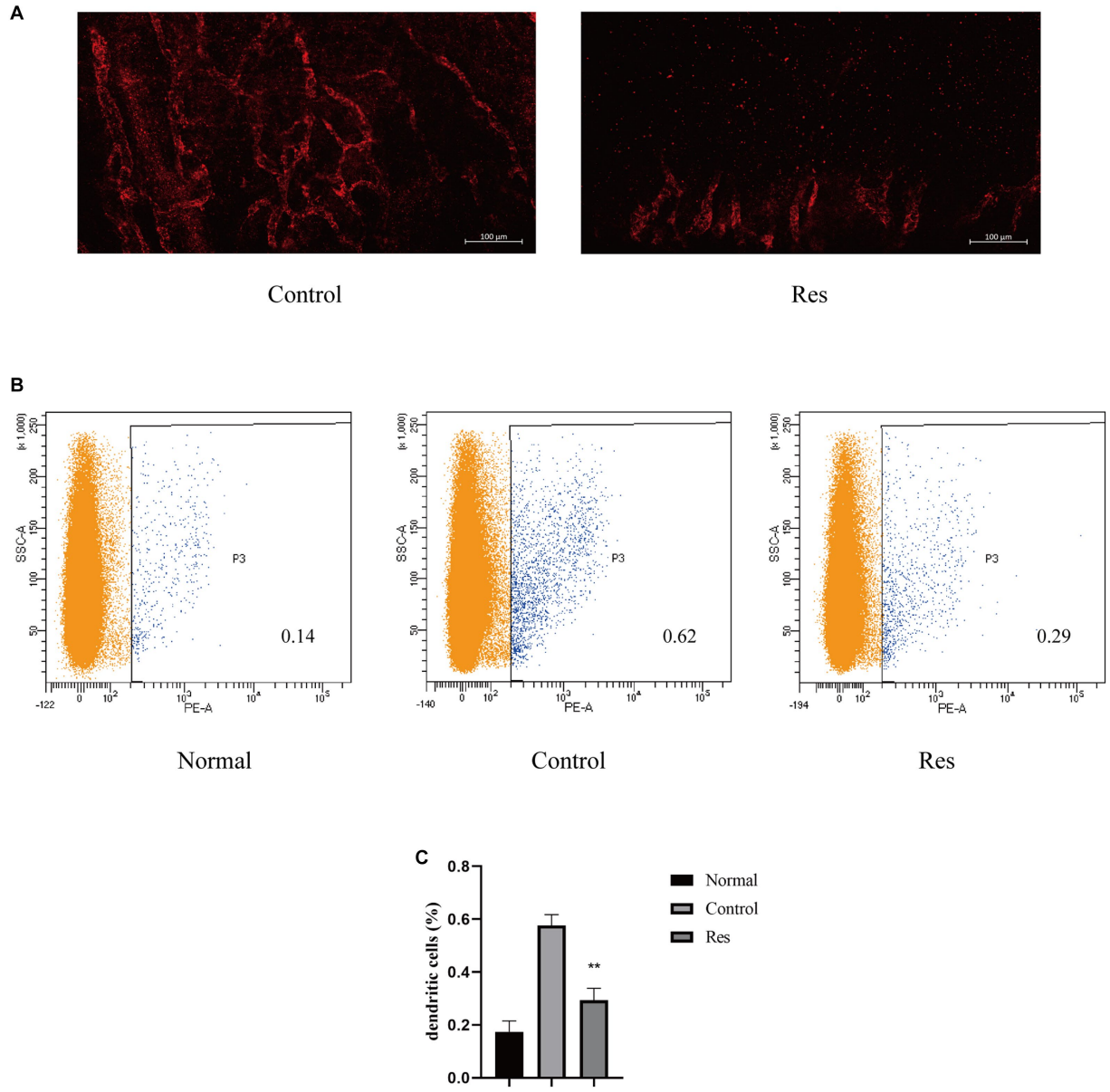

FIGURE 3
Resveratrol suppressed corneal lymphangiogenesis and the migration of DCs to the cervical lymph nodes after corneal transplantation. **(A)** Corneal lymphatic vessels stained with LYVE-1 (red). Resveratrol significantly suppressed corneal lymphangiogenesis 7 days after surgery ($n = 3$, scale bar: 100 μm). **(B,C)** The number and proportion of OX62-labeled DCs in the ipsilateral lymph nodes of rat corneal grafts were significantly lower in the resveratrol group than in the control group ($n = 3$). The data are shown as mean ± SD. $^{**}p < 0.01$ between the resveratrol and control groups.

(Figures 5F–I). Therefore, it can be concluded that resveratrol can inhibit the polarization of human M1 macrophages *in vitro*.

Discussion

Resveratrol has an immunomodulatory effect and has been proven to affect transplant rejection. Wu et al. (29) found that resveratrol enhanced the inhibitory effect of cyclosporine on allogeneic liver rejection. The following studies showed that daily intraperitoneal injections of resveratrol (100 mg/kg) after liver transplantation significantly prolonged graft survival in rats (28, 33). Moreover, an *in vitro* study found that resveratrol reduced peripheral blood monocyte proliferation and stimulated T cell activation (34). However, the effect of resveratrol on CGR has hitherto been unclear. The results of this study showed that intraperitoneal injections of 100 mg/kg resveratrol significantly prolonged corneal graft survival and reduced inflammatory responses in rats.

Macrophages are inflammatory cells that play a crucial role in the occurrence of allogeneic rejection (35, 36). Early macrophage activation can mediate the activation of APCs, which is important for initiating immune rejection (37). Previous studies have shown that pro-inflammatory M1 macrophages promote CGR, while anti-inflammatory M2 macrophages can delay it to some extent (38, 39).

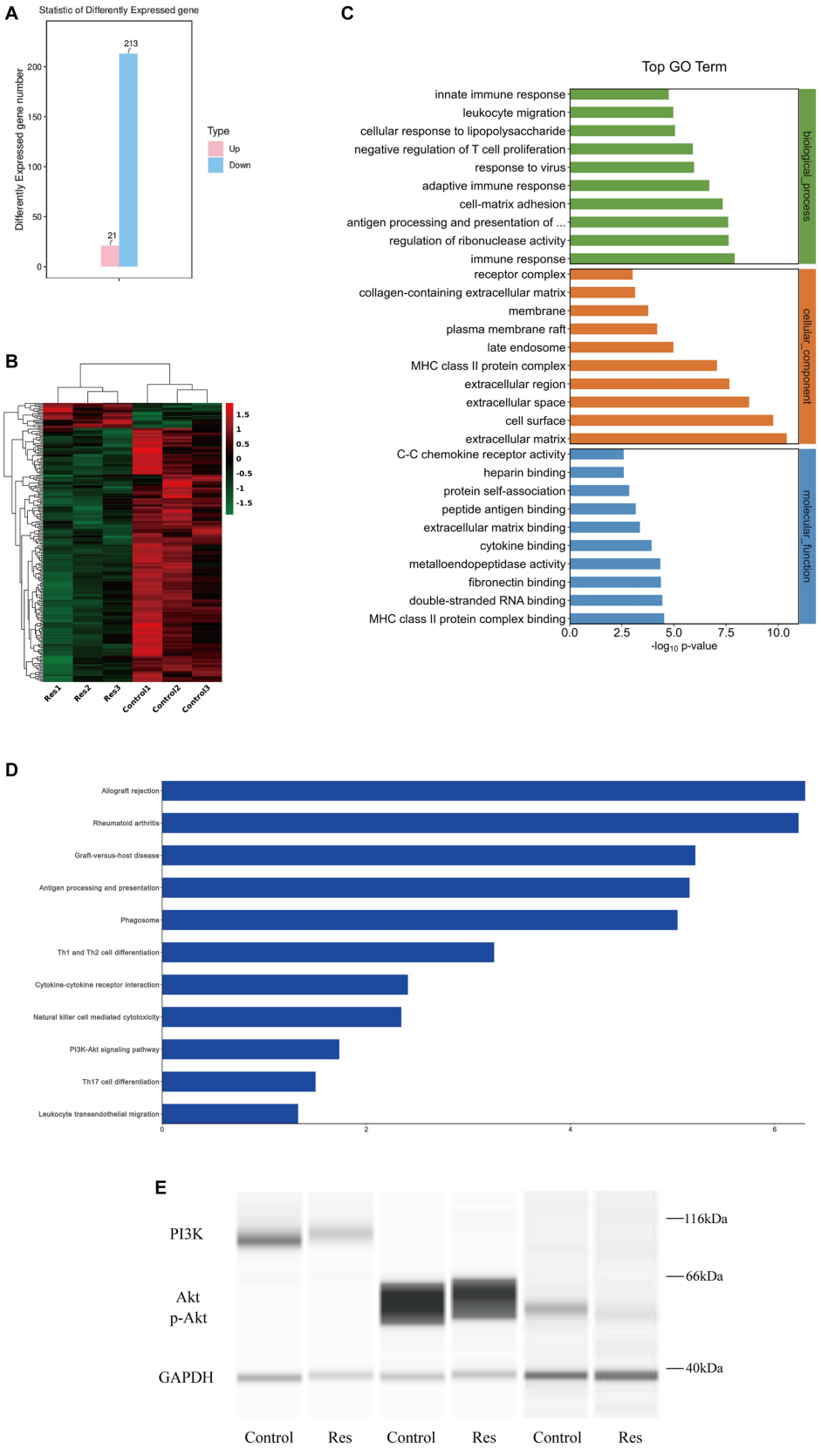

FIGURE 4
Results of RNA sequencing and protein verification of the PI3K/Akt pathway in the control and resveratrol groups. **(A)** Numbers of upregulated and downregulated DEGs in the two groups. **(B)** Differential gene expression heat map, with red indicating relatively high expression and green indicating relatively low expression of protein-coding genes. **(C)** Significant GO term enrichment statistics. The lower the GO term in the same category, the more meaningful it is. **(D)** KEGG pathway enrichment analysis. The higher the ranking, the more significant the change in the pathway. **(E)** Changes in PI3K/Akt signaling pathway protein expression after resveratrol treatment compared to the control group.

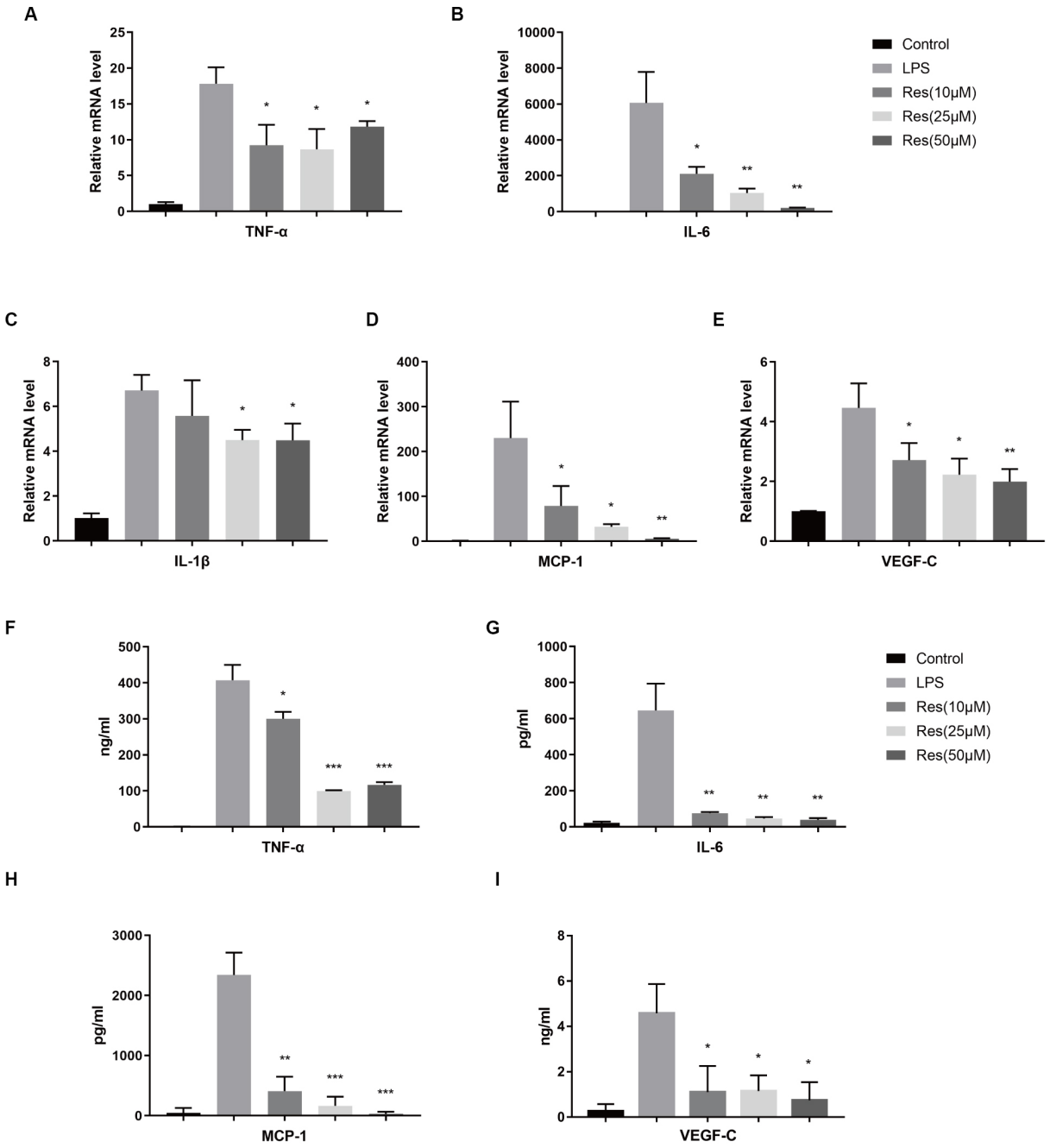

FIGURE 5
Effect of resveratrol on human macrophages *in vitro*. **(A–E)** Transcriptions of TNF-α, IL-6, IL-1β, MCP-1, and VEGF-C in different cell groups after LPS stimulation and resveratrol treatment. **(F–I)** Secretion of TNF-α, IL-6, MCP-1, and VEGF-C proteins in different cell groups after LPS stimulation and resveratrol treatment. The data are shown as mean ± SD. $*p < 0.05$, $**p < 0.01$, and $***p < 0.001$ between the resveratrol and LPS groups.

Thus, inhibiting macrophage recruitment and M1 macrophage polarization can prevent CGR (16, 17). Resveratrol can regulate a wide range of inflammatory components and plays an immunomodulatory role in immune cells. Its anti-inflammatory activity mainly targets macrophages (27). In this study, resveratrol reduced the recruitment of $CD11b^+$-labeled macrophages and the polarization ratio of $CD11b^+$ $iNOS^+$-labeled M1 macrophages compared to saline treatment. These results suggest that resveratrol can reduce macrophage recruitment and M1 macrophage polarization after corneal transplantation in rats, which may be a major reason for its action against CGR.

Previous studies indicated that resveratrol can inhibit the secretion of pro-inflammatory cytokines, such as IL-1, IL-6, and TNF-α, and increase the opposite effect of IL-10 produced by mouse macrophages, thereby regulating the activity of T cells and B cells (40, 41). M1 macrophages can secrete iNOS, IL-6, IL-1β, and TNF-α, which are pro-inflammatory cytokines associated with allograft rejection (39, 42). MCP-1, another important pro-inflammatory cytokine, can be secreted by macrophages during inflammation, significantly impacting the migration and infiltration of macrophages (43–45). Our experimental results are in line with

previous findings. Resveratrol significantly reduced the mRNA expression levels of TNF-α, IL-1β, IL-6, MCP-1, iNOS, and VEGF-C in corneas in the early stages after corneal transplantation. This was mainly related to a reduction in pro-inflammatory macrophages. A reduction in pro-inflammatory cytokines may also affect the subsequent recruitment of inflammatory cells and prevent CGR in the early postoperative period. These results suggest that resveratrol can prevent CGR by inhibiting macrophage recruitment and M1 macrophage polarization. Our *in vitro* cell experiments also showed that resveratrol significantly reduced the secretion of various pro-inflammatory cytokines by M1 macrophages stimulated by LPS. The results indicated that resveratrol can suppress M1 macrophage polarization *in vitro*.

Pathological corneal lymphangiogenesis significantly increases CGR rates (46). It has been reported that lymphatic vessel formation is a more important risk factor for CGR than neovascularization (47, 48). The generation of corneal lymphatic vessels after corneal damage depends on macrophages (49). An animal study suggested that a decrease in corneal neolymphatic vessels was associated with a decrease in the number of macrophages in the cornea (50). This may be because macrophages can secrete paracrine factors and promote lymphatic vessel angiogenesis by binding first to VEGF-C and VEGF-D and then to VEGFR-3 (51). Moreover, M1 macrophages have a greater ability to promote lymphatic vessel formation than M0 and M2 macrophages (52). M1 macrophages can secrete TNF-α, IL-1β, and VEGF-C, thereby promoting lymphatic endothelial cells proliferation (53–55). In summary, macrophages, especially M1 macrophages, can promote CGR by promoting the generation and growth of corneal lymphatic vessels. In this study, the growth of LYVE-1-labeled lymphatic vessels 7 days after surgery was considerably lower in the resveratrol group than in the control group and positively correlated with the growth of corneal neovascularization. This suggests that resveratrol can reduce the generation of new corneal lymphatic vessels after corneal transplantation, thereby preventing CGR. Similar to the above results, a recent study reported that treatment with dimethyl fumarate inhibited M1 macrophage polarization and lymphangiogenesis, prolonging the survival of corneal allografts in rats (56). Moreover, the proportion of DCs in the cervical lymph nodes of rats treated with resveratrol was significantly lower than in those of rats treated with saline. This suggests that a decrease in the generation of corneal lymphatic vessels suppresses the migration of APCs to local lymph nodes.

Our RNA sequencing analysis revealed that allograft rejection was one of the pathways with the greatest DEG enrichment after resveratrol treatment, providing further evidence that resveratrol can act against CGR. Moreover, the analysis also showed that resveratrol can affect T cells in the corneas. This might be due to its effect on macrophages and may also indicate that it can interfere with immune responses after corneal transplantation through various pathways. These results provide possible directions for future research.

In line with the RNA sequencing results, our Simple Western analysis showed that the PI3K, Akt and p-Akt protein contents in the corneas of the resveratrol group were considerably lower than in those of the control group. This suggests that the action of resveratrol against CGR may be related to the PI3K/Akt pathway. The PI3K/Akt signaling pathway, an important intracellular pathway, is related to many biological processes, including cell survival, proliferation, differentiation, and metabolism (57–59). Previous studies have shown that the PI3K/Akt pathway plays a complex and important role in transplant rejection. Regulatory T (Treg) cell therapy is a promising treatment for transplant rejection, and PTEN can promote the optimal function of human Treg cells by downregulating PI3K-Akt activity (60). Akt or PI3K inhibitors have been shown to prolong the survival of heterotopic cardiac allografts in mice (61). However, miR-151-5p upregulation has been shown to activate the PI3K/Akt signaling pathway and regulate the balance between Th17 and Treg cells, possibly preventing CGR (62). Moreover, the PI3K/Akt pathway has also been found to exert different effects on macrophages. The inhibition of the PI3K/Akt-1 pathway has been shown to induce synovial macrophage apoptosis in rheumatoid arthritis (63). Furthermore, it has been reported that different external stimuli can polarize macrophages into M1 or M2 macrophages by regulating the PI3K/Akt pathway (64, 65). These different or even conflicting results may be related to the activation of different subtypes of PI3K or Akt in macrophages (66). Our study provides only preliminary evidence that resveratrol can prevent CGR by regulating the PI3K/Akt pathway. Further research is needed to discover the specific interactions of PI3K/Akt subtypes and the mechanisms underlying their downstream effectors.

Despite the significant findings on the effects and mechanisms of resveratrol on CGR in rats, this study has certain limitations. First, as a preliminary study on drug efficacy, our experimental focus is to explore the impacts of the drug on animals. We confirmed that resveratrol can prevent CGR, and we preliminarily explored the underlying mechanism. In the future, further experiments are needed to explore the mechanisms of action of resveratrol. Second, intraperitoneal resveratrol injection is a simple and direct method selected to help us preliminarily verify the effects of resveratrol on CGR. During the one-month observation period, no significant side effects were observed. However, a longer observation period is required to confirm its safety. Moreover, it would be best to produce resveratrol eye drops. Finally, its efficacy needs to be further verified in trials involving humans before it is considered suitable for clinical use.

In conclusion, our findings suggest that resveratrol can significantly prolong corneal graft survival. Resveratrol can reduce corneal macrophage recruitment and M1 macrophage polarization and decrease pro-inflammatory cytokines and lymphatic vessel generation after corneal transplantation in rats. The PI3K/Akt pathway may be related to the effects of resveratrol on CGR. Resveratrol represents a promising strategy for preventing CGR and delaying its development.

Data availability statement

The datasets presented in this study can be found in online repositories. The names of the repository/repositories and accession number(s) can be found at: NCBI GSE236626.

Ethics statement

Ethical approval was not required for the studies on humans in accordance with the local legislation and institutional requirements because only commercially available established cell lines were used. The animal study was approved by the Institutional Animal

Care and Use Committee of Zhongshan Ophthalmic Center of Sun Yat-sen University (protocol code O2021044). The study was conducted in accordance with the local legislation and institutional requirements.

Author contributions

TH, CX, XD, and JW helped in the study design. CX and RG did the major works on animal experiments. MM, CO, and CH helped in animal experiments. CH helped in the statistical analysis. CX took the lead in writing the manuscript, with help from RG. All authors contributed to the article and approved the submitted version.

Funding

This work was funded by the Natural Science Foundation of Guangdong Province of China (Grant No. 2021A1515010309), the Young Scientists Fund of the National Natural Science Foundation of China (Grant No. 81900865), and the foundation of Zhongshan Ophthalmic Center of Sun Yat-sen University (Grant No. 3030902101216).

Conflict of interest

The authors declare that the research was conducted in the absence of any commercial or financial relationships that could be construed as a potential conflict of interest.

Publisher's note

References

1. Flaxman SR, Bourne RRA, Resnikoff S, Ackland P, Braithwaite T, Cicinelli MV, et al. Global causes of blindness and distance vision impairment 1990–2020: a systematic review and meta-analysis. *Lancet Glob Health*. (2017) 5:e1221–34. doi: 10.1016/s2214-109x(17)30393-5

2. Tan DT, Dart JK, Holland EJ, Kinoshita S. Corneal transplantation. *Lancet*. (2012) 379:1749–61. doi: 10.1016/s0140-6736(12)60437-1

3. Niederkorn JY. Corneal transplantation and immune privilege. *Int Rev Immunol*. (2013) 32:57–67. doi: 10.3109/08830185.2012.737877

4. Taylor AW. Ocular immune privilege and transplantation. *Front Immunol*. (2016) 7:37. doi: 10.3389/fimmu.2016.00037

5. Yin J. Advances in corneal graft rejection. *Curr Opin Ophthalmol*. (2021) 32:331–7. doi: 10.1097/icu.0000000000000767

6. Carnahan MC, Goldstein DA. Ocular complications of topical, peri-ocular, and systemic corticosteroids. *Curr Opin Ophthalmol*. (2000) 11:478–83. doi: 10.1097/00055735-200012000-00016

7. Mihatsch MJ, Kyo M, Morozumi K, Yamaguchi Y, Nickeleit V, Ryffel B. The side-effects of ciclosporine-a and tacrolimus. *Clin Nephrol*. (1998) 49:356–63.

8. Wynn TA, Chawla A, Pollard JW. Macrophage biology in development, homeostasis and disease. *Nature*. (2013) 496:445–55. doi: 10.1038/nature12034

9. Brissette-Storkus CS, Reynolds SM, Lepisto AJ, Hendricks RL. Identification of a Novel Macrophage Population in the Normal Mouse Corneal Stroma. *Invest Ophthalmol Vis Sci*. (2002) 43:2264–71.

10. Slegers TP, Torres PF, Broersma L, van Rooijen N, van Rij G, van der Gaag R. Effect of macrophage depletion on immune effector mechanisms during corneal allograft rejection in rats. *Invest Ophthalmol Vis Sci*. (2000) 41:2239–47.

11. van der Veen G, Broersma L, Dijkstra CD, van Rooijen N, van Rij G, van der Gaag R. Prevention of corneal allograft rejection in rats treated with subconjunctival injections of liposomes containing dichloromethylene diphosphonate. *Invest Ophthalmol Vis Sci*. (1994) 35:3505–15.

12. König S, Nitzki F, Uhmann A, Dittmann K, Theiss-Suennemann J, Herrmann M, et al. Depletion of cutaneous macrophages and dendritic cells promotes growth of basal cell carcinoma in mice. *PLoS One*. (2014) 9:e93555. doi: 10.1371/journal.pone.0093555

13. Shi Y, Luo P, Wang W, Horst K, Bläsius F, Relja B, et al. M1 but not M0 extracellular vesicles induce polarization of raw 264.7 macrophages via the Tlr 4-Nfκb pathway *in vitro*. *Inflammation*. (2020) 43:1611–9. doi: 10.1007/s10753-020-01236-7

14. Labonte AC, Tosello-Trampont AC, Hahn YS. The role of macrophage polarization in infectious and inflammatory diseases. *Mol Cells*. (2014) 37:275–85. doi: 10.14348/molcells.2014.2374

15. Murray PJ, Allen JE, Biswas SK, Fisher EA, Gilroy DW, Goerdt S, et al. Macrophage activation and polarization: nomenclature and experimental guidelines. *Immunity*. (2014) 41:14–20. doi: 10.1016/j.immuni.2014.06.008

16. Oh JY, Lee HJ, Ko AY, Ko JH, Kim MK, Wee WR. Analysis of macrophage phenotype in rejected corneal allografts. *Invest Ophthalmol Vis Sci*. (2013) 54:7779–84. doi: 10.1167/iovs.13-12650

17. Yu J, Li P, Li Z, Li Y, Luo J, Su W, et al. Topical administration of 0.3% tofacitinib suppresses M1 macrophage polarization and allograft corneal rejection by blocking stat 1 activation in the rat cornea. *Transl Vis Sci Technol*. (2022) 11:34. doi: 10.1167/tvst.11.3.34

18. Tian H, Lin S, Wu J, Ma M, Yu J, Zeng Y, et al. Kaempferol alleviates corneal transplantation rejection by inhibiting NLRP 3 Inflammasome activation and macrophage M1 polarization via promoting autophagy. *Exp Eye Res*. (2021) 208:108627. doi: 10.1016/j.exer.2021.108627

19. Niederkorn JY. High-risk corneal allografts and why they lose their immune privilege. *Curr Opin Allergy Clin Immunol*. (2010) 10:493–7. doi: 10.1097/ACI.0b013e32833dfa11

20. Zhang W, Schönberg A, Hamdorf M, Georgiev T, Cursiefen C, Bock F. Preincubation of donor tissue with a VEGF cytokine trap promotes subsequent high-risk corneal transplant survival. *Br J Ophthalmol*. (2022) 106:1617–26. doi: 10.1136/bjophthalmol-2021-319745

21. Hou Y, Bock F, Hos D, Cursiefen C. Lymphatic trafficking in the eye: modulation of lymphatic trafficking to promote corneal transplant survival. *Cells*. (2021) 10:1661. doi: 10.3390/cells10071661

22. Lyons MM, Yu C, Toma RB, Cho SY, Reiboldt W, Lee J, et al. Resveratrol in raw and baked blueberries and bilberries. *J Agric Food Chem*. (2003) 51:5867–70. doi: 10.1021/jf034150f

23. Liu C, Wang L, Wang J, Wu B, Liu W, Fan P, et al. Resveratrols in Vitis berry skins and leaves: their extraction and analysis by HPLC. *Food Chem*. (2013) 136:643–9. doi: 10.1016/j.foodchem.2012.08.017

24. Harikumar KB, Aggarwal BB. Resveratrol: a multitargeted agent for age-associated chronic diseases. *Cell Cycle*. (2008) 7:1020–35. doi: 10.4161/cc.7.8.5740

25. Xu XL, Deng SL, Lian ZX, Yu K. Resveratrol targets a variety of oncogenic and Oncosuppressive signaling for ovarian cancer prevention and treatment. *Antioxidants*. (2021) 10:1718. doi: 10.3390/antiox10111718

26. Lin MC, Liu CC, Lin YC, Liao CS. Resveratrol protects against cerebral ischemic injury via restraining lipid peroxidation, transition elements, and toxic metal levels, but enhancing anti-oxidant activity. *Antioxidants*. (2021) 10:1515. doi: 10.3390/antiox10101515

27. Malaguarnera L. Influence of resveratrol on the immune response. *Nutrients*. (2019) 11:946. doi: 10.3390/nu11050946

28. Wu SL, Yu L, Pan CE, Jiao XY, Lv Y, Fu J, et al. Apoptosis of lymphocytes in allograft in a rat liver transplantation model induced by resveratrol. *Pharmacol Res*. (2006) 54:19–23. doi: 10.1016/j.phrs.2006.01.011

29. Wu SL, Pan CE, Yu L, Meng KW. Immunosuppression by combined use of cyclosporine and resveratrol in a rat liver transplantation model. *Transplant Proc*. (2005) 37:2354–9. doi: 10.1016/j.transproceed.2005.03.112

30. Holland EJ, Chan CC, Wetzig RP, Palestine AG, Nussenblatt RB. Clinical and immunohistologic studies of corneal rejection in the rat penetrating keratoplasty model. *Cornea*. (1991) 10:374–80. doi: 10.1097/00003226-199109000-00003

31. Jiang L, Liu T, Xie L, Ouyang C, Ji J, Huang T. AICAR prolongs corneal allograft survival via the AMPK-mTOR signaling pathway in mice. *Biomed Pharmacother*. (2019) 113:108558. doi: 10.1016/j.biopha.2019.01.019

32. Pleyer U, Schlickeiser S. The taming of the shrew? The immunology of corneal transplantation. *Acta Ophthalmol*. (2009) 87:488–97. doi: 10.1111/j.1755-3768.2009.01596.x

33. Wu SL, Yu L, Jiao XY, Meng KW, Pan CE. The suppressive effect of resveratrol on protein kinase C theta in peripheral blood T lymphocytes in a rat liver transplantation model. *Transplant Proc*. (2006) 38:3052–4. doi: 10.1016/j.transproceed.2006.08.150

34. Kang JJ, Bozso SJ, Boe DE, Al-Adra DP, Moon MC, Freed DH, et al. Resveratrol attenuates stimulated T-cell activation and proliferation: potential therapy against cellular rejection in organ transplantation. *Am J Clin Exp Immunol*. (2020) 9:81–90.

35. Williams KA, White MA, Ash JK, Coster DJ. Leukocytes in the graft bed associated with corneal graft failure. Analysis by immunohistology and actuarial graft survival. *Ophthalmology*. (1989) 96:38–44. doi: 10.1016/s0161-6420(89)32949-6

36. Slegers TP, Broersma L, van Rooijen N, Hooymans JM, van Rij G, van der Gaag R. Macrophages play a role in the early phase of corneal allograft rejection in rats. *Transplantation*. (2004) 77:1641–6. doi: 10.1097/01.tp.0000129410.89410.f2

37. Niederkorn JY. Immune mechanisms of corneal allograft rejection. *Curr Eye Res*. (2007) 32:1005–16. doi: 10.1080/02713680701767884

38. Tian H, Wu J, Ma M. Implications of macrophage polarization in corneal transplantation rejection. *Transpl Immunol*. (2021) 64:101353. doi: 10.1016/j.trim.2020.101353

39. Dai Y, Cheng X, Yu J, Chen X, Xiao Y, Tang F, et al. Hemin promotes corneal allograft survival through the suppression of macrophage recruitment and activation. *Invest Ophthalmol Vis Sci*. (2018) 59:3952–62. doi: 10.1167/iovs.17-23327

40. Sharma S, Chopra K, Kulkarni SK, Agrewala JN. Resveratrol and curcumin suppress immune response through CD28/CTLA-4 and CD80 co-stimulatory pathway. *Clin Exp Immunol*. (2007) 147:155–63. doi: 10.1111/j.1365-2249.2006.03257.x

41. Akdis CA, Blaser K. Mechanisms of interleukin-10-mediated immune suppression. *Immunology*. (2001) 103:131–6. doi: 10.1046/j.1365-2567.2001.01235.x

42. Devraj VM, Kalidindi K, Guditi S, Uppin M, Taduri G. Macrophage polarization in kidney transplant patients. *Transpl Immunol*. (2022) 75:101717. doi: 10.1016/j.trim.2022.101717

43. Singh S, Anshita D, Ravichandiran V. MCP-1: function, regulation, and involvement in disease. *Int Immunopharmacol*. (2021) 101:107598. doi: 10.1016/j.intimp.2021.107598

44. Hanna A, Frangogiannis NG. Inflammatory cytokines and chemokines as therapeutic targets in heart failure. *Cardiovasc Drugs Ther*. (2020) 34:849–63. doi: 10.1007/s10557-020-07071-0

45. Stepp MA, Menko AS. Immune responses to injury and their links to eye disease. *Transl Res*. (2021) 236:52–71. doi: 10.1016/j.trsl.2021.05.005

46. Cursiefen C, Chen L, Dana MR, Streilein JW. Corneal lymphangiogenesis: evidence, mechanisms, and implications for corneal transplant immunology. *Cornea*. (2003) 22:273–81. doi: 10.1097/00003226-200304000-00021

47. Bock F, Onderka J, Dietrich T, Bachmann B, Pytowski B, Cursiefen C. Blockade of VEGFR 3-Signalling specifically inhibits lymphangiogenesis in inflammatory corneal neovascularisation. *Graefes Arch Clin Exp Ophthalmol*. (2008) 246:115–9. doi: 10.1007/s00417-007-0683-5

48. Dietrich T, Bock F, Yuen D, Hos D, Bachmann BO, Zahn G, et al. Cutting edge: lymphatic vessels, not blood vessels, primarily mediate immune rejections after transplantation. *J Immunol*. (2010) 184:535–9. doi: 10.4049/jimmunol.0903180

49. Hos D, Cursiefen C. Lymphatic vessels in the development of tissue and organ rejection. *Adv Anat Embryol Cell Biol*. (2014) 214:119–41. doi: 10.1007/978-3-7091-1646-3_10

50. Kiesewetter A, Cursiefen C, Eming SA, Hos D. Phase-specific functions of macrophages determine injury-mediated corneal hem- and lymphangiogenesis. *Sci Rep*. (2019) 9:308. doi: 10.1038/s41598-018-36526-6

51. Karpanen T, Alitalo K. Molecular biology and pathology of lymphangiogenesis. *Annu Rev Pathol*. (2008) 3:367–97. doi: 10.1146/annurev.pathmechdis.3.121806.151515

52. Zhang Y, Zhang C, Li L, Liang X, Cheng P, Li Q, et al. Lymphangiogenesis in renal fibrosis arises from macrophages via VEGF-C/VEGFR 3-dependent autophagy and polarization. *Cell Death Dis*. (2021) 12:109. doi: 10.1038/s41419-020-03385-x

53. Peppicelli S, Bianchini F, Calorini L. Inflammatory cytokines induce vascular endothelial growth factor-C expression in melanoma-associated macrophages and stimulate melanoma lymph node metastasis. *Oncol Lett*. (2014) 8:1133–8. doi: 10.3892/ol.2014.2297

54. Nihei M, Okazaki T, Ebihara S, Kobayashi M, Niu K, Gui P, et al. Chronic inflammation, lymphangiogenesis, and effect of an anti-VEGFR therapy in a mouse model and in human patients with aspiration pneumonia. *J Pathol*. (2015) 235:632–45. doi: 10.1002/path.4473

55. Cursiefen C, Chen L, Borges LP, Jackson D, Cao J, Radziejewski C, et al. VEGF-A stimulates lymphangiogenesis and hemangiogenesis in inflammatory neovascularization via macrophage recruitment. *J Clin Invest*. (2004) 113:1040–50. doi: 10.1172/jci20465

56. Yu J, Li Y, Li Z, Li H, Chen Y, Chen X, et al. Subconjunctival injections of dimethyl fumarate inhibit lymphangiogenesis and allograft rejection in the rat cornea. *Int Immunopharmacol*. (2021) 96:107580. doi: 10.1016/j.intimp.2021.107580

57. Tóthová Z, Šemeláková M, Solárová Z, Tomc J, Debeljak N, Solár P. The role of Pi3k/Akt and MAPK signaling pathways in erythropoietin signalization. *Int J Mol Sci*. (2021) 22:7682. doi: 10.3390/ijms22147682

58. Hoxhaj G, Manning BD. The Pi3k-Akt network at the interface of oncogenic signalling and cancer metabolism. *Nat Rev Cancer*. (2020) 20:74–88. doi: 10.1038/s41568-019-0216-7

59. Barzegar Behrooz A, Talaie Z, Jusheghani F, Łos MJ, Klonisch T, Ghavami S. Wnt and Pi3k/Akt/mTOR survival pathways as therapeutic targets in glioblastoma. *Int J Mol Sci*. (2022) 23:1353. doi: 10.3390/ijms23031353

60. Lam A, Haque M, Ward-Hartstonge K, Uday P, Wardell C, Gillies J, et al. PTEN is required for human Treg suppression of costimulation *in vitro*. *Eur J Immunol*. (2022) 52:1482–97. doi: 10.1002/eji.202249888

61. Sang AX, McPherson MC, Ivison GT, Qu X, Rigdon J, Esquivel CO, et al. Dual blockade of the Pi3k/Akt/mTOR pathway inhibits posttransplant Epstein-Barr virus B cell lymphomas and promotes allograft survival. *Am J Transplant*. (2019) 19:1305–14. doi: 10.1111/ajt.15216

62. Cao Q, Li Y, Li Y, Li L. miR-151-5p alleviates corneal allograft rejection by activating Pi3k/Akt signaling pathway and balancing Th17/Treg after corneal transplantation via targeting IL-2Rα. *Ann Transl Med*. (2021) 9:1410. doi: 10.21037/atm-21-2054

63. Liu H, Huang Q, Shi B, Eksarko P, Temkin V, Pope RM, et al. Regulation of Mcl-1 Expression in Rheumatoid Arthritis Synovial Macrophages. *Arthritis Rheum*. (2006) 54:3174–81. doi: 10.1002/art.22132

64. Weisser SB, McLarren KW, Voglmaier N, van Netten-Thomas CJ, Antov A, Flavell RA, et al. Alternative activation of macrophages by IL-4 requires SHIP degradation. *Eur J Immunol*. (2011) 41:1742–53. doi: 10.1002/eji.201041105

65. Vergadi E, Vaporidi K, Theodorakis EE, Doxaki C, Lagoudaki E, Ieronymaki E, et al. Akt 2 deficiency protects from acute lung injury via alternative macrophage activation and miR-146a induction in mice. *J Immunol*. (2014) 192:394–406. doi: 10.4049/jimmunol.1300959

66. Vergadi E, Ieronymaki E, Lyroni K, Vaporidi K, Tsatsanis C. Akt signaling pathway in macrophage activation and M1/M2 polarization. *J Immunol*. (2017) 198:1006–14. doi: 10.4049/jimmunol.1601515

frontiers | Frontiers in Medicine

TYPE Original Research
PUBLISHED 25 October 2023
DOI 10.3389/fmed.2023.1295633

OPEN ACCESS

EDITED BY
Georgios D. Panos,
Nottingham University Hospitals NHS Trust, United Kingdom

REVIEWED BY
Luis Haddock,
University of Miami, United States
Michael A. Klufas,
Wills Eye Hospital, United States

*CORRESPONDENCE
Jakob Siedlecki
✉ Jakob.siedlecki@med.uni-muenchen.de

RECEIVED 16 September 2023
ACCEPTED 11 October 2023
PUBLISHED 25 October 2023

CITATION
Klaas JE, Bui V, Maierhofer N, Schworm B, Maier M, Priglinger SG and Siedlecki J (2023) Risk of transient vision loss after intravitreal aflibercept using vial-prepared vs. the novel prefilled syringe formulation.
Front. Med. 10:1295633.
doi: 10.3389/fmed.2023.1295633

Risk of transient vision loss after intravitreal aflibercept using vial-prepared vs. the novel prefilled syringe formulation

Julian E. Klaas[1], Vinh Bui[1], Niklas Maierhofer[2], Benedikt Schworm[1], Mathias Maier[2], Siegfried G. Priglinger[1] and Jakob Siedlecki[1]*

[1]Department of Ophthalmology, Ludwig-Maximilians-University, Munich, Germany, [2]Department of Ophthalmology, Technical University, Munich, Germany

Purpose: To compare the risk of transient vision loss (TVL) probably attributable to a severe intraocular pressure spike after intravitreal aflibercept application using the novel prefilled syringe (PFS) vs. the established vial system (VS).

Methods: Datasets of the intravitreal injection service of the Ludwig Maximilians-University Munich and the Technical University Munich, Germany, were screened for documentation of TVL after intravitreal injection of aflibercept. The observation period included two full months prior to the introduction of the novel PFS and two months afterwards. TVL was defined as loss of perception of hand motion for a duration of >30 s.

Results: Over a period of four months, 1720 intravitreal injections of aflibercept were administered in 672 patients. There were 842 injections with the old VS, and 878 injections using the novel PFS. Using the VS, TVL was noted during two injections (0.24%) in two patients, as compared to 11 cases of TVL (1.25%) in 10 patients with the PFS ($p = 0.015$). Using the PFS, patients had a 5.3-fold risk of TVL as compared to the VS (OR: 5.33; 95% CI: 1.2–24.1; $p = 0.0298$).

Conclusion: There was a more than five-fold risk of TVL using the novel pre-filled aflibercept syringe as compared to the established vial system. During informed consent, this risk should be discussed.

KEYWORDS

Eylea, aflibercept, prefilled syringe, choroidal neovascularization, age related macular degeneration, diabetic macular edema, retinal vein occlusion

1. Introduction

In the last decade, the introduction of intravitreal vascular endothelial growth factor (VEGF) inhibitors has revolutionized the treatment of a multitude of retinal diseases (1). Currently, ranibizumab, aflibercept and brolucizumab possess approval for the treatment of one or more mostly macular disorders, while bevacizumab is being widely used as an off-label alternative (1). In this competitive field, pharmaceutical innovation, e.g., the modification of posology, tissue penetration or sheer efficacy in retinal drying is strategically addressed to secure and expand market share.

In this context, aflibercept was approved and launched as a novel prefilled syringe (PFS) in the USA in August 2019 and in the European Union in April 2020 in order to potentially enable a more streamlined and efficient injection procedure (2, 3). Shortly after introduction, surgeons at the Department of Ophthalmology of both Technical University Munich (TUM) and Ludwig Maximilians-University (LMU) experienced an unusually high incidence of transient vision loss (TVL) due to suspected intraocular pressure spikes directly after the intravitreal application of aflibercept using the novel PFS. Due to the loss of visual acuity suggesting transient central retinal artery occlusion (4), associated long-term damage, e.g., permanent arterial occlusion (5), cannot be excluded. Apart from a recent publication by Gallagher et al. reporting the first case series of transient retinal artery occlusion associated with the aflibercept PFS in 5 eyes of 4 patients (6), we are not aware of any clinical studies that have investigated this issue. Therefore, this retrospective multicenter cross-sectional study was designed to compare the incidence of TVL using the old vial-based injection system vs. the novel PFS system.

2. Materials and methods

In LMU, the novel aflibercept PFS (Bayer, Leverkusen, Germany) was introduced on July 27th, 2020; in TUM, the introduction date was June 1st, 2020. To determine the incidence of TVL, two months (9 calendar weeks) prior to and after switching from the vial to the novel PFS system were defined as observation period. Thus, the observation period at LMU was May 25th until July 26th 2020 for the vial system, and July 27th until September 27th 2020 for the novel PFS. At TUM, the respective observation periods were March 30th until May 31st 2020 for the vial system, and June 1st until August 2nd 2020 for the novel PFS system.

To assess the incidence of TVL, anonymized datasets generated from both intravitreal injection service databases covering the aforementioned observation period were screened for a documentation of TVL associated with an aflibercept injection as defined below as well as required pharmacologic or surgical interventions (e.g., application of eye-pressure lowering agents or paracentesis). Because the research was performed on anonymized data, no prior approval of the respective ethics committees was required.

2.1. Injection procedure

All patients were injected in designated intravitreal injection operating rooms according to established hygiene protocols and standard operating procedures. Prior to entering the operating room, all patients were dressed in a hygienic overcoat and equipped with a surgical cap. After topical anesthesia, eyes, lids and periocular skin were disinfected with 1% povidone iodine in supine position. The eyes were then draped and a lid speculum was inserted. Aflibercept was injected in a distance of 3.5 to 4.0 mm posteriorly to the limbus using either Becton Dickinson syringes filled from the aflibercept vial or the novel PFS. A 30 Gauge needle was used in all cases. The correct injection volume of 50 µL was prepared according to the package insert by one of two specialized nurses and checked by the surgeon prior to injection (LMU), or both prepared and checked by the surgeon (TUM). Hereby, the base of the plunger dome (not the tip of the dome) was aligned with the dosing mark. Where possible, care was taken to ensure that the plunger was not aligned proximal or distal to the mark. Directly after injection, visual acuity of hand motion and above was examined at a distance of 1 foot. No changes in equipment or injection technique occurred during the observation period.

2.2. Definition of TVL

TVL was defined as loss of hand motion immediately or within the first minute after the injection for a duration of >30 s with a hard eye ball on palpation. The need for paracentesis was assessed individually by the surgeon based on the duration of loss of hand motion, palpation of the globe and the individual spontaneous tendency for resolution including the patient's subjective course of symptoms within the first **2** min. Epidemiological data was obtained from the anonymized datasets to correlate TVL during aflibercept therapy with age, gender, ocular comorbidities as well as history of prior TVL during intravitreal injection and the numbers of aflibercept applications before the date of TVL.

2.3. Statistical analysis

All data were gathered and analyzed in Microsoft Excel spreadsheets (Version 16.23 for Mac; Microsoft, Redmond, WA, United States). Statistical analysis was performed in SPSS Statistics 26 (IBM Germany GmbH, Ehningen, Germany). The level to indicate statistical significance was defined as $p < 0.05$. Statistical analyses of intra-group differences were performed using a Chi-Square test and Fisher's exact test. Graphs and diagrams were plotted in Microsoft Excel.

3. Results

In total, 1720 injection procedures of intravitreal aflibercept were performed during the defined time span in 672 patients. Of these, 842 (49.0%) were performed with the old vial system, and 878 (51.0%) were performed with the new PFS. With the vial system, 2 eyes of 2 patients (0.24%) experienced TVL; with the new PFS, 11 eyes (1.25%) of 10 patients experienced TVL ($p = 0.015$; Figure 1). Six different surgeons were involved in all cases of TVL (2 with the vial system, 5 with the PFS).

The two patients experiencing TVL with the vial system were both men (100%) with a mean age of 83 ± 1.4 years. The reason for treatment was neovascular AMD in both eyes (100%). There was one right and one left eye, and there were 32 and 1 previous aflibercept injections prior to TVL. None of these eyes (0%) had experienced TVL prior to this study. One eye (50%) had a history of ocular hypertension with IOP values around 25 mmHg. These two events of TVL occurred to two different surgeons. None of these eyes required paracentesis.

The 10 patients experiencing TVL with the PFS were equally male/female (50/50%) with a mean age of 75.6 ± 9.2 years. The reason for treatment in the 11 eyes was neovascular AMD in 6 eyes (54.5%), diabetic macular edema in 2 eyes (18.2%), macular edema

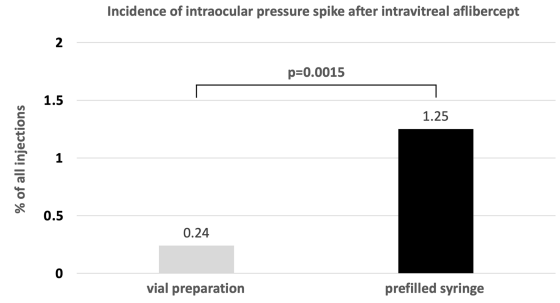

FIGURE 1
Incidence of transient vision loss due to ocular hypertension with the aflibercept vial system vs. the novel PFS system.

due to central retinal vein occlusion in 2 eyes (18.2%) and branch retinal vein occlusion in 1 eye (9.1%). There were 3 right (27.3%) and 8 left eyes (72.7%), and there were mean 15.1 ± 14.7 previous aflibercept injections prior to TVL. One of these eyes (9.1%) had experienced one event of TVL prior to this study. Five eyes (45.5%) had a history of manifest glaucoma. The 11 events of TVL with the aflibercept PFS occurred in 5 surgeons (surgeon 1: 4 events; surgeon 2: 3 events; surgeon 3: 2 events; surgeons 4 and 5: 1 event). Eight out of the 11 cases of TVL (72.7%) required a paracentesis, which was performed at least once by 5 out of the 6 surgeons (83.3%). Table 1 summarizes the demographic and clinical characteristics of all patients experiencing TVL before and after the introduction of PFS.

Overall, the risk of TVL was 5.3 times higher with the PFS as compared to the old vial system (OR: 5.33; 95% CI: 1.2–24.1; $p = 0.0298$). Using the aflibercept PFS, events of TVL were homogenously distributed over the 9 week observation period with an incidence of 1.06% in the first, 1.98% in the second, 2.11% in the third, 2.91% in the fourth, 1.04% in the fifth, 0% in the sixth to eighth and 2.08% in the ninth week (Figure 2). No other serious adverse events (e.g., endophthalmitis, retinal detachment, hemorrhage) were observed during the study period.

TABLE 1 Characteristics of patients with transient vision loss (TVL) after intravitreal administration of aflibercept, using the established vial system vs. the newer PFS system.

Characteristics of patients with TVL	Vial system	Prefilled syringe
Number of eyes with TVL/total, *no. (%)*	2 / 842 (0.24%)[π]	11 / 878 (1.25%)[ƒ]
Sex		
Male, *no. (%)*	2 (100)	5 (50)
Female, *no. (%)*	0 (0)	5 (50)
Age *mean ± SD, in years*	83 ± 1.4	75.6 ± 9.2
Eye		
Right, *no. (%)*	1 (50)	3 (27.3)
Left, *no. (%)*	1 (50)	8 (72.7)
Prior injections, *mean no. ± SD*	16.5 ± 15.5	15.1 ± 14.7
Reason for treatment*		
Neovascular AMD, *no. (%)*	2 (100)	6 (54.5)
Diabetic macular edema, *no. (%)*	0 (0)	2 (18.2)
Central retinal vein occlusion, *no. (%)*	0 (0)	2 (18.2)
Branch retinal vein occlusion, *no. (%)*	0 (0)	1 (9.1)
Other, *no. (%)*	0 (0)	0 (0)
Other ocular comorbidities*		
Ocular hypertension, *no. (%)*	1 (50)	0 (0)
Glaucoma, *no. (%)*	0 (0)	5 (45.5)
Eyes with TVL prior to observation period, *no. (%)**	0 (0)	1 (9.1)°
Surgeons involved in TVL events, *no.*	2	5^
Need for paracentesis, *no.* ¥*	0 (0)	8 (72.7) Ω

[π] 2 eyes with TVL in 2 patients.
ƒ 11 eyes with TVL in 10 patients.
*percentage of the total number of eyes with TVL.
°one prior TVL event was documented in this case.
^surgeon 1: 4 events; surgeon 2: 3 events; surgeon 3: 2 events; surgeons 4 and 5: 1 event.
¥the need for paracentesis was assessed individually by the surgeon based on the duration of loss of perception of hand motion, palpation of the globe and the individual spontaneous tendency for resolution including the patient's subjective course of symptoms within the first 2 min.
Ωa paracentesis was performed at least once by 5 out of the 6 surgeons (83.3%).

4. Discussion

This study suggests a higher incidence of intraocular pressure spikes with transient vision loss immediately after intravitreal injection of aflibercept when using the novel PFS formulation as compared to the established vial system with conventional 1.0 mL insulin syringes. During a time span of 4 months with 1720 injections in 672 patients, significant spikes impacting visual acuity directly after the procedure were seen in 0.24% with the vial system, and in 1.25% with the novel PFS, resulting in an odds ratio of 5.33 (95% CI: 1.2–24.1; $p = 0.0298$).

As spikes were not defined by absolute measurements of intraocular pressure (e.g., with Goldmann applanation), but rather defined as transient vision loss with a palpatory hard eye ball, occlusion of the central retinal artery has to be assumed to be the driving pathomechanism (4). Since subsequent permanent retinal artery occlusion cannot be excluded (5) and optic nerve heads at risk (e.g., glaucoma) could be substantially harmed by such spikes (e.g., wipeout) (7), the complication reported herein represents a significant safety issue, even if rapid treatment can usually avoid long-term damage.

Concerning treatment of the cases reported herein, the standard operating procedures of both clinics suggest paracentesis with drainage of aqueous humor in eyes that do not regain visual acuity within 30–60 s. Interestingly, the majority (73%) of eyes treated with the PFS required urgent paracentesis to relieve the pressure since no spontaneous amelioration of intraocular perfusion was observed. In addition to the risk of the pressure spike itself, the majority of eyes complicated by such spikes will also undoubtedly be exposed to secondary complications, e.g., endophthalmitis, hemorrhage or hypotony in the case of leakage through the paracentesis, even if rare.

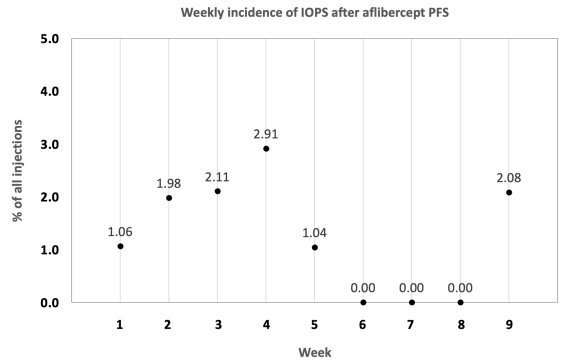

FIGURE 2
Distribution of transient vision loss (TVL) due to an intraocular pressure spike (IOPS) after aflibercept PFS introduction. TVL was consistently seen from week one through week 9.

We therefore believe that, especially in a procedure performed so frequently each day all over the world, these safety concerns should be taken seriously.

In the present study, the incidence of TVL found in eyes treated with the new PFS was higher not only compared to the vial system, but also compared to the known incidence of acute vision loss after intravitreal injection, which has been reported to be 0.14% (8).Two main hypotheses could explain why spikes in intraocular pressure might exacerbate with the novel PFS as compared to the vial system or compared to the ranibizumab prefilled syringe (Novartis, Basel, Switzerland). Recently, Gallagher et al. reported the first case series of transient retinal artery occlusion with the aflibercept PFS in 5 eyes of 4 patients (6). In this article, the authors refer to the different diameters of the conventional 1 mL syringe as compared to the aflibercept PFS, resulting in different calculated internal surface areas of 32 mm^2 for the aflibercept PFS, and 16.6 mm^2 for the 1 mL syringe (6). In fact, the authors were able to show that six injectors performing 20 sham injections each (120 sham injections in total) accidentally sham-injected a volume of 0.07 mL or more in 21% of procedures with the PFS. Thus, even slight errors in plunger alignment can lead to much higher variability in injection volume in the aflibercept PFS (6). This was confirmed by a more recent *in vitro* study, which evaluated the accuracy of injection volumes by 20 ophthalmologists using the PFS vs. a 1 mL BD syringe and a micro scale (9). The authors found that both injection volume and variability were significantly higher with the PFS system than with the previously used system (9). This phenomenon seems to be reproducible when compared to any syringe with a smaller diameter, including other prefilled formulations such as ranibizumab, as was recently shown by Hinkle et al. (10). However, we believe that even with a correctly dosed PFS, sharp rises of intraocular pressure could be provoked by different injection speeds and volume jets due to the higher diameter of the novel PFS resulting in both a shorter distance that the plunger needs to be pushed (aflibercept PFS 2.2 mm; 1 mL syringe: 4.2 mm) and the perception of a higher initial resistance (6). This assumption is supported by previous findings that higher IOP spikes after intravitreal injections have been documented in association with a smaller needle bore size (11). The same should be true for a constant needle bore size (30 gauge) but wider syringe diameters: assuming similar plunger speed applied by the surgeon, the flow rate of aflibercept into the vitreous cavity in an almost doubled surface area should be proportionally higher.

At the recent Pharmacovigilance Risk Assessment Committee (PRAC) meeting held on March 8th 2021, the European Medicines Agency (EMA) issued a statement that a "higher-than-expected proportion of cases of increased pressure inside the eye (intraocular pressure) were reported with the Eylea pre-filled syringes" (12), strengthening the importance of the matter. As "incorrect handling" was given as most probable cause of the problem, the acuity of the problem should be communicated to the ophthalmological community and additional training should be provided. In our study, however, spikes in IOP occurred to six different surgeons who are accustomed to double-checking the correct injection volume. Moreover, these spikes did not occur only shortly after the PFS introduction, but were consistently observed over the course of the 9 weeks evaluated, starting with 1% at week 1, 3% at week 4, and 2% at week 9. All adverse events reported in this study were communicated to the manufacturer and the relevant regulatory authorities.

Limitations of our study include its retrospective nature and the lack of IOP measurements in the cases reported. Since these spikes with central artery occlusion represent a severe acute complication, these patients were kept on the operating table for a possible immediate intervention and were not transferred to a slit lamp for Goldmann applanation tonometry. Furthermore, due to the low absolute number of TVL events, the confidence intervals are rather wide, indicating that better statistical power could be achieved with an even larger sample size, which may be difficult however, due to the low incidence of TVL, especially in the „control group", and may require a multi-centric study with a high case number.

In conclusion, our analysis of a large database of 1720 intravitreal aflibercept procedures suggests that the current aflibercept PFS has a more than fivefold risk of significant transient intraocular pressure spikes over the conventional vial system used with a 1 mL syringe. Since these spikes were accompanied by transient vision loss, central retinal artery occlusion has to be assumed, making this a severe complication. As PFS systems represent an easier-to-use and potentially more efficient way to administer intravitreal substances with a lower intraocular infection risk (13), the current aflibercept PFS system may benefit from a redesign to make it less vulnerable to the complication described herein (13).

Data availability statement

The raw data supporting the conclusions of this article will be made available by the authors, upon reasonable request.

Author contributions

JK: Conceptualization, Data curation, Investigation, Writing – original draft, Writing – review & editing. VB: Data curation, Investigation, Methodology, Validation, Writing – review & editing. NM: Data curation, Investigation, Methodology, Writing – review & editing. BS: Conceptualization, Investigation, Methodology, Writing – review & editing. MM: Supervision, Writing – review & editing. SP: Data curation, Project administration, Supervision, Writing – review

& editing. JS: Conceptualization, Data curation, Methodology, Supervision, Writing – original draft.

Funding

The author(s) declare that no financial support was received for the research, authorship, and/or publication of this article.

Acknowledgments

The authors would like to thank Sonja Schober for her excellent technical assistance.

Conflict of interest

JK received previous speaker honoraria from Novartis Pharma GmbH. BS received previous speaker honoraria and travel expenses from Novartis Pharma GmbH and Topcon Corporation. MM received previous speaker honoraria from Novartis Pharma GmbH, Allergan GmbH, Bayer AG, Heidelberg Engineering GmbH, and Carl Zeiss Meditec AG, and research grants for clinical trials Bayer AG, Novartis Pharma GmbH, and Roche AG. SP received previous speaker honoraria, personal consultation honoraria and travel expenses from Novartis Pharma GmbH, Oertli AG, Bayer AG, Alcon Pharma GmbH and Allergan GmbH. JS received previous speaker honoraria, personal consultations honoraria and travel expenses from Apellis Pharmaceuticals GmbH, Novartis Pharma GmbH, Bayer AG, Roche AG, Carl Zeiss Meditec AG, Oculentis OSD Medical GmbH and Allergan GmbH.

The remaining authors declare that the research was conducted in the absence of any commercial or financial relationships that could be construed as a potential conflict of interest.

Publisher's note

References

1. Adamis AP, Brittain CJ, Dandekar A, Jill Hopkins J. Building on the success of anti-vascular endothelial growth factor therapy: a vision for the next decade. *Eye*. (2020) 34:1966–72. doi: 10.1038/s41433-020-0895-z

2. Bayer (2020). Availble at: https://www.pharmiweb.com/press-release/2020-04-09/bayer-receives-approval-in-europe-for-pre-filled-syringe-to-administer-aflibercept-eylea (accessed April 1st 2021).

3. Regeneron Pharmaceuticals Inc. (2014). Available at: https://investor.regeneron.com/news-releases/news-release-details/regeneron-announces-eylear-aflibercept-injection-approved/ (accessed April 1st 2021).

4. Mansour AM, Shahin M, Kofoed PK, Parodi MB, Shami M, Schwartz SG. Insight into 144 patients with ocular vascular events during Vegf antagonist injections. *Clin Ophthalmol*. (2012) 6:343–63. doi: 10.2147/OPTH.S29075

5. Gao X, Borkar D, Obeid A, Hsu J, Ho AC, Garg SJ. Incidence of retinal artery occlusion following intravitreal Antivascular endothelial growth factor injections. *Acta Ophthalmol*. (2019) 97:e938–9. doi: 10.1111/aos.14058

6. Gallagher K, Raghuram AR, Williams GS, Davies N. Pre-filled Aflibercept syringes-variability in expressed fluid volumes and a case series of transient central retinal artery occlusions. *Eye (Lond)*. (2020) 35:2899–900. doi: 10.1038/s41433-020-01211-4

7. de Vries VA, Bassil FL, Ramdas WD. The effects of intravitreal injections on intraocular pressure and retinal nerve Fiber layer: a systematic review and Meta-analysis. *Sci Rep*. (2020) 10:13248. doi: 10.1038/s41598-020-70269-7

8. Shima C, Sakaguchi H, Gomi F, Kamei M, Ikuno Y, Oshima Y, et al. Complications in patients after intravitreal injection of bevacizumab. *Acta Ophthalmol*. (2008) 86:372–6. doi: 10.1111/j.1600-0420.2007.01067.x

9. Guest JM, Malbin B, Abrams G, Parendo A, Das S, Okeagu C, et al. Accuracy of intravitreal injection volume for Aflibercept pre-filled syringe and Bd Luer-Lok one-milliliter syringe. *Int J Retina Vitreous*. (2022) 8:27. doi: 10.1186/s40942-022-00375-3

10. Hinkle JW, Hsu J. The relationship between stopper position and injection volume in Ranibizumab and Aflibercept prefilled syringes. *Retina*. (2021) 41:2510–4. doi: 10.1097/IAE.0000000000003232

11. Kim JE, Mantravadi AV, Hur EY, Covert DJ. Short-term intraocular pressure changes immediately after intravitreal injections of anti-vascular endothelial growth factor agents. *Am J Ophthalmol*. (2008) 146:930–934.e1. doi: 10.1016/j.ajo.2008.07.007

12. EMA (Press office) (2021). Available at: https://www.ema.europa.eu/en/news/meeting-highlights-pharmacovigilance-risk-assessment-committee-prac-8-11-march-2021 (accessed April 8th 2021).

13. Storey PP, Tauqeer Z, Yonekawa Y, Todorich B, Wolfe JD, Shah SP, et al. The impact of prefilled syringes on Endophthalmitis following intravitreal injection of Ranibizumab. *Am J Ophthalmol*. (2019) 199:200–8. doi: 10.1016/j.ajo.2018.11.023

frontiers | Frontiers in Medicine

TYPE Original Research
PUBLISHED 21 November 2023
DOI 10.3389/fmed.2023.1286159

OPEN ACCESS

EDITED BY
Georgios D. Panos,
Nottingham University Hospitals NHS Trust, United Kingdom

REVIEWED BY
Purvasha Narang,
All India Institute of Medical Sciences Nagpur, India
Minhong Xiang,
Putuo District Central Hospital, China
Yun Feng,
Peking University Third Hospital, China

*CORRESPONDENCE
Mansha He
✉ manshahe@126.com

RECEIVED 31 August 2023
ACCEPTED 06 November 2023
PUBLISHED 21 November 2023

CITATION
Song X, Zhang C, Zhang S and He M (2023) Therapeutic efficacy of optimal pulse technology in the treatment of *chalazions*. *Front. Med.* 10:1286159. doi: 10.3389/fmed.2023.1286159

Therapeutic efficacy of optimal pulse technology in the treatment of *chalazions*

Xi Song, Chunying Zhang, Saisai Zhang and Mansha He*

Guangzhou Aier Eye Hospital Affiliated to Jinan University, Guangzhou, Guangdong, China

Introduction: To evaluate the efficacy of optimized pulse technology in treating chalazia.

Methods: Prospective before-after study. All patients received two sessions of optimal pulse technology (OPT) with an interval of 1 week. The first visit was before treatment and the patients underwent 2 treatment sessions with a 1-week interval. The non-invasive tear breakup time (NIBUT), corneal fluorescein staining (CFS) score, Schirmer's test I without anesthesia, conjunctival hyperemia, and meibomian gland area were compared before and after treatment, and the related factors of curative effect were analyzed.

Results: 23 patients (23 eyes) with chalazia were included. All patients received two sessions of OPT treatment at 1-week intervals. Following the first OPT treatment, a reduction in the chalazion size was observed in 17 patients (73.91%). One patient was completely cured, and 1 patient had an increase in the diameter of the chalazion. The meibomian gland area increased significantly compared to before treatment ($p = 0.023$). Compared with baseline, the conjunctival congestion and ST decreased, NIBUT increased, and there was no statistical difference. After the second treatment, the chalazion size decreased in 21 cases, and 3 patients were cured. A significant increase in the meibomian gland area compared with the baseline area ($p < 0.001$). Additionally, conjunctival congestion decreased significantly. After two sessions, the Schirmer test exhibited a decrease, and NIBUT increased, although these changes did not reach statistical significance. The curative effect was unrelated to sex, age, first onset, single disease, and other factors.

Conclusion: After treatment, the diameter of chalazions was reduced in 91.3% of the patients, and the area of the meibomian gland was significantly increased compared with that before treatment, which suggested that 2 OPT treatments at an interval of 1 week can improve the signs of adult patients in the non-acute infectious stage with chalazia.

KEYWORDS

***chalazions*, optimal pulse technology, meibomian gland cyst, meibomian gland area, conjunctival congestion**

1 Introduction

Chalazion, a chronic inflammatory granuloma, occurs due to the blockage of meibomian glands and the accumulation of glandular secretions. Among Asians, the estimated prevalence of this condition is almost 4% (1). Despite being a common disease, recurrent episodes and treatments might exacerbate the impairment of the meibomian gland structure and function,

resulting in scarring, increased eye discomfort, and decreased quality of life (2). In the presence of an infection, it might develop into orbital cellulitis, posing a potentially life-threatening situation (3).

Chalazions typically resolve on their own and can be managed in the initial stages of the disease through the application of a hot compress and conservative drug treatment (4, 5). Curettage, a conventional surgical treatment, is commonly employed for treating *chalazions*. However, certain patients prefer to explore conservative treatment options before considering surgery, possibly due to apprehension regarding the surgical procedure, anesthesia, pain, and other factors. This approach may be particularly favored by individuals experiencing recurrent *chalazions*. Multiple surgical interventions could increase the psychological burden on patients, exacerbate discomfort, and result in skin scars. Additionally, cases of cardio-ocular reflex have been reported associated with using anesthetics (6). Knezevic et al. suggested that multi-site botulinum toxin injections around the cyst safely and effectively treat recurrent *chalazions*. The underlying mechanism of this treatment might be attributed to the ability of botulinum toxin to reduce the meibomian gland's secretory function and peripheral inflammation through the cholinergic pathway (7). Another alternative to curettage is the local injection of triamcinolone acetonide, as suggested by Amynah et al., which can achieve similar therapeutic outcomes (2, 8). Although the local injection method is simple, severe adverse reactions such as vascular obstruction and vision loss have been reported (9). Therefore, exploring new, non-operative, and safe methods for treating *chalazions* is crucial.

In recent years, the clinical efficacy and safety of intense pulsed light (IPL) for treating ocular surface diseases such as dry eye disease and blepharitis associated with meibomian gland dysfunction (MGD) have been gradually recognized (10–12). Previous retrospective studies have demonstrated that combining IPL with meibomian gland massage could significantly reduce the recurrence rate in patients with recurrent *chalazions* and improve tear film rupture time, meibomian gland secretion function, and other ocular surface signs. Optimal pulse technology (OPT) represents the fifth-generation IPL technology and offers several advantages over the original IPL, including more stable energy delivery and reduced pain (13). However, no prospective study has explored OPT's efficacy in treating *chalazions*.

Therefore, this study was initiated to evaluate, for the first time, the efficacy of OPT in treating *chalazions*. This study aimed to explore a clinical, non-invasive approach to managing meibomian gland cysts (Figure 1).

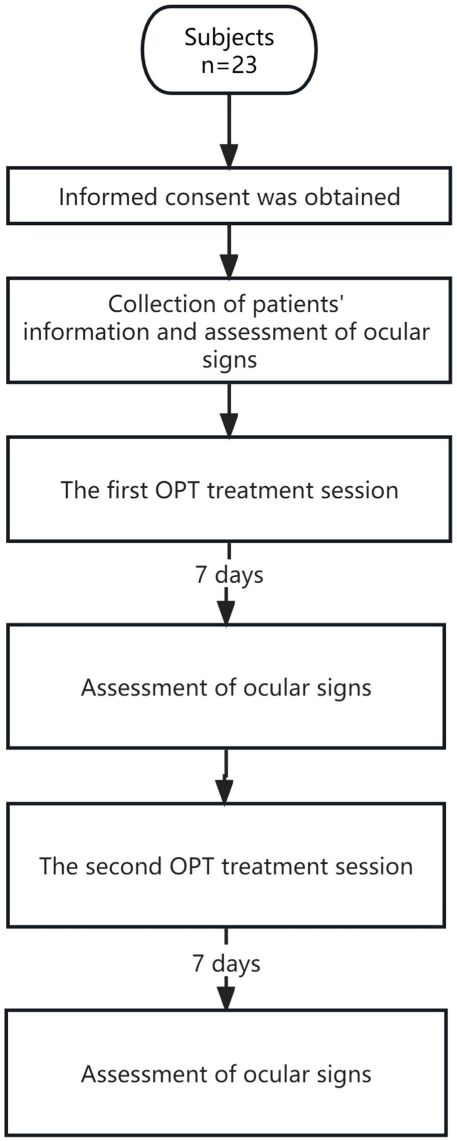

FIGURE 1
A flowchart of procedures used in this study.

2 Methods

2.1 Patients

This study adhered to the principles stated in the Declaration of Helsinki and was approved by the Guangzhou Aier Eye Hospital Ethics Committee affiliated with Jinan University (GZAIER2022IRB05). All patients seeking treatment at the outpatient clinic from June 2022 to May 2023 provided signed informed consent. The inclusion criteria for this study were as follows: (1) patients diagnosed with chalazions, including primary and recurrent chalazion; (2) patients aged ≥18 years; (3) those whose eyelid skin and lesion were intact without ulceration and pus; (4) patients in the non-acute infectious stage with chalazion (defined as the secretions from the meibomian glands are released into the tarsus and surrounding soft tissue of the eyelid, leading to an acute inflammatory reaction characterized by pain and erythema) (14). The following criteria were used as contraindications for Optimal pulse technology (OPT) treatment (15): (1) Fitzpatrick skin color classification above type IV; (2) presence of existing eye allergic diseases; (3) abnormal eyelid structure; (4) recent eye or laser treatment within 4 weeks (including cataract surgery, refractive surgery, and fundus laser treatment); (5) Recent tanning or exposure to tanning devices within 4 weeks before treatment; (6) use of exfoliating cosmetics 4 weeks before treatment; (7) a history of skin allergy within 4 weeks before treatment; (8) diagnosis of solar dermatitis, malignant skin tumor or precancerous lesion, solar keratosis, or melanoma; (9) use of medications known to cause photosensitivity; (10) recent oral administration of isotretinoin within 1 month before treatment; (11) the pupil did not return to the standard size after mydriasis; (12) uncured periorbital trauma; (13) patients with neuropsychiatric disorders; (14) patients taking anticoagulant drugs or having coagulation disorders; (15)

hypersensitivity to ocular surface drops containing sodium fluorescein or coupling agents; (16) participation in other clinical studies within the first 3 weeks of the study; (17) pregnant or lactating women.

2.2 OPT treatment

All patients underwent OPT treatments using M22 (Lumenis Inc., Lumenis, Yokneam, Israel), comprising two sessions with a 7-day interval. The treatment mode employed was OPT, with a wavelength of 590 mm, pulse width of 6.0, 6.0, and 6.0 ms, pulse width delay of 50 and 50 ms, and energy ranging from 10 to 15 J/cm^2. The treatment procedure was as follows: (1) Patients were informed about the purpose, method, and important considerations of the examination. (2) Patients assumed a supine position, removed their makeup, and cleaned their faces. (3) Corneal contact lenses were placed on the treatment eyes, and an eye shield was inserted. Patients were instructed to close their eyes, and a coupling agent (1–2 mm) was evenly applied to the upper and lower eyelid skin. (4) The light guide head delivered energy from the outer canthus to the inner canthus sequentially, ensuring that the spot coverage did not overlap or repeat. Intensive treatment was performed in areas above, below, nasal, temporal, and central to the meibomian gland cyst. This process was repeated twice, resulting in 20 treatment points per eyelid. A 3-s pause was observed before each treatment to allow sufficient skin cooling. (5) After treatment, the eye shield and contact lens were removed. (6) The patient's skin reaction and pain during treatment were observe The patient's skin reaction and pain during treatment were observed. Mild or moderate redness of the treatment site skin and mild tingling sensation experienced by the patient were considered normal reactions. However, if the skin exhibited severe redness and swelling, and the patient could not tolerate the pain, the energy was reduced, or the treatment was stopped. Adverse reactions at the treatment site were monitored after the treatment. Patients were advised to apply sunscreen and moisturize their skin within 48 h after treatment and avoid washing their face with hot water. The patients were followed up before each treatment and 7 days after the completion of the treatment course. Throughout the treatment process, the patients were instructed to use hot compresses and antibiotic eye drops (0.5% Levofloxacin eye drop, Japan). In cases where the volume of chalazia did not decrease by more than 80% following the second treatment session, surgical intervention was considered.

2.3 Other inspection methods and data collection

The diameter of the chalazion decreased by 80% was defined as adequate. The following parameters were measured to evaluate the treatment efficacy: non-invasive tear breakup time (NIBUT), corneal fluorescein staining (CFS) score, Schirmer's test I without anesthesia, conjunctival congestion and meibomian gland area. The CFS score was evaluated based on grades 0 to 3 in each quadrant, resulting in a total score according to the National Eye Institute's grading scale (16). The conjunctival congestion score was evaluated based on grades 0 to 3 in temporal and nasal bulbar conjunctiva using the OCULUS (Keratograph, Oculus Company, Germany). The meibomian gland area was evaluated by capturing photographs of the patient's upper and lower eyelid glands using OCULUS. The images were then analyzed using Image J software to calculate the ratio of the meibomian gland area to the eyelid area. The eye with a more significant number of chalazions was used for analysis. The right eye was chosen for analysis in cases where the eyes were comparable.

2.4 Statistical method

The data obtained in this study were analyzed using SPSS version 27.0 and plotted using Prism 8.0. Descriptive statistics for normally distributed data are presented as the mean ± standard deviation (SD), while median and quartile range was used for non-normally distributed quantitative data (IQR). Conjunctival congestion, fTBUT, meibomian gland area, and ST values before and after each treatment session were compared using the paired *t*-test, whereas CFS scores before and after treatment were compared using the Wilcoxon rank sum test. The chi-square test was used for between-group comparisons. Binary Logistics regression analysis were used to analyze the factors associated with the effectiveness of OPT treatment. p-values < 0.05 were considered statistically significant.

3 Results

23 patients (23 eyes), including 4 males and 19 females, were enrolled in the study. The average age of the patients was 31.61 ± 11.42 years old. The patient demographics were shown in Table 1. The patients did not have a specialist's diagnosis of any systemic diseases, such as diabetes, hypertension, or hyperlipidemia.

TABLE 1 Baseline characteristics of chalazion patients enrolled in the study.

Characteristics	*n* = 23, *n*(%)
Age (years), mean ± SD (range)	31.61 ± 11.42(18–59)
<45 years	20(87.0%)
≥45 years	3(13.0%)
Gender, *n* (%)	
Male	4(17.4%)
Female	19(82.6%)
Laterality, *n* (%)	
Unilateral chalazions	18(78.3%)
Bilateral chalazions	5(21.7%)
First onset, *n* (%)	
Primary chalazions	17(73.9%)
Recurrent chalazions	6(26.1%)
Quantity, *n* (%)	
Single	18(78.3%)
Multiple	5(21.7%)
Diameter of the chalazions, *n* (%)	
≤5 mm	21(91.3%)
>5 mm	2(8.7%)
Position, *n* (%)	
Upper eyelid	14(60.9%)
Lower eyelid	9(39.1%)

Among them, 3 patients were older than 45 years old, 20 were younger than 45 years old, 18 had unilateral disease, 5 had bilateral chalazions, 17 were the primary chalazions, 18 had only one chalazion in one eyelid, and 2 patients had a diameter of chalazion more significant than 5 mm.

Following the first OPT treatment, a reduction in the *chalazion size was observed* in 17 patients (73.91%), increased in 1 patient (4.35%), and remained unchanged in 5 patients (21.74%; Table 2). The meibomian gland area was significantly increased from 43.6 ± 2.87 to 45.97 ± 3.18 ($p = 0.023$). Compared with baseline, the conjunctival hyperemia was reduced from 0.99 ± 0.36 to 0.94 ± 0.28, ST was reduced from 8.94 ± 6.01 to 8.69 ± 7.45, and NIBUT was increased from 8.18 ± 4.46 to 9.53 ± 4.21, although these changes did not reach statistical significance (Table 3).

Following the second OPT treatment, the number of patients with reduced meibomian gland cyst diameter grew to 21 (91.3%), 3 of which were completely cured. In 2 cases, the size of the *chalazion* remained unchanged (8.7%). The patient with enlargement of the chalazion after the first treatment had a reduction in chalazion size after the second treatment, indicating improvement (Table 2). Compared with baseline, the meibomian gland area was significantly improved to 50.92 ± 2.45 ($p < 0.001$), and conjunctival hyperemia was significantly decreased to 0.81 ± 0.29 ($p < 0.001$) after the second treatment (Figure 2). There were no significant differences in the NIBUT and ST at the first and second treatments ($p > 0.05$; Table 3). The CFS score was zero before, after one treatment, and after two sessions.

Age over 45 years old, gender, first onset, single lesion, diameter of meibomian gland cyst before treatment, and lesion located in the upper or lower eyelid had no relationship with the reduction of meibomian gland cyst diameter ($p > 0.05$; Table 2).

The addition of the meibomian gland area was not associated with age over 45 years, gender, first onset, single lesion, diameter of meibomian gland cyst less than 5 mm before treatment, and lesion located in the upper or lower eyelid ($p > 0.05$; Table 4).

The adequacy of the OPT treatment was not correlated with sex, age, first onset, the diameter of the chalazion before treatment, upper eyelid or lower eyelid location, or the presence of a single or multiple chalazions according to our research ($p > 0.05$).

During the treatment and follow-up, 9 patients underwent hot compress, 21 patients had received antibiotic eye drops, and a total of 2 patients underwent surgical intervention after two sessions of OPT treatment. No adverse reactions, such as skin pigmentation, skin rupture, corneal epithelial defect, uveitis, and cataract were observed during the treatment and follow-up.

TABLE 2 The number of patients whose diameter of chalazions decreased, increased, or remained unchanged after OPT treatment.

	7 days after first session		7 days after second session	
	Reduction(*n*)	Increased or unchanged(*n*)	Reduction(*n*)	Increased or unchanged(*n*)
Age				
<45 years	16	4	19	1
≥45 years	1	2	2	1
P-value	0.155		0.249	
Gender				
Male	4	0	4	0
Female	13	6	17	2
P-value	0.539		1.000	
Episodes				
Primary	12	5	16	1
Recurrent	5	1	5	1
P-value	1.000		0.462	
Quantity				
Solitary	12	5	15	2
Multiple	5	1	6	0
P-value	1.000		1.000	
Diameter of chalazions				
≤5 mm	16	5	20	1
>5 mm	1	1	1	1
P-value	0.462		0.170	
Position				
Upper eyelid	12	2	13	1
Lower eyelid	5	4	8	1
P-value	0.162		1.000	

TABLE 3 Comparison of ocular signs between baseline and 7 days after first and second treatment of OPT sessions.

	Baseline	After one session	After two sessions	*p*-value (baseline vs. T1)	*p*-value (baseline vs. T2)	*p*-value (T1 vs. T2)
Conjunctival congestion	0.99(0.36)	0.94(0.28)	0.81(0.29)	0.177	**<0.001*** **	**0.014***
ST (mm)	8.94(6.01)	8.69(7.45)	9.13(9.14)	0.124	0.083	0.960
NIBUT (s)	8.18(4.46)	9.53(4.21)	9.71(4.18)	0.680	0.760	0.856
CFS	0.09(0)	0.04(0)	0.00(0)	0.157	0.317	0.564
Meibomian gland area (%)	43.69(2.87)	45.97(3.18)	50.92(2.45)	**0.023***	**<0.001*** **	**0.004****

CFS, corneal fluorescein staining; NIBUT, non-invasive tear breakup time; ST, Schirmer's test I; T1, 7 days after first treatment; T2, 7 days after second treatment. *$p < 0.05$, **$p < 0.01$, ***$p < 0.001$. The values in bold were used to remind the reader that these p-values were statistically significant.

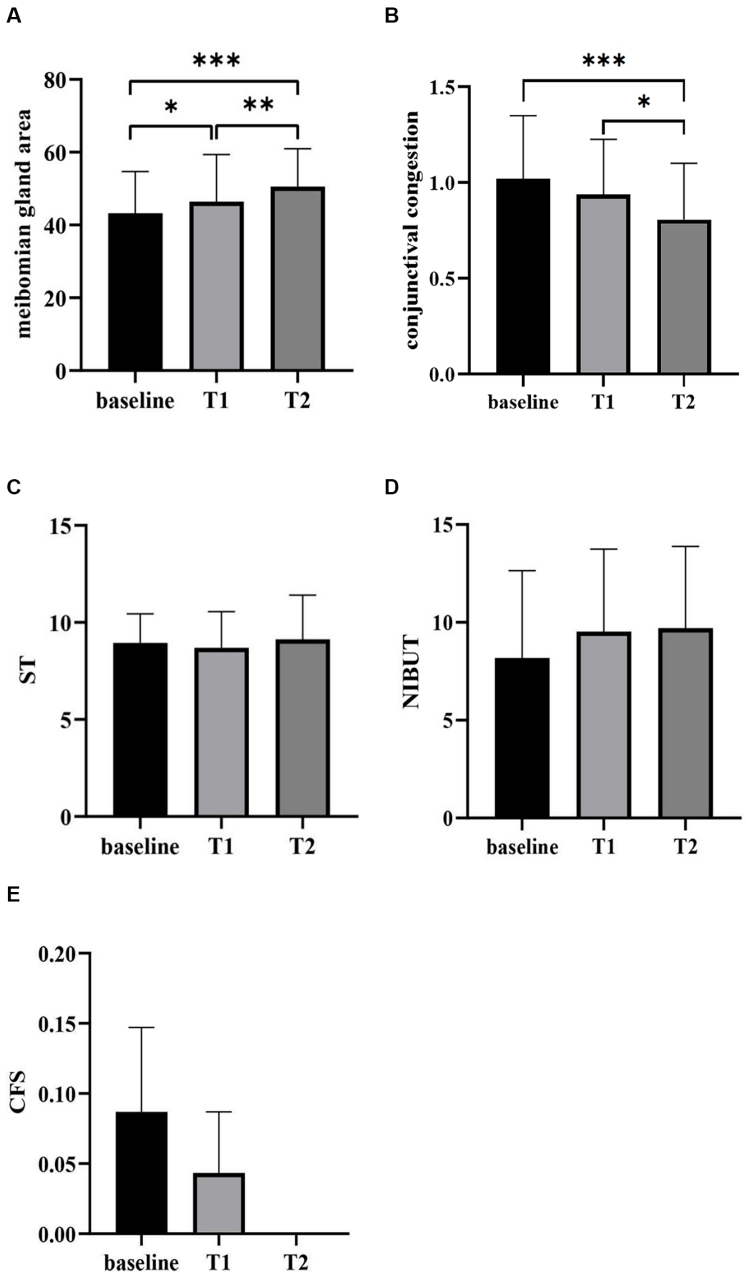

FIGURE 2
Comparison of the meibomian gland area **(A)**, conjunctival congestion **(B)**, ST **(C)**, NIBUT **(D)** and CFS **(E)** before and after OPT treatment sessions. T1, 7 days after the first treatment; T2, 7 days after the second treatment; *$p < 0.05$, **$p < 0.01$, ***$p < 0.001$.

TABLE 4 The number of patients whose meibomian gland area decreased, increased, or remained unchanged after OPT treatment.

	7 days after first session		7 days after second session	
	Increased(*n*)	Reduction or unchanged(*n*)	Increased(*n*)	Reduction or unchanged(*n*)
Age				
<45 years	14	6	18	2
≥45 years	3	0	2	1
P-value	0.539		0.365	
Gender				
Male	2	2	3	1
Female	15	4	17	2
P-value	0.270		0.453	
Episodes				
Primary	12	5	14	3
Recurrent	5	1	6	0
P-value	1.000		0.539	
Quantity				
Solitary	13	4	14	3
Multiple	4	2	6	0
P-value	0.632		0.539	
Diameter of chalazions				
≤5 mm	15	6	18	3
>5 mm	2	0	2	0
P-value	0.379		0.567	
Position				
Upper eyelid	11	3	13	1
Lower eyelid	6	3	7	2
P-value	0.643		0.538	

4 Discussion

Chalazia is a common eye condition. While the pathogenesis of MGD and blepharitis concerning chalazions remains unclear, previous studies have indicated a strong association (1, 17). When the regular discharge of oil from the meibomian gland is disrupted, excessive meibum accumulates in the surrounding eyelid tissue, resulting in inflammatory cell infiltration, redness, and swelling (18). Over time, this process can result in cyst formation. The treatment approach for chalazion in the non-acute infection stage typically involves warm compress and administration of antibiotic eye drops. Jacob Evans indicated that surgical intervention was required in approximately 40% of patients following the administration of topical antibiotic and steroid therapy (1). IPL is a broad-spectrum pulsed light with a wavelength of 500–2,000 nm, which is a non-invasive and non-laser treatment method. Initially, IPL was primarily used for treating rosacea. However, in 2002, its application expanded to include the treatment of dry eyes, meibomian gland dysfunction, blepharitis, and other ocular surface diseases. Currently, OPT and intense regulatory pulsed light (IRPL) are the main IPL devices in clinical practice. The OPT is the latest generation (fifth-generation) IPL technology, offering enhanced stable energy and reduced discomfort compared with the original IPL (19). Compared with IRPL technology, OPT technology has the advantages of no pulse spike, constant energy, stable and repeatable, larger flash density, and a more stable cooling system (20). Subsequent studies have increasingly demonstrated the safety and efficacy of IPL and OPT in improving symptoms and signs in patients. Although the exact mechanism of how OPT treats ocular surface diseases remains to be elucidated, it is believed that OPT can inhibit the release of inflammatory mediators within the local tissues and impede the inflammatory cascade reaction (21). In this study, conjunctival congestion improved significantly after two OPT treatments, which supports the aforementioned hypothesis. By generating heat that can penetrate the skin, OPT selectively targets the meibomian gland, resulting in the melting of eyelid esters and an improvement in the palpebral ester character (22, 23). Consequently, this process reduces the cyst diameter and increases the area of the meibomian gland. In our study, a significant improvement was observed in the meibomian gland area of the patients who underwent OPT treatment. Furthermore, as the number of treatments increased, the meibomian gland area increased more significantly, indicating that OPT exhibits a persistent and cumulative effect when targeting the meibomian gland. Moreover, OPT used hemoglobin as its target color base. During treatment, light is absorbed by hemoglobin, converting it into heat. This localized increase in

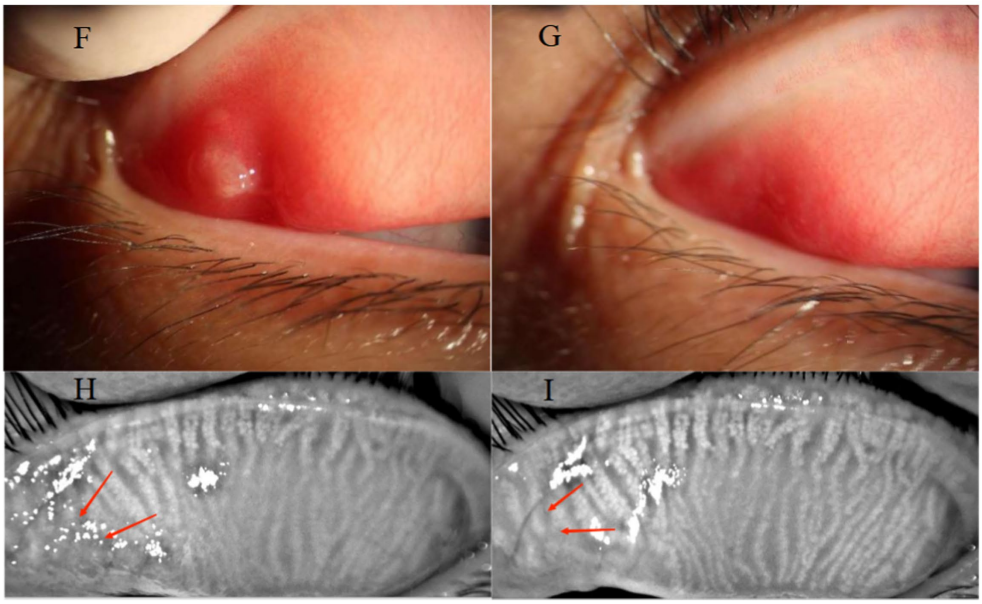

FIGURE 3
A 32-year-old female presented with a primary chalazion in the upper eyelid of the right eye (F). Before OPT treatments, the patient showed palpebral conjunctival hyperemia (F) and meibomian gland dropout at the site of the cyst (H). Following treatment, complete regression of the cyst was observed (G), along with decreased hyperemia on the palpebral conjunctival (G) and increased of the meibomian gland area at the cyst site (I).

temperature results in the solidification and sealing of abnormally dilated capillaries along the palpebral margin. This process not only helps reduce bacteria and mites present on the surface of the eyelid skin but also contributes to the overall efficacy of the treatment.

IPL energy penetrates the eyelid, gets absorbed by hemoglobin, and transforms into heat, causing localized destruction of superficial blood vessels. This process reduces eyelid neovascularization and subsequently lowers the accumulation of inflammatory mediators, thereby eliminating a significant source of inflammation in both the eyelid and meibomian glands. Simultaneously, the volume of meibomian gland cysts diminishes post-treatment, leading to a reduction in the levels of inflammatory factors, which may have accounted for the observed improvement in conjunctival hyperemia following treatment. In Arita's research, the therapeutic effects of IPL on refractive multiple recurrent chalazia were examined, it was noted that corneal fluorescein staining (CFS) significantly improved in patients with recurrent meibomian gland cysts after OPT treatment, Schirmer's Test (ST) did not exhibit statistically significant changes, and non-invasive tear breakup time (NIBUT) alterations were not assessed in their study (24). In addition, a study by Yirui Zhu focusing on patients with chalazion in the acute inflammatory phase, reported significant improvements in NIBUT after OPT treatment (25). These outcomes contrast with the patient population in our current study. In our study, although no statistically significant differences were observed in NIBUT and CFS after one or two OPT treatments compared to baseline, NIBUT displayed an upward trend, suggesting improved tear film stability. Similarly, CFS exhibited a downward trend, indicating reduced ocular surface staining. ST showed a decrease after the first treatment, which we attribute to factors such as the short evaluation interval and the OPT treatment effect not yet reaching its full potential. Interestingly, ST increased from baseline after the second treatment. Our study encompassed a diverse range of chalazion types, including patients in non-acute infectious stages, as well as primary and recurrent cases, with varying diameters and locations of chalazion. Following two treatments, NIBUT, CFS, and ST all demonstrated an improving trend compared to their respective baseline measurements.

The frequency of OPT treatment is also a critical aspect to investigate. Previous studies have indicated that the effects of OPT are cumulative and persistent. Jin et al. conducted a study suggesting that four sessions of OPT combined with meibomian gland expression can effectively alleviate symptoms, reduce palpebral margin congestion, improve meibomian gland secretion function, and increase tear film rupture time in patients with MGD (23). Furthermore, the improvement becomes more evident with an increase in the number of treatment sessions, and there is still a statistically significant difference observed 3 months after completing the treatment course. In the Chinese experts' consensus on IPL for treating MGD-related dry eyes, it is recommended to undergo IPL treatments 2–12 times (15). Reiko et al. have suggested that patients with recurrent chalazions might require three or more courses of IPL treatment (24, 25). Given the specific characteristics of the patients enrolled in our study, which included individuals with single, small-diameter, and primary chalazions, and considering the aforementioned recommendations regarding the number of IPL treatments, a total of two OPT treatments were administered (Figure 3). During the follow-up, it was found that one patient recovered after 1 week of treatment. The patient was a 30-year-old woman who underwent chalazion curettage 6 months before our intervention. The diameter of her chalazion was 2 mm before treatment. Notably, the patient remained free from relapse during the irregular follow-up assessments conducted after the treatment. Furthermore, three additional patients were completely cured after undergoing two treatments. These positive outcomes have left the patients delighted with the rapid onset of OPT efficacy and the level of comfort they experienced.

The effectiveness of performing two OPT treatments for treating chalazions has demonstrated its clinical relevance.

As previous studies have indicated, *chalazions* are commonly observed in adult women, particularly around the age of 25 years. In our analysis of related factors influencing OPT efficacy while treating *chalazions,* no significant associations were observed with sex, age, first onset, the presence of a single chalazion, site, and the diameter of the meibomian gland cysts. These findings are consistent with previous studies.

This study has certain limitations. First, the sample size was small, the observation period was short, and more objective and microscopic observations of the expression of inflammatory factors in ocular surface tissues, such as optical surface goblet cells, epithelial cells, and tears, were lacking. These aspects warrant further investigation and will be our focus in future research endeavors.

5 Conclusion

In our study, the primary chalazion was observed in 73.9% patients, while cysts larger than 5 mm in diameter were found in 8.7%, additionally, single cysts were present in 78.3% patients. After treatment, the diameter of chalazions was reduced in 91.3% of the patients, and the area of the meibomian gland was significantly increased compared with that before treatment. To the best of our knowledge, this is the first study to explore the efficacy of OPT treatment on different types of chalazions, which suggested that two OPT treatments at an interval of 1 week can improve the signs of adult patients in the non-acute infectious stage with chalazion.

Data availability statement

The original contributions presented in the study are included in the article/Supplementary material, further inquiries can be directed to the corresponding author.

Ethics statement

The studies involving humans were approved by Guangzhou Aier Eye Hospital Ethics Committee affiliated with Jinan University. The studies were conducted in accordance with the local legislation and institutional requirements. The participants provided their written informed consent to participate in this study.

Author contributions

XS: Funding acquisition, Methodology, Resources, Writing – original draft, Writing – review & editing. CZ: Formal analysis, Investigation, Writing – review & editing. SZ: Formal analysis, Investigation, Writing – review & editing. MH: Conceptualization, Supervision, Writing – review & editing.

Funding

The author(s) declare financial support was received for the research, authorship, and/or publication of this article. The present study was funded by the Youth Scientific Research Fund of Guangzhou Aier Eye Hospital (no. G2022004).

Acknowledgments

We would like to thank Guangzhou Aier Eye Hospital for the support of this study, and MH, XS, CZ, and SZ for their efforts in this study.

Conflict of interest

The authors declare that the research was conducted in the absence of any commercial or financial relationships that could be construed as a potential conflict of interest.

Publisher's note

Supplementary material

The Supplementary material for this article can be found online at: https://www.frontiersin.org/articles/10.3389/fmed.2023.1286159/full#supplementary-material

References

1. Evans J, Vo KBH, Schmitt M. Chalazion: racial risk factors for formation, recurrence, and surgical intervention. *Can J Ophthalmol.* (2021) 57:242–6. doi: 10.1016/j.jcjo.2021.04.023

2. Ben Simon GJ, Rosen N, Rosner M, Spierer A. Intralesional triamcinolone Acetonide injection versus incision and curettage for primary Chalazia: a prospective, Randomized Study. *Am J Ophthalmol.* (2011) 151:714–718.e1. doi: 10.1016/j.ajo.2010.10.026

3. Rumelt S, Rubin PA. Potential sources for orbital cellulitis. *Int Ophthalmol Clin.* (1996) 36:207–21. doi: 10.1097/00004397-199603630-00019

4. Cottrell DG, Bosanquet RC, Fawcett IM. Chalazions: the frequency of spontaneous resolution. *Br Med J.* (1983) 287:1595. doi: 10.1136/bmj.287.6405.1595

5. Perry HD, Serniuk RA. Conservative treatment of chalazia. *Ophthalmology*. (1980) 87:218–21. doi: 10.1016/S0161-6420(80)35250-0

6. Katowitz WR, O'Brien M, Kiskis E, Elliott EM. An asystolic event after eyelid skin bupivicaine injection during chalazion surgery. *J AAPOS.* (2016) 20:75–7. doi: 10.1016/j.jaapos.2015.09.010

7. Goawalla A, Lee V. A prospective randomized treatment study comparing three treatment options for chalazia: triamcinolone acetonide injections, incision and curettage and treatment with hot compresses. *Clin Exp Ophthalmol.* (2007) 35:706–12. doi: 10.1111/j.1442-9071.2007.01617.x

8. Singhania R, Sharma N, Vashisht S, Dewan T. Intralesional triamcinolone Acetonide (TA) versus incision and curettage (I & C) for medium and large size Chalazia. *Nepal J Ophthalmol.* (2018) 10:3–10. doi: 10.3126/nepjoph.v10i1.21661

9. Shiramizu KM, Kreiger AE, McCannel CA. Severe visual loss caused by ocular perforation during chalazion removal. *Am J Ophthalmol*. (2004) 137:204–5. doi: 10.1016/S0002-9394(03)00863-8

10. Yin Y, Liu N, Gong L, Song N. Changes in the Meibomian gland after exposure to intense pulsed light in Meibomian gland dysfunction (MGD) patients. *Curr Eye Res*. (2018) 43:308–13. doi: 10.1080/02713683.2017.1406525

11. Craig JP, Chen YH, Turnbull PRK. Prospective trial of intense pulsed light for the treatment of meibomian gland dysfunction. *Invest Ophthalmol Vis Sci*. (2015) 56:1965–70. doi: 10.1167/iovs.14-15764

12. Arita R, Fukuoka S, Morishige N. Therapeutic efficacy of intense pulsed light in patients with refractory meibomian gland dysfunction. *Ocul Surf*. (2019) 17:104–10. doi: 10.1016/j.jtos.2018.11.004

13. Chen J, Liu J, Wu J. Treatment of melasma by a combination of intense pulsed light with advanced optimal pulse technology and human-like collagen repair dressing: a case series study. *Medicine*. (2022) 101:e29492. doi: 10.1097/MD.0000000000029492

14. Zhu Y, Zhao H, Huang X, Lin L, Huo Y, Qin Z, et al. Novel treatment of chalazion using light-guided-tip intense pulsed light. *Sci Rep*. (2023) 13:12393. doi: 10.1038/s41598-023-39332-x

15. Eye CECG of IPL for D, Dry Eye Rehabilitation Specialty VRC of CRMA. Experts consensus on intense pulsed light for meibomian gland dysfunction and related dry eye. *Chin J Exp Ophthalmol*. (2022) 40:97–103. doi: 10.3760/cma.j.cn115989-20211015-00563

16. Lemp MA. Report of the National eye Institute/industry workshop on clinical trials in dry eyes. *CLAO J*. (1995) 21:221–32.

17. Liang L, Ding X, Tseng SCG. High prevalence of demodex brevis infestation in chalazia. *Am J Ophthalmol*. (2014) 157:342–348.e1. doi: 10.1016/j.ajo.2013.09.031

18. Suzuki T, Katsuki N, Tsutsumi R, Uchida K, Ohashi K, Eishi Y, et al. Reconsidering the pathogenesis of chalazion. *Ocul Surf*. (2022) 24:31–3. doi: 10.1016/j.jtos.2021.12.010

19. Liu R, Rong B, Tu P, Tang Y, Song W, Toyos R, et al. Analysis of cytokine levels in tears and clinical correlations after intense pulsed light treating Meibomian gland dysfunction. *Am J Ophthalmol*. (2017) 183:81–90. doi: 10.1016/j.ajo.2017.08.021

20. Wu Y, Li J, Hu M, Zhao Y, Lin X, Chen Y, et al. Comparison of two intense pulsed light patterns for treating patients with meibomian gland dysfunction. *Int Ophthalmol*. (2020) 40:1695–705. doi: 10.1007/s10792-020-01337-0

21. Zhang X, Song N, Gong L. Therapeutic effect of intense pulsed light on ocular Demodicosis. *Curr Eye Res*. (2019) 44:250–6. doi: 10.1080/02713683.2018.1536217

22. Dell SJ. Intense pulsed light for evaporative dry eye disease. *Clin Ophthalmol*. (2017) 11:1167–73. doi: 10.2147/OPTH.S139894

23. Huo Y, Mo Y, Wu Y, Fang F, Jin X. Therapeutic effect of intense pulsed light with optimal pulse technology on meibomian gland dysfunction with and without ocular Demodex infestation. *Ann Transl Med*. (2021) 9:238. doi: 10.21037/atm-20-1745

24. Arita R, Fukuoka S. Therapeutic efficacy and safety of intense pulsed light for refractive multiple recurrent Chalazia. *J Clin Med*. (2022) 11:5338. doi: 10.3390/jcm11185338

25. Zhu Y, Huang X, Lin L, di M, Chen R, Dong J, et al. Efficacy of intense pulsed light in the treatment of recurrent Chalaziosis. *Front Med*. (2022) 9:839908. doi: 10.3389/fmed.2022.839908

frontiers | Frontiers in Medicine

TYPE Original Research
PUBLISHED 09 January 2024
DOI 10.3389/fmed.2023.1340198

OPEN ACCESS

EDITED BY
Georgios D. Panos,
Nottingham University Hospitals NHS Trust, United Kingdom

REVIEWED BY
Changzheng Chen,
Renmin Hospital of Wuhan University, China
Rizwan Malik,
Sheikh Khalifa Medical City, United Arab Emirates

*CORRESPONDENCE
Songtao Yuan
songtaoyuan@njmu.edu.cn
Yasha Wang
wangyasha@pku.edu.cn

†These authors have contributed equally to this work and share first authorship

‡These authors have contributed equally to this work and share last authorship

RECEIVED 17 November 2023
ACCEPTED 28 December 2023
PUBLISHED 09 January 2024

CITATION
Fan W, Zhang C, Ge L, Su N, Chen J, Song S, Wang Y and Yuan S (2024) Prediction model for elevated intraocular pressure risk after silicone oil filling based on clinical features. *Front. Med.* 10:1340198. doi: 10.3389/fmed.2023.1340198

Prediction model for elevated intraocular pressure risk after silicone oil filling based on clinical features

Wen Fan[1†], Chaohe Zhang[2,3†], Lexin Ge[1†], Na Su[1], Jiaqin Chen[1], Siyao Song[3,4,5], Yasha Wang[2,4*‡] and Songtao Yuan[1*‡]

[1]Department of Ophthalmology, The First Affiliated Hospital of Nanjing Medical University, Nanjing, China, [2]Key Laboratory of High Confidence Software Technologies, Ministry of Education, Peking University, Beijing, China, [3]School of Computer Science, Peking University, Beijing, China, [4]National Engineering Research Center of Software Engineering, Peking University, Beijing, China, [5]Software College, Northeastern University, Shenyang, China

Background: To evaluate risk factors and further develop prediction models for intraocular pressure elevation (IOP) after vitreoretinal surgery with silicone oil tamponade to support clinical management.

Methods: A retrospective study analyzed 1,061 eyes of 1,061 consecutive patients that presented to the Jiangsu Province Hospital between December 2015 and December 2020, the IOP was measured from the preoperative visit and at the 1-week, 1-month, 3-month, and 6-month visits, and the final postoperative visit before silicone oil removal. Four machine learning methods were used to carried out the prediction of IOP elevation: Decision Tree, Logistic Regression, Random Forest, and Gradient-Boosted Decision Trees (GBDT) based on features including demographic and clinical characteristics, preoperative factors and surgical factors. Predictors were selected based on the *p*-value of the univariate analysis.

Results: Elevated intraocular pressure developed in 26.01% of the eyes postoperatively. Elevated intraocular pressure primarily occurred within 1–2 weeks after surgery. Additionally, the majority of IOP values were distributed around 25–40 mmHg. GBDT utilizing features with *p*-values less than 0.5 from the hypothesis testing demonstrated the best predictive performance for 0.7944 in accuracy. The analysis revealed that age, sex, hypertension, diabetes, myopia, retinal detachment, lens status and biological parameters have predictive value.

Conclusion: Age, sex, hypertension, diabetes, myopia, retinal detachment, lens status and biological parameters have influence on postoperative intraocular pressure elevation for patients with silicone oil tamponade after pars plana vitrectomy. The prediction model showed promising accuracy for the occurrence of IOP elevation. This may have some reference significance for reducing the incidence of high intraocular pressure after pars plana vitrectomy combined with silicone oil filling.

KEYWORDS

prediction model, intraocular pressure, ocular hypertension, pars plana vitrectomy, silicone oil, biological parameter

1 Introduction

Silicone oil (SO) has become an essential tamponade agent in vitreoretinal surgery due to its high surface tension since its introduction by Cibis in 1962 (1). However, despite its successful use by retina surgeons for several decades, complications associated with silicone oil endotamponade have been reported. These include increased intraocular pressure (IOP), ocular hypotony, cataract formation in phakic eyes, band keratopathy in corneas, and silicone oil emulsification (2, 3). Elevated IOP is particularly prevalent and severe among these complications (4). The incidence of elevated IOP varies from 2.2 to 56.0% related to SO endotamponade in different studies (5–8). Discrepancies in the definitions of ocular hypertension, postoperative time points, and retinal diseases contribute to this variation. Additionally, each study incorporates different inclusion and exclusion criteria. The underlying pathological mechanisms of IOP elevation are multifactorial and remain uncertain. They may include overfilling of silicone oil, anterior chamber inflammatory activity, pupillary block, anterior migration of SO, and preexisting glaucoma (9–12). In public hospitals, the limited use of inert gas is attributed to policy constraints. Consequently, silicone oil filling is the predominant choice for patients undergoing vitrectomy combined with intraocular filling surgery. As a result, there is a considerable prevalence of silicone oil-filled eyes in China, necessitating an analysis of the risk factors associated with elevated intraocular pressure following silicone oil filling.

Since the occurrence of postoperative IOP elevation is the result of multiple factors, conventional single-factor analysis fails to provide a comprehensive analysis, and there is no consensus regarding the risk factors derived from current study analyses. With the advancement of data science, machine learning models have gained popularity in predictive tasks across various domains, including healthcare. However, the medical field places a high premium on model interpretability, leading to the development of interpretable predictive models for clinical analysis. In this study (2, 13), we presented a predictive model for further analysis, offering clinicians not only predicted values for assistance but also interpretability to discern the importance of different features and provide more precise clinical reference.

2 Materials and methods

This study was approved by the ethics of committees of The First Affiliated Hospital of Nanjing Medical University (Jiangsu Province Hospital) and conducted in accordance with the tenets of the Declaration of Helsinki (2022-SR-200). As this is a retrospective study with data processed anonymously, informed consent was waived.

This retrospective study enrolled 1,061 eyes of 1,061 consecutive patients that presented to the Jiangsu Province Hospital between December 2015 and December 2020. These cases were confirmed by experienced researchers. All eyes had a vitreoretinal condition treated by pars plana vitrectomy (PPV) with SO endotamponade. Eyes with corneal pathology, a previous history of glaucoma or preoperative ocular hypertension (IOP > 21 mmHg), or patients with severe data deficiencies were excluded. Demographic data, a detailed ocular and systemic history, and the etiology of the PPV were recorded for each patient pre-operatively.

Vitreoretinal surgery was indicated for various conditions, including retinal detachment (RD), macular hole (MH), choroidal detachment, vitreous hemorrhage (VH), and diabetic retinopathy (DR). All procedures were performed under either local or general anesthesia. PPV, air/fluid exchange, and SO were employed in all patients. Following surgery, the eyes were maintained at a slightly hypotonic state, and intraocular pressure was assessed through manual palpation.

Patient age, sex, lens status, presence of diabetes, hypertension, biological parameters, surgical indication and surgical factors were recorded. Biological parameters were measured by ZEISS IOL Master500 before surgery. The IOP measured by Canon TX-20 automatic non-contact tonometer were obtained for both the operative and fellow eyes from the preoperative visit and at the 1-week, 1-month, 3-month, 6-month visits, and at the final postoperative visit. The follow-up ended after silicone oil removal. Silicone Oil was removed about 3–6 months after implantation. IOP less than 21 mmHg was predefined as normal. If the intraocular pressure exceeds 21 mmHg at any point during the follow-up process, it is diagnosed as elevated intraocular pressure, and the appropriate treatment method is selected based on the specific numerical value. Commonly used IOP-lowering drugs include Brinzolamide and Timolol Maleate Eye Drops, Carteolol Hydrochloride Eye Drops, Brimonidine Tartrate Eye Drops and Travoprost Eye Drops. For patients whose IOP was not effectively controlled with IOP-lowering medications, we performed further operations or surgeries to control IOP, such as paracentesis of anterior chamber, trabeculectomy and drainage valve implantation.

Data were analyzed using Python 3.6.9 with package: SciPy (1.2.1), Statsmodels (0.11.1), NumPy (1.19.4) and scikit-learn (0.24.1). Continuous variables were expressed as means (standard deviations), and were compared with the Mann–Whitney U test. Categorical variables were expressed as number (%) and compared by $\chi 2$ test. A p-value of less than 0.05 was considered a statistically significant difference. Four machine learning methods were used to carried out the prediction of IOP elevation: Decision Tree, Logistic Regression, Random Forest, and Gradient-Boosted Decision Trees (GBDT). Among these, GBDT achieved the best predictive performance. The selection of predictive features was based on the p-value from the above hypothesis testing.

TABLE 1 The baseline characteristics of the study cohort.

Characteristics	Value
Male	563 (53.06%)
Age at surgery, years	58.52 ± 12.81 (11–93)
A history of diabetes mellitus	205 (19.32%)
A history of high blood pressure	301 (28.37%)
Myopia	247 (23. 28%)
Retinal detachment	771 (72.67%)
Macular hole	122 (11.50%)
Choroidal detachment	61 (5.75%)
Vitreous hemorrhage	171 (16.12%)

3 Results

3.1 Demographic and clinical characteristics

The baseline characteristics of the study cohort were presented in Table 1. The study included 1,061 patients who underwent pars plana vitrectomy, with a mean age of 58.52 years ±12.81 and range of 11 to 93 years. Of the total number of patients, 563 (53.06%) were male, and 538 (46.94%) were female. Diabetes mellitus was present in 205 patients (19.32%), systemic hypertension in 301 patients (28.37%), and myopia in 247 patients (23.28%). The primary indication for surgery in the study eye was retinal detachment in 771 patients (72.67%), followed by vitreous hemorrhage in 171 patients (16.12%)

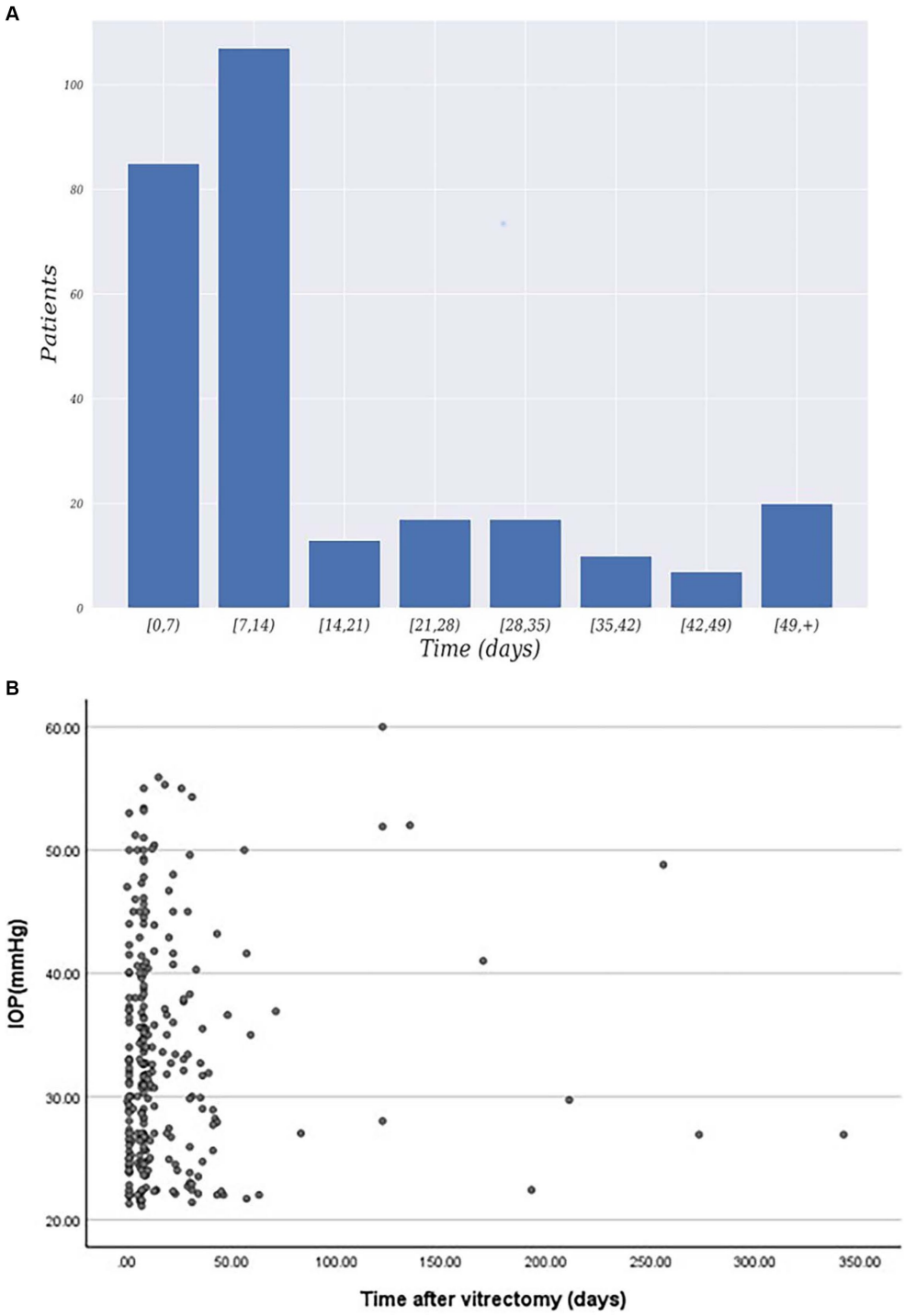

FIGURE 1
(A) Distribution of patients exhibiting elevated intraocular pressure time after surgery. **(B)** Time and IOP values for postoperative intraocular pressure elevation.

and macular hole in 122 patients (11.50%). Among the 276 patients with IOP elevation, Figure 1 illustrated that elevated intraocular pressure primarily occurs within 1–2 weeks after surgery. Additionally, the majority of IOP values are distributed around 25–40 mmHg.

3.2 Preoperative risk factors

The analysis of preoperative risk factors for intraocular pressure elevation is presented in Table 2. Out of the 1,061 patients included in the study, 276 (26.01%) developed postoperative IOP elevation, 785 (73.99%) showed normal postoperative IOP. We compared various variables among all the patients and found that age at surgery, sex, myopia, retinal detachment, vitreous hemorrhage, hypertension and diabetes were associated with a higher risk of increased IOP. No significant associations were observed between other characteristics and the development of elevated IOP. Specifically, the age of patients with IOP elevation was significantly lower compared to those with normal IOP ($p < 0.001$, OR = 0.96 [0.95–0.97]). Gender also showed a significant difference ($p = 0.02$, OR = 1.39 [1.05–1.83]). Among patients with IOP elevation, the underlying ocular diseases necessitating pars plana vitrectomy (PPV) included retinal detachment, macular hole, choroidal detachment, vitreous hemorrhage, and diabetic retinopathy. Patients with retinal detachment ($p < 0.001$, OR = 6.71 [4.16–10.83]), diabetes ($p = 0.045$, OR = 0.69 [0.47–0.99]), hypertension ($p = 0.018$, OR = 0.68 [0.49–0.94]), vitreous hemorrhage ($p = 0.002$, OR = 0.51 [0.33–0.78]), and myopia ($p < 0.001$, OR = 1.84 [1.36–2.51]) were more susceptible to developing increased IOP. On the other hand, the presence of macular hole and choroidal detachment did not appear to influence the risk of elevated IOP.

3.3 Surgical factors

Effects of surgical factors are shown in Table 3. Among all 1,061 patients, 891 patients were with phakic, 22 patients were aphakic, 148 patients were Pseudophakic. Lens status had significant statistical differences. Besides, other continuous variables were also analyzed,

TABLE 2 The preoperative risk factors for intraocular pressure elevation.

	Eyes		OR	95% CI	*p*-value
	With IOP > 21 mmHg (*n* = 276)	With IOP ≤ 21 mmHg (*n* = 785)			
Preoperative characteristics					
Age, years	53.34 ± 13.38	60.34 ± 12.08	0.96	0.95–0.97	<0.001
Sex					
Male	163	400	1.39	1.05–1.83	0.020
Female	113	385			
Diabetes					
Yes	42	163	0.69	0.47–0.99	0.045
No	234	622			
Hypertension					
Yes	63	238	0.68	0.49–0.94	0.018
No	213	547			
Myopia					
Yes	88	159	1.84	1.36–2.51	<0.001
No	188	626			
Retinal detachment					
Yes	256	515	6.71	4.16–10.83	<0.001
No	20	270			
Macular hole					
Yes	28	94	0.83	0.53–1.30	0.412
No	248	691			
Choroidal detachment					
Yes	21	40	1.53	0.89–2.65	0.123
No	255	745			
Vitreous hemorrhage					
Yes	28	143	0.51	0.33–0.78	0.002
No	248	642			

such as axial length (AL), anterior chamber depth (ACD), lens thickness (LT), central corneal thickness (CCT), white-to-white value (WTW). Eyes with longer axial length, deeper ACD and longer WTW were significantly associated with elevated IOP. Patients with elevated IOP had a mean AL of 24.82 ± 3.77, which was significantly longer than patients with normal IOP (23.88 ± 2.76) ($p < 0.001$, OR = 1.10 [1.05–1.16]). Similar findings were observed for ACD ($p<0.001$, OR = 1.83 [1.35–2.49]), and WTW ($p = 0.04$, OR = 1.34 [0.99–1.80]). However, no significant difference was found in CCT and LT between the two groups. A total of 36 (3.4%) patients had 1000cSt silicone oil implanted, while the remaining 1,025 (96.6%) patients received 5000cSt silicone oil. SO viscosity was not found to be associated with the development of increased IOP ($p = 0.799$). Meanwhile, pars plana vitrectomy combined cataract extraction conferred a reduced risk for increased IOP ($p < 0.001$, OR = 0.44 [0.33–0.58]).

3.4 Prediction models

Four machine learning methods:

- Decision tree: a decision tree is a flowchart-like model that makes decisions based on a series of questions about the data. In our study, it was used to predict IOP elevation by asking a series of intuitive, yes-or-no questions based on patient characteristics.
- Logistic regression: logistic regression is a statistical model that estimates the probability of a binary outcome (such as IOP elevation) based predictor variables. In our context, it assessed the likelihood of IOP elevation by analyzing patient characteristics.
- Random forest: a random forest is an ensemble learning method, which operates by constructing multiple decision trees during training and outputting the class that is the mode of the classes of the individual trees. In our study, it was used to improve predictive accuracy and control over-fitting, which can be a problem in decision trees.
- Gradient-Boosted Decision Trees (GBDT): GBDT is another ensemble technique that builds the model in a stage-wise fashion. It constructs new trees that predict the residuals or errors of prior trees then combines these trees in a weighted manner to make the final prediction. In predicting IOP elevation, GBDT was particularly useful for handling various types of patient data and improving prediction accuracy over traditional decision trees.

Were employed to conduct the prediction of IOP elevation. For our data processing approach, each surgical procedure on an individual eye of a patient was treated as a separate sample. The dataset was divided into a training set and a testing set at a ratio of 9:1. Each model was then trained on the training set and tested on the testing set, with the test results reported. In this phase, we employed the grid search technique to find the most suitable hyperparameters for the current model, such as maximum depth and the number of estimators. All methods were experimented within the same framework to ensure fairness in comparison.

TABLE 3 The surgical factors for intraocular pressure elevation.

	Eyes		OR	95% CI	*p*-value
	With IOP > 21 mmHg (*n* = 276)	With IOP ≤ 21 mmHg (*n* = 785)			
Intraoperative characteristics					
Lens status					
Phakic	213	678	0.53	0.38–0.76	<0.001
Aphakic	13	9	4.80	1.97–11.71	
Pseudophakic	50	98	1.55	1.07–2.25	
Biological parameter					
Axial length	24.82 ± 3.77	23.88 ± 2.76	1.10	1.05–1.16	<0.001
Anterior chamber depth	3.25 ± 0.55	3.09 ± 0.48	1.83	1.35–2.49	<0.001
Lens thickness	4.82 ± 0.75	4.85 ± 0.66	0.95	0.71–1.26	0.509
Central corneal thickness	543.89 ± 54.53	540.16 ± 38.28	1.00	1.00–1.01	0.074
WTW	11.59 ± 0.56	11.51 ± 0.53	1.34	0.99–1.80	0.041
Viscosity of silicone oil					
1,000 cSt	7	29	0.61	0.25–1.48	0.799
5,000 cSt	269	756	1.19	0.44–3.26	
DK-line injection					
Yes	208	605	0.93	0.67–1.30	0.669
No	68	180			
Combined cataract extraction					
Yes	136	542	0.44	0.33–0.58	<0.001
No	140	243			

Furthermore, considering not all features of the samples might positively contribute to prediction accuracy due to the presence of redundant features in the patient characteristics, feature selection was performed before training the model. This process incorporated the clinical experience of senior doctors and the data analysis results from earlier in this study to filter out redundant feature information. Specifically, we initially identified 19 fixed important features based on the expertise of senior doctors (see Table 4, Fixed Features). These features were used as a foundational input for training and predicting in each model. Following this, based on the *p*-values from our hypothesis testing, we gradually increased the *p*-value threshold, which allowed for the introduction of additional features for experimentation ($p < 0.1$, 0.2, 0.3, 0.4, 0.5, and all features). The results of the prediction models on IOP elevation are shown in Table 4.

By incorporating the clinical expertise of senior doctors and considering features with *p*-values less than 0.5 from hypothesis testing, the Gradient-Boosted Decision Trees model achieved the highest accuracy of 0.7944. The feature importance provided by the prediction model was presented in Figure 2. The vertical axis represents the feature name, while the horizontal axis represents the corresponding feature importance value. It is worth noting that the sum of the importance of all features is equal to 1. The model assigns higher importance to certain features compared to others in the prediction process. The results of the prediction model indicate that factors such as age, biological parameters, and lens status play a more significant role. Specifically, the importance values for each feature are as follows: Age-0.1526, AL-0.1651, ACD-0.1154, LT-0.0735, CCT-0.1431, WTW-0.0679, Phakic-0.0079, Aphakia-0.0023, Pseudophakic-0.0112, Cata-ract-0.0094, RD-0.0084. These findings align with the results obtained from our single-factor analysis above. The code of prediction model can be found in supplementary materials.

4 Discussion

This study aimed to evaluate the risk factors and incidence of postoperative IOP elevation following vitreoretinal surgery with

TABLE 4 Results of the prediction model on IOP elevation.

p-value	Model	Accuracy	Precision	Recall	F1-score
All (36 features)	DT	0.757	0.5	0.0769	0.1333
	LR	0.7664	0.5385	0.2692	0.359
	RF	0.7944	0.75	0.2308	0.3529
	GB	0.7757	0.5385	0.2692	0.359
Fixed features (19 features)	DT	0.757	0.5	0.0769	0.1333
	LR	0.7757	0.5833	0.2692	0.3684
	RF	0.785	0.6364	0.2692	0.3784
	GB	0.7757	0.5455	0.4615	0.5
$p < 0.1$ (28 features)	DT	0.757	0.5	0.0769	0.1333
	LR	0.7664	0.5385	0.2692	0.359
	RF	0.7944	0.6	0.4615	0.5217
	GB	0.785	0.5517	0.6154	0.5818
$p < 0.2$ (30 features)	DT	0.757	0.5	0.0769	0.1333
	LR	0.7664	0.5385	0.2692	0.359
	RF	0.7757	0.6	0.2308	0.3333
	GB	0.785	0.5517	0.6154	0.5818
$p < 0.3$ (31 features)	DT	0.757	0.5	0.0769	0.1333
	LR	0.7664	0.5385	0.2692	0.359
	RF	0.7664	1	0.0385	0.0741
	GB	0.785	0.5714	0.4615	0.5106
$p < 0.4$ (31 features)	DT	0.757	0.5	0.0769	0.1333
	LR	0.7664	0.5385	0.2692	0.359
	RF	0.7664	1	0.0385	0.0741
	GB	0.785	0.5714	0.4615	0.5106
$p < 0.5$ (32 features)	DT	0.757	0.5	0.0769	0.1333
	LR	0.7664	0.5385	0.2692	0.359
	RF	0.7757	0.5625	0.3462	0.4286
	GB	0.7944	0.5769	0.5769	0.5769

DT: decision tree, LR: Logistic Regression, RF: Random Forest, GB: Gradient Boosting.

silicone oil tamponade in patients who have no prior history of glaucoma or ocular hypertension. Based on these findings, a predictive model was developed in the hope of early detection and treatment for these patients. The presence of preexisting glaucoma is widely recognized as a significant risk factor for IOP elevation following PPV and SO tamponade. Previous studies have reported an incidence of approximately 5.9% to 7% in patients who experienced elevated IOP after surgery and had a history of preoperative glaucoma or ocular hypertension (14, 15). In our study, we excluded patients with a history of glaucoma or ocular hypertension in order to identify additional risk factors. Elevated IOP commonly occurs within the first week after surgery in patients. Therefore, close monitoring and follow-up are essential during this period, along with timely initiation of appropriate treatment to achieve better treatment and prognosis.

Previous studies have considered diabetes, aphakic eye, and the viscosity of silicone oil as risk factors for IOP elevation after PPV combined with silicone oil tamponade (16, 17). In our study, analysis revealed that age, sex, hypertension, diabetes, myopia, retinal detachment, lens status and biological parameters were identified as risk factors for elevated IOP after PPV.

Our results indicated that younger patients are more prone to developing high IOP postoperatively. This finding is comparable with Pillai et al. (18), which suggested that the higher incidence of trabeculitis and anterior chamber inflammation in younger patients may contribute to the manifestation of high IOP symptoms following surgery due to their heightened inflammatory response. However, our study lacks clear evidence to support this conclusion, highlighting the need for future investigations.

Although several biological parameters, such as ACD, CCT, LT, and WTW distance, significantly influenced postoperative IOP in the present study, few prior studies have evaluated their effects on IOP elevation after vitreoretinal surgery with silicone oil filling. Previous studies have found a positive association between CCT and IOP values (19–21). Additionally, a tendency of higher IOP readings with longer axial length has been reported (22), while Hoffmann et al. (23) highlighted the high correlation of IOP measures with thicker central cornea, greater lens thickness, and longer posterior segment length. WTW distance has been found to be positively correlated with ACD. This suggested that WTW also has a positive association with IOP (24). However, these studies only reported the correlation between biological parameters and intraocular pressure, without analyzing the impact on the occurrence of elevated IOP after vitrectomy and silicone oil tamponade. In contrast, the present study is the first to investigate these relationships and found a high positive correlation between postoperative IOP elevation and AL, ACD, and WTW. Further exploration and explanation of the relationship between biological parameters and IOP is necessary.

Many articles have reported that aphakia is a strong risk factor for IOP elevation after PPV and SO tamponade (14, 25), and our study confirmed this finding. We also founded that patients with pseudophakia are also associated with an increased risk of IOP

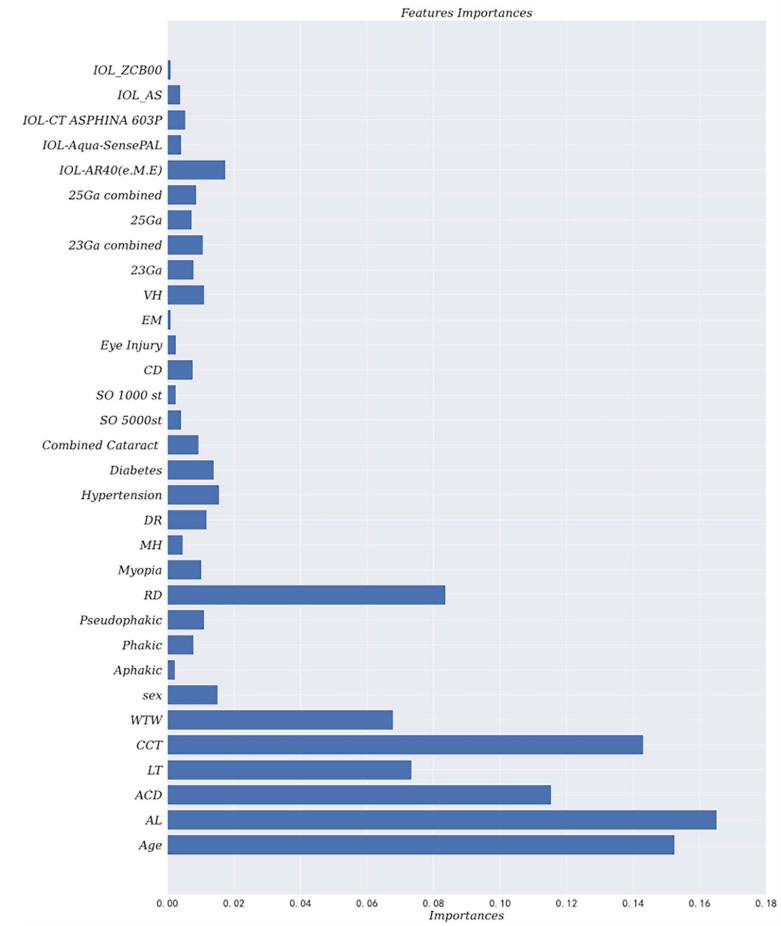

Features	Importance
Age	0.1526
Axial length (AL)	0.1651
Anterior chamber depth (ACD)	0.1154
Lens thickness（LT）	0.0735
Central Corneal Thickness（CCT）	0.1431
WTW	0.0679
Sex	0.0152
Aphakic	0.0023
Phakia	0.0079
Pseudophakic	0.0112
Retinal Detachment	0.0084
Myopia	0.0010
Macular Hole	0.0047
Diabetic Retinopathy	0.0119
Hypertension	0.0156
Diabetes	0.0140
Combined Cataract	0.0094
Silicone Oil_5000st	0.0042
Silicone Oil_1000st	0.0026
Choroidal detachment (CD)	0.0077
Eye Injury	0.0026
Epiretinal membrane (EM)	0.0011
Vitreous hemorrhage (VH)	0.0111
23Ga procedure pak	0.0080
23Ga combined procedure pak	0.0107
25Ga procedure pak	0.0073
25Ga combined procedure pak	0.0088
Intraocular Lens_AR40(e,M,E)	0.0175
Intraocular Lens_Aqua-SensePAL	0.0042
Intraocular Lens_AS	0.0039
Intraocular Lens_CT ASPHINA 603P	0.0054
Intraocular Lens_ZCB00	0.0011

FIGURE 2
Feature importance provided by prediction model.

elevation. Chang (26) was the first to report that the diffusion of oxygen from the vitreous cavity into the anterior chamber is the main reason for elevated IOP in vitrectomized eyes. This diffusion caused alterations in the trabecular meshwork, resulting in reduced aqueous outflow, increased IOP, and the development of glaucoma (27, 28). Because the crystalline lens contains proteins that metabolize oxygen (29, 30), it has the potential to reduce oxidative stress on the trabecular meshwork and prevent oxidative damage. Additionally, it serves as a barrier, preventing oxygen from entering the anterior chamber. These factors could explain why our model estimates that lens status is a significant factor influencing postoperative IOP elevation.

Compared to previous studies (31–33), it has been shown that combined phacoemulsification and intraocular lens implantation (PE&IOL) have an additive effect on transient elevation of IOP, which was consistent with the findings of our prediction model. Furthermore, the long-term effect of cataract surgery on reducing IOP can result in reduced IOP during the late postoperative period. This could be attributed to the induction of greater inflammation in the trabecular meshwork by cataract surgery, resulting in increased IOP during the initial postoperative period. Additionally, the combination of PPV and cataract surgery can induce anterior segment inflammation and disrupt the blood-aqueous barrier (25, 34–36). The long-term reduction of IOP following cataract surgery can be attributed to improvements in outflow facility, deepening of the anterior chamber, and posteriorizing of the lens-iris diaphragm (37, 38).

Patients diagnosed with RD or VH showed a strong association with the development of elevated IOP in our study. Fujikawa et al. (39) reached a similar conclusion, indicating that the RD group had a significantly higher risk of post-vitrectomy IOP increase. Recent study findings (40) have suggested that the absence of an oxygen diffusion barrier in the vitreous leads to significantly elevated partial oxygen pressure within the vitreous cavity. In the case of patients diagnosed with RD and VH, we conducted a comprehensive vitrectomy, completely removing the peripheral vitreous, while performing a core vitrectomy for other patients. This procedure could lead to increased oxygen stress on the trabecular meshwork in the eyes of RD patients (41), potentially resulting in elevated IOP.

Elevated IOP is a common and severe complication of PPV with silicone oil tamponade. Clinicians typically manage high postoperative IOP through the administration of IOP-lowering eye drops or early removal of intraocular silicone oil to avoid optic nerve damage, but the latter approach may induce secondary complications like recurrent retinal detachment. Thus, it is essential from a clinical perspective to examine the potential risk factors associated with postoperative hypertension and develop corresponding interventions to mitigate its occurrence. Furthermore, given the high incidence of myopia and cataract in China, our study introduces biological parameters as factors for a comprehensive systemic analysis. Leveraging a larger data set, our study provides a more thorough and precise analysis of the potential risk factors linked to postoperative high IOP. Moreover, our statistical findings and prediction model lay the foundation for future prospective studies.

5 Conclusion

In conclusion, IOP elevation is a common complication following PPV with SO tamponade. Our study identified several risk factors, including age, sex, hypertension, diabetes, myopia, retinal detachment, lens status and biological parameter. Additionally, we conducted prediction model using GBDT to predict IOP elevation, achieving an accuracy of 0.7944. Knowledge of incidence, risk factors, and mechanism of IOP rise following PPV is essential for the postoperative follow-up and management of patients.

Data availability statement

The raw data supporting the conclusions of this article will be made available by the authors, without undue reservation.

Ethics statement

The studies involving humans were approved by the ethics committee of The First Affiliated Hospital of Nanjing Medical University, 2022-SR-200. Exception to the requirement of informed consent. The studies were conducted in accordance with the local legislation and institutional requirements. Written informed consent for participation was not required from the participants or the participants' legal guardians/next of kin in accordance with the national legislation and institutional requirements.

Author contributions

WF: Conceptualization, Funding acquisition, Methodology, Resources, Writing – review & editing, Project administration. CZ: Formal analysis, Investigation, Methodology, Software, Writing – original draft, Conceptualization, Validation, Visualization. LG: Data curation, Formal analysis, Methodology, Writing – original draft, Conceptualization, Validation, Visualization. NS: Data curation, Investigation, Writing – review & editing. JC: Data curation, Writing – review & editing. SS: Software, Writing – review & editing. YW: Conceptualization, Resources, Supervision, Validation, Visualization, Writing – review & editing. SY: Conceptualization, Funding acquisition, Resources, Supervision, Validation, Visualization, Writing – review & editing.

Funding

The author(s) declare financial support was received for the research, authorship, and/or publication of this article. This work is supported by the National Natural Science Foundation of China (No.82241052), Natural Science Foundation of Jiangsu Province (BK20220730), Nanjing Health Science and Technology Development Special Fund Program (GBX21339); Jiangsu Province Hospital (the First Affiliated Hospital with Nanjing Medical University) Clinical Capacity Enhancement Project (JSPH-MB-2021-8) and Jiangsu Province Hospital Excellent Young and Middle-aged Talents Support Special Fund Program (YNRCQN008).

Conflict of interest

The authors declare that the research was conducted in the absence of any commercial or financial relationships that could be construed as a potential conflict of interest.

Publisher's note

References

1. Cibis PA, Becker B, Okun E, Canaan S. The use of liquid silicone in retinal detachment surgery. *Arch Ophthalmol*. (1962) 68:590–9. doi: 10.1001/archopht.1962.00960030594005

2. Abu-Yaghi NE, Abu Gharbieh YA, al-Amer AM, AlRyalat SAS, Nawaiseh MB, Darweesh MJ, et al. Characteristics, fates and complications of long-term silicone oil tamponade after pars plana vitrectomy. *BMC Ophthalmol*. (2020) 20:336. doi: 10.1186/s12886-020-01608-5

3. Branisteanu DC, Moraru AD, Maranduca MA, Branisteanu D, Stoleriu G, Branisteanu C, et al. Intraocular pressure changes during and after silicone oil endotamponade (review). *Exp Ther Med*. (2020) 20:1. doi: 10.3892/etm.2020.9334

4. Marti M, Walton R, Böni C, Zweifel SA, Stahel M, Barthelmes D. Increased intraocular pressure is a risk factor for unexplained visual loss during silicone oil ENDOTAMPONADE. *Retina*. (2017) 37:2334–40. doi: 10.1097/IAE.0000000000001492

5. Muether PS, Hoerster R, Kirchhof B, Fauser S. Course of intraocular pressure after vitreoretinal surgery: is early postoperative intraocular pressure elevation predictable? *Retina*. (2011) 31:1545–52. doi: 10.1097/IAE.0b013e31820f4b05

6. Antoun J, Azar G, Jabbour E, Kourie HR, Slim E, Schakal A, et al. Vitreoretinal surgery with silicone oil tamponade in primary uncomplicated rhegmatogenous retinal detachment: clinical outcomes and complications. *Retina*. (2016) 36:1906–12. doi: 10.1097/IAE.0000000000001008

7. Honavar SG, Goyal M, Majji AB, Sen PK, Naduvilath T, Dandona L. Glaucoma after pars plana vitrectomy and silicone oil injection for complicated retinal detachments. *Ophthalmology*. (1999) 106:169–76. doi: 10.1016/S0161-6420(99)90017-9

8. Barr CC, Lai MY, Lean JS, Linton KLP, Trese M, Abrams G, et al. Postoperative intraocular pressure abnormalities in the silicone study. Silicone Study Report 4. *Ophthalmology*. (1993) 100:1629–35. doi: 10.1016/S0161-6420(93)31425-9

9. Ichhpujani P, Jindal A, Jay KL. Silicone oil induced glaucoma: a review. *Graefes Arch Clin Exp Ophthalmol*. (2009) 247:1585–93. doi: 10.1007/s00417-009-1155-x

10. Budenz DL, Taba KE, Feuer WJ, Eliezer R, Cousins S, Henderer J, et al. Surgical management of secondary glaucoma after pars plana vitrectomy and silicone oil injection for complex retinal detachment. *Ophthalmology*. (2001) 108:1628–32. doi: 10.1016/S0161-6420(01)00658-3

11. Jonas JB, Knorr HL, Rank RM, Budde WM. Intraocular pressure and silicone oil endotamponade. *J Glaucoma*. (2001) 10:102–8. doi: 10.1097/00061198-200104000-00006

12. Jackson TL, Thiagarajan M, Murthy R, Snead MP, Wong D, Williamson TH. Pupil block glaucoma in phakic and pseudophakic patients after vitrectomy with silicone oil injection. *Am J Ophthalmol*. (2001) 132:414–6. doi: 10.1016/S0002-9394(01)00991-6

13. Rajkomar A, Dean J, Kohane I. Machine learning in medicine. *N Engl J Med*. (2019) 380:1347–58. doi: 10.1056/NEJMra1814259

14. Jabbour E, Azar G, Antoun J, Kourie HR, Abdelmassih Y, Jalkh A. Incidence and risk factors of ocular hypertension following pars Plana vitrectomy and silicone oil injection. *Ophthalmologica*. (2018) 240:129–34. doi: 10.1159/000489792

15. Fang Y, Long Q, Wang X, Jiang R, Sun X. Intraocular pressure 1 year after vitrectomy in eyes without a history of glaucoma or ocular hypertension. *Clin Ophthalmol*. (2017) 11:2091–7. doi: 10.2147/OPTH.S144985

16. Iwata K, Haruta M, Uehara K, Koshiyama T, Tsuru H, Yamakawa R. Influence of postoperative lens status on intraocular pressure and corneal endothelium following vitrectomy with silicone oil tamponade. *Nippon Ganka Gakkai Zasshi*. (2013) 117:95–101.

17. Al-Jazzaf A, Netland P, Charles S. Incidence and management of elevated intraocular pressure after silicone oil injection. *J Glaucoma*. (2005) 14:40–6. doi: 10.1097/01.ijg.0000145811.62095.fa

18. Pillai GS, Varkey R, Unnikrishnan UG, Radhakrishnan N. Incidence and risk factors for intraocular pressure rise after transconjunctival vitrectomy. *Indian J Ophthalmol*. (2020) 68:812–7. doi: 10.4103/ijo.IJO_244_19

19. Lee M, Ahn J. Effects of central corneal stromal thickness and epithelial thickness on intraocular pressure using Goldmann Applanation and non-contact Tonometers. *PLoS One*. (2016) 11:e0151868. doi: 10.1371/journal.pone.0151868

20. Ma Y, Ma Y, Feng C, Shen M, Yuan Y. Ocular biometric parameters are associated with non-contact tonometry measured intraocular pressure in non-pathologic myopic patients. *Int Ophthalmol*. (2020) 40:431–7. doi: 10.1007/s10792-019-01203-8

21. Rimayanti U, Kiuchi Y, Uemura S, Takenaka J, Mochizuki H, Kaneko M. Ocular surface displacement with and without contact lenses during non-contact tonometry. *PLoS One*. (2014) 9:e96066. doi: 10.1371/journal.pone.0096066

22. Foster PJ, Broadway DC, Garway-Heath DF, Yip JLY, Luben R, Hayat S, et al. Intraocular pressure and corneal biomechanics in an adult British population: the EPIC-Norfolk eye study. *Invest Ophthalmol Vis Sci*. (2011) 52:8179–85. doi: 10.1167/iovs.11-7853

23. Hoffmann EM, Aghayeva F, Wagner FM, Fiess A, Nagler M, Münzel T, et al. Intraocular pressure and its relation to ocular geometry: results from the Gutenberg health study. *Invest Ophthalmol Vis Sci*. (2022) 63:40. doi: 10.1167/iovs.63.1.40

24. Xu G, Wu G, du Z, Zhu S, Guo Y, Yu H, et al. Distribution of white-to-white corneal diameter and anterior chamber depth in Chinese myopic patients. *Front Med (Lausanne)*. (2021) 8:732719. doi: 10.3389/fmed.2021.732719

25. Koreen L, Yoshida N, Escariao P, Niziol LM, Koreen IV, Musch DC, et al. Incidence of, risk factors for, and combined mechanism of late-onset open-angle glaucoma after vitrectomy. *Retina*. (2012) 32:160–7. doi: 10.1097/IAE.0b013e318217fffb

26. Chang S. LXII Edward Jackson lecture: open angle glaucoma after vitrectomy. *Am J Ophthalmol*. (2006) 141:1033–1043.e1. doi: 10.1016/j.ajo.2006.02.014

27. Izzotti A, Saccà S, Cartiglia C, De Flora S. Oxidative deoxyribonucleic acid damage in the eyes of glaucoma patients. *Am J Med*. (2003) 114:638–46. doi: 10.1016/S0002-9343(03)00114-1

28. Saccà S, Izzotti A, Rossi P, Traverso C. Glaucomatous outflow pathway and oxidative stress. *Exp Eye Res*. (2007) 84:389–99. doi: 10.1016/j.exer.2006.10.008

29. Shui Y, Fu J, Garcia C, Dattilo L, Rajagopal R, McMillan S, et al. Oxygen distribution in the rabbit eye and oxygen consumption by the lens. *Invest Ophthalmol Vis Sci*. (2006) 47:1571–80. doi: 10.1167/iovs.05-1475

30. Barbazetto I, Liang J, Chang S, Zheng L, Spector A, Dillon J. Oxygen tension in the rabbit lens and vitreous before and after vitrectomy. *Exp Eye Res*. (2004) 78:917–24. doi: 10.1016/j.exer.2004.01.003

31. Yang HK, Woo SJ, Park KH, Park KH. Intraocular pressure changes after vitrectomy with and without combined phacoemulsification and intraocular lens implantation. *Korean J Ophthalmol*. (2010) 24:341–6. doi: 10.3341/kjo.2010.24.6.341

32. Shingleton B, Rosenberg R, Teixeira R, O'Donoghue M. Evaluation of intraocular pressure in the immediate postoperative period after phacoemulsification. *J Cataract Refract Surg*. (2007) 33:1953–7. doi: 10.1016/j.jcrs.2007.06.039

33. Thirumalai B, Baranyovits P. Intraocular pressure changes and the implications on patient review after phacoemulsification. *J Cataract Refract Surg*. (2003) 29:504–7. doi: 10.1016/S0886-3350(02)01481-5

34. Laurell C, Zetterström C. Inflammation and blood-aqueous barrier disruption. *J Cataract Refract Surg*. (2000) 26:306–7. doi: 10.1016/S0886-3350(00)00347-3

35. Desai U, Alhalel A, Schiffman R, Campen T, Sundar G, Muhich A. Intraocular pressure elevation after simple pars plana vitrectomy. *Ophthalmology*. (1997) 104:781–6. doi: 10.1016/S0161-6420(97)30233-4

36. Laurell C, Lydahl E. Evaluation of aqueous outflow facility in patients with high intraocular pressure after cataract surgery. *Ophthalmic Surg Lasers Imaging*. (2006) 37:476–80. doi: 10.3928/15428877-20061101-05

37. Alaghband P, Beltran-Agulló L, Galvis E, Overby D, Lim K. Effect of phacoemulsification on facility of outflow. *Br J Ophthalmol*. (2018) 102:1520–6. doi: 10.1136/bjophthalmol-2017-311548

38. Ki IY, Yamashita T, Uemura A, Sakamoto T. Long-term intraocular pressure changes after combined phacoemulsification, intraocular lens implantation, and vitrectomy. *Jpn J Ophthalmol*. (2013) 57:57–62. doi: 10.1007/s10384-012-0207-7

39. Fujikawa M, Sawada O, Kakinoki M, Sawada T, Kawamura H, Ohji M. Long-term intraocular pressure changes after vitrectomy for epiretinal membrane and macular hole. *Graefes Arch Clin Exp Ophthalmol*. (2014) 252:389–93. doi: 10.1007/s00417-013-2475-4

40. Yamamoto K, Iwase T, Terasaki H. Long-term changes in intraocular pressure after vitrectomy for Rhegmatogenous retinal detachment, epi-retinal membrane, or macular hole. *PLoS One*. (2016) 11:e0167303. doi: 10.1371/journal.pone.0167303

41. Luk F, Kwok A, Lai T, Lam D. Presence of crystalline lens as a protective factor for the late development of open angle glaucoma after vitrectomy. *Retina (Philadelphia, PA)*. (2009) 29:218–24. doi: 10.1097/IAE.0b013e31818ba9ca

frontiers | Frontiers in Medicine

TYPE Original Research
PUBLISHED 15 January 2024
DOI 10.3389/fmed.2023.1306276

OPEN ACCESS

EDITED BY
Horace MASSA,
Hôpitaux universitaires de Genève (HUG), Switzerland

REVIEWED BY
Pablo De Gracia,
University of Detroit Mercy, United States
João Machado,
Federal University of Rio de Janeiro, Brazil
Xuhua Tan,
Sun Yat-sen University, China
Honghua Yu,
Guangdong Provincial People's Hospital, China

*CORRESPONDENCE
Xiangjia Zhu
✉ zhuxiangjia1982@126.com
Yi Lu
✉ luyieent@163.com

RECEIVED 03 October 2023
ACCEPTED 28 December 2023
PUBLISHED 15 January 2024

CITATION
Huang Z, Qi J, Cheng K, Liu S, Zhang K, Du Y, Lu Y and Zhu X (2024) The relationships between lens diameter and ocular biometric parameters: an ultrasound biomicroscopy-based study.
Front. Med. 10:1306276.
doi: 10.3389/fmed.2023.1306276

The relationships between lens diameter and ocular biometric parameters: an ultrasound biomicroscopy-based study

Zhiqian Huang[1,2,3,4,5], Jiao Qi[1,2,3,4,5], Kaiwen Cheng[1,2,3,4,5], Shuyu Liu[1,2,3,4,5], Keke Zhang[1,2,3,4,5], Yu Du[1,2,3,4,5], Yi Lu[1,2,3,4,5]* and Xiangjia Zhu[1,2,3,4,5]*

[1]Department of Ophthalmology, Eye and Ear, Nose and Throat Hospital of Fudan University, Shanghai, China, [2]Eye Institute, Eye and Ear, Nose and Throat Hospital of Fudan University, Shanghai, China, [3]NHC Key Laboratory of Myopia (Fudan University), Key Laboratory of Myopia, Chinese Academy of Medical Sciences, Shanghai, China, [4]Shanghai Key Laboratory of Visual Impairment and Restoration, Shanghai, China, [5]State Key Laboratory of Medical Neurobiology, Shanghai, China

Purpose: This study aims to explore the relationships between lens diameter (LD) measured with ultrasound biomicroscopy (UBM) and ocular biometric parameters.

Methods: Ocular biometric parameters including axial length (AL), white-to-white distance (WTW), anterior chamber depth (ACD), lens thickness (LT) and anterior segment length (ASL) were measured with IOL-Master 700, and the direct measurement of LD was conducted through UBM (ArcScan Insight 100). Relationships between LD and ocular biometric parameters were then investigated. Eyes with AL ≥ 28 mm were defined as eyes with extreme myopia, and eyes with AL < 28 mm were defined as eyes without extreme myopia.

Results: A total of 194 eyes from 194 subjects were included. The mean LD was 9.58 ± 0.49 mm, ranging from 8.60 to 10.96 mm. According to univariate analysis, larger LD was associated with elder age, male gender, larger WTW, ACD and ASL (all $p < 0.05$). Meanwhile, the LD was positively correlated with AL in eyes without extreme myopia ($p < 0.05$), but not in eyes with extreme myopia ($p > 0.05$). Backward stepwise regressions revealed that a larger LD was associated with larger WTW, ASL and AL in eyes without extreme myopia (all $p < 0.05$), while ASL was the only significant variable in eyes with extreme myopia ($p < 0.05$).

Conclusion: Larger WTW, ASL and AL in eyes without extreme myopia, as well as longer ASL in eyes with extreme myopia indicated a larger LD, which provides guidance in personalized surgical choice and promises ideal visual outcomes.

KEYWORDS

lens diameter, ultrasound biomicroscopy, white-to-white distance, anterior segment length, axial length

Introduction

Cataract has always been one of the most common causes of vision loss worldwide (1). In recent decades, with the rapid development of accurate biometric techniques and application of various functional intraocular lenses (IOLs), cataract surgery has become more of a refractive surgery aiming at better visual quality, rather than solely visual acuity restorations (2, 3).

However, postoperative misalignment of intraocular lenses (IOLs), encompassing tilt, decentration, and rotation, notably compromises refractive cataract surgery outcomes, particularly with multifocal and toric IOLs (4, 5). It is widely acknowledged that the size of the capsular bag plays a vital role in the postoperative IOL position (3, 6), but the difficulty in measuring lens diameter (LD) directly, as an indicator for the size of the capsular bag, presents challenges for surgeons in choosing a corresponding compatible IOL. Thus, investigation of the relationships of LD with measurable ocular biometric parameters might provide useful information for cataract surgeons to predict LD and further select compatible IOLs.

However, associations between LD and biometric parameters remain controversial due to technique restrictions. Previously, several studies have focused on the measurements of human cadaver eyes and found that the LD was positively correlated with the axial length (AL) and age, but could not be predicted by white-to-white (WTW) distance (7, 8). The ocular magnetic resonance imaging (MRI) was applied to find that the transverse diameter of the eyeball and AL resulted in the best prediction for LD (9), while the results of optical coherence tomography (OCT) showed poor prediction performance (10). Nevertheless, postmortem changes of cadaver lens largely reduced the accuracy, and the sample sizes were limited due to the difficulty in obtaining cadaver lens, and the poor resolution of MRI and the incomplete lens imaging of OCT impaired the reliability of these measurements.

Here we introduced a newly developed very high frequency (VHF) ultrasound biomicroscopy (UBM), ArcScan Insight 100. Compared with conventional UBM, it offers superior signal penetration and better ability to capture the entire anterior segment in a single image, and is less invasive by using a disposable eyepiece, which allows to measure the LD more accurately and conveniently (11–13).

Therefore, in this study, we aimed to investigate the relationships between LD measured with UBM and ocular biometric parameters, thereby guiding surgeons to choose a compatible IOL, and helping patients obtain better visual outcomes.

Materials and methods

Ethics statement

The cross-sectional study was performed in accordance with the tenets of the Declaration of Helsinki, approved by the Institutional Review Board of the Eye & ENT Hospital of Fudan University, Shanghai, China, and registered at http://www.clinicaltrials.gov (accession number NCT02182921, protocol number 20201001–1, date of approval December 22nd, 2020). All participants provided signed informed consent, after receiving a full description of the study, for the use of their clinical data.

Participants

Participants planned to have cataract surgery at Eye & ENT Hospital of Fudan University, Shanghai, China and healthy volunteers were enrolled in this study from January 2022 to December 2022. Exclusion criteria are listed as follows: (1) abnormalities in the position and shape of the lens, such as lens dislocation or subluxation, lens coloboma, etc.; (2) mature or hyper-mature stage of cataract (LOCS III grading: NO score $\geq$ 5 or NC score $\geq$ 5 or C score $\geq$ 4) that impacts the relationships between LD and other ocular parameters; (3) history of strabismus, nystagmus or severe retinal pathologies that affect fixation; (4) history of intraocular surgeries or ocular trauma; (5) unclear UBM images of the anterior segment. One eye was randomly selected from each patient to avoid double-organ bias.

Ocular biometric measurements by IOL master

Ocular biometric parameters were obtained using the IOL Master 700 (Carl Zeiss AG, Jena, Germany), a non-invasive optical biometer that uses partial coherence interferometry, by experienced technicians. Before measurement, the correct fixation of the examinees was visually checked on the fovea scan by the technician. During each examination, AL, WTW; anterior chamber depth (ACD), and lens thickness (LT) were measured automatically. Meanwhile, the standard deviation (SD) for AL, ACD and LT were also automatically calculated, and the device would warn of low-quality results if the SD for AL >0.027 mm, for ACD >0.021 mm or LT >0.038 mm, which would further be deleted and repeated until reproducible readings were obtained. The anterior segment length (ASL) was calculated by the sum of LT and ACD. Eyes with AL $\geq$ 28 mm were defined as eyes with extreme myopia, and eyes with AL < 28 mm were defined as eyes without extreme myopia.

Lens diameter measurement by ultrasound biomicroscopy

Cross-sectional views of the lens with anterior segment imaging were obtained using UBM measurements (Insight 100, ArcScan Inc., Golden, CO, USA), which is a newly developed very high frequency (VHF) ultrasound device for imaging and obtaining biometric measurements of the eye. It uses precision high-frequency ultrasound technology to offer superior signal penetration and to image the true anatomy of the entire anterior segment in a single image with the high resolution at an ultrasonic frequency of 20–60 MHz, a maximum arc scanning range of 80°, and a linear scanning range of 28 mm (Figure 1A). During scanning, seated subjects placed their chin into a headrest and the fellow eye into a soft and rimmed eye-cup, which was

Abbreviations: IOL, Intraocular lens; UBM, Ultrasound biomicroscopy; LD, Lens diameter; WTW, White-to-white distance; ACD, Anterior chamber depth; LT, Lens thickness; ASL, Anterior segment length; AL, Axial length; MRI, Magnetic resonance imaging; OCT, Optical coherence tomography.

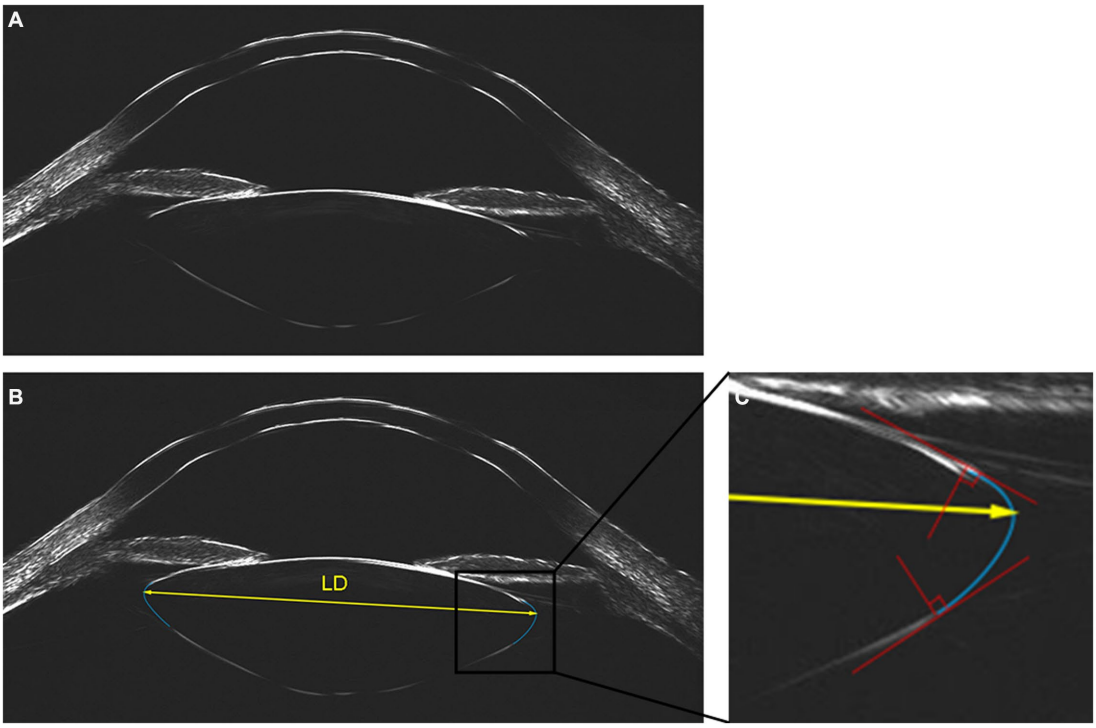

FIGURE 1
Lens imaging and measurement of lens diameter with ArcScan Insight 100. **(A)** Original image. **(B)** Two best fitting arcs (in blue) were generated to delineate the equator of the lens, then the lens diameter (LD) was measured as the distance between the vertex of the circular arcs on both sides of the lens (in yellow). **(C)** Two auxiliary lines (in red) were introduced at the intersection of our fitting arc and the observed anterior or posterior curve to ensure the alignment, with the perpendicular angle defining the fitting arc (in blue) as the best fit.

then filled with the balanced salt solution. A soft membrane separated the eye from the transducer in a scanning chamber filled with distilled water. With participants staring at a narrow fixation target, the examiner adjusted the scanning frame to be centered on the corneal reflex. The UBM measurement was then performed in the 'capsule' mode, with a tissue penetration depth of 15 mm on the axial horizontal section (transverse diameter passing through the corneal apex from 9 to 3 o'clock).

Using the built-in tool of Insight 100, the outline of the lens was delineated and LD was measured by two experienced ophthalmologists independently. The built-in manual caliper tool can generate a fitting arc through three points, which could be adjusted via moving these three points for the best fit. Two auxiliary lines (Figure 1C, depicted in red) were introduced at the intersection of our fitting arc and the observed anterior or posterior curve, which were strategically positioned to ensure that the fitting arc tangentially aligned with the observed curve. The perpendicular orientation of these lines determined the ideal positioning, defining the fitting arc as the best fit (Figure 1C, depicted in blue). Two best fitting arcs were generated to delineate the equator of the lens, effectively outlining its elliptical shape. LD was quantified as the distance between the vertex of the circular arcs on both sides of the lens (Figure 1B, depicted in yellow). The Bland–Altman analysis of two observers showed excellent interobserver reproducibility (Supplementary Figure S1), and the averaged measurements from both observers were utilized for subsequent analyses.

Statistical analysis

Quantitative data were presented as means ± standard deviations (SD). After assessing the normal distribution of the data with Shapiro–Wilk normality test, comparisons between two groups were performed using Student's t-test, and among more than two groups using one-way analysis of variance (ANOVA). Categorical data were expressed as the frequencies and percentages of each category, and compared using X^2 test. The Pearson coefficient was determined to evaluate the strength of all correlation pairs. Multiple linear regressions were performed using backward stepwise selection. Statistical analyses were performed with SPSS version 26.0 (IBM Inc., Chicago, IL, USA) and graphs were prepared using Prism 8.0 (GraphPad Software, Inc., USA). p values <0.05 were considered statistically significant.

Results

Characteristics

Table 1 presents the demographic and ocular biometric parameters of all participants in this study. This study included 194 eyes of 194 patients (91 men and 103 women). The mean age was 59.2 ± 16.1, ranging from 22 to 90 years old. The study population included 20 (10.31%) eyes with AL < 22 mm, 80 (41.24%) eyes with AL between 22 and 24.5 mm, 28 (14.43%) eyes with AL between 24.5 and

26 mm, 32 (16.50%) eyes with AL between 26 and 28 mm and 34 (17.53%) eyes with AL ≥ 28 mm.

The distribution of LD among this study population is presented in Figure 2. The mean LD was 9.58 ± 0.49 mm, ranging from 8.60 to 10.96 mm. The 25 and 75% percentiles of LD were 9.22 and 9.84, respectively.

Univariate analysis of the correlations between lens diameter and other variables

The LD was positively correlated with age (Pearson's correlation coefficient, $r = 0.206$, $p = 0.004$; Figure 3A), and the male subjects had significantly larger LD than female subjects (9.68 ± 0.48 mm for males and 9.49 ± 0.48 mm for females, $p = 0.009$, Figure 3B). As presented in the scatterplots for LD against WTW, ACD, LT, and ASL, the Pearson's correlation analysis revealed that LD was positively correlated with WTW ($r = 0.288$, $p < 0.001$; Figure 3C), ACD ($r = 0.331$, $p < 0.001$; Figure 3D), ASL ($r = 0.448$, $p < 0.001$; Figure 3F), whereas, no correlation was found between LD and LT ($r = 0.074$, $p = 0.301$; Figure 3E).

Change of LD with AL is presented in Figure 4A. With the increase of AL, the LD was firstly increased gradually to peak in the group with AL of 26-28 mm, then decreased slightly (ANOVA, $p < 0.05$). Pearson's correlation analysis showed that the LD correlated positively with AL in eyes without extreme myopia ($r = 0.398$, $p < 0.001$; Figure 4B), but not correlated in eyes with extreme myopia ($r = 0.175$, $p = 0.323$; Figure 4B).

TABLE 1 Demographic and ocular biometric data of all participants.

Parameters	Value
Eyes (n)	194
Age (years)	59.2 ± 16.1 (22–90)
Gender (Male/Female)	91 (46.9%) / 103 (53.1%)
WTW (mm)	11.62 ± 0.50 (10.1–12.7)
ACD (mm)	3.18 ± 0.48 (1.75–4.60)
LT (mm)	4.31 ± 0.52 (3.02–5.87)
ASL (mm)	7.49 ± 0.44 (5.99–9.09)
AL (mm)	25.39 ± 3.11 (21.07–35.33)

WTW, white-to-white distance; ACD, anterior chamber depth; LT, lens thickness; ASL, anterior segment length; AL, axial length.
Data were presented as mean ± standard deviation (range or proportion).

Independent predictive factors of lens diameter with multivariate analysis

Backward stepwise multiple linear regressions, which included age, sex, WTW, ASL and AL as independent variables, were performed to evaluate the independent predictors of LD in eyes without and with extreme myopia, respectively. As shown in Table 2, after adjusting for age and sex, a larger LD was associated with larger WTW (β = 0.165, $p = 0.019$), longer ASL (β = 0.232, $p = 0.010$) and longer AL (β = 0.074, $p = 0.001$) in eyes without extreme myopia. Whereas, in eyes with extreme myopia, only ASL (β = 0.693, $p = 0.014$) was independently correlated with LD.

Discussion

Cataract is a common ocular disease which can cause vision impairment and seriously affect the patient's quality of life. With

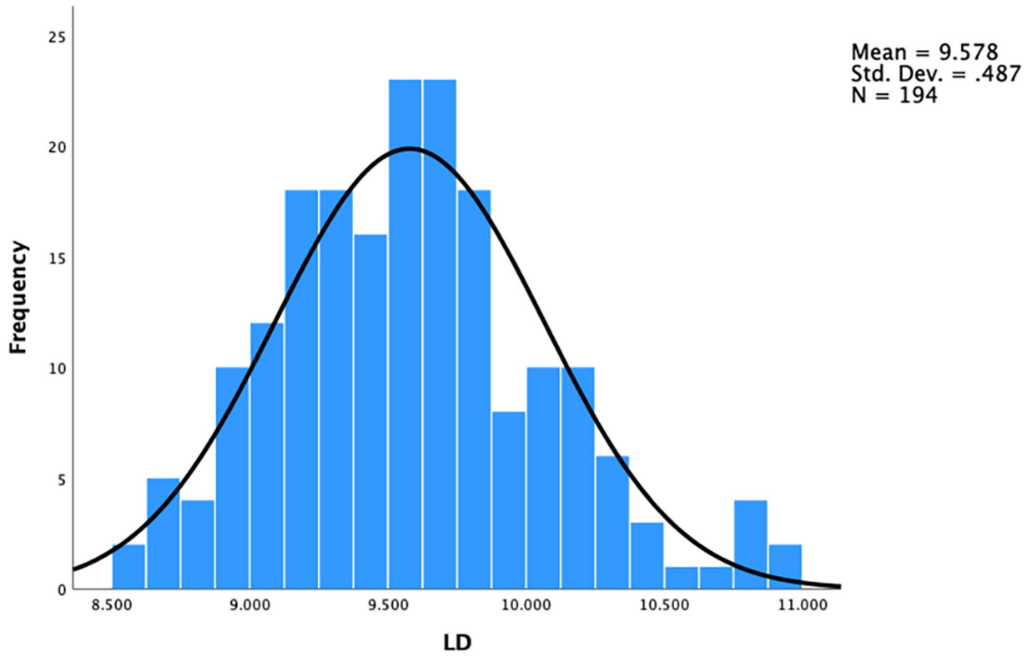

FIGURE 2
Distribution of lens diameter (LD) among this study population.

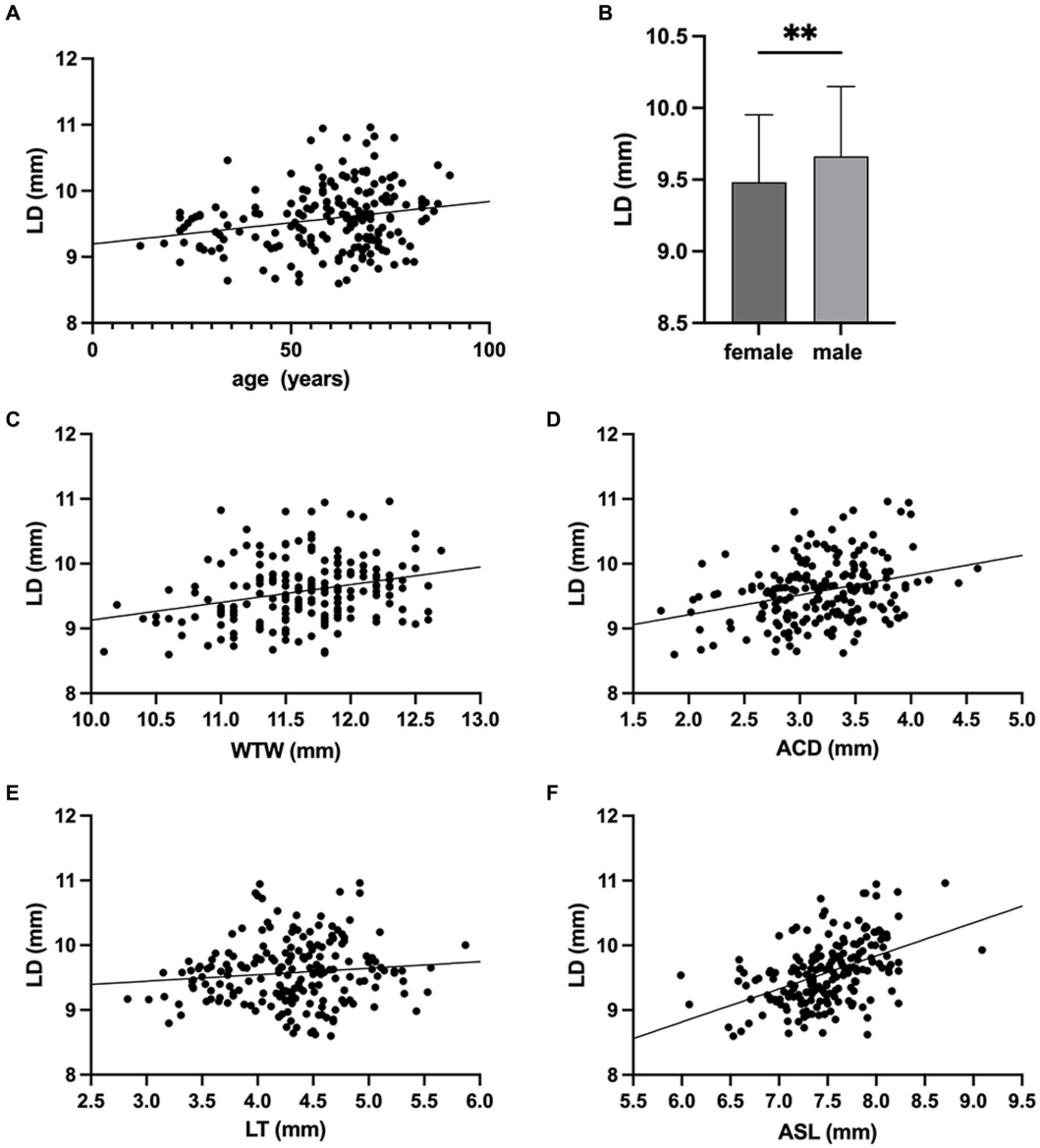

FIGURE 3
Associations of lens diameter (LD) with age, sex and ocular biometric parameters. **(A)** LD was positively correlated with age ($r = 0.206$, $p = 0.004$). **(B)** The LD of males was significantly larger than that of females (** $p < 0.01$). Correlations between lens diameter (LD) and **(C)** white-to-white distance (WTW) ($r = 0.288$, $p < 0.001$), **(D)** anterior chamber depth (ACD) ($r = 0.331$, $p < 0.001$), **(E)** lens thickness (LT) ($r = 0.074$, $p = 0.301$), **(F)** anterior segment length (ASL) ($r = 0.448$, $p < 0.001$).

advances in surgical technology and application of various functional IOLs, cataract surgery has entered the era of refractive surgery, which can not only rebuild vision but also provide good visual quality. The postoperative stability of the IOL position is the critical fundament of achieving optimal visual outcomes, with the match between the capsular bag and IOL serving as the determinant (2, 3, 5). However, whether the regular biometry could predict the LD has not yet been reached, and the best approach to measure or calculate the LD was also sought for (14–16). In this study, we used a novel UBM to measure LD and investigate the relationships between the LD and ocular biometric parameters, and observed that a larger LD was associated with larger WTW, ASL and AL in eyes without extreme myopia, while ASL was the only significant predictor in eyes with extreme myopia.

In our study, we firstly used a novel UBM to measure LD and investigate its predictors. Revolving around LD, early efforts were based on *ex vivo* measurements of human cadaver eyes (7, 8). However, due to the postmortem changes of cadaver lens, the deviation from its physiological shape should not be overlooked. And since the lens shape was dependent on the accommodation force, the extracted lens without any accommodation was not comparable to the lens *in vivo* (17). Compared with previous studies based on cadaver eyes, our study avoided the postmortem changes of cadaver lens from its physiological shape, rendering our findings more precise and compelling (12, 13). Besides, the primitive methods of measurement may lack accuracy, and the sample sizes of both studies was relatively small. Also, plenty of *in vivo* measurements have been performed, such as MRI and OCT, but a reliable and easily available approach to

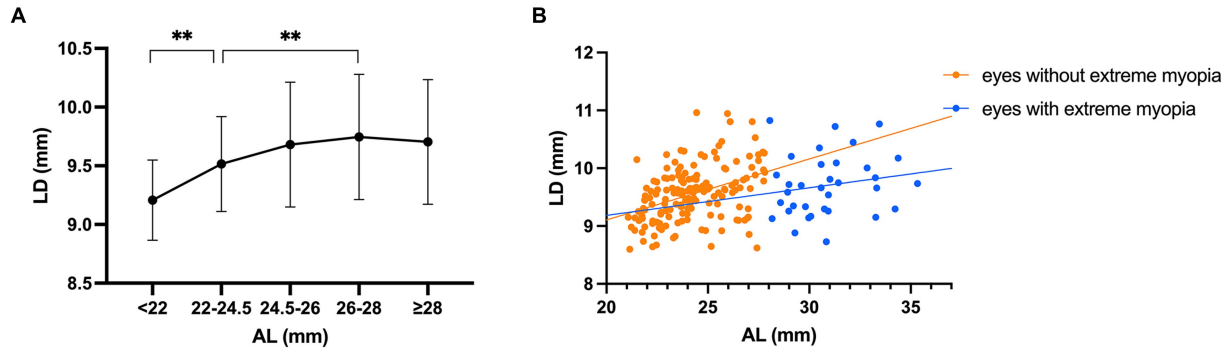

FIGURE 4
Changes of lens diameter (LD) with axial length (AL). **(A)** Compared with the AL 22–24.5 mm group, the AL < 22 mm group had significantly smaller LDs and the AL 26–28 mm group had significantly larger LDs (** $p < 0.01$). With the increase of AL, the LD was firstly increased gradually to peak in the AL 26–28 mm group, then decreased slightly. **(B)** The correlation between LD and AL was significantly positive in eyes without extreme myopia ($r = 0.398$, $p < 0.001$), but not significant in eyes with extreme myopia ($r = 0.175$, $p = 0.323$).

TABLE 2 Multiple linear regressions analysis of LD in eyes without and with extreme myopia.

	Variables	β Coefficient	Std. Error	*P* value
Eyes without extreme myopia	WTW	0.165	0.069	0.019
	ASL	0.232	0.089	0.010
	AL	0.074	0.021	0.001
Eyes with extreme myopia	ASL	0.693	0.268	0.014

WTW, white-to-white distance; ASL, anterior segment length; AL, axial length.

predict LD was hardly found. The resolution of MRI remained relatively lower, and given its expensive and inconvenient nature, routine utilization was impractical (9). Regarding the commonly employed measuring methodology based on OCT imaging, the distance between the intersections of the extended anterior and posterior lenticular surface curvatures was regarded as the lens equatorial diameter, which obviously failed to match with the actual elliptical shape of the lens (10, 14, 18, 19). On the contrary, the strength of Insight 100 lies in its ability to detect the peripheral area behind the iris, thus enhancing its capability to depict the real elliptical shape of the lens after the rigorous fitting procedure mentioned above, rather than a spindle-shaped one. As evidenced by recent studies, measurements of lens diameters with Insight 100 were notably shorter compared to those obtained using OCT. This disparity suggests that the enhanced accuracy offered by Insight 100 could carry considerable implications in guiding more informed surgical decisions (12, 13). Besides, compared with conventional UBM, the newly developed Insight 100 exhibits superior signal penetration and reduced invasiveness using a disposable eyepiece, indicating the potential for broader applications (11–13).

In our study, we evaluated the relationships between LD and ocular biometric parameters *in vivo* and found a non-linear correlation between LD and AL. To our best knowledge, our study was the largest sample-size LD prediction study based on ocular biometric parameters. Previously, the conventional idea that longer eyes have a larger capsular diameter was widely believed, as several studies based on cadaver eyes and *in vivo* measurements including OCT and MRI have consistently exhibited a positive association between LD and AL (6, 8–10, 14, 19–21). Contrary to prior expectations, we found that the correlation between LD and AL was not linear. In eyes without extreme myopia, as historically proposed, the LD was on the rise as the AL increased, but that was not the case in eyes with extreme myopia, which could be explained by morphological characteristics of the elongation of myopic eyes. Normally, the eyeball grows globally and uniformly with AL increasing. However, as suggested by our previous finding, extreme elongation of the eyeball was mainly due to the extension of the posterior segment (22). Thus, in eyes with extreme myopia, the LD, as an anterior structure, was not further increased with the eyeball extension.

In our study, we also provided evidence for predicting LD using ocular biometric parameters. We demonstrated that larger AL, WTW and ASL were associated with larger LD in eyes without extreme myopia, and larger ASL was only independent predictor for larger LD in eyes with extreme myopia. The positive correlations of WTW and ASL with LD was consistent with our previous finding that toric IOLs rotate more in eyes with larger WTW and longer ASL (23). One reasonable explanation could be that WTW serves as an indicator of the horizontal diameter of the eyeball, thus representing the horizontal size of the anterior segment to a certain extent (24), and ASL has been established to represent the sagittal dimension of the anterior segment (22, 23). Based on the above findings, we should pay special attention to the selection of an appropriate IOL in the clinical management of patients with these characteristics to avoid postoperative IOL decentration, tilt and rotation.

Several limitations exist in this study. First, the single-hospital setting and exclusion criteria may introduce selection bias, warranting caution when extrapolating findings to broader populations. Second, potential confounding factors, which we may not have fully accounted for, require further elucidation in future research. Third, given the inherent imaging limitations of Insight 100 and the potential deviations introduced by manual measurement, our measuring protocol has not been established as a gold standard for *in vivo* lens biometry, so further explorations into advanced imaging techniques or software tools that offer improved resolution or better delineation of the lens equator still remain a priority.

Conclusion

To conclude, with the novel UBM introduced, our study demonstrated that a larger LD was associated with elder age, male gender, larger WTW, ACD and ASL, while the correlation between AL and LD was not linear. Conventional parameters including AL, WTW and ASL in eyes without extreme myopia, as well as ASL in eyes with extreme myopia would help better to predict LD, hopefully to aid in personalized surgical decision-making and to promise ideal visual outcomes.

Data availability statement

The raw data supporting the conclusions of this article will be made available by the authors, without undue reservation.

Ethics statement

The studies involving humans were approved by the Institutional Review Board of the Eye & ENT Hospital of Fudan University, Shanghai, China. The studies were conducted in accordance with the local legislation and institutional requirements. The participants provided their written informed consent to participate in this study.

Author contributions

ZH: Conceptualization, Data curation, Formal analysis, Investigation, Writing – original draft. JQ: Data curation, Writing – review & editing. KC: Data curation, Writing – review & editing. SL: Data curation, Writing – review & editing. KZ: Data curation, Writing – review & editing. YD: Data curation, Writing – review & editing. YL: Funding acquisition, Resources, Supervision, Writing – review & editing. XZ: Conceptualization, Funding acquisition, Resources, Supervision, Writing – review & editing.

Funding

The author(s) declare financial support was received for the research, authorship, and/or publication of this article. The study was supported by research grants from the National Key Research and Development Program of China (2022YFC2502800), National Natural Science Foundation of China (82122017, 82271069, 81900838, 81870642, 81970780, 81470613 and 81670835), Science and Technology Innovation Action Plan of Shanghai Science and Technology Commission (19441900700 and 21S31904900), Clinical Research Plan of Shanghai Shenkang Hospital Development Center (SHDC2020CR4078, SHDC12019X08 and SHDC12020111), Double-E Plan of Eye & ENT Hospital (SYA202006), Shanghai Municipal Key Clinical Specialty Program (hslczdzk01901), and the Fudan University Outstanding 2025 Program.

Acknowledgments

High tribute shall be paid to Eye and ENT Hospital of Fudan University.

Conflict of interest

The authors declare that the research was conducted in the absence of any commercial or financial relationships that could be construed as a potential conflict of interest.

The author(s) declared that they were an editorial board member of Frontiers, at the time of submission. This had no impact on the peer review process and the final decision.

Publisher's note

Supplementary material

The Supplementary material for this article can be found online at: https://www.frontiersin.org/articles/10.3389/fmed.2023.1306276/full#supplementary-material

SUPPLEMENTARY FIGURE S1
The Bland-Altman analysis of two observers in measuring LDs showed excellent interobserver reproducibility.

References

1. Hashemi H, Pakzad R, Yekta A, Aghamirsalim M, Pakbin M, Ramin S, et al. Global and regional prevalence of age-related cataract: a comprehensive systematic review and meta-analysis. *Eye (Lond)*. (2020) 34:1357–70. doi: 10.1038/s41433-020-0806-3

2. Meng J, He W, Rong X, Miao A, Lu Y, Zhu X. Decentration and tilt of plate-haptic multifocal intraocular lenses in myopic eyes. *Eye Vis (Lond)*. (2020) 7:17. doi: 10.1186/s40662-020-00186-3

3. Chen X, Gu X, Wang W, Xiao W, Jin G, Wang L, et al. Characteristics and factors associated with intraocular lens tilt and decentration after cataract surgery. *J Cataract Refract Surg*. (2020) 46:1126–31. doi: 10.1097/j.jcrs.0000000000000219

4. Yao Y, Lu Q, Wei L, Cheng K, Lu Y, Zhu X. Efficacy and complications of cataract surgery in high myopia. *J Cataract Refract Surg*. (2021) 47:1473–80. doi: 10.1097/j.jcrs.0000000000000664

5. Zhu X, He W, Zhang Y, Chen M, Du Y, Lu Y. Inferior Decentration of multifocal intraocular lenses in myopic eyes. *Am J Ophthalmol*. (2018) 188:1–8. doi: 10.1016/j.ajo.2018.01.007

6. Vasavada A, Singh R. Relationship between lens and capsular bag size. *J Cataract Refract Surg*. (1998) 24:547–51. doi: 10.1016/S0886-3350(98)80300-3

7. Lim SJ, Kang SJ, Kim HB, Kurata Y, Sakabe I, Apple DJ. Analysis of zonular-free zone and lens size in relation to axial length of eye with age. *J Cataract Refract Surg*. (1998) 24:390–6. doi: 10.1016/S0886-3350(98)80329-5

8. Khng C, Osher RH. Evaluation of the relationship between corneal diameter and lens diameter. *J Cataract Refract Surg*. (2008) 34:475–9. doi: 10.1016/j.jcrs.2007.10.043

9. Erb-Eigner K, Hirnschall N, Hackl C, Schmidt C, Asbach P, Findl O. Predicting lens diameter: ocular biometry with high-resolution MRI. *Invest Ophthalmol Vis Sci*. (2015) 56:6847–54. doi: 10.1167/iovs.15-17228

10. Got W, Chang DH, Rocha KM, Gouvea L, Penatti R. Correlation of intraoperative optical coherence tomography of crystalline lens diameter, thickness, and volume with biometry and age. *Am J Ophthalmol*. (2021) 225:147–56. doi: 10.1016/j.ajo.2020.12.021

11. Qi J, He W, Zhang K, Guo D, Du Y, Lu Y, et al. Actual lens positions of three intraocular lenses in highly myopic eyes: an ultrasound biomicroscopy-based study. *Br J Ophthalmol*. (2022) 108:45–50. doi: 10.1136/bjo-2022-322037

12. Li X, Chang P, Li Z, Qian S, Zhu Z, Wang Q, et al. Agreement between anterior segment parameters obtained by a new ultrasound biomicroscopy and a swept-source fourier-domain anterior segment optical coherence tomography. *Expert Rev Med Devices*. (2020) 17:1333–40. doi: 10.1080/17434440.2020.1848541

13. Ruan X, Liang C, Xia Z, Tan X, Jin G, Jin L, et al. In-vivo lens biometry using the novel ultrasound biomicroscopy. *Front Med (Lausanne)*. (2022) 9:777645. doi: 10.3389/fmed.2022.777645

14. Nagase D, Akura J, Omatsu Y, Inoue Y. Intraoperative measurement of crystalline lens diameter in living humans. *Yonago Acta Med*. (2022) 65:53–62. doi: 10.33160/yam.2022.02.010

15. Rozema JJ, Atchison DA, Kasthurirangan S, Pope JM, Tassignon MJ. Methods to estimate the size and shape of the unaccommodated crystalline lens in vivo. *Invest Ophthalmol Vis Sci*. (2012) 53:2533–40. doi: 10.1167/iovs.11-8645

16. Muralidharan G, Martínez-Enríquez E, Birkenfeld J, Velasco-Ocana M, Pérez-Merino P, Marcos S. Morphological changes of human crystalline lens in myopia. *Biomed Opt Express*. (2019) 10:6084–95. doi: 10.1364/BOE.10.006084

17. Monsálvez-Romín D, Moulakaki AI, Esteve-Taboada JJ, Ferrer-Blasco T, Montés-Micó R. In vivo OCT assessment of anterior segment central axial lengths with accommodation. *Arq Bras Oftalmol*. (2017) 80:364–8. doi: 10.5935/0004-2749.20170089

18. Haddad JS, Rocha KM, Yeh K, Waring GO. Lens anatomy parameters with intraoperative spectral-domain optical coherence tomography in cataractous eyes. *Clin Ophthalmol*. (2019) 13:253–60. doi: 10.2147/OPTH.S184208

19. Martinez-Enriquez E, Sun M, Velasco-Ocana M, Birkenfeld J, Pérez-Merino P, Marcos S. Optical coherence tomography based estimates of crystalline lens volume, equatorial diameter, and plane position. *Invest Ophthalmol Vis Sci*. (2016) 57:OCT600. doi: 10.1167/iovs.15-18933

20. Vass C, Menapace R, Schmetterer K, Findl O, Rainer G, Steineck I. Prediction of pseudophakic capsular bag diameter based on biometric variables. *J Cataract Refract Surg*. (1999) 25:1376–81. doi: 10.1016/S0886-3350(99)00204-7

21. Mohamed A, Nandyala S, Ho A, Manns F, Parel JA, Augusteyn RC. Relationship of the cornea and globe dimensions to the changes in adult human crystalline lens diameter, thickness and power with age. *Exp Eye Res*. (2021) 209:108653. doi: 10.1016/j.exer.2021.108653

22. Qi J, He W, Meng J, Wei L, Qian D, Lu Y, et al. Distribution of ocular anterior and posterior segment lengths among a cataract surgical population in Shanghai. *Front Med (Lausanne)*. (2021) 8:688805. doi: 10.3389/fmed.2021.688805

23. Yao Y, Meng J, He W, Zhang K, Wei L, Cheng K, et al. Associations between anterior segment parameters and rotational stability of a plate-haptic toric intraocular lens. *J Cataract Refract Surg*. (2021) 47:1436–40. doi: 10.1097/j.jcrs.0000000000000653

24. Wei L, He W, Meng J, Qian D, Lu Y, Zhu X. Evaluation of the white-to-white distance in 39,986 Chinese Cataractous eyes. *Invest Ophthalmol Vis Sci*. (2021) 62:7. doi: 10.1167/iovs.62.1.7

Frontiers in Medicine

Translating medical research and innovation into improved patient care

A multidisciplinary journal which advances our medical knowledge. It supports the translation of scientific advances into new therapies and diagnostic tools that will improve patient care.

Discover the latest Research Topics

See more →

Frontiers

Avenue du Tribunal-Fédéral 34
1005 Lausanne, Switzerland
frontiersin.org

Contact us

+41 (0)21 510 17 00
frontiersin.org/about/contact